

JPL D-27667-A

SPITZER SPACE TELESCOPE

Focal Plane Survey Final Report

APPENDIX A: IRS

David S. Bayard
Bryan H. Kang
Paul B. Brugarolas
Dhemetrios Boussalis

July 8, 2004



Jet Propulsion Laboratory
California Institute of Technology

Copyright © 2004 California Institute of Technology. Government sponsorship acknowledged.

Appendix A contains final IPF calibration reports for the IRS Fine Focal Plane Survey:

NF	RN	Description	Report #	Page #
018	701	IRS_Red_PeakUp_FOV_Center	ID701018	A-5
019	701	IRS_Red_PeakUp_FOV_Sweet_Spot	ID701019	A-47
022	701	IRS_Blue_PeakUp_FOV_Center	ID701022	A-89
023	701	IRS_Blue_PeakUp_FOV_Sweet_Spot	ID701023	A-131
028	502	IRS_ShortLo_1st_Ord_Center_Pos	ID502028	A-173
034	502	IRS_ShortLo_2nd_Ord_Center_Pos	ID502034	A-217
040	502	IRS_LongLo_1st_Ord_Center_Pos	ID502040	A-259
046	501	IRS_LongLo_2nd_Ord_Center_Pos	ID501046	A-305
052	502	IRS_ShortHi_Center_Position	ID502052	A-349
058	501	IRS_LongHi_Center_Position	ID501058	A-393

Note: A complete set of IPF calibration reports is available on the SIRTF project website (https://sirtfweb/pub/IPF_focal_plane_survey).

This page left blank.

JET PROPULSION LABORATORY

SIRTF IPF REPORT

JPL ID701018

April 26, 2004

**SIRTF INSTRUMENT POINTING FRAME
KALMAN FILTER EXECUTION SUMMARY**

IPF RUN NUMBER: 701018

REPORT TYPE: IOC EXECUTION (FINE)

PRIME FRAME: IRS_Red_PeakUp_FOV_Center (18)

INFERRRED FRAMES:

IPF TEAM

Autonomy and Control Section (345)

Jet Propulsion Laboratory

California Institute of Technology

4800 Oak Grove Drive

Pasadena, CA 91109

Contents

1 IPF EXECUTION SUMMARY	5
2 IPF INPUT FILE HISTORY	9
3 IPF EXECUTION RESULTS	10
3.1 IPF EXECUTION OUTPUT PLOTS	10
3.2 IPF OUTPUT DATA (IF MINI FILE)	36
3.3 IPF EXECUTION LOG	38
4 COMMENTS	41

List of Figures

1.1 A-priori and a-posteriori IPF frames	5
1.2 A-priori and a-posteriori IPF frames (ZOOMED)	8
2.1 Scenario Plot	9
3.1 TPF coords of measurements and a-priori predicts	12
3.2 Oriented Pixel Coords of measurements and a-priori predicts	12
3.3 Oriented (W,V) Pixel Coords of A-Priori Prediction Error Quiver Plot	13
3.4 A-priori prediction error (Science Centroids)	13
3.5 Oriented Pixel Coords of measurements and a-priori predicts (PCRS only)	14
3.6 Oriented Pixel Coords of measurements and a-priori predicts (Zoomed, PCRS only)	14
3.7 Oriented (W,V) Pixel Coords of A-Priori PCRS Prediction Error Quiver Plot	15
3.8 A-priori PCRS prediction error	15
3.9 IPF execution convergence, chart 1	16
3.10 IPF execution convergence, chart 2	16
3.11 Parameter uncertainty convergence	17
3.12 IPF parameter symbol table	17
3.13 KF parameter error sigma plots	18
3.14 LS parameter error sigma plot	18
3.15 KF and LS parameter error sigma plot	19

3.16	Oriented Pixel Coords of meas. and a-posteriori predicts	20
3.17	Oriented Pixel Coords of meas. and a-posteriori predicts (attitude corrected)	20
3.18	KF innovations with (o) and w/o (+) attitude corrections	21
3.19	Histograms of science a-posteriori residuals (or innovations)	21
3.20	A-Posteriori Science Centroid Prediction Error Quiver (Att. Cor.)	22
3.21	Normalized A-Posteriori Science Centroid Prediction Errors	22
3.22	KF innovations with (o) and w/o (+) attitude corrections (PCRS)	23
3.23	Histograms of PCRS a-posteriori residuals (or innovations)	23
3.24	A-posteriori PCRS Prediction Summary	24
3.25	A-posteriori PCRS Prediction (PCRS 1 Only)	25
3.26	A-posteriori PCRS Prediction (PCRS 2 Only)	25
3.27	A-Posteriori PCRS Prediction Errors Quiver (Att. Cor.)	26
3.28	Normalized A-Posteriori PCRS Prediction Errors	26
3.29	W-axis KF innovations and 1-sigma bound	27
3.30	V-axis KF innovations and 1-sigma bound	27
3.31	Array plot with (solid) and w/o (dashed) optical distortion corrections	28
3.32	Optical Distortion Plot: total (x5 magnification)	28
3.33	Optical Distortion Plot: constant plate scales (x5 magnification)	29
3.34	Optical Distortion Plot: linear plate scale (x5 magnification)	29
3.35	Optical Distortion Plot: gamma terms (x5 magnification)	30
3.36	Scan Mirror Chops	30
3.37	IPF Frame Reconstruction	31
3.38	Center Pixel Reconstruction	31
3.39	Estimated attitude corrections (Body frame)	32
3.40	Estimated attitude error sigma plot (Body frame)	32
3.41	Thermo-mechanical boresight drift (equiv. angle in (W,V) coords)	33
3.42	Thermo-mechanical boresight drift (equiv. angle in Body frame)	33
3.43	Gyro drift bias contribution (equiv. rate in (W,V) coords)	34
3.44	Gyro drift bias contribution (equiv. angle in (W,V) coords)	34
3.45	Gyro drift bias contribution (equiv. angle in Body frame)	35

List of Tables

1.1	IPF filter input files	6
1.2	IPF filter execution configuration	6
1.3	IPF filter execution mask vector assignment	6
1.4	IPF calibration error summary ([arcsec], 1-sigma, radial)	7
1.5	Science measurement prediction error summary (1-sigma)	7
1.6	IPF Brown angle summary	8
2.1	IPF input file editing status	9
3.1	Table of figures I (IPF run)	10
3.2	Table of figures II (IPF run)	11
3.3	PCRS measurement prediction error summary	24

1 IPF EXECUTION SUMMARY

This report summarizes the SIRTF Instrument Pointing Frame (IPF) Kalman Filter execution associated with run file: RN701018. In particular, this Focal Point Survey calibrates the instrument: IRS_Red_PeakUp_FOV_Center (18), as part of the IOC Fine Survey. The main calibration results from the IPF filter execution have been documented in IF701018 typically stored in the mission archive DOM collection IPF_IF. This report only summarizes the main aspects of the run, and does not substitute for the full information contained in the IF file.

Section 1 summarizes the filter execution results. The filter configurations are tabulated in Table 1.2 and the mask vector assignments are tabulated in Table 1.3. A total of 27 state parameters are estimated in this run. The overall End-to-End pointing performances are tabulated in Table 1.4. The prediction residuals throughout the estimation processes are tabulated in Table 1.5. Section 3 summarizes resulting plots, a mini summary of the IF IPF output file, and the execution log. Section 4 captures the user comments that are specific to this particular run.

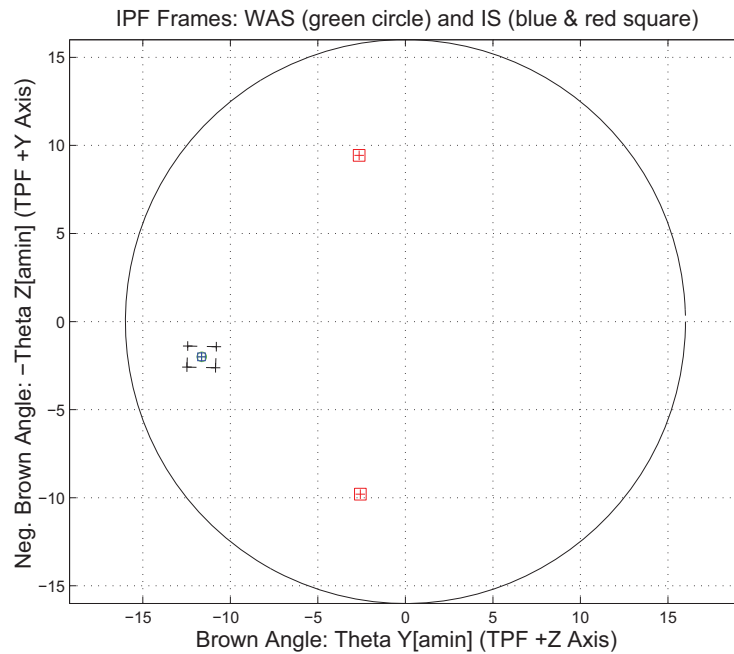


Figure 1.1: A-priori and a-posteriori IPF frames

RAW	FINAL (After Editing)
AA501018	AA501018
AS501018	AS501018
CA501018	CA501018
CB502018	CB502018
CS701018	CS701018

Table 1.1: IPF filter input files

EXECUTION CONFIGURATION ITEM	CURRENT STATUS
IPF Filter Version Used	IPF.V4.0.0
Frame Table Version Used	BodyFrames_FTU_17a
Scan-Mirror Employed?	NO
IPF Filter Mode	NORMAL-MODE(0)
SLIT-MODE Operation	DISABLED
Kalman Filter Operation	ENABLED
Least-Squares Data Analysis	ENABLED
IBAD Screening	ENABLED
User-Specified Data Editing	DISABLED
Total Number of Iterations	35
LS Residual Sigma Scale	5.41871908E-001
Total Number of Maneuvers	7

Table 1.2: IPF filter execution configuration

Con. Plate Scale			Γ Dependent				Γ^2 Dependent				Linear Plate Scale						Mirror	
a_{00}	b_{00}	c_{00}	a_{10}	b_{10}	c_{10}	d_{10}	a_{20}	b_{20}	c_{20}	d_{20}	a_{01}	b_{01}	c_{01}	d_{01}	e_{01}	f_{01}	α	β
1	2	3	4	5	6	7	8	9	10	11	12	13	14	15	16	17	18	19
1	1	1	0	0	0	0	0	0	0	0	1	1	1	1	1	1	0	0
IPF (T)			Alignment R										Gyro Drift Bias					
θ_1	θ_2	θ_3	a_{rx}	a_{ry}	a_{rz}	b_{rx}	b_{ry}	b_{rz}	c_{rx}	c_{ry}	c_{rz}	b_{gx}	b_{gy}	b_{gz}	c_{gx}	c_{gy}	c_{gz}	
20	21	22	23	24	25	26	27	28	29	30	31	32	33	34	35	36	37	
1	1	1	1	1	1	1	1	1	1	1	1	1	1	1	1	1	1	

Table 1.3: IPF filter execution mask vector assignment

FOCAL PLANE SURVEY ANALYSIS: IOC Fine Survey.

INSTRUMENT NAME: IRS_Red_PeakUp_FOV_Center **NF: 18**

PIX2RADW: 8.72660000E-008 [rad/pixel] = 1.8000E-002 [arcsec/pixel]

PIX2RADV: 8.72660000E-008 [rad/pixel] = 1.8000E-002 [arcsec/pixel]

FRAME	DESCRIPTION	IPF ¹	SF ²	TOTAL	REQ
018(P)	IRS_Red_PeakUp_FOV_Center	0.0279	0.0855	0.0899	0.25

Table 1.4: IPF calibration error summary ([arcsec], 1-sigma, radial)

RMS METRIC	A PRIORI ³	A POSTERIORI ³	ATT. CORRECTED ⁴	UNITS
Radial	1.3635	0.1075	0.0509	arcsec
W-Axis	1.3367	0.0645	0.0390	arcsec
V-Axis	0.2690	0.0859	0.0327	arcsec
Radial	75.7489	5.9702	2.8271	pixels
W-Axis	74.2600	3.5845	2.1658	pixels
V-Axis	14.9450	4.7743	1.8171	pixels

Table 1.5: Science measurement prediction error summary (1-sigma)

¹IPF filter removes systematic pointing errors due to: thermomechanical alignment drift (Body to TPF), gyro bias and bias drift, centroiding error, attitude error, and optical distortion. IPF SIGMA presented here is “Scaled” by the Least Squares Scale factor. The Least Squares Scale Factor was: 0.541872. It is assumed that the gyro Angle Random Walk contribution is captured with the Least Squares scaling. The gyro ARW contribution can be approximately calculated as 0.0788 arcseconds, given that ARW = 100 $\mu\text{deg}/\sqrt{\text{hr}}$, with 6.043555e+002 second Maneuver time (max), and 7 independent Maneuvres.

²Gyro Scale Factor(GSF) assumes 95 ppm error over 0.250 degree maneuver.

³This can be interpreted as estimate of ”pixel to sky” pointing reconstruction error if no science data is used.

⁴This can be interpreted as estimate of achieved S/I centroiding error

IPF BROWN ANGLE SUMMARY					
FRAME TABLE USED: BodyFrames_FTU_17a					
NF	NAME	WAS	IS	CHANGE	UNIT
018	theta_Y	-11.634104	-11.649227	-0.015122	arcmin
018	theta_Z	+2.000761	+2.000391	-0.000370	arcmin
018	angle	+1.797497	+1.796568	-0.000929	deg

Table 1.6: IPF Brown angle summary

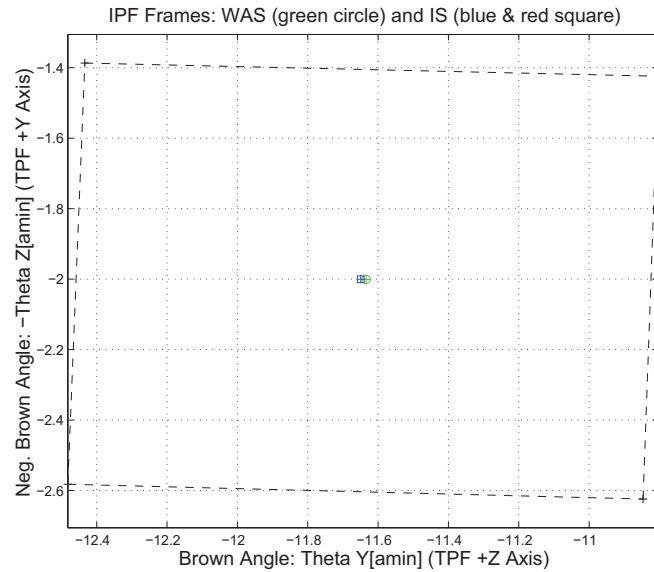


Figure 1.2: A-priori and a-posteriori IPF frames (ZOOMED)

2 IPF INPUT FILE HISTORY

WAS	SIZE	IS	SIZE	REMOVED	PATCHED
AA501018	UNCHANGED	AA501018	UNCHANGED	0	0
CA501018	UNCHANGED	CA501018	UNCHANGED	0	N/A
CB502018	UNCHANGED	CB502018	UNCHANGED	0	N/A

Table 2.1: IPF input file editing status

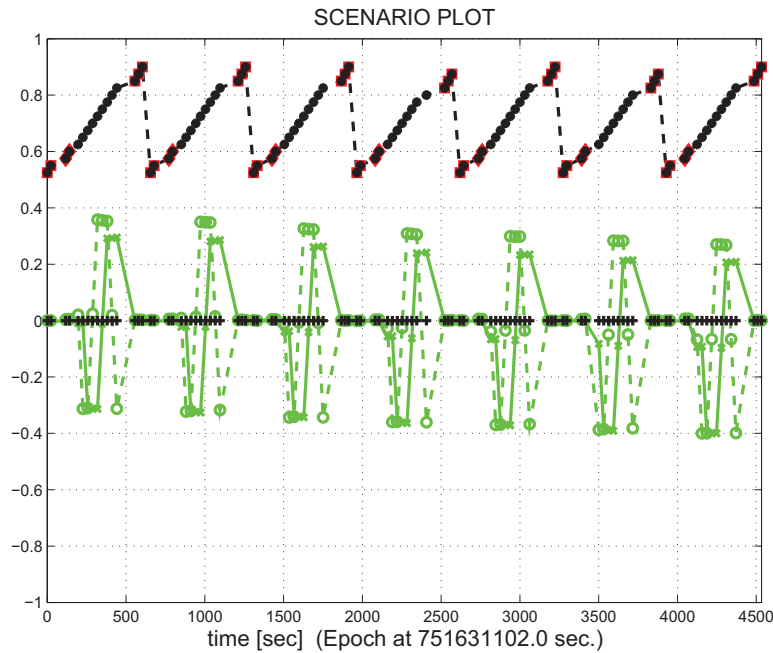


Figure 2.1: Scenario Plot

3 IPF EXECUTION RESULTS

3.1 IPF EXECUTION OUTPUT PLOTS

This subsection summarizes the IPF filter results. As shown in Table 3.1, the output plots are segmented to three groups: predicted performance, post-run results and IPF trending plots.

FIGURE NO.	DESCRIPTION
Predicted performance prior to IPF run	
Figure 3.1	Meas. and a-priori predicts in TPF coords
Figure 3.2	Meas. and a-priori predicts in Oriented Pixel Coords including rectangular array boundary approximation
Figure 3.3	A-Priori Prediction Error Quiver Plot in Oriented Pixel Coords including rectangular array boundary approximation
Figure 3.4	A-priori prediction error
Figure 3.5	Oriented Pixel Coords of measurements and a-priori predicts (PCRS only)
Figure 3.6	Oriented Pixel Coords of measurements and a-priori predicts (Zoomed, PCRS only)
Figure 3.7	Oriented (W,V) Pixel Coords of A-Priori PCRS Prediction Error Quiver Plot
Figure 3.8	A-priori PCRS prediction error
IPF filter performance (post run results)	
Figure 3.9	IPF execution convergence, chart 1: (top) normalized residual error vs. iteration number and (bottom) norm of effective parameter corrections
Figure 3.10	IPF execution convergence, chart 2: parameter correction size vs. iteration number
Figure 3.11	Parameter uncertainty convergence: square-root of diagonal elements of covariance matrix vs. maneuver number
Figure 3.12	IPF parameter symbol table
Figure 3.13	KF parameter error sigma plot (a-priori-dashed, a-posteriori-solid). Includes true parameter errors (FLUTE runs only)
Figure 3.14	LS parameter error sigma plot. Includes true parameter errors (FLUTE runs only)
Figure 3.15	KF and LS parameter errors sigma plot (Figure 3.13 & Figure 3.14 combined)
Figure 3.16	Measurements and a-posteriori predicts in Oriented Pixel Coords including rectangular array boundaries (a-priori-dashed, a-posteriori-solid)
Figure 3.17	Attitude corrected meas. and a-posteriori predicts in Oriented Pixel Coords including rectangular array boundaries (a-priori-dashed, a-posteriori-solid)

Table 3.1: Table of figures I (IPF run)

FIGURE NO.	DESCRIPTION
IPF filter performance (post run results) - CONTINUE	
Figure 3.18	KF innovations with (o) and w/o (+) attitude corrections
Figure 3.19	Histograms of science a-posteriori residuals (or innovations)
Figure 3.20	A-Posteriori Science Centroid Prediction Error Quiver (Att. Cor.)
Figure 3.21	Normalized A-Posteriori Science Centroid Prediction Errors
Figure 3.22	KF innovations with (o) and w/o (+) attitude corrections (PCRS)
Figure 3.23	Histograms of PCRS a-posteriori residuals (or innovations)
Figure 3.24	A-posteriori PCRS Prediction Summary
Figure 3.25	A-posteriori PCRS Prediction (PCRS 1 Only)
Figure 3.26	A-posteriori PCRS Prediction (PCRS 2 Only)
Figure 3.27	A-Posteriori PCRS Prediction Errors Quiver (Att. Cor.)
Figure 3.28	Normalized A-Posteriori PCRS Prediction Errors
Figure 3.29	W-axis KF innovations and 1-sigma bound
Figure 3.30	V-axis KF innovations and 1-sigma bound
Figure 3.31	Array plot with (solid) and w/o (dashed) optical distortion corrections
Figure 3.32	Optical Distortion Plot: total (x5 magnification)
Figure 3.33	Optical Distortion Plot: constant plate scales (x5 magnification)
Figure 3.34	Optical Distortion Plot: linear plate scale (x5 magnification)
Figure 3.35	Optical Distortion Plot: gamma terms (x5 magnification)
Figure 3.36	Scan Mirror Chops
Figure 3.37	IPF Frame Reconstruction
Figure 3.38	Center Pixel Reconstruction
IPF parameter trending plots	
Figure 3.39	Estimated attitude corrections (Body frame)
Figure 3.40	Estimated attitude error sigma plot (Body frame)
Figure 3.41	Systematic error attributed to thermo-mechanical boresight drift (equiv. angle in (W,V) coords)
Figure 3.42	Systematic error attributed to thermo-mechanical boresight drift (equiv. angle in Body frame)
Figure 3.43	Systematic error attributed to gyro drift bias (equiv. rate in (W,V) coords)
Figure 3.44	Systematic error attributed to gyro drift bias (equiv. angle in (W,V) coords)
Figure 3.45	Systematic error attributed to gyro drift bias (equiv. angle in Body frame)

Table 3.2: Table of figures II (IPF run)

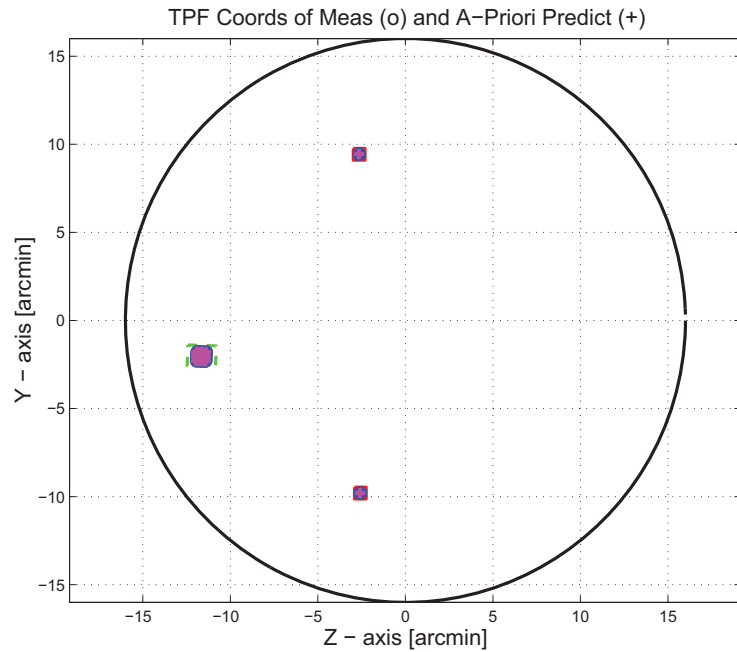


Figure 3.1: TPF coords of measurements and a-priori predicts

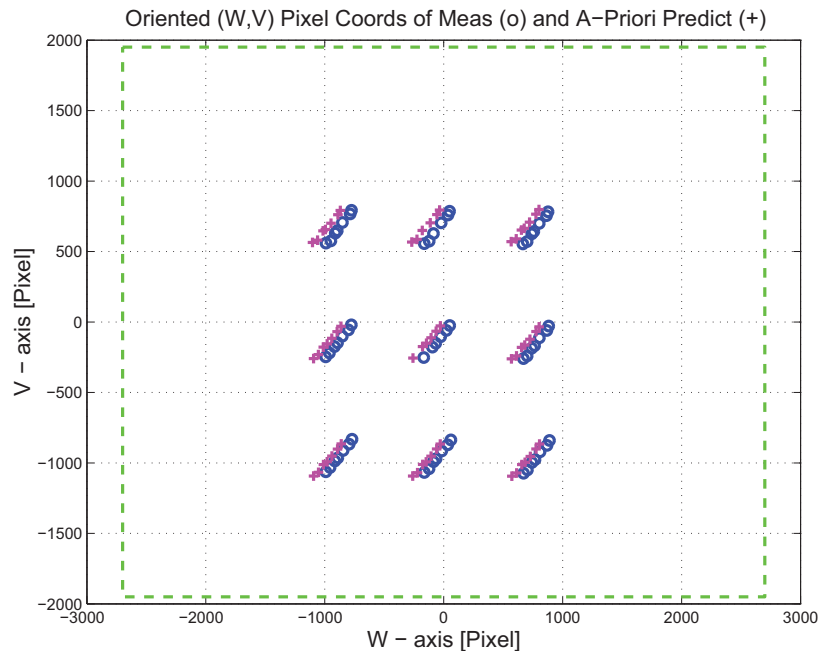


Figure 3.2: Oriented PixelCoords of measurements and a-priori predicts

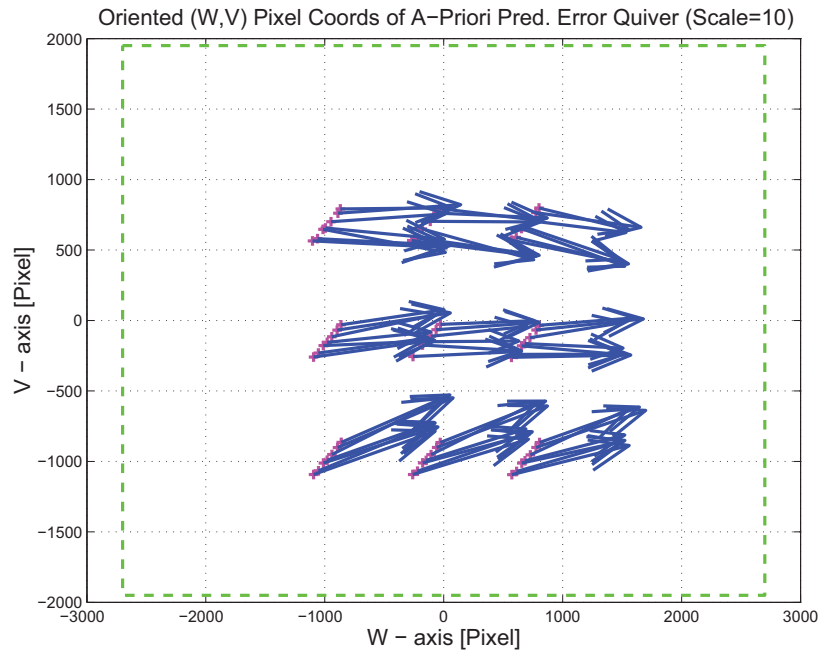


Figure 3.3: Oriented (W,V) Pixel Coords of A-Priori Prediction Error Quiver Plot

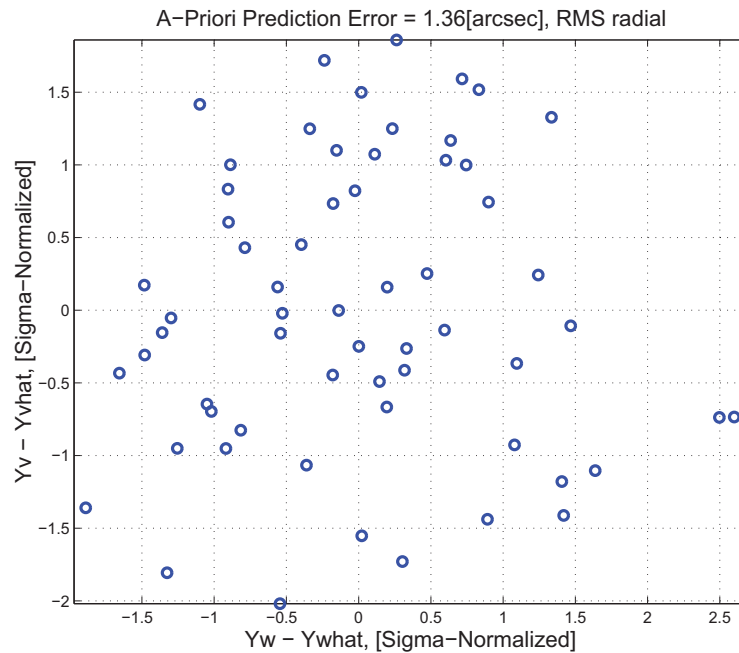


Figure 3.4: A-priori prediction error (Science Centroids)

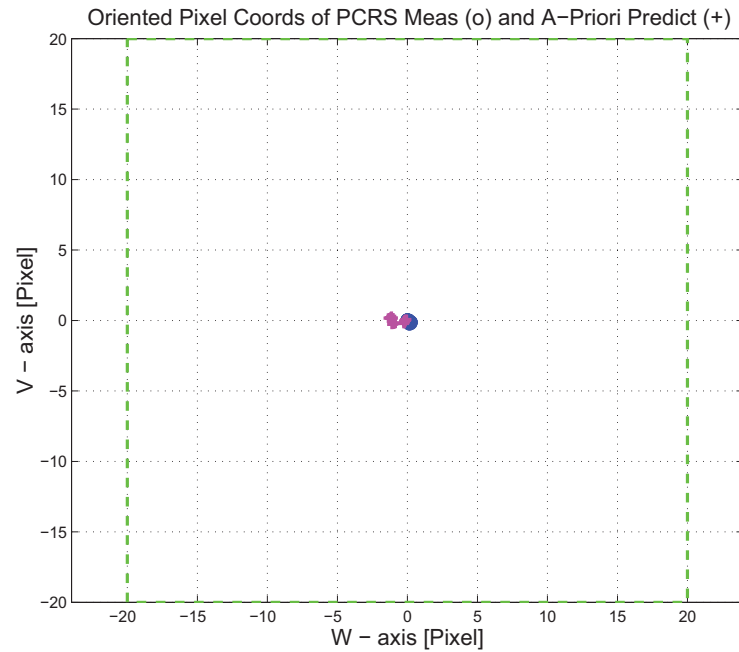


Figure 3.5: Oriented Pixel Coords of measurements and a-priori predicts (PCRS only)

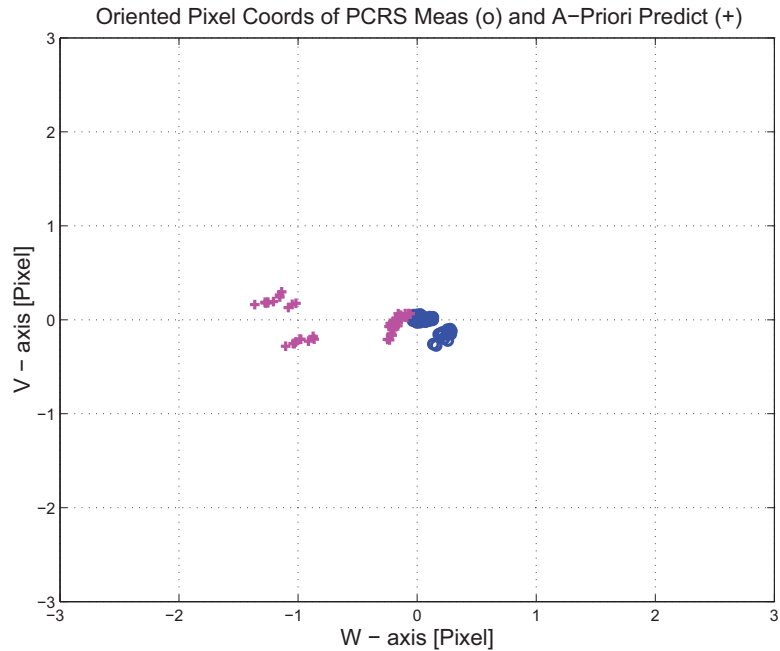


Figure 3.6: Oriented Pixel Coords of measurements and a-priori predicts (Zoomed, PCRS only)

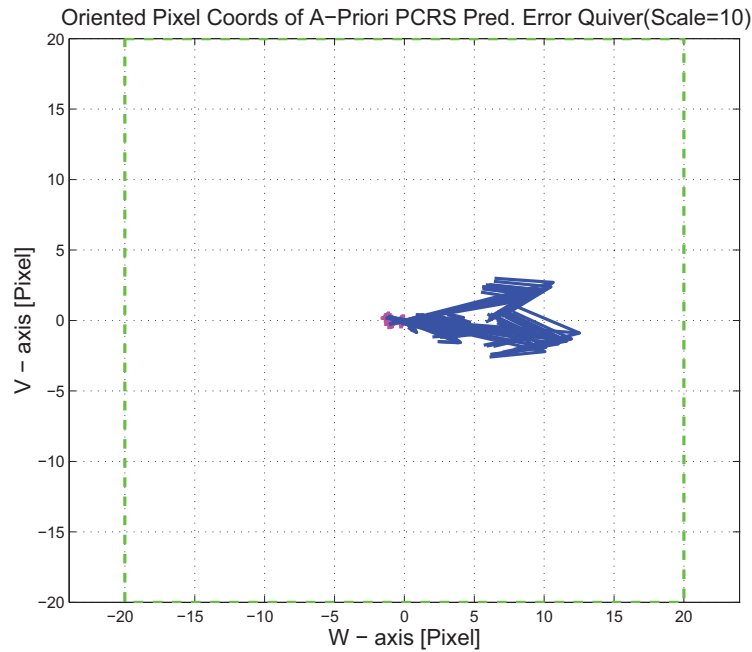


Figure 3.7: Oriented (W,V) Pixel Coords of A-Priori PCRS Prediction Error Quiver Plot

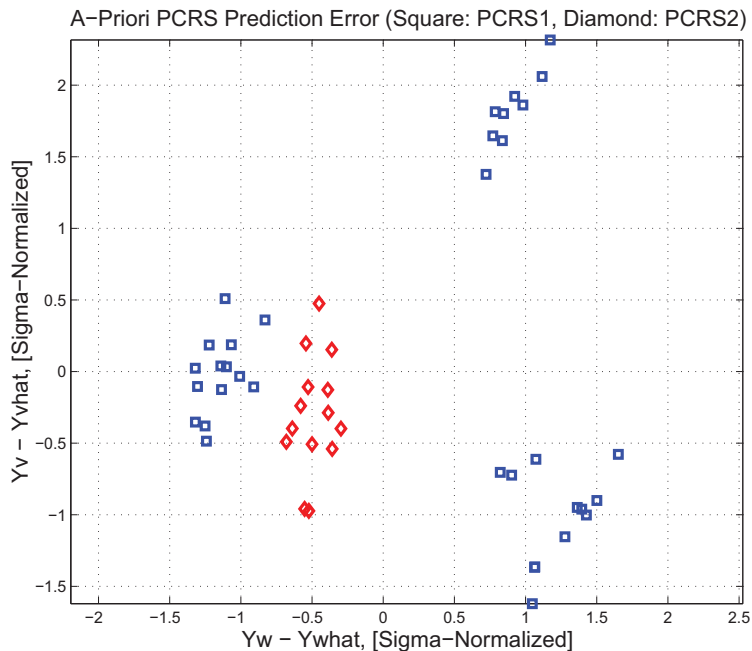


Figure 3.8: A-priori PCRS prediction error

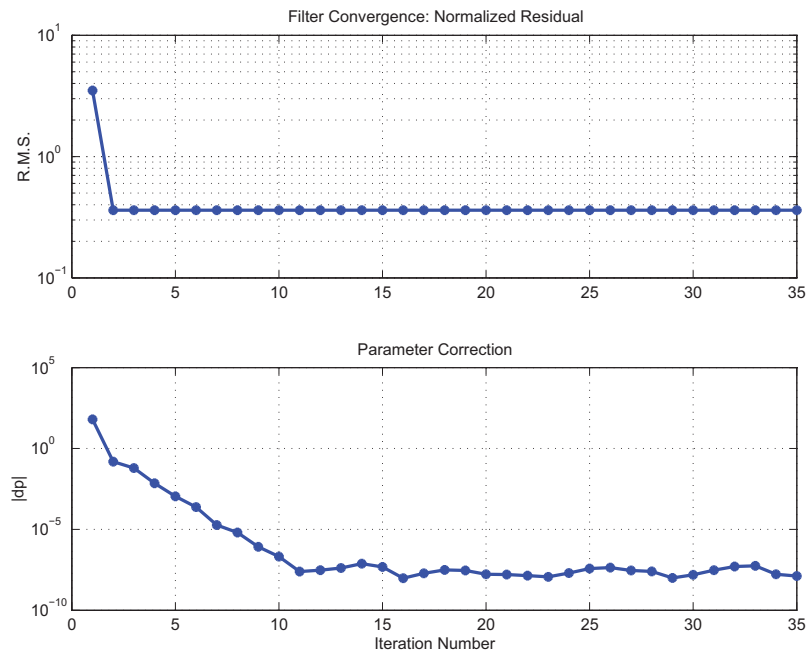


Figure 3.9: IPF execution convergence, chart 1

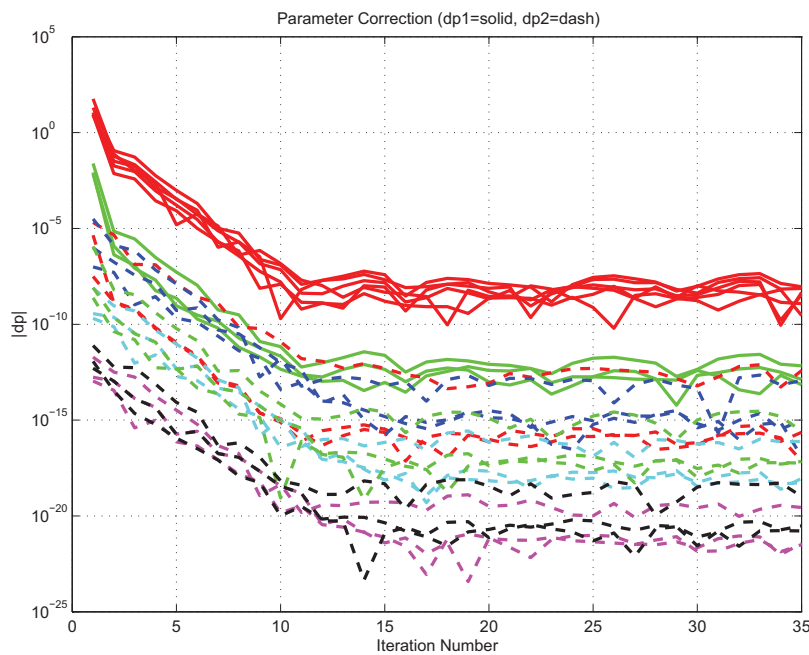


Figure 3.10: IPF execution convergence, chart 2

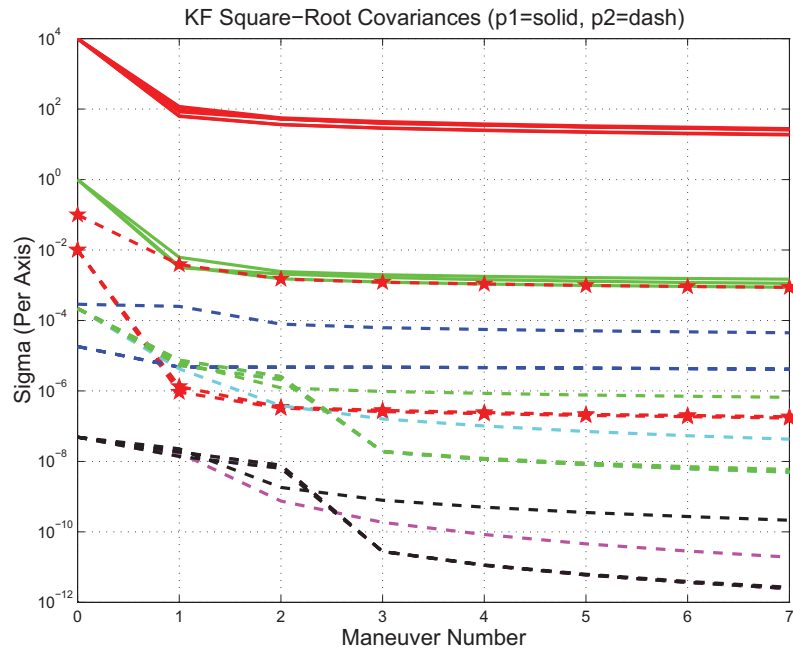


Figure 3.11: Parameter uncertainty convergence

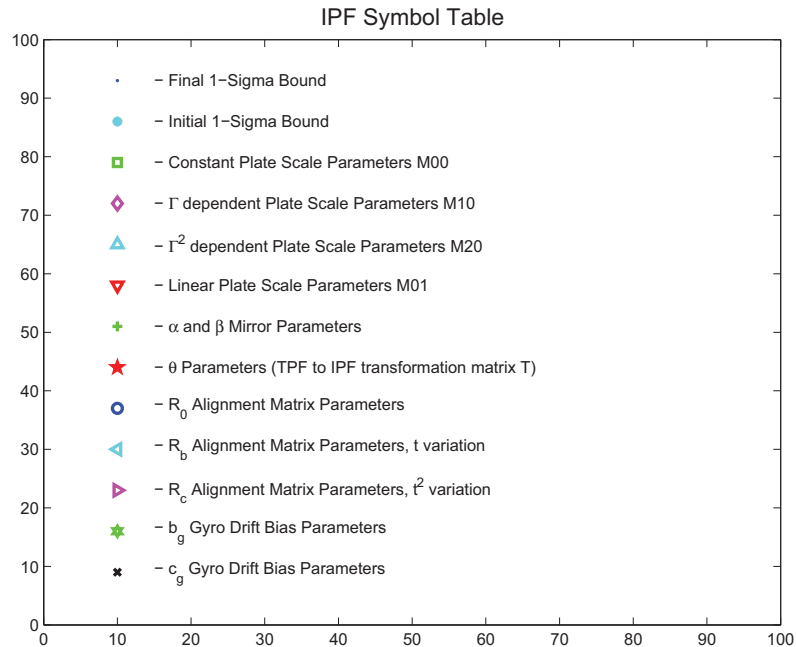


Figure 3.12: IPF parameter symbol table

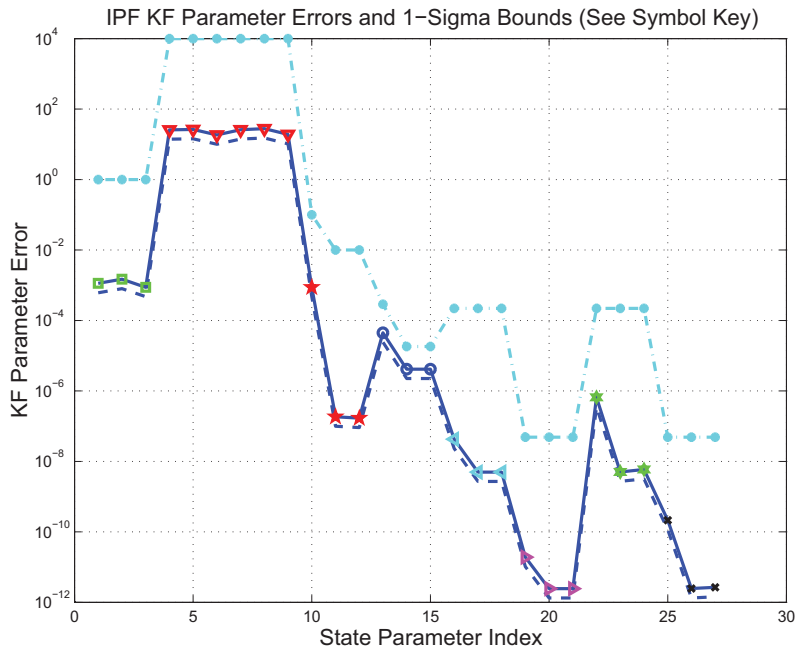


Figure 3.13: KF parameter error sigma plots

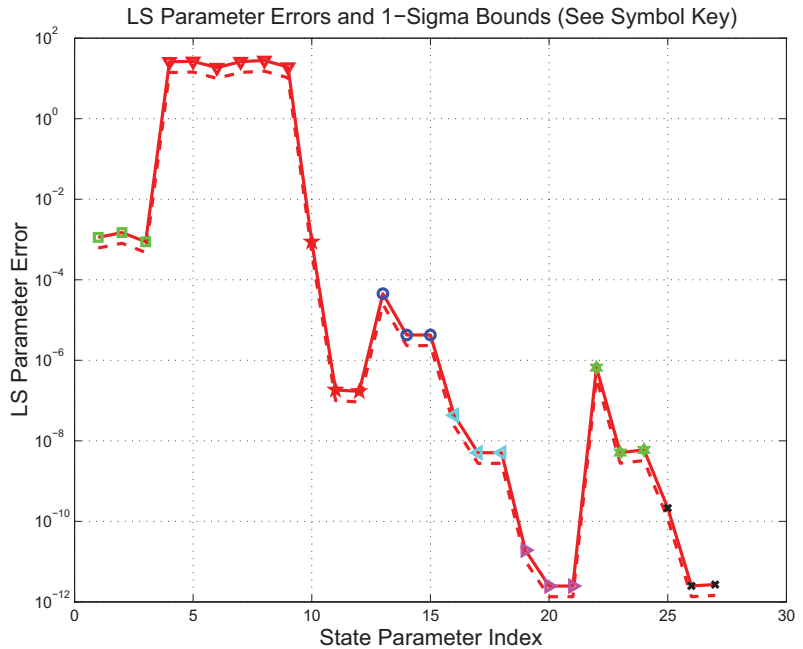


Figure 3.14: LS parameter error sigma plot

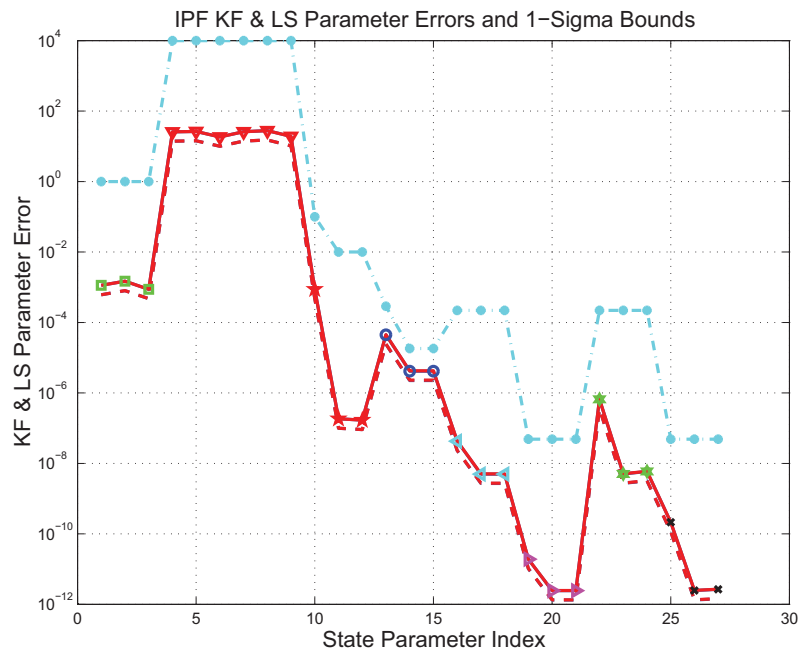


Figure 3.15: KF and LS parameter error sigma plot

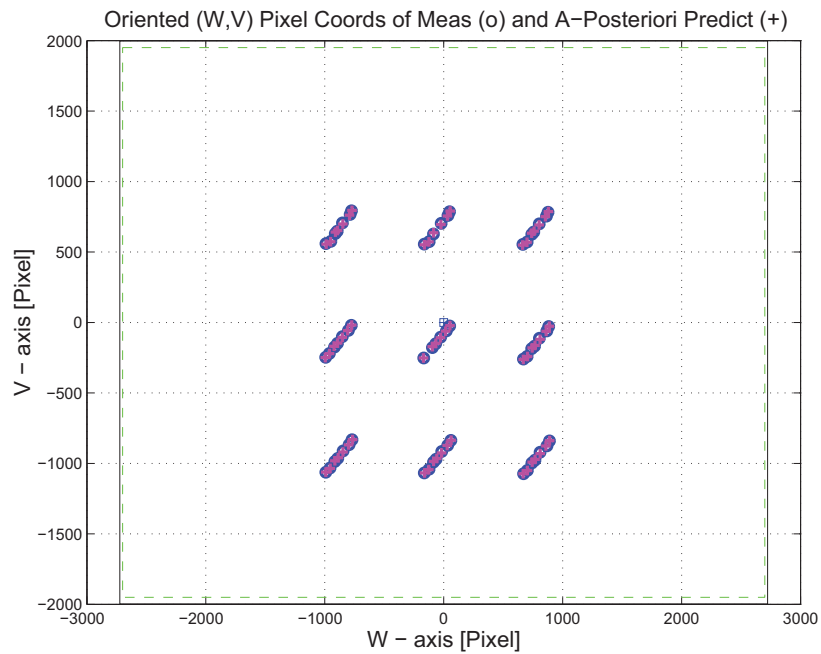


Figure 3.16: Oriented Pixel Coords of meas. and a-posteriori predicts

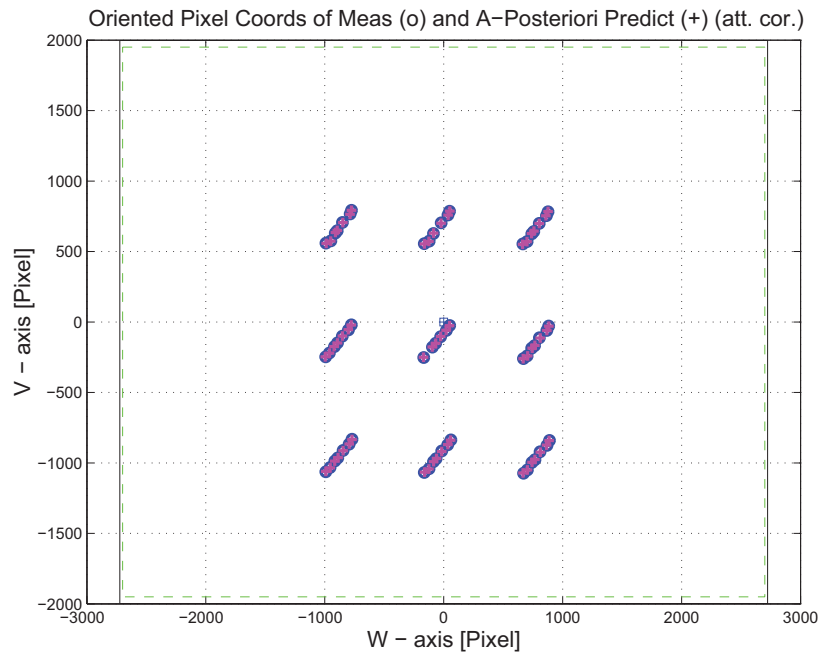


Figure 3.17: Oriented Pixel Coords of meas. and a-posteriori predicts (attitude corrected)

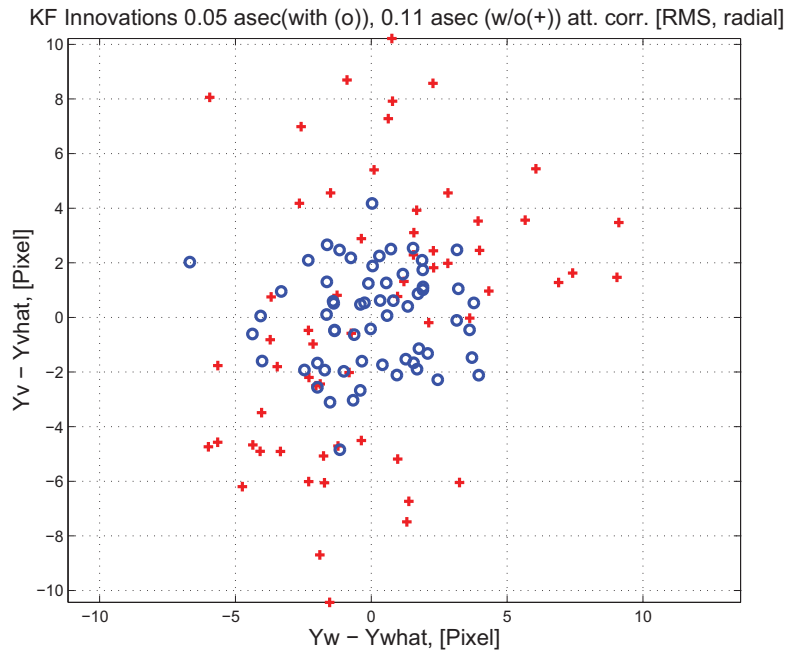


Figure 3.18: KF innovations with (o) and w/o (+) attitude corrections

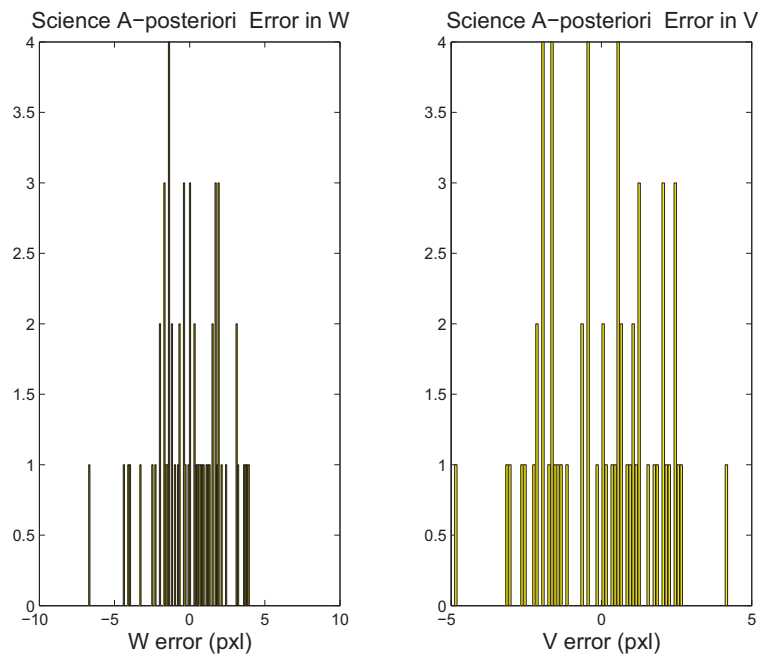


Figure 3.19: Histograms of science a-posteriori residuals (or innovations)

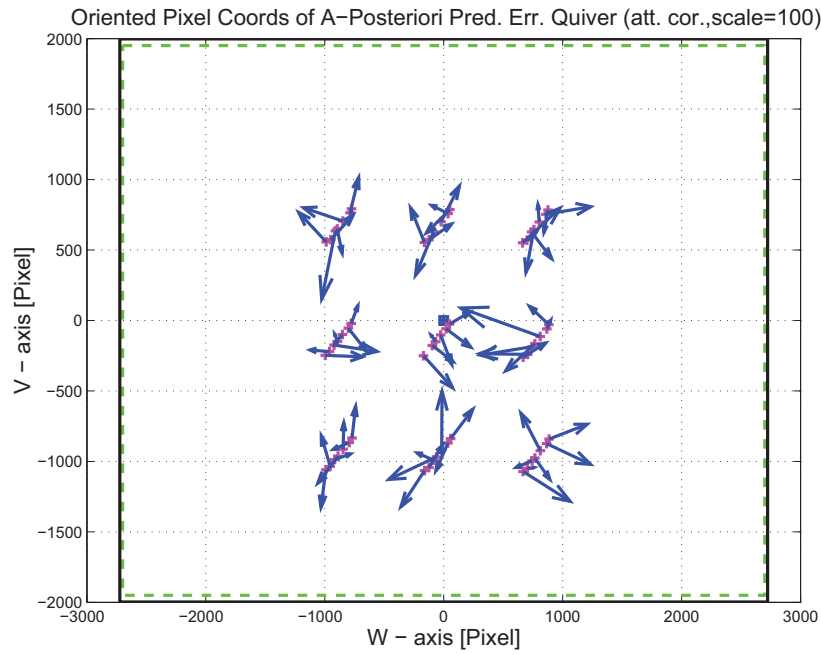


Figure 3.20: A-Posteriori Science Centroid Prediction Error Quiver (Att. Cor.)

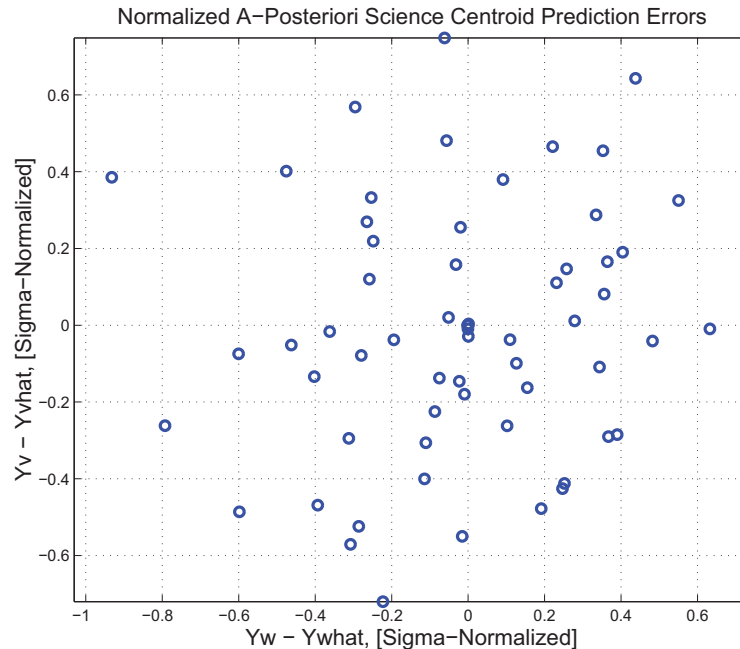


Figure 3.21: Normalized A-Posteriori Science Centroid Prediction Errors

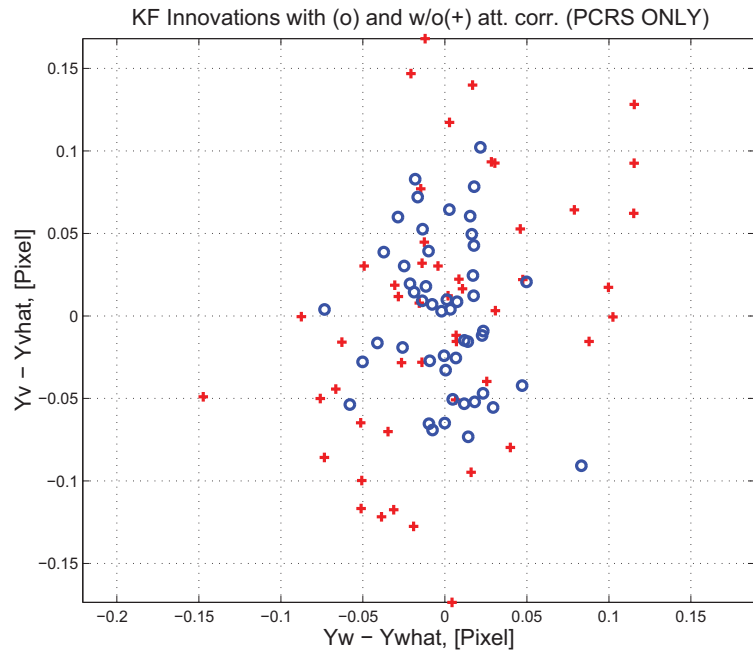


Figure 3.22: KF innovations with (o) and w/o (+) attitude corrections (PCRS)

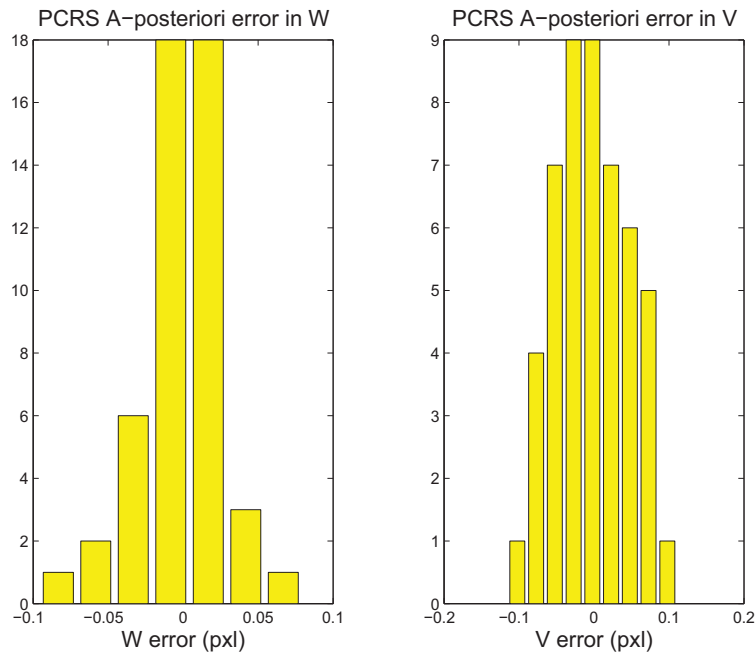


Figure 3.23: Histograms of PCRS a-posteriori residuals (or innovations)

IPF PCRS SUMMARY						
PCRS 1 (Total of 35 centroids)						
RMS	MEAN		SIGMA			
METRIC	APOST.	ATT. COR.	APOST.	ATT. COR.	STAT. CONF.	UNITS
Radial	0.0037	0.0034	0.1041	0.0565	0.0095	arcsec
W-axis	0.0002	-0.0000	0.0592	0.0284	0.0048	arcsec
V-axis	0.0037	0.0034	0.0857	0.0488	0.0083	arcsec
PCRS 2 (Total of 14 centroids)						
METRIC	APOST.	ATT. COR.	APOST.	ATT. COR.	STAT. CONF.	UNITS
Radial	0.0092	0.0095	0.0674	0.0434	0.0116	arcsec
W-axis	0.0003	0.0000	0.0455	0.0239	0.0064	arcsec
V-axis	-0.0092	-0.0095	0.0497	0.0362	0.0097	arcsec
Combined (Total of 49 centroids)						
METRIC	APOST.	ATT. COR.	APOST.	ATT. COR.	STAT. CONF.	UNITS
Radial	0.0003	0.0003	0.0953	0.0534	0.0076	arcsec
W-axis	0.0003	-0.0000	0.0556	0.0272	0.0039	arcsec
V-axis	0.0000	-0.0003	0.0774	0.0460	0.0066	arcsec

Table 3.3: PCRS measurement prediction error summary

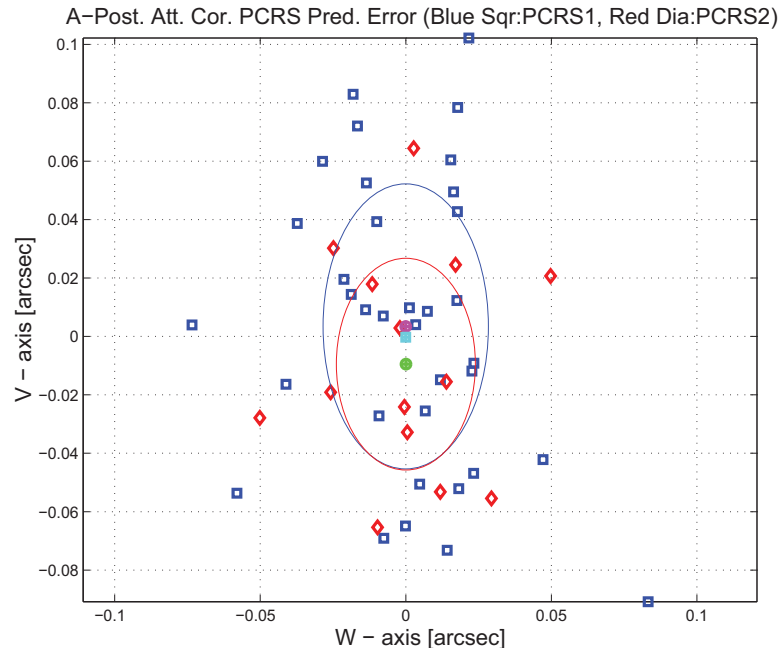


Figure 3.24: A-posteriori PCRS Prediction Summary

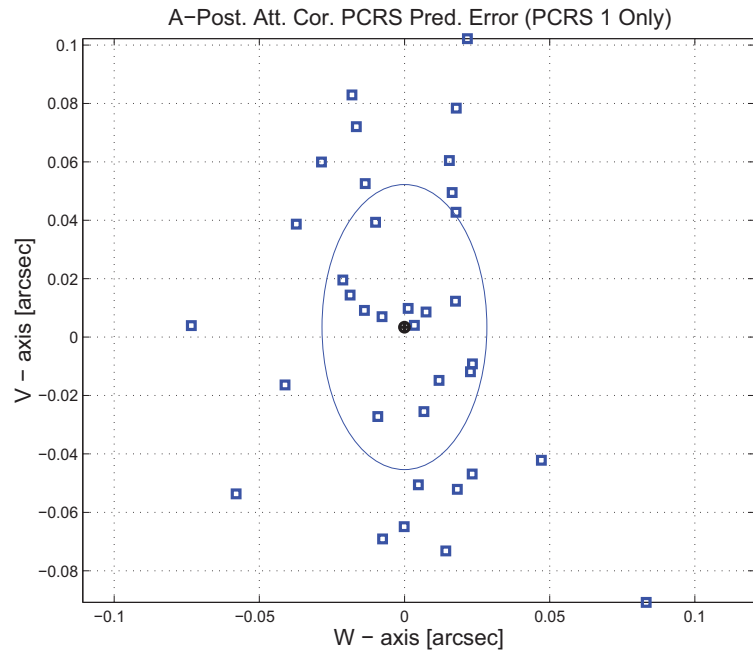


Figure 3.25: A-posteriori PCRS Prediction (PCRS 1 Only)

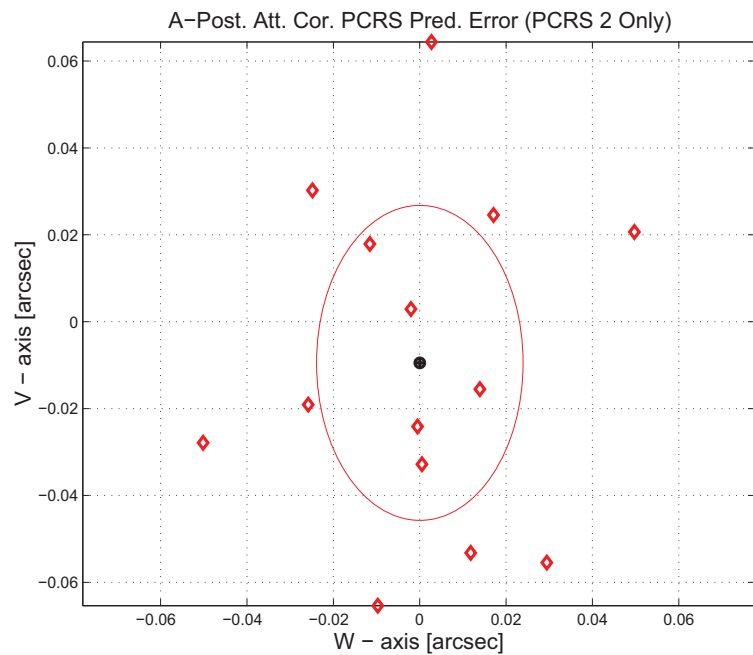


Figure 3.26: A-posteriori PCRS Prediction (PCRS 2 Only)

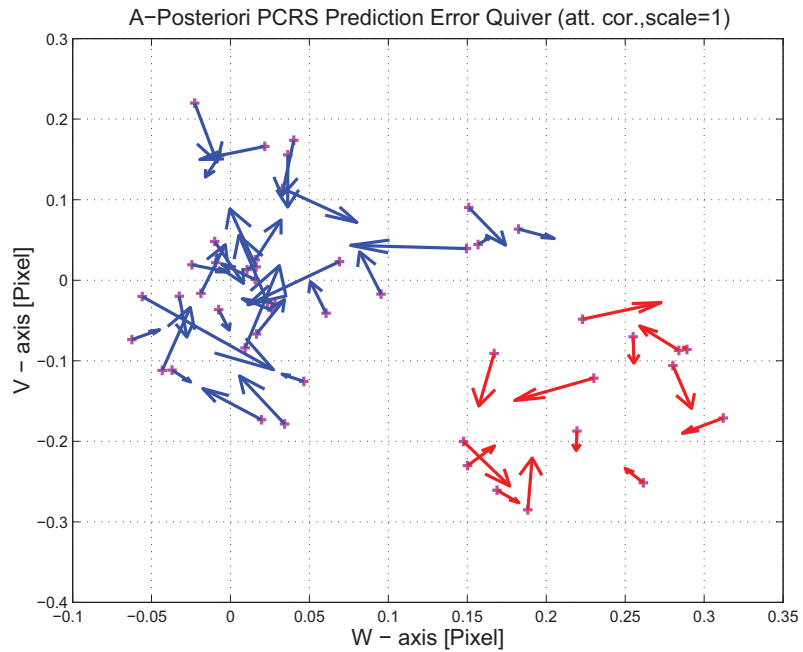


Figure 3.27: A-Posteriori PCRS Prediction Errors Quiver (Att. Cor.)

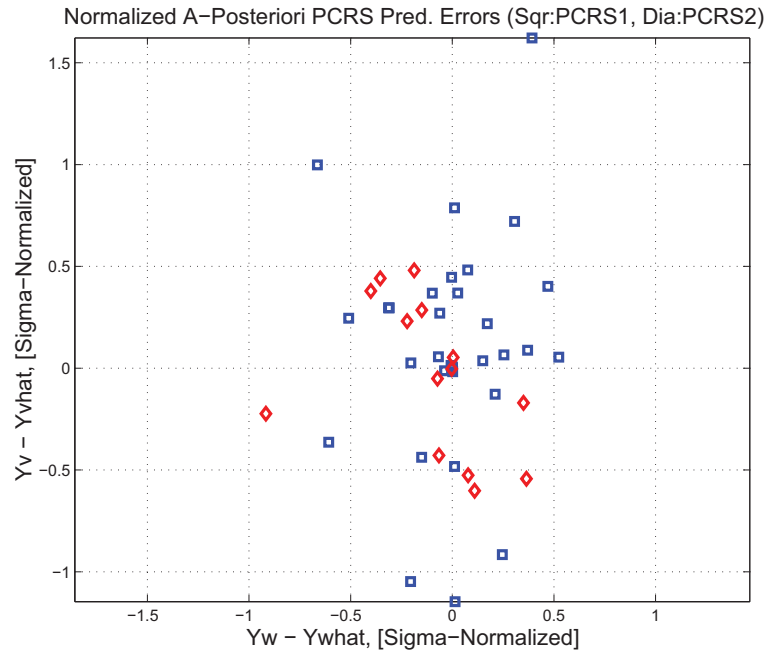


Figure 3.28: Normalized A-Posteriori PCRS Prediction Errors

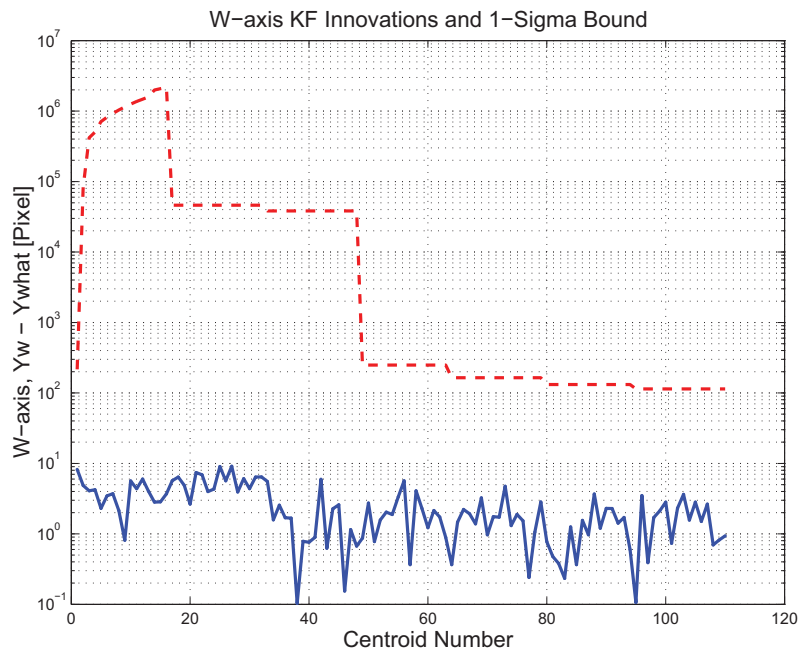


Figure 3.29: W-axis KF innovations and 1-sigma bound

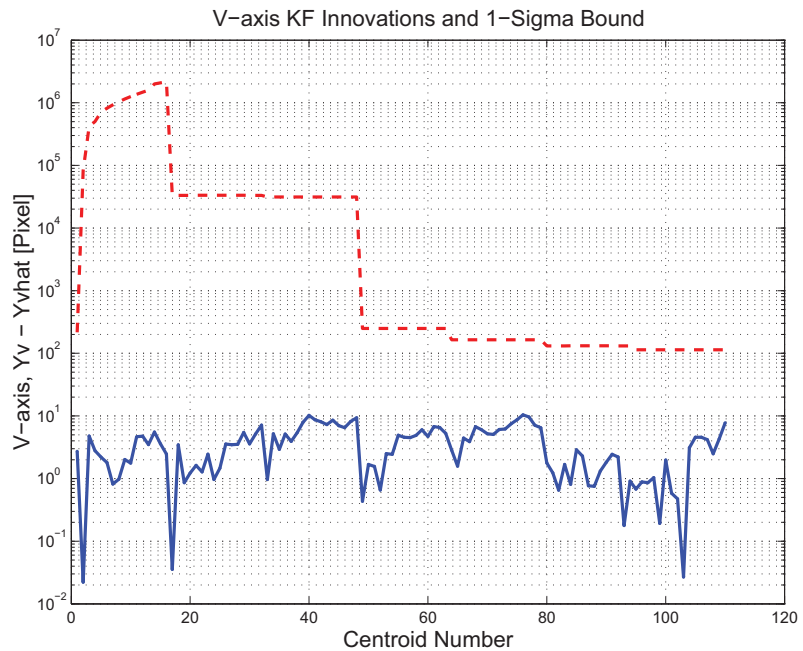


Figure 3.30: V-axis KF innovations and 1-sigma bound

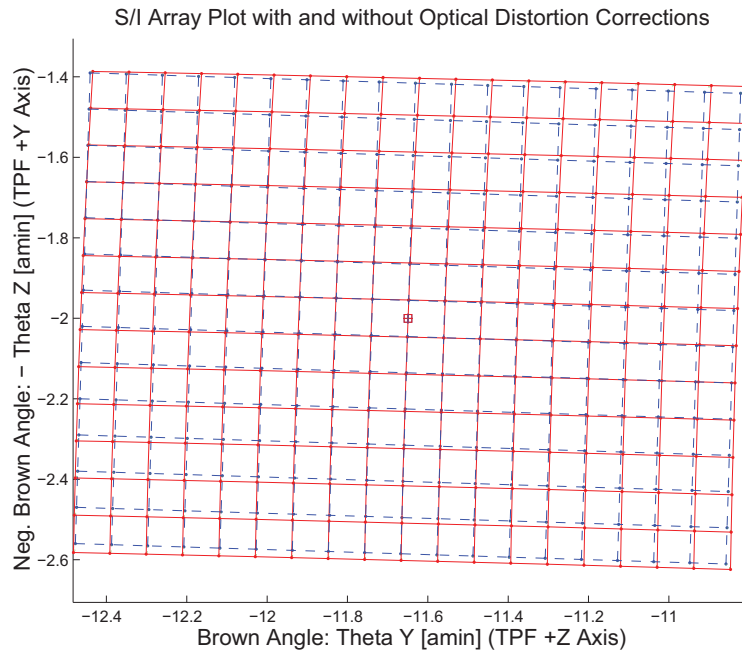


Figure 3.31: Array plot with (solid) and w/o (dashed) optical distortion corrections

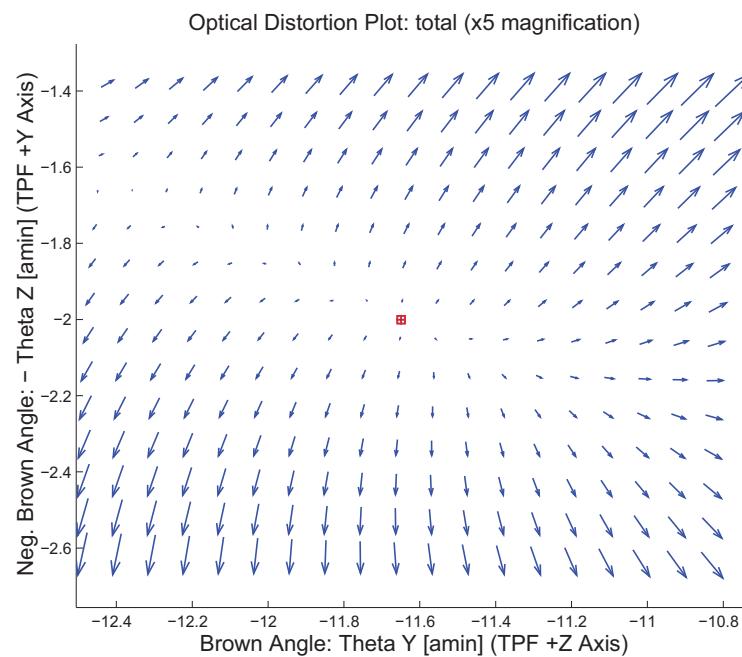


Figure 3.32: Optical Distortion Plot: total (x5 magnification)

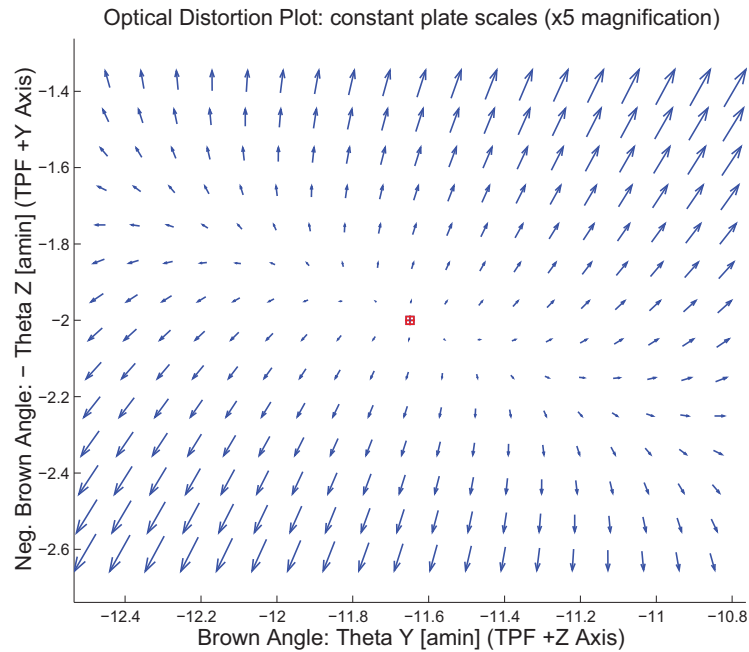


Figure 3.33: Optical Distortion Plot: constant plate scales (x5 magnification)

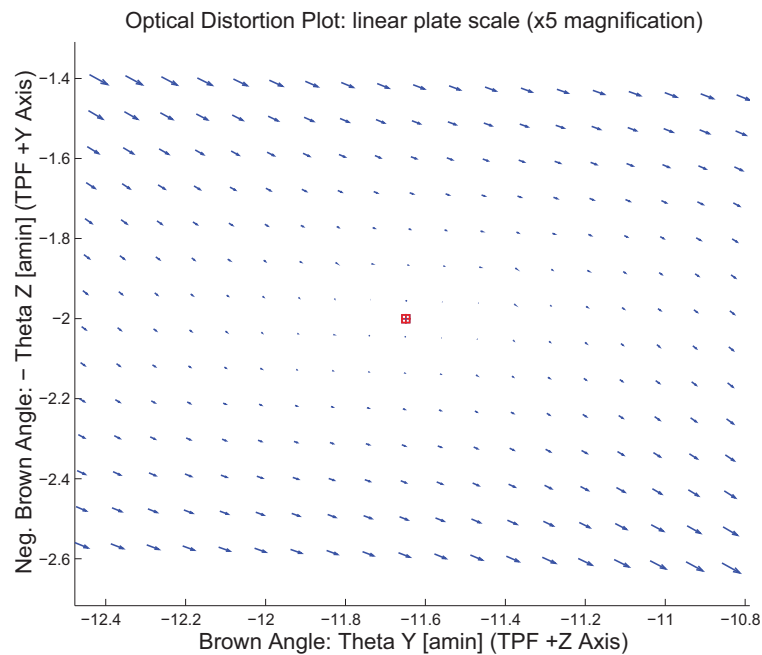


Figure 3.34: Optical Distortion Plot: linear plate scale (x5 magnification)

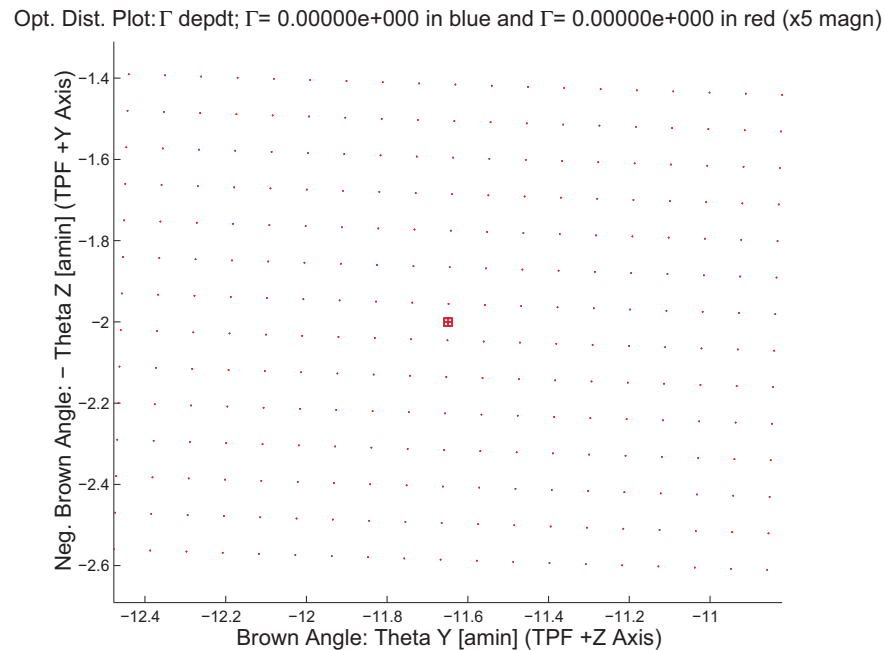


Figure 3.35: Optical Distortion Plot: gamma terms (x5 magnification)

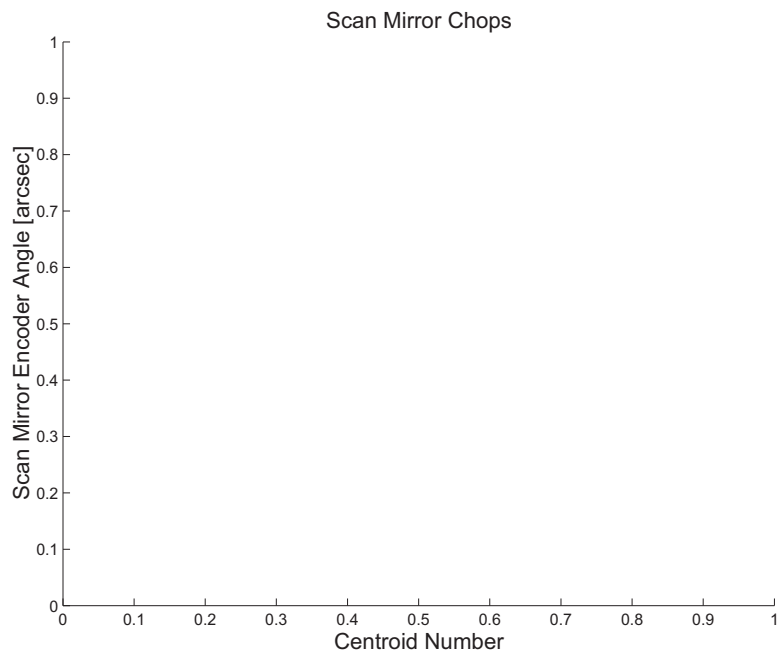


Figure 3.36: Scan Mirror Chops

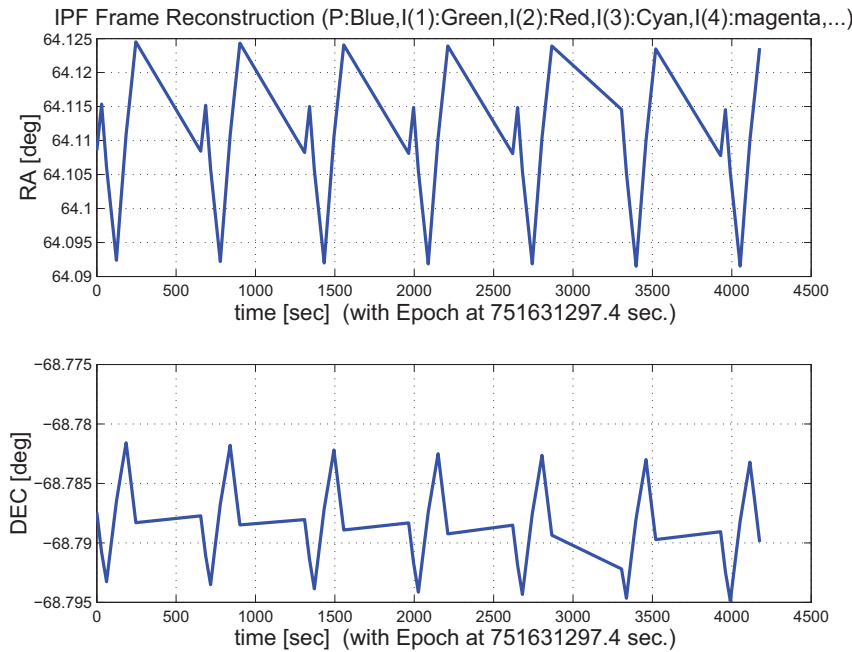


Figure 3.37: IPF Frame Reconstruction

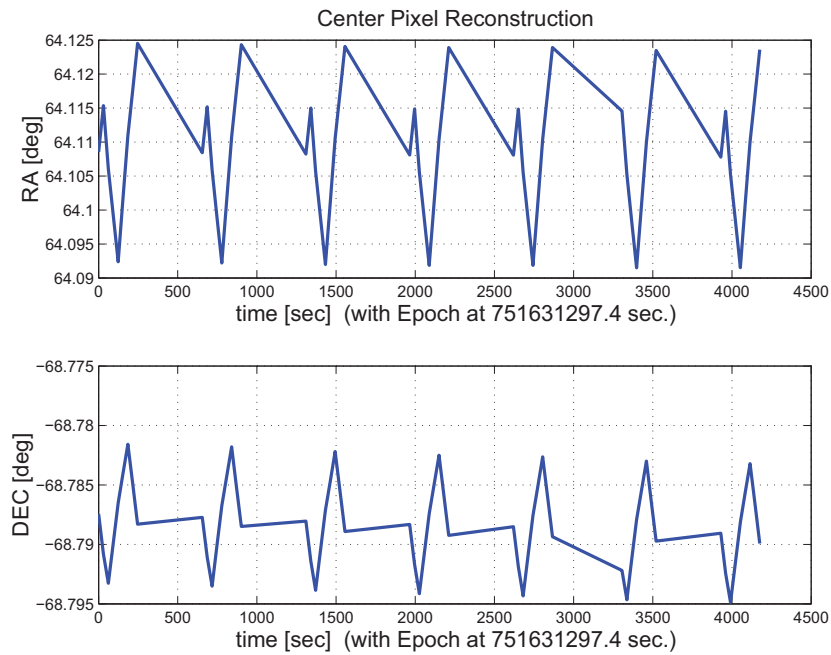


Figure 3.38: Center Pixel Reconstruction

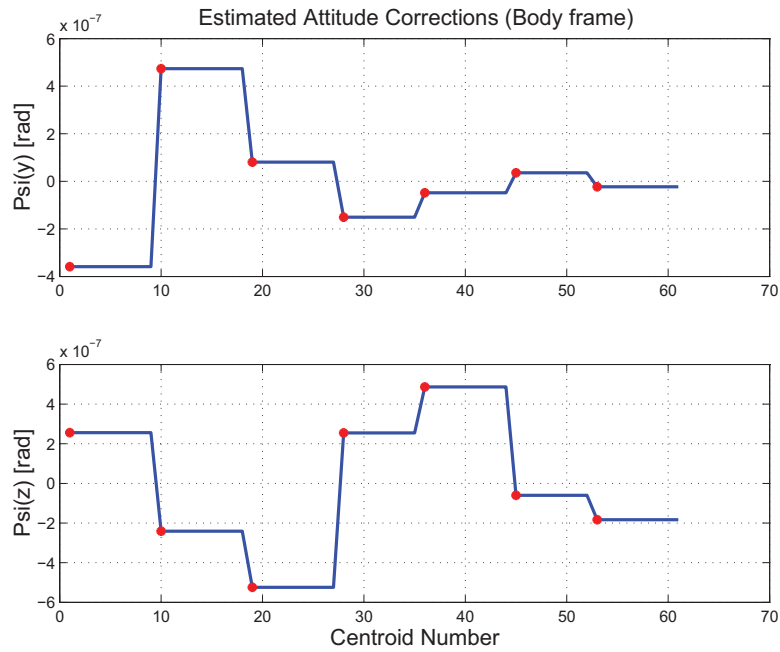


Figure 3.39: Estimated attitude corrections (Body frame)

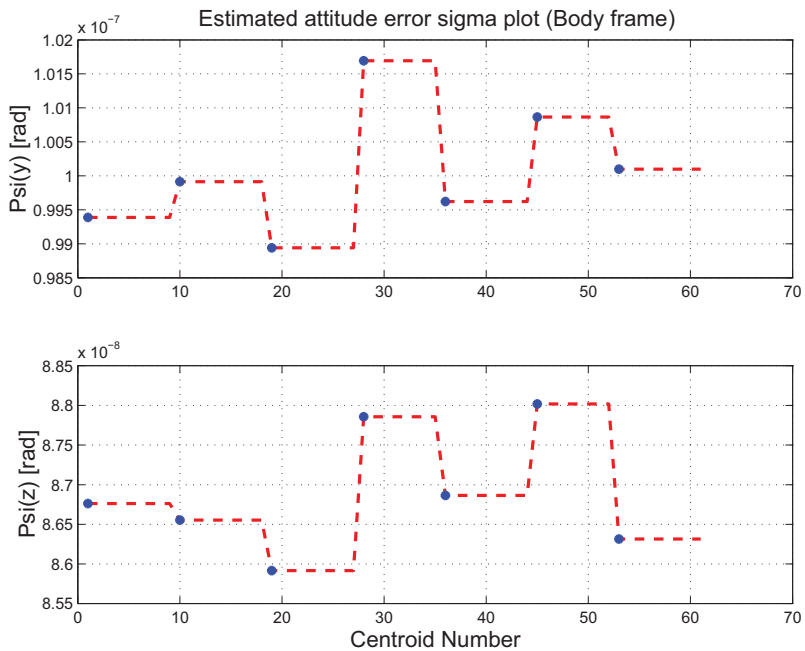


Figure 3.40: Estimated attitude error sigma plot (Body frame)

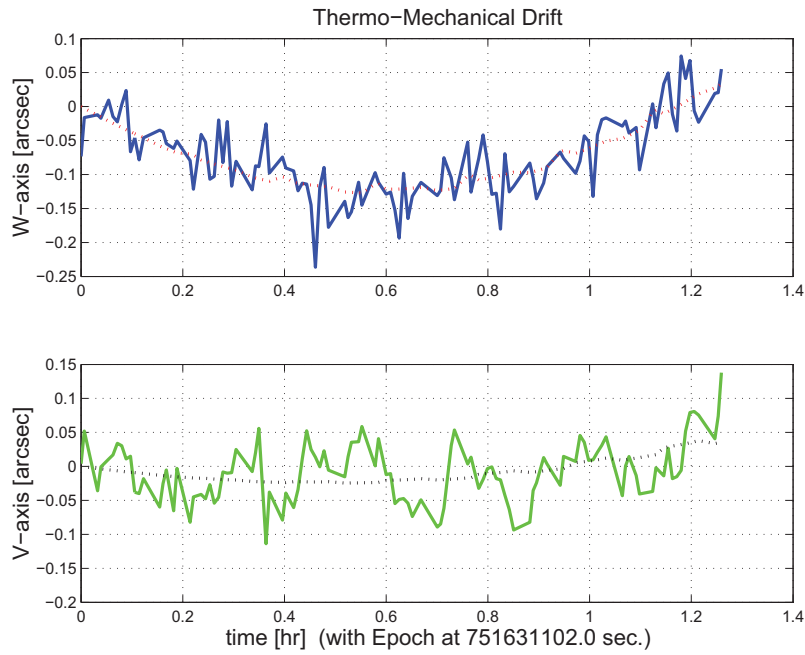


Figure 3.41: Thermo-mechanical boresight drift (equiv. angle in (W,V) coords)

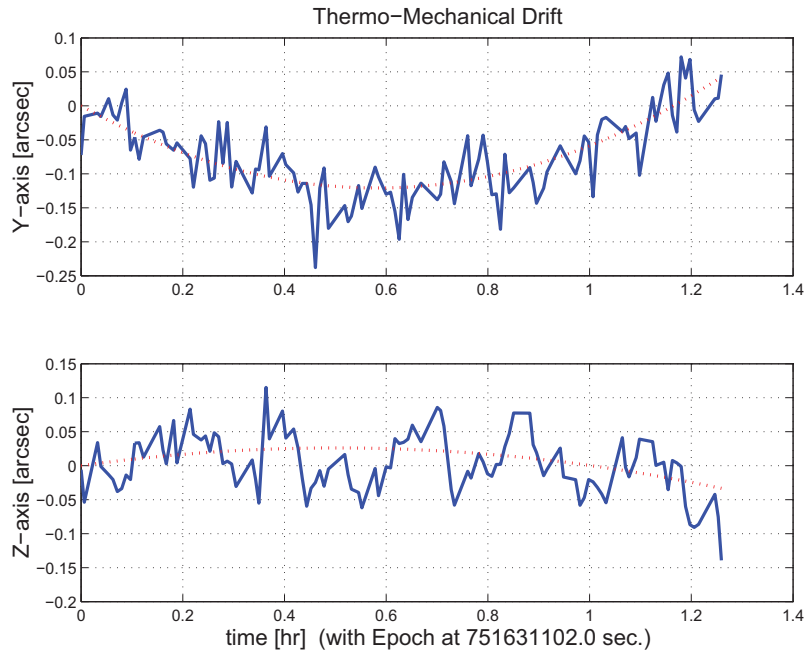


Figure 3.42: Thermo-mechanical boresight drift (equiv. angle in Body frame)

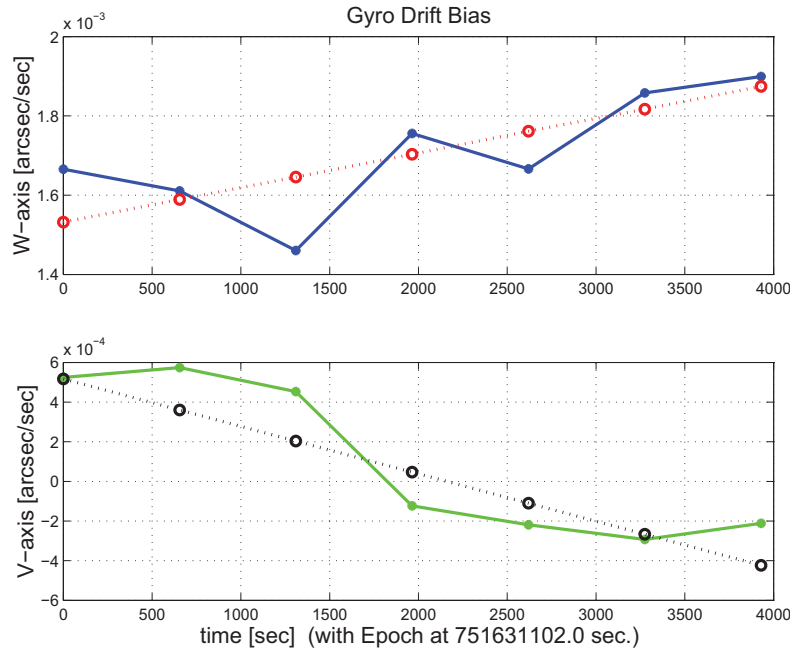


Figure 3.43: Gyro drift bias contribution (equiv. rate in (W,V) coords)

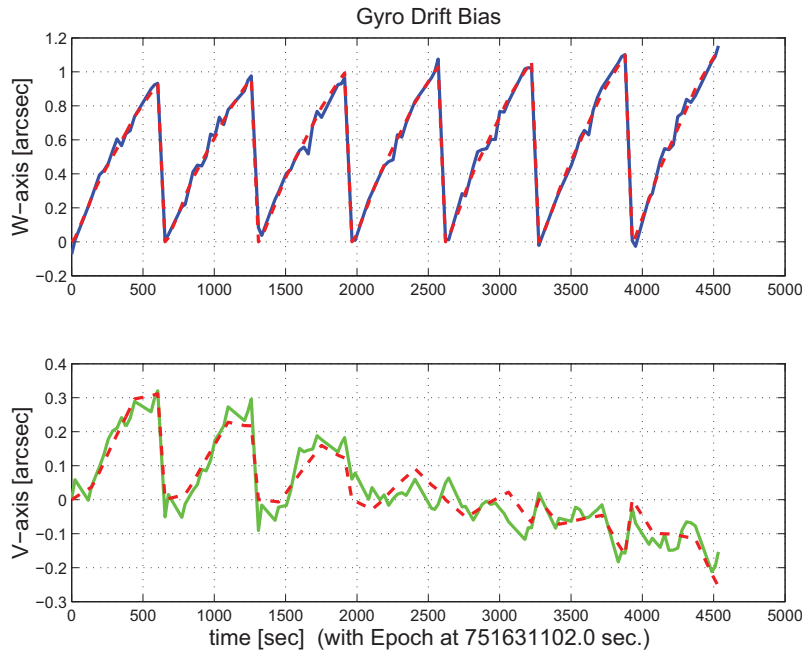


Figure 3.44: Gyro drift bias contribution (equiv. angle in (W,V) coords)

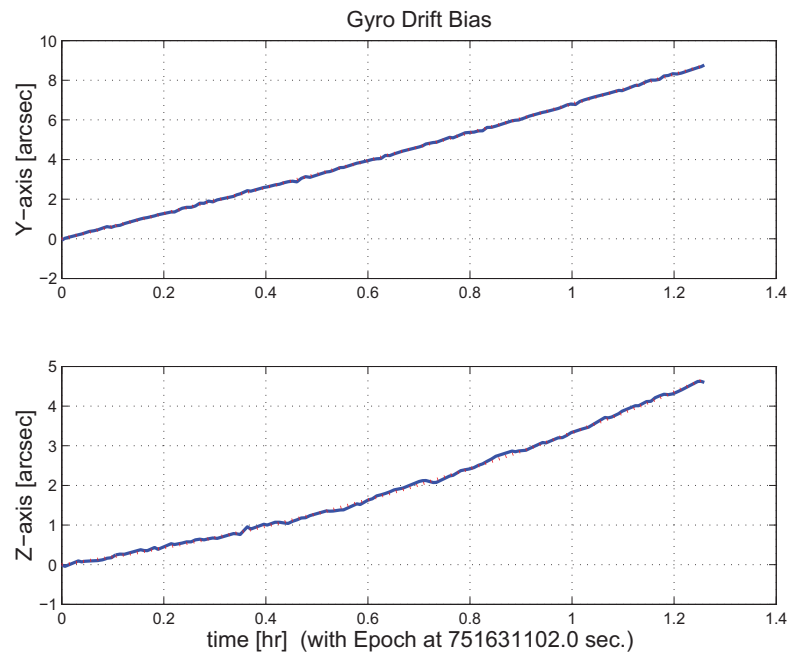


Figure 3.45: Gyro drift bias contribution (equiv. angle in Body frame)

3.2 IPF OUTPUT DATA (IF MINI FILE)

OUTPUT FILE NAME: IFmini701018.dat DATE: 26-Apr-2004 TIME: 10:29
 INSTRUMENT NAME: IRS_Red_PeakUp_FOV_Center NF: 18
 IPF FILTER VERSION: IPF.V4.0.0 SW RELEASE DATE: January 30, 2004
 FRAME TABLE USED: BodyFrames_FTU_17a

----- IPF BROWN ANGLE SUMMARY -----

Frame Number	WAS			IS		
	theta_Y (arcmin)	theta_Z (arcmin)	angle (deg)	theta_Y (arcmin)	theta_Z (arcmin)	angle (deg)
018	-11.634104	+2.000761	+1.797497	-11.649227	+2.000391	+1.796568

OFFSET	NF	Delta_CW	Delta_CV
0	18	+0.000	+0.000 pixels

OFFSET FRAME NAME: IRS_Red_PeakUp_FOV_Center

Brown Angle	theta_Y(arcmin)	theta_Z(arcmin)	angle(deg)
WAS(FTB)	-11.634104	+2.000761	+1.797497
IS (EST)	-11.649227	+2.000391	+1.796568
dT_EST	-0.015122	-0.000370	-0.000929
T_ssSIGMA	+0.000343	+0.000314	+0.027035
dT_EST/T_ssSIGMA	-44.145328	-1.179646	-0.034381

VARNAME	MEAN	SIGMA	SCALED_SIGMA
a00	+8.3450700080643682E-003	+1.1273567124418847E-003	+6.1088293297998969E-004
b00	+2.4451506019239577E-002	+1.4793499350343783E-003	+8.0161817217560096E-004
c00	+6.9999743657076785E-003	+8.7540744264380868E-004	+4.7435870138780892E-004
a01	+1.1248577582585527E+001	+2.5755386292958942E+001	+1.3956120316697406E+001
b01	+5.7551828493173169E+001	+2.6436266228613896E+001	+1.4325070026678015E+001
c01	-8.86949768775352811E+000	+1.8462630582075413E+001	+1.0004380863688421E+001
d01	-8.2959472672241539E+000	+2.5976959878197114E+001	+1.4076184818134580E+001
e01	-1.9967256641951010E+001	+2.7887173104844319E+001	+1.5111275704304798E+001
f01	+8.2634102587626721E+000	+1.9039395020480583E+001	+1.0316913310502295E+001
del_theta1	+3.8673030706634637E-013	+8.7076274322244471E-004	+4.7184186924939243E-004
del_theta2	+2.3100620027209200E-016	+1.8389176895891647E-007	+9.9645783745925455E-008
del_theta3	-7.2814657915123895E-018	+6.852041764747993E-007	+9.1316480279361660E-008
del_arx	-1.1794819525771548E-013	+4.4691893314850053E-005	+2.4217281511074331E-005
del_ary	-1.2444422772602969E-017	+4.1320408664020520E-006	+2.2390368689901116E-006
del_arz	+1.0424518391060012E-015	+4.1328896599874182E-006	+2.2394968063898723E-006
brx	-7.4250778782522904E-009	+4.2628402179686213E-008	+2.3099133632133062E-008
bry	-5.5139723484908851E-010	+4.9752052316802564E-009	+2.6959239525199515E-009
brz	+1.3323473199365649E-010	+4.9765515288145841E-009	+2.6966534731171182E-009
crx	+1.8010742375275293E-012	+1.9044106701084413E-011	+1.0319466437861868E-011
cry	+2.6361801087110402E-013	+2.4468321782871572E-012	+1.3258696214654676E-012
crz	-7.4853164468114418E-014	+2.4475046095252647E-012	+1.3262339930635865E-012
bgx	-1.1525072612839652E-006	+6.5550525259180096E-007	+3.5519988204949896E-007
bgy	+8.4040468426487263E-009	+5.0146161860984653E-009	+2.7172796415940759E-009
bgz	+2.4630372118899584E-009	+5.8819295556110879E-009	+3.1872523921292719E-009
cgx	+7.7404924268011984E-012	+2.1272758775495873E-010	+1.1527110390111448E-010
cgy	+4.1964546732329322E-013	+2.4576115666657468E-012	+1.3317106692152788E-012
cgz	+1.1250680144746528E-012	+2.6554335245667130E-012	+1.4389048310246589E-012

LSQF RESIDUAL SIGMA SCALE = +5.4187190818849251E-001

qT	qT(1)	qT(2)	qT(3)	qT(4)
FrmTbl:	+1.5685950396860798E-002	+1.6873384069184499E-003	-3.1750423083573603E-004	+9.9987549376925400E-001

```

Estim: +1.5677840616661914E-002 +1.6895410010107225E-003 -3.1747117089890592E-004 +9.9987561725289620E-001
DelTheta    deltheta(1)          deltheta(2)          deltheta(3)
             -1.6222925177406008E-005 +4.4001101220594843E-006 -3.0313087402225201E-008      [rad]
EulAngT     theta(1)           theta(2)           theta(3)          [rad]
Mean        +3.1356026320632086E-002 +3.3886227124768492E-003 -5.8189003055389909E-004
SigmaT      +8.7076274322244471E-004 +1.8389176895891647E-007 +1.6852041764747993E-007
-----
qR          qR(1)            qR(2)            qR(3)            qR(4)
ASFILE: +7.0887658512219787E-004 +1.2699844082817435E-003 -1.6144585970323533E-004 +9.9999892711639404E-001
Estim: +6.9296645298730169E-004 +1.2705352751716415E-003 -1.6135299880226298E-004 +9.9999893975084764E-001
DelThetaR   delthetaR(1)       delthetaR(2)       delthetaR(3)
             -3.1820661768110888E-005 +1.0966972123745599E-006 +1.4451600099373513E-007      [rad]
EulAngR     angR(1)          angR(2)          angR(3)          [rad]
Mean        +1.3855263444650481E-003 +2.5412942159593632E-003 -3.2094582068137577E-004
SigmaR      +4.4691893314850053E-005 +4.1320408664020520E-006 +4.1328896599874182E-006
-----
Initial Gyro Bias      Bg0(1)          Bg0(2)          Bg0(3)
             -4.6477461523863894E-007 -1.9199045198092790E-007 +3.6719961826747749E-007
Gyro Bias Correction    Bg(1)           Bg(2)           Bg(3)
             -1.1525072612839652E-006 +8.4040468426487263E-009 +2.4630372118899584E-009
Total Gyro Bias        BgT(1)          BgT(2)          BgT(3)
             -1.6172818765226042E-006 -1.8358640513827919E-007 +3.6966265547936743E-007
-----
Initial Gyro Bias Rate  Cg0(1)          Cg0(2)          Cg0(3)
             +0.0000000000000000E+000 +0.0000000000000000E+000 +0.0000000000000000E+000
Gyro Bias Rate Correction Cg(1)           Cg(2)           Cg(3)
             +7.7404924268011984E-012 +4.1964546732329322E-013 +1.1250680144746528E-012
Total Gyro Bias Rate    CgT(1)          CgT(2)          CgT(3)
             +7.7404924268011984E-012 +4.1964546732329322E-013 +1.1250680144746528E-012
-----
q(1)          q(2)            q(3)            q(4)
PCRS1A: +5.3371888965461637E-007 +3.7444233778550031E-004 -1.4253684912431913E-003 +9.9999891405806784E-001
PCRS2A: -5.2779261998836216E-007 +3.8462959425181312E-004 +1.3722087221825403E-003 +9.9999898455099423E-001
-----
***** CS-FILE PARAMETERS: ***** AS-FILE PARAMETERS: *****
Row (01) PIX2RADX: +8.726599999999995E-008 Row (1) TASTART: +7.5163090219075012E+008
Row (02) PIX2RADY: +8.726599999999995E-008 Row (2) TASTOP: +7.5163583509073484E+008
Row (03) CXO: +1.0500000000000000E+004 Row (3) S/C TIME: +7.5161268789079285E+008
Row (04) CYO: +9.2000000000000000E+003 Row (4) QR1: +7.0887658512219787E-004
Row (05) BETA0: +9.9999000000000000E+004 Row (5) QR2: +1.2699844082817435E-003
Row (06) GAMMA_E0: +9.9999000000000000E+004 Row (6) QR3: -1.6144585970323533E-004
Row (07) D11: +0.0000000000000000E+000 Row (7) QR4: +9.9999892711639404E-001
Row (08) D12: +1.0000000000000000E+000
Row (09) D21: +1.0000000000000000E+000
Row (10) D22: +0.0000000000000000E+000
Row (11) DG: +9.9999000000000000E+004
-----
INITIAL STA-TO-PCRS ALIGNMENT (R) KNOWLEDGE (1-SIGMA)
SIGMA(X)      SIGMA(Y)      SIGMA(Z)
5.93446115E+000 3.75377923E-001 3.75875241E-001 [arcsec]
-----
PIX2RADX = 8.726600000000E-008[rad/pixel]
XPIXSIZE = 0.0180[arcsec]
PIX2RADY = 8.726600000000E-008[rad/pixel]
YPIXSIZE = 0.0180[arcsec]
CXO = 10500.0[pixel] = 189.00[arcsec]
CYO = 9200.0[pixel] = 165.60[arcsec]
-----
NOMINAL BETA0 = 9.999900000000E+004[rad/encoder unit]
ENCODER UNIT SIZE = 99999.00[arcsec]
GAMMA_E0 = 99999.00[encoder unit] = 99999.00[arcsec]

```

```

FLIP MATRIX D = | +0 | +1 |
                |----|----|
                | +1 | +0 |
-----
```

3.3 IPF EXECUTION LOG

```
*****
IPF EXECUTION-LOG FILE NAME: LG701018.dat
INSTRUMENT TYPE: IRS_Red_PeakUp_FOV_Center
IPF FILTER EXECUTION DATE: 26-Apr-2004 TIME: 10:28
IPF FILTER VERSION USED: IPF.V4.0.0
*****
```

```
-- Loading & Preparing Input Files --
AAFILE: AA501018 Loaded! AAFILE dimension = 49330 X 21
ASFFILE: AS501018 Loaded!
CAFFILE: CA501018 Loaded! CAFFILE dimension = 61 X 15
CBFILE: CB502018 Loaded! CBFILE dimension = 49 X 15
CCFILE: CC701018 Created! CCFFILE dimension = 110 X 19
CSFILE: CS701018 Loaded!
Loading Input Files Completed!
```

```
-- Selected Mask Vectors --
index = 1 2 3 4 5 6 7 8 9 10 11 12 13 14 15 16 17 18 19 20
-----
mask1 = [ 1 1 1 0 0 0 0 0 0 0 0 1 1 1 1 1 1 1 ]
mask2 = [ 0 0 1 1 1 1 1 1 1 1 1 1 1 1 1 1 1 ]
```

```
-- Selected Initial Gyro Bias Parameters --
User Entered 1 : Use AFILE database - from S/C filter
IPF Linearized Using Following Nominal Gyro Bias Estimates
bg0 = [-4.6477461523863894E-007 -1.9199045198092790E-007 +3.6719961826747749E-007 ]
cg0 = [+0.000000000000000E+000 +0.000000000000000E+000 +0.000000000000000E+000 ]
```

```
-- Gyro Pre-Processor Run Completed --
AGFILE CREATED: AG701018.m ACFFILE CREATED: AC701018.m
```

```
Total Gyro Preprocessor Execution Time: 18 seconds
```

```
FRAME TABLE ENTRIES FOR PCRS LOADED TO TPCRS
q_PCRS4 = [ +5.3371888965461637E-007 q_PCRS5 = [ +7.3379987833742897E-007
            +3.7444233778550031E-004 +5.2236196154513707E-004
            -1.4253684912431913E-003 -1.4047712280184723E-003
            +9.9999891405806784E-001 ]; +9.9999887687698918E-001 ];
q_PCRS8 = [ -5.2779261998836216E-007 q_PCRS9 = [ -7.1963421681856818E-007
            +3.8462959425181312E-004 +5.3239763239987400E-004
            +1.3722087221825403E-003 +1.3516841804518383E-003
            +9.9999898455099423E-001 ]; +9.9999894475050310E-001 ];
----- Initial Conditions for State ----- ----- Initial Square-Root Cov (diag) -----
p1(01) = a00 = +0.000000000000000E+000 Sigma_initial(01,01) = 1.000000000000000E+000
p1(02) = b00 = +0.000000000000000E+000 Sigma_initial(02,02) = 1.000000000000000E+000
p1(03) = c00 = +0.000000000000000E+000 Sigma_initial(03,03) = 1.000000000000000E+000
```

p1(04) = a10 = +0.0000000000000000E+000	Sigma_initial(04,04) = 9.9999000000000000E+004
p1(05) = b10 = +0.0000000000000000E+000	Sigma_initial(05,05) = 9.9999000000000000E+004
p1(06) = c10 = +0.0000000000000000E+000	Sigma_initial(06,06) = 9.9999000000000000E+004
p1(07) = d10 = +0.0000000000000000E+000	Sigma_initial(07,07) = 9.9999000000000000E+004
p1(08) = a20 = +0.0000000000000000E+000	Sigma_initial(08,08) = 9.9999000000000000E+004
p1(09) = b20 = +0.0000000000000000E+000	Sigma_initial(09,09) = 9.9999000000000000E+004
p1(10) = c20 = +0.0000000000000000E+000	Sigma_initial(10,10) = 9.9999000000000000E+004
p1(11) = d20 = +0.0000000000000000E+000	Sigma_initial(11,11) = 9.9999000000000000E+004
p1(12) = a01 = +0.0000000000000000E+000	Sigma_initial(12,12) = 1.0000000000000000E+004
p1(13) = b01 = +0.0000000000000000E+000	Sigma_initial(13,13) = 1.0000000000000000E+004
p1(14) = c01 = +0.0000000000000000E+000	Sigma_initial(14,14) = 1.0000000000000000E+004
p1(15) = d01 = +0.0000000000000000E+000	Sigma_initial(15,15) = 1.0000000000000000E+004
p1(16) = e01 = +0.0000000000000000E+000	Sigma_initial(16,16) = 1.0000000000000000E+004
p1(17) = f01 = +0.0000000000000000E+000	Sigma_initial(17,17) = 1.0000000000000000E+004
<hr/>	
p2f(01) = am1 = +0.0000000000000000E+000	Sigma_initial(18,18) = 9.9999000000000000E+004
p2f(02) = am2 = +0.0000000000000000E+000	Sigma_initial(19,19) = 9.9999000000000000E+004
p2f(03) = am3 = +1.0000000000000000E+000	Sigma_initial(20,20) = 1.0000000000000001E-001
p2f(04) = beta = +1.0000000000000000E+000	Sigma_initial(21,21) = 1.0000000000000000E-002
p2f(05) = qT1 = +1.5685950396860812E-002	Sigma_initial(22,22) = 1.0000000000000000E-002
p2f(06) = qT2 = +1.6873384069184514E-003	Sigma_initial(23,23) = 2.8771079560603423E-004
p2f(07) = aT3 = -3.1750423083573630E-004	Sigma_initial(24,24) = 1.8198835244140440E-005
p2f(08) = qT4 = +9.9987549376925489E-001	Sigma_initial(25,25) = 1.8222945902831599E-005
p2f(09) = qR1 = +7.0887658512219787E-004	Sigma_initial(26,26) = 2.2058858106798428E-004
p2f(10) = qR2 = +1.2699844082817435E-003	Sigma_initial(27,27) = 2.2058858106798428E-004
p2f(11) = qR3 = -1.6144585970323533E-004	Sigma_initial(28,28) = 2.2058858106798428E-004
p2f(12) = qR4 = +9.999892711639404E-001	Sigma_initial(29,29) = 4.8659322097586675E-008
p2f(13) = brx = +0.0000000000000000E+000	Sigma_initial(30,30) = 4.8659322097586675E-008
p2f(14) = bry = +0.0000000000000000E+000	Sigma_initial(31,31) = 4.8659322097586675E-008
p2f(15) = brz = +0.0000000000000000E+000	Sigma_initial(32,32) = 2.2058858106798428E-004
p2f(16) = crx = +0.0000000000000000E+000	Sigma_initial(33,33) = 2.2058858106798428E-004
p2f(17) = cry = +0.0000000000000000E+000	Sigma_initial(34,34) = 2.2058858106798428E-004
p2f(18) = crz = +0.0000000000000000E+000	Sigma_initial(35,35) = 4.8659322097586675E-008
p2f(19) = bgx = +0.0000000000000000E+000	Sigma_initial(36,36) = 4.8659322097586675E-008
p2f(20) = bgy = +0.0000000000000000E+000	Sigma_initial(37,37) = 4.8659322097586675E-008
p2f(21) = bgz = +0.0000000000000000E+000	
p2f(22) = cgx = +0.0000000000000000E+000	
p2f(23) = cgy = +0.0000000000000000E+000	
p2f(24) = cgz = +0.0000000000000000E+000	

----- IPF KALMAN FILTER STARTED -----
 Iteration#001: |dp|= +6.358107220007E+001 RMS(|Res|)=+8.168186120069E-006
 Iteration#002: |dp|= +1.541119553523E-001 RMS(|Res|)=+5.229023085988E-007
 Iteration#003: |dp|= +6.122415404421E-002 RMS(|Res|)=+5.217294502705E-007
 Iteration#004: |dp|= +7.025999328974E-003 RMS(|Res|)=+5.211670082808E-007
 Iteration#005: |dp|= +1.101980503638E-003 RMS(|Res|)=+5.209901482929E-007
 Iteration#006: |dp|= +2.363159257439E-004 RMS(|Res|)=+5.209845188689E-007
 Iteration#007: |dp|= +1.863150526806E-005 RMS(|Res|)=+5.209920418939E-007
 Iteration#008: |dp|= +6.442397276725E-006 RMS(|Res|)=+5.209931072462E-007
 Iteration#009: |dp|= +8.351929917688E-007 RMS(|Res|)=+5.209928135423E-007
 Iteration#010: |dp|= +2.062494342098E-007 RMS(|Res|)=+5.209927268799E-007
 Iteration#011: |dp|= +2.483617237075E-008 RMS(|Res|)=+5.209927330681E-007
 Iteration#012: |dp|= +2.981965077361E-008 RMS(|Res|)=+5.209927382619E-007
 Iteration#013: |dp|= +4.107742369416E-008 RMS(|Res|)=+5.209927385965E-007
 Iteration#014: |dp|= +7.512336986836E-008 RMS(|Res|)=+5.209927381447E-007
 Iteration#015: |dp|= +4.735651451031E-008 RMS(|Res|)=+5.209927384277E-007
 Iteration#016: |dp|= +9.584265297097E-009 RMS(|Res|)=+5.209927382629E-007
 Iteration#017: |dp|= +1.925959043487E-008 RMS(|Res|)=+5.209927382479E-007
 Iteration#018: |dp|= +3.113212255193E-008 RMS(|Res|)=+5.209927382877E-007
 Iteration#019: |dp|= +2.891716980583E-008 RMS(|Res|)=+5.209927381457E-007
 Iteration#020: |dp|= +1.687750211465E-008 RMS(|Res|)=+5.209927383441E-007
 Iteration#021: |dp|= +1.625661919031E-008 RMS(|Res|)=+5.209927382026E-007
 Iteration#022: |dp|= +1.373208225057E-008 RMS(|Res|)=+5.209927382698E-007

```

Iteration#023: |dp|= +1.169087994728E-008 RMS(|Res|)=+5.209927383185E-007
Iteration#024: |dp|= +1.977067517166E-008 RMS(|Res|)=+5.209927383634E-007
Iteration#025: |dp|= +3.810904076537E-008 RMS(|Res|)=+5.209927382525E-007
Iteration#026: |dp|= +4.322248826298E-008 RMS(|Res|)=+5.209927383919E-007
Iteration#027: |dp|= +2.892972332652E-008 RMS(|Res|)=+5.209927382105E-007
Iteration#028: |dp|= +2.507896720191E-008 RMS(|Res|)=+5.209927383114E-007
Iteration#029: |dp|= +9.910855131396E-009 RMS(|Res|)=+5.209927382337E-007
Iteration#030: |dp|= +1.535780374726E-008 RMS(|Res|)=+5.209927383221E-007
Iteration#031: |dp|= +2.970026846634E-008 RMS(|Res|)=+5.209927382634E-007
Iteration#032: |dp|= +5.000485592273E-008 RMS(|Res|)=+5.209927381598E-007
Iteration#033: |dp|= +5.545106435285E-008 RMS(|Res|)=+5.209927383066E-007
Iteration#034: |dp|= +1.659023685973E-008 RMS(|Res|)=+5.209927381447E-007
Iteration#035: |dp|= +1.311185954557E-008 RMS(|Res|)=+5.209927381589E-007
IPF Kalman Filter Completed with Error |dp1| + |dp2| = +1.3111859545568550E-008
-----
```

```

----- IPF LEAST SQUARES FILTER STARTED -----
Iteration#001 COND#=+1.399189791241E+007, |dp|=+6.362682708611E+001
Iteration#002 COND#=+1.398849120028E+007, |dp|=+4.325932031734E-002
Iteration#003 COND#=+1.398847428610E+007, |dp|=+5.811455036191E-003
Iteration#004 COND#=+1.398847443029E+007, |dp|=+5.638351679098E-006
Iteration#005 COND#=+1.398847443107E+007, |dp|=+3.687812098373E-008
Iteration#006 COND#=+1.398847442991E+007, |dp|=+5.404358074632E-009
Iteration#007 COND#=+1.398847443001E+007, |dp|=+6.785972738512E-009
Iteration#008 COND#=+1.398847442879E+007, |dp|=+8.555804042340E-009
Iteration#009 COND#=+1.398847443014E+007, |dp|=+6.262402887518E-009
Iteration#010 COND#=+1.398847443003E+007, |dp|=+4.055284459953E-009
Iteration#011 COND#=+1.398847443027E+007, |dp|=+4.918050618090E-009
Iteration#012 COND#=+1.398847443037E+007, |dp|=+6.442937627030E-009
Iteration#013 COND#=+1.398847442894E+007, |dp|=+3.729186900478E-009
Iteration#014 COND#=+1.398847442962E+007, |dp|=+6.364235833771E-009
Iteration#015 COND#=+1.398847443039E+007, |dp|=+8.190099205068E-009
Iteration#016 COND#=+1.398847442940E+007, |dp|=+4.258448271717E-009
Iteration#017 COND#=+1.398847442954E+007, |dp|=+6.488553963044E-009
Iteration#018 COND#=+1.398847443009E+007, |dp|=+9.101965967460E-009
Iteration#019 COND#=+1.398847443013E+007, |dp|=+4.836051729132E-009
Iteration#020 COND#=+1.398847443044E+007, |dp|=+6.039787541870E-009
Iteration#021 COND#=+1.398847443105E+007, |dp|=+7.414016703929E-009
Iteration#022 COND#=+1.398847442948E+007, |dp|=+6.847988139404E-009
Iteration#023 COND#=+1.398847442996E+007, |dp|=+3.738326445615E-009
Iteration#024 COND#=+1.398847443034E+007, |dp|=+3.351003291190E-009
Iteration#025 COND#=+1.398847443031E+007, |dp|=+4.634205174782E-009
Iteration#026 COND#=+1.398847443042E+007, |dp|=+4.705292084961E-009
Iteration#027 COND#=+1.398847443075E+007, |dp|=+6.589796118887E-009
Iteration#028 COND#=+1.398847443077E+007, |dp|=+7.727054403346E-009
Iteration#029 COND#=+1.398847442958E+007, |dp|=+3.650543171509E-009
Iteration#030 COND#=+1.398847443068E+007, |dp|=+5.053468859087E-009
Iteration#031 COND#=+1.398847442974E+007, |dp|=+8.932675701542E-009
Iteration#032 COND#=+1.398847442924E+007, |dp|=+9.529473253073E-009
Iteration#033 COND#=+1.398847443095E+007, |dp|=+5.503540207808E-009
Iteration#034 COND#=+1.398847442937E+007, |dp|=+5.636197305970E-009
Iteration#035 COND#=+1.398847442953E+007, |dp|=+3.314385213953E-009
IPF Least Squares Filter Completed with Error |dp1| + |dp2| = +3.3143852139529970E-009
-----
```

Total Execution Time: 97 seconds

4 COMMENTS

This IPF run is a post-IOC re-run of the IOC flight data taken from run IF501018, but with a modified CS-file CS701018.m, which specifies that the Prime frame 018 is to be moved over from its previous definition by 1/2 pixel. This change puts the Prime frame exactly at the middle of a physical pixel, which was desired by the IRS team to improve in-flight Peakup centroiding accuracy.

The IPF run was performed in the most recent IPF version IPF.V4.0.0. All IPF settings, data editing, and parameters were kept the same as the IF501018 run (see report ID501018.pdf for details). As a reminder, constant and linear plate scales were estimated, which did not change significantly from run IF501018.

We recommend updating frame 018 with the new quaternion listed in the IF file IF701018.dat. The recommended Brown angle change is on the order of 0.9 arcsec, which is consistent with the desired 1/2 pixel shift (the PU pixels are approximately 1.8 arcsec wide). As before, in our best judgement, the Fine survey is accurate to 0.09 arcsec which satisfies the fine survey requirement of 0.25 arcsecond by a good margin.

IPF TEAM CONTACT INFORMATION

IPF Team email	ipf@sirtfweb.jpl.nasa.gov	
David S. Bayard	X4-8208	David.S.Bayard@jpl.nasa.gov (TEAM LEADER)
Dhemetrio Boussalis	X4-3977	boussali@grover.jpl.nasa.gov
Paul Brugarolas	X4-9243	Paul.Brugarolas@jpl.nasa.gov
Bryan H. Kang	X4-0541	Bryan.H.Kang@jpl.nasa.gov
Edward.C.Wong	X4-3053	Edward.C.Wong@jpl.nasa.gov (TASK MANAGER)

ACKNOWLEDGEMENTS

This work was performed at the Jet Propulsion Laboratory, California Institute of Technology, under contract with the National Aeronautics and Space Administration.

References

- [1] D.S. Bayard, B.H. Kang, *SIRTF Instrument Pointing Frame Kalman Filter Algorithm*, JPL D-Document D-24809, September 30, 2003.
- [2] B.H. Kang, D.S. Bayard, *SIRTF Instrument Pointing Frame (IPF) Software Description Document and User's Guide*, JPL D-Document D-24808, September 30, 2003.
- [3] D.S. Bayard, B.H. Kang, *SIRTF Instrument Pointing Frame (IPF) Kalman Filter Unit Test Report*, JPL D-Document D-24810, September 30, 2003.
- [4] *Space Infrared Telescope Facility In-Orbit Checkout and Science Verification Mission Plan*, JPL D-Document D-22622, 674-FE-301 Version 1.4, February 8, 2002.
- [5] *Space Infrared Telescope Facility Observatory Description Document*, Lockheed Martin LMMS/P458569, 674-SEIT-300 Version 1.2, November 1, 2002.
- [6] *SIRTF Software Interface Specification for Science Centroid INPUT Files (CAFILER, CSFILE)*, JPL SOS-SIS-2002, November 18, 2002.
- [7] *SIRTF Software Interface Specification for Inferred Frames Offset INPUT Files (OFILE)*, JPL SOS-SIS-2003, November 18, 2002.
- [8] *SIRTF Software Interface Specification for PCRS Centroid INPUT Files (CBFILE)*, JPL SIS-FES-015, November 18, 2002.
- [9] *SIRTF Software Interface Specification for Attitude INPUT Files (AFILE, ASFILE)*, JPL SIS-FES-014, January 7, 2002.
- [10] *SIRTF Software Interface Specification for IPF Filter Output Files (IFFILE, LGFILE, TARFILE)*, JPL SOS-SIS-2005, November 18, 2002.
- [11] R.J. Brown, *Focal Surface to Object Space Field of View Conversion*. Systems Engineering Report SER No. S20447-OPT-051, Ball Aerospace & Technologies Corp., November 23, 1999.

JET PROPULSION LABORATORY

SIRTF IPF REPORT

JPL ID701019

April 26, 2004

**SIRTF INSTRUMENT POINTING FRAME
KALMAN FILTER EXECUTION SUMMARY**

IPF RUN NUMBER: 701019

REPORT TYPE: IOC EXECUTION (FINE)

PRIME FRAME: IRS_Red_PeakUp_FOV_Sweet_Spot (19)

INFERRRED FRAMES:

IPF TEAM

Autonomy and Control Section (345)

Jet Propulsion Laboratory

California Institute of Technology

4800 Oak Grove Drive

Pasadena, CA 91109

Contents

1 IPF EXECUTION SUMMARY	5
2 IPF INPUT FILE HISTORY	9
3 IPF EXECUTION RESULTS	10
3.1 IPF EXECUTION OUTPUT PLOTS	10
3.2 IPF OUTPUT DATA (IF MINI FILE)	36
3.3 IPF EXECUTION LOG	38
4 COMMENTS	41

List of Figures

1.1 A-priori and a-posteriori IPF frames	5
1.2 A-priori and a-posteriori IPF frames (ZOOMED)	8
2.1 Scenario Plot	9
3.1 TPF coords of measurements and a-priori predicts	12
3.2 Oriented PixelCoords of measurements and a-priori predicts	12
3.3 Oriented (W,V) PixelCoords of A-Priori Prediction Error Quiver Plot	13
3.4 A-priori prediction error (Science Centroids)	13
3.5 Oriented PixelCoords of measurements and a-priori predicts (PCRS only)	14
3.6 Oriented PixelCoords of measurements and a-priori predicts (Zoomed, PCRS only)	14
3.7 Oriented (W,V) PixelCoords of A-Priori PCRS Prediction Error Quiver Plot	15
3.8 A-priori PCRS prediction error	15
3.9 IPF execution convergence, chart 1	16
3.10 IPF execution convergence, chart 2	16
3.11 Parameter uncertainty convergence	17
3.12 IPF parameter symbol table	17
3.13 KF parameter error sigma plots	18
3.14 LS parameter error sigma plot	18
3.15 KF and LS parameter error sigma plot	19
3.16 Oriented PixelCoords of meas. and a-posteriori predicts	20
3.17 Oriented PixelCoords of meas. and a-posteriori predicts (attitude corrected)	20

3.18	KF innovations with (o) and w/o (+) attitude corrections	21
3.19	Histograms of science a-posteriori residuals (or innovations)	21
3.20	A-Posteriori Science Centroid Prediction Error Quiver (Att. Cor.)	22
3.21	Normalized A-Posteriori Science Centroid Prediction Errors	22
3.22	KF innovations with (o) and w/o (+) attitude corrections (PCRS)	23
3.23	Histograms of PCRS a-posteriori residuals (or innovations)	23
3.24	A-posteriori PCRS Prediction Summary	24
3.25	A-posteriori PCRS Prediction (PCRS 1 Only)	25
3.26	A-posteriori PCRS Prediction (PCRS 2 Only)	25
3.27	A-Posteriori PCRS Prediction Errors Quiver (Att. Cor.)	26
3.28	Normalized A-Posteriori PCRS Prediction Errors	26
3.29	W-axis KF innovations and 1-sigma bound	27
3.30	V-axis KF innovations and 1-sigma bound	27
3.31	Array plot with (solid) and w/o (dashed) optical distortion corrections	28
3.32	Optical Distortion Plot: total (x5 magnification)	28
3.33	Optical Distortion Plot: constant plate scales (x5 magnification)	29
3.34	Optical Distortion Plot: linear plate scale (x5 magnification)	29
3.35	Optical Distortion Plot: gamma terms (x5 magnification)	30
3.36	Scan Mirror Chops	30
3.37	IPF Frame Reconstruction	31
3.38	Center Pixel Reconstruction	31
3.39	Estimated attitude corrections (Body frame)	32
3.40	Estimated attitude error sigma plot (Body frame)	32
3.41	Thermo-mechanical boresight drift (equiv. angle in (W,V) coords)	33
3.42	Thermo-mechanical boresight drift (equiv. angle in Body frame)	33
3.43	Gyro drift bias contribution (equiv. rate in (W,V) coords)	34
3.44	Gyro drift bias contribution (equiv. angle in (W,V) coords)	34
3.45	Gyro drift bias contribution (equiv. angle in Body frame)	35

List of Tables

1.1	IPF filter input files	6
1.2	IPF filter execution configuration	6

1.3	IPF filter execution mask vector assignment	6
1.4	IPF calibration error summary ([arcsec], 1-sigma, radial)	7
1.5	Science measurement prediction error summary (1-sigma)	7
1.6	IPF Brown angle summary	8
2.1	IPF input file editing status	9
3.1	Table of figures I (IPF run)	10
3.2	Table of figures II (IPF run)	11
3.3	PCRS measurement prediction error summary	24

1 IPF EXECUTION SUMMARY

This report summarizes the SIRTF Instrument Pointing Frame (IPF) Kalman Filter execution associated with run file: RN701019. In particular, this Focal Point Survey calibrates the instrument: IRS_Red_PeakUp_FOV_Sweet_Spot (19), as part of the IOC Fine Survey. The main calibration results from the IPF filter execution have been documented in IF701019 typically stored in the mission archive DOM collection IPF_IF. This report only summarizes the main aspects of the run, and does not substitute for the full information contained in the IF file.

Section 1 summarizes the filter execution results. The filter configurations are tabulated in Table 1.2 and the mask vector assignments are tabulated in Table 1.3. A total of 21 state parameters are estimated in this run. The overall End-to-End pointing performances are tabulated in Table 1.4. The prediction residuals throughout the estimation processes are tabulated in Table 1.5. Section 3 summarizes resulting plots, a mini summary of the IF IPF output file, and the execution log. Section 4 captures the user comments that are specific to this particular run.

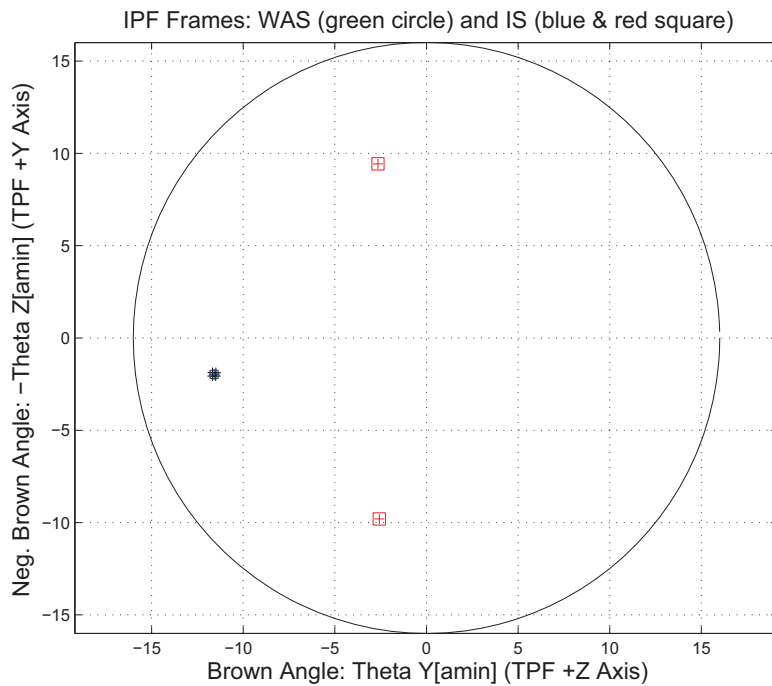


Figure 1.1: A-priori and a-posteriori IPF frames

RAW	FINAL (After Editing)
AA501019	AA501019
AS501019	AS501019
CA501019	CA501019
CB502019	CB502019
CS701019	CS701019

Table 1.1: IPF filter input files

EXECUTION CONFIGURATION ITEM	CURRENT STATUS
IPF Filter Version Used	IPF.V4.0.0
Frame Table Version Used	BodyFrames_FTU_17a
Scan-Mirror Employed?	NO
IPF Filter Mode	NORMAL-MODE(0)
SLIT-MODE Operation	DISABLED
Kalman Filter Operation	ENABLED
Least-Squares Data Analysis	ENABLED
IBAD Screening	ENABLED
User-Specified Data Editing	DISABLED
Total Number of Iterations	30
LS Residual Sigma Scale	7.27871156E-01
Total Number of Maneuvers	21

Table 1.2: IPF filter execution configuration

Con. Plate Scale			Γ Dependent				Γ^2 Dependent				Linear Plate Scale						Mirror			
a_{00}	b_{00}	c_{00}	a_{10}	b_{10}	c_{10}	d_{10}	a_{20}	b_{20}	c_{20}	d_{20}	a_{01}	b_{01}	c_{01}	d_{01}	e_{01}	f_{01}	α	β		
1	2	3	4	5	6	7	8	9	10	11	12	13	14	15	16	17	18	19		
1	1	1	0	0	0	0	0	0	0	0	0	0	0	0	0	0	0	0		
IPF (T)			Alignment R						Gyro Drift Bias											
θ_1	θ_2	θ_3	a_{rx}	a_{ry}	a_{rz}	b_{rx}	b_{ry}	b_{rz}	c_{rx}	c_{ry}	c_{rz}	b_{gx}	b_{gy}	b_{gz}	c_{gx}	c_{gy}	c_{gz}			
20	21	22	23	24	25	26	27	28	29	30	31	32	33	34	35	36	37			
1	1	1	1	1	1	1	1	1	1	1	1	1	1	1	1	1	1			

Table 1.3: IPF filter execution mask vector assignment

FOCAL PLANE SURVEY ANALYSIS: IOC Fine Survey.

INSTRUMENT NAME: IRS_Red_PeakUp_FOV_Sweet_Spot NF: 19

PIX2RADW: 8.72660000E-08 [rad/pixel] = 1.8000E-02 [arcsec/pixel]

PIX2RADV: 8.72660000E-08 [rad/pixel] = 1.8000E-02 [arcsec/pixel]

FRAME	DESCRIPTION	IPF ¹	SF ²	TOTAL	REQ
019(P)	IRS_Red_PeakUp_FOV_Sweet_Spot	0.0138	0.0855	0.0866	0.14

Table 1.4: IPF calibration error summary ([arcsec], 1-sigma, radial)

RMS METRIC	A PRIORI ³	A POSTERIORI ³	ATT. CORRECTED ⁴	UNITS
Radial	1.2220	0.1035	0.0662	arcsec
W-Axis	1.2153	0.0773	0.0538	arcsec
V-Axis	0.1276	0.0689	0.0385	arcsec
Radial	67.8890	5.7517	3.6757	pixels
W-Axis	67.5178	4.2937	2.9886	pixels
V-Axis	7.0904	3.8271	2.1397	pixels

Table 1.5: Science measurement prediction error summary (1-sigma)

¹IPF filter removes systematic pointing errors due to: thermomechanical alignment drift (Body to TPF), gyro bias and bias drift, centroiding error, attitude error, and optical distortion. IPF SIGMA presented here is “Scaled” by the Least Squares Scale factor. The Least Squares Scale Factor was: 0.727871. It is assumed that the gyro Angle Random Walk contribution is captured with the Least Squares scaling. The gyro ARW contribution can be approximately calculated as 0.0453 arcseconds, given that ARW = $100 \mu\text{deg}/\sqrt{\text{hr}}$, with 5.980000e+02 second Maneuver time (max), and 21 independent Maneuvres.

²Gyro Scale Factor(GSF) assumes 95 ppm error over 0.250 degree maneuver.

³This can be interpreted as estimate of ”pixel to sky” pointing reconstruction error if no science data is used.

⁴This can be interpreted as estimate of achieved S/I centroiding error

IPF BROWN ANGLE SUMMARY					
FRAME TABLE USED: BodyFrames_FTU_17a					
NF	NAME	WAS	IS	CHANGE	UNIT
019	theta_Y	-11.571876	-11.587019	-0.015143	arcmin
019	theta_Z	+1.971732	+1.971349	-0.000383	arcmin
019	angle	+1.977920	+1.977920	+0.000000	deg

Table 1.6: IPF Brown angle summary

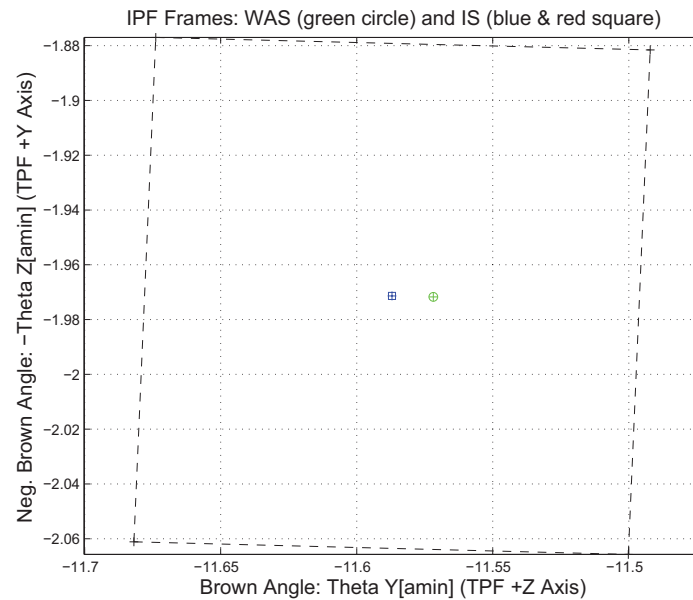


Figure 1.2: A-priori and a-posteriori IPF frames (ZOOMED)

2 IPF INPUT FILE HISTORY

WAS	SIZE	IS	SIZE	REMOVED	PATCHED
AA501019	UNCHANGED	AA501019	UNCHANGED	0	0
CA501019	UNCHANGED	CA501019	UNCHANGED	0	N/A
CB502019	UNCHANGED	CB502019	UNCHANGED	0	N/A

Table 2.1: IPF input file editing status

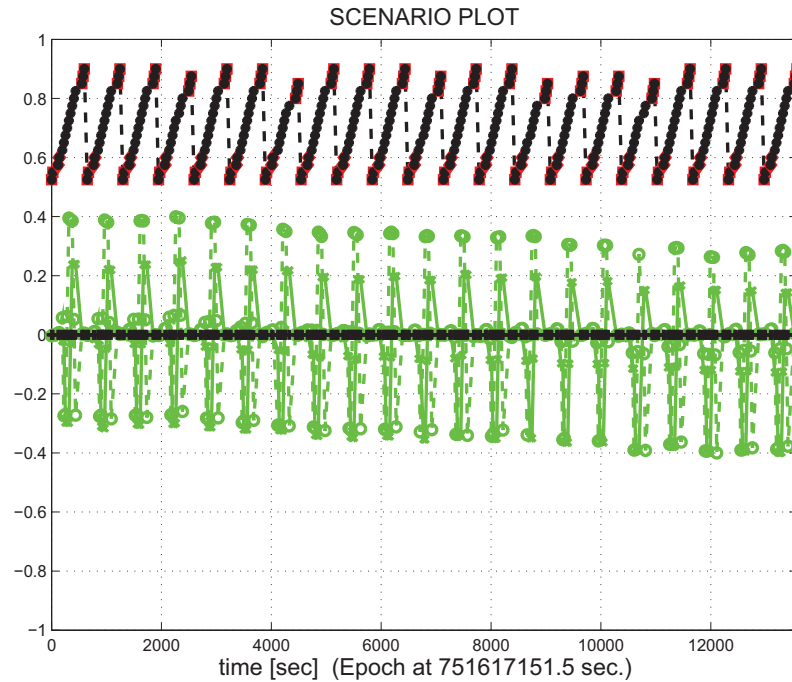


Figure 2.1: Scenario Plot

3 IPF EXECUTION RESULTS

3.1 IPF EXECUTION OUTPUT PLOTS

This subsection summarizes the IPF filter results. As shown in Table 3.1, the output plots are segmented to three groups: predicted performance, post-run results and IPF trending plots.

FIGURE NO.	DESCRIPTION
Predicted performance prior to IPF run	
Figure 3.1	Meas. and a-priori predicts in TPF coords
Figure 3.2	Meas. and a-priori predicts in Oriented Pixel Coords including rectangular array boundary approximation
Figure 3.3	A-Priori Prediction Error Quiver Plot in Oriented Pixel Coords including rectangular array boundary approximation
Figure 3.4	A-priori prediction error
Figure 3.5	Oriented Pixel Coords of measurements and a-priori predicts (PCRS only)
Figure 3.6	Oriented Pixel Coords of measurements and a-priori predicts (Zoomed, PCRS only)
Figure 3.7	Oriented (W,V) Pixel Coords of A-Priori PCRS Prediction Error Quiver Plot
Figure 3.8	A-priori PCRS prediction error
IPF filter performance (post run results)	
Figure 3.9	IPF execution convergence, chart 1: (top) normalized residual error vs. iteration number and (bottom) norm of effective parameter corrections
Figure 3.10	IPF execution convergence, chart 2: parameter correction size vs. iteration number
Figure 3.11	Parameter uncertainty convergence: square-root of diagonal elements of covariance matrix vs. maneuver number
Figure 3.12	IPF parameter symbol table
Figure 3.13	KF parameter error sigma plot (a-priori-dashed, a-posteriori-solid). Includes true parameter errors (FLUTE runs only)
Figure 3.14	LS parameter error sigma plot. Includes true parameter errors (FLUTE runs only)
Figure 3.15	KF and LS parameter errors sigma plot (Figure 3.13 & Figure 3.14 combined)
Figure 3.16	Measurements and a-posteriori predicts in Oriented Pixel Coords including rectangular array boundaries (a-priori-dashed, a-posteriori-solid)
Figure 3.17	Attitude corrected meas. and a-posteriori predicts in Oriented Pixel Coords including rectangular array boundaries (a-priori-dashed, a-posteriori-solid)

Table 3.1: Table of figures I (IPF run)

FIGURE NO.	DESCRIPTION
IPF filter performance (post run results) - CONTINUE	
Figure 3.18	KF innovations with (o) and w/o (+) attitude corrections
Figure 3.19	Histograms of science a-posteriori residuals (or innovations)
Figure 3.20	A-Posteriori Science Centroid Prediction Error Quiver (Att. Cor.)
Figure 3.21	Normalized A-Posteriori Science Centroid Prediction Errors
Figure 3.22	KF innovations with (o) and w/o (+) attitude corrections (PCRS)
Figure 3.23	Histograms of PCRS a-posteriori residuals (or innovations)
Figure 3.24	A-posteriori PCRS Prediction Summary
Figure 3.25	A-posteriori PCRS Prediction (PCRS 1 Only)
Figure 3.26	A-posteriori PCRS Prediction (PCRS 2 Only)
Figure 3.27	A-Posteriori PCRS Prediction Errors Quiver (Att. Cor.)
Figure 3.28	Normalized A-Posteriori PCRS Prediction Errors
Figure 3.29	W-axis KF innovations and 1-sigma bound
Figure 3.30	V-axis KF innovations and 1-sigma bound
Figure 3.31	Array plot with (solid) and w/o (dashed) optical distortion corrections
Figure 3.32	Optical Distortion Plot: total (x5 magnification)
Figure 3.33	Optical Distortion Plot: constant plate scales (x5 magnification)
Figure 3.34	Optical Distortion Plot: linear plate scale (x5 magnification)
Figure 3.35	Optical Distortion Plot: gamma terms (x5 magnification)
Figure 3.36	Scan Mirror Chops
Figure 3.37	IPF Frame Reconstruction
Figure 3.38	Center Pixel Reconstruction
IPF parameter trending plots	
Figure 3.39	Estimated attitude corrections (Body frame)
Figure 3.40	Estimated attitude error sigma plot (Body frame)
Figure 3.41	Systematic error attributed to thermo-mechanical boresight drift (equiv. angle in (W,V) coords)
Figure 3.42	Systematic error attributed to thermo-mechanical boresight drift (equiv. angle in Body frame)
Figure 3.43	Systematic error attributed to gyro drift bias (equiv. rate in (W,V) coords)
Figure 3.44	Systematic error attributed to gyro drift bias (equiv. angle in (W,V) coords)
Figure 3.45	Systematic error attributed to gyro drift bias (equiv. angle in Body frame)

Table 3.2: Table of figures II (IPF run)

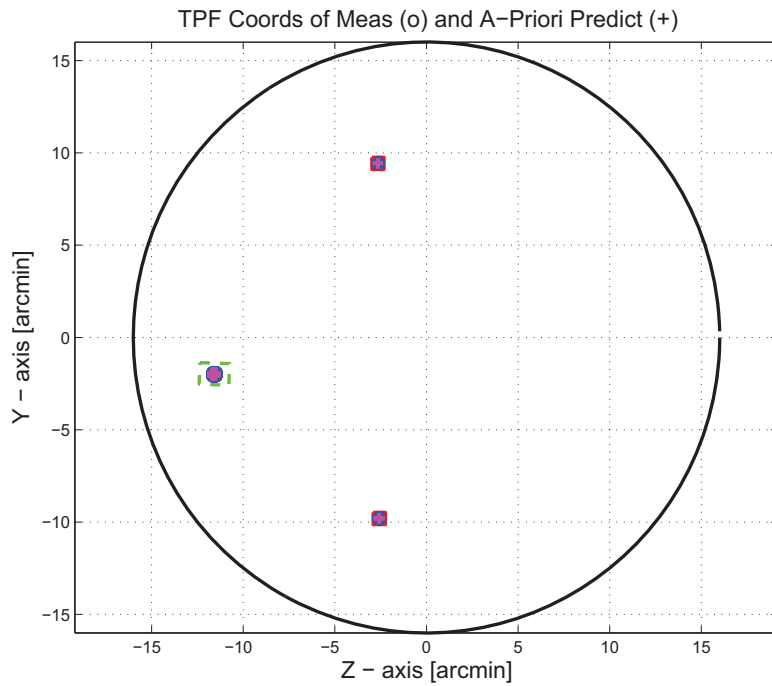


Figure 3.1: TPF coords of measurements and a-priori predicts

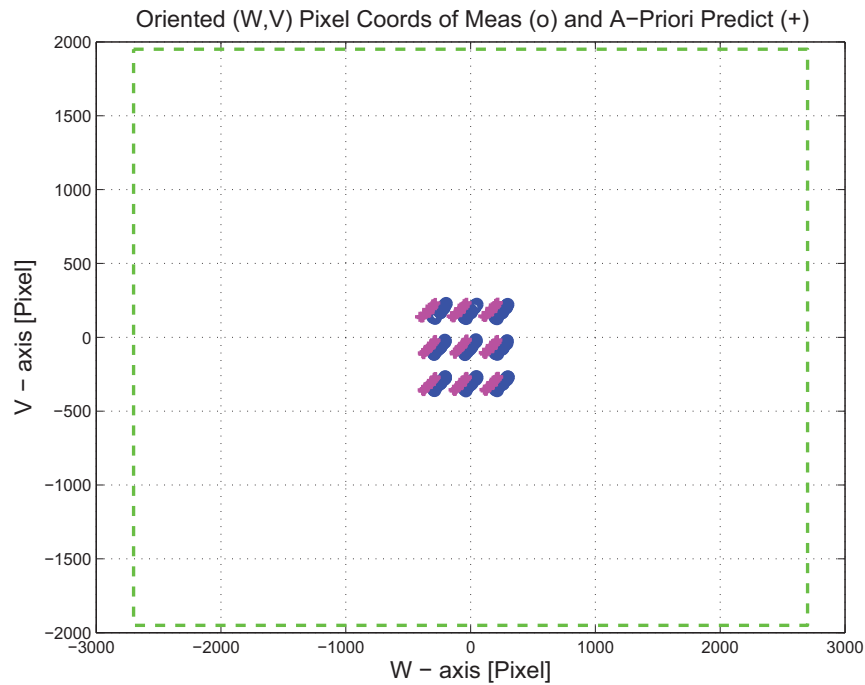


Figure 3.2: Oriented PixelCoords of measurements and a-priori predicts

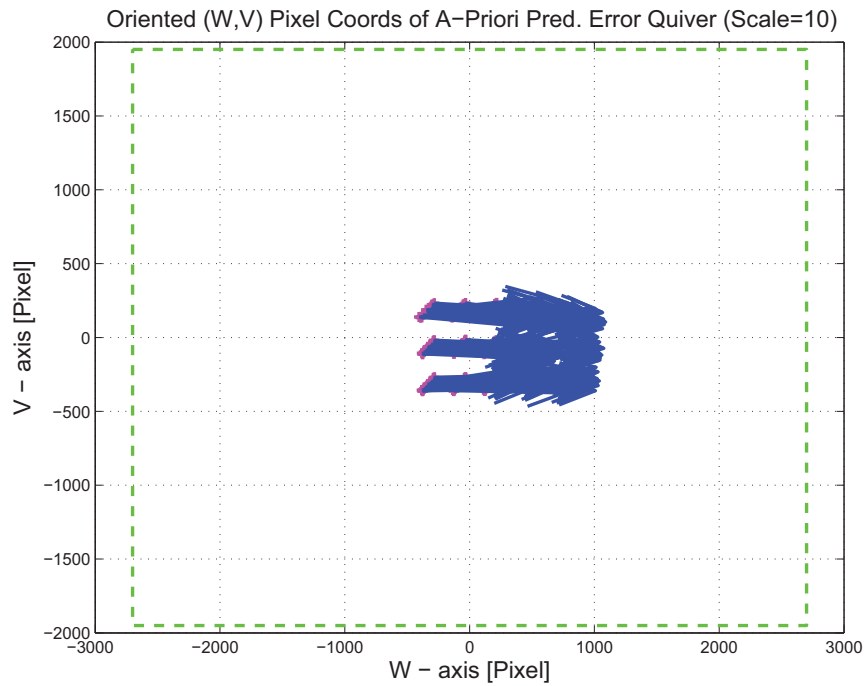


Figure 3.3: Oriented (W,V) Pixel Coords of A-Priori Prediction Error Quiver Plot

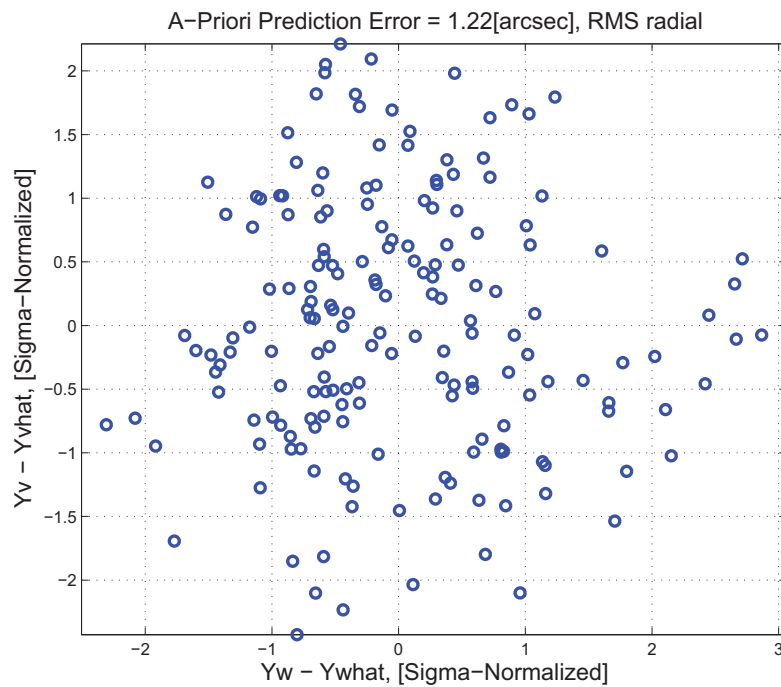


Figure 3.4: A-priori prediction error (Science Centroids)

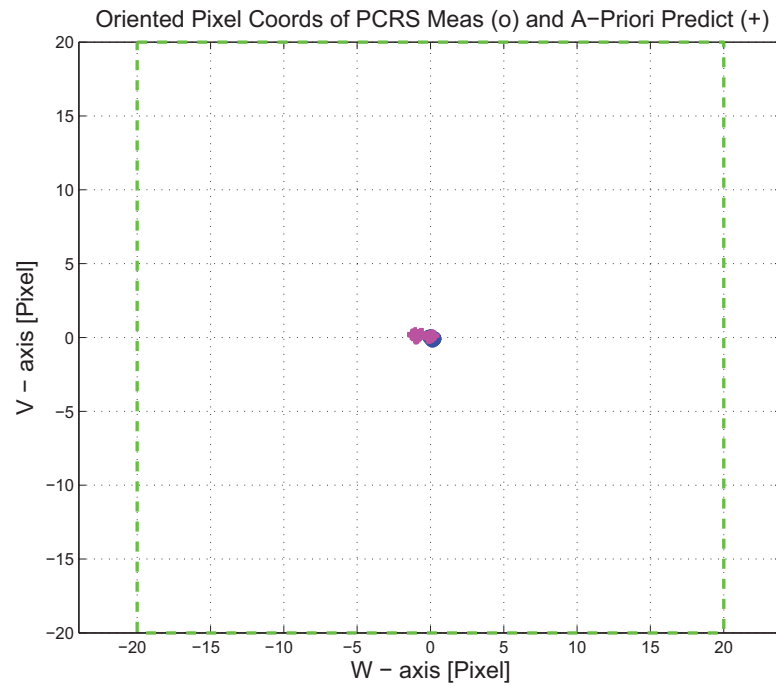


Figure 3.5: Oriented Pixel Coords of measurements and a-priori predicts (PCRS only)

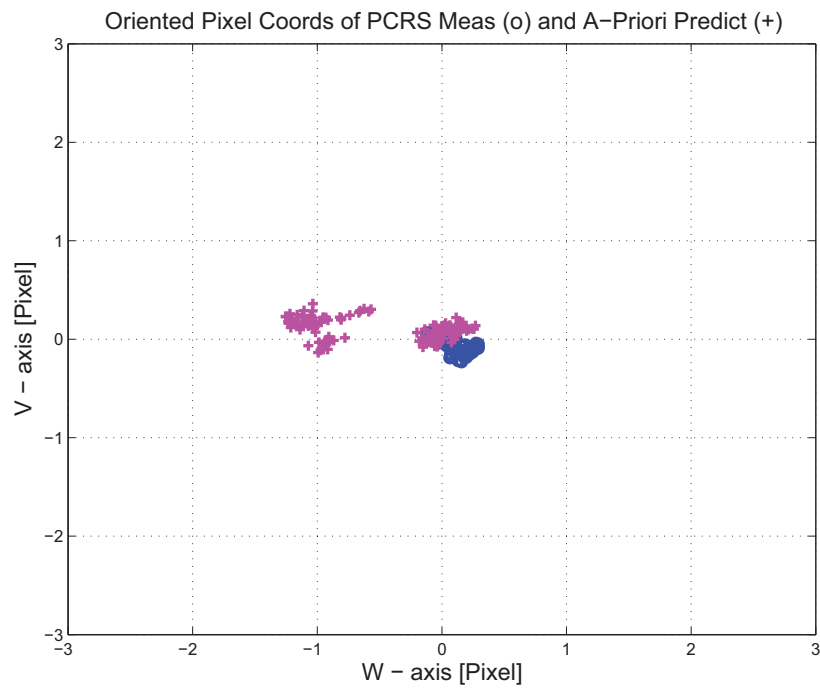


Figure 3.6: Oriented Pixel Coords of measurements and a-priori predicts (Zoomed, PCRS only)

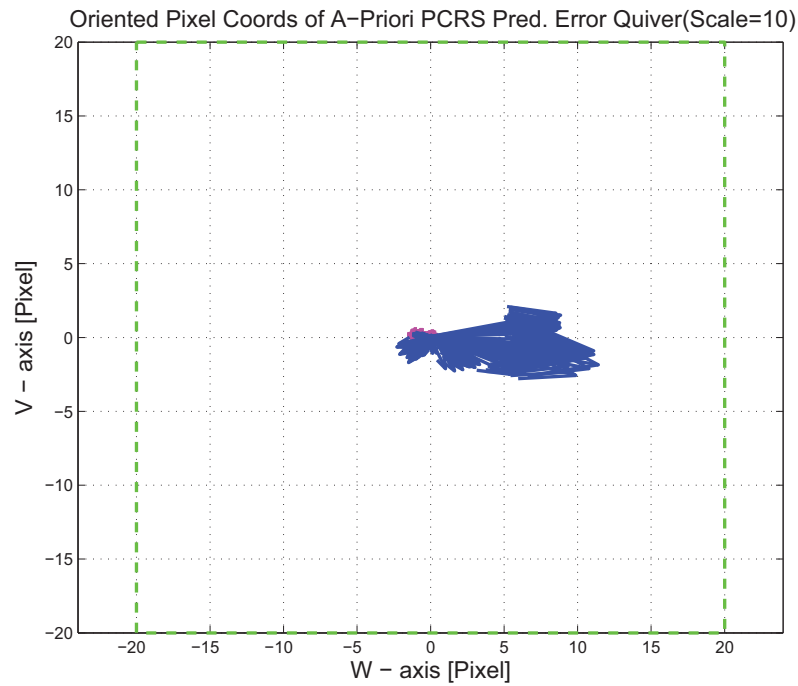


Figure 3.7: Oriented (W,V) Pixel Coords of A-Priori PCRS Prediction Error Quiver Plot

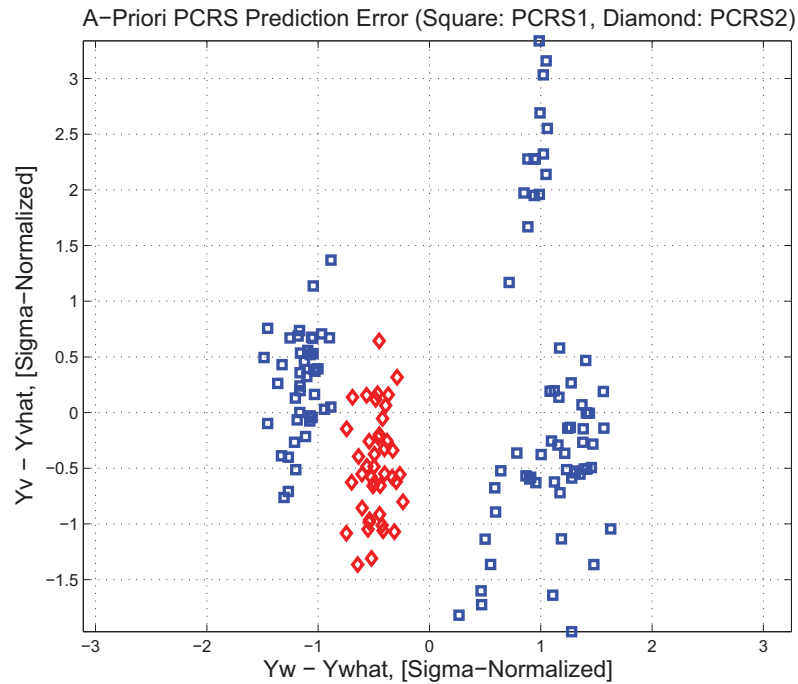


Figure 3.8: A-priori PCRS prediction error

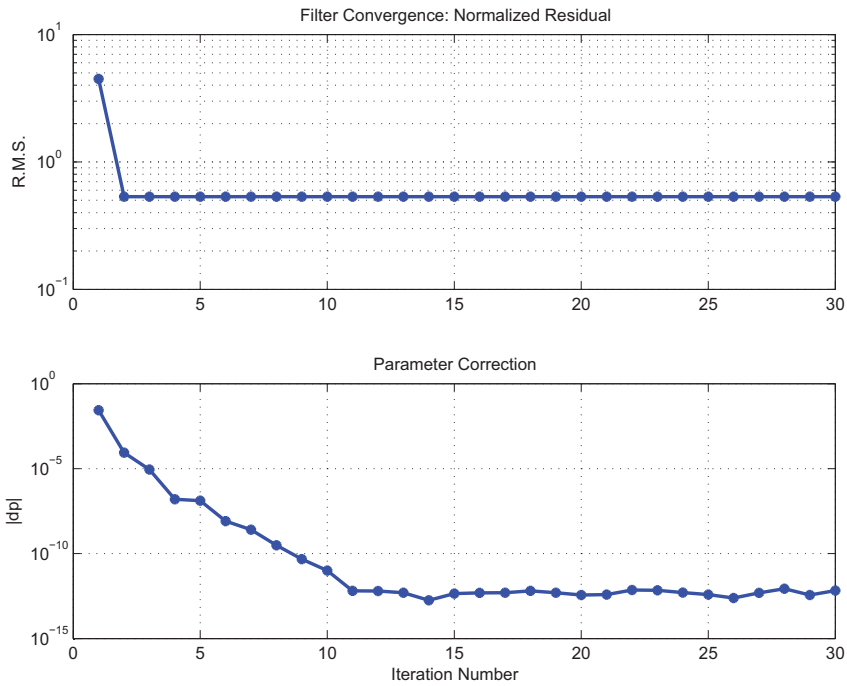


Figure 3.9: IPF execution convergence, chart 1

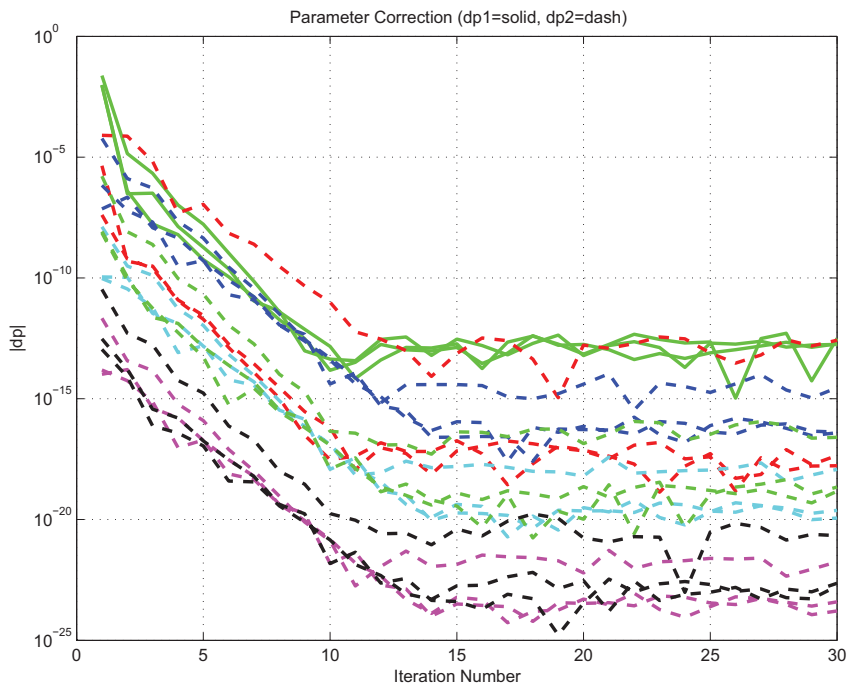


Figure 3.10: IPF execution convergence, chart 2

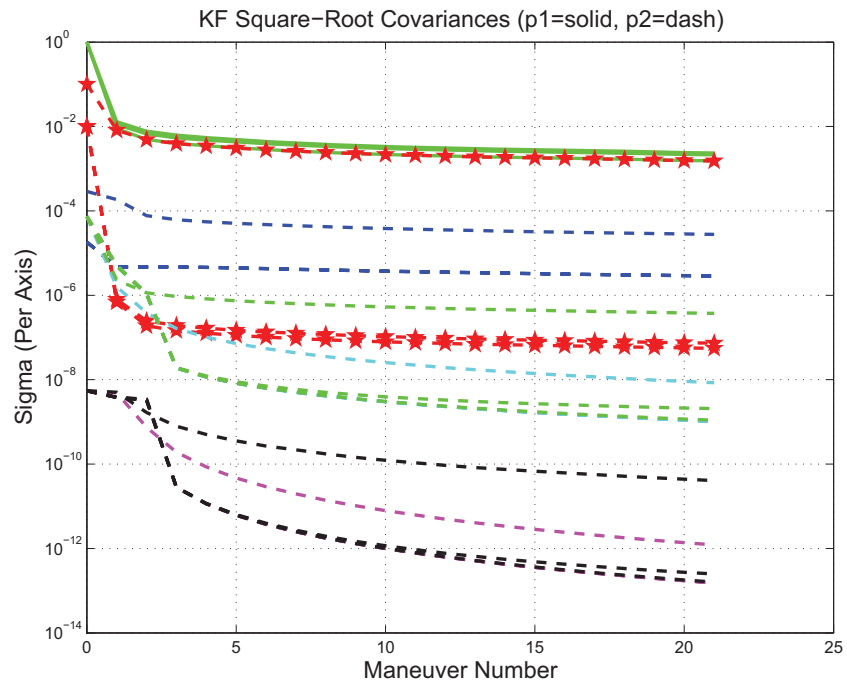


Figure 3.11: Parameter uncertainty convergence

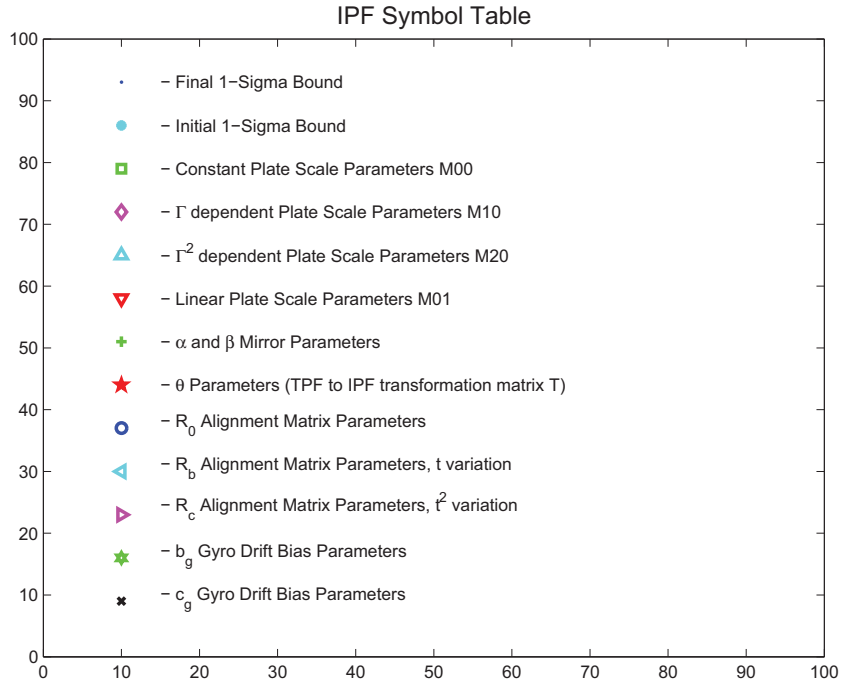


Figure 3.12: IPF parameter symbol table

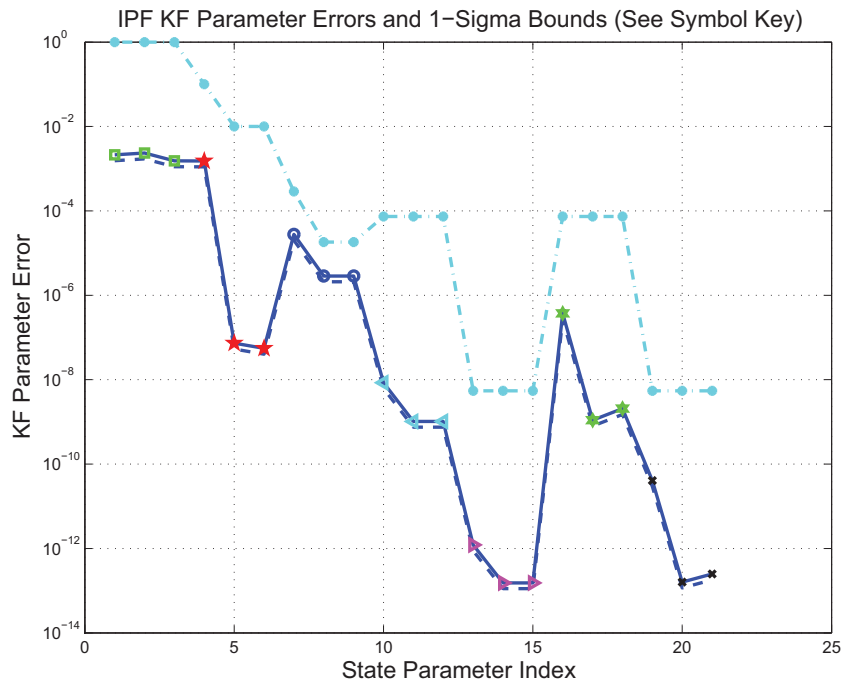


Figure 3.13: KF parameter error sigma plots

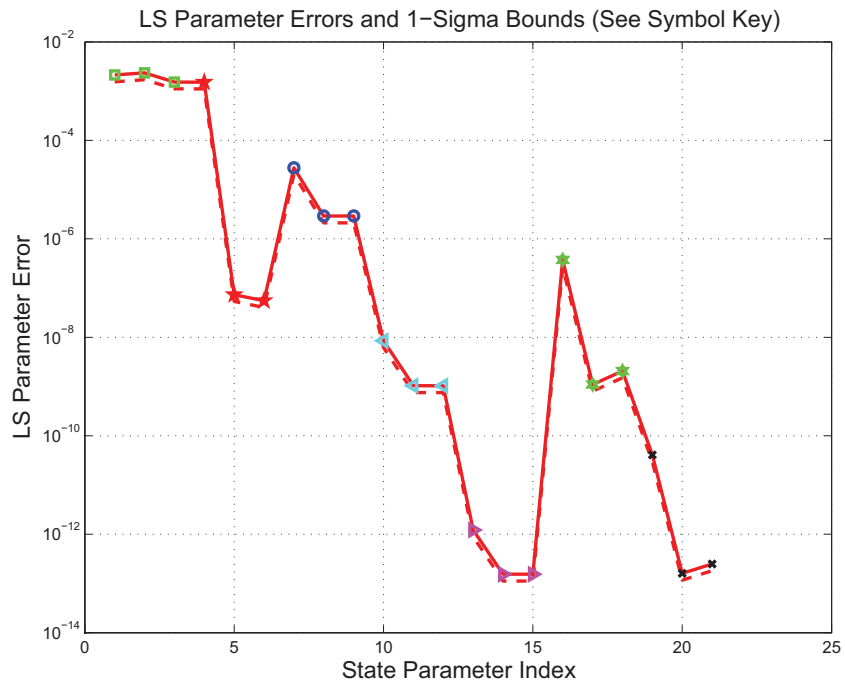


Figure 3.14: LS parameter error sigma plot

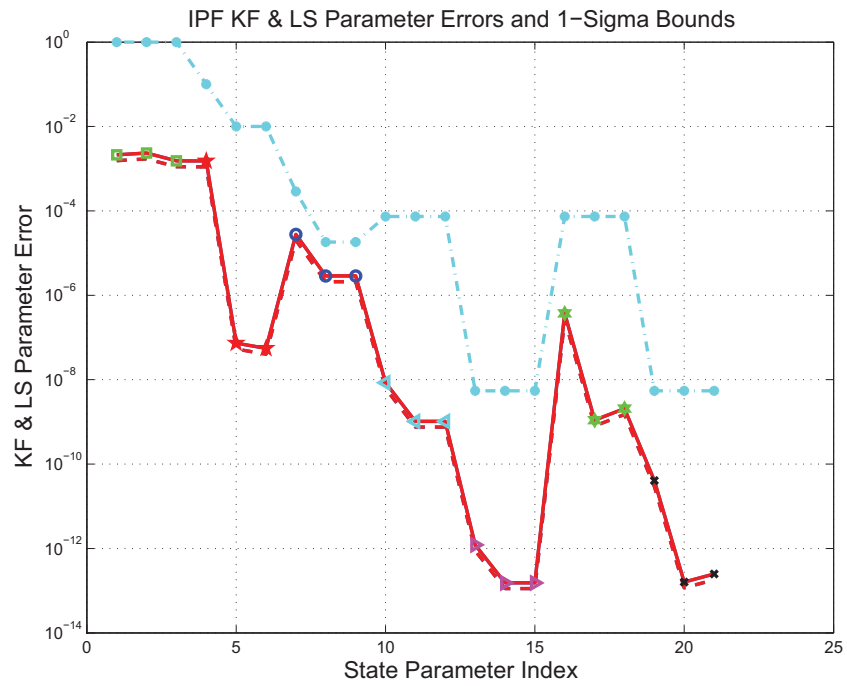


Figure 3.15: KF and LS parameter error sigma plot

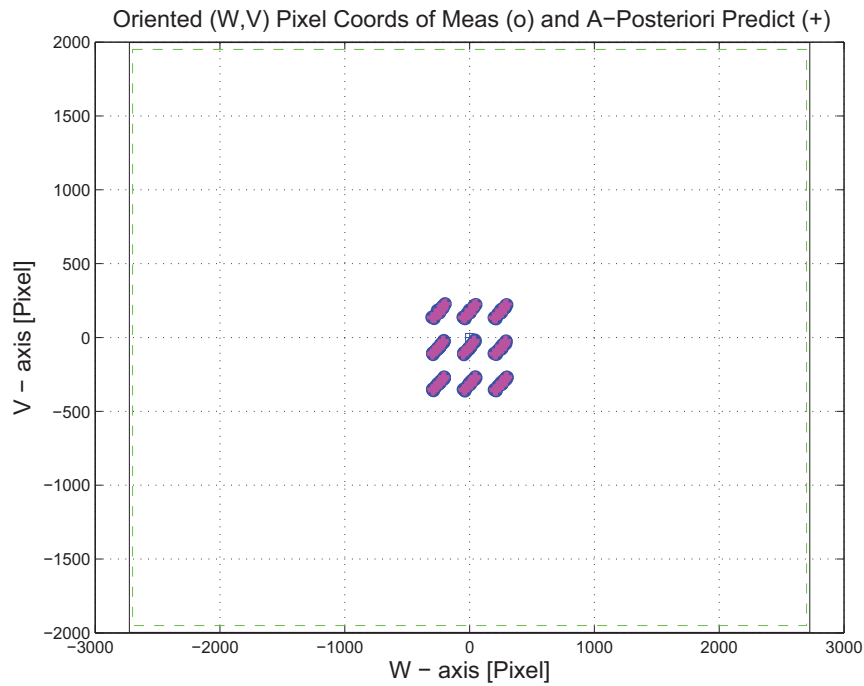


Figure 3.16: Oriented Pixel Coords of meas. and a-posteriori predicts

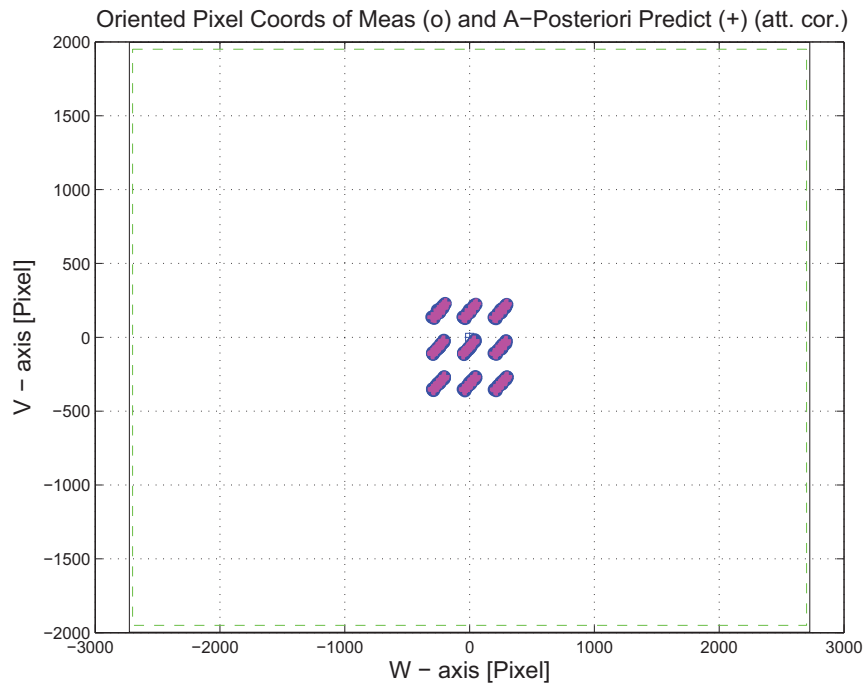


Figure 3.17: Oriented Pixel Coords of meas. and a-posteriori predicts (attitude corrected)

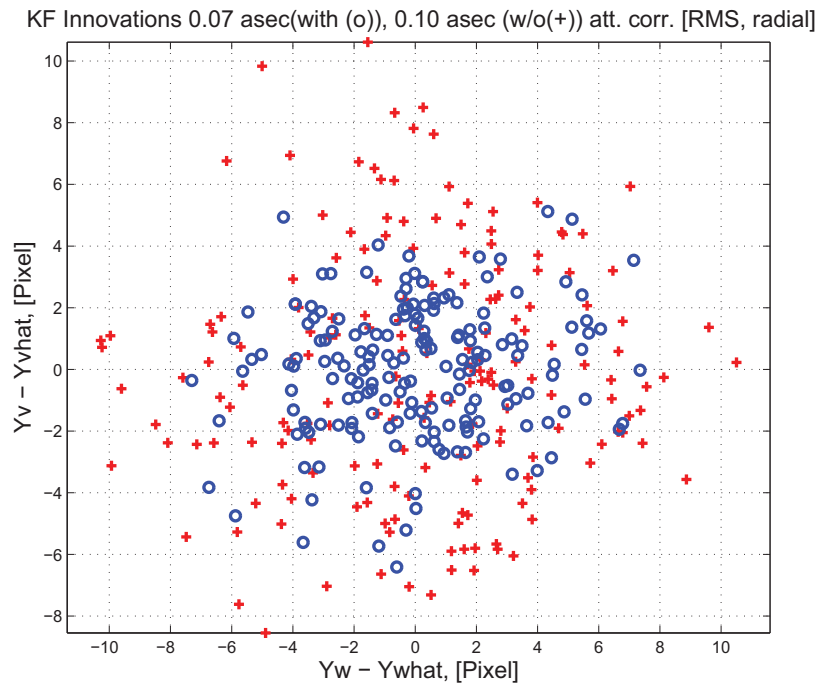


Figure 3.18: KF innovations with (o) and w/o (+) attitude corrections

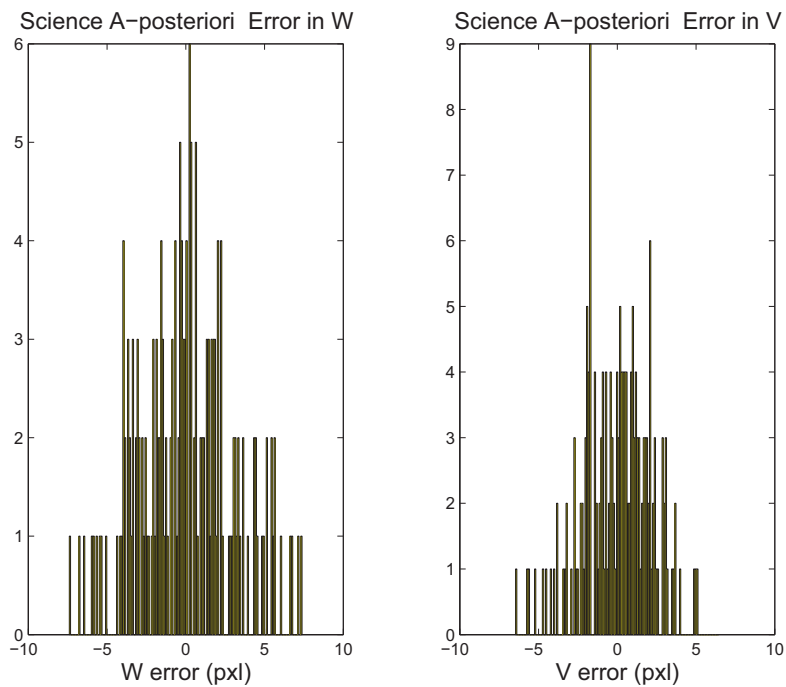


Figure 3.19: Histograms of science a-posteriori residuals (or innovations)

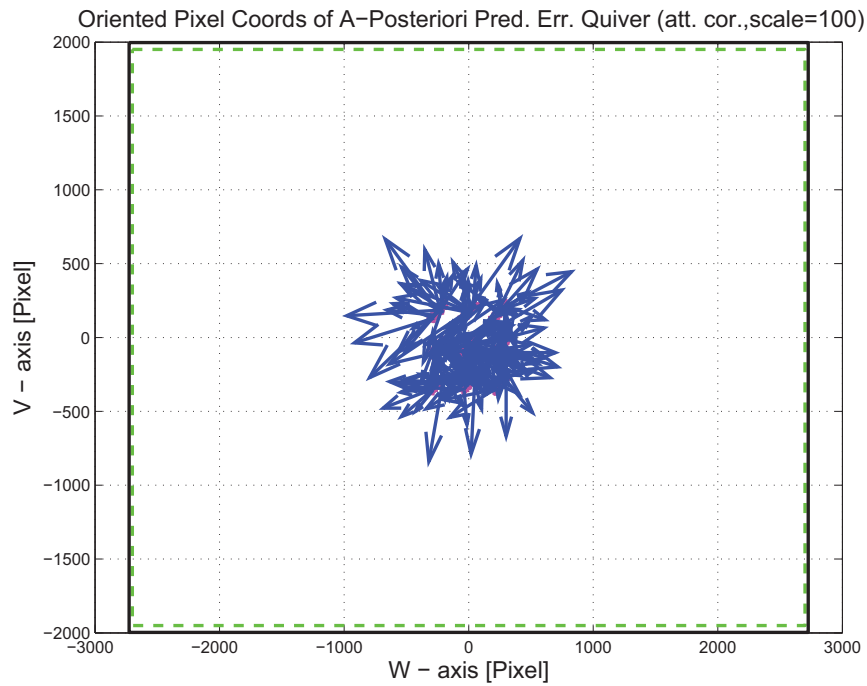


Figure 3.20: A-Posteriori Science Centroid Prediction Error Quiver (Att. Cor.)

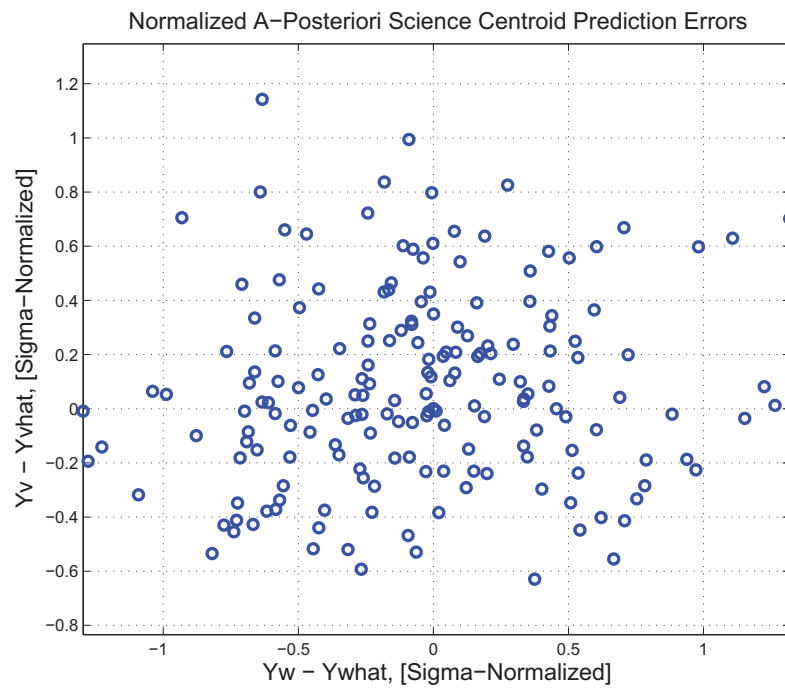


Figure 3.21: Normalized A-Posteriori Science Centroid Prediction Errors

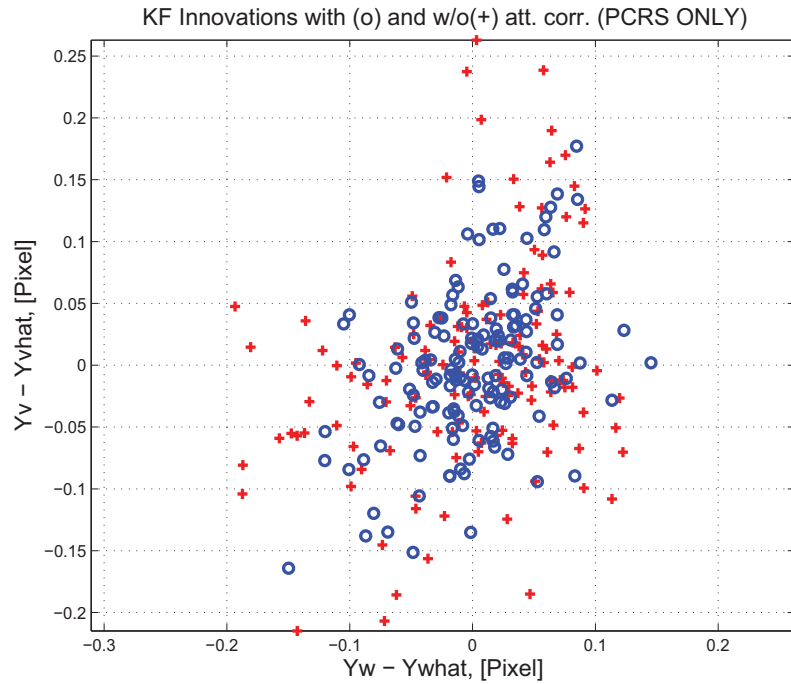


Figure 3.22: KF innovations with (o) and w/o (+) attitude corrections (PCRS)

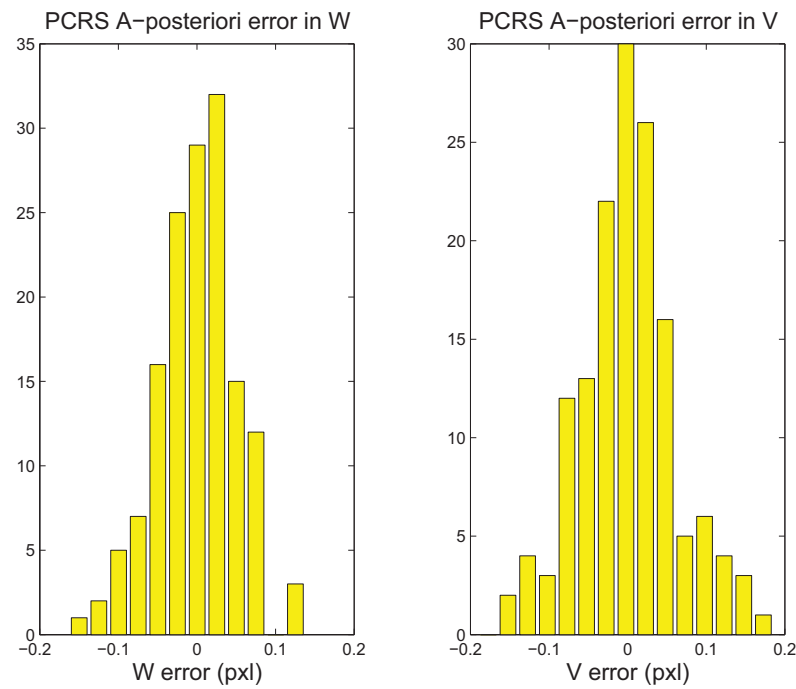


Figure 3.23: Histograms of PCRS a-posteriori residuals (or innovations)

IPF PCRS SUMMARY						
PCRS 1 (Total of 105 centroids)						
RMS	MEAN		SIGMA			
METRIC	APOST.	ATT. COR.	APOST.	ATT. COR.	STAT. CONF.	UNITS
Radial	0.0039	0.0039	0.1171	0.0878	0.0086	arcsec
W-axis	-0.0000	-0.0000	0.0731	0.0559	0.0055	arcsec
V-axis	0.0039	0.0039	0.0914	0.0677	0.0066	arcsec
PCRS 2 (Total of 42 centroids)						
METRIC	APOST.	ATT. COR.	APOST.	ATT. COR.	STAT. CONF.	UNITS
Radial	0.0109	0.0109	0.0731	0.0526	0.0081	arcsec
W-axis	0.0000	0.0000	0.0600	0.0290	0.0045	arcsec
V-axis	-0.0109	-0.0109	0.0417	0.0439	0.0068	arcsec
Combined (Total of 147 centroids)						
METRIC	APOST.	ATT. COR.	APOST.	ATT. COR.	STAT. CONF.	UNITS
Radial	0.0003	0.0003	0.1066	0.0797	0.0066	arcsec
W-axis	-0.0000	-0.0000	0.0697	0.0497	0.0041	arcsec
V-axis	-0.0003	-0.0003	0.0807	0.0622	0.0051	arcsec

Table 3.3: PCRS measurement prediction error summary

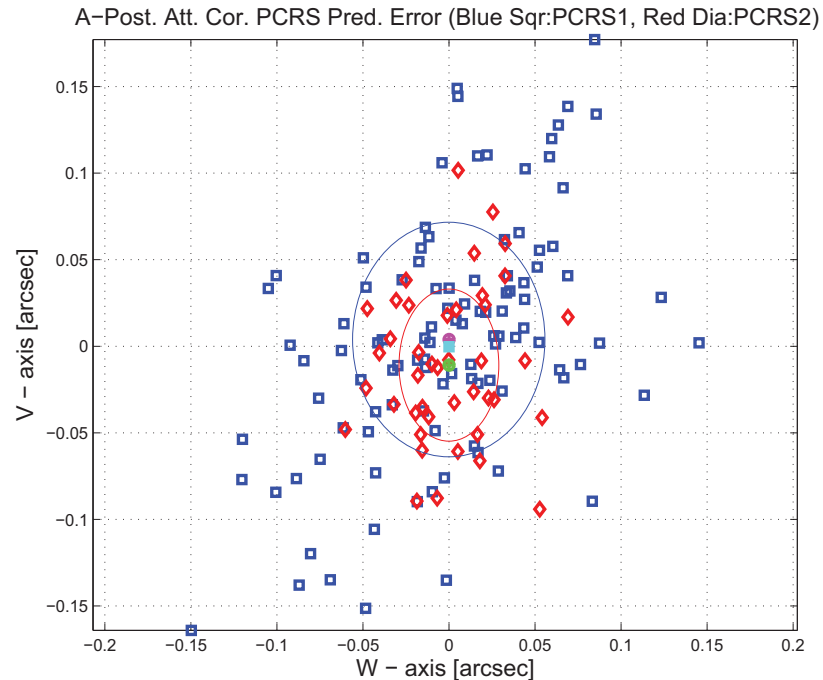


Figure 3.24: A-posteriori PCRS Prediction Summary

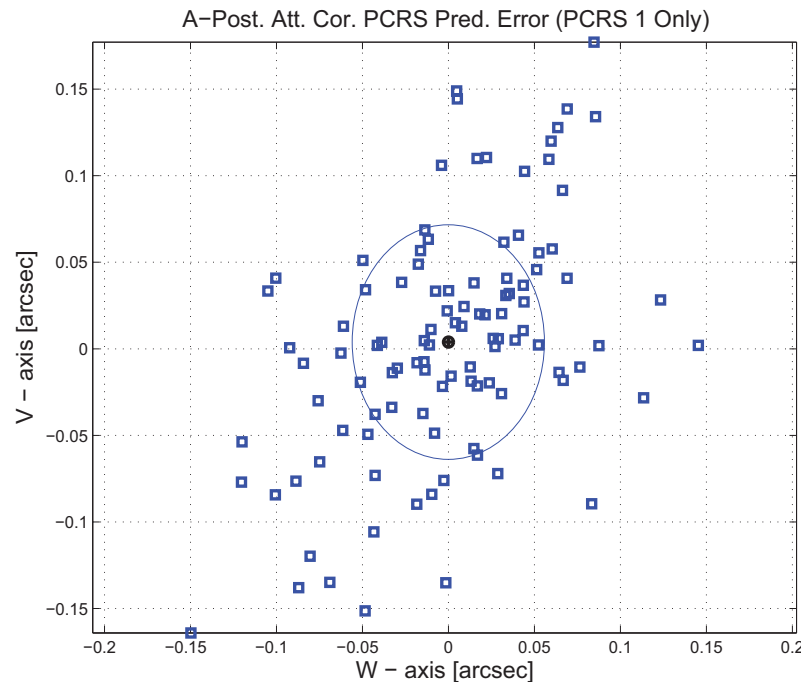


Figure 3.25: A-posteriori PCRS Prediction (PCRS 1 Only)

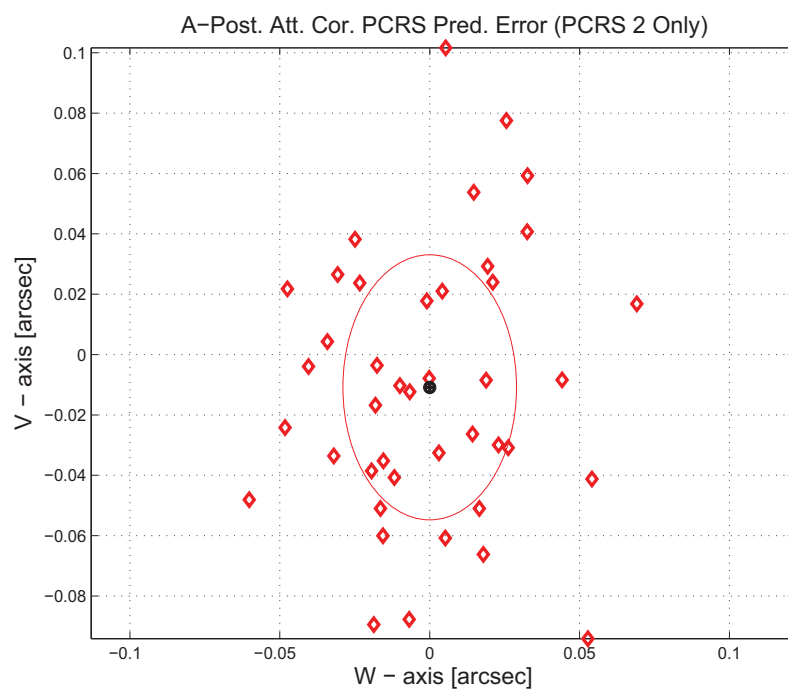


Figure 3.26: A-posteriori PCRS Prediction (PCRS 2 Only)

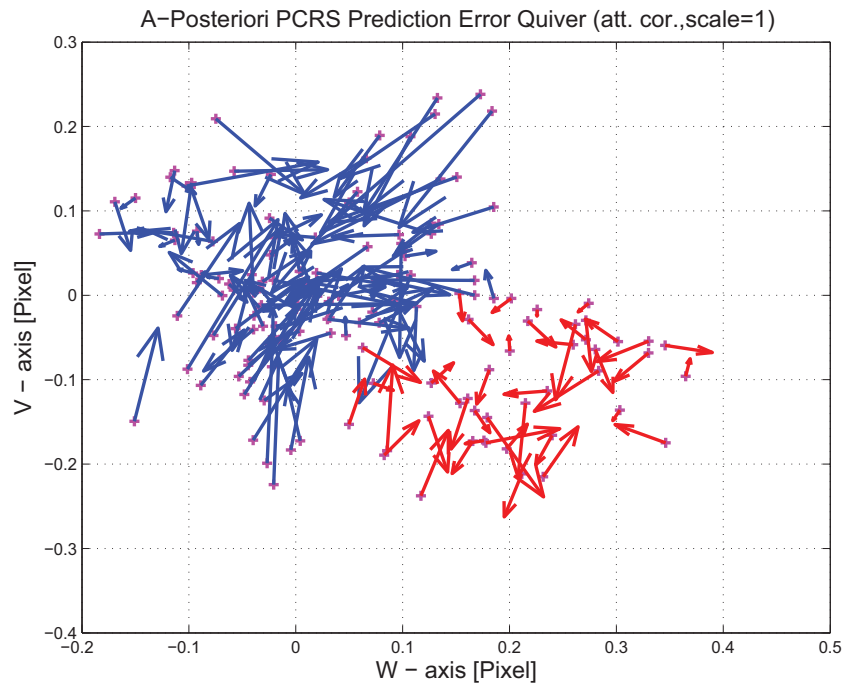


Figure 3.27: A-Posteriori PCRS Prediction Errors Quiver (Att. Cor.)

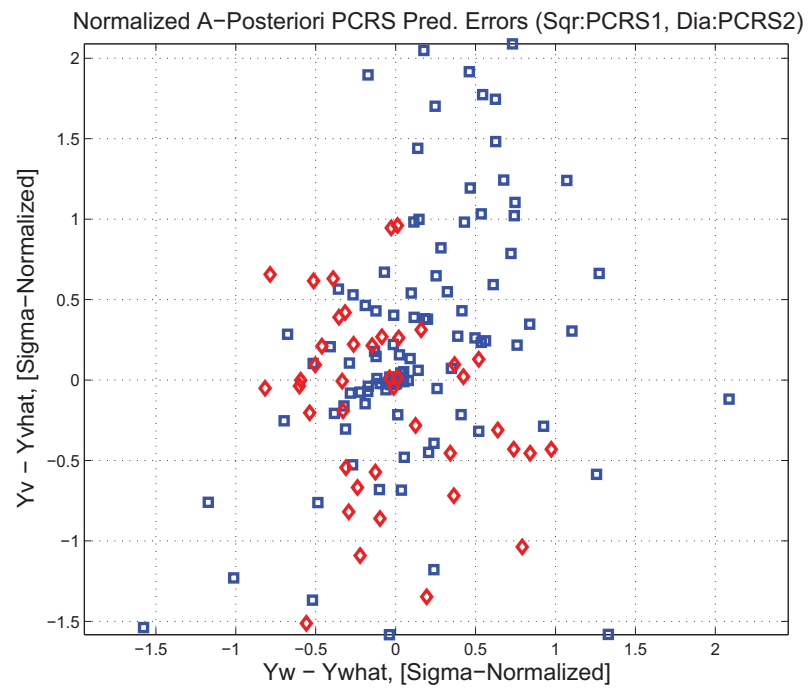


Figure 3.28: Normalized A-Posteriori PCRS Prediction Errors

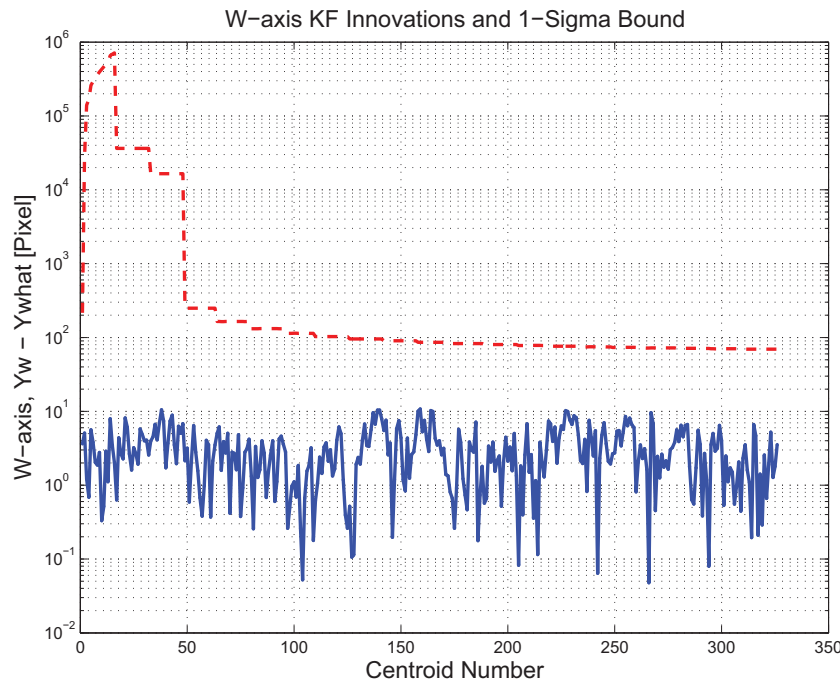


Figure 3.29: W-axis KF innovations and 1-sigma bound

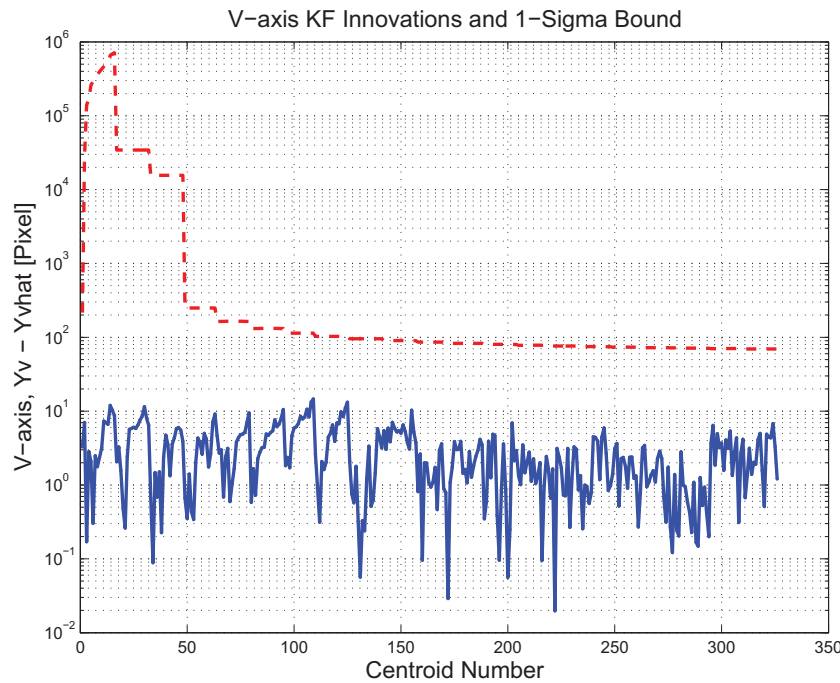


Figure 3.30: V-axis KF innovations and 1-sigma bound

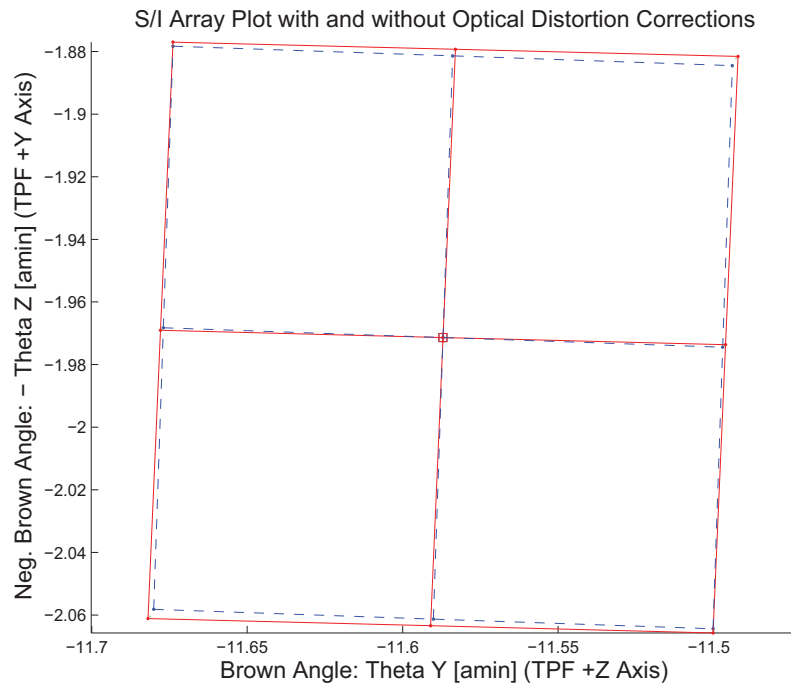


Figure 3.31: Array plot with (solid) and w/o (dashed) optical distortion corrections

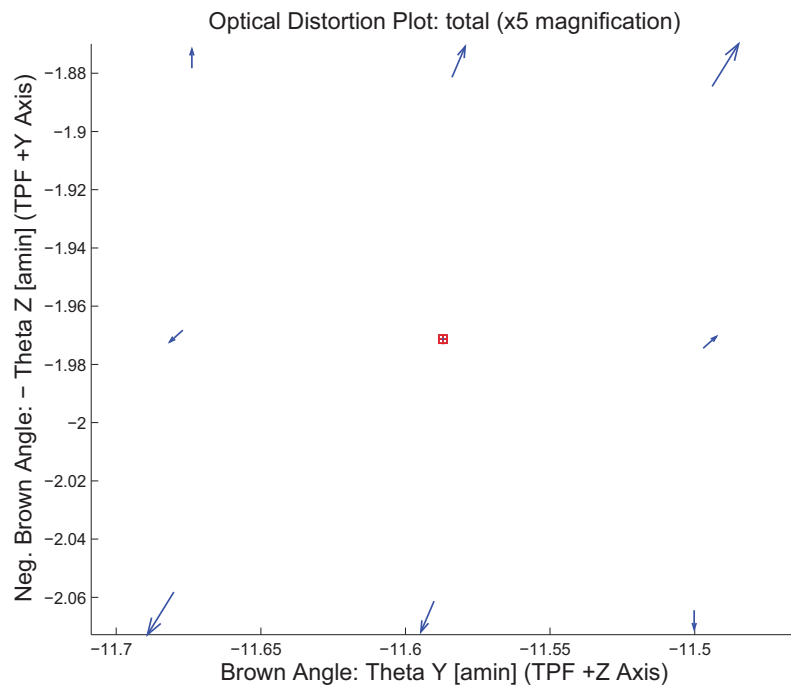


Figure 3.32: Optical Distortion Plot: total (x5 magnification)

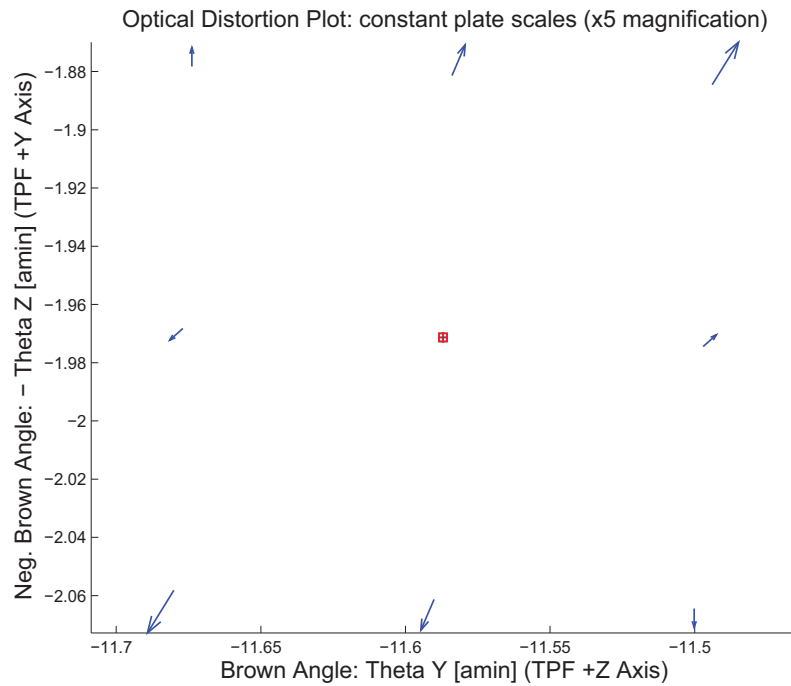


Figure 3.33: Optical Distortion Plot: constant plate scales (x5 magnification)

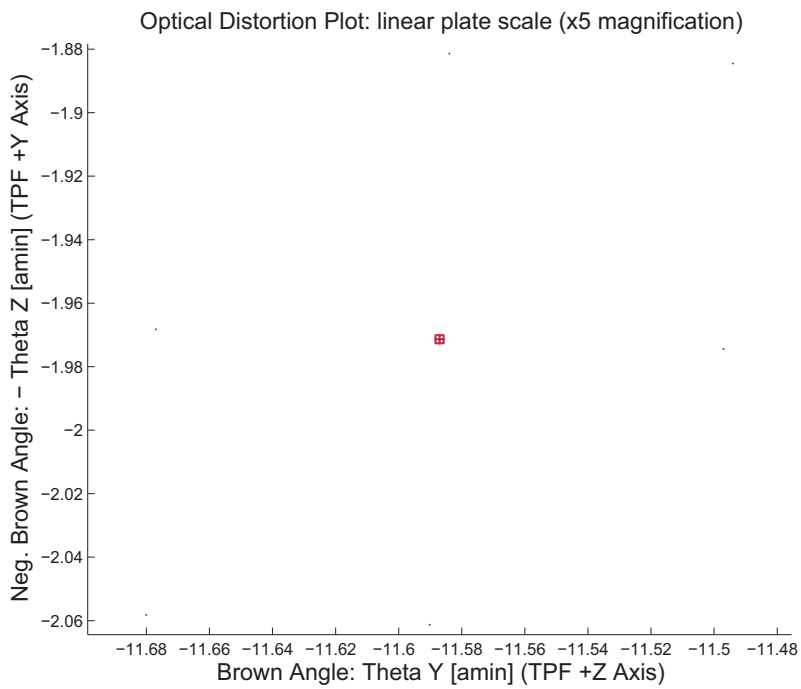


Figure 3.34: Optical Distortion Plot: linear plate scale (x5 magnification)

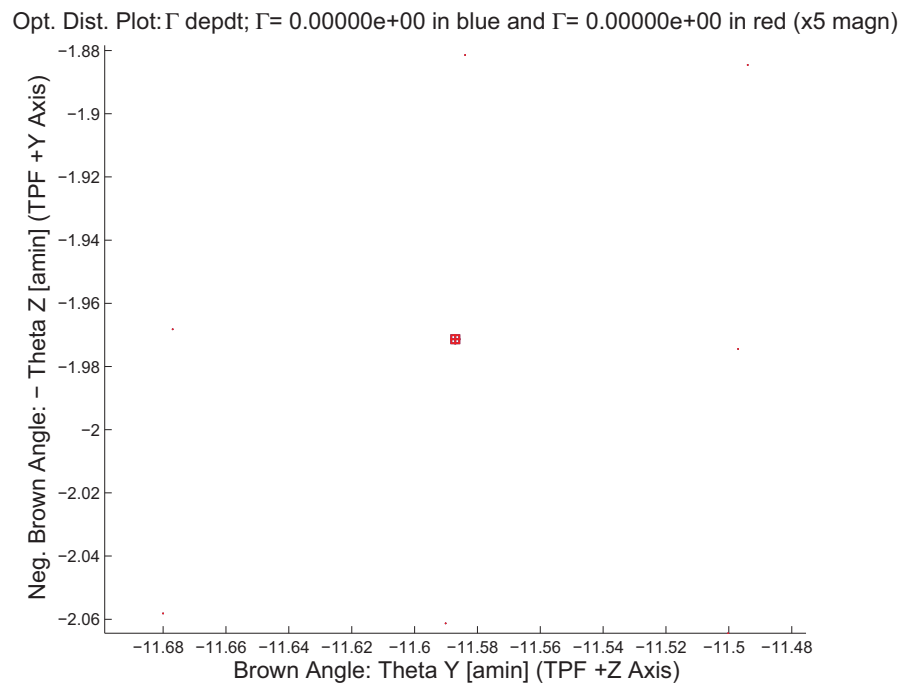


Figure 3.35: Optical Distortion Plot: gamma terms (x5 magnification)

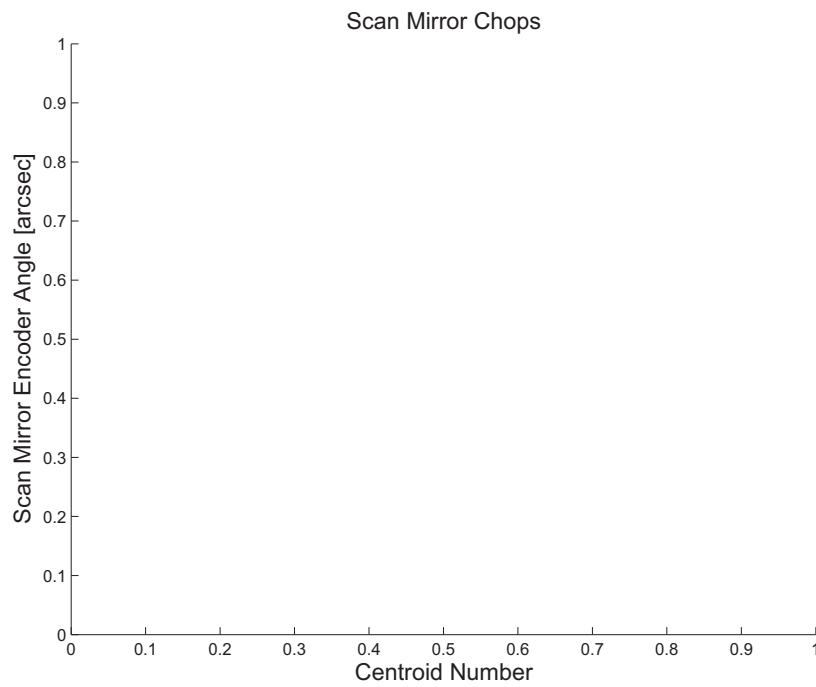


Figure 3.36: Scan Mirror Chops

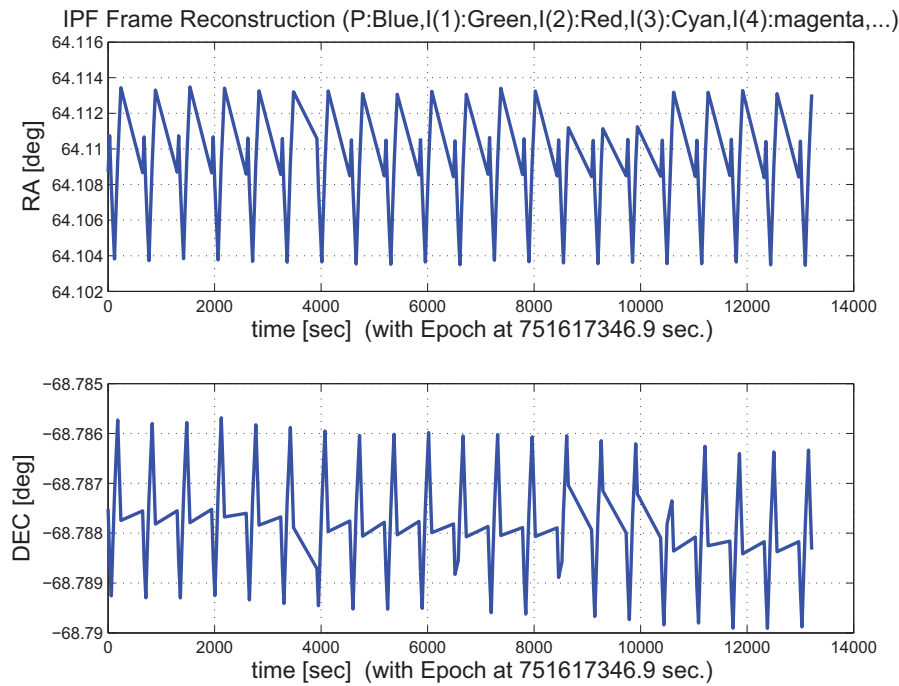


Figure 3.37: IPF Frame Reconstruction

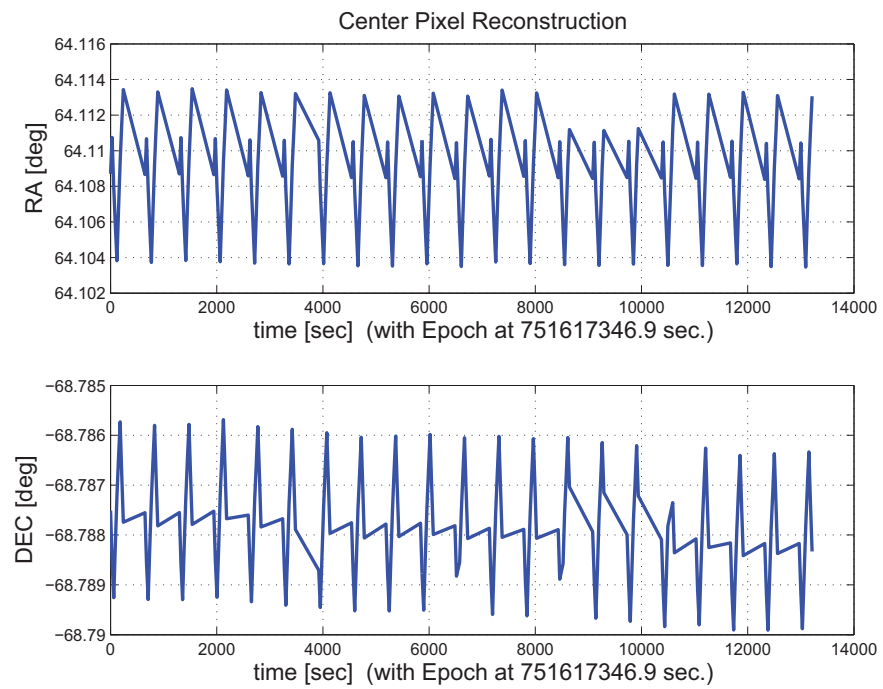


Figure 3.38: Center Pixel Reconstruction

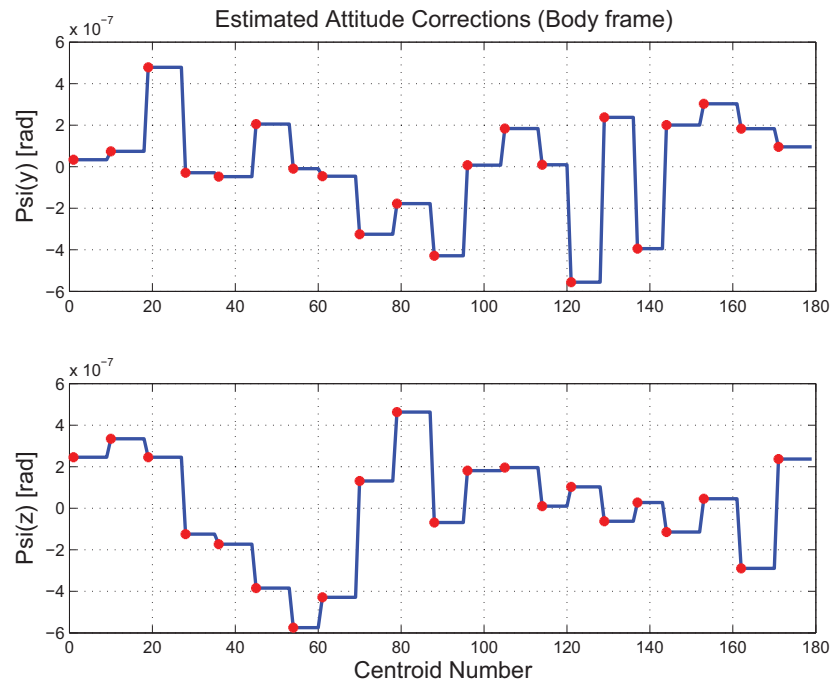


Figure 3.39: Estimated attitude corrections (Body frame)

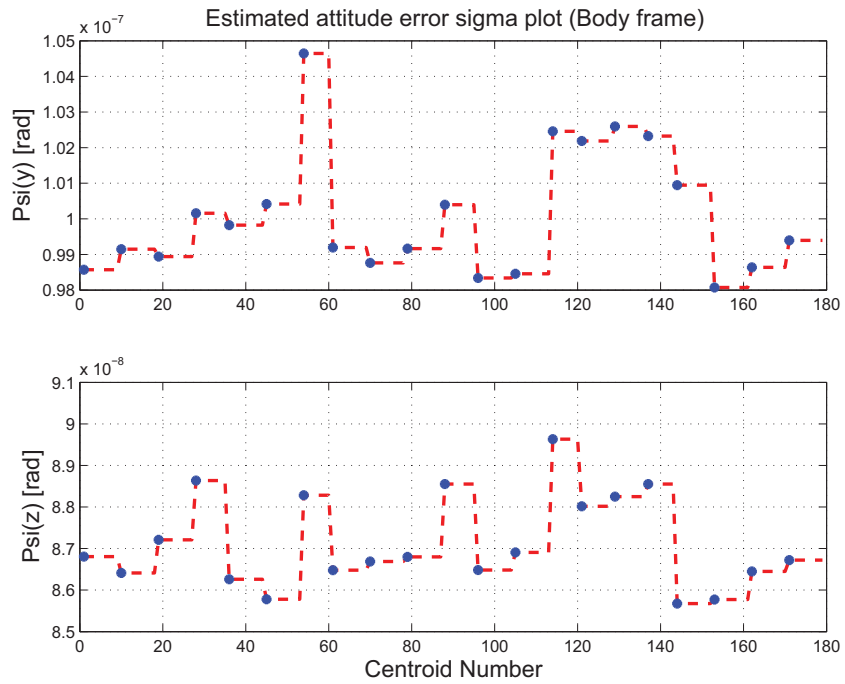


Figure 3.40: Estimated attitude error sigma plot (Body frame)

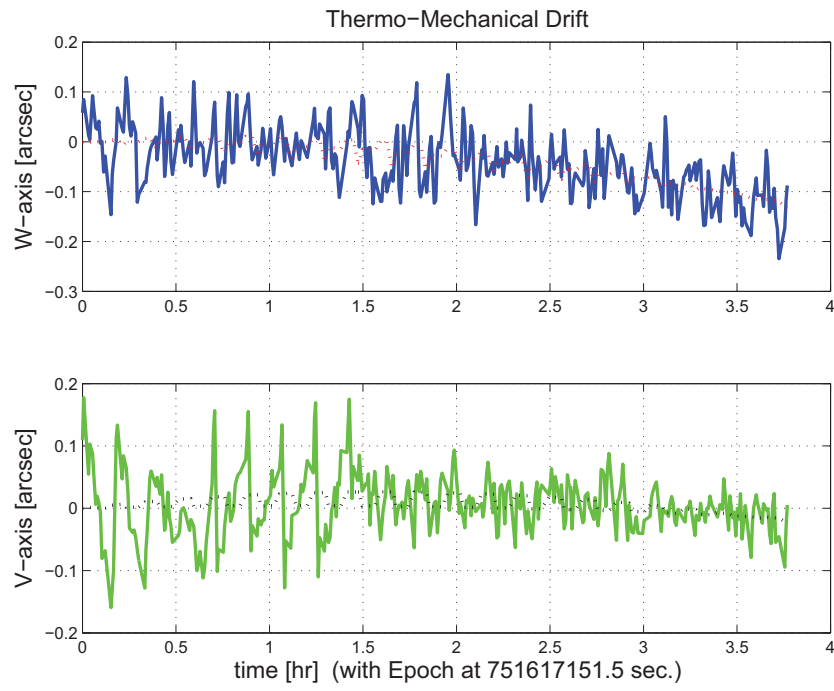


Figure 3.41: Thermo-mechanical boresight drift (equiv. angle in (W,V) coords)

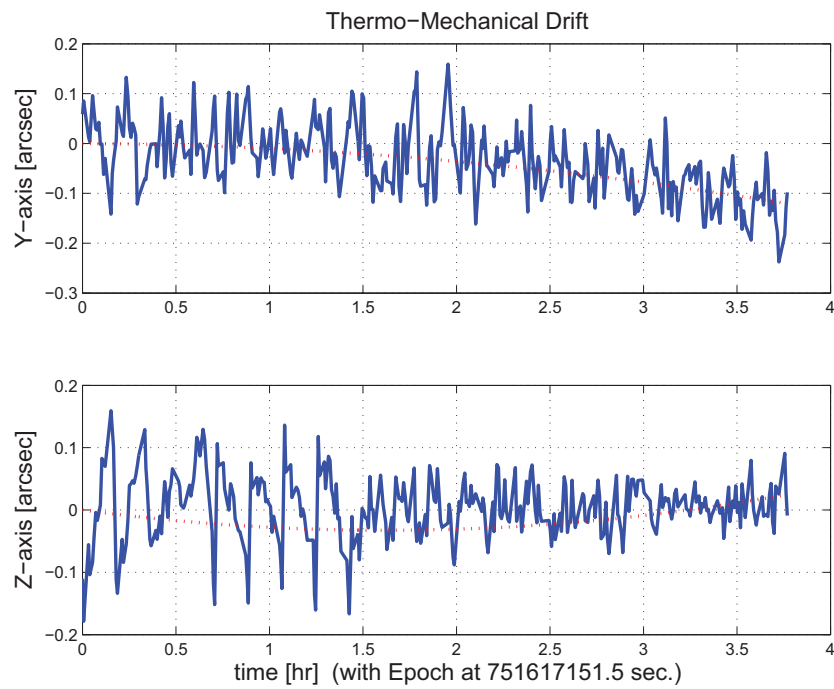


Figure 3.42: Thermo-mechanical boresight drift (equiv. angle in Body frame)

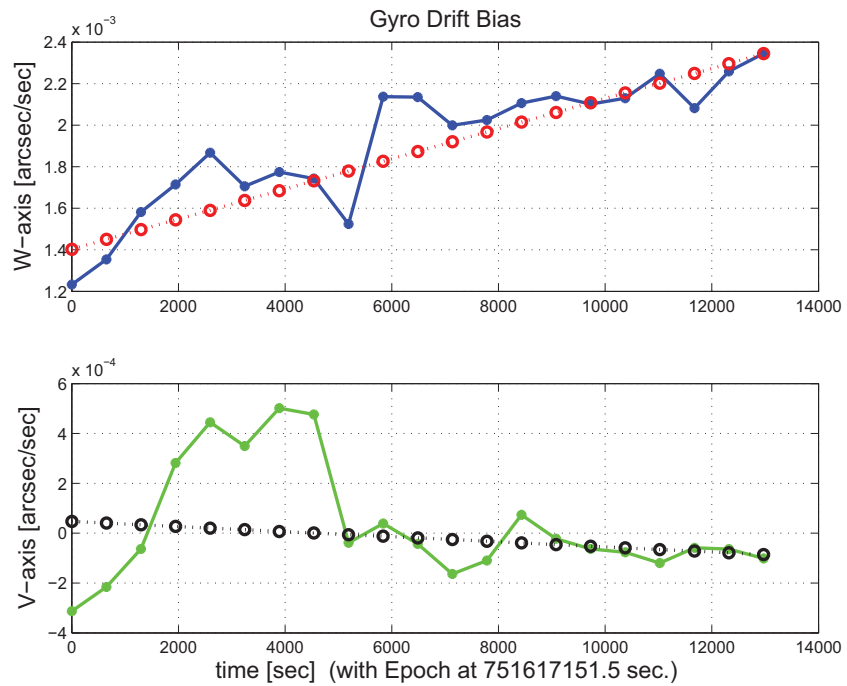


Figure 3.43: Gyro drift bias contribution (equiv. rate in (W,V) coords)

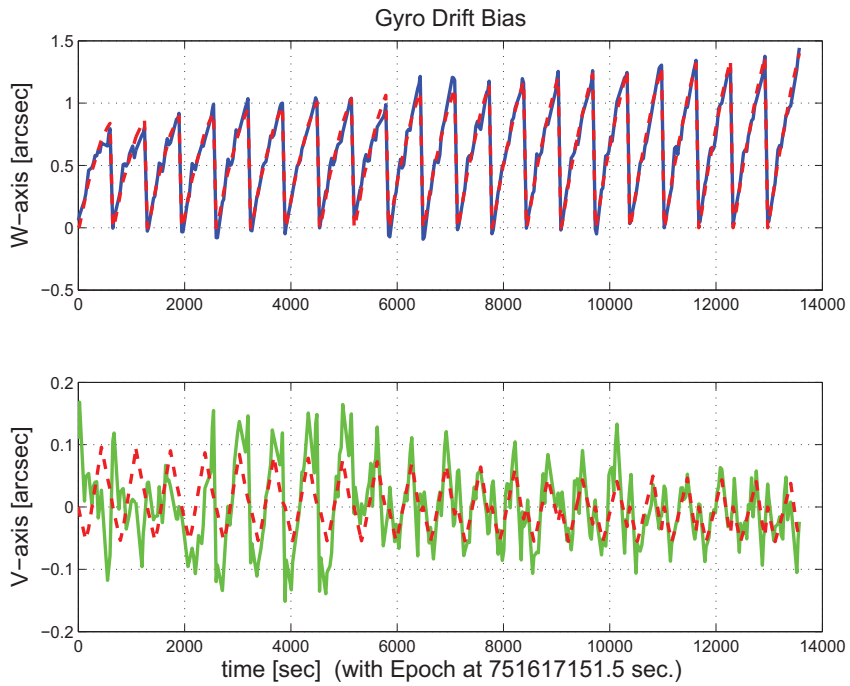


Figure 3.44: Gyro drift bias contribution (equiv. angle in (W,V) coords)

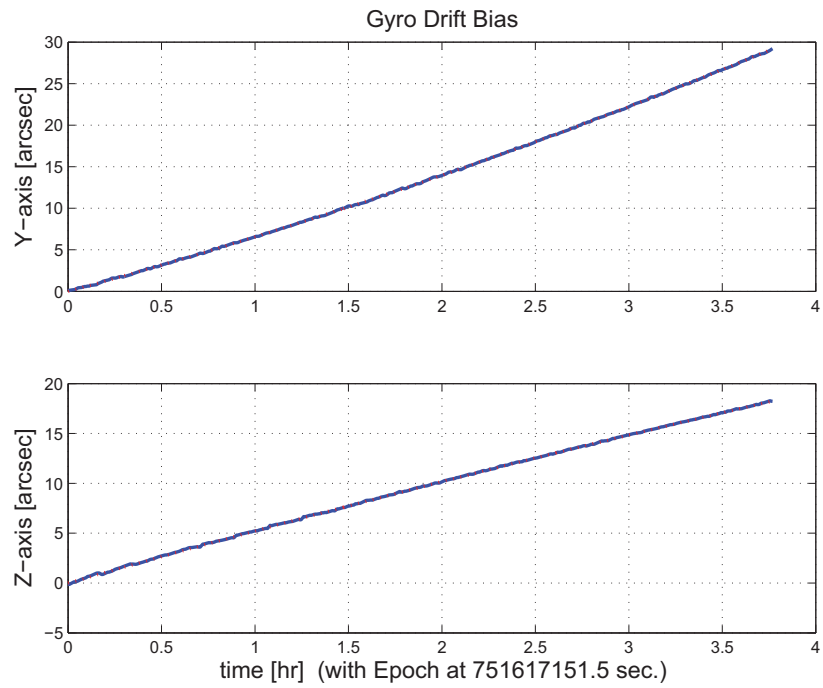


Figure 3.45: Gyro drift bias contribution (equiv. angle in Body frame)

3.2 IPF OUTPUT DATA (IF MINI FILE)

OUTPUT FILE NAME: IFmini701019.dat DATE: 26-Apr-2004 TIME: 10:42
 INSTRUMENT NAME: IRS_Red_PeakUp_FOV_Sweet_Spot NF: 19
 IPF FILTER VERSION: IPF.V4.0.0 SW RELEASE DATE: January 30, 2004
 FRAME TABLE USED: BodyFrames_FTU_17a

----- IPF BROWN ANGLE SUMMARY -----

Frame Number	WAS			IS		
	theta_Y (arcmin)	theta_Z (arcmin)	angle (deg)	theta_Y (arcmin)	theta_Z (arcmin)	angle (deg)
019	-11.571876	+1.971732	+1.977920	-11.587019	+1.971349	+1.977920

OFFSET	NF	Delta_CW	Delta_CV
0	19	+0.000	+0.000 pixels

OFFSET FRAME NAME: IRS_Red_PeakUp_FOV_Sweet_Spot

Brown Angle	theta_Y(arcmin)	theta_Z(arcmin)	angle(deg)
WAS(FTB)	-11.571876	+1.971732	+1.977920
IS (EST)	-11.587019	+1.971349	+1.977920
dT_EST	-0.015143	-0.000383	+0.000000
T_sSIGMA	+0.000183	+0.000139	+0.063394
dT_EST/T_sSIGMA	-82.598387	-2.764716	+0.000000

VARNAME	MEAN	SIGMA	SCALED_SIGMA
a00	+9.8511506132953654E-003	+2.1245507856627083E-003	+1.5463992372048250E-003
b00	+2.3848691277818575E-002	+2.3447799787420045E-003	+1.7066977146459404E-003
c00	+9.3091236059139413E-003	+1.5306183906951731E-003	+1.1140929780524751E-003
del_theta1	-2.6193581808761635E-013	+1.5200905980215845E-003	+1.1064301014247415E-003
del_theta2	+1.6920190360828382E-018	+7.3269928790004029E-008	+5.3331067798208050E-008
del_theta3	+4.5086902037856365E-018	+5.5400890525996666E-008	+4.0324710253111569E-008
del_arx	+2.8517214936305772E-015	+2.7685589892767429E-005	+2.0151542331046968E-005
del_ary	+4.1634018550488512E-017	+2.8649300172978903E-006	+2.0852999247145404E-006
del_arz	-3.8920283806163344E-017	+2.8655335293248264E-006	+2.0857392037114918E-006
brx	+1.3343108181549648E-008	+8.4901469038347389E-009	+6.1797330449559418E-009
bry	-2.7480755600980097E-012	+1.0270373527610807E-009	+7.4755086562696113E-010
brz	-5.3981601538133312E-011	+1.0273392408343690E-009	+7.4777060124797078E-010
crx	-2.1646887767102277E-012	+1.2173784660109220E-012	+8.8609467183983895E-013
cry	-5.9595312759201611E-015	+1.5328211442398753E-013	+1.1156962988223362E-013
crz	+9.2666978326263776E-015	+1.5332848621252379E-013	+1.1160338256958015E-013
bgx	-1.6269914085501530E-006	+3.7279260320715356E-007	+2.7134498319621043E-007
bgy	+8.2539129027976648E-009	+1.0945357063374789E-009	+7.9668097030015434E-010
bgz	+7.2136854057590919E-009	+2.0602815472558340E-009	+1.4996195123242430E-009
cgx	+3.3373240757784547E-011	+4.0660621998603075E-011	+2.9595693954334068E-011
cgy	+3.1962590430427453E-013	+1.5955919583509399E-013	+1.1613853638779393E-013
cgz	-1.0231653822625830E-013	+2.4875959467002927E-013	+1.8106493383970649E-013

LSQF RESIDUAL SIGMA SCALE = +7.2787115640658062E-001

qT	qT(1)	qT(2)	qT(3)	qT(4)
FrmTbl:	+1.7260206333841101E-002	+1.6778598237061700E-003	-3.1578291163250502E-004	+9.9984957385842599E-001
Estim:	+1.7260207001741457E-002	+1.6800629845937301E-003	-3.1576519115542593E-004	+9.9984957015291498E-001
DelTheta	deltheta(1)	deltheta(2)	deltheta(3)	
	+1.2519980712928453E-011	+4.4062835238013424E-006	-4.0618499059943870E-008	[rad]
EulAngT	theta(1)	theta(2)	theta(3)	[rad]
Mean	+3.4521212301945867E-002	+3.3705272328611790E-003	-5.7344220021853421E-004	
SigmaT	+1.5200905980215845E-003	+7.3269928790004029E-008	+5.5400890525996666E-008	

qR	qR(1)	qR(2)	qR(3)	qR(4)
ASFILE:	+7.0887658512219787E-004	+1.2699844082817435E-003	-1.6144585970323533E-004	+9.9999892711639404E-001
Estim:	+6.7872515932306118E-004	+1.2699113709819115E-003	-1.6110651468370286E-004	+9.9999895035042852E-001

```

DelThetaR      delthetaR(1)          delthetaR(2)          delthetaR(3)
-6.0303658369715328E-005 -1.5536983723923915E-007 +6.0222136680933779E-007 [rad]
EulAngR       angR(1)           angR(2)           angR(3)           [rad]
Mean          +1.3570445060179504E-003 +2.5400415014399935E-003 -3.2048988891739426E-004
SigmaR        +2.7685589892767429E-005 +2.8649300172978903E-006 +2.8655335293248264E-006

-----
Initial Gyro Bias   Bg0(1)          Bg0(2)          Bg0(3)
-4.0949606727735954E-007 -1.9548996021967469E-007 +3.6376303569340962E-007
Gyro Bias Correction Bg(1)           Bg(2)           Bg(3)
-1.6269914085501530E-006 +8.2539129027976648E-009 +7.2136854057590919E-009
Total Gyro Bias    BgT(1)          BgT(2)          BgT(3)
-2.0364874758275125E-006 -1.8723604731687702E-007 +3.7097672109916873E-007

Initial Gyro Bias Rate   Cg0(1)          Cg0(2)          Cg0(3)
+0.0000000000000000E+000 +0.0000000000000000E+000 +0.0000000000000000E+000
Gyro Bias Rate Correction Cg(1)           Cg(2)           Cg(3)
+3.3373240757784547E-011 +3.1962590430427453E-013 -1.0231653822625830E-013
Total Gyro Bias Rate    CgT(1)          CgT(2)          CgT(3)
+3.3373240757784547E-011 +3.1962590430427453E-013 -1.0231653822625830E-013

-----
q(1)             q(2)             q(3)             q(4)
PCRS1A: +5.3371888965461637E-007 +3.7444233778550031E-004 -1.4253684912431913E-003 +9.9999891405806784E-001
PCRS2A: -5.2779261998836216E-007 +3.8462959425181312E-004 +1.3722087221825403E-003 +9.9999898455099423E-001

***** CS-FILE PARAMETERS: ***** AS-FILE PARAMETERS: *****
Row (01) PIX2RADX: +8.72659999999995E-008 Row (1) TASTART: +7.5161695119071960E+008
Row (02) PIX2RADY: +8.72659999999995E-008 Row (2) TASTOP: +7.5163091909073484E+008
Row (03) CXO: +1.060000000000000E+004 Row (3) S/C TIME: +7.5161268789079285E+008
Row (04) CYO: +9.400000000000000E+003 Row (4) QR1: +7.0887658512219787E-004
Row (05) BETA0: +9.999900000000000E+004 Row (5) QR2: +1.2699844082817435E-003
Row (06) GAMMA_E0: +9.999900000000000E+004 Row (6) QR3: -1.6144585970323533E-004
Row (07) D11: +0.000000000000000E+000 Row (7) QR4: +9.9999892711639404E-001
Row (08) D12: +1.000000000000000E+000
Row (09) D21: +1.000000000000000E+000
Row (10) D22: +0.000000000000000E+000
Row (11) DG: +9.999900000000000E+004

-----
INITIAL STA-TO-PCRS ALIGNMENT (R) KNOWLEDGE (1-SIGMA)
SIGMA(X)      SIGMA(Y)      SIGMA(Z)
5.93446115E+000 3.75377923E-001 3.75875241E-001 [arcsec]

PIX2RADX = 8.726600000000E-008[rad/pixel]
XPIXSIZE = 0.0180[arcsec]
PIX2RADY = 8.726600000000E-008[rad/pixel]
YPIXSIZE = 0.0180[arcsec]
CX0 = 10600.0[pixel] = 190.80[arcsec]
CY0 = 9400.0[pixel] = 169.20[arcsec]

NOMINAL BETA0 = 9.999900000000E+004[rad/encoder unit]
ENCODER UNIT SIZE = 99999.00[arcsec]
GAMMA_E0 = 99999.00[encoder unit] = 99999.00[arcsec]

-----
| +0 | +1 |
FLIP MATRIX D = |----|----| and DG = +99999
| +1 | +0 |


```

3.3 IPF EXECUTION LOG

```
*****
IPF EXECUTION-LOG FILE NAME: LG701019.dat
INSTRUMENT TYPE: IRS_Red_PeakUp_FOV_Sweet_Spot
IPF FILTER EXECUTION DATE: 26-Apr-2004 TIME: 10:33
IPF FILTER VERSION USED: IPF.V4.0.0
*****


----- Loading & Preparing Input Files -----
AAFILE: AA501019 Loaded! AAFILE dimension = 139680 X 21
ASFILE: AS501019 Loaded!
CAFFILE: CA501019 Loaded! CAFFILE dimension = 179 X 15
CBFILE: CB502019 Loaded! CBFILE dimension = 147 X 15
CCFILE: CC701019 Created! CCFILE dimension = 326 X 19
CSFILE: CS701019 Loaded!
Loading Input Files Completed!
-----


----- Selected Mask Vectors -----
index = 1 2 3 4 5 6 7 8 9 10 11 12 13 14 15 16 17 18 19 20
-----
mask1 = [ 1 1 1 0 0 0 0 0 0 0 0 0 0 0 0 0 0 0 0 0 ]
mask2 = [ 0 0 1 1 1 1 1 1 1 1 1 1 1 1 1 1 1 1 1 1 ]
-----


----- Selected Initial Gyro Bias Parameters -----
User Entered 1 : Use AFILE database - from S/C filter
IPF Linearized Using Following Nominal Gyro Bias Estimates
bg0 = [-4.0949606727735954E-007 -1.9548996021967469E-007 +3.6376303569340962E-007 ]
cg0 = [+0.0000000000000000E+000 +0.0000000000000000E+000 +0.0000000000000000E+000 ]
-----


----- Gyro Pre-Processor Run Completed -----
AGFILE CREATED: AG701019.m ACFILE CREATED: AC701019.m
-----


Total Gyro Preprocessor Execution Time: 232 seconds

FRAME TABLE ENTRIES FOR PCRS LOADED TO TPCRS
q_PCRS4 = [ +5.3371888965461637E-007 q_PCRS5 = [ +7.3379987833742897E-007
            +3.7444233778550031E-004 +5.2236196154513707E-004
            -1.4253684912431913E-003 -1.4047712280184723E-003
            +9.9999891405806784E-001 ]; +9.9999887687698918E-001 ];
q_PCRS8 = [ -5.2779261998836216E-007 q_PCRS9 = [ -7.1963421681856818E-007
            +3.8462959425181312E-004 +5.3239763239987400E-004
            +1.3722087221825403E-003 +1.3516841804518383E-003
            +9.9999898455099423E-001 ]; +9.9999894475050310E-001 ];
----- Initial Conditions for State ----- ----- Initial Square-Root Cov (diag) -----
p1(01) = a00 = +0.0000000000000000E+000 Sigma_initial(01,01) = 1.0000000000000000E+000
p1(02) = b00 = +0.0000000000000000E+000 Sigma_initial(02,02) = 1.0000000000000000E+000
p1(03) = c00 = +0.0000000000000000E+000 Sigma_initial(03,03) = 1.0000000000000000E+000
p1(04) = a10 = +0.0000000000000000E+000 Sigma_initial(04,04) = 9.9999000000000000E+004
p1(05) = b10 = +0.0000000000000000E+000 Sigma_initial(05,05) = 9.9999000000000000E+004
p1(06) = c10 = +0.0000000000000000E+000 Sigma_initial(06,06) = 9.9999000000000000E+004
p1(07) = d10 = +0.0000000000000000E+000 Sigma_initial(07,07) = 9.9999000000000000E+004
p1(08) = a20 = +0.0000000000000000E+000 Sigma_initial(08,08) = 9.9999000000000000E+004
p1(09) = b20 = +0.0000000000000000E+000 Sigma_initial(09,09) = 9.9999000000000000E+004
p1(10) = c20 = +0.0000000000000000E+000 Sigma_initial(10,10) = 9.9999000000000000E+004
p1(11) = d20 = +0.0000000000000000E+000 Sigma_initial(11,11) = 9.9999000000000000E+004
p1(12) = a01 = +0.0000000000000000E+000 Sigma_initial(12,12) = 9.9999000000000000E+004
p1(13) = b01 = +0.0000000000000000E+000 Sigma_initial(13,13) = 9.9999000000000000E+004
p1(14) = c01 = +0.0000000000000000E+000 Sigma_initial(14,14) = 9.9999000000000000E+004
p1(15) = d01 = +0.0000000000000000E+000 Sigma_initial(15,15) = 9.9999000000000000E+004
p1(16) = e01 = +0.0000000000000000E+000 Sigma_initial(16,16) = 9.9999000000000000E+004
p1(17) = f01 = +0.0000000000000000E+000 Sigma_initial(17,17) = 9.9999000000000000E+004
```

```

-----
p2f(01) = am1 = +0.000000000000000E+000 Sigma_initial(18,18) = 9.999900000000000E+004
p2f(02) = am2 = +0.000000000000000E+000
p2f(03) = am3 = +1.000000000000000E+000
p2f(04) = beta = +1.000000000000000E+000 Sigma_initial(19,19) = 9.999900000000000E+004
p2f(05) = qT1 = +1.7260206333841115E-002 Sigma_initial(20,20) = 1.000000000000001E-001
p2f(06) = qT2 = +1.6778598237061715E-003 Sigma_initial(21,21) = 1.000000000000000E-002
p2f(07) = aT3 = -3.1578291163250529E-004 Sigma_initial(22,22) = 1.000000000000000E-002
p2f(08) = qT4 = +9.9984957385842688E-001
p2f(09) = qR1 = +7.0887658512219787E-004 Sigma_initial(23,23) = 2.8771079560603423E-004
p2f(10) = qR2 = +1.2699844082817435E-003 Sigma_initial(24,24) = 1.8198835244140440E-005
p2f(11) = qR3 = -1.6144585970323533E-004 Sigma_initial(25,25) = 1.8222945902831599E-005
p2f(12) = qR4 = +9.9999892711639404E-001
p2f(13) = brx = +0.000000000000000E+000 Sigma_initial(26,26) = 7.3706089381596270E-005
p2f(14) = bry = +0.000000000000000E+000 Sigma_initial(27,27) = 7.3706089381596270E-005
p2f(15) = brz = +0.000000000000000E+000 Sigma_initial(28,28) = 7.3706089381596270E-005
p2f(16) = crx = +0.000000000000000E+000 Sigma_initial(29,29) = 5.4325876119278582E-009
p2f(17) = cry = +0.000000000000000E+000 Sigma_initial(30,30) = 5.4325876119278582E-009
p2f(18) = crz = +0.000000000000000E+000 Sigma_initial(31,31) = 5.4325876119278582E-009
p2f(19) = bgx = +0.000000000000000E+000 Sigma_initial(32,32) = 7.3706089381596270E-005
p2f(20) = bgy = +0.000000000000000E+000 Sigma_initial(33,33) = 7.3706089381596270E-005
p2f(21) = bgz = +0.000000000000000E+000 Sigma_initial(34,34) = 7.3706089381596270E-005
p2f(22) = cgx = +0.000000000000000E+000 Sigma_initial(35,35) = 5.4325876119278582E-009
p2f(23) = cgy = +0.000000000000000E+000 Sigma_initial(36,36) = 5.4325876119278582E-009
p2f(24) = cgz = +0.000000000000000E+000 Sigma_initial(37,37) = 5.4325876119278582E-009
-----
```

```

----- IPF KALMAN FILTER STARTED -----
Iteration#001: |dp|= +2.754113539665E-002 RMS(|Resl|)=+7.395451628495E-006
Iteration#002: |dp|= +8.730374325759E-005 RMS(|Resl|)=+4.806889737678E-007
Iteration#003: |dp|= +8.812971159070E-006 RMS(|Resl|)=+5.003147520481E-007
Iteration#004: |dp|= +1.585270196512E-007 RMS(|Resl|)=+5.023570542817E-007
Iteration#005: |dp|= +1.288034533817E-007 RMS(|Resl|)=+5.019968121211E-007
Iteration#006: |dp|= +8.162205643402E-009 RMS(|Resl|)=+5.019243888881E-007
Iteration#007: |dp|= +2.547996474799E-009 RMS(|Resl|)=+5.019292881750E-007
Iteration#008: |dp|= +3.066015977632E-010 RMS(|Resl|)=+5.019313523289E-007
Iteration#009: |dp|= +4.713437336667E-011 RMS(|Resl|)=+5.019313382563E-007
Iteration#010: |dp|= +1.003850049119E-011 RMS(|Resl|)=+5.019312860628E-007
Iteration#011: |dp|= +6.394707823805E-013 RMS(|Resl|)=+5.019312837383E-007
Iteration#012: |dp|= +6.284044030123E-013 RMS(|Resl|)=+5.019312849199E-007
Iteration#013: |dp|= +4.953899000943E-013 RMS(|Resl|)=+5.019312850395E-007
Iteration#014: |dp|= +1.786441032884E-013 RMS(|Resl|)=+5.019312850018E-007
Iteration#015: |dp|= +4.462722100034E-013 RMS(|Resl|)=+5.019312850041E-007
Iteration#016: |dp|= +4.881704056185E-013 RMS(|Resl|)=+5.019312849945E-007
Iteration#017: |dp|= +4.960615995364E-013 RMS(|Resl|)=+5.019312850018E-007
Iteration#018: |dp|= +6.394239175226E-013 RMS(|Resl|)=+5.019312850141E-007
Iteration#019: |dp|= +4.977535479903E-013 RMS(|Resl|)=+5.019312850136E-007
Iteration#020: |dp|= +3.668721286821E-013 RMS(|Resl|)=+5.019312850117E-007
Iteration#021: |dp|= +3.838021649491E-013 RMS(|Resl|)=+5.019312850072E-007
Iteration#022: |dp|= +7.127902207911E-013 RMS(|Resl|)=+5.019312849996E-007
Iteration#023: |dp|= +6.850978780225E-013 RMS(|Resl|)=+5.019312850051E-007
Iteration#024: |dp|= +5.112391860016E-013 RMS(|Resl|)=+5.019312850156E-007
Iteration#025: |dp|= +3.877489907912E-013 RMS(|Resl|)=+5.019312850026E-007
Iteration#026: |dp|= +2.405417240829E-013 RMS(|Resl|)=+5.019312850039E-007
Iteration#027: |dp|= +4.859967369567E-013 RMS(|Resl|)=+5.019312850111E-007
Iteration#028: |dp|= +8.497146105755E-013 RMS(|Resl|)=+5.019312850162E-007
Iteration#029: |dp|= +3.676179193738E-013 RMS(|Resl|)=+5.019312850067E-007
Iteration#030: |dp|= +6.695009247238E-013 RMS(|Resl|)=+5.019312850020E-007
IPF Kalman Filter Completed with Error |dp1| + |dp2| = +6.6950092472379039E-013
-----
```

```

----- IPF LEAST SQUARES FILTER STARTED -----
Iteration#001 COND#=+3.138100205089E+007, |dp|=+2.753893430129E-002
Iteration#002 COND#=+3.135580153264E+007, |dp|=+8.112843778891E-005
Iteration#003 COND#=+3.135596678149E+007, |dp|=+7.376759635897E-006
Iteration#004 COND#=+3.135597313000E+007, |dp|=+3.036219910126E-008
Iteration#005 COND#=+3.135597311550E+007, |dp|=+4.751071076473E-010
Iteration#006 COND#=+3.135597312502E+007, |dp|=+1.754889273101E-011
-----
```

```

Iteration#007 COND#=+3.135597312226E+007, |dp|=+5.462059812783E-013
Iteration#008 COND#=+3.135597311835E+007, |dp|=+1.844566331753E-013
Iteration#009 COND#=+3.135597312030E+007, |dp|=+4.058600911756E-013
Iteration#010 COND#=+3.135597312560E+007, |dp|=+4.450056577418E-013
Iteration#011 COND#=+3.135597310720E+007, |dp|=+4.191543138226E-013
Iteration#012 COND#=+3.135597311581E+007, |dp|=+5.686884607979E-013
Iteration#013 COND#=+3.135597311923E+007, |dp|=+2.105824581350E-013
Iteration#014 COND#=+3.135597311838E+007, |dp|=+6.085355746581E-013
Iteration#015 COND#=+3.135597312243E+007, |dp|=+5.311487826778E-013
Iteration#016 COND#=+3.135597312046E+007, |dp|=+3.603321251666E-013
Iteration#017 COND#=+3.135597310711E+007, |dp|=+5.674088863526E-013
Iteration#018 COND#=+3.135597312378E+007, |dp|=+8.610771331290E-013
Iteration#019 COND#=+3.135597312253E+007, |dp|=+9.712321053642E-013
Iteration#020 COND#=+3.135597311251E+007, |dp|=+5.958142772056E-013
Iteration#021 COND#=+3.135597311343E+007, |dp|=+4.484518465056E-013
Iteration#022 COND#=+3.135597311335E+007, |dp|=+4.578517252676E-013
Iteration#023 COND#=+3.135597312858E+007, |dp|=+4.292720267256E-013
Iteration#024 COND#=+3.135597310573E+007, |dp|=+2.690596399669E-013
Iteration#025 COND#=+3.135597310669E+007, |dp|=+6.087455521317E-013
Iteration#026 COND#=+3.135597311454E+007, |dp|=+5.510771086285E-013
Iteration#027 COND#=+3.135597312347E+007, |dp|=+3.866429540032E-013
Iteration#028 COND#=+3.135597311687E+007, |dp|=+5.456483376927E-013
Iteration#029 COND#=+3.135597312141E+007, |dp|=+3.241742260932E-013
Iteration#030 COND#=+3.135597311623E+007, |dp|=+2.090123419312E-013
IPF Least Squares Filter Completed with Error |dp1| + |dp2| = +2.0901234193123903E-013
-----
```

Total Execution Time: 565 seconds

4 COMMENTS

This IPF run is a post-IOC re-run of the IOC light data taken from run IF502019, but with a modified CS-file CS701019.m, which specifies that the Prime frame 019 is to be moved over from its previous definition by 1/2 pixel. This change puts the Prime frame exactly at the middle of a physical pixel, which was desired by the IRS team to improve light Peakup centroiding accuracy.

The IPF run was performed in the most recent IPF version IPF.V4.0.0. All IPF settings, data editing, and parameters were kept the same as the IF502019 run (see report ID502019.pdf for details). As a reminder, only constant plate scales were estimated, which did not change significantly from run IF502019.

We recommend updating frame 019 with the new quaternion listed in the IF file IF701019.dat. The recommended Brown angle change is on the order of 0.9 arcsec, which is consistent with the desired 1/2 pixel shift (the PU pixels are approximately 1.8 arcsec wide). As before, in our best judgement, the Fine survey is accurate to 0.09 arcsec which satisfies the fine survey requirement of 0.14 arcsecond by a good margin.

IPF TEAM CONTACT INFORMATION

IPF Team email	ipf@sirtfweb.jpl.nasa.gov	
David S. Bayard	X4-8208	David.S.Bayard@jpl.nasa.gov (TEAM LEADER)
Dhemetrio Boussalis	X4-3977	boussali@grover.jpl.nasa.gov
Paul Brugarolas	X4-9243	Paul.Brugarolas@jpl.nasa.gov
Bryan H. Kang	X4-0541	Bryan.H.Kang@jpl.nasa.gov
Edward.C.Wong	X4-3053	Edward.C.Wong@jpl.nasa.gov (TASK MANAGER)

ACKNOWLEDGEMENTS

This work was performed at the Jet Propulsion Laboratory, California Institute of Technology, under contract with the National Aeronautics and Space Administration.

References

- [1] D.S. Bayard, B.H. Kang, *SIRTF Instrument Pointing Frame Kalman Filter Algorithm*, JPL D-Document D-24809, September 30, 2003.
- [2] B.H. Kang, D.S. Bayard, *SIRTF Instrument Pointing Frame (IPF) Software Description Document and User's Guide*, JPL D-Document D-24808, September 30, 2003.
- [3] D.S. Bayard, B.H. Kang, *SIRTF Instrument Pointing Frame (IPF) Kalman Filter Unit Test Report*, JPL D-Document D-24810, September 30, 2003.
- [4] *Space Infrared Telescope Facility In-Orbit Checkout and Science Verification Mission Plan*, JPL D-Document D-22622, 674-FE-301 Version 1.4, February 8, 2002.
- [5] *Space Infrared Telescope Facility Observatory Description Document*, Lockheed Martin LMMS/P458569, 674-SEIT-300 Version 1.2, November 1, 2002.
- [6] *SIRTF Software Interface Specification for Science Centroid INPUT Files (CAFFILE, CS-FILE)*, JPL SOS-SIS-2002, November 18, 2002.
- [7] *SIRTF Software Interface Specification for Inferred Frames Offset INPUT Files (OFILE)*, JPL SOS-SIS-2003, November 18, 2002.
- [8] *SIRTF Software Interface Specification for PCRS Centroid INPUT Files (CBFILE)*, JPL SIS-FES-015, November 18, 2002.
- [9] *SIRTF Software Interface Specification for Attitude INPUT Files (AFILE, ASFILE)*, JPL SIS-FES-014, January 7, 2002.
- [10] *SIRTF Software Interface Specification for IPF Filter Output Files (IFFILE, LGFILE, TARFILE)*, JPL SOS-SIS-2005, November 18, 2002.
- [11] R.J. Brown, *Focal Surface to Object Space Field of View Conversion*. Systems Engineering Report SER No. S20447-OPT-051, Ball Aerospace & Technologies Corp., November 23, 1999.

JET PROPULSION LABORATORY

SIRTF IPF REPORT

JPL ID701022

April 26, 2004

**SIRTF INSTRUMENT POINTING FRAME
KALMAN FILTER EXECUTION SUMMARY**

IPF RUN NUMBER: 701022

REPORT TYPE: IOC EXECUTION (FINE)

PRIME FRAME: IRS_Blue_PeakUp_FOV_Center (22)

INFERRRED FRAMES:

IPF TEAM

Autonomy and Control Section (345)

Jet Propulsion Laboratory

California Institute of Technology

4800 Oak Grove Drive

Pasadena, CA 91109

Contents

1 IPF EXECUTION SUMMARY	5
2 IPF INPUT FILE HISTORY	9
3 IPF EXECUTION RESULTS	10
3.1 IPF EXECUTION OUTPUT PLOTS	10
3.2 IPF OUTPUT DATA (IF MINI FILE)	36
3.3 IPF EXECUTION LOG	38
4 COMMENTS	41

List of Figures

1.1 A-priori and a-posteriori IPF frames	5
1.2 A-priori and a-posteriori IPF frames (ZOOMED)	8
2.1 Scenario Plot	9
3.1 TPF coords of measurements and a-priori predicts	12
3.2 Oriented PixelCoords of measurements and a-priori predicts	12
3.3 Oriented (W,V) PixelCoords of A-Priori Prediction Error Quiver Plot	13
3.4 A-priori prediction error (Science Centroids)	13
3.5 Oriented PixelCoords of measurements and a-priori predicts (PCRS only)	14
3.6 Oriented PixelCoords of measurements and a-priori predicts (Zoomed, PCRS only)	14
3.7 Oriented (W,V) PixelCoords of A-Priori PCRS Prediction Error Quiver Plot	15
3.8 A-priori PCRS prediction error	15
3.9 IPF execution convergence, chart 1	16
3.10 IPF execution convergence, chart 2	16
3.11 Parameter uncertainty convergence	17
3.12 IPF parameter symbol table	17
3.13 KF parameter error sigma plots	18
3.14 LS parameter error sigma plot	18
3.15 KF and LS parameter error sigma plot	19
3.16 Oriented PixelCoords of meas. and a-posteriori predicts	20
3.17 Oriented PixelCoords of meas. and a-posteriori predicts (attitude corrected)	20

3.18	KF innovations with (o) and w/o (+) attitude corrections	21
3.19	Histograms of science a-posteriori residuals (or innovations)	21
3.20	A-Posteriori Science Centroid Prediction Error Quiver (Att. Cor.)	22
3.21	Normalized A-Posteriori Science Centroid Prediction Errors	22
3.22	KF innovations with (o) and w/o (+) attitude corrections (PCRS)	23
3.23	Histograms of PCRS a-posteriori residuals (or innovations)	23
3.24	A-posteriori PCRS Prediction Summary	24
3.25	A-posteriori PCRS Prediction (PCRS 1 Only)	25
3.26	A-posteriori PCRS Prediction (PCRS 2 Only)	25
3.27	A-Posteriori PCRS Prediction Errors Quiver (Att. Cor.)	26
3.28	Normalized A-Posteriori PCRS Prediction Errors	26
3.29	W-axis KF innovations and 1-sigma bound	27
3.30	V-axis KF innovations and 1-sigma bound	27
3.31	Array plot with (solid) and w/o (dashed) optical distortion corrections	28
3.32	Optical Distortion Plot: total (x5 magnification)	28
3.33	Optical Distortion Plot: constant plate scales (x5 magnification)	29
3.34	Optical Distortion Plot: linear plate scale (x5 magnification)	29
3.35	Optical Distortion Plot: gamma terms (x5 magnification)	30
3.36	Scan Mirror Chops	30
3.37	IPF Frame Reconstruction	31
3.38	Center Pixel Reconstruction	31
3.39	Estimated attitude corrections (Body frame)	32
3.40	Estimated attitude error sigma plot (Body frame)	32
3.41	Thermo-mechanical boresight drift (equiv. angle in (W,V) coords)	33
3.42	Thermo-mechanical boresight drift (equiv. angle in Body frame)	33
3.43	Gyro drift bias contribution (equiv. rate in (W,V) coords)	34
3.44	Gyro drift bias contribution (equiv. angle in (W,V) coords)	34
3.45	Gyro drift bias contribution (equiv. angle in Body frame)	35

List of Tables

1.1	IPF filter input files	6
1.2	IPF filter execution configuration	6

1.3	IPF filter execution mask vector assignment	6
1.4	IPF calibration error summary ([arcsec], 1-sigma, radial)	7
1.5	Science measurement prediction error summary (1-sigma)	7
1.6	IPF Brown angle summary	8
2.1	IPF input file editing status	9
3.1	Table of figures I (IPF run)	10
3.2	Table of figures II (IPF run)	11
3.3	PCRS measurement prediction error summary	24

1 IPF EXECUTION SUMMARY

This report summarizes the SIRTF Instrument Pointing Frame (IPF) Kalman Filter execution associated with run file: RN701022. In particular, this Focal Point Survey calibrates the instrument: IRS_Blue_PeakUp_FOV_Center (22), as part of the IOC Fine Survey. The main calibration results from the IPF filter execution have been documented in IF701022 typically stored in the mission archive DOM collection IPF_IF. This report only summarizes the main aspects of the run, and does not substitute for the full information contained in the IF file.

Section 1 summarizes the filter execution results. The filter configurations are tabulated in Table 1.2 and the mask vector assignments are tabulated in Table 1.3. A total of 27 state parameters are estimated in this run. The overall End-to-End pointing performances are tabulated in Table 1.4. The prediction residuals throughout the estimation processes are tabulated in Table 1.5. Section 3 summarizes resulting plots, a mini summary of the IF IPF output file, and the execution log. Section 4 captures the user comments that are specific to this particular run.

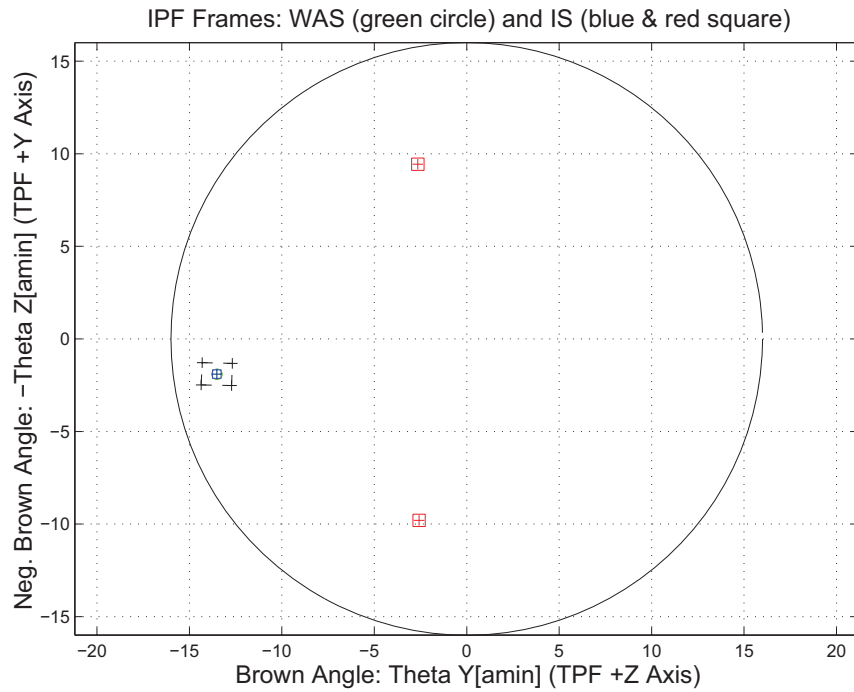


Figure 1.1: A-priori and a-posteriori IPF frames

RAW	FINAL (After Editing)
AA501022	AA501022
AS501022	AS501022
CA502022	CA502022
CB502022	CB502022
CS701022	CS701022

Table 1.1: IPF filter input files

EXECUTION CONFIGURATION ITEM	CURRENT STATUS
IPF Filter Version Used	IPF.V4.0.0
Frame Table Version Used	BodyFrames_FTU_17a
Scan-Mirror Employed?	NO
IPF Filter Mode	NORMAL-MODE(0)
SLIT-MODE Operation	DISABLED
Kalman Filter Operation	ENABLED
Least-Squares Data Analysis	ENABLED
IBAD Screening	ENABLED
User-Specified Data Editing	DISABLED
Total Number of Iterations	30
LS Residual Sigma Scale	8.70666314E-001
Total Number of Maneuvers	6

Table 1.2: IPF filter execution configuration

Con. Plate Scale			Γ Dependent				Γ^2 Dependent				Linear Plate Scale						Mirror			
a_{00}	b_{00}	c_{00}	a_{10}	b_{10}	c_{10}	d_{10}	a_{20}	b_{20}	c_{20}	d_{20}	a_{01}	b_{01}	c_{01}	d_{01}	e_{01}	f_{01}	α	β		
1	2	3	4	5	6	7	8	9	10	11	12	13	14	15	16	17	18	19		
1	1	1	0	0	0	0	0	0	0	0	1	1	1	1	1	1	0	0		
IPF (T)			Alignment R						Gyro Drift Bias											
θ_1	θ_2	θ_3	a_{rx}	a_{ry}	a_{rz}	b_{rx}	b_{ry}	b_{rz}	c_{rx}	c_{ry}	c_{rz}	b_{gx}	b_{gy}	b_{gz}	c_{gx}	c_{gy}	c_{gz}			
20	21	22	23	24	25	26	27	28	29	30	31	32	33	34	35	36	37			
1	1	1	1	1	1	1	1	1	1	1	1	1	1	1	1	1	1			

Table 1.3: IPF filter execution mask vector assignment

FOCAL PLANE SURVEY ANALYSIS: IOC Fine Survey.

INSTRUMENT NAME: IRS_Blue_PeakUp_FOV_Center NF: 22

PIX2RADW: 8.72660000E-008 [rad/pixel] = 1.8000E-002 [arcsec/pixel]

PIX2RADV: 8.72660000E-008 [rad/pixel] = 1.8000E-002 [arcsec/pixel]

FRAME	DESCRIPTION	IPF ¹	SF ²	TOTAL	REQ
022(P)	IRS_Blue_PeakUp_FOV_Center	0.0449	0.0855	0.0966	0.25

Table 1.4: IPF calibration error summary ([arcsec], 1-sigma, radial)

RMS METRIC	A PRIORI ³	A POSTERIORI ³	ATT. CORRECTED ⁴	UNITS
Radial	1.5993	0.0972	0.0682	arcsec
W-Axis	0.7167	0.0754	0.0455	arcsec
V-Axis	1.4297	0.0613	0.0509	arcsec
Radial	88.8505	5.3991	3.7911	pixels
W-Axis	39.8168	4.1907	2.5279	pixels
V-Axis	79.4294	3.4041	2.8253	pixels

Table 1.5: Science measurement prediction error summary (1-sigma)

¹IPF filter removes systematic pointing errors due to: thermomechanical alignment drift (Body to TPF), gyro bias and bias drift, centroiding error, attitude error, and optical distortion. IPF SIGMA presented here is “Scaled” by the Least Squares Scale factor. The Least Squares Scale Factor was: 0.870666. It is assumed that the gyro Angle Random Walk contribution is captured with the Least Squares scaling. The gyro ARW contribution can be approximately calculated as 0.0853 arcseconds, given that ARW = $100 \mu\text{deg}/\sqrt{\text{hr}}$, with 6.060556e+002 second Maneuver time (max), and 6 independent Maneuvres.

²Gyro Scale Factor(GSF) assumes 95 ppm error over 0.250 degree maneuver.

³This can be interpreted as estimate of ”pixel to sky” pointing reconstruction error if no science data is used.

⁴This can be interpreted as estimate of achieved S/I centroiding error

IPF BROWN ANGLE SUMMARY					
FRAME TABLE USED: BodyFrames_FTU_17a					
NF	NAME	WAS	IS	CHANGE	UNIT
022	theta_Y	-13.520824	-13.520255	+0.000570	arcmin
022	theta_Z	+1.912112	+1.896747	-0.015365	arcmin
022	angle	+1.696937	+1.704385	+0.007448	deg

Table 1.6: IPF Brown angle summary

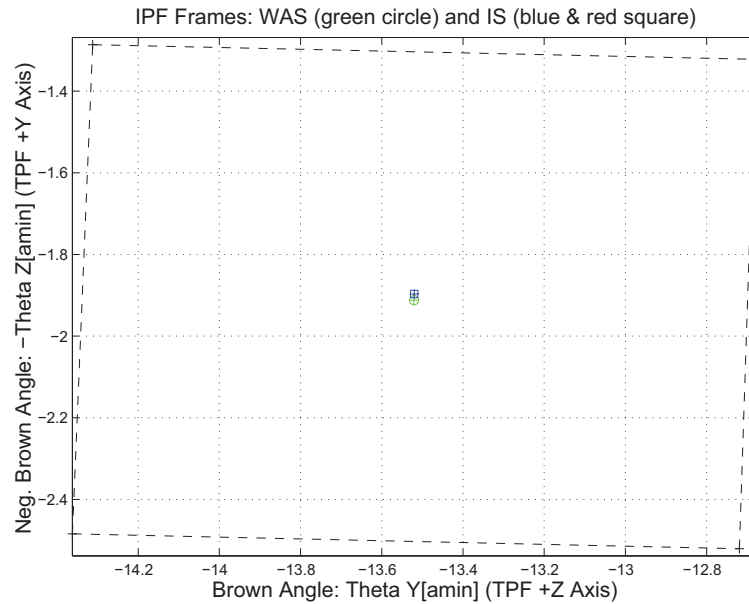


Figure 1.2: A-priori and a-posteriori IPF frames (ZOOMED)

2 IPF INPUT FILE HISTORY

WAS	SIZE	IS	SIZE	REMOVED	PATCHED
AA501022	UNCHANGED	AA501022	UNCHANGED	0	0
CA502022	UNCHANGED	CA502022	UNCHANGED	0	N/A
CB502022	UNCHANGED	CB502022	UNCHANGED	0	N/A

Table 2.1: IPF input file editing status

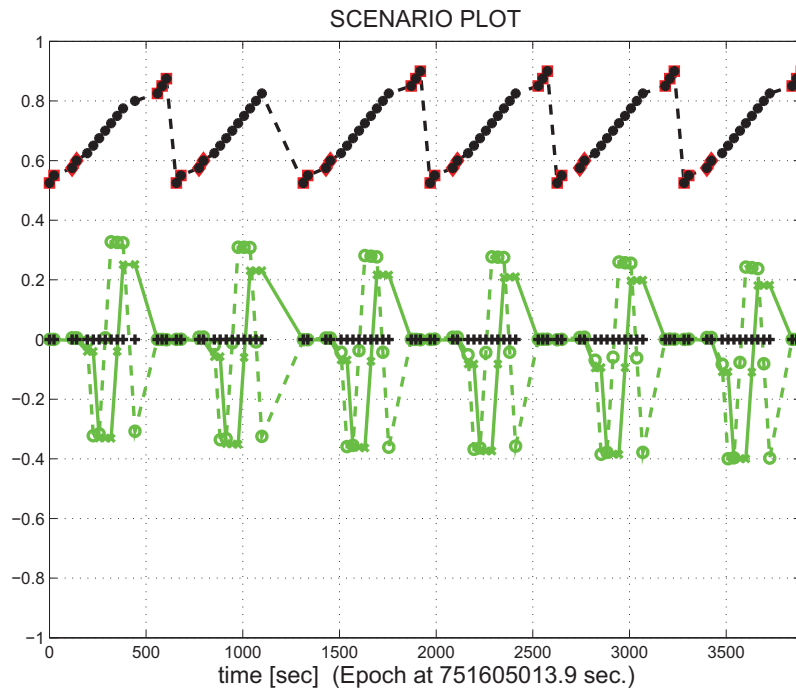


Figure 2.1: Scenario Plot

3 IPF EXECUTION RESULTS

3.1 IPF EXECUTION OUTPUT PLOTS

This subsection summarizes the IPF filter results. As shown in Table 3.1, the output plots are segmented to three groups: predicted performance, post-run results and IPF trending plots.

FIGURE NO.	DESCRIPTION
Predicted performance prior to IPF run	
Figure 3.1	Meas. and a-priori predicts in TPF coords
Figure 3.2	Meas. and a-priori predicts in Oriented Pixel Coords including rectangular array boundary approximation
Figure 3.3	A-Priori Prediction Error Quiver Plot in Oriented Pixel Coords including rectangular array boundary approximation
Figure 3.4	A-priori prediction error
Figure 3.5	Oriented Pixel Coords of measurements and a-priori predicts (PCRS only)
Figure 3.6	Oriented Pixel Coords of measurements and a-priori predicts (Zoomed, PCRS only)
Figure 3.7	Oriented (W,V) Pixel Coords of A-Priori PCRS Prediction Error Quiver Plot
Figure 3.8	A-priori PCRS prediction error
IPF filter performance (post run results)	
Figure 3.9	IPF execution convergence, chart 1: (top) normalized residual error vs. iteration number and (bottom) norm of effective parameter corrections
Figure 3.10	IPF execution convergence, chart 2: parameter correction size vs. iteration number
Figure 3.11	Parameter uncertainty convergence: square-root of diagonal elements of covariance matrix vs. maneuver number
Figure 3.12	IPF parameter symbol table
Figure 3.13	KF parameter error sigma plot (a-priori-dashed, a-posteriori-solid). Includes true parameter errors (FLUTE runs only)
Figure 3.14	LS parameter error sigma plot. Includes true parameter errors (FLUTE runs only)
Figure 3.15	KF and LS parameter errors sigma plot (Figure 3.13 & Figure 3.14 combined)
Figure 3.16	Measurements and a-posteriori predicts in Oriented Pixel Coords including rectangular array boundaries (a-priori-dashed, a-posteriori-solid)
Figure 3.17	Attitude corrected meas. and a-posteriori predicts in Oriented Pixel Coords including rectangular array boundaries (a-priori-dashed, a-posteriori-solid)

Table 3.1: Table of figures I (IPF run)

FIGURE NO.	DESCRIPTION
IPF filter performance (post run results) - CONTINUE	
Figure 3.18	KF innovations with (o) and w/o (+) attitude corrections
Figure 3.19	Histograms of science a-posteriori residuals (or innovations)
Figure 3.20	A-Posteriori Science Centroid Prediction Error Quiver (Att. Cor.)
Figure 3.21	Normalized A-Posteriori Science Centroid Prediction Errors
Figure 3.22	KF innovations with (o) and w/o (+) attitude corrections (PCRS)
Figure 3.23	Histograms of PCRS a-posteriori residuals (or innovations)
Figure 3.24	A-posteriori PCRS Prediction Summary
Figure 3.25	A-posteriori PCRS Prediction (PCRS 1 Only)
Figure 3.26	A-posteriori PCRS Prediction (PCRS 2 Only)
Figure 3.27	A-Posteriori PCRS Prediction Errors Quiver (Att. Cor.)
Figure 3.28	Normalized A-Posteriori PCRS Prediction Errors
Figure 3.29	W-axis KF innovations and 1-sigma bound
Figure 3.30	V-axis KF innovations and 1-sigma bound
Figure 3.31	Array plot with (solid) and w/o (dashed) optical distortion corrections
Figure 3.32	Optical Distortion Plot: total (x5 magnification)
Figure 3.33	Optical Distortion Plot: constant plate scales (x5 magnification)
Figure 3.34	Optical Distortion Plot: linear plate scale (x5 magnification)
Figure 3.35	Optical Distortion Plot: gamma terms (x5 magnification)
Figure 3.36	Scan Mirror Chops
Figure 3.37	IPF Frame Reconstruction
Figure 3.38	Center Pixel Reconstruction
IPF parameter trending plots	
Figure 3.39	Estimated attitude corrections (Body frame)
Figure 3.40	Estimated attitude error sigma plot (Body frame)
Figure 3.41	Systematic error attributed to thermo-mechanical boresight drift (equiv. angle in (W,V) coords)
Figure 3.42	Systematic error attributed to thermo-mechanical boresight drift (equiv. angle in Body frame)
Figure 3.43	Systematic error attributed to gyro drift bias (equiv. rate in (W,V) coords)
Figure 3.44	Systematic error attributed to gyro drift bias (equiv. angle in (W,V) coords)
Figure 3.45	Systematic error attributed to gyro drift bias (equiv. angle in Body frame)

Table 3.2: Table of figures II (IPF run)

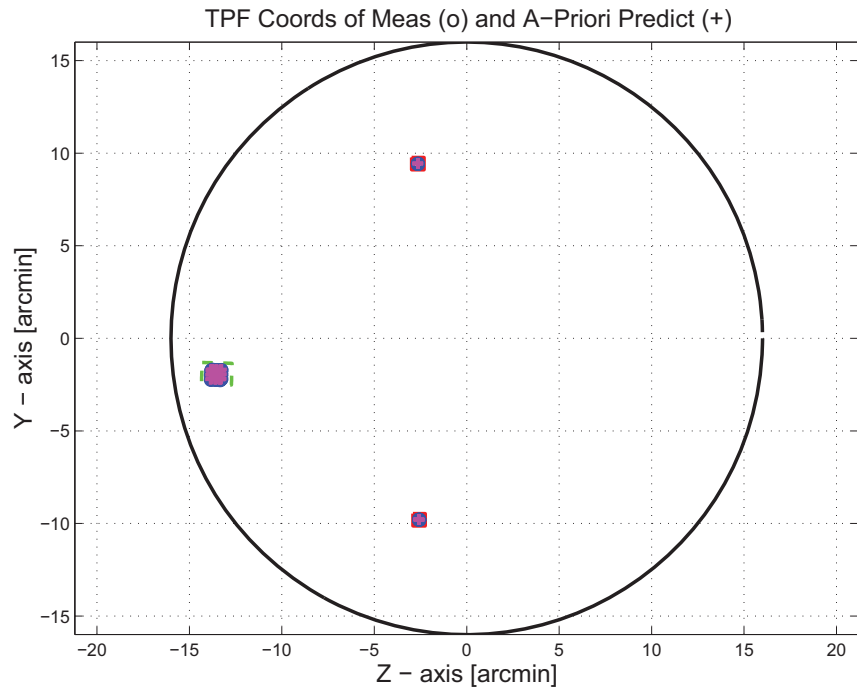


Figure 3.1: TPF coords of measurements and a-priori predicts

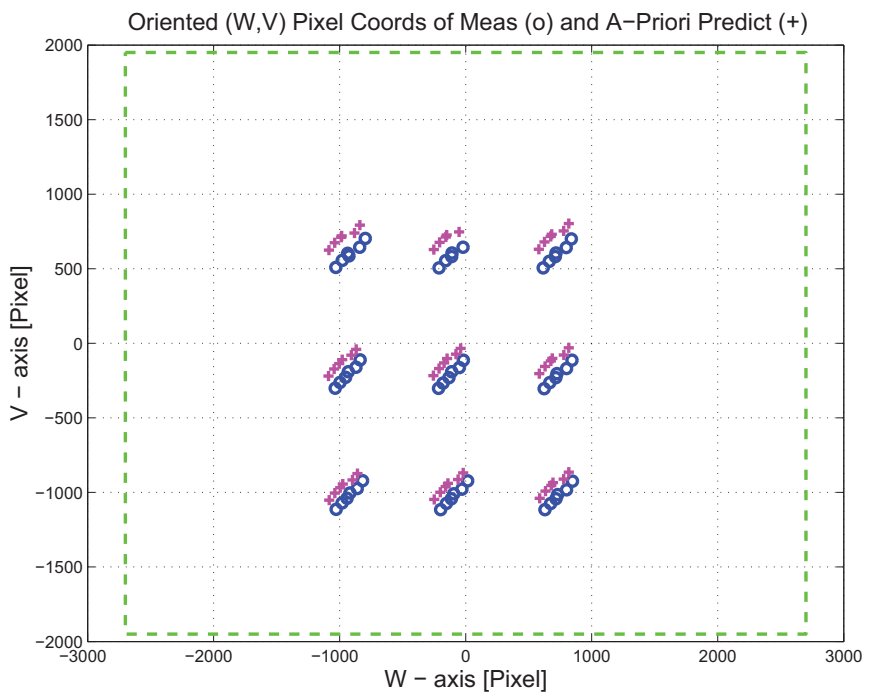


Figure 3.2: Oriented PixelCoords of measurements and a-priori predicts

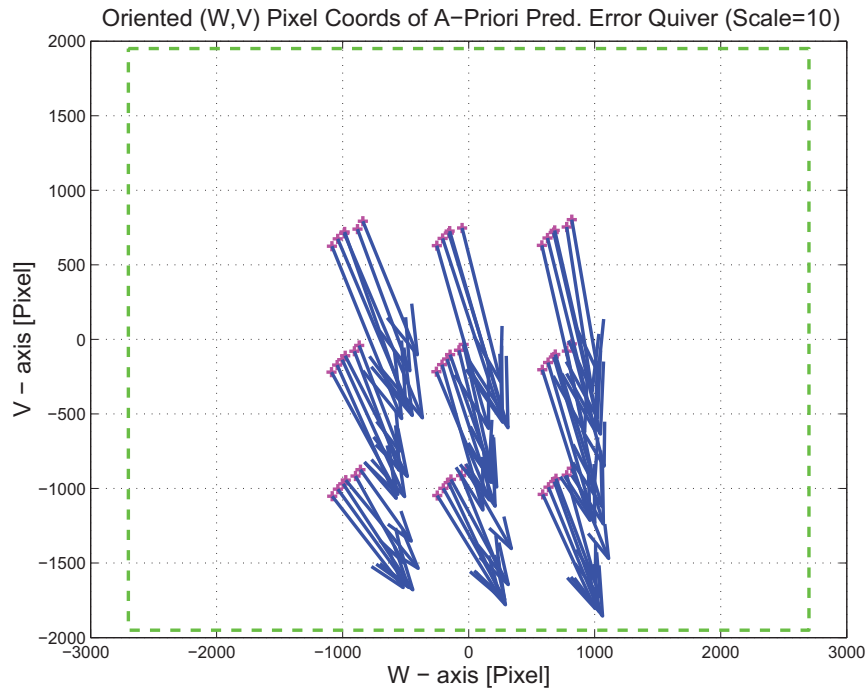


Figure 3.3: Oriented (W,V) Pixel Coords of A-Priori Prediction Error Quiver Plot

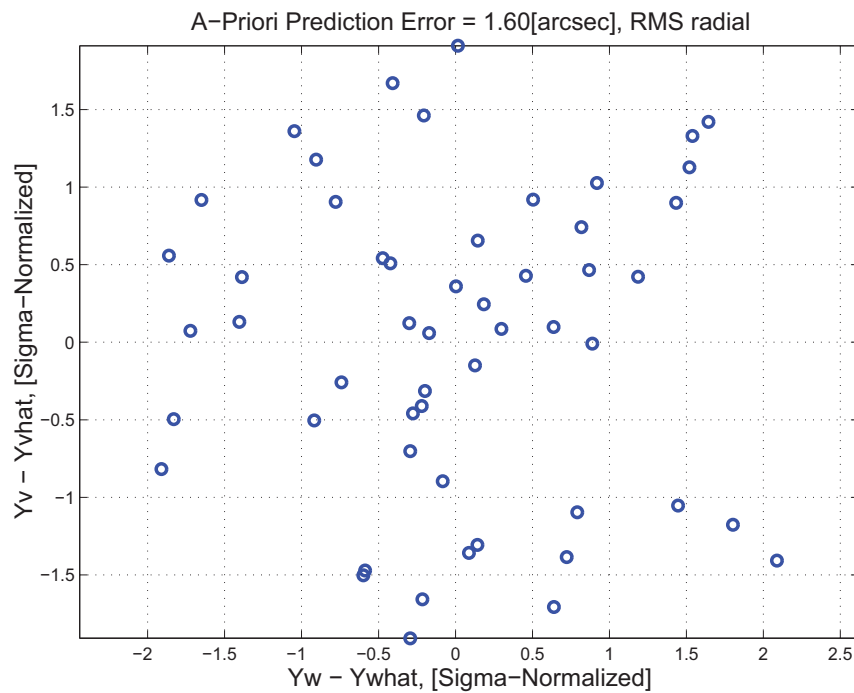


Figure 3.4: A-priori prediction error (Science Centroids)

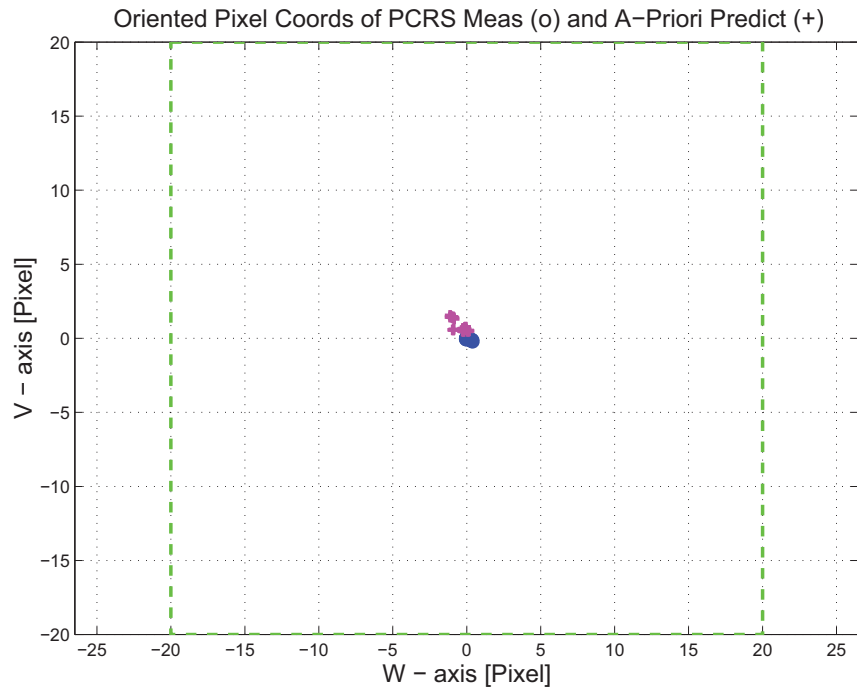


Figure 3.5: Oriented Pixel Coords of measurements and a-priori predicts (PCRS only)

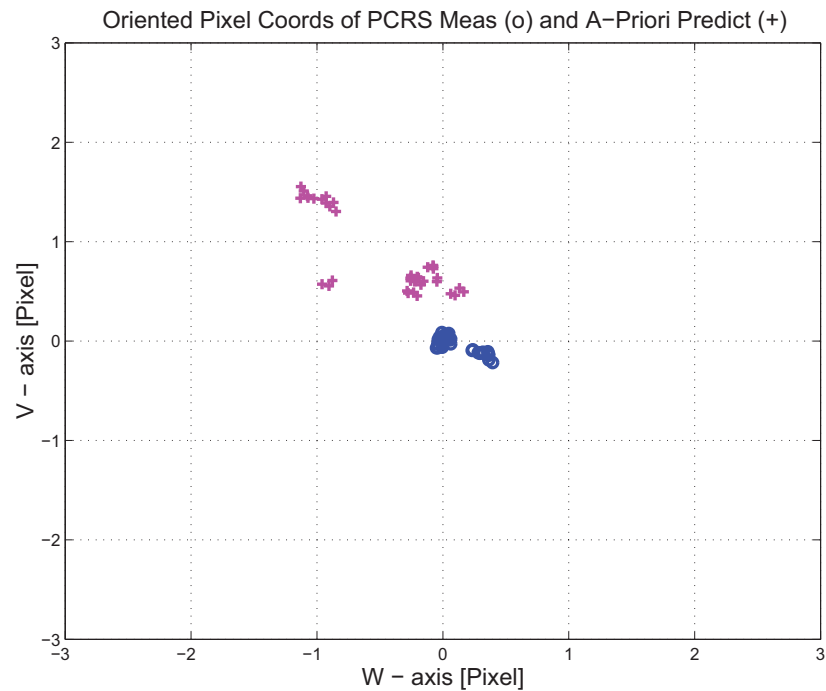


Figure 3.6: Oriented Pixel Coords of measurements and a-priori predicts (Zoomed, PCRS only)

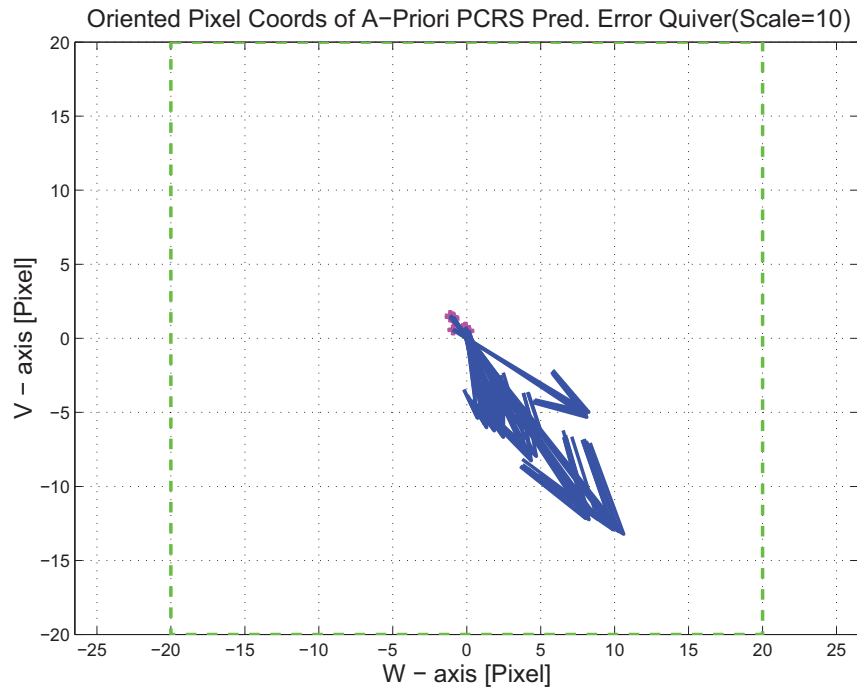


Figure 3.7: Oriented (W,V) Pixel Coords of A-Priori PCRS Prediction Error Quiver Plot

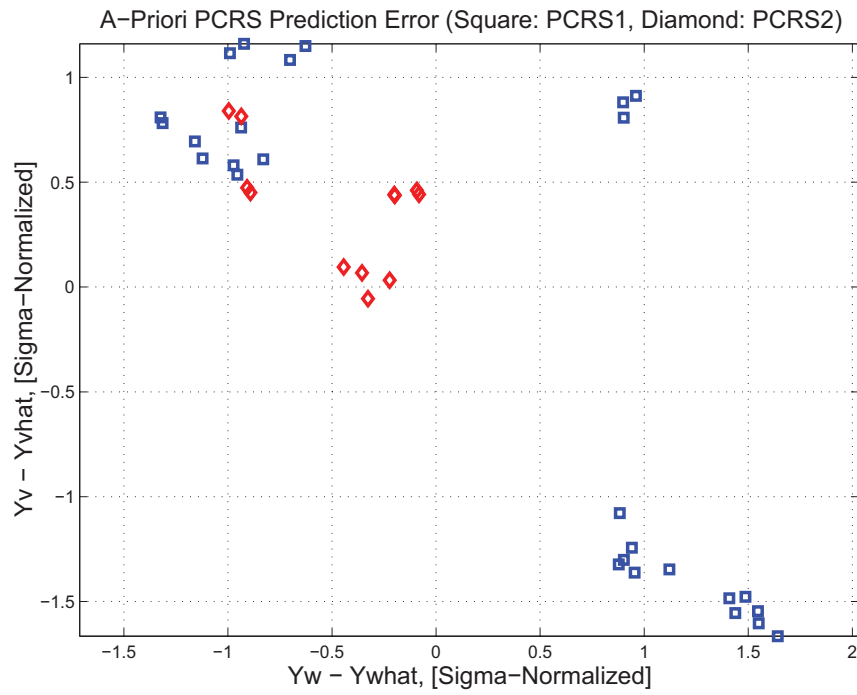


Figure 3.8: A-priori PCRS prediction error

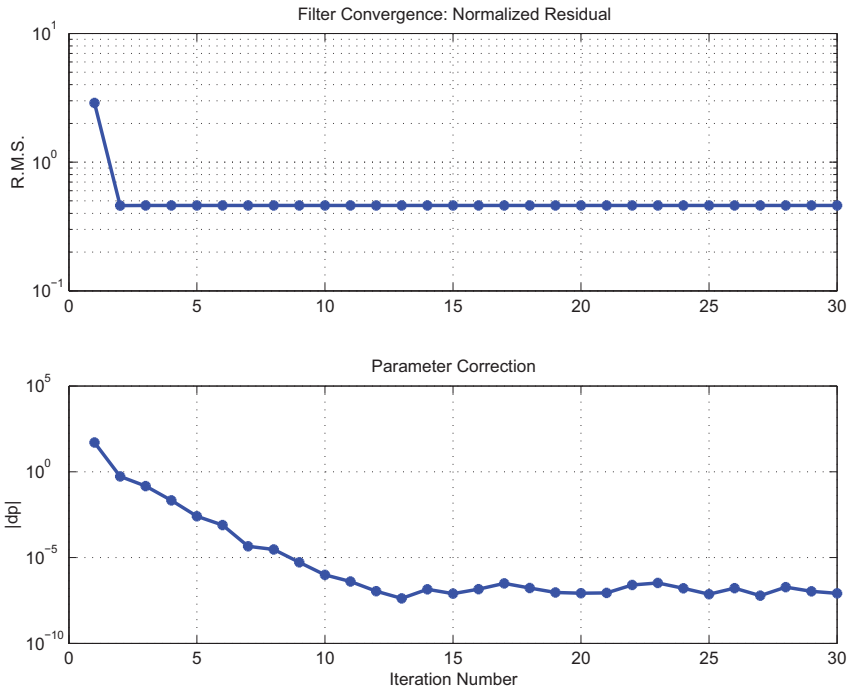


Figure 3.9: IPF execution convergence, chart 1

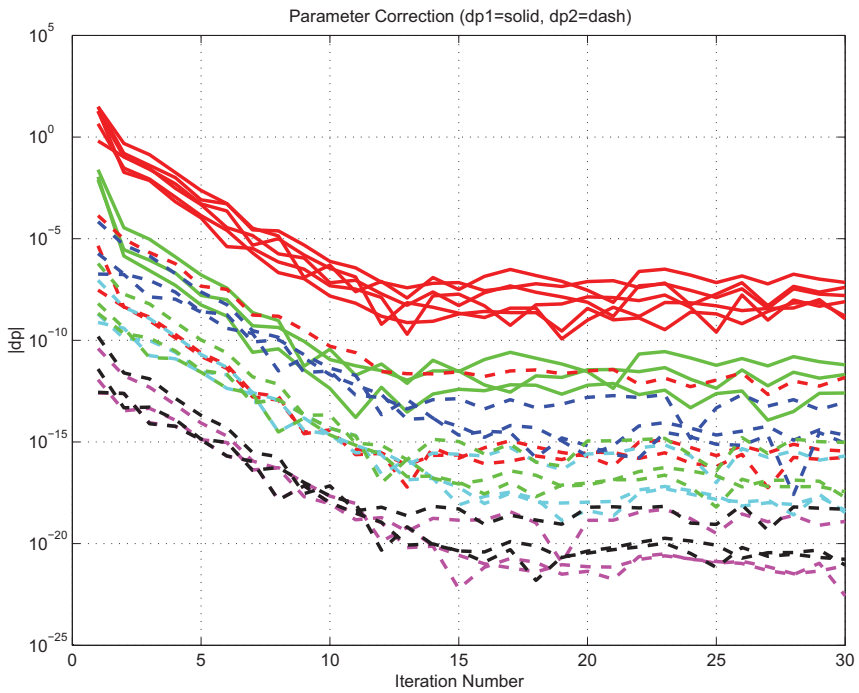


Figure 3.10: IPF execution convergence, chart 2

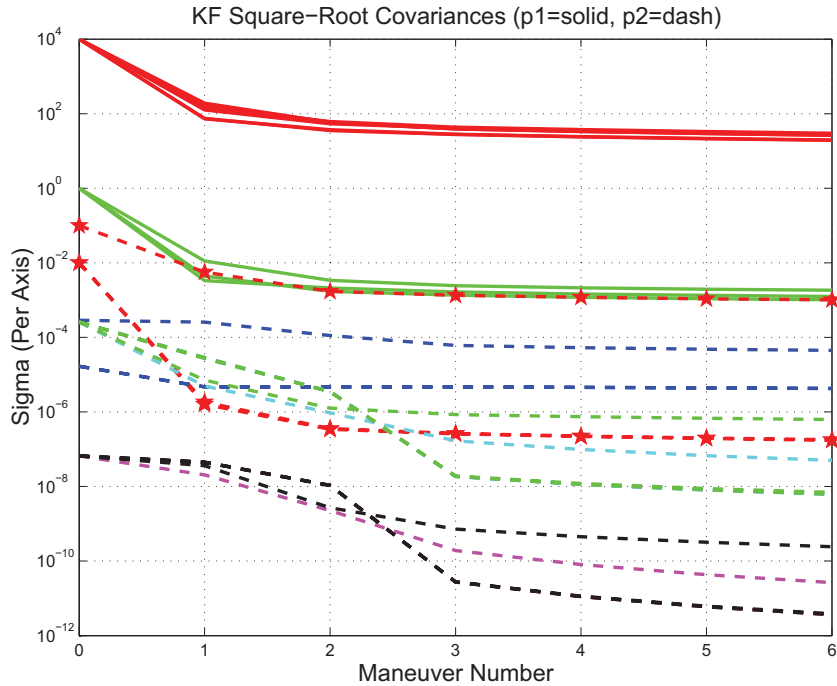


Figure 3.11: Parameter uncertainty convergence

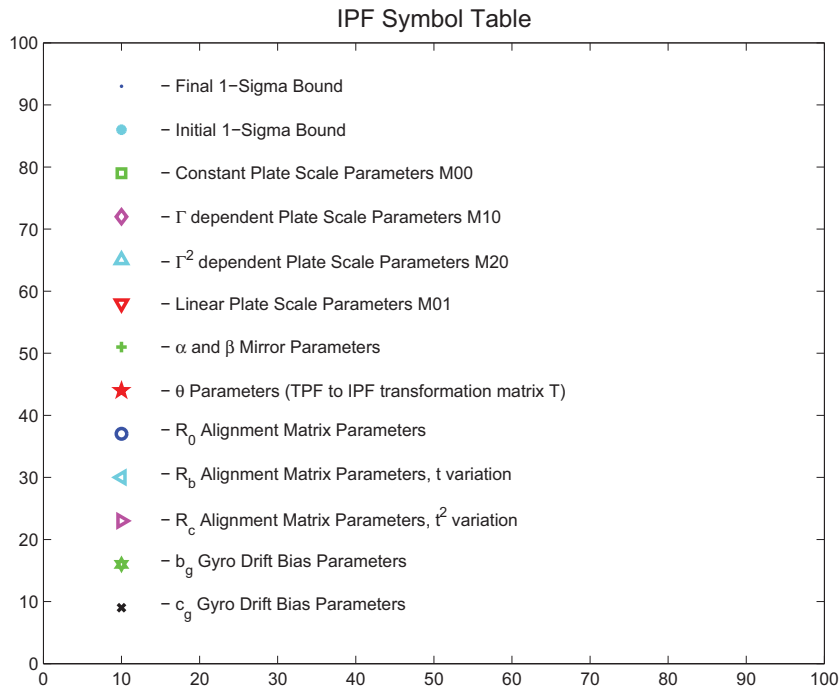


Figure 3.12: IPF parameter symbol table

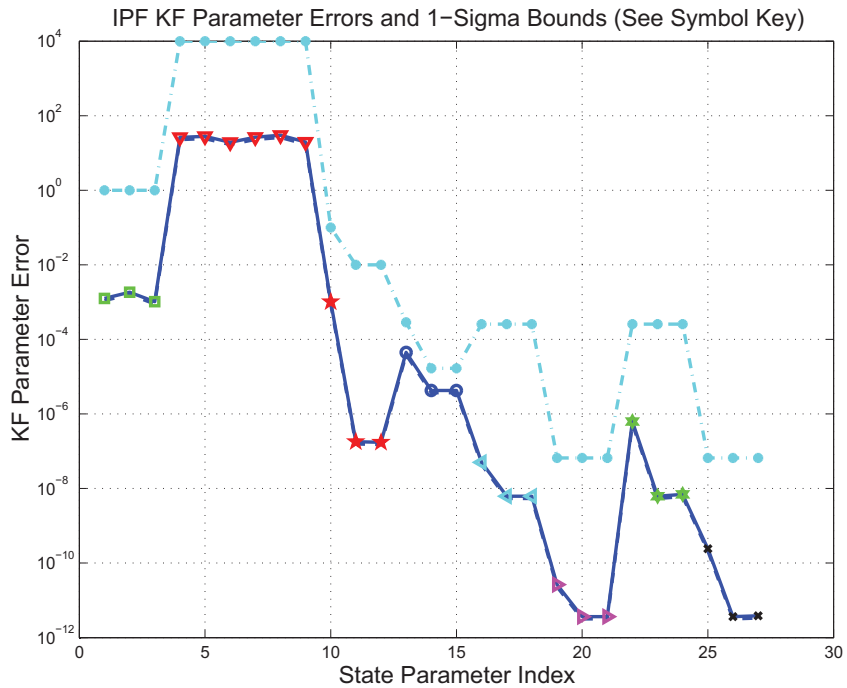


Figure 3.13: KF parameter error sigma plots

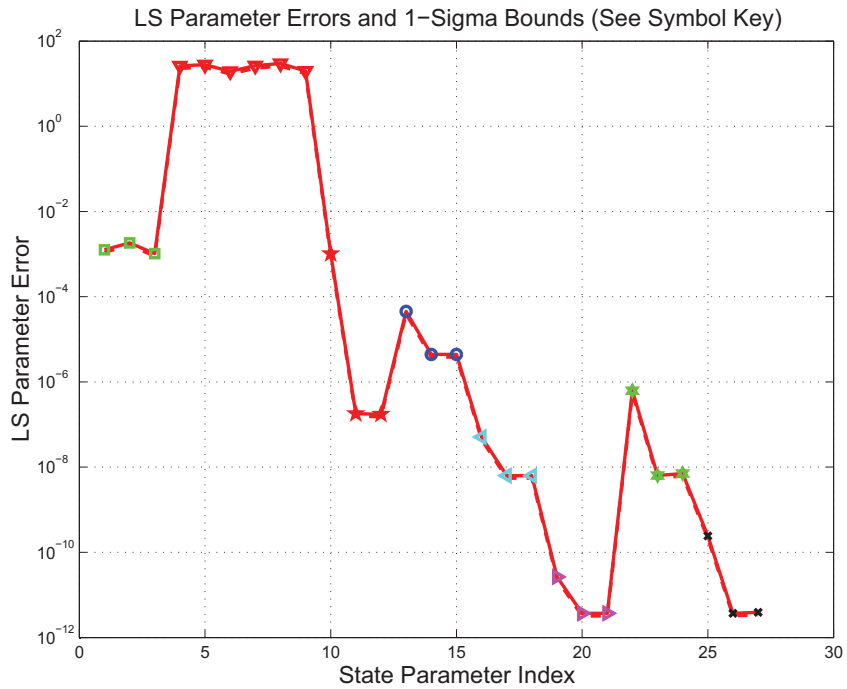


Figure 3.14: LS parameter error sigma plot

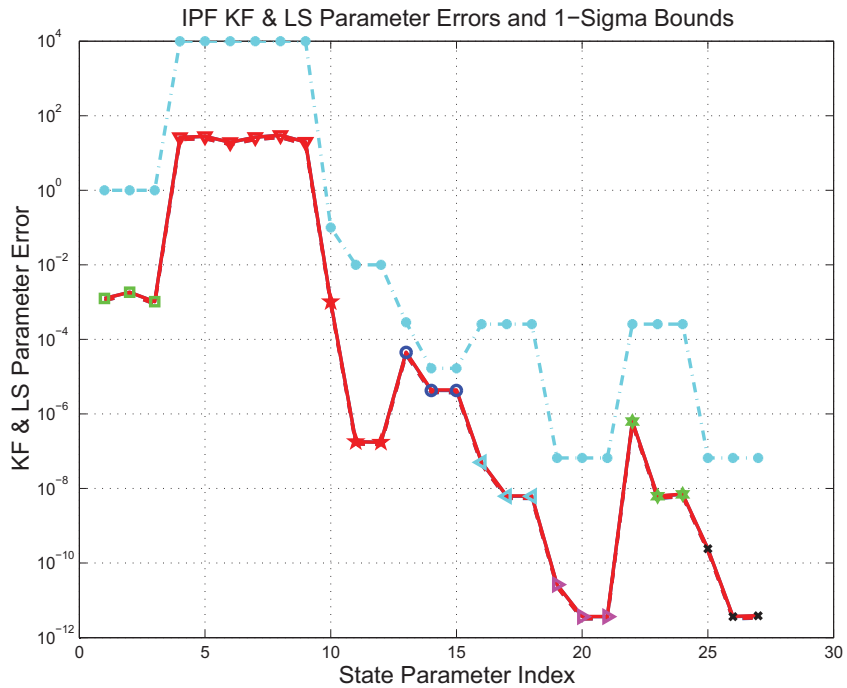


Figure 3.15: KF and LS parameter error sigma plot

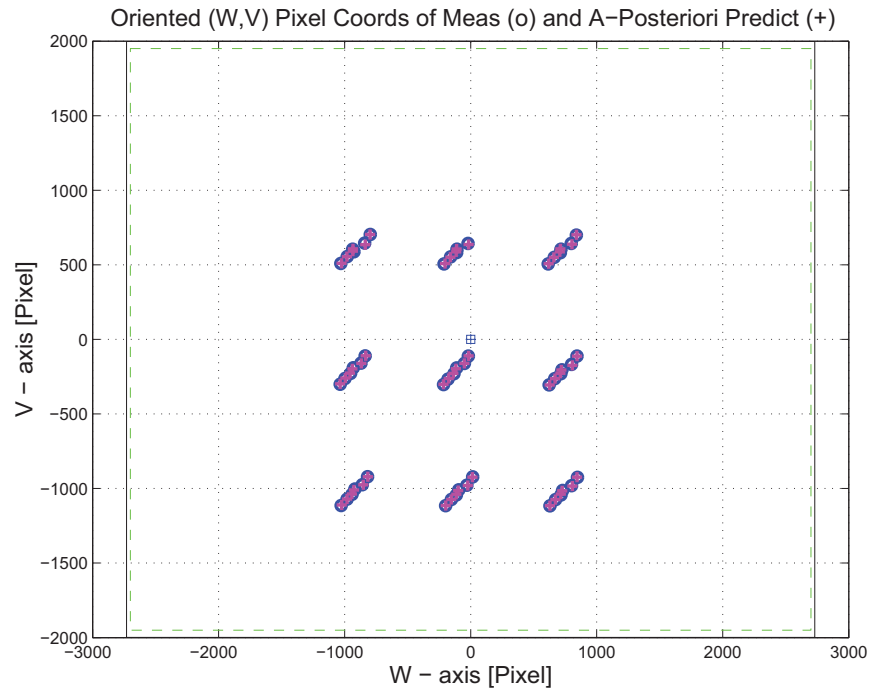


Figure 3.16: Oriented Pixel Coords of meas. and a-posteriori predicts

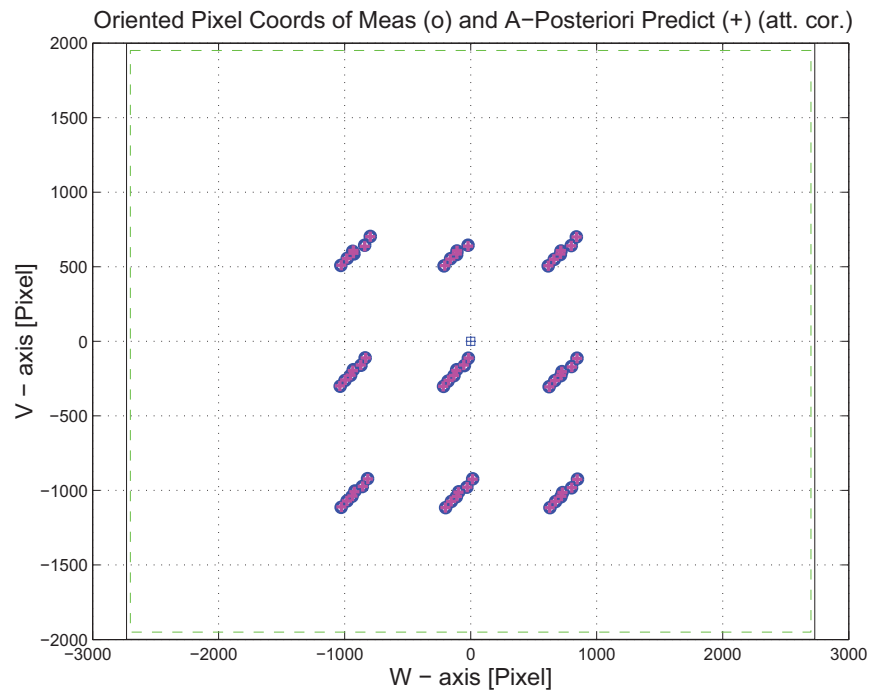


Figure 3.17: Oriented Pixel Coords of meas. and a-posteriori predicts (attitude corrected)

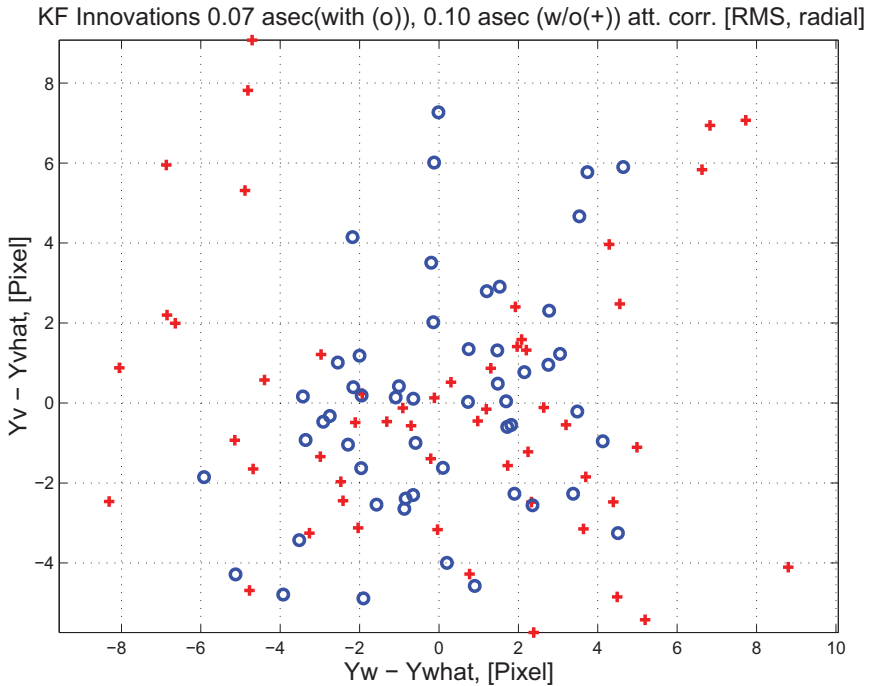


Figure 3.18: KF innovations with (o) and w/o (+) attitude corrections

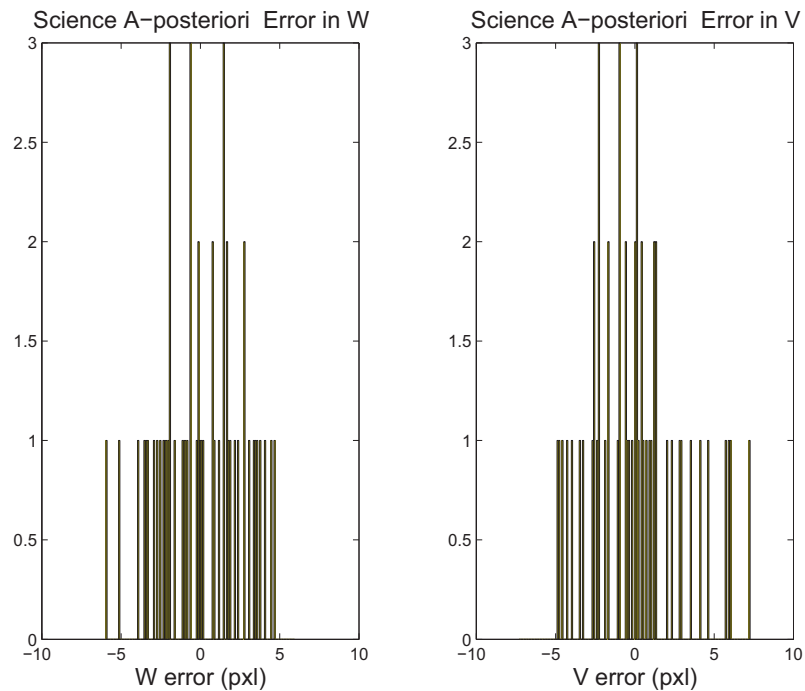


Figure 3.19: Histograms of science a-posteriori residuals (or innovations)

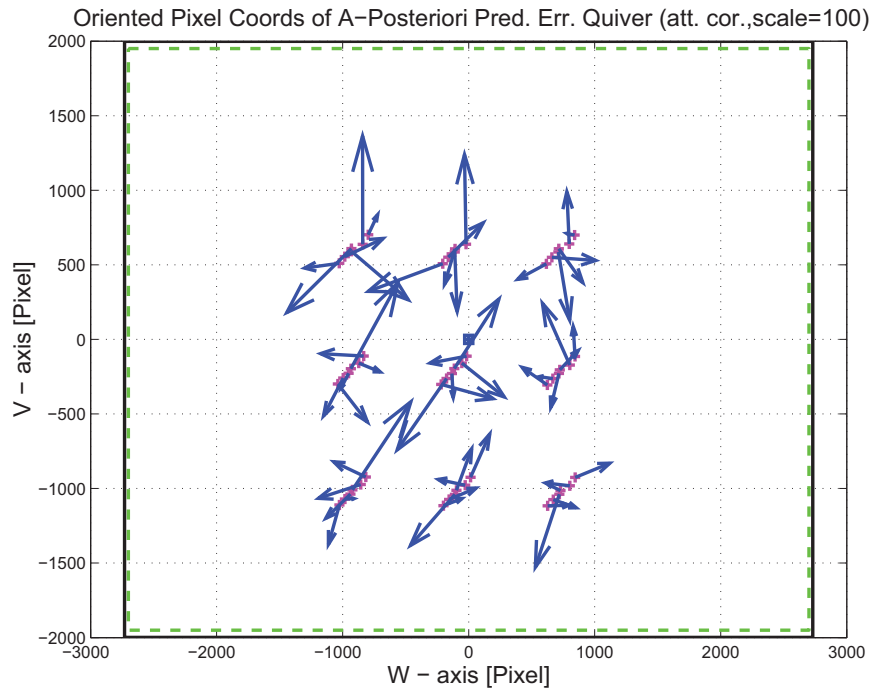


Figure 3.20: A-Posteriori Science Centroid Prediction Error Quiver (Att. Cor.)

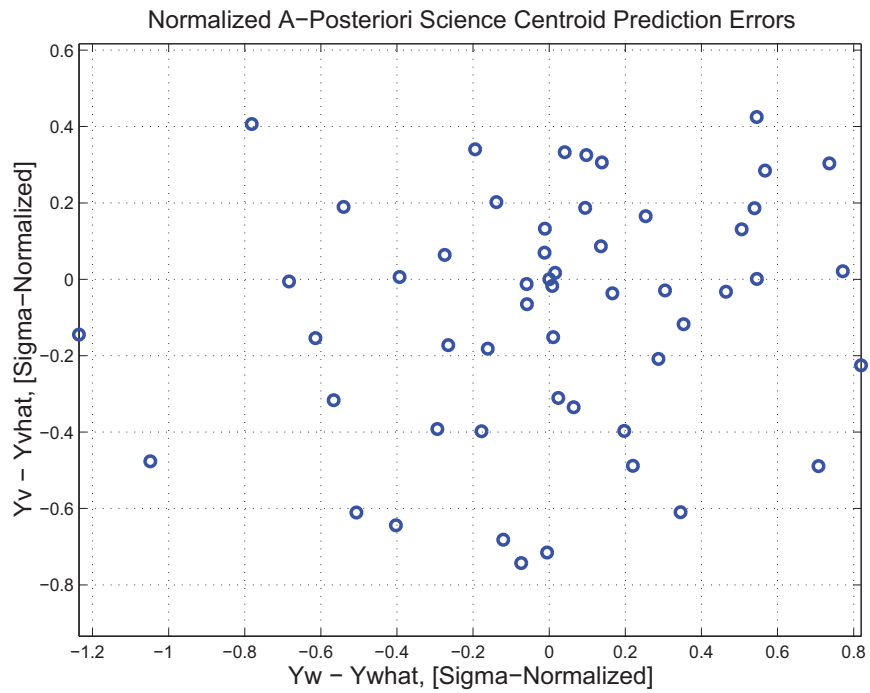


Figure 3.21: Normalized A-Posteriori Science Centroid Prediction Errors

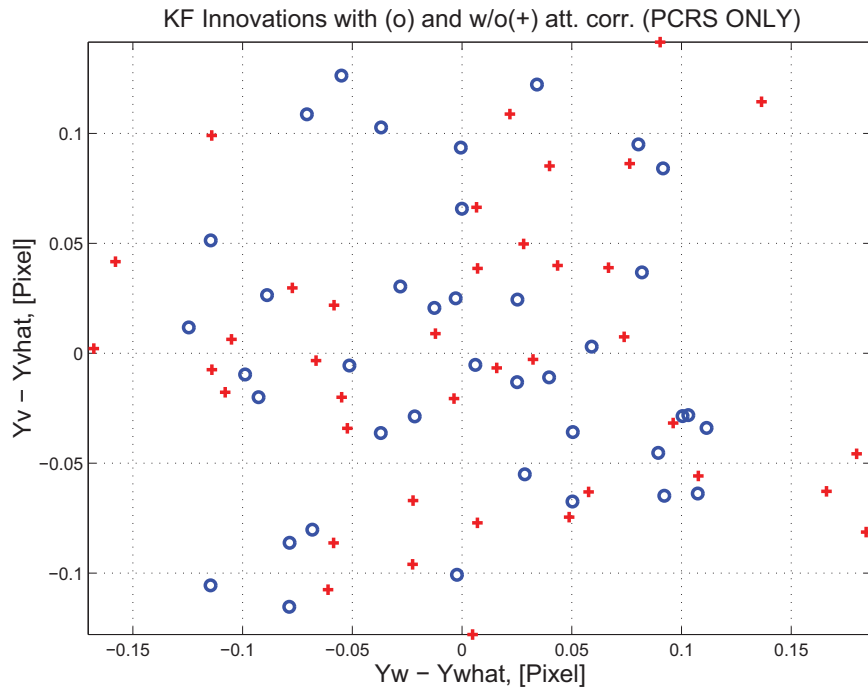


Figure 3.22: KF innovations with (o) and w/o (+) attitude corrections (PCRS)

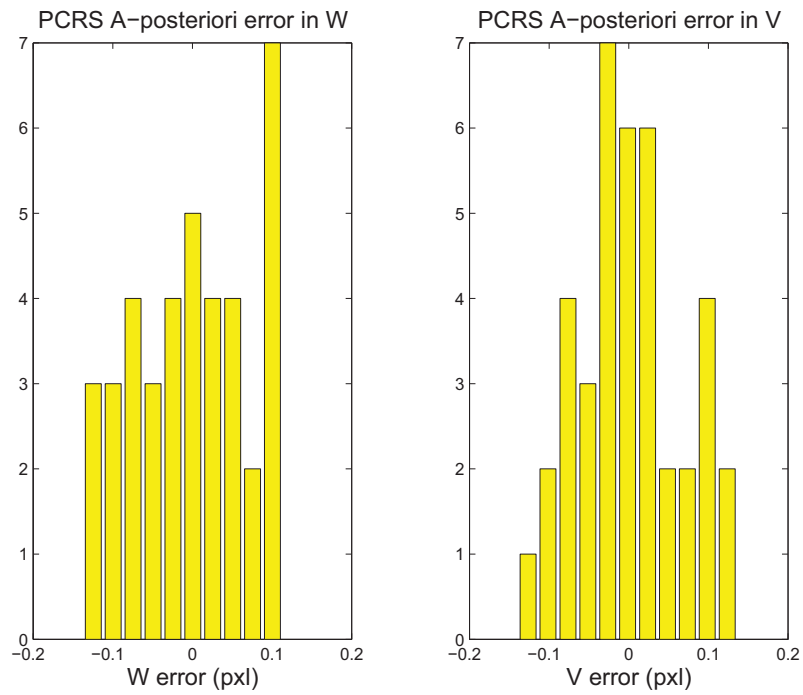


Figure 3.23: Histograms of PCRS a-posteriori residuals (or innovations)

IPF PCRS SUMMARY						
PCRS 1 (Total of 27 centroids)						
RMS	MEAN		SIGMA			
METRIC	APOST.	ATT. COR.	APOST.	ATT. COR.	STAT. CONF.	UNITS
Radial	0.0087	0.0038	0.1116	0.1004	0.0193	arcsec
W-axis	0.0087	-0.0002	0.0937	0.0771	0.0148	arcsec
V-axis	0.0003	0.0038	0.0606	0.0643	0.0124	arcsec
PCRS 2 (Total of 12 centroids)						
METRIC	APOST.	ATT. COR.	APOST.	ATT. COR.	STAT. CONF.	UNITS
Radial	0.0091	0.0095	0.1031	0.0846	0.0244	arcsec
W-axis	-0.0001	0.0002	0.0706	0.0544	0.0157	arcsec
V-axis	-0.0091	-0.0095	0.0752	0.0648	0.0187	arcsec
Combined (Total of 39 centroids)						
METRIC	APOST.	ATT. COR.	APOST.	ATT. COR.	STAT. CONF.	UNITS
Radial	0.0066	0.0003	0.1092	0.0960	0.0154	arcsec
W-axis	0.0060	-0.0001	0.0873	0.0709	0.0114	arcsec
V-axis	-0.0026	-0.0003	0.0656	0.0647	0.0104	arcsec

Table 3.3: PCRS measurement prediction error summary

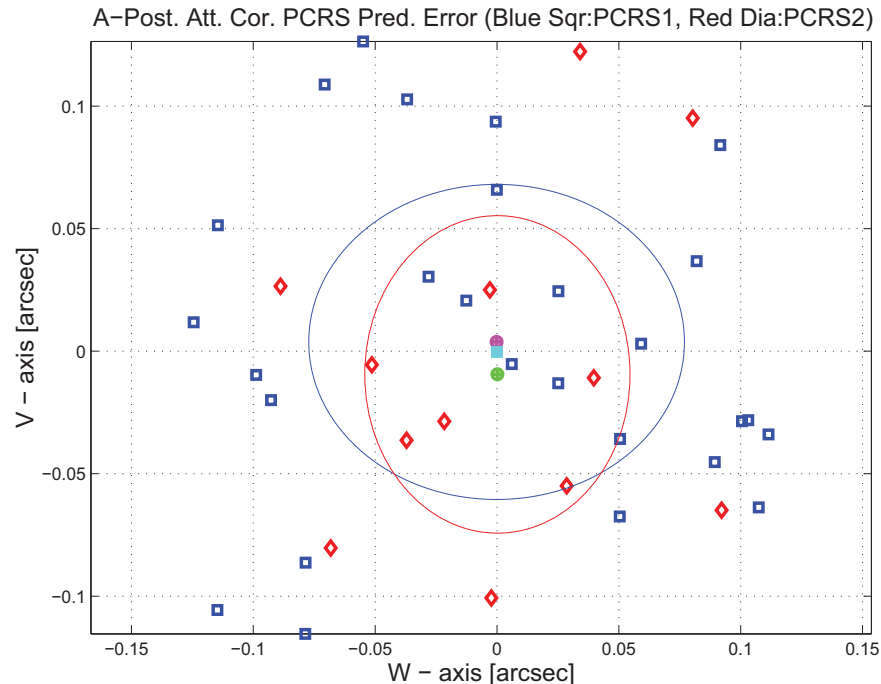


Figure 3.24: A-posteriori PCRS Prediction Summary

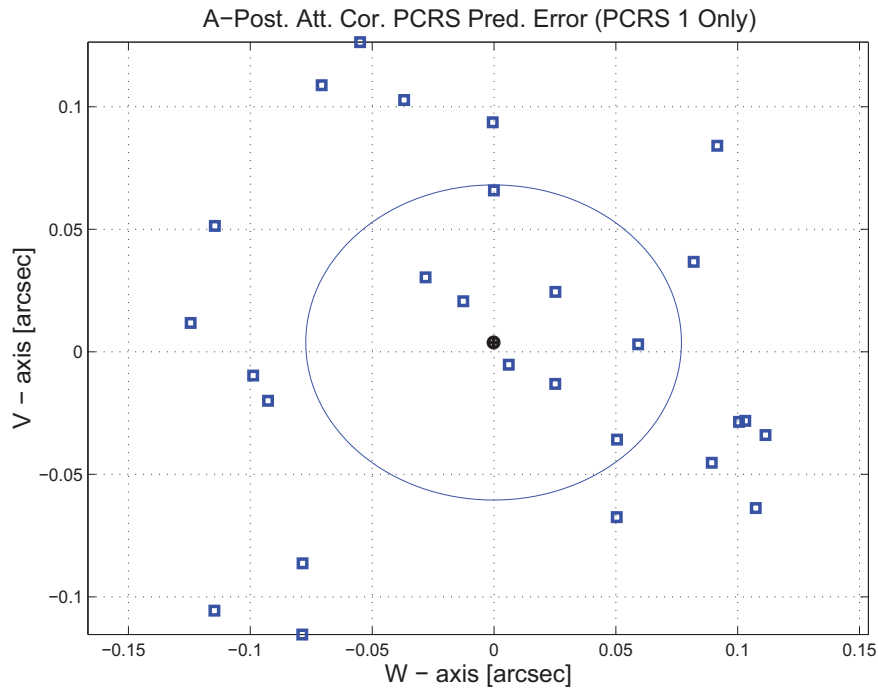


Figure 3.25: A-posteriori PCRS Prediction (PCRS 1 Only)

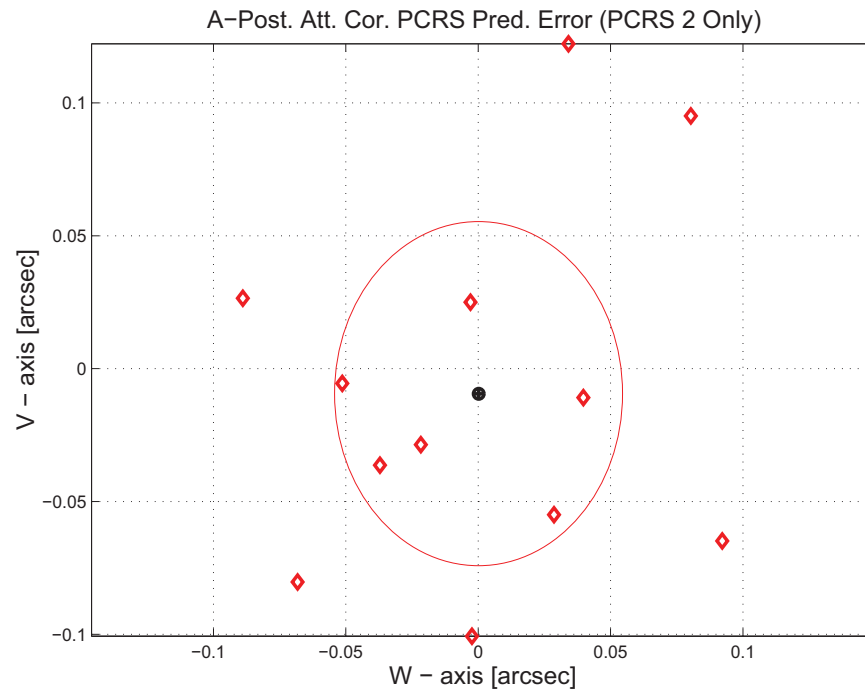


Figure 3.26: A-posteriori PCRS Prediction (PCRS 2 Only)

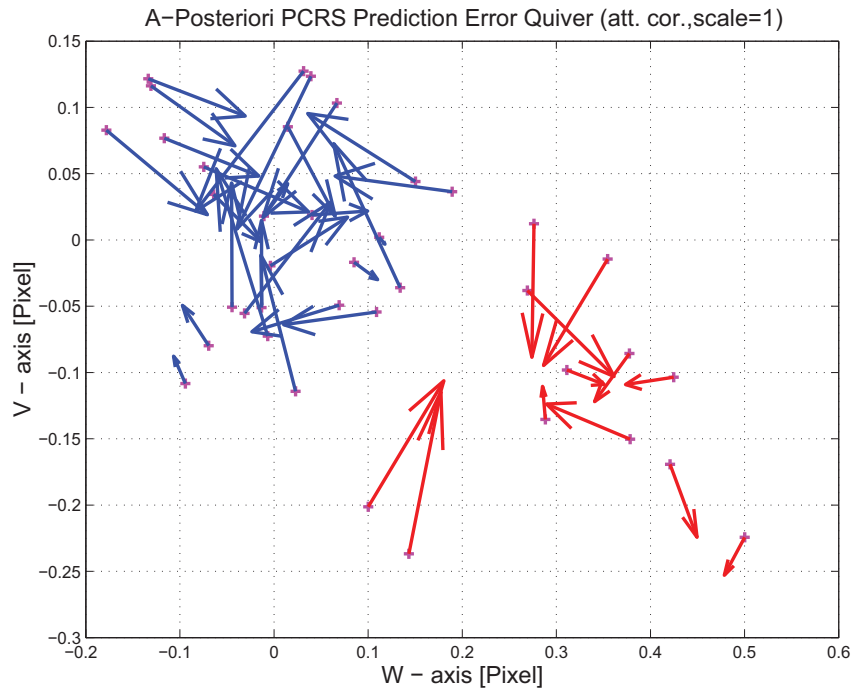


Figure 3.27: A-Posteriori PCRS Prediction Errors Quiver (Att. Cor.)

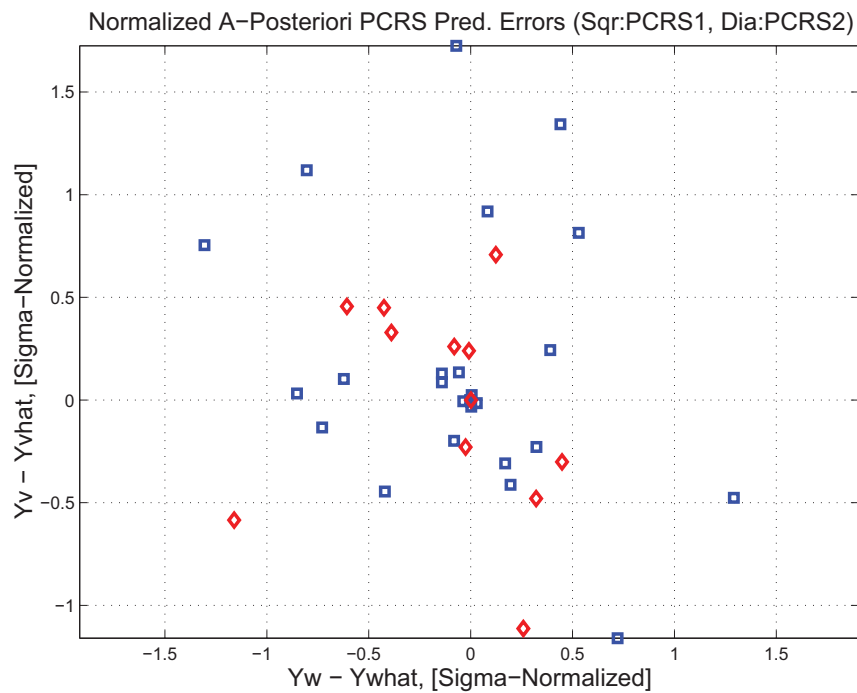


Figure 3.28: Normalized A-Posteriori PCRS Prediction Errors

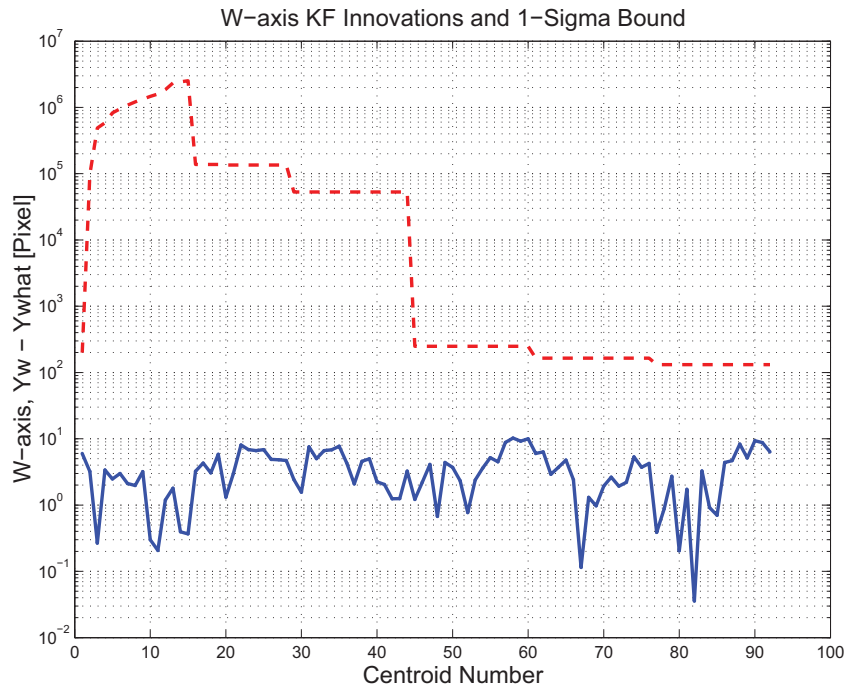


Figure 3.29: W-axis KF innovations and 1-sigma bound

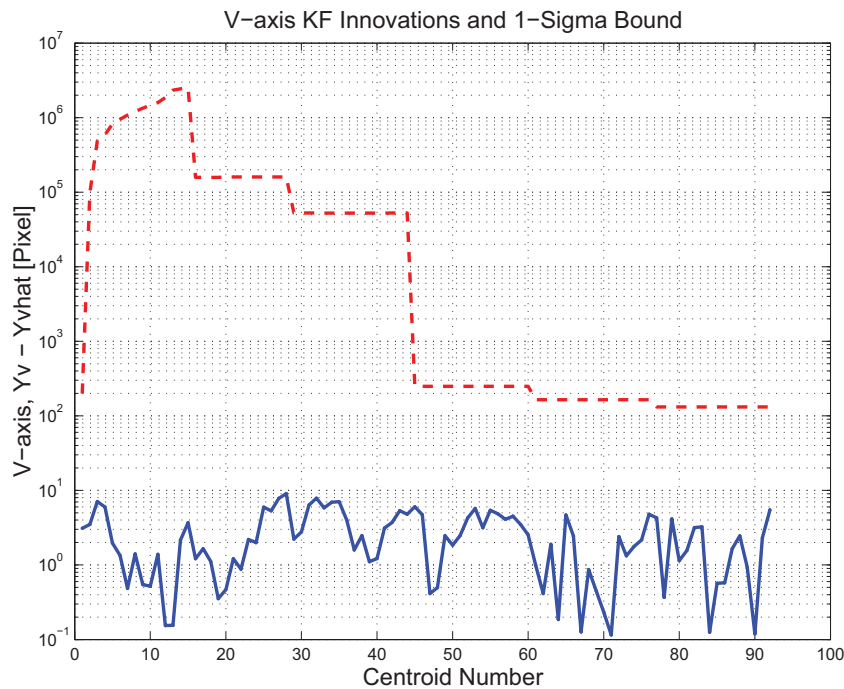


Figure 3.30: V-axis KF innovations and 1-sigma bound

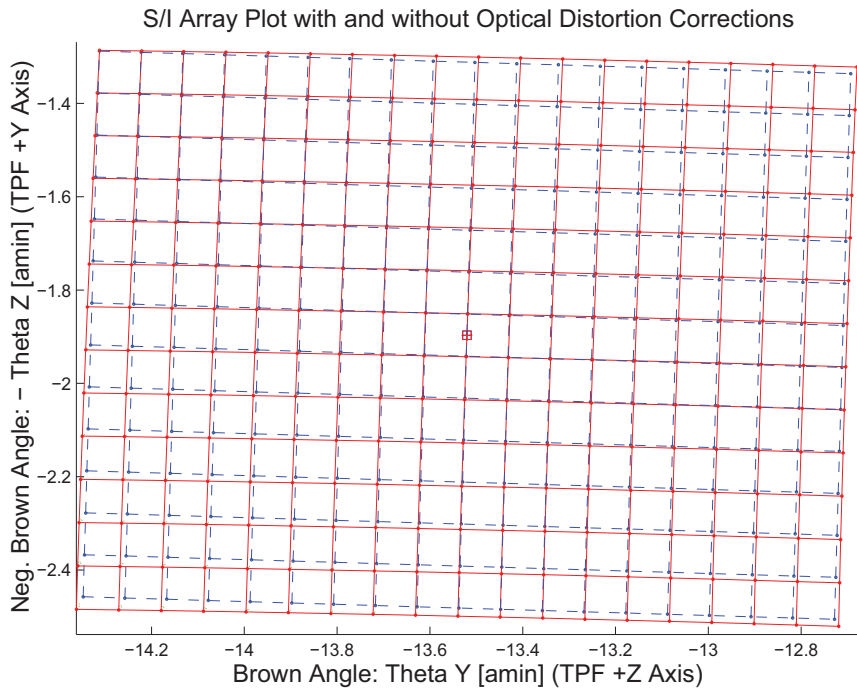


Figure 3.31: Array plot with (solid) and w/o (dashed) optical distortion corrections

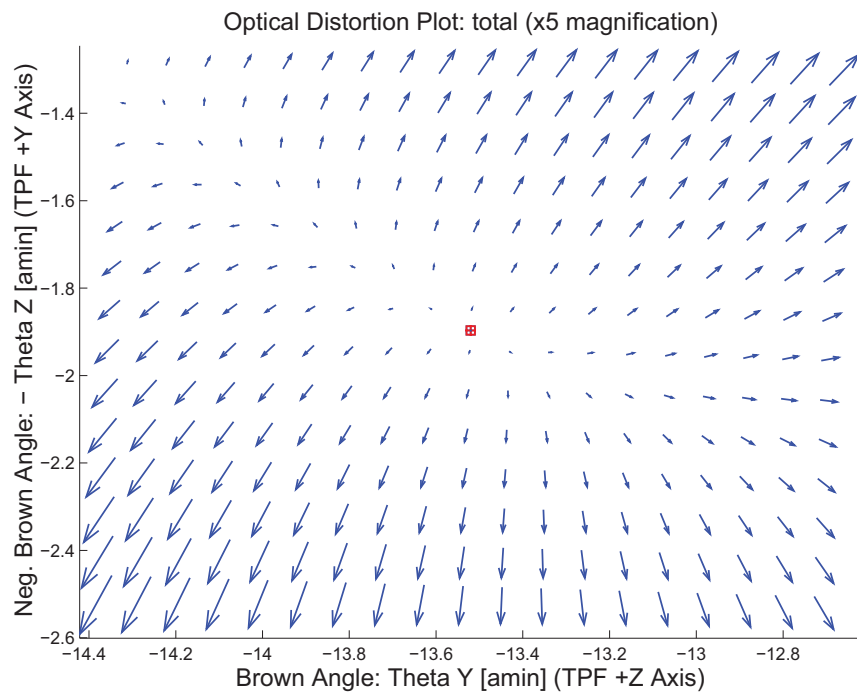


Figure 3.32: Optical Distortion Plot: total (x5 magnification)

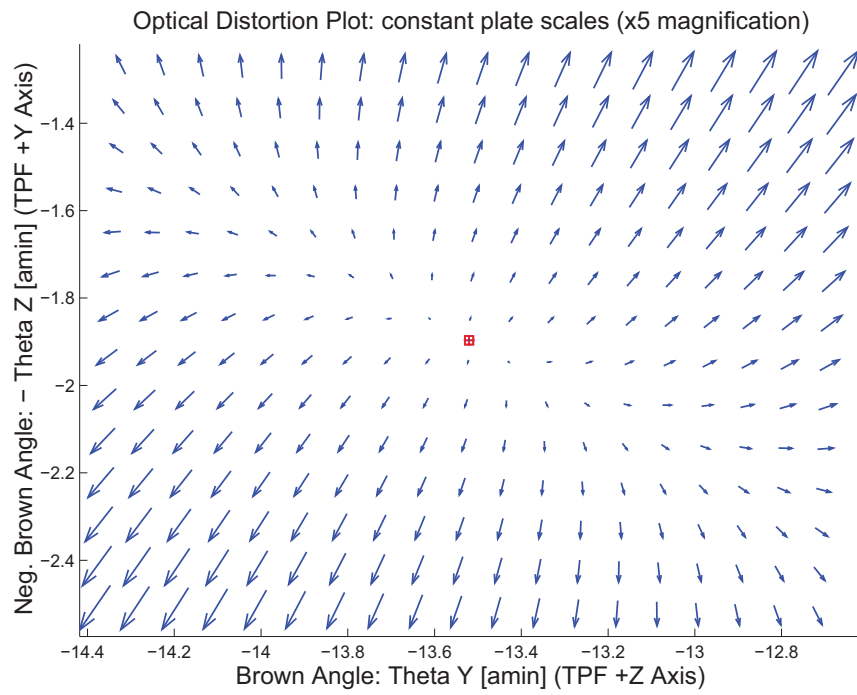


Figure 3.33: Optical Distortion Plot: constant plate scales (x5 magnification)

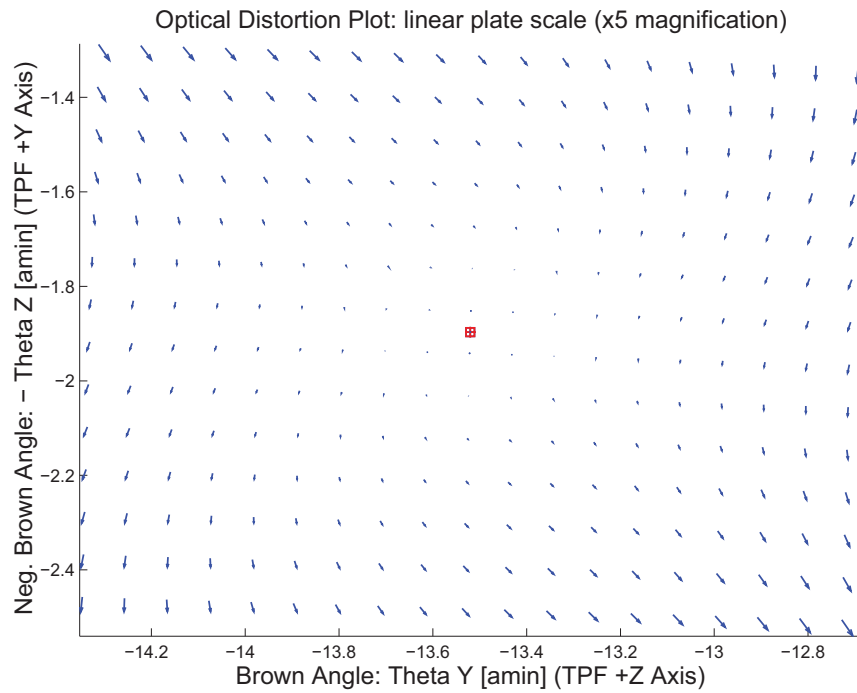


Figure 3.34: Optical Distortion Plot: linear plate scale (x5 magnification)

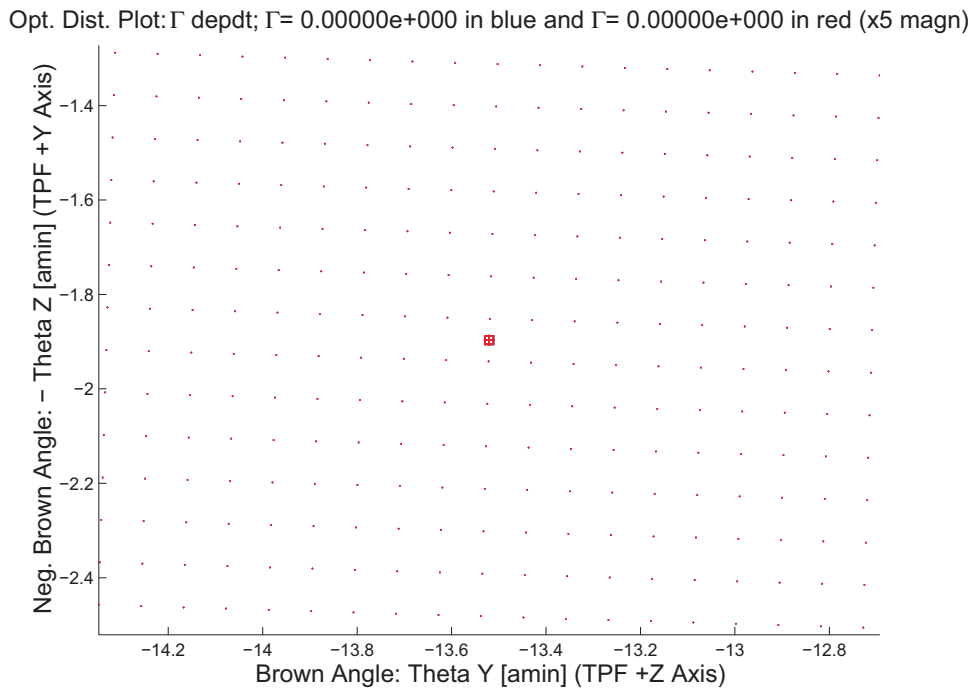


Figure 3.35: Optical Distortion Plot: gamma terms (x5 magnification)

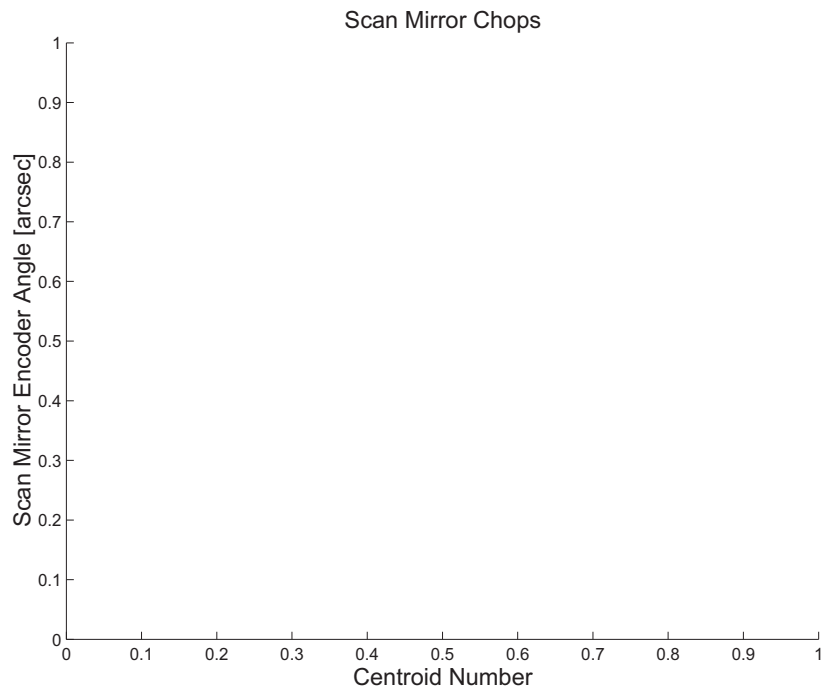


Figure 3.36: Scan Mirror Chops

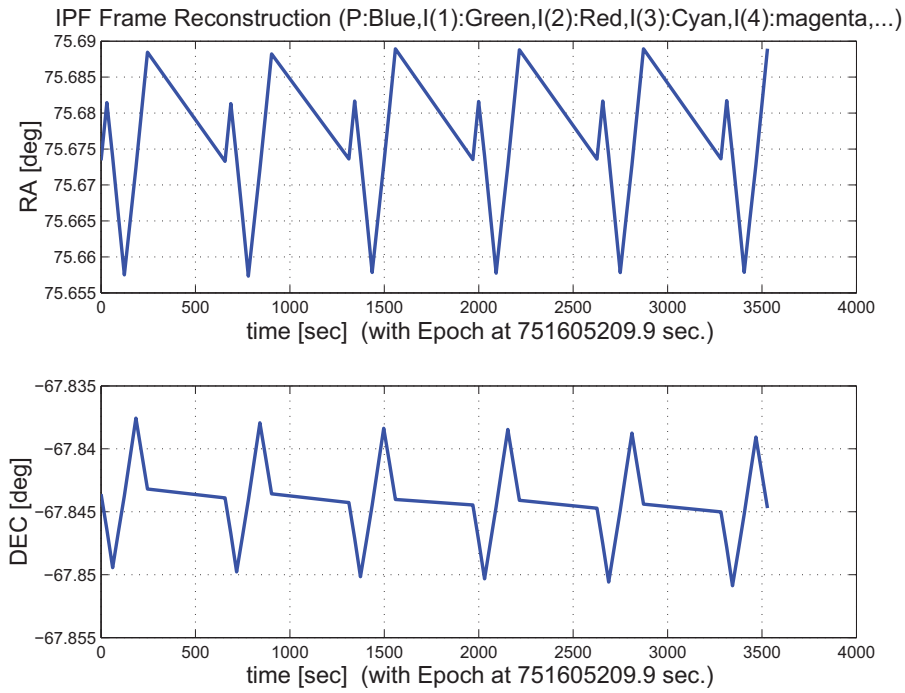


Figure 3.37: IPF Frame Reconstruction

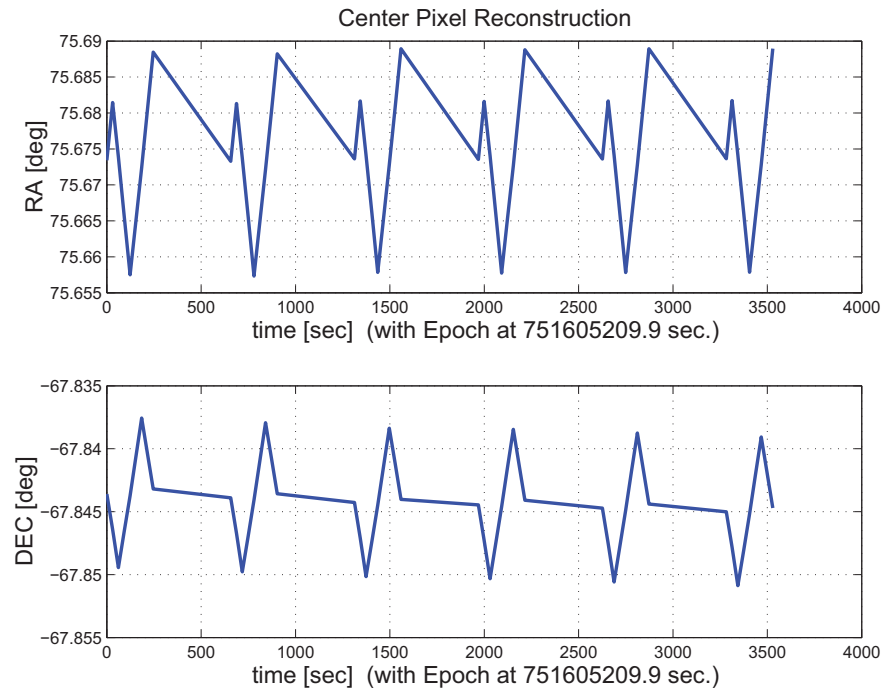


Figure 3.38: Center Pixel Reconstruction

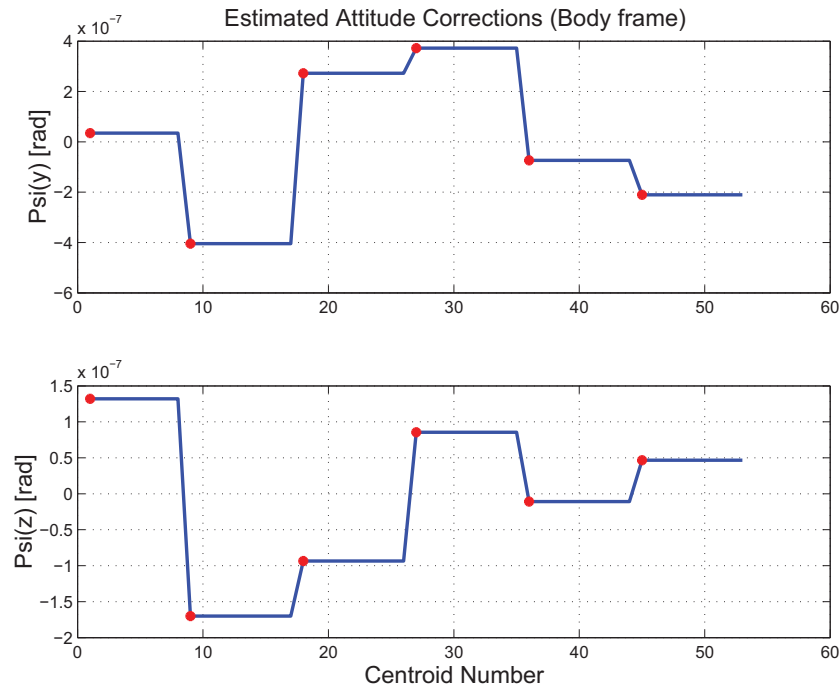


Figure 3.39: Estimated attitude corrections (Body frame)

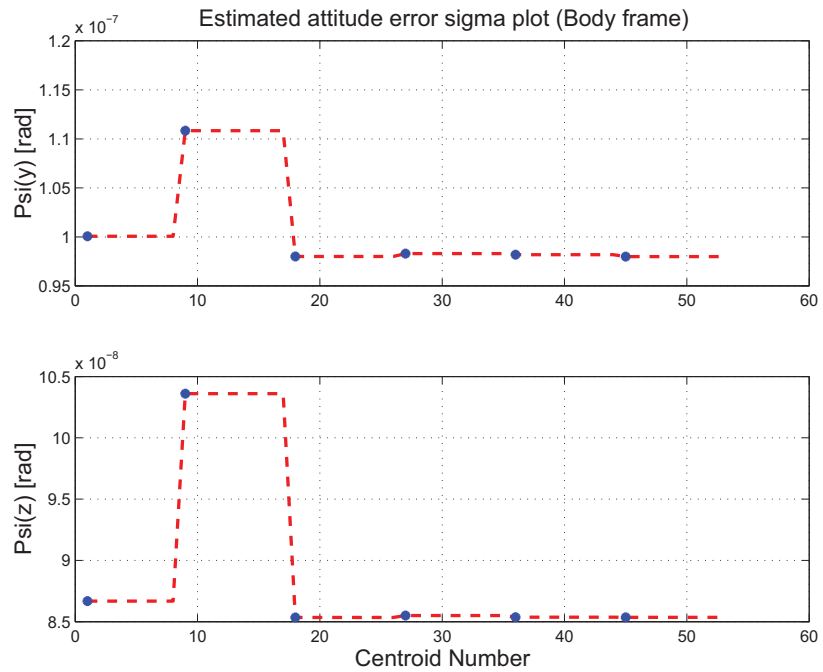


Figure 3.40: Estimated attitude error sigma plot (Body frame)

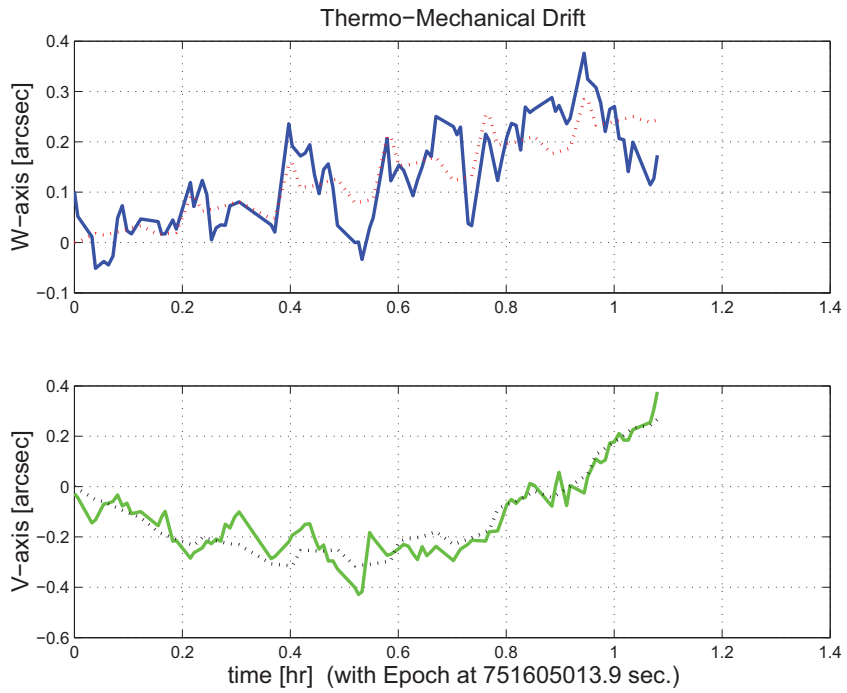


Figure 3.41: Thermo-mechanical boresight drift (equiv. angle in (W,V) coords)

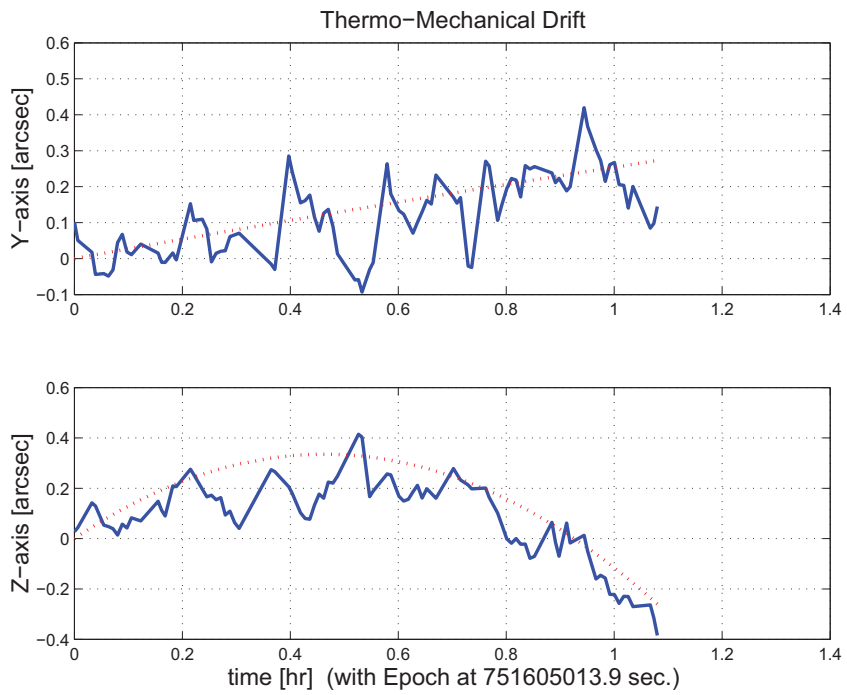


Figure 3.42: Thermo-mechanical boresight drift (equiv. angle in Body frame)

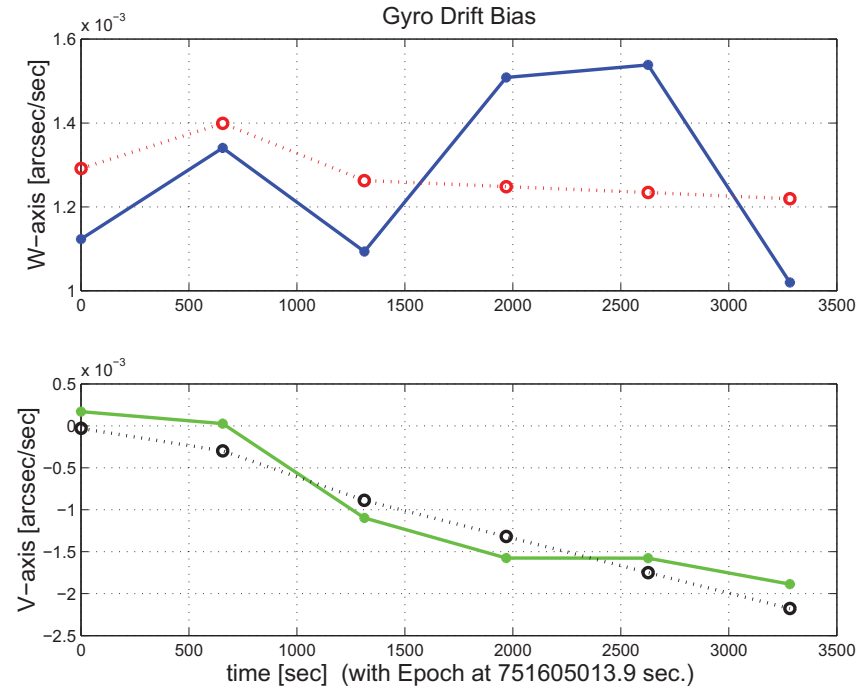


Figure 3.43: Gyro drift bias contribution (equiv. rate in (W,V) coords)

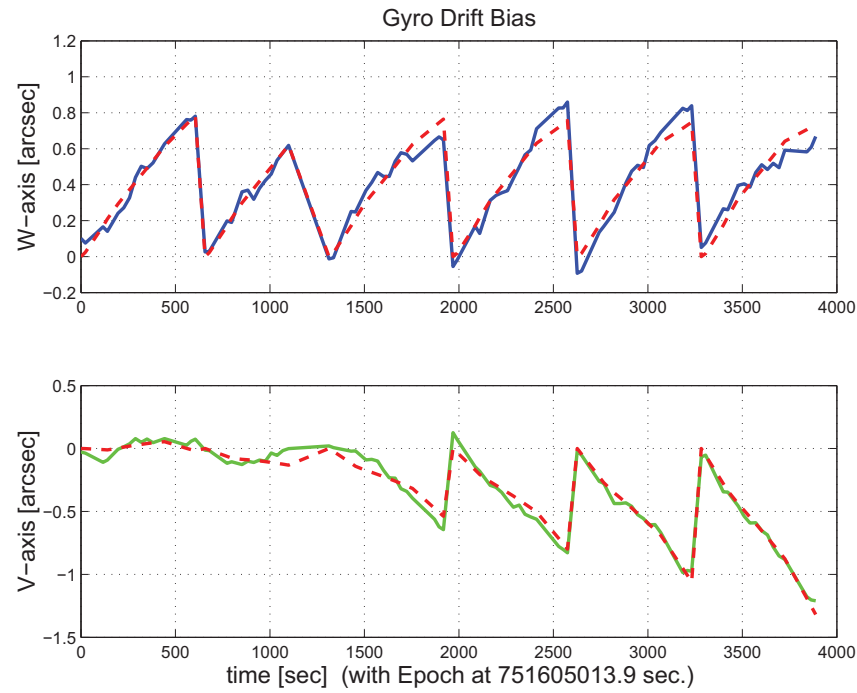


Figure 3.44: Gyro drift bias contribution (equiv. angle in (W,V) coords)

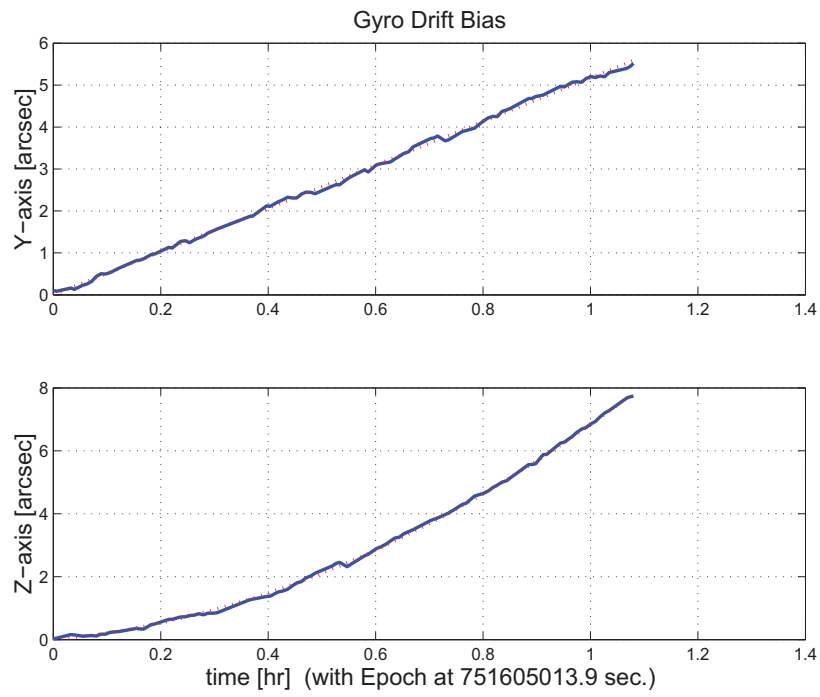


Figure 3.45: Gyro drift bias contribution (equiv. angle in Body frame)

3.2 IPF OUTPUT DATA (IF MINI FILE)

OUTPUT FILE NAME: IFmini701022.dat DATE: 26-Apr-2004 TIME: 10:54
 INSTRUMENT NAME: IRS_Blue_PeakUp_FOV_Center NF: 22
 IPF FILTER VERSION: IPF.V4.0.0 SW RELEASE DATE: January 30, 2004
 FRAME TABLE USED: BodyFrames_FTU_17a

----- IPF BROWN ANGLE SUMMARY -----

Frame Number	WAS			IS		
	theta_Y (arcmin)	theta_Z (arcmin)	angle (deg)	theta_Y (arcmin)	theta_Z (arcmin)	angle (deg)
022	-13.520824	+1.912112	+1.696937	-13.520255	+1.896747	+1.704385

OFFSET	NF	Delta_CW	Delta_CV
0	22	+0.000	+0.000 pixels

OFFSET FRAME NAME: IRS_Blue_PeakUp_FOV_Center

Brown Angle	theta_Y(arcmin)	theta_Z(arcmin)	angle(deg)
WAS(FTB)	-13.520824	+1.912112	+1.696937
IS (EST)	-13.520255	+1.896747	+1.704385
dT_EST	+0.000570	-0.015365	+0.007448
T_sSIGMA	+0.000537	+0.000521	+0.050836
dT_EST/T_sSIGMA	+1.061280	-29.491698	+0.146507

VARNAME	MEAN	SIGMA	SCALED_SIGMA
a00	+1.1155010312634394E-002	+1.2582048619935711E-003	+1.0954765891086843E-003
b00	+2.4801831523666041E-002	+1.8326458109479138E-003	+1.5956229725901324E-003
c00	+7.7641301342509326E-003	+1.0244777038614023E-003	+8.9197822591923837E-004
a01	-4.4833568212058994E+000	+2.6269885666290744E+001	+2.2872304515169123E+001
b01	+3.0305010364801944E+001	+2.7961106829659876E+001	+2.4344793811181319E+001
c01	-1.9253984865202113E+001	+1.9393062855851802E+001	+1.6884886548632174E+001
d01	-1.8232650258124362E+001	+2.6468965332746787E+001	+2.3045636474500938E+001
e01	-3.0559413010757886E+001	+2.9836620581710680E+001	+2.5977740456028688E+001
f01	+5.6985677449906302E-001	+1.9717606393751545E+001	+1.7167455674420129E+001
del_theta1	+1.4988146899812260E-012	+1.0190524068930719E-003	+8.8725460260693340E-004
del_theta2	-1.7430033222978914E-016	+1.7931731671568731E-007	+1.5612554713274227E-007
del_theta3	+3.5667259727933614E-016	+1.7406731501995784E-007	+1.5155454750924701E-007
del_arx	-9.0353085798779154E-014	+4.4708776513045988E-005	+3.8926425637977168E-005
del_ary	+8.6066837776008166E-016	+4.2599779107783966E-006	+3.7090192641472257E-006
del_arz	-2.1482484813070435E-015	+4.2608344999763899E-006	+3.7097650675066232E-006
brx	-9.2184198596680267E-008	+5.0452018189534104E-008	+4.3926872697303660E-008
bry	+3.5587491250525585E-010	+6.1894525998250045E-009	+5.3889478790941270E-009
brz	+1.9425674504291457E-009	+6.1909413820594312E-009	+5.3902441116341215E-009
crx	+4.0811413534335819E-011	+2.6384830316078294E-011	+2.2972382949682595E-011
cry	-8.6879254461608206E-015	+3.6462620434694452E-012	+3.1746775322799367E-012
crz	-1.1663563410844646E-012	+3.6471589973256433E-012	+3.1754584797874986E-012
bgx	-6.1305645665748891E-007	+6.2255153654766888E-007	+5.4203465143269754E-007
bgy	+6.9146028383937827E-009	+6.2209413548491539E-009	+5.4163640773549395E-009
bgz	+2.2026495325727875E-009	+6.9527669570530370E-009	+6.0535399767187863E-009
cgx	-1.5103954669323643E-010	+2.4150119236632217E-010	+2.1026695291890441E-010
cgy	+3.0465106954145749E-014	+3.6567428779444961E-012	+3.1838028417971401E-012
cgz	+3.9051264093662173E-012	+3.8551216319588451E-012	+3.3565245402770975E-012

LSQF RESIDUAL SIGMA SCALE = +8.7066631372966485E-001

	qT(1)	qT(2)	qT(3)	qT(4)
FrmTbl:	+1.4808544673835499E-002	+1.9621890181873501E-003	-3.0719476084145798E-004	+9.9988837499506800E-001
Estim:	+1.4873527538599281E-002	+1.9621194502754441E-003	-3.0508651078153001E-004	+9.9988741125590863E-001
DelTheta	deltheta(1)	deltheta(2)	deltheta(3)	
	+1.2997153444014098E-004	-3.3263844146985590E-008	+4.4725129158218857E-006	[rad]
EulAngT	theta(1)	theta(2)	theta(3)	[rad]

```

Mean      +2.9747125653788151E-002 +3.9328826393401194E-003 -5.5174134262893598E-004
SigmaT    +1.0190524068930719E-003 +1.7931731671568731E-007 +1.7406731501995784E-007
-----
qR          qR(1)           qR(2)           qR(3)           qR(4)
ASFILE:   +7.0895574754104018E-004 +1.2697734637185931E-003 -1.6151434101630002E-004 +9.9999892711639404E-001
Estim:    +7.4525361602702505E-004 +1.2699444559992961E-003 -1.6059020237547381E-004 +9.9999890302385508E-001
DelThetaR  delthetaR(1)     delthetaR(2)     delthetaR(3)     [rad]
          +7.2593291649709768E-005 +3.5501055571530053E-007 +1.9402180961161867E-006
EulAngR   angR(1)         angR(2)         angR(3)         [rad]
Mean      +1.4901030744234153E-003 +2.5401282182491622E-003 -3.1928822651607926E-004
SigmaR    +4.4708776513045988E-005 +4.2599779107783966E-006 +4.2608344999763899E-006
-----
Initial Gyro Bias   Bg0(1)           Bg0(2)           Bg0(3)
                  -4.2826755475289247E-007 -1.9468615164441871E-007 +3.5719489233088098E-007
Gyro Bias Correction Bg(1)            Bg(2)            Bg(3)
                  -6.1305645665748891E-007 +6.9146028383937827E-009 +2.2026495325727875E-009
Total Gyro Bias     BgT(1)          BgT(2)          BgT(3)
                  -1.0413240114103814E-006 -1.8777154880602493E-007 +3.5939754186345377E-007
-----
Initial Gyro Bias Rate Cg0(1)           Cg0(2)           Cg0(3)
                  +0.0000000000000000E+000 +0.0000000000000000E+000 +0.0000000000000000E+000
Gyro Bias Rate Correction Cg(1)            Cg(2)            Cg(3)
                  -1.5103954669323643E-010 +3.0465106954145749E-014 +3.9051264093662173E-012
Total Gyro Bias Rate   CgT(1)          CgT(2)          CgT(3)
                  -1.5103954669323643E-010 +3.0465106954145749E-014 +3.9051264093662173E-012
-----
q(1)          q(2)          q(3)          q(4)
PCRS1A: +5.3371888965461637E-007 +3.7444233778550031E-004 -1.4253684912431913E-003 +9.9999891405806784E-001
PCRS2A: -5.2779261998836216E-007 +3.8462959425181312E-004 +1.3722087221825403E-003 +9.9999898455099423E-001
-----
***** CS-FILE PARAMETERS: ***** AS-FILE PARAMETERS: *****
Row (01) PIX2RADX: +8.726599999999995E-008 Row (1) TASTART: +7.5160415709075928E+008
Row (02) PIX2RADY: +8.726599999999995E-008 Row (2) TASTOP: +7.5160910199075925E+008
Row (03) CXO: +1.0700000000000000E+004 Row (3) S/C TIME: +7.5158472999073792E+008
Row (04) CYO: +3.0000000000000000E+003 Row (4) QR1: +7.0895574754104018E-004
Row (05) BETA0: +9.9999000000000000E+004 Row (5) QR2: +1.2697734637185931E-003
Row (06) GAMMA_E0: +9.9999000000000000E+004 Row (6) QR3: -1.6151434101630002E-004
Row (07) D11: +0.0000000000000000E+000 Row (7) QR4: +9.9999892711639404E-001
Row (08) D12: +1.0000000000000000E+000
Row (09) D21: +1.0000000000000000E+000
Row (10) D22: +0.0000000000000000E+000
Row (11) DG: +9.9999000000000000E+004
-----
INITIAL STA-TO-PCRS ALIGNMENT (R) KNOWLEDGE (1-SIGMA)
  SIGMA(X)      SIGMA(Y)      SIGMA(Z)
5.93454643E+000 3.44777762E-001 3.45078359E-001 [arcsec]
-----
PIX2RADX = 8.726600000000E-008[rad/pixel]
XPIXSIZE = 0.0180[arcsec]
PIX2RADY = 8.726600000000E-008[rad/pixel]
YPIXSIZE = 0.0180[arcsec]
CX0 = 10700.0[pixel] = 192.60[arcsec]
CY0 = 3000.0[pixel] = 54.00[arcsec]
-----
NOMINAL BETA0 = 9.999900000000E+004[rad/encoder unit]
ENCODER UNIT SIZE = 99999.00[arcsec]
GAMMA_E0 = 99999.00[encoder unit] = 99999.00[arcsec]
-----
| +0 | +1 |
FLIP MATRIX D = |---|---| and DG = +99999
| +1 | +0 |

```

3.3 IPF EXECUTION LOG

```
*****
IPF EXECUTION-LOG FILE NAME: LG701022.dat
INSTRUMENT TYPE: IRS_Blue_PeakUp_FOV_Center
IPF FILTER EXECUTION DATE: 26-Apr-2004 TIME: 10:53
IPF FILTER VERSION USED: IPF.V4.0.0
*****


----- Loading & Preparing Input Files -----
AAFILE: AA501022 Loaded! AAFILE dimension = 49450 X 21
ASFILE: AS501022 Loaded!
CAFFILE: CA502022 Loaded! CAFFILE dimension = 53 X 15
CBFILE: CB502022 Loaded! CBFILE dimension = 39 X 15
CCFILE: CC701022 Created! CCFILE dimension = 92 X 19
CSFILE: CS701022 Loaded!
Loading Input Files Completed!
-----


----- Selected Mask Vectors -----
index = 1 2 3 4 5 6 7 8 9 10 11 12 13 14 15 16 17 18 19 20
-----
mask1 = [ 1 1 1 0 0 0 0 0 0 0 0 0 1 1 1 1 1 1 1 ]
mask2 = [ 0 0 1 1 1 1 1 1 1 1 1 1 1 1 1 1 1 1 1 1 ]
-----


----- Selected Initial Gyro Bias Parameters -----
User Entered 1 : Use AFILE database - from S/C filter
IPF Linearized Using Following Nominal Gyro Bias Estimates
bg0 = [-4.2826755475289247E-007 -1.9468615164441871E-007 +3.5719489233088098E-007 ]
cg0 = [+0.000000000000000E+000 +0.000000000000000E+000 +0.000000000000000E+000 ]
-----


----- Gyro Pre-Processor Run Completed -----
AGFILE CREATED: AG701022.m ACFILE CREATED: AC701022.m
-----


Total Gyro Preprocessor Execution Time: 25 seconds

FRAME TABLE ENTRIES FOR PCRS LOADED TO TPCRS
q_PCRS4 = [ +5.3371888965461637E-007 q_PCRS5 = [ +7.3379987833742897E-007
            +3.7444233778550031E-004 +5.2236196154513707E-004
            -1.4253684912431913E-003 -1.4047712280184723E-003
            +9.9999891405806784E-001 ]; +9.9999887687698918E-001 ];
q_PCRS8 = [ -5.2779261998836216E-007 q_PCRS9 = [ -7.1963421681856818E-007
            +3.8462959425181312E-004 +5.3239763239987400E-004
            +1.3722087221825403E-003 +1.3516841804518383E-003
            +9.9999898455099423E-001 ]; +9.9999894475050310E-001 ];
----- Initial Conditions for State ----- ----- Initial Square-Root Cov (diag) -----
p1(01) = a00 = +0.000000000000000E+000 Sigma_initial(01,01) = 1.000000000000000E+000
p1(02) = b00 = +0.000000000000000E+000 Sigma_initial(02,02) = 1.000000000000000E+000
p1(03) = c00 = +0.000000000000000E+000 Sigma_initial(03,03) = 1.000000000000000E+000
p1(04) = a10 = +0.000000000000000E+000 Sigma_initial(04,04) = 9.999900000000000E+004
p1(05) = b10 = +0.000000000000000E+000 Sigma_initial(05,05) = 9.999900000000000E+004
p1(06) = c10 = +0.000000000000000E+000 Sigma_initial(06,06) = 9.999900000000000E+004
p1(07) = d10 = +0.000000000000000E+000 Sigma_initial(07,07) = 9.999900000000000E+004
p1(08) = a20 = +0.000000000000000E+000 Sigma_initial(08,08) = 9.999900000000000E+004
p1(09) = b20 = +0.000000000000000E+000 Sigma_initial(09,09) = 9.999900000000000E+004
p1(10) = c20 = +0.000000000000000E+000 Sigma_initial(10,10) = 9.999900000000000E+004
p1(11) = d20 = +0.000000000000000E+000 Sigma_initial(11,11) = 9.999900000000000E+004
p1(12) = a01 = +0.000000000000000E+000 Sigma_initial(12,12) = 1.000000000000000E+004
p1(13) = b01 = +0.000000000000000E+000 Sigma_initial(13,13) = 1.000000000000000E+004
p1(14) = c01 = +0.000000000000000E+000 Sigma_initial(14,14) = 1.000000000000000E+004
p1(15) = d01 = +0.000000000000000E+000 Sigma_initial(15,15) = 1.000000000000000E+004
p1(16) = e01 = +0.000000000000000E+000 Sigma_initial(16,16) = 1.000000000000000E+004
p1(17) = f01 = +0.000000000000000E+000 Sigma_initial(17,17) = 1.000000000000000E+004
```

```

-----
p2f(01) = am1 = +0.000000000000000E+000 Sigma_initial(18,18) = 9.999900000000000E+004
p2f(02) = am2 = +0.000000000000000E+000 Sigma_initial(19,19) = 9.999900000000000E+004
p2f(03) = am3 = +1.000000000000000E+000 Sigma_initial(20,20) = 1.000000000000001E-001
p2f(04) = beta = +1.000000000000000E+000 Sigma_initial(21,21) = 1.000000000000000E-002
p2f(05) = qT1 = +1.4808544673835506E-002 Sigma_initial(22,22) = 1.000000000000000E-002
p2f(06) = qT2 = +1.9621890181873510E-003 Sigma_initial(23,23) = 2.8771492986883954E-004
p2f(07) = aT3 = -3.0719476084145814E-004 Sigma_initial(24,24) = 1.6715297603189757E-005
p2f(08) = qT4 = +9.9988837499506844E-001 Sigma_initial(25,25) = 1.6729870951362112E-005
p2f(09) = qR1 = +7.0895574754104018E-004 Sigma_initial(26,26) = 2.5720164508112511E-004
p2f(10) = qR2 = +1.2697734637185931E-003 Sigma_initial(27,27) = 2.5720164508112511E-004
p2f(11) = qR3 = -1.6151434101630002E-004 Sigma_initial(28,28) = 2.5720164508112511E-004
p2f(12) = qR4 = +9.9999892711639404E-001 Sigma_initial(29,29) = 6.6152686232437047E-008
p2f(13) = brx = +0.000000000000000E+000 Sigma_initial(30,30) = 6.6152686232437047E-008
p2f(14) = bry = +0.000000000000000E+000 Sigma_initial(31,31) = 6.6152686232437047E-008
p2f(15) = brz = +0.000000000000000E+000 Sigma_initial(32,32) = 2.5720164508112511E-004
p2f(16) = crx = +0.000000000000000E+000 Sigma_initial(33,33) = 2.5720164508112511E-004
p2f(17) = cry = +0.000000000000000E+000 Sigma_initial(34,34) = 2.5720164508112511E-004
p2f(18) = crz = +0.000000000000000E+000 Sigma_initial(35,35) = 6.6152686232437047E-008
p2f(19) = bgx = +0.000000000000000E+000 Sigma_initial(36,36) = 6.6152686232437047E-008
p2f(20) = bgy = +0.000000000000000E+000 Sigma_initial(37,37) = 6.6152686232437047E-008
p2f(21) = bgz = +0.000000000000000E+000 Sigma_initial(38,38) = 6.6152686232437047E-008
p2f(22) = cgx = +0.000000000000000E+000 Sigma_initial(39,39) = 6.6152686232437047E-008
p2f(23) = cgy = +0.000000000000000E+000 Sigma_initial(40,40) = 6.6152686232437047E-008
p2f(24) = cgz = +0.000000000000000E+000 Sigma_initial(41,41) = 6.6152686232437047E-008
-----
```

```

----- IPF KALMAN FILTER STARTED -----
Iteration#001: |dp|= +5.105167735487E+001 RMS(|Res|)=+8.994003074823E-006
Iteration#002: |dp|= +5.341725147919E-001 RMS(|Res|)=+4.333146781545E-007
Iteration#003: |dp|= +1.457312021715E-001 RMS(|Res|)=+4.790841102784E-007
Iteration#004: |dp|= +2.141777103714E-002 RMS(|Res|)=+4.736022186201E-007
Iteration#005: |dp|= +2.568346476252E-003 RMS(|Res|)=+4.711255738791E-007
Iteration#006: |dp|= +7.832979921532E-004 RMS(|Res|)=+4.710032595459E-007
Iteration#007: |dp|= +4.547852775671E-005 RMS(|Res|)=+4.711391402787E-007
Iteration#008: |dp|= +2.952459900952E-005 RMS(|Res|)=+4.711651445707E-007
Iteration#009: |dp|= +5.261129917164E-006 RMS(|Res|)=+4.711598111362E-007
Iteration#010: |dp|= +9.805671217444E-007 RMS(|Res|)=+4.711574000285E-007
Iteration#011: |dp|= +4.034787523429E-007 RMS(|Res|)=+4.711574226176E-007
Iteration#012: |dp|= +1.097709717585E-007 RMS(|Res|)=+4.711575817549E-007
Iteration#013: |dp|= +4.152017578503E-008 RMS(|Res|)=+4.711576025236E-007
Iteration#014: |dp|= +1.404681828109E-007 RMS(|Res|)=+4.711575948985E-007
Iteration#015: |dp|= +7.890237952224E-008 RMS(|Res|)=+4.711575929059E-007
Iteration#016: |dp|= +1.445866080084E-007 RMS(|Res|)=+4.711575931447E-007
Iteration#017: |dp|= +3.125292345014E-007 RMS(|Res|)=+4.711575925090E-007
Iteration#018: |dp|= +1.683780263592E-007 RMS(|Res|)=+4.711575939850E-007
Iteration#019: |dp|= +9.267418181400E-008 RMS(|Res|)=+4.711575930180E-007
Iteration#020: |dp|= +8.401679224178E-008 RMS(|Res|)=+4.711575933968E-007
Iteration#021: |dp|= +8.679511762212E-008 RMS(|Res|)=+4.711575932894E-007
Iteration#022: |dp|= +2.510579051983E-007 RMS(|Res|)=+4.711575931002E-007
Iteration#023: |dp|= +3.310550034050E-007 RMS(|Res|)=+4.711575918800E-007
Iteration#024: |dp|= +1.634719870840E-007 RMS(|Res|)=+4.711575937188E-007
Iteration#025: |dp|= +7.346942572499E-008 RMS(|Res|)=+4.711575926364E-007
Iteration#026: |dp|= +1.656937628493E-007 RMS(|Res|)=+4.711575931055E-007
Iteration#027: |dp|= +5.977900568530E-008 RMS(|Res|)=+4.711575932354E-007
Iteration#028: |dp|= +1.879401661708E-007 RMS(|Res|)=+4.711575923030E-007
Iteration#029: |dp|= +1.072129964044E-007 RMS(|Res|)=+4.711575929940E-007
Iteration#030: |dp|= +8.278284546953E-008 RMS(|Res|)=+4.711575931913E-007
IPF Kalman Filter Completed with Error |dp1| + |dp2| = +8.2782845469528019E-008
-----
```

```

----- IPF LEAST SQUARES FILTER STARTED -----
Iteration#001 COND#=+1.511996639546E+007, |dp|=+5.091698812134E+001
Iteration#002 COND#=+1.511610453467E+007, |dp|=+5.205895567093E-002
Iteration#003 COND#=+1.511611207969E+007, |dp|=+1.422183366054E-002
Iteration#004 COND#=+1.511611224491E+007, |dp|=+3.057002677576E-005
Iteration#005 COND#=+1.511611223974E+007, |dp|=+1.425755157750E-005
Iteration#006 COND#=+1.511611223887E+007, |dp|=+5.385920613789E-009
-----
```

```

Iteration#007 COND#=+1.511611223699E+007, |dp|=+3.990289162971E-009
Iteration#008 COND#=+1.511611223821E+007, |dp|=+5.106116583937E-009
Iteration#009 COND#=+1.511611223846E+007, |dp|=+3.793836729065E-009
Iteration#010 COND#=+1.511611223851E+007, |dp|=+5.320266406753E-009
Iteration#011 COND#=+1.511611223771E+007, |dp|=+1.034803757470E-008
Iteration#012 COND#=+1.511611223935E+007, |dp|=+1.180533790588E-008
Iteration#013 COND#=+1.511611223654E+007, |dp|=+9.114906501569E-009
Iteration#014 COND#=+1.511611223765E+007, |dp|=+7.159435713852E-009
Iteration#015 COND#=+1.511611223666E+007, |dp|=+9.059260845162E-009
Iteration#016 COND#=+1.511611223633E+007, |dp|=+5.839218616079E-009
Iteration#017 COND#=+1.511611223756E+007, |dp|=+4.481408014748E-009
Iteration#018 COND#=+1.511611223895E+007, |dp|=+3.549078479283E-009
Iteration#019 COND#=+1.511611223649E+007, |dp|=+6.368253142975E-009
Iteration#020 COND#=+1.511611223740E+007, |dp|=+7.393214378280E-009
Iteration#021 COND#=+1.511611223741E+007, |dp|=+7.213973098818E-009
Iteration#022 COND#=+1.511611223836E+007, |dp|=+5.794139408001E-009
Iteration#023 COND#=+1.511611223835E+007, |dp|=+6.087388903682E-009
Iteration#024 COND#=+1.511611223697E+007, |dp|=+7.933781378153E-009
Iteration#025 COND#=+1.511611223684E+007, |dp|=+1.169818073884E-008
Iteration#026 COND#=+1.511611223961E+007, |dp|=+8.112166197660E-009
Iteration#027 COND#=+1.511611223744E+007, |dp|=+6.454864751563E-009
Iteration#028 COND#=+1.511611223818E+007, |dp|=+5.633562825825E-009
Iteration#029 COND#=+1.511611223744E+007, |dp|=+6.476840478961E-009
Iteration#030 COND#=+1.511611223743E+007, |dp|=+6.121151807046E-009
IPF Least Squares Filter Completed with Error |dp1| + |dp2| = +6.1211518070463143E-009
-----
```

Total Execution Time: 75 seconds

4 COMMENTS

This IPF run is a post-IOC re-run of the IOC flight data taken from run IF503022, but with a modified CS-file CS701022.m, which specifies that the Prime frame 022 is to be moved over from its previous definition by 1/2 pixel. This change puts the Prime frame exactly at the middle of a physical pixel, which was desired by the IRS team to improve in-flight Peakup centroiding accuracy.

The IPF run was performed in the most recent IPF version IPF.V4.0.0. All IPF settings, data editing, and parameters were kept the same as the IF503022 run (see report ID503022.pdf for details). As a reminder, constant and linear plate scales were estimated, which did not change significantly from run IF503022.

We recommend updating frame 022 with the new quaternion listed in the IF file IF701022.dat. The recommended Brown angle change is on the order of 0.9 arcsec, which is consistent with the desired 1/2 pixel shift (the PU pixels are approximately 1.8 arcsec wide). As before, in our best judgement, the Fine survey is accurate to 0.097 arcsec which satisfies the fine survey requirement of 0.25 arcsecond by a good margin.

IPF TEAM CONTACT INFORMATION

IPF Team email	ipf@sirtfweb.jpl.nasa.gov	
David S. Bayard	X4-8208	David.S.Bayard@jpl.nasa.gov (TEAM LEADER)
Dhemetrio Boussalis	X4-3977	boussali@grover.jpl.nasa.gov
Paul Brugarolas	X4-9243	Paul.Brugarolas@jpl.nasa.gov
Bryan H. Kang	X4-0541	Bryan.H.Kang@jpl.nasa.gov
Edward.C.Wong	X4-3053	Edward.C.Wong@jpl.nasa.gov (TASK MANAGER)

ACKNOWLEDGEMENTS

This work was performed at the Jet Propulsion Laboratory, California Institute of Technology, under contract with the National Aeronautics and Space Administration.

References

- [1] D.S. Bayard, B.H. Kang, *SIRTF Instrument Pointing Frame Kalman Filter Algorithm*, JPL D-Document D-24809, September 30, 2003.
- [2] B.H. Kang, D.S. Bayard, *SIRTF Instrument Pointing Frame (IPF) Software Description Document and User's Guide*, JPL D-Document D-24808, September 30, 2003.
- [3] D.S. Bayard, B.H. Kang, *SIRTF Instrument Pointing Frame (IPF) Kalman Filter Unit Test Report*, JPL D-Document D-24810, September 30, 2003.
- [4] *Space Infrared Telescope Facility In-Orbit Checkout and Science Verification Mission Plan*, JPL D-Document D-22622, 674-FE-301 Version 1.4, February 8, 2002.
- [5] *Space Infrared Telescope Facility Observatory Description Document*, Lockheed Martin LMMS/P458569, 674-SEIT-300 Version 1.2, November 1, 2002.
- [6] *SIRTF Software Interface Specification for Science Centroid INPUT Files (CAFILe, CS-FILE)*, JPL SOS-SIS-2002, November 18, 2002.
- [7] *SIRTF Software Interface Specification for Inferred Frames Offset INPUT Files (OFILE)*, JPL SOS-SIS-2003, November 18, 2002.
- [8] *SIRTF Software Interface Specification for PCRS Centroid INPUT Files (CBFILE)*, JPL SIS-FES-015, November 18, 2002.
- [9] *SIRTF Software Interface Specification for Attitude INPUT Files (AFILE, ASFILE)*, JPL SIS-FES-014, January 7, 2002.
- [10] *SIRTF Software Interface Specification for IPF Filter Output Files (IFFILE, LGFILE, TARFILE)*, JPL SOS-SIS-2005, November 18, 2002.
- [11] R.J. Brown, *Focal Surface to Object Space Field of View Conversion*. Systems Engineering Report SER No. S20447-OPT-051, Ball Aerospace & Technologies Corp., November 23, 1999.

JET PROPULSION LABORATORY

SIRTF IPF REPORT

JPL ID701023

April 26, 2004

**SIRTF INSTRUMENT POINTING FRAME
KALMAN FILTER EXECUTION SUMMARY**

IPF RUN NUMBER: 701023

REPORT TYPE: IOC EXECUTION (FINE)

PRIME FRAME: IRS_Blue_PeakUp_FOV_Sweet_Spot (23)

INFERRRED FRAMES:

IPF TEAM

Autonomy and Control Section (345)

Jet Propulsion Laboratory

California Institute of Technology

4800 Oak Grove Drive

Pasadena, CA 91109

Contents

1 IPF EXECUTION SUMMARY	5
2 IPF INPUT FILE HISTORY	9
3 IPF EXECUTION RESULTS	10
3.1 IPF EXECUTION OUTPUT PLOTS	10
3.2 IPF OUTPUT DATA (IF MINI FILE)	36
3.3 IPF EXECUTION LOG	38
4 COMMENTS	41

List of Figures

1.1 A-priori and a-posteriori IPF frames	5
1.2 A-priori and a-posteriori IPF frames (ZOOMED)	8
2.1 Scenario Plot	9
3.1 TPF coords of measurements and a-priori predicts	12
3.2 Oriented PixelCoords of measurements and a-priori predicts	12
3.3 Oriented (W,V) PixelCoords of A-Priori Prediction Error Quiver Plot	13
3.4 A-priori prediction error (Science Centroids)	13
3.5 Oriented PixelCoords of measurements and a-priori predicts (PCRS only)	14
3.6 Oriented PixelCoords of measurements and a-priori predicts (Zoomed, PCRS only)	14
3.7 Oriented (W,V) PixelCoords of A-Priori PCRS Prediction Error Quiver Plot	15
3.8 A-priori PCRS prediction error	15
3.9 IPF execution convergence, chart 1	16
3.10 IPF execution convergence, chart 2	16
3.11 Parameter uncertainty convergence	17
3.12 IPF parameter symbol table	17
3.13 KF parameter error sigma plots	18
3.14 LS parameter error sigma plot	18
3.15 KF and LS parameter error sigma plot	19

3.16	Oriented Pixel Coords of meas. and a-posteriori predicts	20
3.17	Oriented Pixel Coords of meas. and a-posteriori predicts (attitude corrected)	20
3.18	KF innovations with (o) and w/o (+) attitude corrections	21
3.19	Histograms of science a-posteriori residuals (or innovations)	21
3.20	A-Posteriori Science Centroid Prediction Error Quiver (Att. Cor.)	22
3.21	Normalized A-Posteriori Science Centroid Prediction Errors	22
3.22	KF innovations with (o) and w/o (+) attitude corrections (PCRS)	23
3.23	Histograms of PCRS a-posteriori residuals (or innovations)	23
3.24	A-posteriori PCRS Prediction Summary	24
3.25	A-posteriori PCRS Prediction (PCRS 1 Only)	25
3.26	A-posteriori PCRS Prediction (PCRS 2 Only)	25
3.27	A-Posteriori PCRS Prediction Errors Quiver (Att. Cor.)	26
3.28	Normalized A-Posteriori PCRS Prediction Errors	26
3.29	W-axis KF innovations and 1-sigma bound	27
3.30	V-axis KF innovations and 1-sigma bound	27
3.31	Array plot with (solid) and w/o (dashed) optical distortion corrections	28
3.32	Optical Distortion Plot: total (x5 magnification)	28
3.33	Optical Distortion Plot: constant plate scales (x5 magnification)	29
3.34	Optical Distortion Plot: linear plate scale (x5 magnification)	29
3.35	Optical Distortion Plot: gamma terms (x5 magnification)	30
3.36	Scan Mirror Chops	30
3.37	IPF Frame Reconstruction	31
3.38	Center Pixel Reconstruction	31
3.39	Estimated attitude corrections (Body frame)	32
3.40	Estimated attitude error sigma plot (Body frame)	32
3.41	Thermo-mechanical boresight drift (equiv. angle in (W,V) coords)	33
3.42	Thermo-mechanical boresight drift (equiv. angle in Body frame)	33
3.43	Gyro drift bias contribution (equiv. rate in (W,V) coords)	34
3.44	Gyro drift bias contribution (equiv. angle in (W,V) coords)	34
3.45	Gyro drift bias contribution (equiv. angle in Body frame)	35

List of Tables

1.1	IPF filter input files	6
1.2	IPF filter execution configuration	6
1.3	IPF filter execution mask vector assignment	6
1.4	IPF calibration error summary ([arcsec], 1-sigma, radial)	7
1.5	Science measurement prediction error summary (1-sigma)	7
1.6	IPF Brown angle summary	8
2.1	IPF input file editing status	9
3.1	Table of figures I (IPF run)	10
3.2	Table of figures II (IPF run)	11
3.3	PCRS measurement prediction error summary	24

1 IPF EXECUTION SUMMARY

This report summarizes the SIRTF Instrument Pointing Frame (IPF) Kalman Filter execution associated with run file: RN701023. In particular, this Focal Point Survey calibrates the instrument: IRS_Blue_PeakUp_FOV_Sweet_Spot (23), as part of the IOC Fine Survey. The main calibration results from the IPF filter execution have been documented in IF701023 typically stored in the mission archive DOM collection IPF_IF. This report only summarizes the main aspects of the run, and does not substitute for the full information contained in the IF file.

Section 1 summarizes the filter execution results. The filter configurations are tabulated in Table 1.2 and the mask vector assignments are tabulated in Table 1.3. A total of 21 state parameters are estimated in this run. The overall End-to-End pointing performances are tabulated in Table 1.4. The prediction residuals throughout the estimation processes are tabulated in Table 1.5. Section 3 summarizes resulting plots, a mini summary of the IF IPF output file, and the execution log. Section 4 captures the user comments that are specific to this particular run.

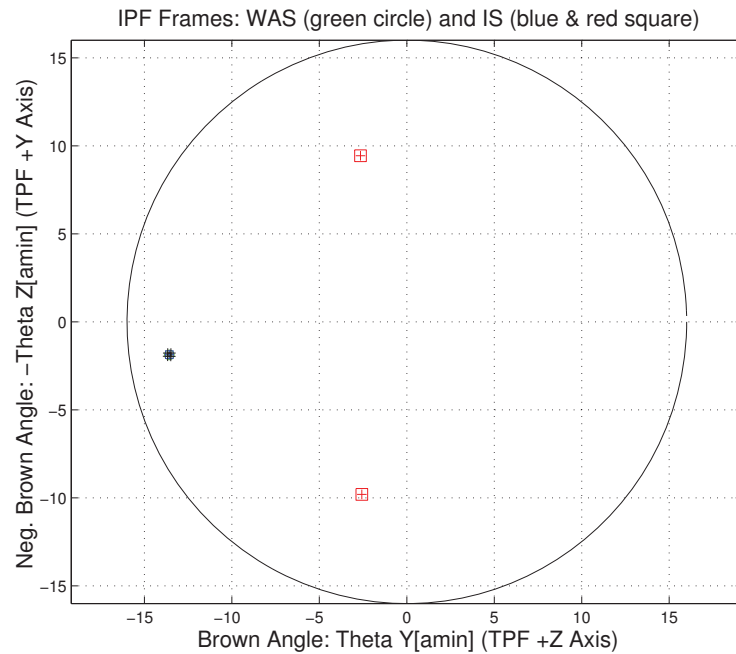


Figure 1.1: A-priori and a-posteriori IPF frames

RAW	FINAL (After Editing)
AA501023	AA501023
AS501023	AS501023
CA501023	CA501023
CB501023	CB501023
CS701023	CS701023

Table 1.1: IPF filter input files

EXECUTION CONFIGURATION ITEM	CURRENT STATUS
IPF Filter Version Used	IPF.V4.0.0
Frame Table Version Used	BodyFrames_FTU_17a
Scan-Mirror Employed?	NO
IPF Filter Mode	NORMAL-MODE(0)
SLIT-MODE Operation	DISABLED
Kalman Filter Operation	ENABLED
Least-Squares Data Analysis	ENABLED
IBAD Screening	ENABLED
User-Specified Data Editing	DISABLED
Total Number of Iterations	30
LS Residual Sigma Scale	8.31187328E-001
Total Number of Maneuvers	21

Table 1.2: IPF filter execution configuration

Con. Plate Scale			Γ Dependent				Γ^2 Dependent				Linear Plate Scale						Mirror	
a_{00}	b_{00}	c_{00}	a_{10}	b_{10}	c_{10}	d_{10}	a_{20}	b_{20}	c_{20}	d_{20}	a_{01}	b_{01}	c_{01}	d_{01}	e_{01}	f_{01}	α	β
1	2	3	4	5	6	7	8	9	10	11	12	13	14	15	16	17	18	19
1	1	1	0	0	0	0	0	0	0	0	0	0	0	0	0	0	0	0
IPF (T)			Alignment R												Gyro Drift Bias			
θ_1	θ_2	θ_3	a_{rx}	a_{ry}	a_{rz}	b_{rx}	b_{ry}	b_{rz}	c_{rx}	c_{ry}	c_{rz}	b_{gx}	b_{gy}	b_{gz}	c_{gx}	c_{gy}	c_{gz}	
20	21	22	23	24	25	26	27	28	29	30	31	32	33	34	35	36	37	
1	1	1	1	1	1	1	1	1	1	1	1	1	1	1	1	1	1	

Table 1.3: IPF filter execution mask vector assignment

FOCAL PLANE SURVEY ANALYSIS: IOC Fine Survey.

INSTRUMENT NAME: IRS_Blue_PeakUp_FOV_Sweet_Spot NF: 23

PIX2RADW: 8.72660000E-008 [rad/pixel] = 1.8000E-002 [arcsec/pixel]

PIX2RADV: 8.72660000E-008 [rad/pixel] = 1.8000E-002 [arcsec/pixel]

FRAME	DESCRIPTION	IPF ¹	SF ²	TOTAL	REQ
023(P)	IRS_Blue_PeakUp_FOV_Sweet_Spot	0.0157	0.0855	0.0869	0.14

Table 1.4: IPF calibration error summary ([arcsec], 1-sigma, radial)

RMS METRIC	A PRIORI ³	A POSTERIORI ³	ATT. CORRECTED ⁴	UNITS
Radial	1.2491	0.1536	0.0669	arcsec
W-Axis	0.4280	0.1276	0.0576	arcsec
V-Axis	1.1735	0.0855	0.0339	arcsec
Radial	69.3972	8.5322	3.7155	pixels
W-Axis	23.7752	7.0870	3.2014	pixels
V-Axis	65.1975	4.7511	1.8857	pixels

Table 1.5: Science measurement prediction error summary (1-sigma)

¹IPF filter removes systematic pointing errors due to: thermomechanical alignment drift (Body to TPF), gyro bias and bias drift, centroiding error, attitude error, and optical distortion. IPF SIGMA presented here is “Scaled” by the Least Squares Scale factor. The Least Squares Scale Factor was: 0.831187. It is assumed that the gyro Angle Random Walk contribution is captured with the Least Squares scaling. The gyro ARW contribution can be approximately calculated as 0.0454 arcseconds, given that ARW = $100 \mu\text{deg}/\sqrt{\text{hr}}$, with 6.004369e+002 second Maneuver time (max), and 21 independent Maneuvers.

²Gyro Scale Factor(GSF) assumes 95 ppm error over 0.250 degree maneuver.

³This can be interpreted as estimate of ”pixel to sky” pointing reconstruction error if no science data is used.

⁴This can be interpreted as estimate of achieved S/I centroiding error

IPF BROWN ANGLE SUMMARY					
FRAME TABLE USED: BodyFrames_FTU_17a					
NF	NAME	WAS	IS	CHANGE	UNIT
023	theta_Y	-13.579030	-13.578384	+0.000646	arcmin
023	theta_Z	+1.879766	+1.864398	-0.015368	arcmin
023	angle	+1.817224	+1.817225	+0.000001	deg

Table 1.6: IPF Brown angle summary

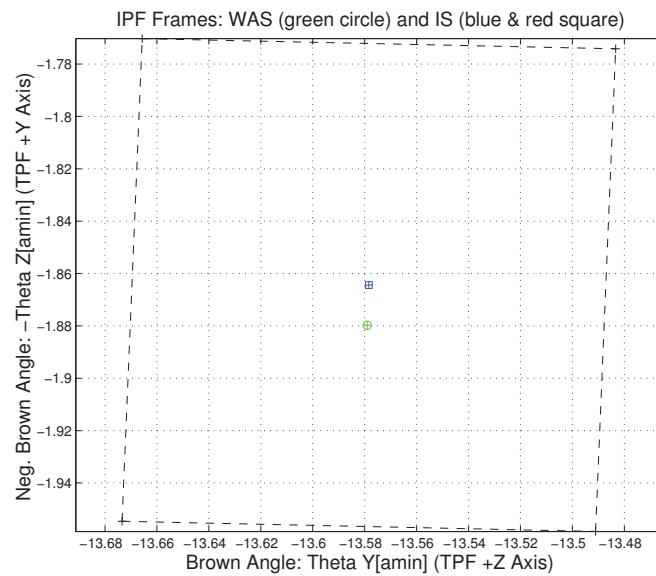


Figure 1.2: A-priori and a-posteriori IPF frames (ZOOMED)

2 IPF INPUT FILE HISTORY

WAS	SIZE	IS	SIZE	REMOVED	PATCHED
AA501023	UNCHANGED	AA501023	UNCHANGED	0	0
CA501023	UNCHANGED	CA501023	UNCHANGED	0	N/A
CB501023	UNCHANGED	CB501023	UNCHANGED	0	N/A

Table 2.1: IPF input file editing status

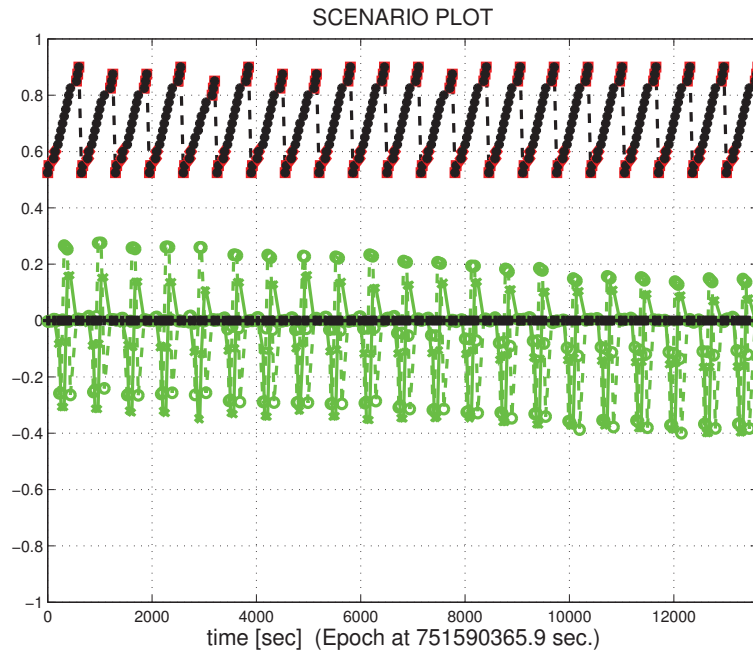


Figure 2.1: Scenario Plot

3 IPF EXECUTION RESULTS

3.1 IPF EXECUTION OUTPUT PLOTS

This subsection summarizes the IPF filter results. As shown in Table 3.1, the output plots are segmented to three groups: predicted performance, post-run results and IPF trending plots.

FIGURE NO.	DESCRIPTION
Predicted performance prior to IPF run	
Figure 3.1	Meas. and a-priori predicts in TPF coords
Figure 3.2	Meas. and a-priori predicts in Oriented Pixel Coords including rectangular array boundary approximation
Figure 3.3	A-Priori Prediction Error Quiver Plot in Oriented Pixel Coords including rectangular array boundary approximation
Figure 3.4	A-priori prediction error
Figure 3.5	Oriented Pixel Coords of measurements and a-priori predicts (PCRS only)
Figure 3.6	Oriented Pixel Coords of measurements and a-priori predicts (Zoomed, PCRS only)
Figure 3.7	Oriented (W,V) Pixel Coords of A-Priori PCRS Prediction Error Quiver Plot
Figure 3.8	A-priori PCRS prediction error
IPF filter performance (post run results)	
Figure 3.9	IPF execution convergence, chart 1: (top) normalized residual error vs. iteration number and (bottom) norm of effective parameter corrections
Figure 3.10	IPF execution convergence, chart 2: parameter correction size vs. iteration number
Figure 3.11	Parameter uncertainty convergence: square-root of diagonal elements of covariance matrix vs. maneuver number
Figure 3.12	IPF parameter symbol table
Figure 3.13	KF parameter error sigma plot (a-priori-dashed, a-posteriori-solid). Includes true parameter errors (FLUTE runs only)
Figure 3.14	LS parameter error sigma plot. Includes true parameter errors (FLUTE runs only)
Figure 3.15	KF and LS parameter errors sigma plot (Figure 3.13 & Figure 3.14 combined)
Figure 3.16	Measurements and a-posteriori predicts in Oriented Pixel Coords including rectangular array boundaries (a-priori-dashed, a-posteriori-solid)
Figure 3.17	Attitude corrected meas. and a-posteriori predicts in Oriented Pixel Coords including rectangular array boundaries (a-priori-dashed, a-posteriori-solid)

Table 3.1: Table of figures I (IPF run)

FIGURE NO.	DESCRIPTION
IPF filter performance (post run results) - CONTINUE	
Figure 3.18	KF innovations with (o) and w/o (+) attitude corrections
Figure 3.19	Histograms of science a-posteriori residuals (or innovations)
Figure 3.20	A-Posteriori Science Centroid Prediction Error Quiver (Att. Cor.)
Figure 3.21	Normalized A-Posteriori Science Centroid Prediction Errors
Figure 3.22	KF innovations with (o) and w/o (+) attitude corrections (PCRS)
Figure 3.23	Histograms of PCRS a-posteriori residuals (or innovations)
Figure 3.24	A-posteriori PCRS Prediction Summary
Figure 3.25	A-posteriori PCRS Prediction (PCRS 1 Only)
Figure 3.26	A-posteriori PCRS Prediction (PCRS 2 Only)
Figure 3.27	A-Posteriori PCRS Prediction Errors Quiver (Att. Cor.)
Figure 3.28	Normalized A-Posteriori PCRS Prediction Errors
Figure 3.29	W-axis KF innovations and 1-sigma bound
Figure 3.30	V-axis KF innovations and 1-sigma bound
Figure 3.31	Array plot with (solid) and w/o (dashed) optical distortion corrections
Figure 3.32	Optical Distortion Plot: total (x5 magnification)
Figure 3.33	Optical Distortion Plot: constant plate scales (x5 magnification)
Figure 3.34	Optical Distortion Plot: linear plate scale (x5 magnification)
Figure 3.35	Optical Distortion Plot: gamma terms (x5 magnification)
Figure 3.36	Scan Mirror Chops
Figure 3.37	IPF Frame Reconstruction
Figure 3.38	Center Pixel Reconstruction
IPF parameter trending plots	
Figure 3.39	Estimated attitude corrections (Body frame)
Figure 3.40	Estimated attitude error sigma plot (Body frame)
Figure 3.41	Systematic error attributed to thermo-mechanical boresight drift (equiv. angle in (W,V) coords)
Figure 3.42	Systematic error attributed to thermo-mechanical boresight drift (equiv. angle in Body frame)
Figure 3.43	Systematic error attributed to gyro drift bias (equiv. rate in (W,V) coords)
Figure 3.44	Systematic error attributed to gyro drift bias (equiv. angle in (W,V) coords)
Figure 3.45	Systematic error attributed to gyro drift bias (equiv. angle in Body frame)

Table 3.2: Table of figures II (IPF run)

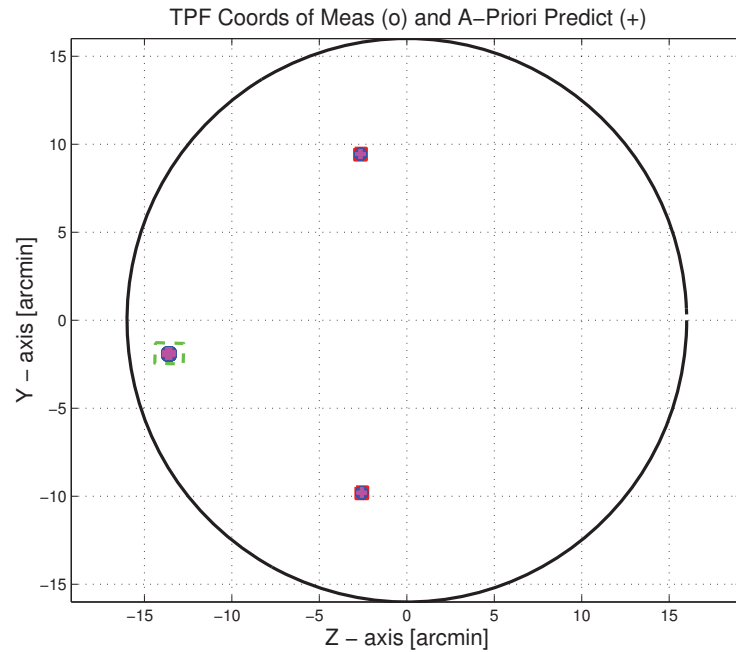


Figure 3.1: TPF coords of measurements and a-priori predicts

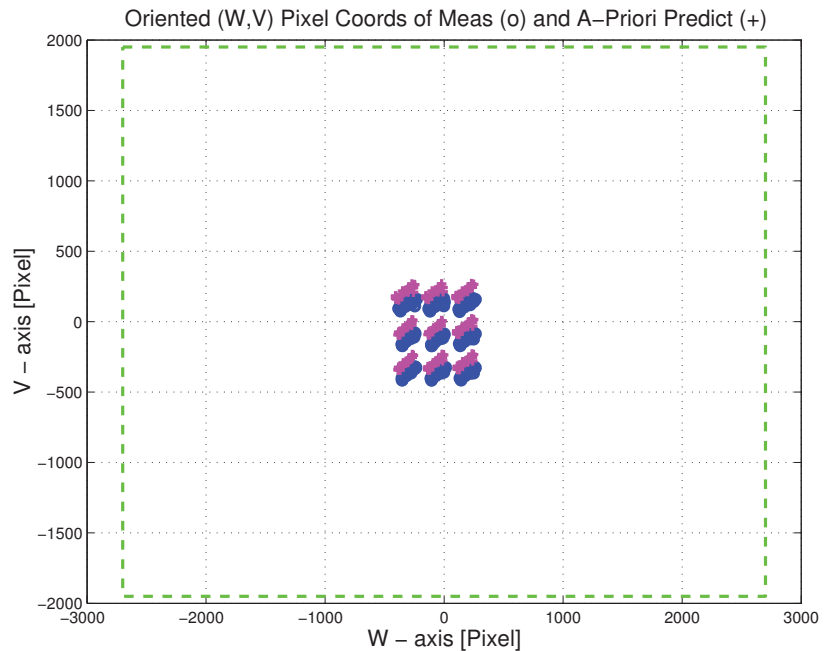


Figure 3.2: Oriented PixelCoords of measurements and a-priori predicts

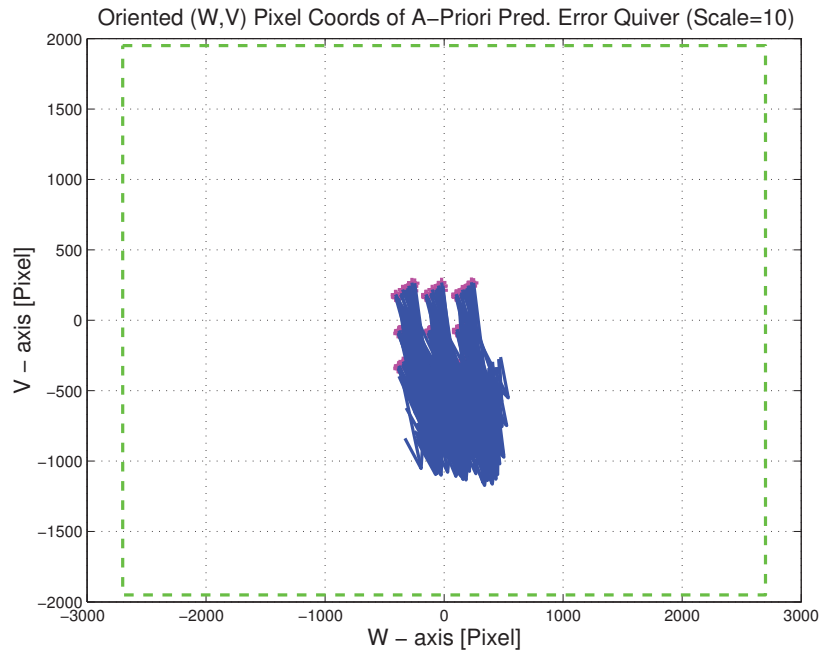


Figure 3.3: Oriented (W,V) Pixel Coords of A-Priori Prediction Error Quiver Plot

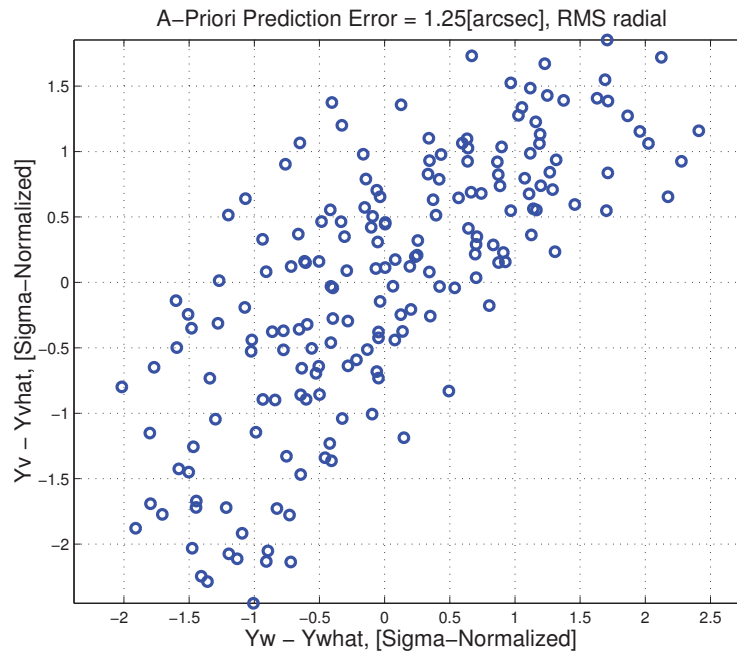


Figure 3.4: A-priori prediction error (Science Centroids)

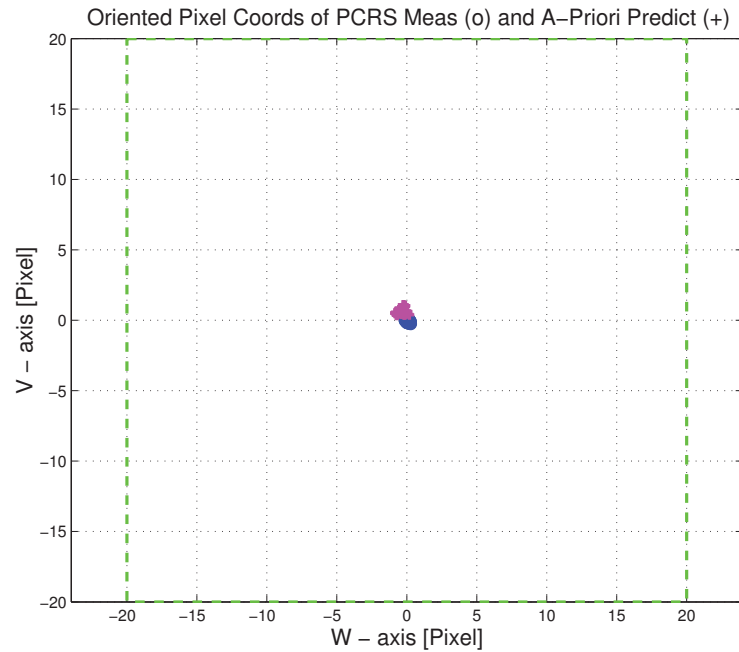


Figure 3.5: Oriented Pixel Coords of measurements and a-priori predicts (PCRS only)

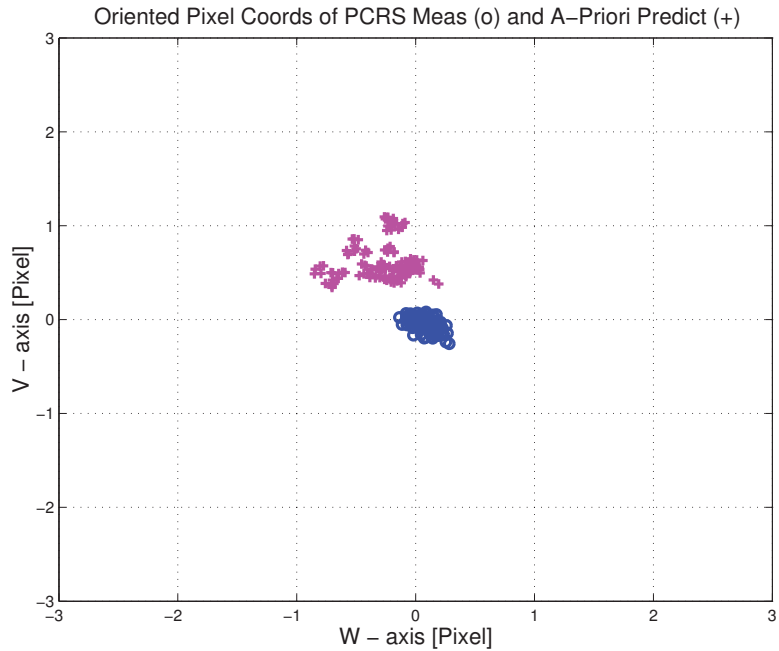


Figure 3.6: Oriented Pixel Coords of measurements and a-priori predicts (Zoomed, PCRS only)

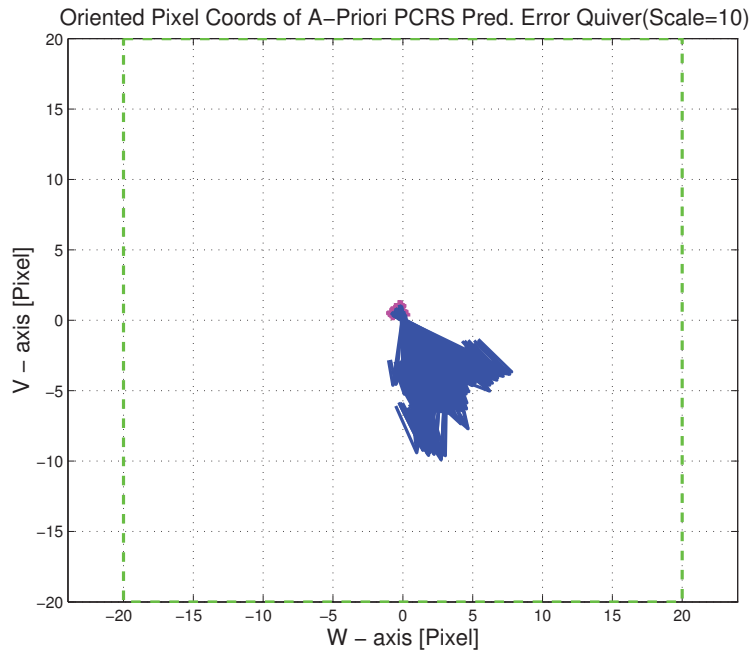


Figure 3.7: Oriented (W,V) Pixel Coords of A-Priori PCRS Prediction Error Quiver Plot

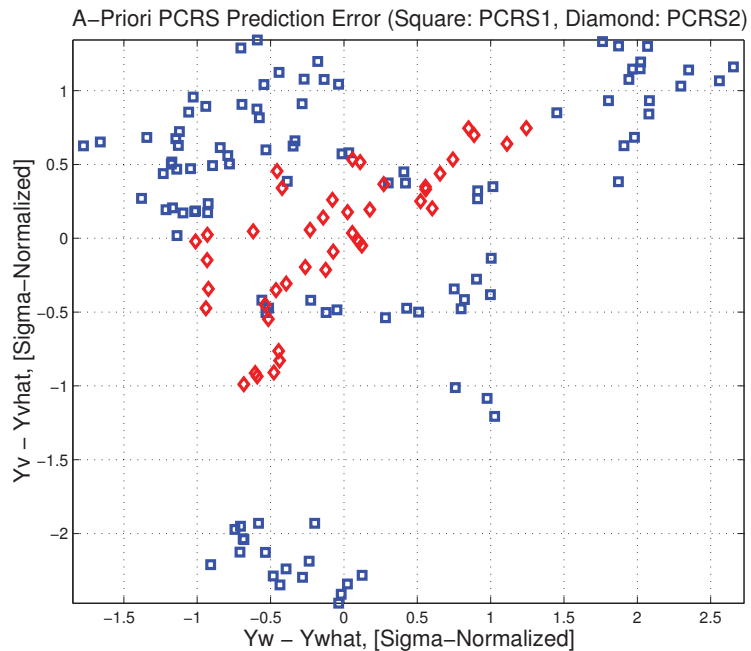


Figure 3.8: A-priori PCRS prediction error

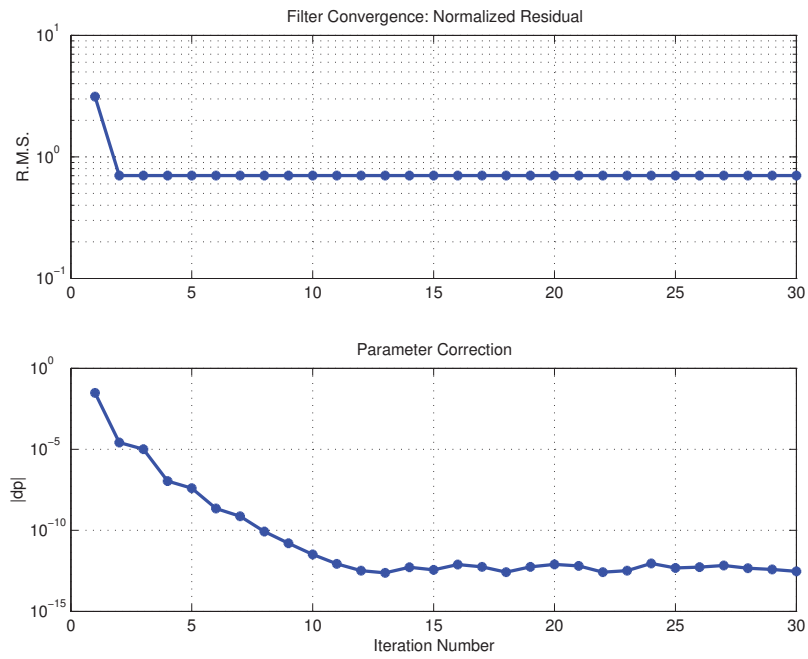


Figure 3.9: IPF execution convergence, chart 1

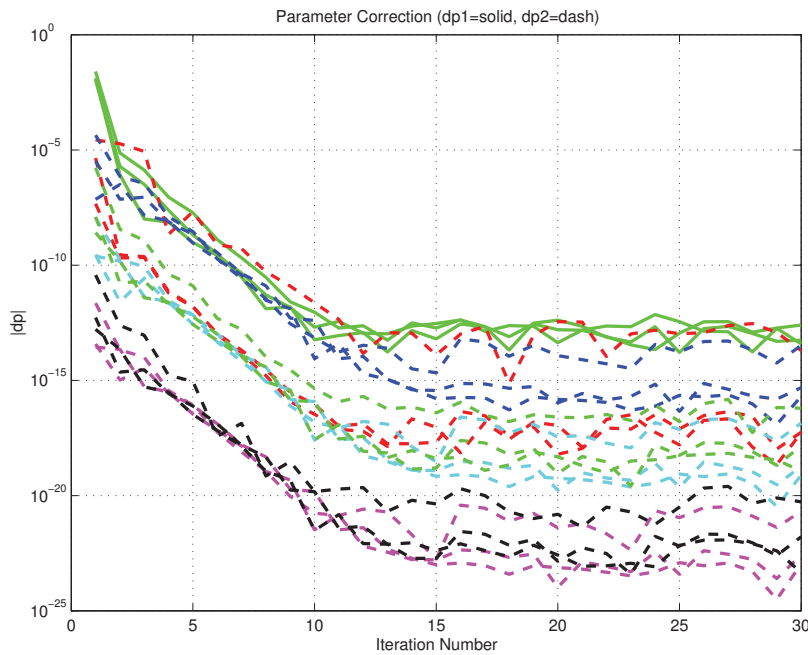


Figure 3.10: IPF execution convergence, chart 2

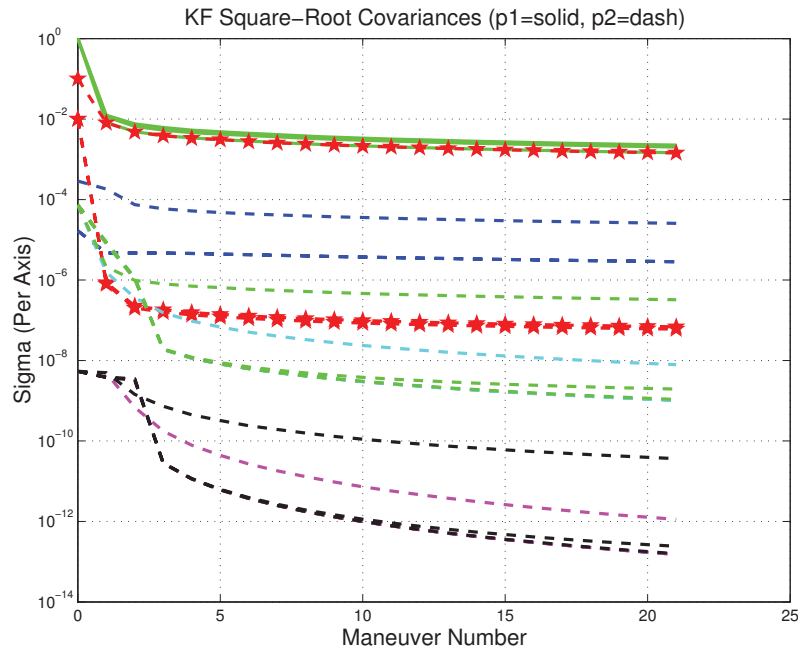


Figure 3.11: Parameter uncertainty convergence

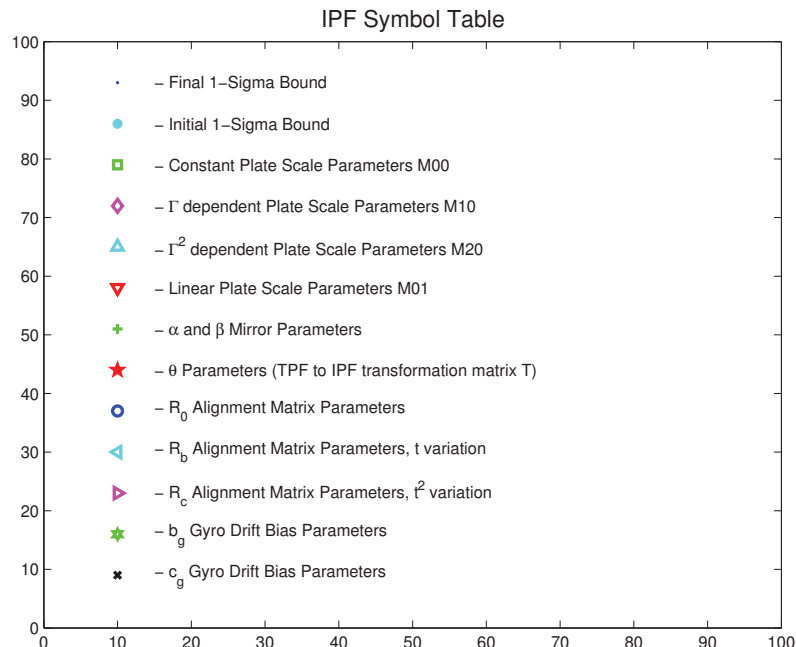


Figure 3.12: IPF parameter symbol table

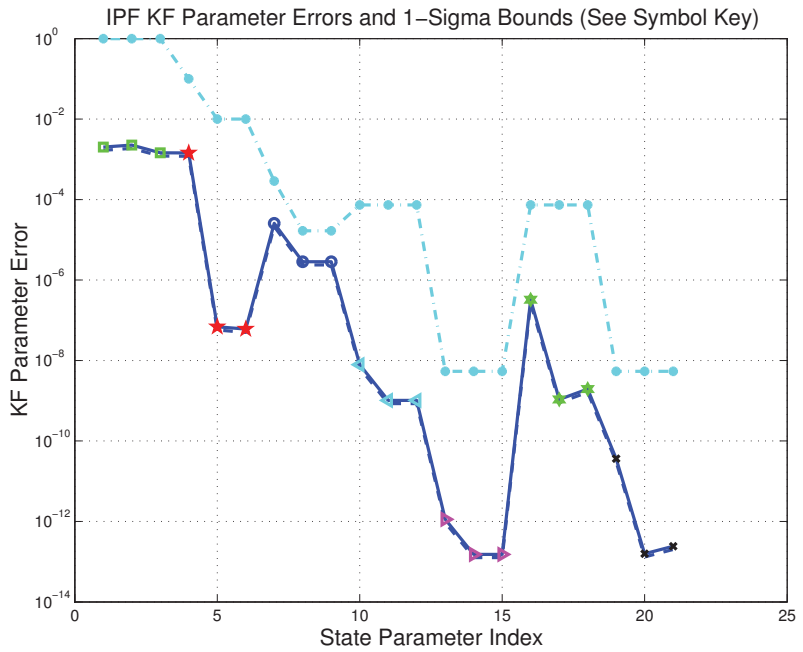


Figure 3.13: KF parameter error sigma plots

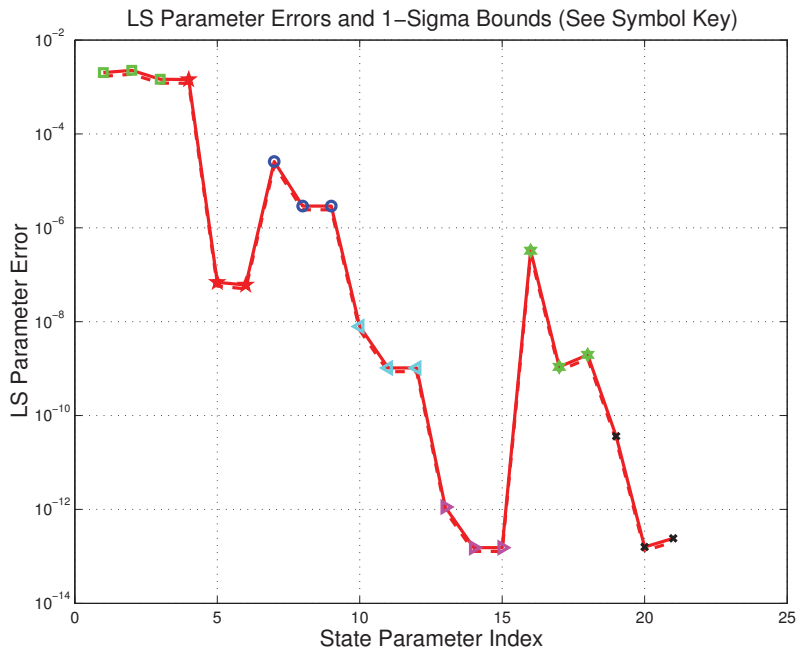


Figure 3.14: LS parameter error sigma plot

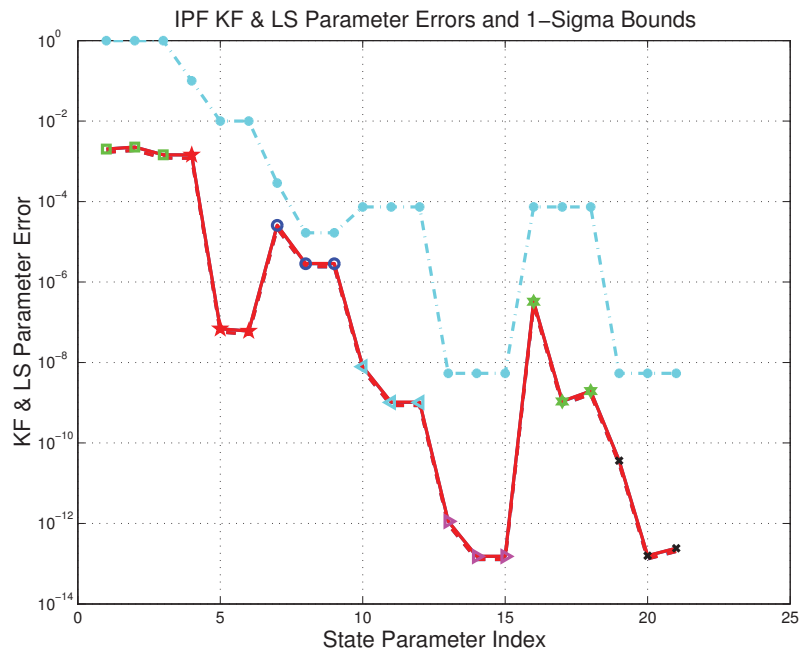


Figure 3.15: KF and LS parameter error sigma plot

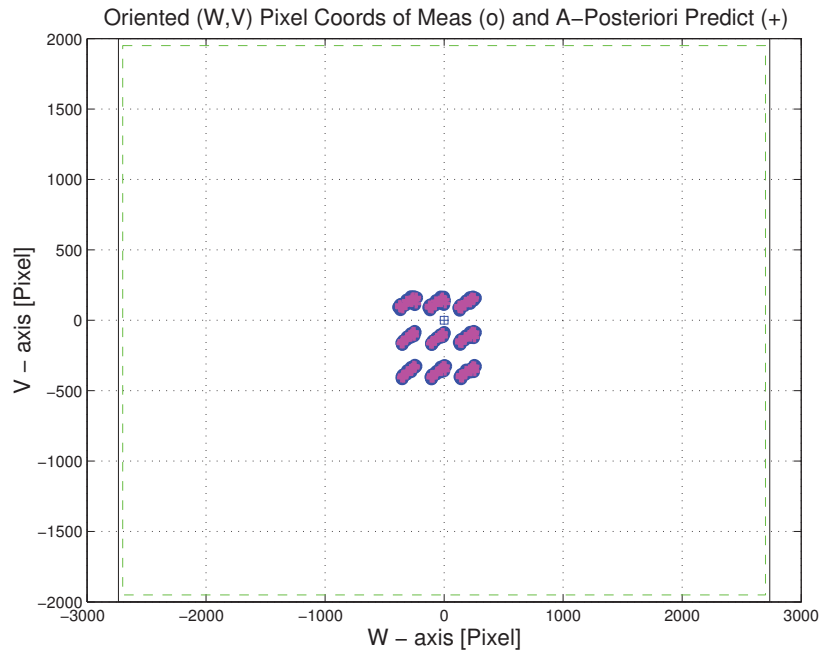


Figure 3.16: Oriented Pixel Coords of meas. and a-posteriori predicts

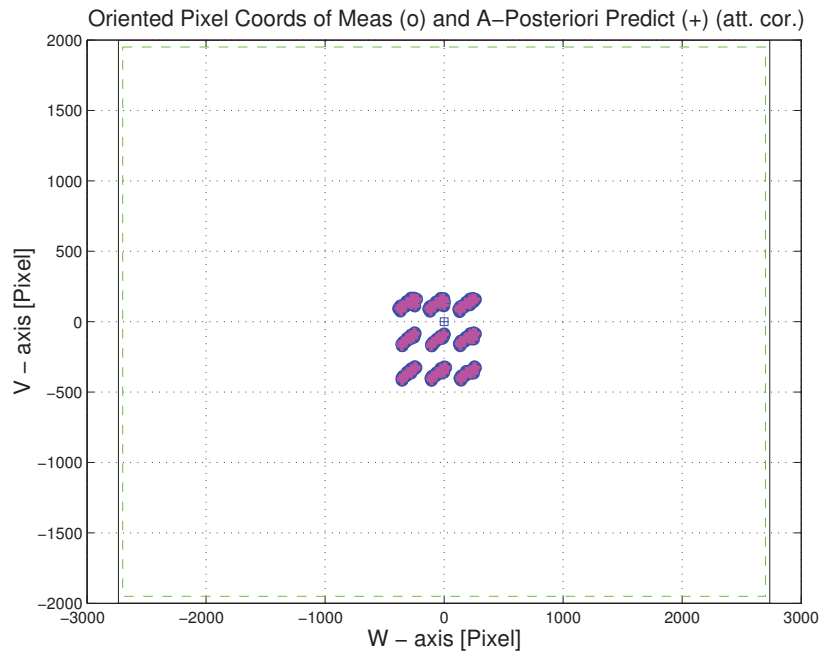


Figure 3.17: Oriented Pixel Coords of meas. and a-posteriori predicts (attitude corrected)

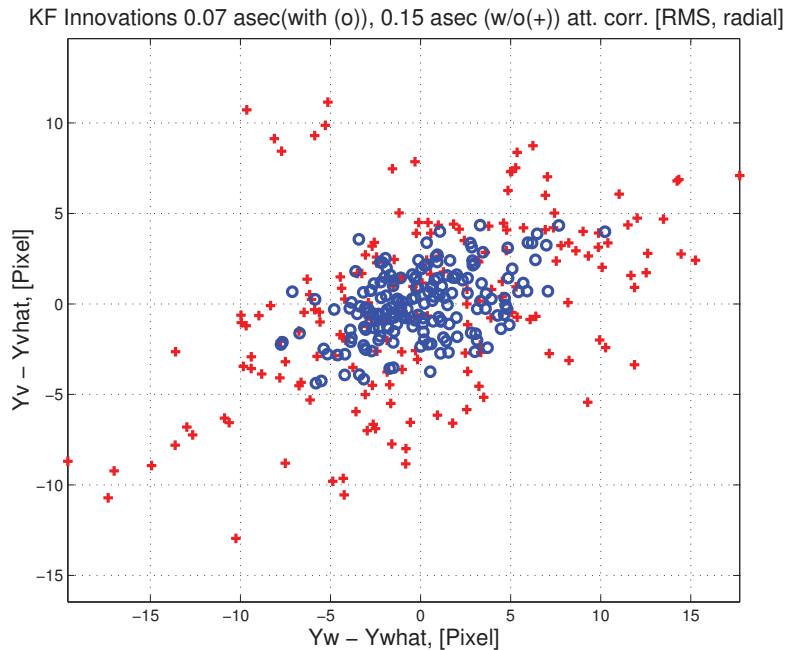


Figure 3.18: KF innovations with (o) and w/o (+) attitude corrections

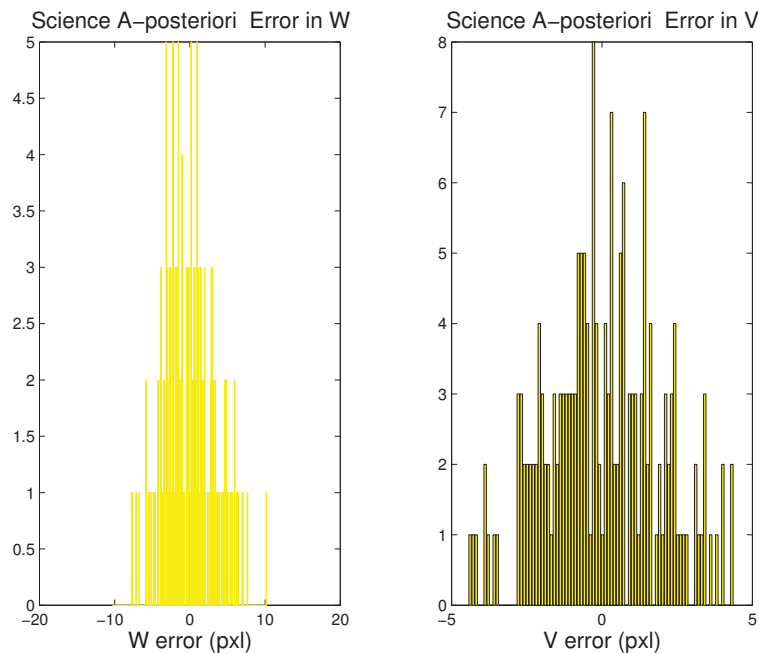


Figure 3.19: Histograms of science a-posteriori residuals (or innovations)

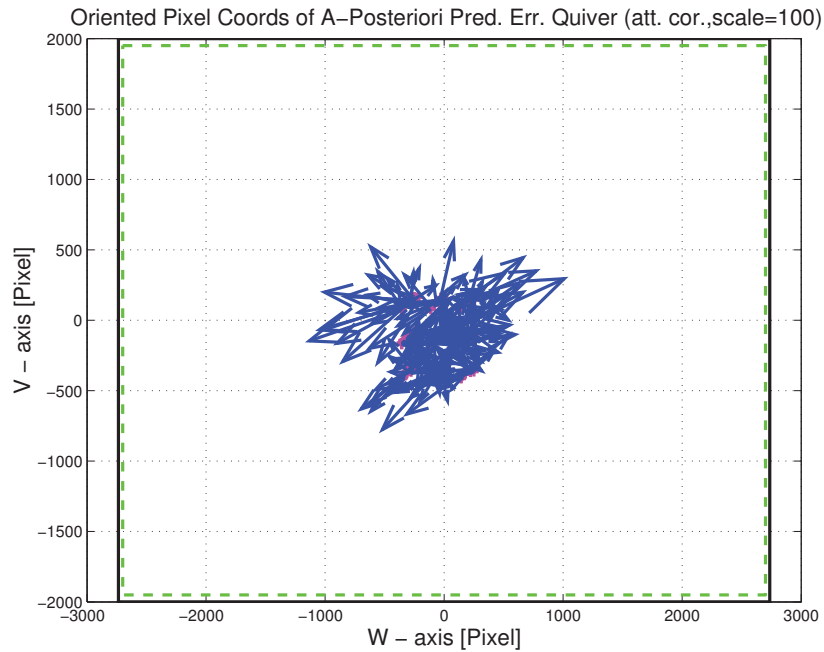


Figure 3.20: A-Posteriori Science Centroid Prediction Error Quiver (Att. Cor.)

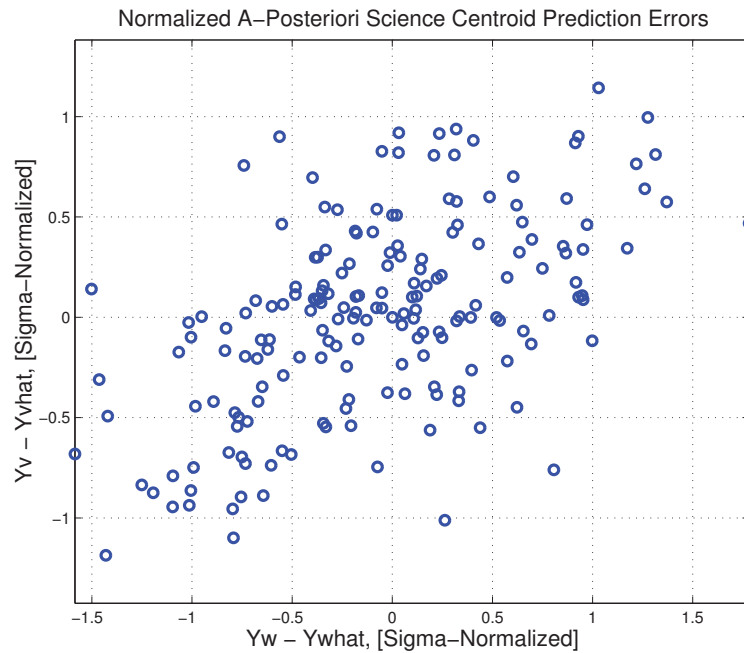


Figure 3.21: Normalized A-Posteriori Science Centroid Prediction Errors

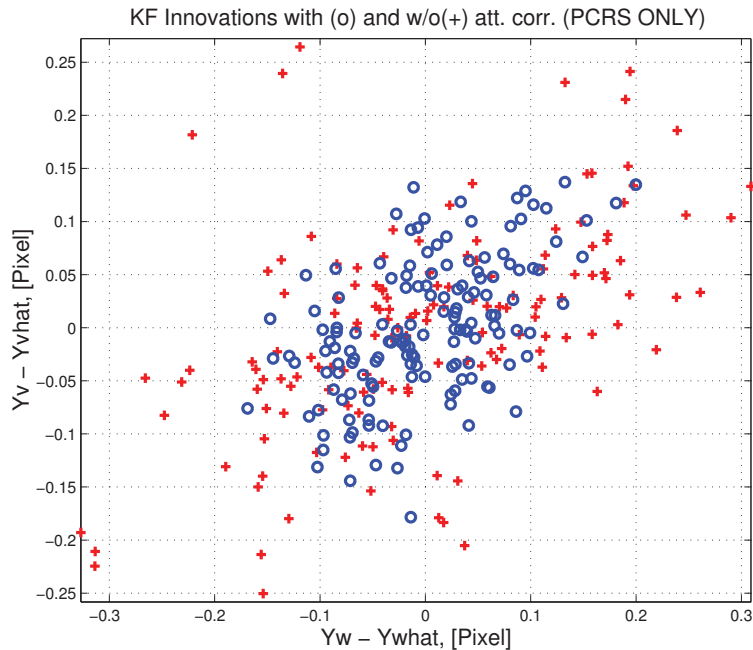


Figure 3.22: KF innovations with (o) and w/o (+) attitude corrections (PCRS)

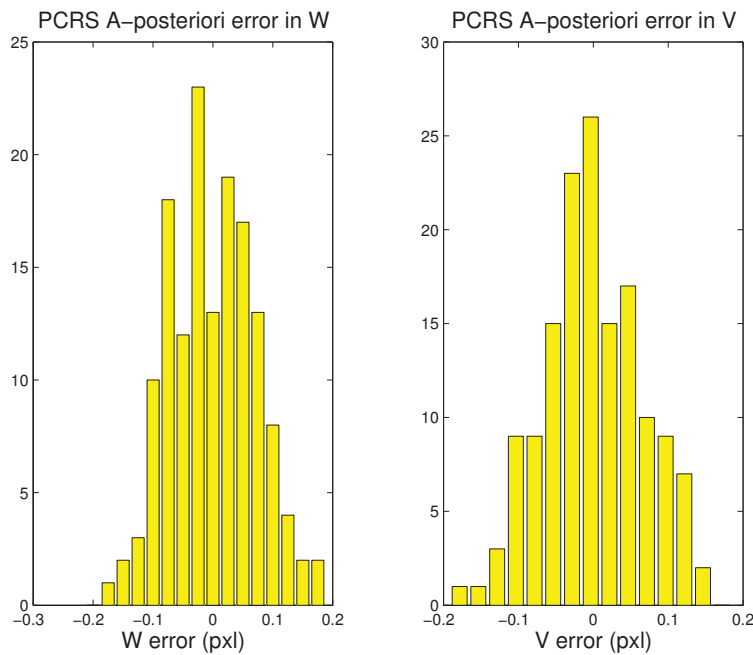


Figure 3.23: Histograms of PCRS a-posteriori residuals (or innovations)

IPF PCRS SUMMARY						
PCRS 1 (Total of 105 centroids)						
RMS	MEAN		SIGMA			
METRIC	APOST.	ATT. COR.	APOST.	ATT. COR.	STAT. CONF.	UNITS
Radial	0.0051	0.0052	0.1778	0.1049	0.0102	arcsec
W-axis	-0.0002	-0.0000	0.1420	0.0794	0.0078	arcsec
V-axis	0.0051	0.0052	0.1070	0.0685	0.0067	arcsec
PCRS 2 (Total of 42 centroids)						
METRIC	APOST.	ATT. COR.	APOST.	ATT. COR.	STAT. CONF.	UNITS
Radial	0.0144	0.0144	0.1162	0.0717	0.0111	arcsec
W-axis	-0.0001	0.0001	0.1008	0.0455	0.0070	arcsec
V-axis	-0.0144	-0.0144	0.0579	0.0554	0.0086	arcsec
Combined (Total of 147 centroids)						
METRIC	APOST.	ATT. COR.	APOST.	ATT. COR.	STAT. CONF.	UNITS
Radial	0.0005	0.0004	0.1628	0.0970	0.0080	arcsec
W-axis	-0.0002	-0.0000	0.1316	0.0714	0.0059	arcsec
V-axis	-0.0004	-0.0004	0.0960	0.0657	0.0054	arcsec

Table 3.3: PCRS measurement prediction error summary

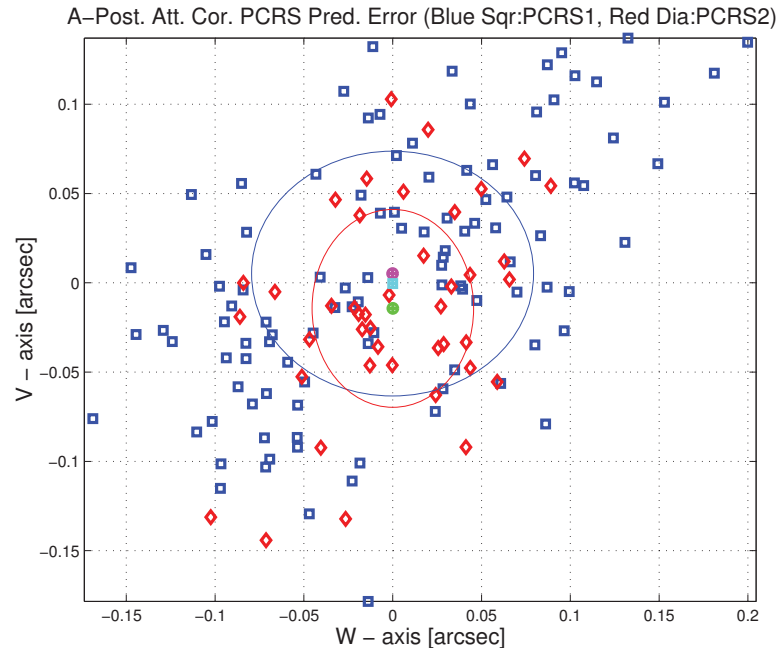


Figure 3.24: A-posteriori PCRS Prediction Summary

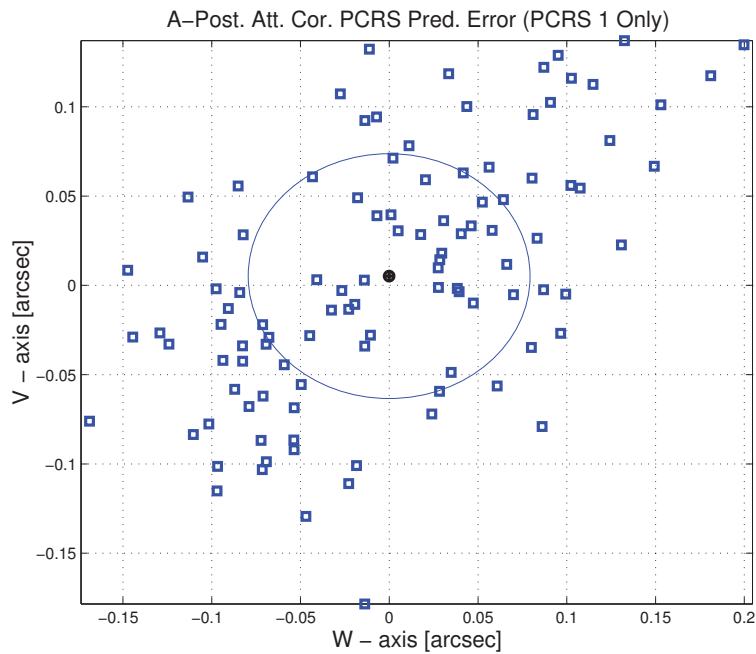


Figure 3.25: A-posteriori PCRS Prediction (PCRS 1 Only)

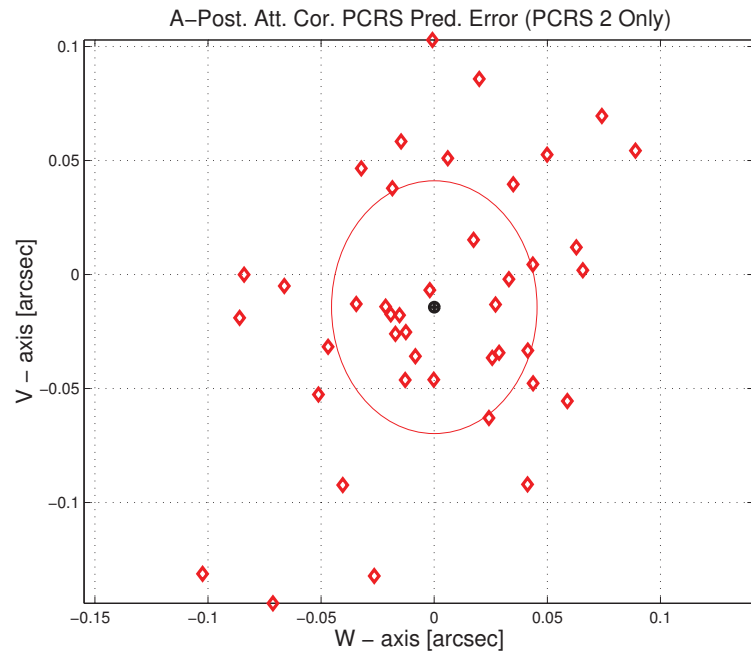


Figure 3.26: A-posteriori PCRS Prediction (PCRS 2 Only)

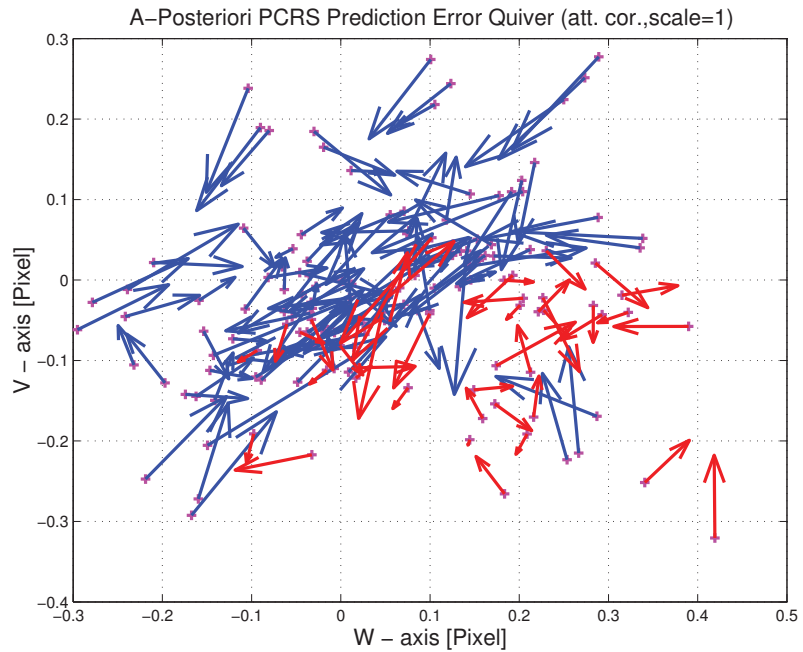


Figure 3.27: A-Posteriori PCRS Prediction Errors Quiver (Att. Cor.)

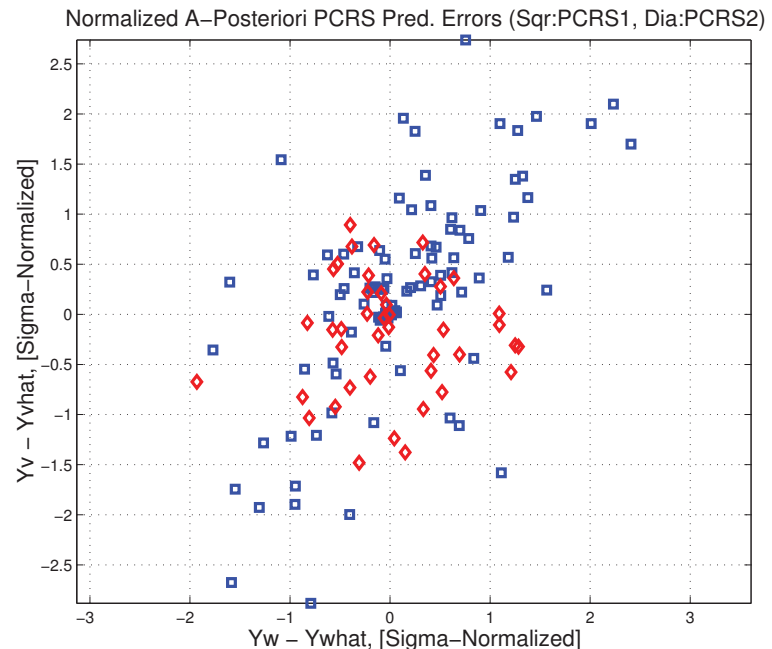


Figure 3.28: Normalized A-Posteriori PCRS Prediction Errors

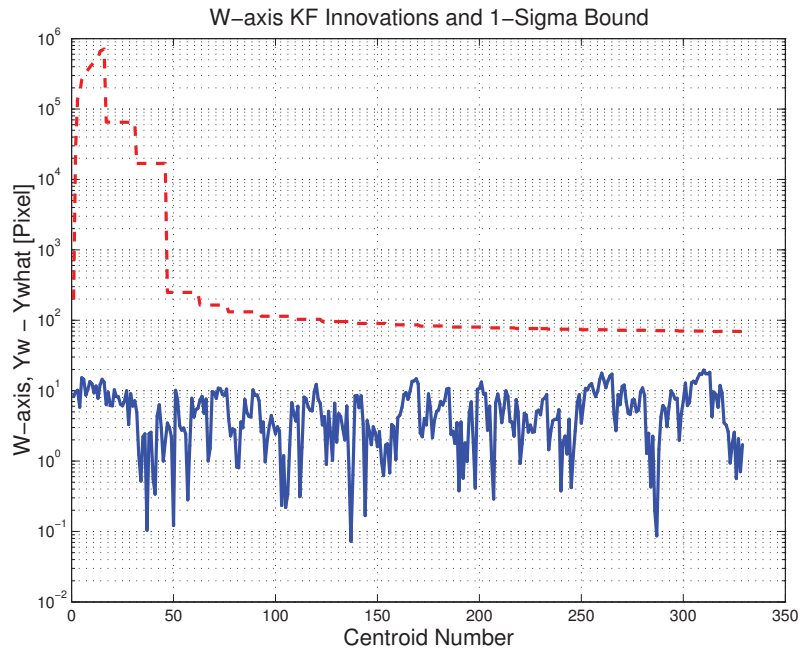


Figure 3.29: W-axis KF innovations and 1-sigma bound

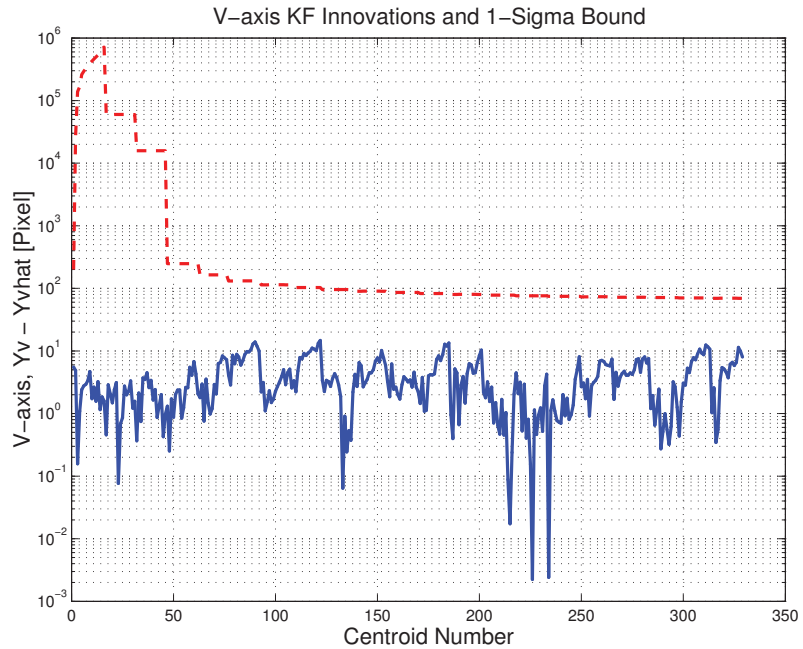


Figure 3.30: V-axis KF innovations and 1-sigma bound

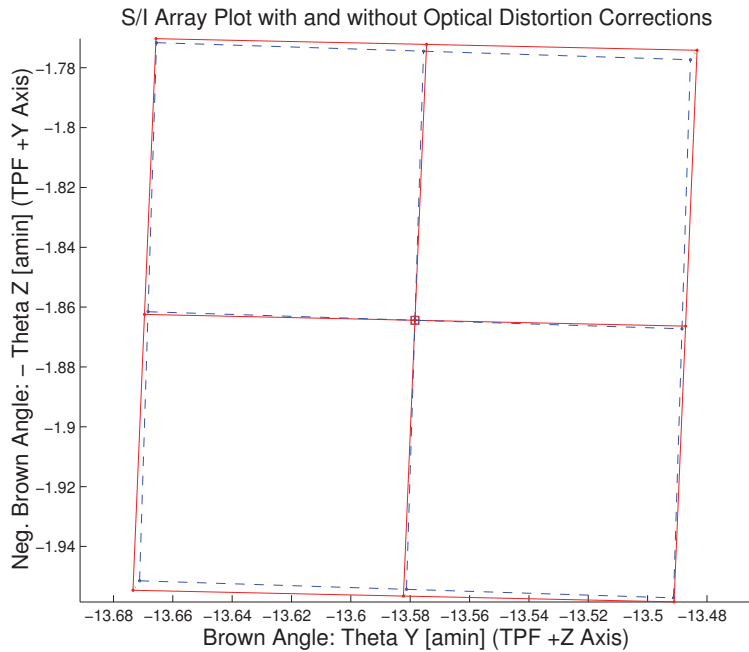


Figure 3.31: Array plot with (solid) and w/o (dashed) optical distortion corrections

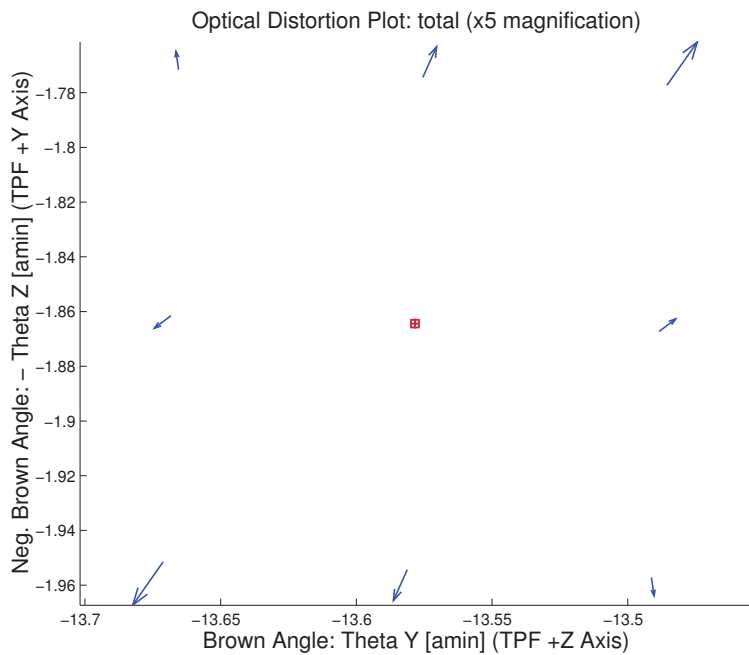


Figure 3.32: Optical Distortion Plot: total (x5 magnification)

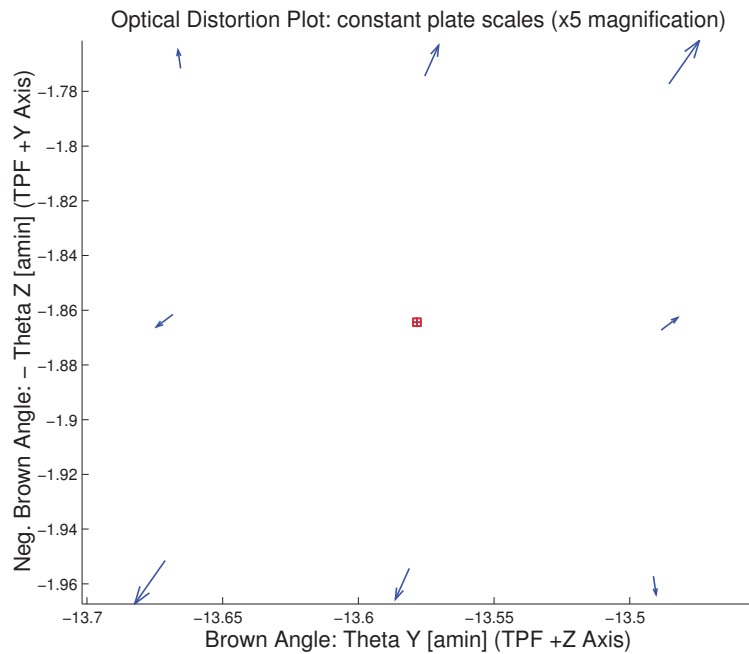


Figure 3.33: Optical Distortion Plot: constant plate scales (x5 magnification)

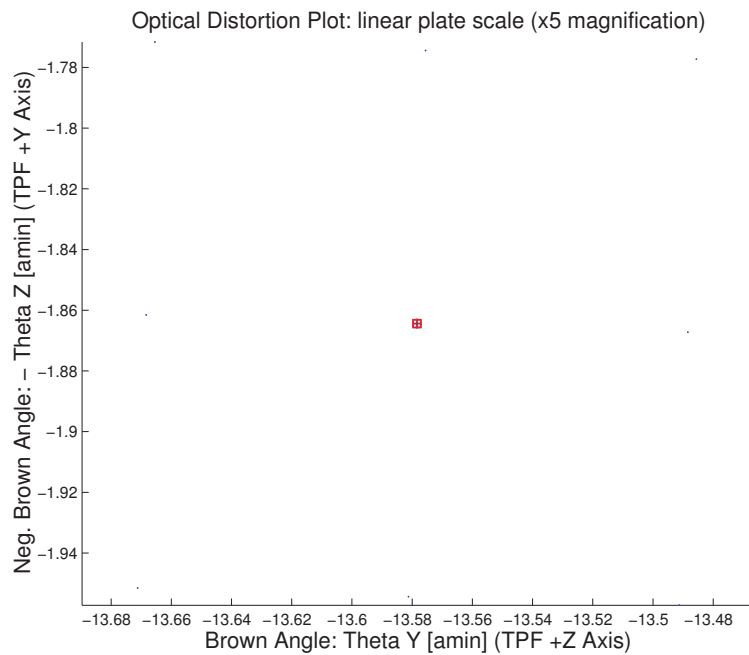


Figure 3.34: Optical Distortion Plot: linear plate scale (x5 magnification)

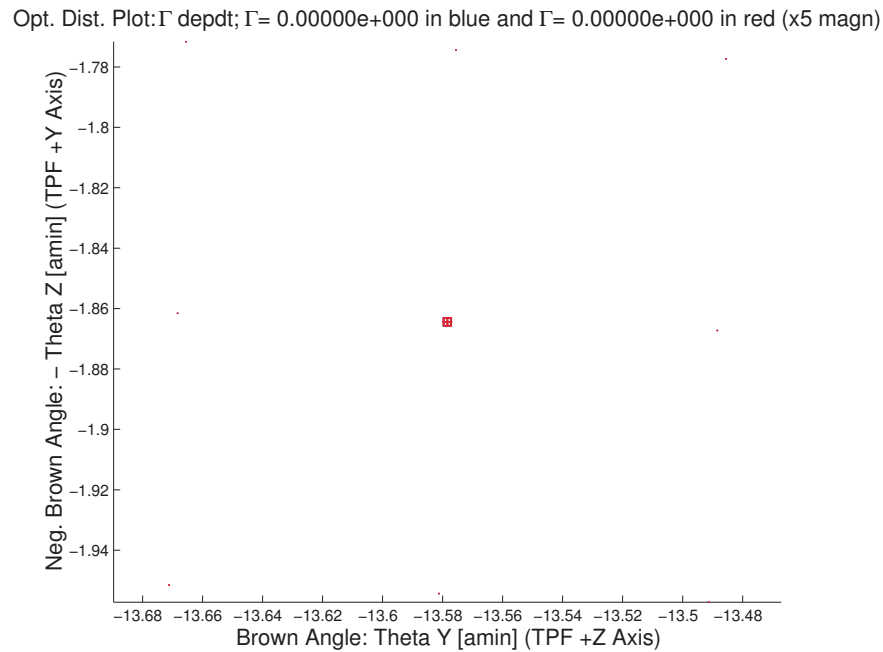


Figure 3.35: Optical Distortion Plot: gamma terms (x5 magnification)

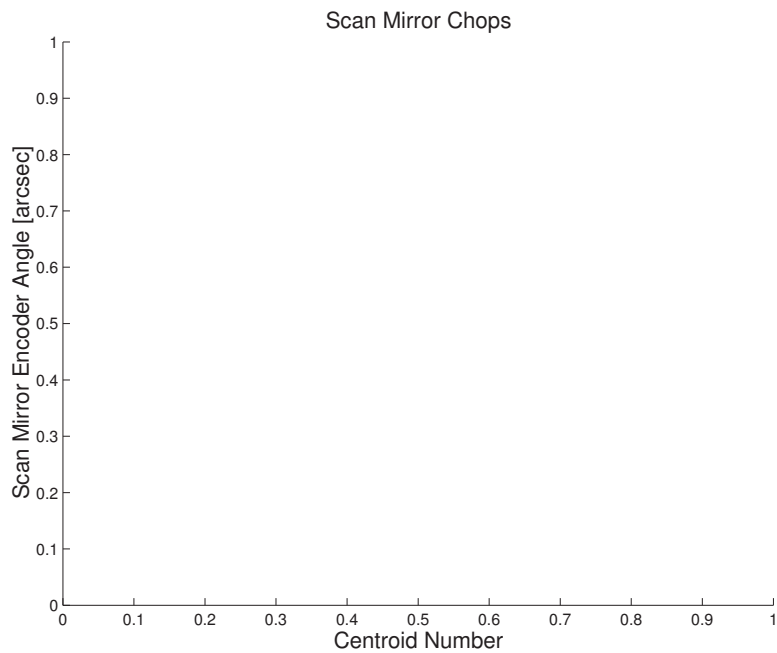


Figure 3.36: Scan Mirror Chops

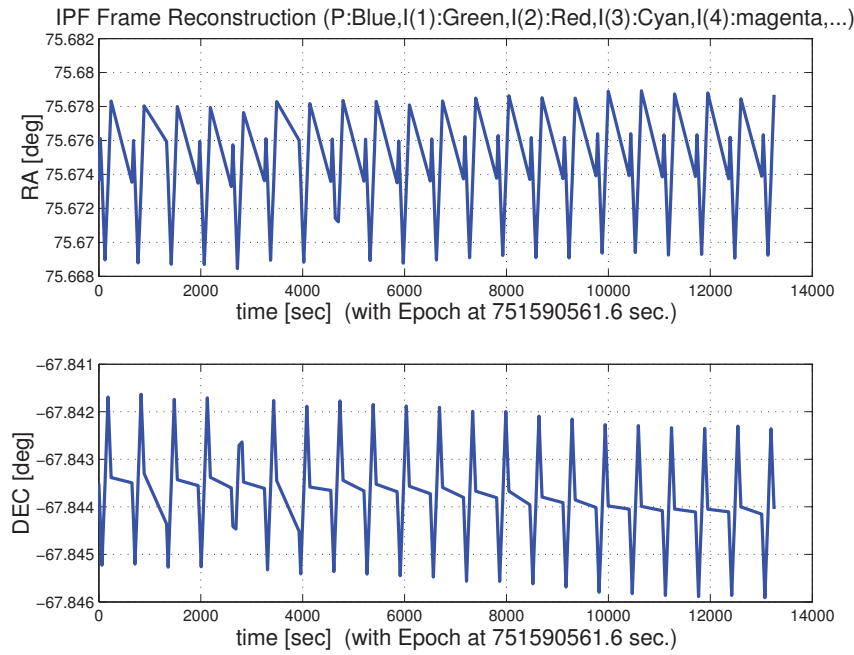


Figure 3.37: IPF Frame Reconstruction

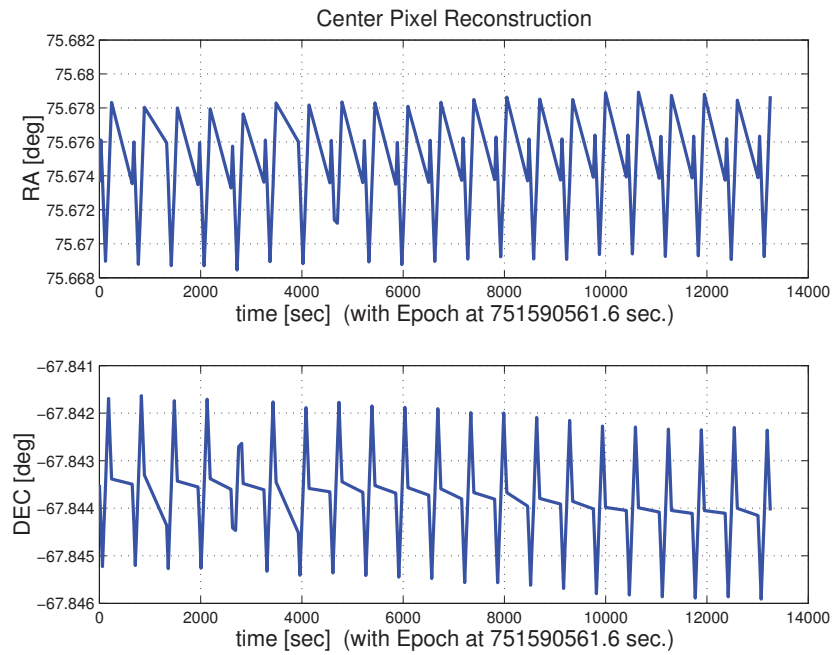


Figure 3.38: Center Pixel Reconstruction

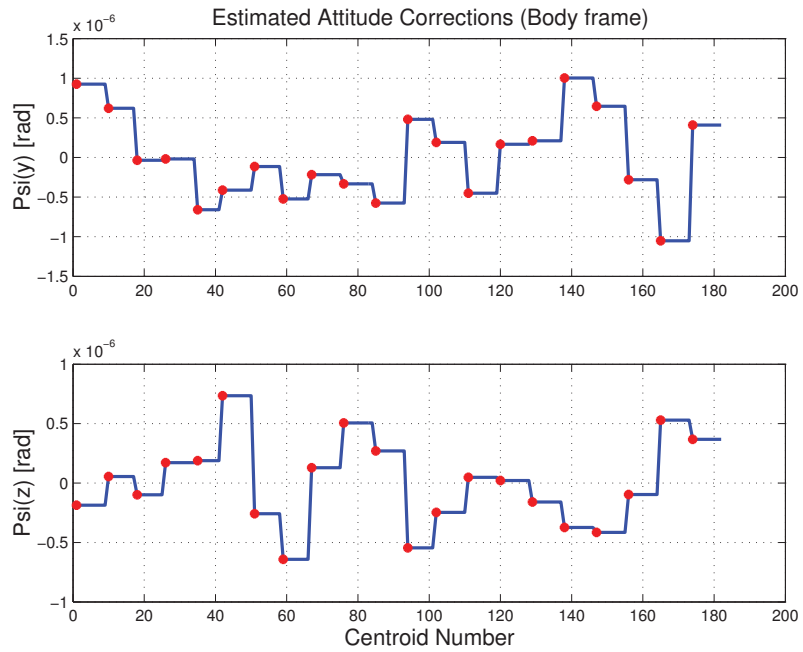


Figure 3.39: Estimated attitude corrections (Body frame)

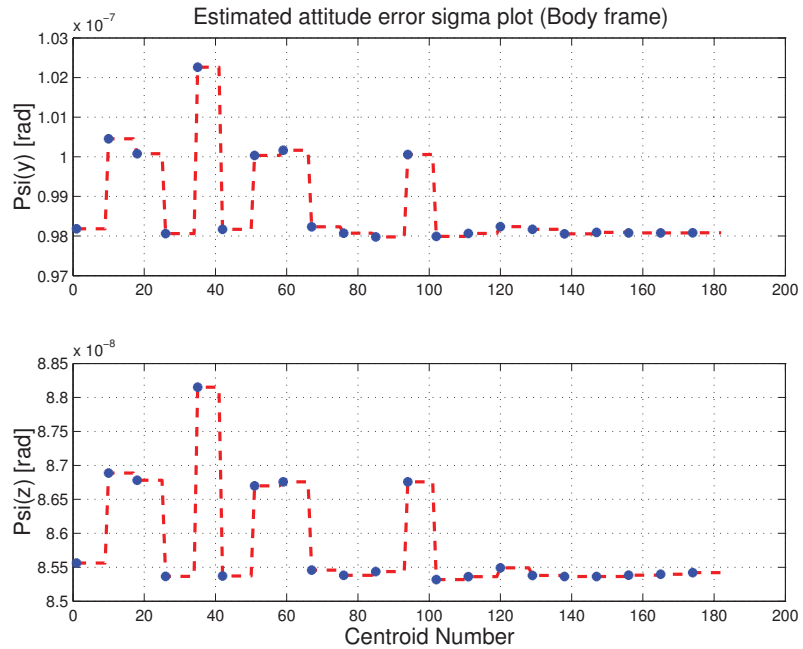


Figure 3.40: Estimated attitude error sigma plot (Body frame)

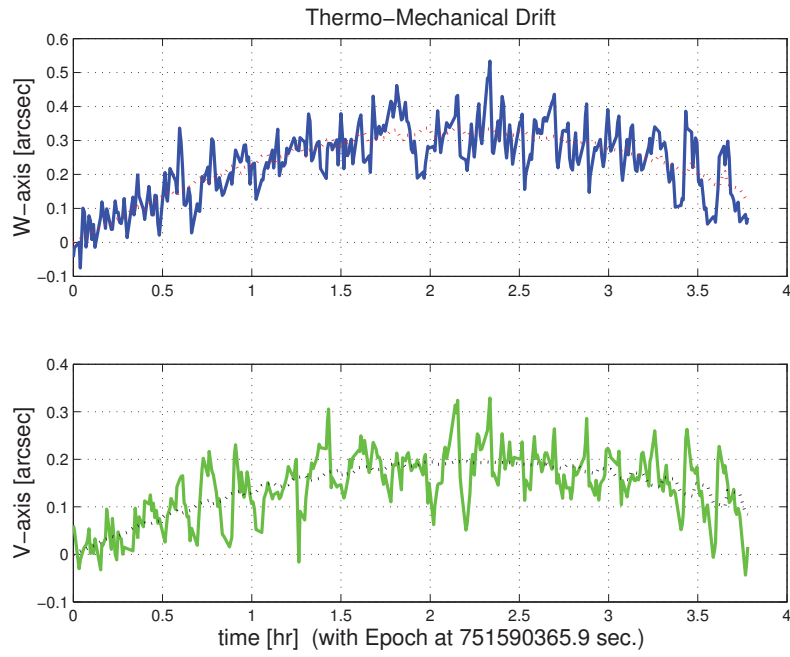


Figure 3.41: Thermo-mechanical boresight drift (equiv. angle in (W,V) coords)

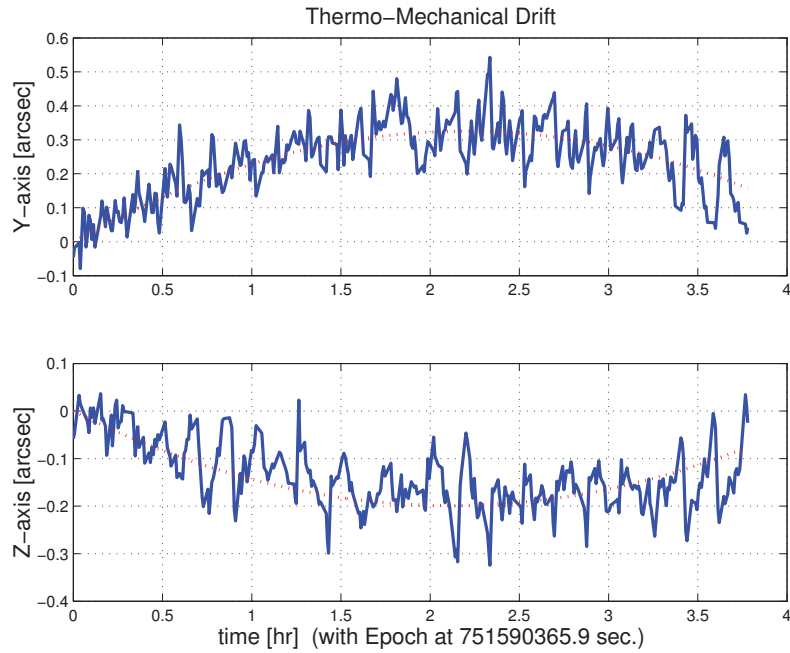


Figure 3.42: Thermo-mechanical boresight drift (equiv. angle in Body frame)

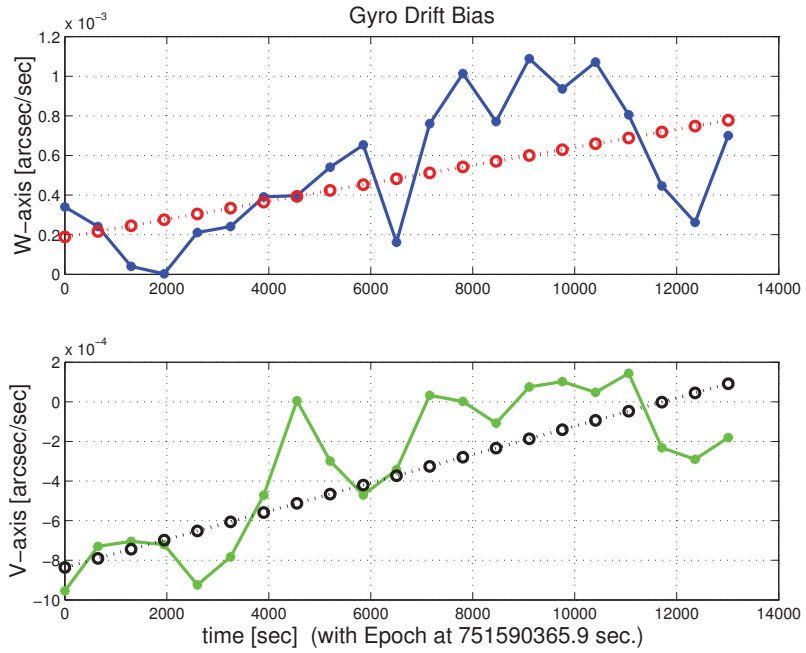


Figure 3.43: Gyro drift bias contribution (equiv. rate in (W,V) coords)

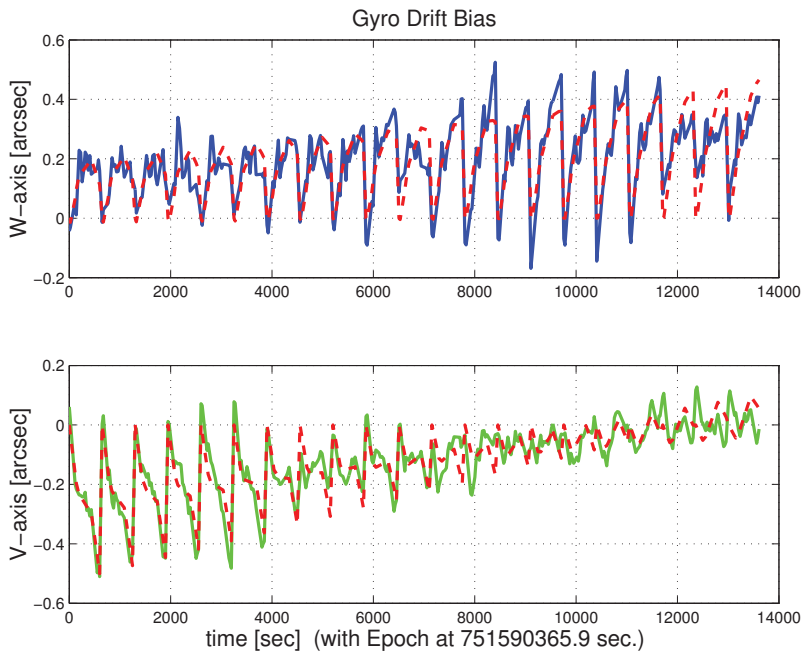


Figure 3.44: Gyro drift bias contribution (equiv. angle in (W,V) coords)

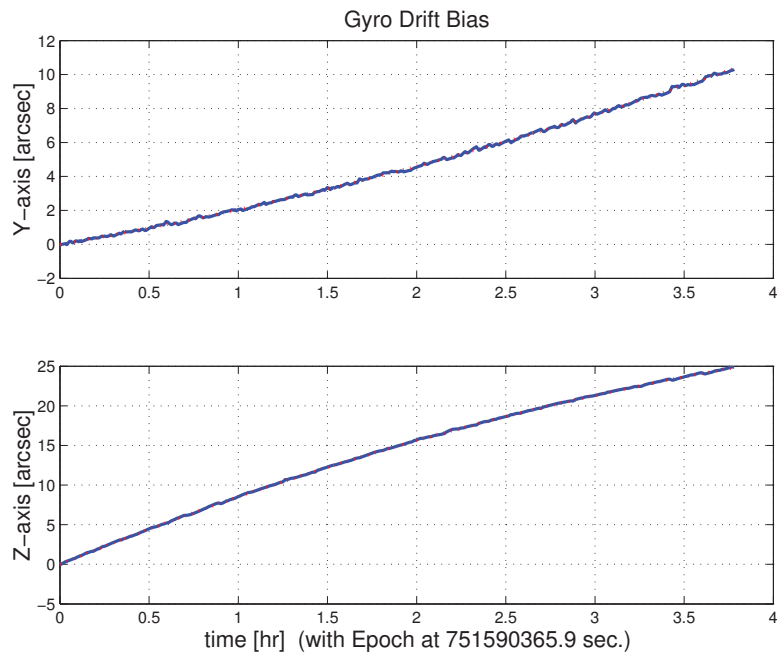


Figure 3.45: Gyro drift bias contribution (equiv. angle in Body frame)

3.2 IPF OUTPUT DATA (IF MINI FILE)

OUTPUT FILE NAME: IFmini701023.dat DATE: 26-Apr-2004 TIME: 10:33
 INSTRUMENT NAME: IRS_Blue_PeakUp_FOV_Sweet_Spot NF: 23
 IPF FILTER VERSION: IPF.V4.0.0 SW RELEASE DATE: January 30, 2004
 FRAME TABLE USED: BodyFrames_FTU_17a

----- IPF BROWN ANGLE SUMMARY -----

Frame Number	WAS			IS		
	theta_Y (arcmin)	theta_Z (arcmin)	angle (deg)	theta_Y (arcmin)	theta_Z (arcmin)	angle (deg)
023	-13.579030	+1.879766	+1.817224	-13.578384	+1.864398	+1.817225

OFFSET	NF	Delta_CW	Delta_CV
0	23	+0.000	+0.000 pixels

OFFSET FRAME NAME: IRS_Blue_PeakUp_FOV_Sweet_Spot

Brown Angle	theta_Y(arcmin)	theta_Z(arcmin)	angle(deg)
WAS(FTB)	-13.579030	+1.879766	+1.817224
IS (EST)	-13.578384	+1.864398	+1.817225
dT_EST	+0.000646	-0.015368	+0.000001
T_sSIGMA	+0.000197	+0.000172	+0.068454
dT_EST/T_sSIGMA	+3.275906	-89.265395	+0.000015

VARNAME	MEAN	SIGMA	SCALED_SIGMA
a00	+1.3233453116169183E-002	+2.0210239419119458E-003	+1.6798494896489680E-003
b00	+2.5412786439262099E-002	+2.2521610335906584E-003	+1.8719677112312976E-003
c00	+1.0575668906357950E-002	+1.4532626487390198E-003	+1.2079334975619569E-003
del_theta1	-1.9717029658278262E-014	+1.4373974158310480E-003	+1.1947465170166370E-003
del_theta2	+5.6287986323008427E-018	+6.9045510214356038E-008	+5.7389753129996327E-008
del_theta3	+5.3087442553306001E-018	+6.0252425811043069E-008	+5.0081052801898407E-008
del_arx	-3.2913458234090729E-014	+2.5646159718097155E-005	+2.1316762963799890E-005
del_ary	-4.814611081120020E-016	+2.8573062668832138E-006	+2.3749567606080790E-006
del_arz	-2.0177993723201321E-016	+2.8579889050694066E-006	+2.3755241608178983E-006
brx	+1.150955574625223E-008	+7.8750367432783803E-009	+6.5456307467828250E-009
bry	+3.9779188468430228E-010	+1.0222062833981025E-009	+8.4964490913343456E-010
brz	-2.5228713457295045E-010	+0.0225279342241174E-009	+4.991226122398686E-010
crx	-2.2606358657494025E-012	+1.1254584649614274E-012	+9.3546681401408992E-013
cry	-5.0253779901968459E-014	+1.5219122833942210E-013	+1.2649942039438074E-013
crz	+3.3118293047657479E-014	+1.5224024737269263E-013	+1.2654016439365505E-013
bgx	-1.6938822354207249E-006	+3.2401676962554928E-007	+2.6931863289964967E-007
bgy	+2.4285994279514564E-009	+1.0783794679597734E-009	+8.9633534830191390E-010
bgz	+1.2405381910519908E-008	+1.9518110213297786E-009	+1.6223205871427089E-009
cgx	+3.6850213661915362E-011	+3.6437830286672392E-011	+3.0286662785932099E-011
cgy	+1.8576678979728197E-013	+1.5768486421231551E-013	+1.3106566091534503E-013
cgz	-5.2437272745702083E-013	+2.4200895573573261E-013	+2.0115477721582709E-013

LSQF RESIDUAL SIGMA SCALE = +8.3118732777593074E-001

qT	qT(1)	qT(2)	qT(3)	qT(4)
FrmTbl:	+1.5858111556389300E-002	+1.9704047155945600E-003	-3.0468455263753702E-004	+9.9987226432702103E-001
Estim:	+1.5858115961655411E-002	+1.9703461700757078E-003	-3.0244811248178585E-004	+9.9987226505151960E-001
DelTheta	deltheta(1)	deltheta(2)	deltheta(3)	
	+8.6165794052580653E-012	-4.6144816740580204E-008	+4.4741836096685204E-006	[rad]
EulAngT	theta(1)	theta(2)	theta(3)	[rad]
Mean	+3.1716553380869504E-002	+3.9497917605119887E-003	-5.4233125947142824E-004	
SigmaT	+1.4373974158310480E-003	+6.9045510214356038E-008	+6.0252425811043069E-008	

qR	qR(1)	qR(2)	qR(3)	qR(4)
----	-------	-------	-------	-------

ASFILe: +7.0895574754104018E-004 +1.2697734637185931E-003 -1.6151434101630002E-004 +9.9999892711639404E-001
Estim: +6.8670554901240478E-004 +1.2695790361891162E-003 -1.5989254028270033E-004 +9.9999894551891177E-001
DelThetaR delthetaR(1) delthetaR(2) delthetaR(3)
-4.4504431976655421E-005 -3.9371833291417761E-007 +3.1873829588984474E-006 [rad]
EulAngR angR(1) angR(2) angR(3) [rad]
Mean +1.3730085156199556E-003 +2.5393777222429822E-003 -3.1804212021873296E-004
SigmaR +2.5646159718097155E-005 +2.8573062668832138E-006 +2.8579889050694066E-006

Initial Gyro Bias	Bg0(1)	Bg0(2)	Bg0(3)
-------------------	--------	--------	--------

-4.2707347347459290E-007 -1.9959894359544705E-007 +3.5802264619633206E-007
Gyro Bias Correction Bg(1) Bg(2) Bg(3)
-1.6938822354207249E-006 +2.4285994279514564E-009 +1.2405381910519908E-008
Total Gyro Bias BgT(1) BgT(2) BgT(3)
-2.1209557088953176E-006 -1.9717034416749559E-007 +3.7042802810685194E-007

Initial Gyro Bias Rate	Cg0(1)	Cg0(2)	Cg0(3)
------------------------	--------	--------	--------

+0.0000000000000000E+000 +0.0000000000000000E+000 +0.0000000000000000E+000
Gyro Bias Rate Correction Cg(1) Cg(2) Cg(3)
+3.6850213661915362E-011 +1.8576678979728197E-013 -5.2437272745702083E-013
Total Gyro Bias Rate CgT(1) CgT(2) CgT(3)
+3.6850213661915362E-011 +1.8576678979728197E-013 -5.2437272745702083E-013

q(1)	q(2)	q(3)	q(4)
------	------	------	------

PCRS1A: +5.3371888965461637E-007 +3.7444233778550031E-004 -1.4253684912431913E-003 +9.9999891405806784E-001
PCRS2A: -5.2779261998836216E-007 +3.8462959425181312E-004 +1.3722087221825403E-003 +9.9999898455099423E-001

***** CS-FILE PARAMETERS: ***** AS-FILE PARAMETERS: *****

Row (01) PIX2RADX:	+8.7265999999999995E-008	Row (1) TASTART:	+7.5159016509075928E+008
Row (02) PIX2RADY:	+8.7265999999999995E-008	Row (2) TASTOP:	+7.5160417499077451E+008
Row (03) CX0:	+1.0800000000000000E+004	Row (3) S/C TIME:	+7.5158472999073792E+008
Row (04) CY0:	+2.8000000000000000E+003	Row (4) QR1:	+7.0895574754104018E-004
Row (05) BETA0:	+9.9999000000000000E+004	Row (5) QR2:	+1.2697734637185931E-003
Row (06) GAMMA_E0:	+9.9999000000000000E+004	Row (6) QR3:	-1.6151434101630002E-004
Row (07) D11:	+0.0000000000000000E+000	Row (7) QR4:	+9.9999892711639404E-001
Row (08) D12:	+1.0000000000000000E+000		
Row (09) D21:	+1.0000000000000000E+000		
Row (10) D22:	+0.0000000000000000E+000		
Row (11) DG:	+9.9999000000000000E+004		

INITIAL STA-TO-PCRS ALIGNMENT (R) KNOWLEDGE (1-SIGMA)

SIGMA(X)	SIGMA(Y)	SIGMA(Z)
----------	----------	----------

5.93454643E+000 3.44777762E-001 3.45078359E-001 [arcsec]

PIX2RADX = 8.726600000000E-008 [rad/pixel]
XPIXSIZE = 0.0180 [arcsec]
PIX2RADY = 8.726600000000E-008 [rad/pixel]
YPIXSIZE = 0.0180 [arcsec]
CX0 = 10800.0 [pixel] = 194.40 [arcsec]
CY0 = 2800.0 [pixel] = 50.40 [arcsec]

NOMINAL BETA0 = 9.999900000000E+004 [rad/encoder unit]
ENCODER UNIT SIZE = 99999.00 [arcsec]
GAMMA_E0 = 99999.00 [encoder unit] = 99999.00 [arcsec]

FLIP MATRIX D = | +0 | +1 |
| --- | --- | and DG = +99999
| +1 | +0 |

3.3 IPF EXECUTION LOG

```
*****
IPF EXECUTION-LOG FILE NAME: LG701023.dat
INSTRUMENT TYPE: IRS_Blue_PeakUp_FOV_Sweet_Spot
IPF FILTER EXECUTION DATE: 26-Apr-2004 TIME: 10:30
IPF FILTER VERSION USED: IPF.V4.0.0
*****


----- Loading & Preparing Input Files -----
AAFILE: AA501023 Loaded! AAFILE dimension = 140100 X 21
ASFIL: AS501023 Loaded!
CAFIL: CA501023 Loaded! CAFIL dimension = 182 X 15
CBFILE: CB501023 Loaded! CBFILE dimension = 147 X 15
CCFILE: CC701023 Created! CCFILE dimension = 329 X 19
CSFILE: CS701023 Loaded!
Loading Input Files Completed!
-----


----- Selected Mask Vectors -----
index = 1 2 3 4 5 6 7 8 9 10 11 12 13 14 15 16 17 18 19 20
-----
mask1 = [ 1 1 1 0 0 0 0 0 0 0 0 0 0 0 0 0 0 0 0 0 0 ]
mask2 = [ 0 0 1 1 1 1 1 1 1 1 1 1 1 1 1 1 1 1 1 1 1 ]


----- Selected Initial Gyro Bias Parameters -----
User Entered 1 : Use AFILE database - from S/C filter
IPF Linearized Using Following Nominal Gyro Bias Estimates
bg0 = [-4.2707347347459290E-007 -1.9959894359544705E-007 +3.5802264619633206E-007 ]
cg0 = [+0.000000000000000E+000 +0.000000000000000E+000 +0.000000000000000E+000 ]


----- Gyro Pre-Processor Run Completed -----
AGFILE CREATED: AG701023.m ACFILE CREATED: AC701023.m
-----


Total Gyro Preprocessor Execution Time: 65 seconds

FRAME TABLE ENTRIES FOR PCRS LOADED TO TPCRS
q_PCRS4 = [ +5.337188965461637E-007 q_PCRS5 = [ +7.3379987833742897E-007
            +3.7444233778550031E-004 +5.2236196154513707E-004
            -1.4253684912431913E-003 -1.4047712280184723E-003
            +9.9999891405806784E-001 ]; +9.9999887687698918E-001 ];
q_PCRS8 = [ -5.2779261998836216E-007 q_PCRS9 = [ -7.1963421681856818E-007
            +3.8462959425181312E-004 +5.3239763239987400E-004
            +1.3722087221825403E-003 +1.3516841804518383E-003
            +9.9999898455099423E-001 ]; +9.9999894475050310E-001 ];


----- Initial Conditions for State ----- ----- Initial Square-Root Cov (diag) -----
p1(01) = a00 = +0.000000000000000E+000 Sigma_initial(01,01) = 1.000000000000000E+000
p1(02) = b00 = +0.000000000000000E+000 Sigma_initial(02,02) = 1.000000000000000E+000
p1(03) = c00 = +0.000000000000000E+000 Sigma_initial(03,03) = 1.000000000000000E+000
p1(04) = a10 = +0.000000000000000E+000 Sigma_initial(04,04) = 9.999900000000000E+004
p1(05) = b10 = +0.000000000000000E+000 Sigma_initial(05,05) = 9.999900000000000E+004
p1(06) = c10 = +0.000000000000000E+000 Sigma_initial(06,06) = 9.999900000000000E+004
p1(07) = d10 = +0.000000000000000E+000 Sigma_initial(07,07) = 9.999900000000000E+004
p1(08) = a20 = +0.000000000000000E+000 Sigma_initial(08,08) = 9.999900000000000E+004
p1(09) = b20 = +0.000000000000000E+000 Sigma_initial(09,09) = 9.999900000000000E+004
p1(10) = c20 = +0.000000000000000E+000 Sigma_initial(10,10) = 9.999900000000000E+004
p1(11) = d20 = +0.000000000000000E+000 Sigma_initial(11,11) = 9.999900000000000E+004
p1(12) = a01 = +0.000000000000000E+000 Sigma_initial(12,12) = 9.999900000000000E+004
p1(13) = b01 = +0.000000000000000E+000 Sigma_initial(13,13) = 9.999900000000000E+004
```

```

p1(14) = c01 = +0.0000000000000000E+000 Sigma_initial(14,14) = 9.9999000000000000E+004
p1(15) = d01 = +0.0000000000000000E+000 Sigma_initial(15,15) = 9.9999000000000000E+004
p1(16) = e01 = +0.0000000000000000E+000 Sigma_initial(16,16) = 9.9999000000000000E+004
p1(17) = f01 = +0.0000000000000000E+000 Sigma_initial(17,17) = 9.9999000000000000E+004
-----
p2f(01) = am1 = +0.0000000000000000E+000 Sigma_initial(18,18) = 9.9999000000000000E+004
p2f(02) = am2 = +0.0000000000000000E+000 Sigma_initial(19,19) = 9.9999000000000000E+004
p2f(03) = am3 = +1.0000000000000000E+000 Sigma_initial(20,20) = 1.0000000000000000E-001
p2f(04) = beta = +1.0000000000000000E+000 Sigma_initial(21,21) = 1.0000000000000000E-002
p2f(05) = qT1 = +1.5858111556389307E-002 Sigma_initial(22,22) = 1.0000000000000000E-002
p2f(06) = qT2 = +1.9704047155945609E-003 Sigma_initial(23,23) = 2.8771492986883954E-004
p2f(07) = aT3 = -3.0468455263753713E-004 Sigma_initial(24,24) = 1.6715297603189757E-005
p2f(08) = qT4 = +9.9987226432702148E-001 Sigma_initial(25,25) = 1.6729870951362112E-005
p2f(09) = qr1 = +7.0895574754104018E-004 Sigma_initial(26,26) = 7.3484943416182282E-005
p2f(10) = qr2 = +1.2697734637185931E-003 Sigma_initial(27,27) = 7.3484943416182282E-005
p2f(11) = qr3 = -1.6151434101630002E-004 Sigma_initial(28,28) = 7.3484943416182282E-005
p2f(12) = qr4 = +9.999892711639404E-001 Sigma_initial(29,29) = 5.4000369088795115E-009
p2f(13) = brx = +0.0000000000000000E+000 Sigma_initial(30,30) = 5.4000369088795115E-009
p2f(14) = bry = +0.0000000000000000E+000 Sigma_initial(31,31) = 5.4000369088795115E-009
p2f(15) = brz = +0.0000000000000000E+000 Sigma_initial(32,32) = 7.3484943416182282E-005
p2f(16) = crx = +0.0000000000000000E+000 Sigma_initial(33,33) = 7.3484943416182282E-005
p2f(17) = cry = +0.0000000000000000E+000 Sigma_initial(34,34) = 7.3484943416182282E-005
p2f(18) = crz = +0.0000000000000000E+000 Sigma_initial(35,35) = 5.4000369088795115E-009
p2f(19) = bgx = +0.0000000000000000E+000 Sigma_initial(36,36) = 5.4000369088795115E-009
p2f(20) = bgy = +0.0000000000000000E+000 Sigma_initial(37,37) = 5.4000369088795115E-009
p2f(21) = bgz = +0.0000000000000000E+000
p2f(22) = cgx = +0.0000000000000000E+000
p2f(23) = cgy = +0.0000000000000000E+000
p2f(24) = cgz = +0.0000000000000000E+000
-----
```

```

----- IPF KALMAN FILTER STARTED -----
Iteration#001: |dp|= +3.059764367091E-002 RMS(|Res|)=+7.448908559771E-006
Iteration#002: |dp|= +2.616794601895E-005 RMS(|Res|)=+7.281627792083E-007
Iteration#003: |dp|= +1.011295633443E-005 RMS(|Res|)=+7.428683972903E-007
Iteration#004: |dp|= +1.097910938958E-007 RMS(|Res|)=+7.450147899834E-007
Iteration#005: |dp|= +4.011477173829E-008 RMS(|Res|)=+7.446699728774E-007
Iteration#006: |dp|= +2.243735306895E-009 RMS(|Res|)=+7.445638085316E-007
Iteration#007: |dp|= +7.404528157724E-010 RMS(|Res|)=+7.445671015859E-007
Iteration#008: |dp|= +8.352348435109E-011 RMS(|Res|)=+7.445703987781E-007
Iteration#009: |dp|= +1.585303989393E-011 RMS(|Res|)=+7.445705027233E-007
Iteration#010: |dp|= +3.280319862639E-012 RMS(|Res|)=+7.445704124549E-007
Iteration#011: |dp|= +8.561792425821E-013 RMS(|Res|)=+7.445704039085E-007
Iteration#012: |dp|= +3.249749315118E-013 RMS(|Res|)=+7.445704060632E-007
Iteration#013: |dp|= +2.374682619749E-013 RMS(|Res|)=+7.445704064064E-007
Iteration#014: |dp|= +5.246961334934E-013 RMS(|Res|)=+7.445704063866E-007
Iteration#015: |dp|= +3.666205221412E-013 RMS(|Res|)=+7.445704063980E-007
Iteration#016: |dp|= +7.749161872428E-013 RMS(|Res|)=+7.445704063828E-007
Iteration#017: |dp|= +5.556256846194E-013 RMS(|Res|)=+7.445704062881E-007
Iteration#018: |dp|= +2.618568637585E-013 RMS(|Res|)=+7.445704063646E-007
Iteration#019: |dp|= +5.613313016974E-013 RMS(|Res|)=+7.445704063314E-007
Iteration#020: |dp|= +7.917616525110E-013 RMS(|Res|)=+7.445704063793E-007
Iteration#021: |dp|= +6.442099339595E-013 RMS(|Res|)=+7.445704063853E-007
Iteration#022: |dp|= +2.634681173598E-013 RMS(|Res|)=+7.445704063565E-007
Iteration#023: |dp|= +3.243532160356E-013 RMS(|Res|)=+7.445704063420E-007
Iteration#024: |dp|= +9.017686351094E-013 RMS(|Res|)=+7.445704063356E-007
Iteration#025: |dp|= +4.771484390078E-013 RMS(|Res|)=+7.445704064032E-007
Iteration#026: |dp|= +5.381191010232E-013 RMS(|Res|)=+7.445704063855E-007
Iteration#027: |dp|= +6.765545080992E-013 RMS(|Res|)=+7.445704062998E-007
Iteration#028: |dp|= +4.561239342842E-013 RMS(|Res|)=+7.445704063698E-007
Iteration#029: |dp|= +3.855784711239E-013 RMS(|Res|)=+7.445704063384E-007
Iteration#030: |dp|= +2.967022964648E-013 RMS(|Res|)=+7.445704063455E-007
IPF Kalman Filter Completed with Error |dp1| + |dp2| = +2.9670229646475785E-013
-----
```

```

----- IPF LEAST SQUARES FILTER STARTED -----
Iteration#001 COND#=+3.035068031264E+007, |dp|=+3.059653660747E-002
Iteration#002 COND#=+3.034282414933E+007, |dp|=+2.240828210269E-005
Iteration#003 COND#=+3.034272876054E+007, |dp|=+9.440197042146E-006
Iteration#004 COND#=+3.034273998841E+007, |dp|=+2.433189326171E-008
Iteration#005 COND#=+3.034273991941E+007, |dp|=+1.830259835688E-010
Iteration#006 COND#=+3.034273990927E+007, |dp|=+3.052838006860E-011
Iteration#007 COND#=+3.034273992068E+007, |dp|=+4.090024151783E-013
Iteration#008 COND#=+3.034273990781E+007, |dp|=+3.538750873698E-013
Iteration#009 COND#=+3.034273991169E+007, |dp|=+3.014835312381E-013
Iteration#010 COND#=+3.034273990991E+007, |dp|=+5.539012975301E-013
Iteration#011 COND#=+3.034273990941E+007, |dp|=+6.351636707019E-013
Iteration#012 COND#=+3.034273990690E+007, |dp|=+4.499244898422E-013
Iteration#013 COND#=+3.034273989237E+007, |dp|=+3.655241961772E-013
Iteration#014 COND#=+3.034273988907E+007, |dp|=+3.525177105931E-013
Iteration#015 COND#=+3.034273991601E+007, |dp|=+3.868420056042E-013
Iteration#016 COND#=+3.034273993265E+007, |dp|=+5.152260063071E-013
Iteration#017 COND#=+3.034273995188E+007, |dp|=+2.799579417923E-013
Iteration#018 COND#=+3.034273993166E+007, |dp|=+1.332481414284E-013
Iteration#019 COND#=+3.034273988645E+007, |dp|=+3.149314034694E-013
Iteration#020 COND#=+3.034273993869E+007, |dp|=+6.494680511050E-013
Iteration#021 COND#=+3.034273990271E+007, |dp|=+7.392227344296E-013
Iteration#022 COND#=+3.034273993401E+007, |dp|=+5.551304357215E-013
Iteration#023 COND#=+3.034273994780E+007, |dp|=+6.466313958593E-013
Iteration#024 COND#=+3.034273991391E+007, |dp|=+2.488793610166E-013
Iteration#025 COND#=+3.034273992126E+007, |dp|=+8.253775902577E-013
Iteration#026 COND#=+3.034273990607E+007, |dp|=+3.277615707091E-013
Iteration#027 COND#=+3.034273991755E+007, |dp|=+5.486385509870E-013
Iteration#028 COND#=+3.034273994459E+007, |dp|=+6.662648193292E-013
Iteration#029 COND#=+3.034273990106E+007, |dp|=+5.229611676569E-013
Iteration#030 COND#=+3.034273990801E+007, |dp|=+3.639056775248E-013
IPF Least Squares Filter Completed with Error |dp1| + |dp2| = +3.6390567752482442E-013
-----
```

Total Execution Time: 176 seconds

4 COMMENTS

This IPF run is a post-IOC re-run of the IOC flight data taken from run IF502023, but with a modified CS-file CS701023.m, which specifies that the Prime frame 023 is to be moved over from its previous definition by 1/2 pixel. This change puts the Prime frame exactly at the middle of a physical pixel, which was desired by the IRS team to improve in-flight Peakup centring accuracy.

The IPF run was performed in the most recent IPF version IPF.V4.0.0. All IPF settings, data editing, and parameters were kept the same as the IF502023 run (see report ID502023.pdf for details). As a reminder, only constant plate scales were estimated, which did not change significantly from run IF502023.

We recommend updating frame 023 with the new quaternion listed in the IF file IF701023.dat. The recommended Brown angle change is on the order of 0.9 arcsec, which is consistent with the desired 1/2 pixel shift (the PU pixels are approximately 1.8 arcsec wide). We also recommend including all plate scales as part of the frame table update since they were estimated simultaneously with the Brown angles. As before, in our best judgement, the Fine survey is accurate to 0.09 arcsec which satisfies the fine survey requirement of 0.14 arcsecond by a good margin.

IPF TEAM CONTACT INFORMATION

IPF Team email	ipf@sirtfweb.jpl.nasa.gov	
David S. Bayard	X4-8208	David.S.Bayard@jpl.nasa.gov (TEAM LEADER)
Dhemetrio Boussalis	X4-3977	boussali@grover.jpl.nasa.gov
Paul Brugarolas	X4-9243	Paul.Brugarolas@jpl.nasa.gov
Bryan H. Kang	X4-0541	Bryan.H.Kang@jpl.nasa.gov
Edward.C.Wong	X4-3053	Edward.C.Wong@jpl.nasa.gov (TASK MANAGER)

ACKNOWLEDGEMENTS

This work was performed at the Jet Propulsion Laboratory, California Institute of Technology, under contract with the National Aeronautics and Space Administration.

References

- [1] D.S. Bayard, B.H. Kang, *SIRTF Instrument Pointing Frame Kalman Filter Algorithm*, JPL D-Document D-24809, September 30, 2003.
- [2] B.H. Kang, D.S. Bayard, *SIRTF Instrument Pointing Frame (IPF) Software Description Document and User's Guide*, JPL D-Document D-24808, September 30, 2003.
- [3] D.S. Bayard, B.H. Kang, *SIRTF Instrument Pointing Frame (IPF) Kalman Filter Unit Test Report*, JPL D-Document D-24810, September 30, 2003.
- [4] *Space Infrared Telescope Facility In-Orbit Checkout and Science Verification Mission Plan*, JPL D-Document D-22622, 674-FE-301 Version 1.4, February 8, 2002.
- [5] *Space Infrared Telescope Facility Observatory Description Document*, Lockheed Martin LMMS/P458569, 674-SEIT-300 Version 1.2, November 1, 2002.
- [6] *SIRTF Software Interface Specification for Science Centroid INPUT Files (CAFILER, CSFILE)*, JPL SOS-SIS-2002, November 18, 2002.
- [7] *SIRTF Software Interface Specification for Inferred Frames Offset INPUT Files (OFILE)*, JPL SOS-SIS-2003, November 18, 2002.
- [8] *SIRTF Software Interface Specification for PCRS Centroid INPUT Files (CBFILE)*, JPL SIS-FES-015, November 18, 2002.
- [9] *SIRTF Software Interface Specification for Attitude INPUT Files (AFILE, ASFILE)*, JPL SIS-FES-014, January 7, 2002.
- [10] *SIRTF Software Interface Specification for IPF Filter Output Files (IFFILE, LGFILE, TARFILE)*, JPL SOS-SIS-2005, November 18, 2002.
- [11] R.J. Brown, *Focal Surface to Object Space Field of View Conversion*. Systems Engineering Report SER No. S20447-OPT-051, Ball Aerospace & Technologies Corp., November 23, 1999.

JET PROPULSION LABORATORY

SIRTF IPF REPORT

JPL ID502028

November 6, 2003

**SIRTF INSTRUMENT POINTING FRAME
KALMAN FILTER EXECUTION SUMMARY**

IPF RUN NUMBER: 502028

REPORT TYPE: IOC EXECUTION (FINE)

PRIME FRAME: IRS_ShortLo_1st_Ord_Center_Pos (28)

INFERRRED FRAMES: (26) (27) (29)

IPF TEAM

Autonomy and Control Section (345)

Jet Propulsion Laboratory

California Institute of Technology

4800 Oak Grove Drive

Pasadena, CA 91109

Contents

1 IPF EXECUTION SUMMARY	5
2 IPF INPUT FILE HISTORY	9
3 IPF EXECUTION RESULTS	10
3.1 IPF EXECUTION OUTPUT PLOTS	10
3.2 IPF OUTPUT DATA (IF MINI FILE)	36
3.3 IPF EXECUTION LOG	39
4 COMMENTS	42

List of Figures

1.1 A-priori and a-posteriori IPF frames	5
1.2 A-priori and a-posteriori IPF frames (ZOOMED)	8
2.1 Scenario Plot	9
3.1 TPF coords of measurements and a-priori predicts	12
3.2 Oriented PixelCoords of measurements and a-priori predicts	12
3.3 Oriented (W,V) PixelCoords of A-Priori Prediction Error Quiver Plot	13
3.4 A-priori prediction error (Science Centroids)	13
3.5 Oriented PixelCoords of measurements and a-priori predicts (PCRS only)	14
3.6 Oriented PixelCoords of measurements and a-priori predicts (Zoomed, PCRS only)	14
3.7 Oriented (W,V) PixelCoords of A-Priori PCRS Prediction Error Quiver Plot	15
3.8 A-priori PCRS prediction error	15
3.9 IPF execution convergence, chart 1	16
3.10 IPF execution convergence, chart 2	16
3.11 Parameter uncertainty convergence	17
3.12 IPF parameter symbol table	17
3.13 KF parameter error sigma plots	18
3.14 LS parameter error sigma plot	18
3.15 KF and LS parameter error sigma plot	19
3.16 Oriented PixelCoords of meas. and a-posteriori predicts	20
3.17 Oriented PixelCoords of meas. and a-posteriori predicts (attitude corrected)	20

3.18	KF innovations with (o) and w/o (+) attitude corrections	21
3.19	Histograms of science a-posteriori residuals (or innovations)	21
3.20	A-Posteriori Science Centroid Prediction Error Quiver (Att. Cor.)	22
3.21	Normalized A-Posteriori Science Centroid Prediction Errors	22
3.22	KF innovations with (o) and w/o (+) attitude corrections (PCRS)	23
3.23	Histograms of PCRS a-posteriori residuals (or innovations)	23
3.24	A-posteriori PCRS Prediction Summary	24
3.25	A-posteriori PCRS Prediction (PCRS 1 Only)	25
3.26	A-posteriori PCRS Prediction (PCRS 2 Only)	25
3.27	A-Posteriori PCRS Prediction Errors Quiver (Att. Cor.)	26
3.28	Normalized A-Posteriori PCRS Prediction Errors	26
3.29	W-axis KF innovations and 1-sigma bound	27
3.30	V-axis KF innovations and 1-sigma bound	27
3.31	Array plot with (solid) and w/o (dashed) optical distortion corrections	28
3.32	Optical Distortion Plot: total (x5 magnification)	28
3.33	Optical Distortion Plot: constant plate scales (x5 magnification)	29
3.34	Optical Distortion Plot: linear plate scale (x5 magnification)	29
3.35	Optical Distortion Plot: gamma terms (x5 magnification)	30
3.36	Scan Mirror Chops	30
3.37	IPF Frame Reconstruction	31
3.38	Center Pixel Reconstruction	31
3.39	Estimated attitude corrections (Body frame)	32
3.40	Estimated attitude error sigma plot (Body frame)	32
3.41	Thermo-mechanical boresight drift (equiv. angle in (W,V) coords)	33
3.42	Thermo-mechanical boresight drift (equiv. angle in Body frame)	33
3.43	Gyro drift bias contribution (equiv. rate in (W,V) coords)	34
3.44	Gyro drift bias contribution (equiv. angle in (W,V) coords)	34
3.45	Gyro drift bias contribution (equiv. angle in Body frame)	35

List of Tables

1.1	IPF filter input files	6
1.2	IPF filter execution configuration	6

1.3	IPF filter execution mask vector assignment	6
1.4	IPF calibration error summary ([arcsec], 1-sigma, radial)	7
1.5	Science measurement prediction error summary (1-sigma)	7
1.6	IPF Brown angle summary	8
2.1	IPF input file editing status	9
3.1	Table of figures I (IPF run)	10
3.2	Table of figures II (IPF run)	11
3.3	PCRS measurement prediction error summary	24

1 IPF EXECUTION SUMMARY

This report summarizes the SIRTF Instrument Pointing Frame (IPF) Kalman Filter execution associated with run file: RN502028. In particular, this Focal Point Survey calibrates the instrument: IRS_ShortLo_1st_Ord_Center_Pos (28), as part of the IOC Fine Survey. The main calibration results from the IPF filter execution have been documented in IF502028 typically stored in the mission archive DOM collection IPF_IF. This report only summarizes the main aspects of the run, and does not substitute for the full information contained in the IF file.

Section 1 summarizes the filter execution results. The filter configurations are tabulated in Table 1.2 and the mask vector assignments are tabulated in Table 1.3. A total of 18 state parameters are estimated in this run. The overall End-to-End pointing performances are tabulated in Table 1.4. The prediction residuals throughout the estimation processes are tabulated in Table 1.5. Section 3 summarizes resulting plots, a mini summary of the IF IPF output file, and the execution log. Section 4 captures the user comments that are specific to this particular run.

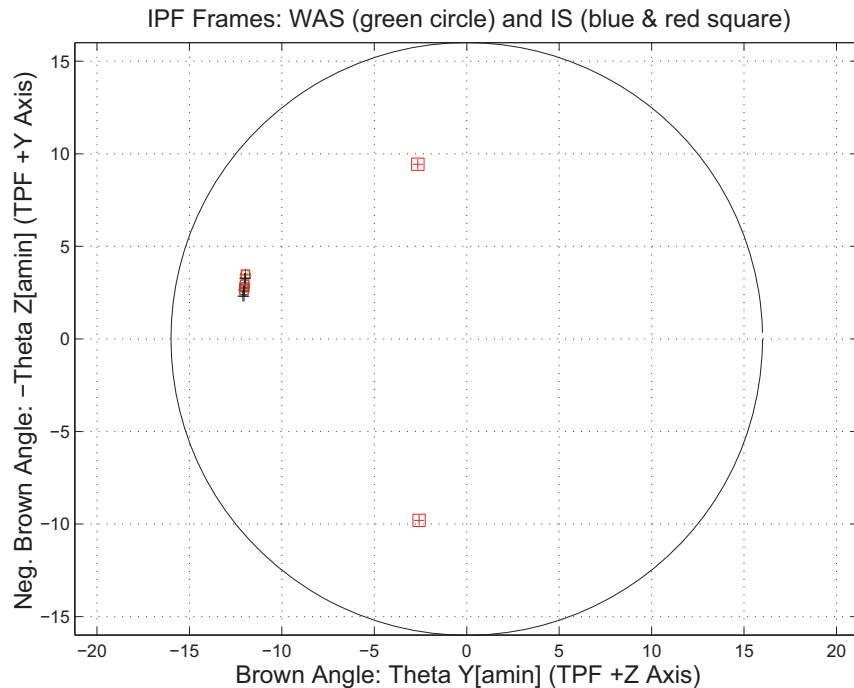


Figure 1.1: A-priori and a-posteriori IPF frames

RAW	FINAL (After Editing)
AA501028	AA501028
AS501028	AS501028
CA501028	CA501028
CB502028	CB502028
CS501028	CS501028

Table 1.1: IPF filter input files

EXECUTION CONFIGURATION ITEM	CURRENT STATUS
IPF Filter Version Used	IPF.V3.0.0B
Frame Table Version Used	BodyFrames_FTU_12b
Scan-Mirror Employed?	NO
IPF Filter Mode	NORMAL-MODE(0)
SLIT-MODE Operation	ENABLED
Kalman Filter Operation	ENABLED
Least-Squares Data Analysis	ENABLED
IBAD Screening	ENABLED
User-Specified Data Editing	DISABLED
Total Number of Iterations	25
LS Residual Sigma Scale	3.48528754E+000
Total Number of Maneuvers	32

Table 1.2: IPF filter execution configuration

Con. Plate Scale			Γ Dependent				Γ^2 Dependent				Linear Plate Scale						Mirror			
a_{00}	b_{00}	c_{00}	a_{10}	b_{10}	c_{10}	d_{10}	a_{20}	b_{20}	c_{20}	d_{20}	a_{01}	b_{01}	c_{01}	d_{01}	e_{01}	f_{01}	α	β		
1	2	3	4	5	6	7	8	9	10	11	12	13	14	15	16	17	18	19		
1	0	0	0	0	0	0	0	0	0	0	0	0	0	0	0	0	0	0		
IPF (T)			Alignment R						Gyro Drift Bias											
θ_1	θ_2	θ_3	a_{rx}	a_{ry}	a_{rz}	b_{rx}	b_{ry}	b_{rz}	c_{rx}	c_{ry}	c_{rz}	b_{gx}	b_{gy}	b_{gz}	c_{gx}	c_{gy}	c_{gz}			
20	21	22	23	24	25	26	27	28	29	30	31	32	33	34	35	36	37			
0	1	1	1	1	1	1	1	1	1	1	1	1	1	1	1	1	1			

Table 1.3: IPF filter execution mask vector assignment

FOCAL PLANE SURVEY ANALYSIS: IOC Fine Survey.

INSTRUMENT NAME: IRS_ShortLo_1st_Ord_Center_Pos NF: 28

PIX2RADW: 4.84813681E-006 [rad/pixel] = 1.0000E+000 [arcsec/pixel]

PIX2RADV: 4.84813681E-006 [rad/pixel] = 1.0000E+000 [arcsec/pixel]

FRAME	DESCRIPTION	IPF ¹	SF ²	TOTAL	REQ
028(P)	IRS_ShortLo_1st_Ord_Center_Pos	0.0791	0.0855	0.1165	0.14
026(I)	IRS_ShortLo_1st_Ord_1st_Pos	0.0821	0.0855	0.1186	N/A
027(I)	IRS_ShortLo_1st_Ord_2nd_Pos	0.0772	0.0855	0.1152	N/A
029(I)	IRS_ShortLo_Module_Center	0.0809	0.0855	0.1177	N/A

Table 1.4: IPF calibration error summary ([arcsec], 1-sigma, radial)

RMS METRIC	A PRIORI ³	A POSTERIORI ³	ATT. CORRECTED ⁴	UNITS
Radial	1.5786	0.6289	0.5543	arcsec
W-Axis	1.3875	0.5477	0.5429	arcsec
V-Axis	0.7528	0.3092	0.1115	arcsec
Radial	1.5786	0.6289	0.5543	pixels
W-Axis	1.3875	0.5477	0.5429	pixels
V-Axis	0.7528	0.3092	0.1115	pixels

Table 1.5: Science measurement prediction error summary (1-sigma)

¹IPF filter removes systematic pointing errors due to: thermomechanical alignment drift (Body to TPF), gyro bias and bias drift, centroiding error, attitude error, and optical distortion. IPF SIGMA presented here is “Scaled” by the Least Squares Scale factor. The Least Squares Scale Factor was: 3.485288. It is assumed that the gyro Angle Random Walk contribution is captured with the Least Squares scaling. The gyro ARW contribution can be approximately calculated as 0.0387 arcseconds, given that ARW = 100 $\mu\text{deg}/\sqrt{\text{hr}}$, with 6.872852e+002 second Maneuver time (max), and 32 independent Maneuvres.

²Gyro Scale Factor(GSF) assumes 95 ppm error over 0.250 degree maneuver.

³This can be interpreted as estimate of “pixel to sky” pointing reconstruction error if no science data is used.

⁴This can be interpreted as estimate of achieved S/I centroiding error

IPF BROWN ANGLE SUMMARY					
FRAME TABLE USED: BodyFrames_FTU_12b					
NF	NAME	WAS	IS	CHANGE	UNIT
028	theta_Y	-12.031014	-12.032552	-0.001538	arcmin
028	theta_Z	-2.776537	-2.792599	-0.016062	arcmin
028	angle	-84.719994	-84.719993	+0.000001	deg
026	theta_Y	-12.044971	-12.047468	-0.002497	arcmin
026	theta_Z	-2.625513	-2.631200	-0.005688	arcmin
026	angle	-84.719994	-84.719993	+0.000001	deg
027	theta_Y	-12.017057	-12.017636	-0.000579	arcmin
027	theta_Z	-2.927561	-2.953997	-0.026436	arcmin
027	angle	-84.719994	-84.719993	+0.000001	deg
029	theta_Y	-11.969972	-11.967317	+0.002655	arcmin
029	theta_Z	-3.437059	-3.498495	-0.061435	arcmin
029	angle	-84.719994	-84.719993	+0.000001	deg

Table 1.6: IPF Brown angle summary

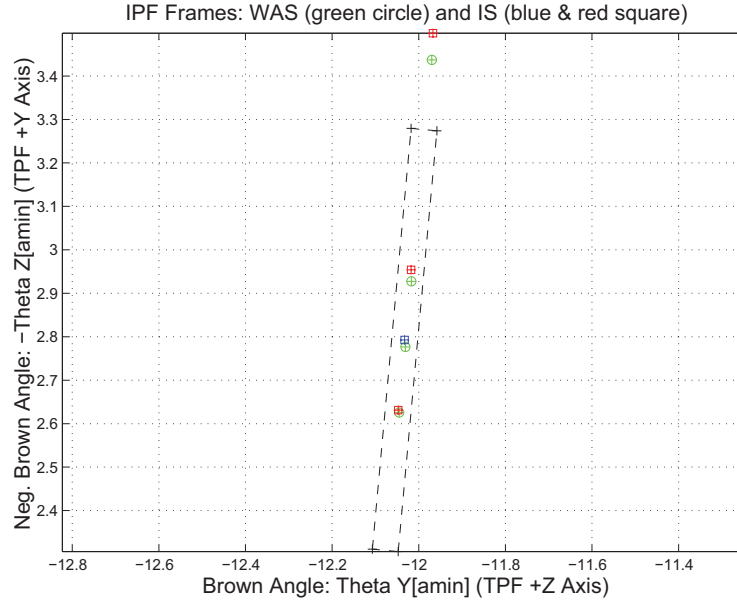


Figure 1.2: A-priori and a-posteriori IPF frames (ZOOMED)

2 IPF INPUT FILE HISTORY

WAS	SIZE	IS	SIZE	REMOVED	PATCHED
AA501028	UNCHANGED	AA501028	UNCHANGED	0	0
CA501028	UNCHANGED	CA501028	UNCHANGED	0	N/A
CB502028	UNCHANGED	CB502028	UNCHANGED	0	N/A

Table 2.1: IPF input file editing status

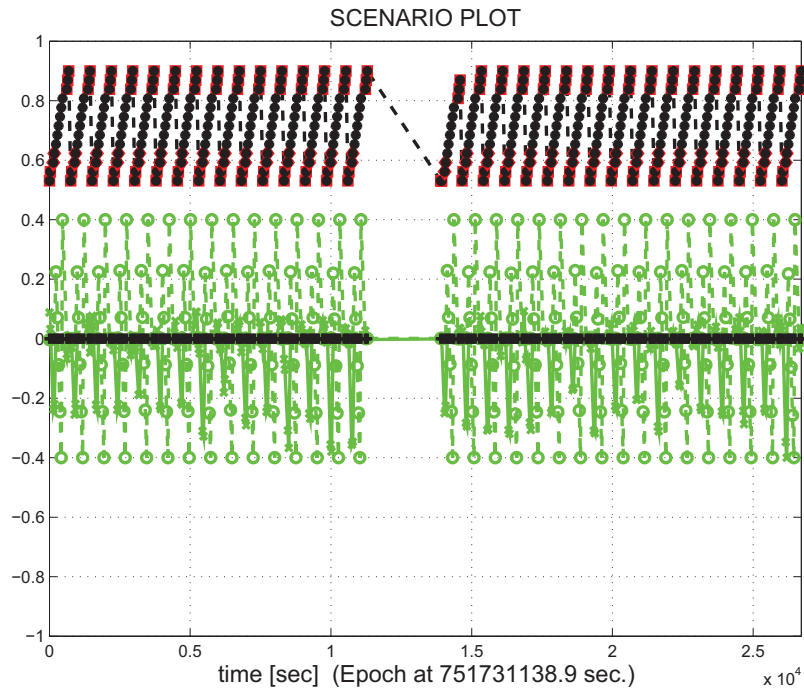


Figure 2.1: Scenario Plot

3 IPF EXECUTION RESULTS

3.1 IPF EXECUTION OUTPUT PLOTS

This subsection summarizes the IPF filter results. As shown in Table 3.1, the output plots are segmented to three groups: predicted performance, post-run results and IPF trending plots.

FIGURE NO.	DESCRIPTION
Predicted performance prior to IPF run	
Figure 3.1	Meas. and a-priori predicts in TPF coords
Figure 3.2	Meas. and a-priori predicts in Oriented Pixel Coords including rectangular array boundary approximation
Figure 3.3	A-Priori Prediction Error Quiver Plot in Oriented Pixel Coords including rectangular array boundary approximation
Figure 3.4	A-priori prediction error
Figure 3.5	Oriented Pixel Coords of measurements and a-priori predicts (PCRS only)
Figure 3.6	Oriented Pixel Coords of measurements and a-priori predicts (Zoomed, PCRS only)
Figure 3.7	Oriented (W,V) Pixel Coords of A-Priori PCRS Prediction Error Quiver Plot
Figure 3.8	A-priori PCRS prediction error
IPF filter performance (post run results)	
Figure 3.9	IPF execution convergence, chart 1: (top) normalized residual error vs. iteration number and (bottom) norm of effective parameter corrections
Figure 3.10	IPF execution convergence, chart 2: parameter correction size vs. iteration number
Figure 3.11	Parameter uncertainty convergence: square-root of diagonal elements of covariance matrix vs. maneuver number
Figure 3.12	IPF parameter symbol table
Figure 3.13	KF parameter error sigma plot (a-priori-dashed, a-posteriori-solid). Includes true parameter errors (FLUTE runs only)
Figure 3.14	LS parameter error sigma plot. Includes true parameter errors (FLUTE runs only)
Figure 3.15	KF and LS parameter errors sigma plot (Figure 3.13 & Figure 3.14 combined)
Figure 3.16	Measurements and a-posteriori predicts in Oriented Pixel Coords including rectangular array boundaries (a-priori-dashed, a-posteriori-solid)
Figure 3.17	Attitude corrected meas. and a-posteriori predicts in Oriented Pixel Coords including rectangular array boundaries (a-priori-dashed, a-posteriori-solid)

Table 3.1: Table of figures I (IPF run)

FIGURE NO.	DESCRIPTION
IPF filter performance (post run results) - CONTINUE	
Figure 3.18	KF innovations with (o) and w/o (+) attitude corrections
Figure 3.19	Histograms of science a-posteriori residuals (or innovations)
Figure 3.20	A-Posteriori Science Centroid Prediction Error Quiver (Att. Cor.)
Figure 3.21	Normalized A-Posteriori Science Centroid Prediction Errors
Figure 3.22	KF innovations with (o) and w/o (+) attitude corrections (PCRS)
Figure 3.23	Histograms of PCRS a-posteriori residuals (or innovations)
Figure 3.24	A-posteriori PCRS Prediction Summary
Figure 3.25	A-posteriori PCRS Prediction (PCRS 1 Only)
Figure 3.26	A-posteriori PCRS Prediction (PCRS 2 Only)
Figure 3.27	A-Posteriori PCRS Prediction Errors Quiver (Att. Cor.)
Figure 3.28	Normalized A-Posteriori PCRS Prediction Errors
Figure 3.29	W-axis KF innovations and 1-sigma bound
Figure 3.30	V-axis KF innovations and 1-sigma bound
Figure 3.31	Array plot with (solid) and w/o (dashed) optical distortion corrections
Figure 3.32	Optical Distortion Plot: total (x5 magnification)
Figure 3.33	Optical Distortion Plot: constant plate scales (x5 magnification)
Figure 3.34	Optical Distortion Plot: linear plate scale (x5 magnification)
Figure 3.35	Optical Distortion Plot: gamma terms (x5 magnification)
Figure 3.36	Scan Mirror Chops
Figure 3.37	IPF Frame Reconstruction
Figure 3.38	Center Pixel Reconstruction
IPF parameter trending plots	
Figure 3.39	Estimated attitude corrections (Body frame)
Figure 3.40	Estimated attitude error sigma plot (Body frame)
Figure 3.41	Systematic error attributed to thermo-mechanical boresight drift (equiv. angle in (W,V) coords)
Figure 3.42	Systematic error attributed to thermo-mechanical boresight drift (equiv. angle in Body frame)
Figure 3.43	Systematic error attributed to gyro drift bias (equiv. rate in (W,V) coords)
Figure 3.44	Systematic error attributed to gyro drift bias (equiv. angle in (W,V) coords)
Figure 3.45	Systematic error attributed to gyro drift bias (equiv. angle in Body frame)

Table 3.2: Table of figures II (IPF run)

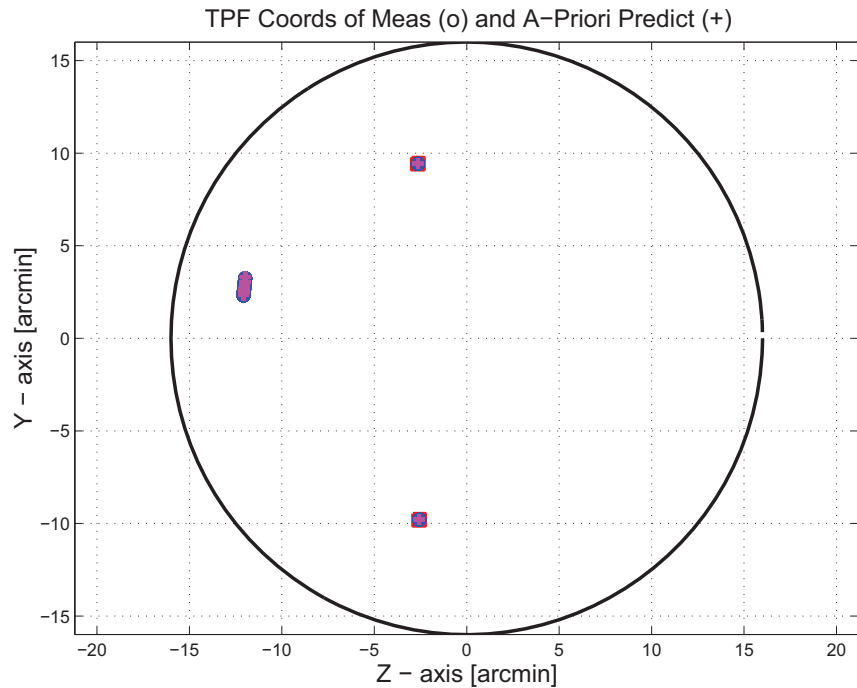


Figure 3.1: TPF coords of measurements and a-priori predicts

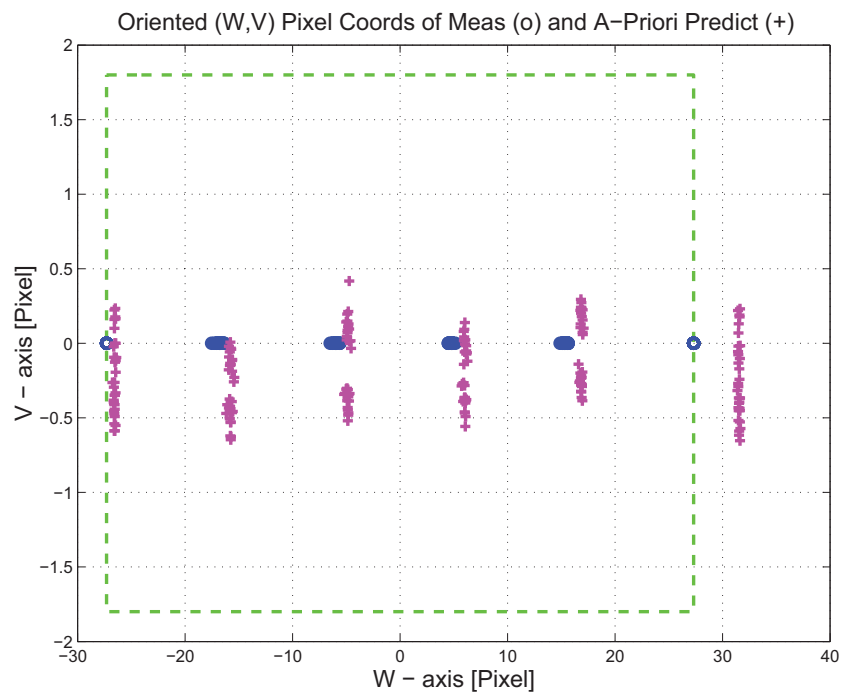


Figure 3.2: Oriented PixelCoords of measurements and a-priori predicts

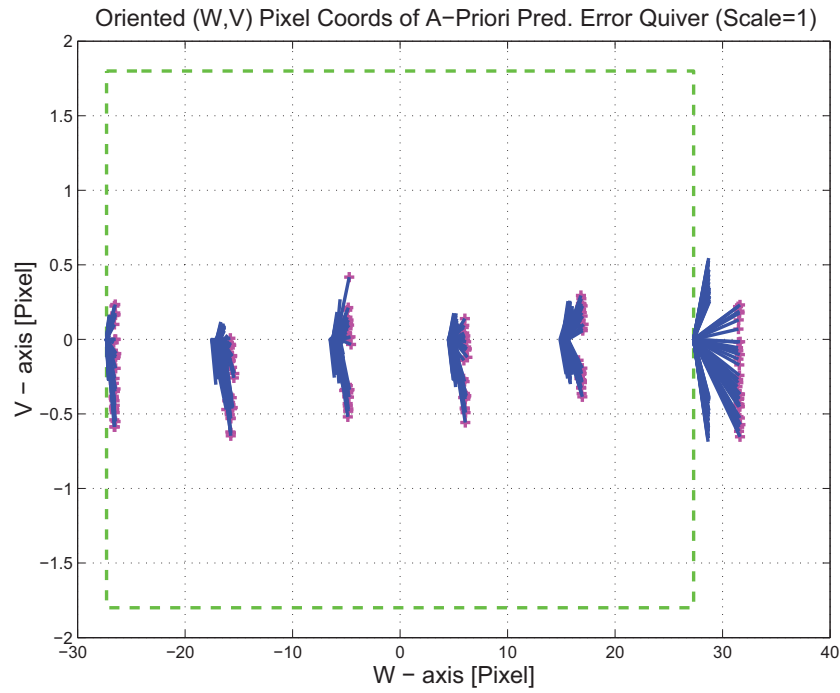


Figure 3.3: Oriented (W,V) Pixel Coords of A-Priori Prediction Error Quiver Plot

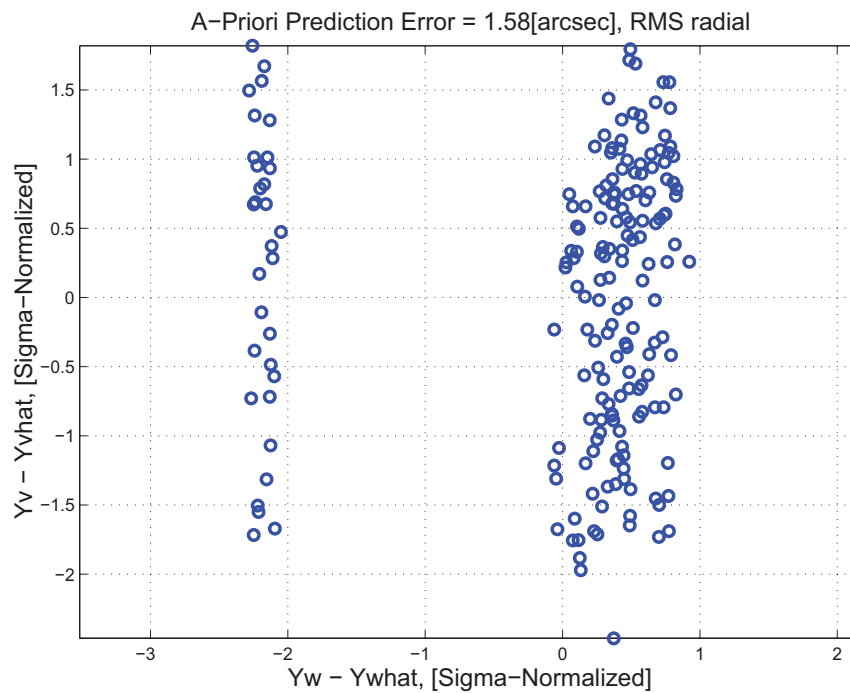


Figure 3.4: A-priori prediction error (Science Centroids)

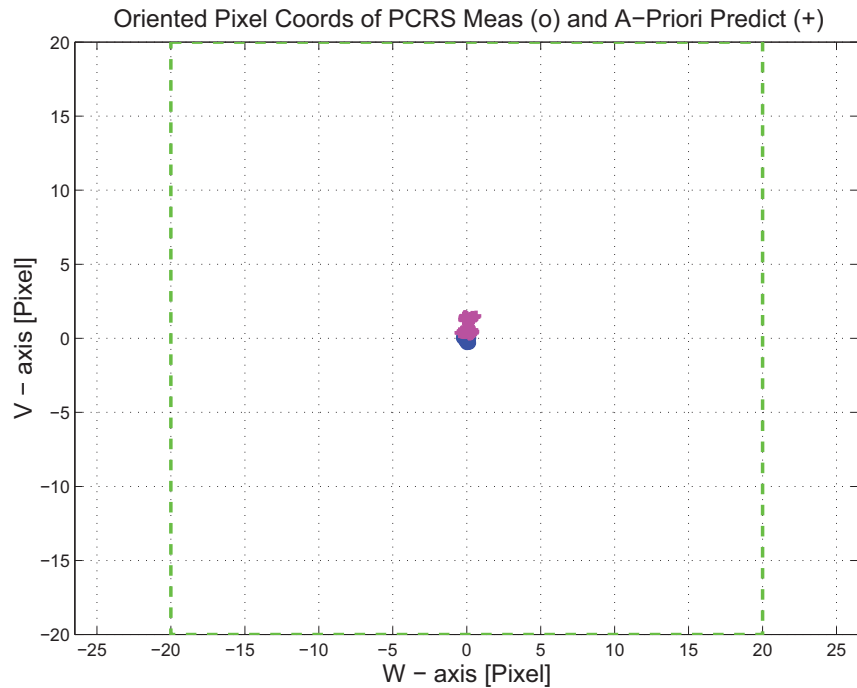


Figure 3.5: Oriented Pixel Coords of measurements and a-priori predicts (PCRS only)

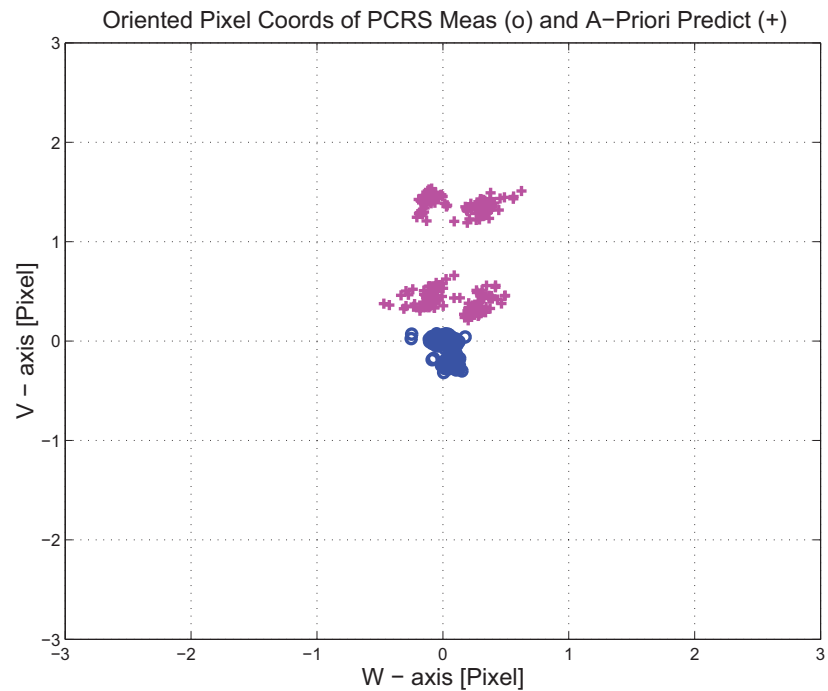


Figure 3.6: Oriented Pixel Coords of measurements and a-priori predicts (Zoomed, PCRS only)

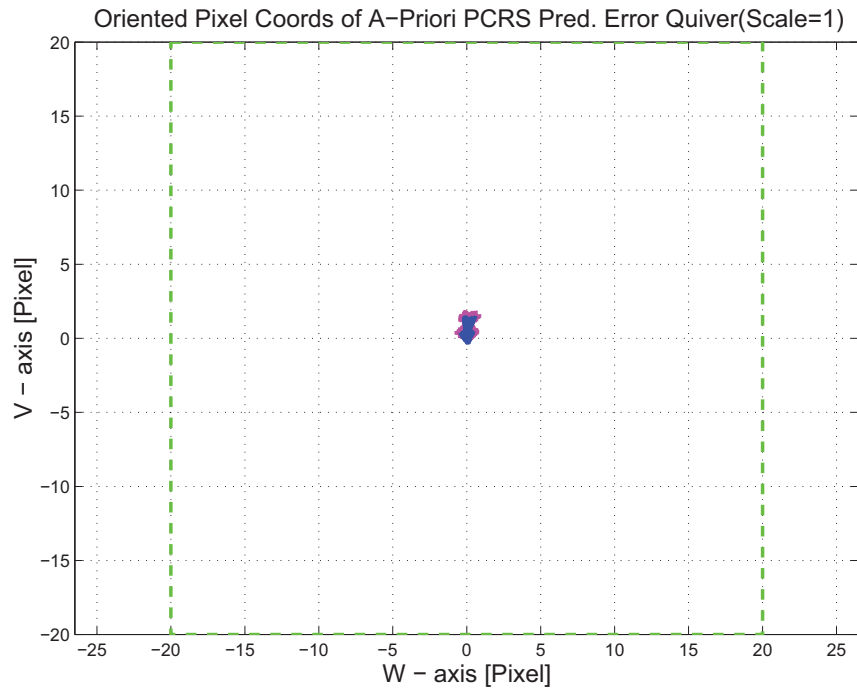


Figure 3.7: Oriented (W,V) Pixel Coords of A-Priori PCRS Prediction Error Quiver Plot

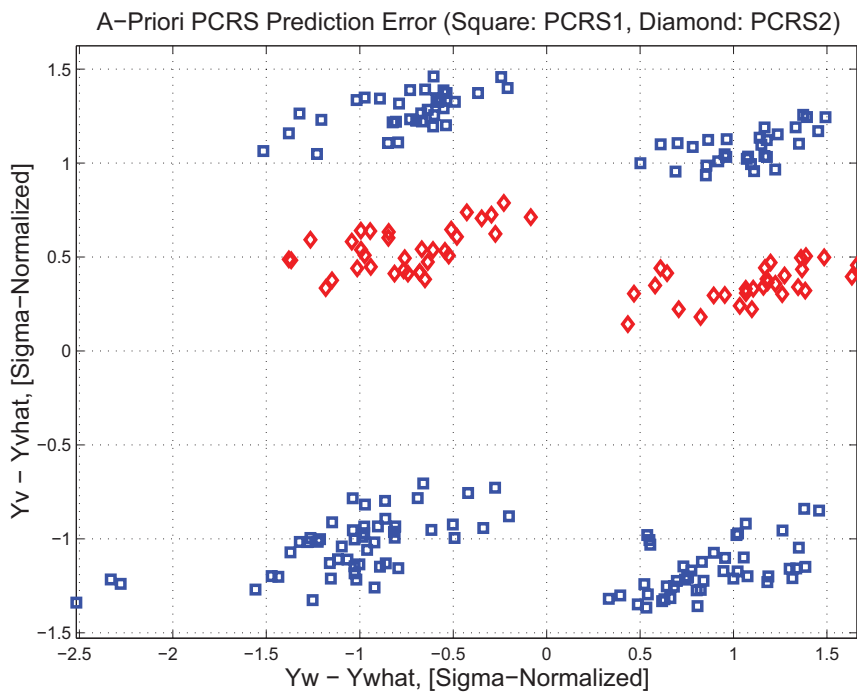


Figure 3.8: A-priori PCRS prediction error

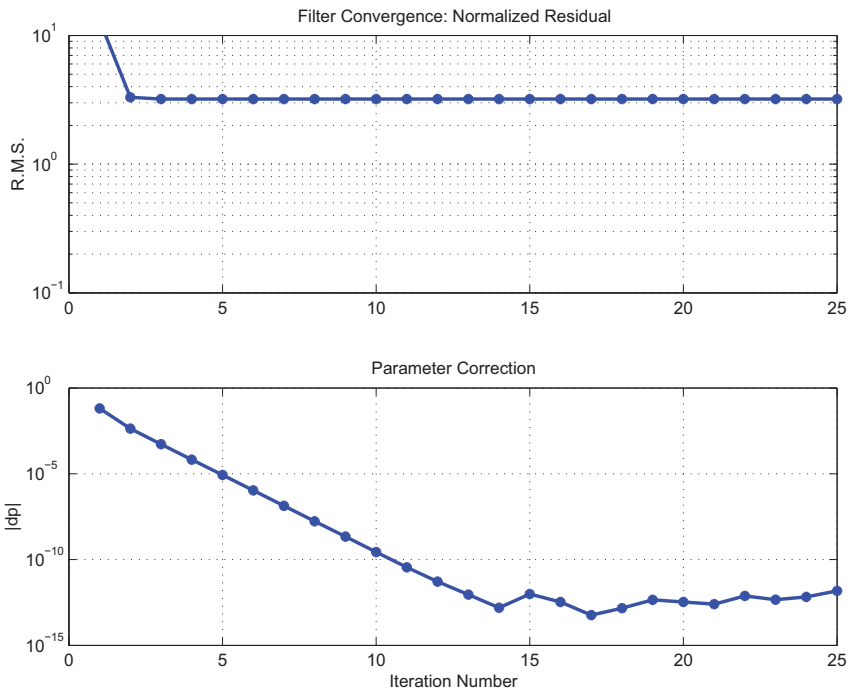


Figure 3.9: IPF execution convergence, chart 1

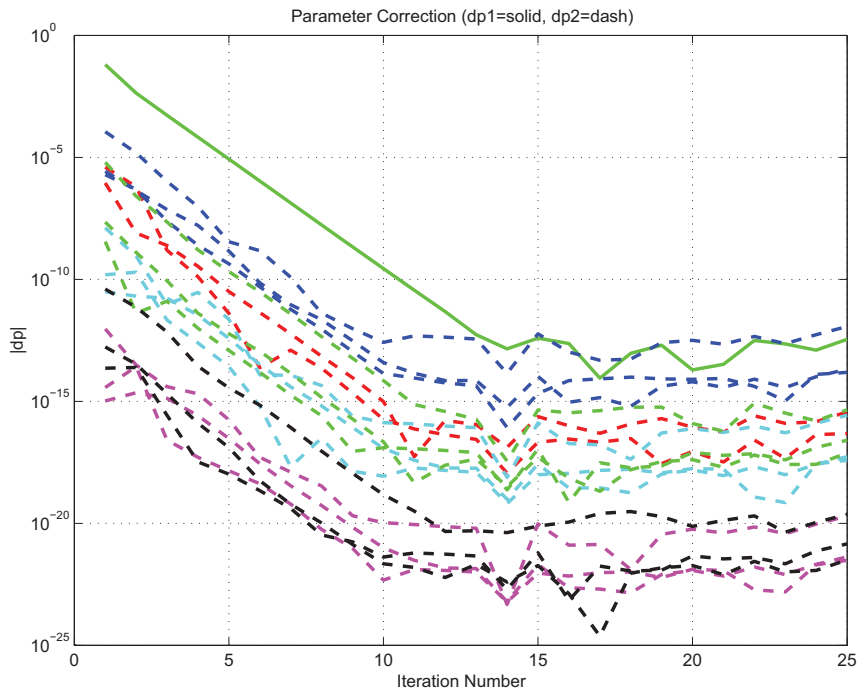


Figure 3.10: IPF execution convergence, chart 2

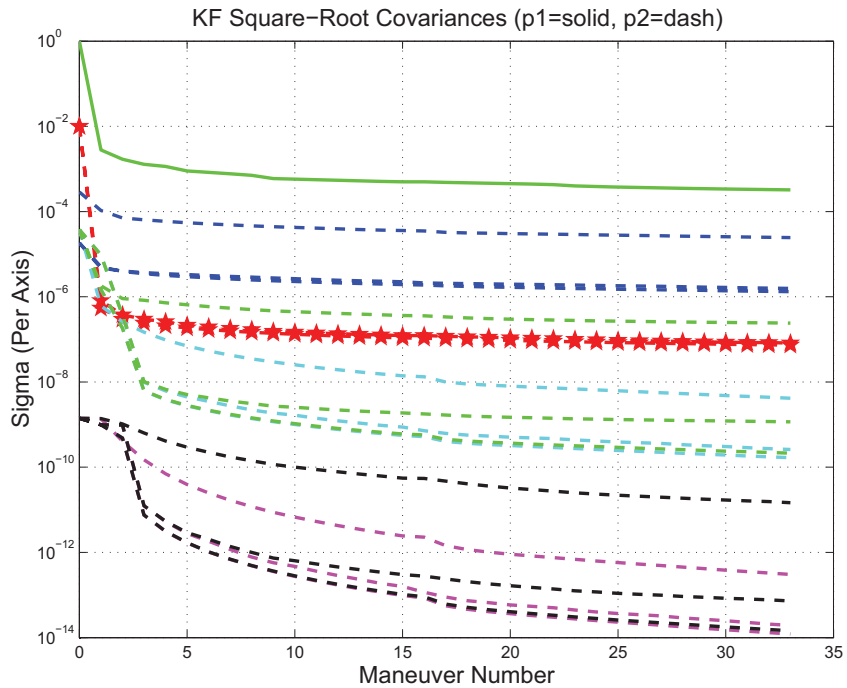


Figure 3.11: Parameter uncertainty convergence

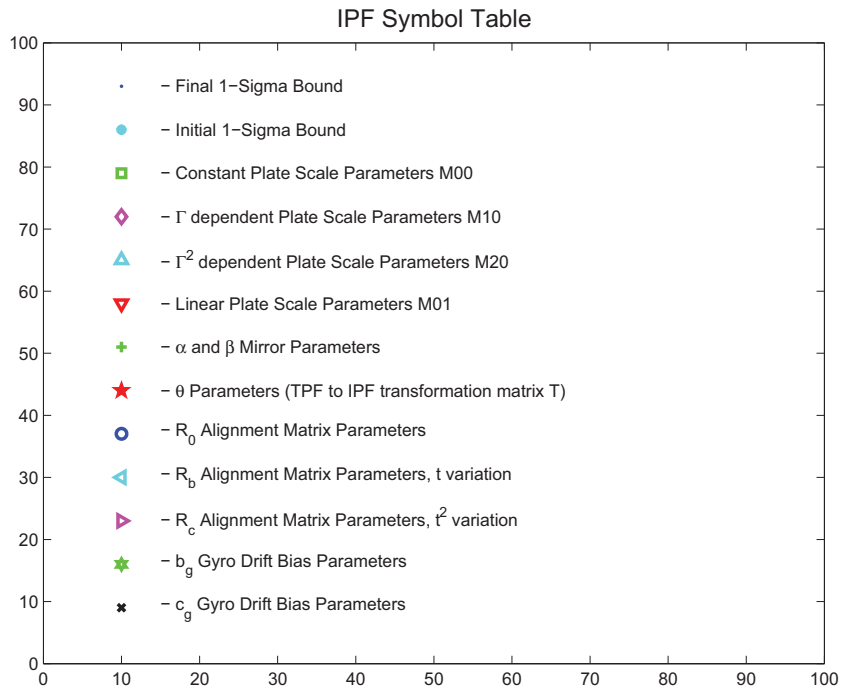


Figure 3.12: IPF parameter symbol table

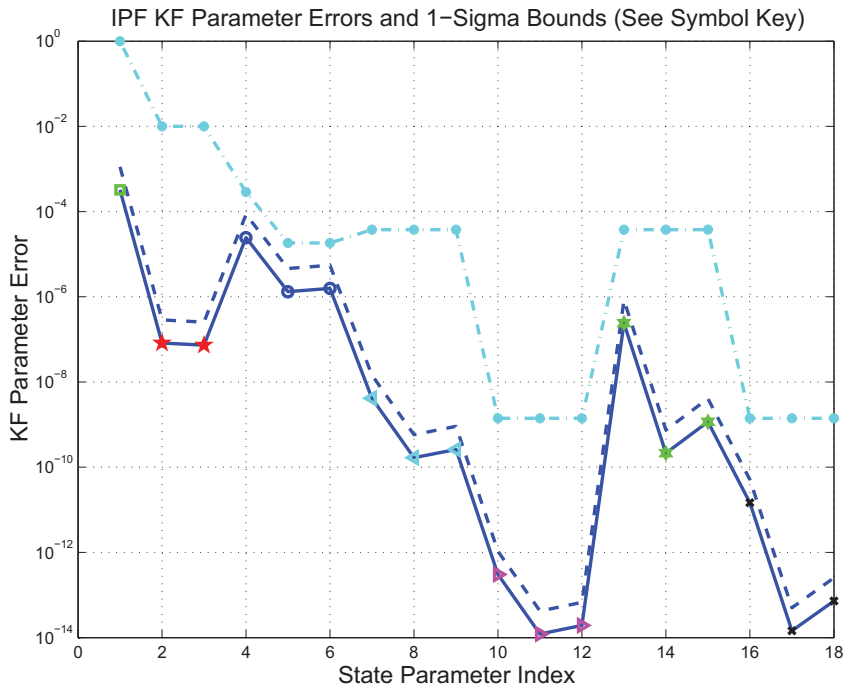


Figure 3.13: KF parameter error sigma plots

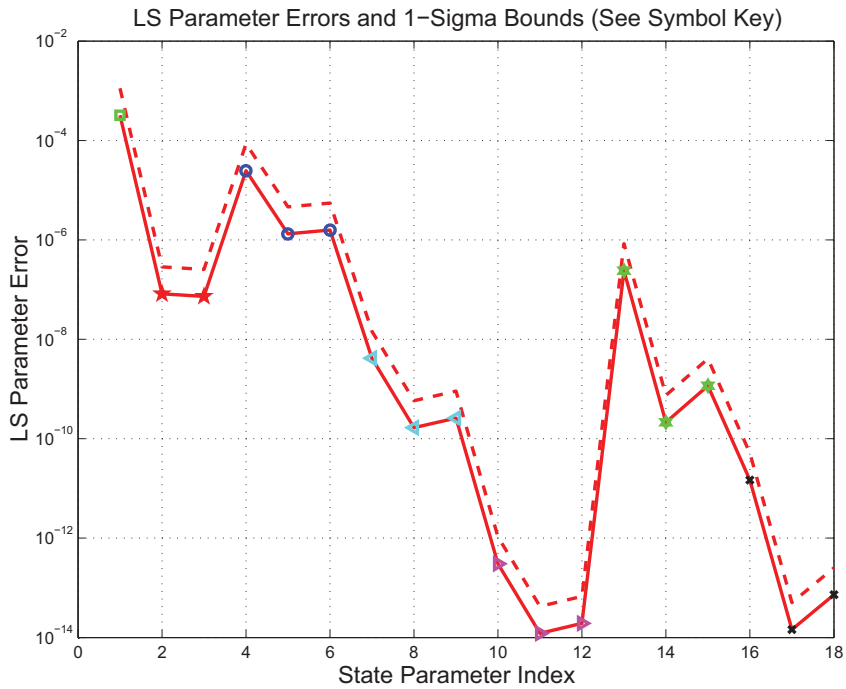


Figure 3.14: LS parameter error sigma plot

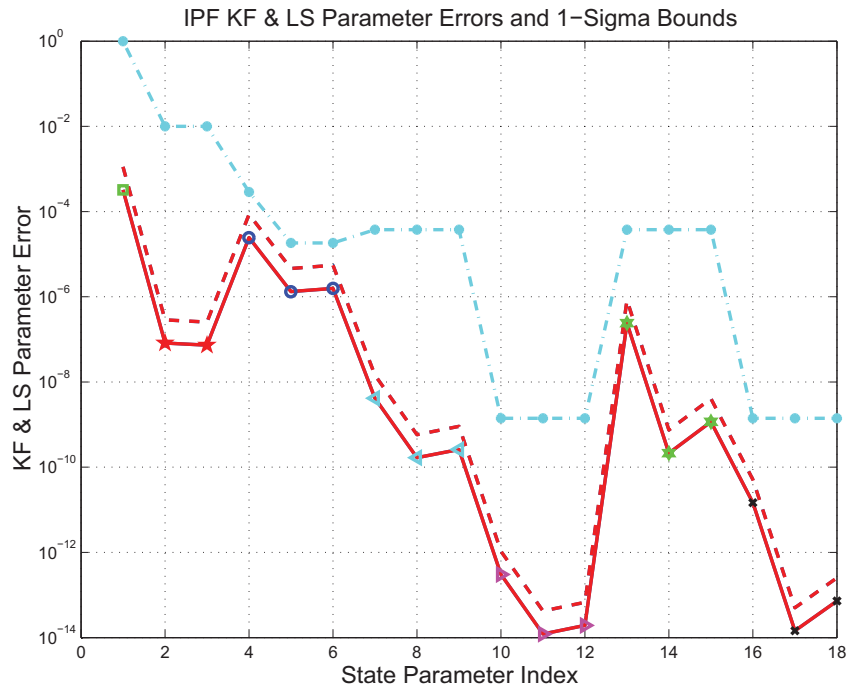


Figure 3.15: KF and LS parameter error sigma plot

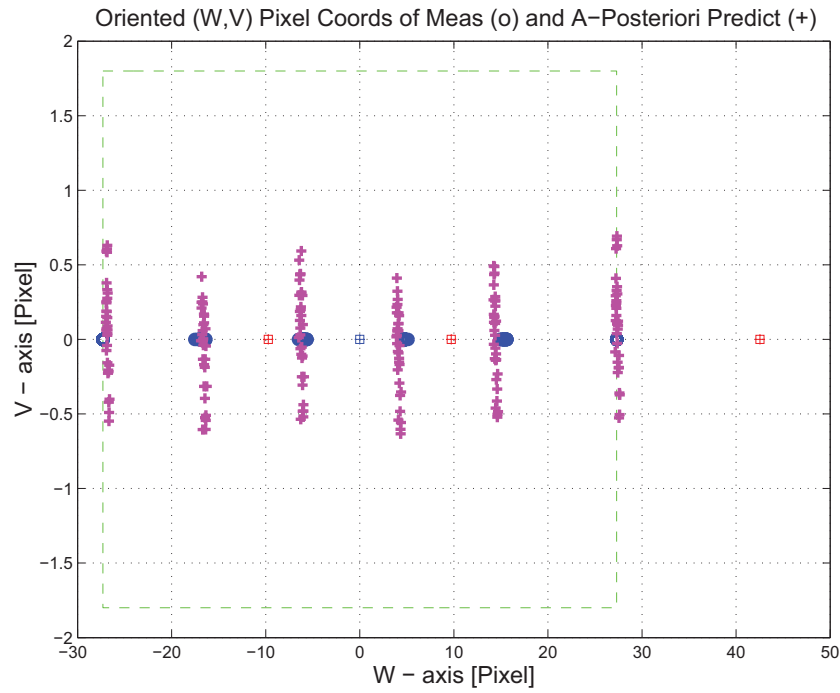


Figure 3.16: Oriented Pixel Coords of meas. and a-posteriori predicts

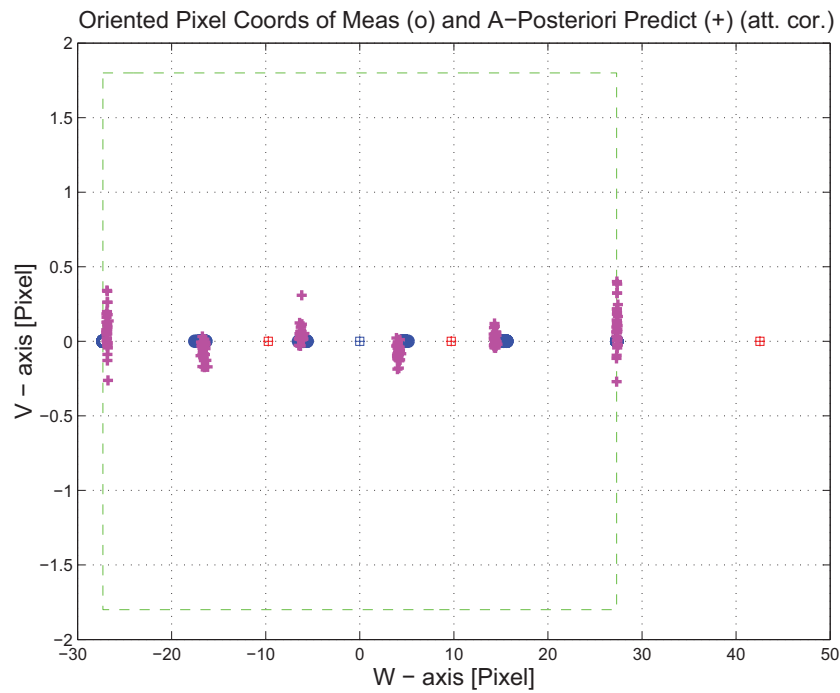


Figure 3.17: Oriented Pixel Coords of meas. and a-posteriori predicts (attitude corrected)

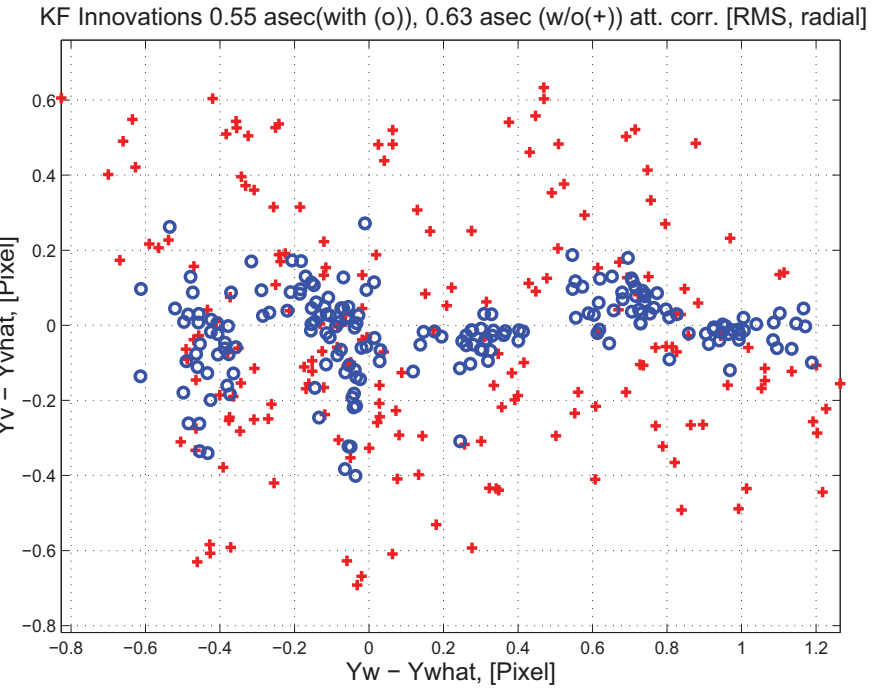


Figure 3.18: KF innovations with (o) and w/o (+) attitude corrections

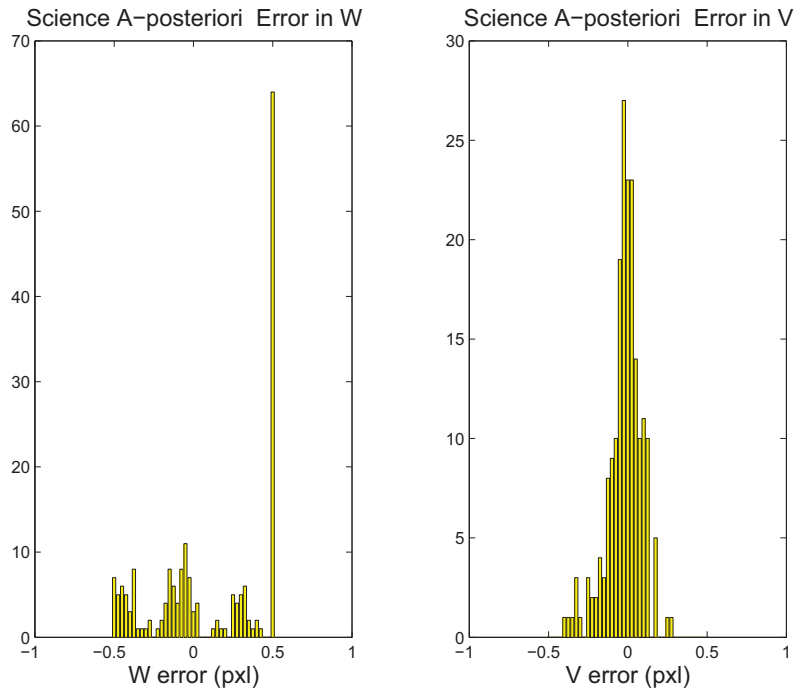


Figure 3.19: Histograms of science a-posteriori residuals (or innovations)

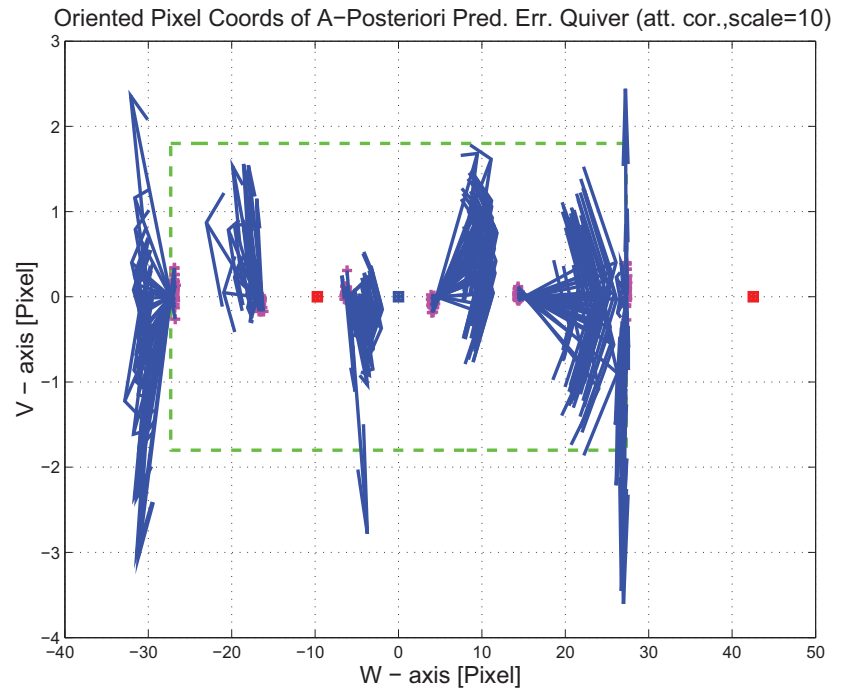


Figure 3.20: A-Posteriori Science Centroid Prediction Error Quiver (Att. Cor.)

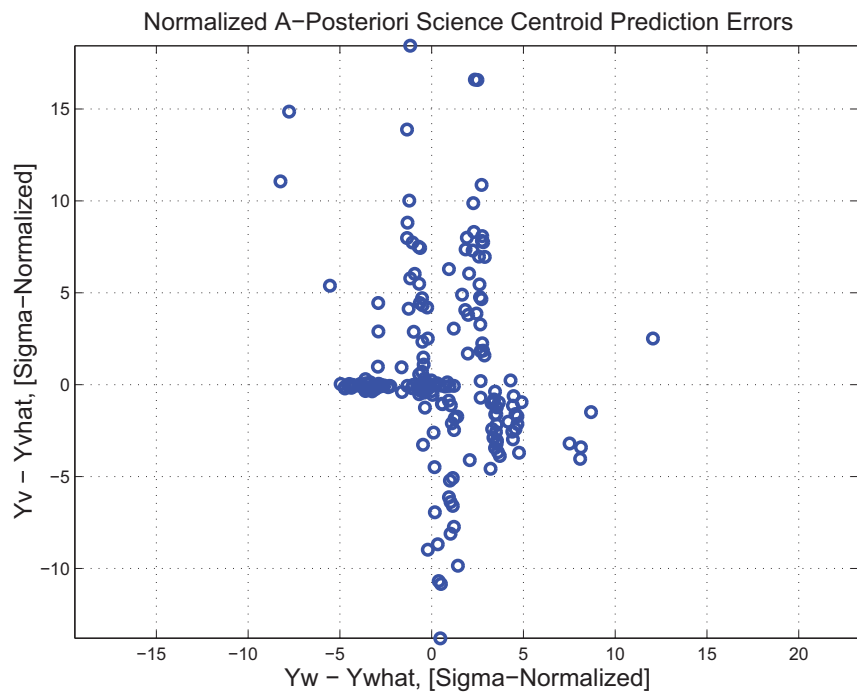


Figure 3.21: Normalized A-Posteriori Science Centroid Prediction Errors

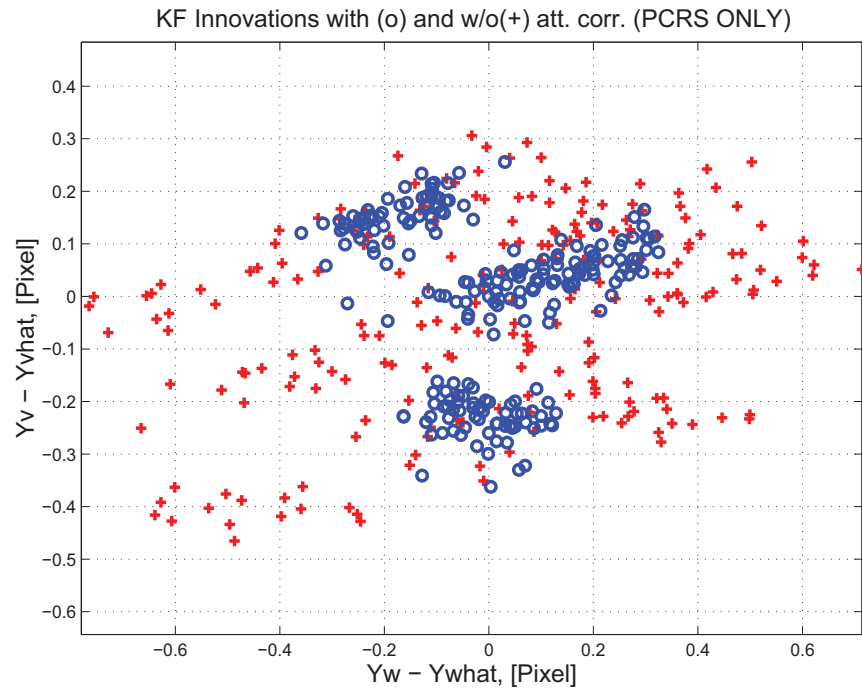


Figure 3.22: KF innovations with (o) and w/o (+) attitude corrections (PCRS)

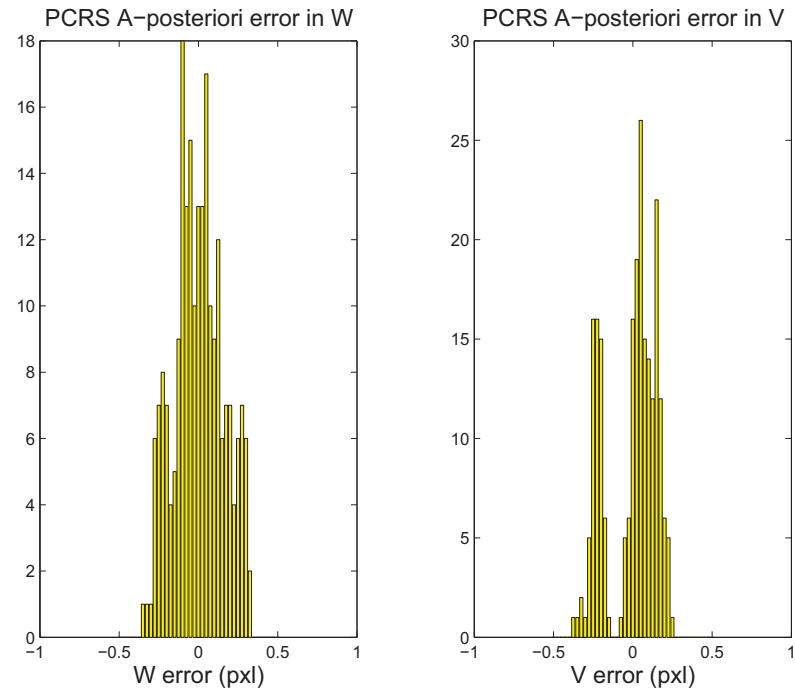


Figure 3.23: Histograms of PCRS a-posteriori residuals (or innovations)

IPF PCRS SUMMARY						
PCRS 1 (Total of 160 centroids)						
RMS	MEAN		SIGMA			
METRIC	APOST.	ATT. COR.	APOST.	ATT. COR.	STAT. CONF.	UNITS
Radial	0.0592	0.0835	0.3666	0.1923	0.0152	arcsec
W-axis	0.0046	0.0086	0.3474	0.1786	0.0141	arcsec
V-axis	0.0590	0.0830	0.1171	0.0715	0.0056	arcsec
PCRS 2 (Total of 64 centroids)						
METRIC	APOST.	ATT. COR.	APOST.	ATT. COR.	STAT. CONF.	UNITS
Radial	0.2568	0.2316	0.3243	0.0839	0.0105	arcsec
W-axis	-0.0140	-0.0116	0.3071	0.0734	0.0092	arcsec
V-axis	-0.2564	-0.2313	0.1041	0.0406	0.0051	arcsec
Combined (Total of 224 centroids)						
METRIC	APOST.	ATT. COR.	APOST.	ATT. COR.	STAT. CONF.	UNITS
Radial	0.0311	0.0073	0.3827	0.2206	0.0147	arcsec
W-axis	-0.0007	0.0028	0.3365	0.1562	0.0104	arcsec
V-axis	-0.0311	-0.0068	0.1822	0.1558	0.0104	arcsec

Table 3.3: PCRS measurement prediction error summary

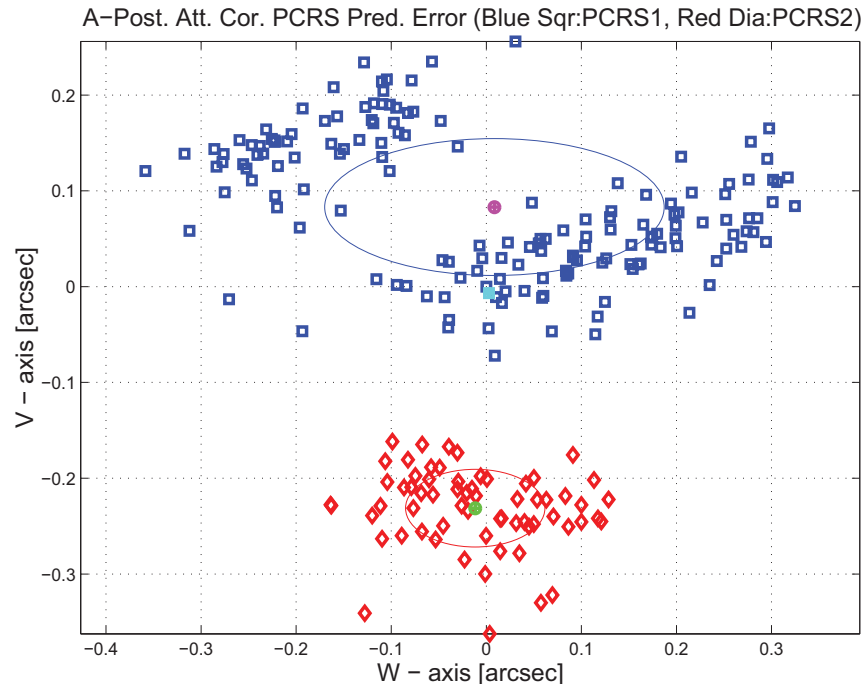


Figure 3.24: A-posteriori PCRS Prediction Summary

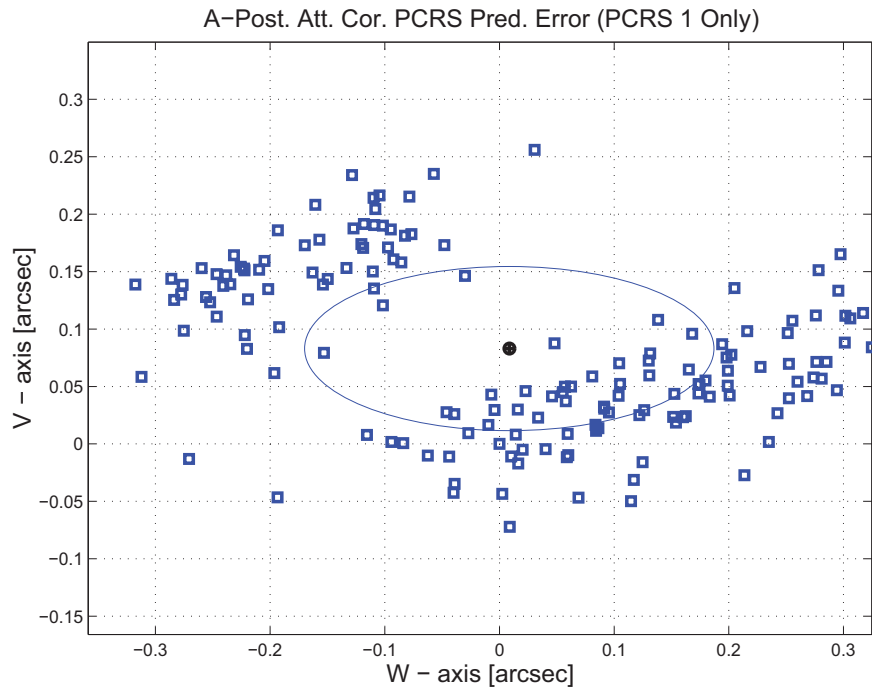


Figure 3.25: A-posteriori PCRS Prediction (PCRS 1 Only)

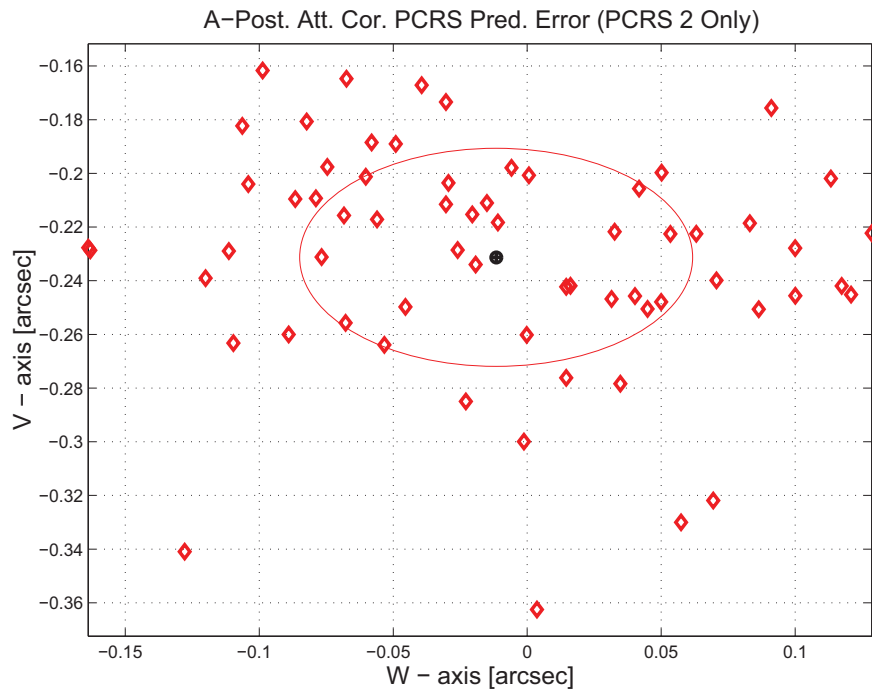


Figure 3.26: A-posteriori PCRS Prediction (PCRS 2 Only)

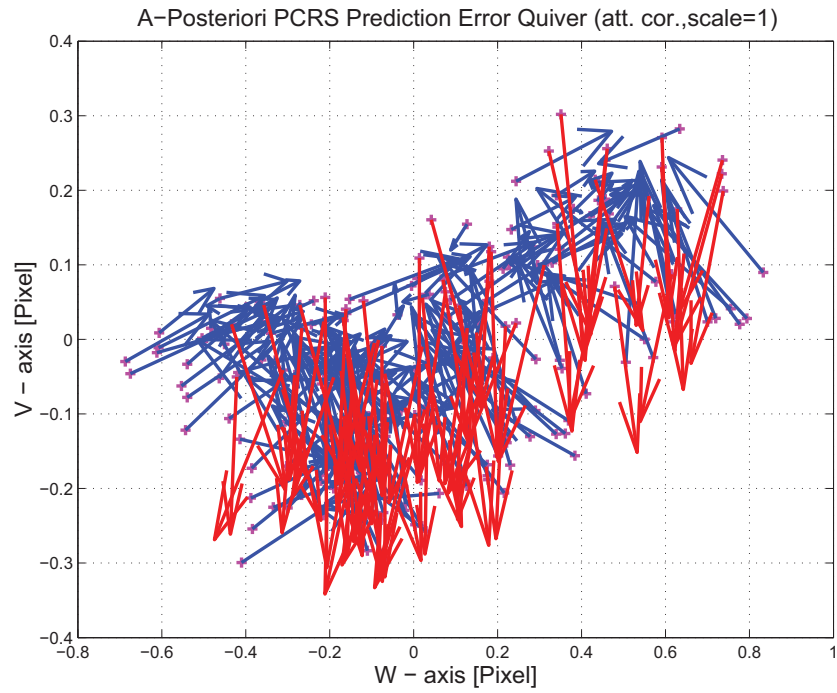


Figure 3.27: A-Posteriori PCRS Prediction Errors Quiver (Att. Cor.)

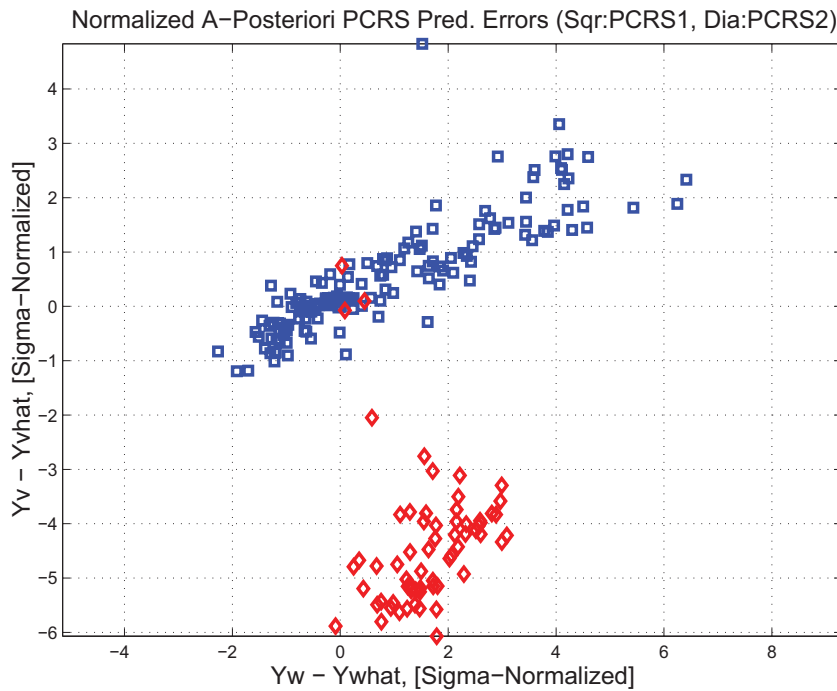


Figure 3.28: Normalized A-Posteriori PCRS Prediction Errors

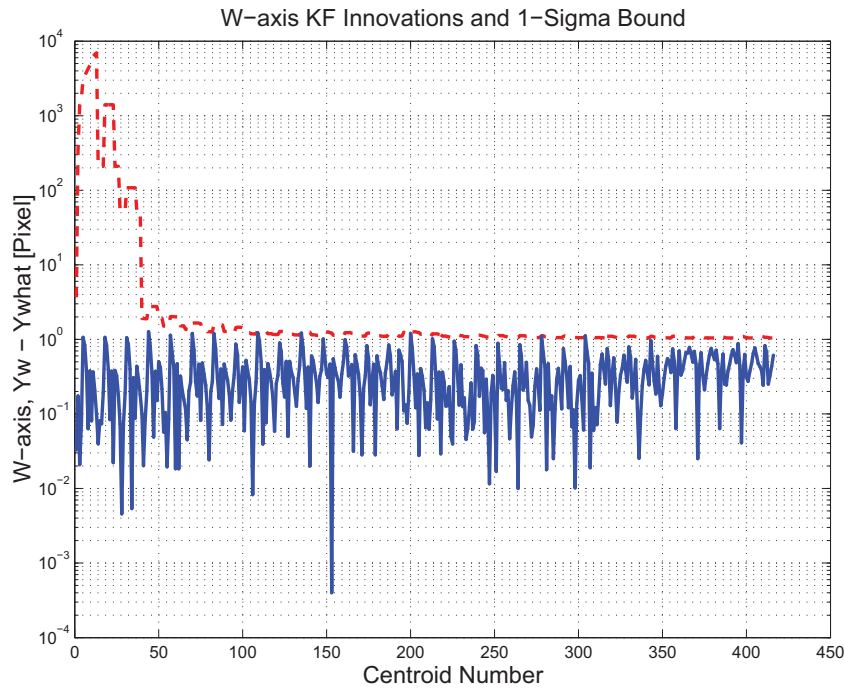


Figure 3.29: W-axis KF innovations and 1-sigma bound

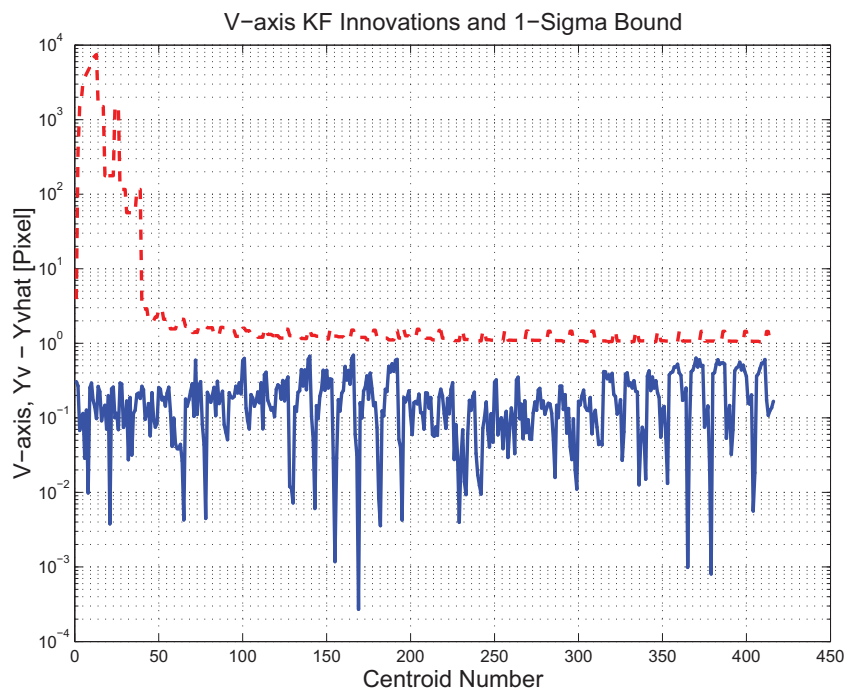


Figure 3.30: V-axis KF innovations and 1-sigma bound

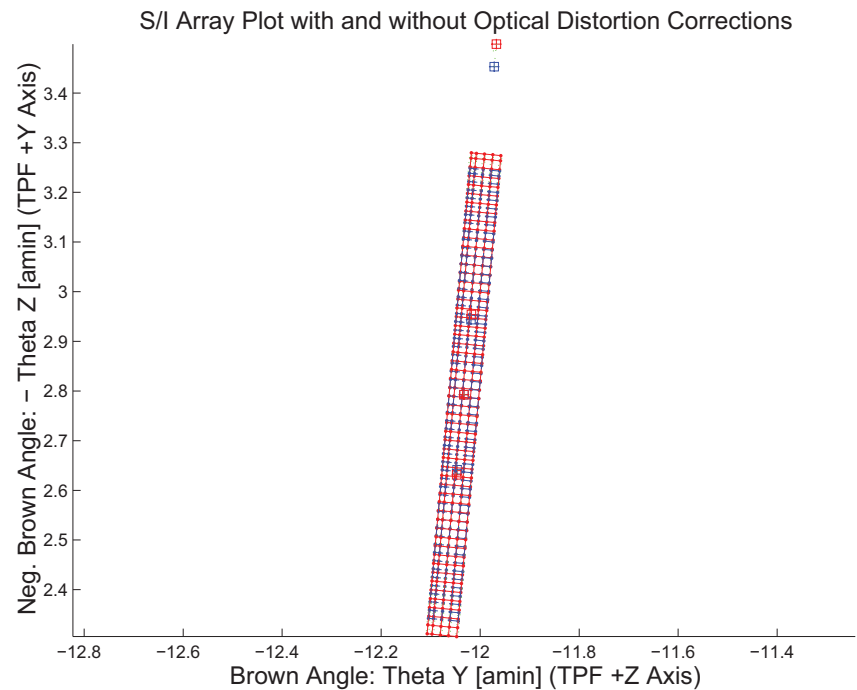


Figure 3.31: Array plot with (solid) and w/o (dashed) optical distortion corrections

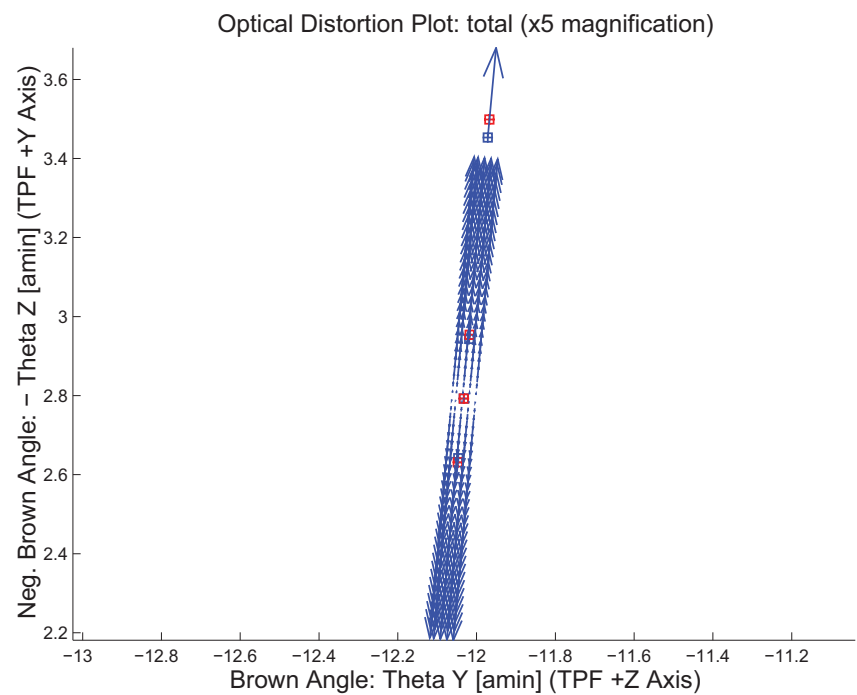


Figure 3.32: Optical Distortion Plot: total (x5 magnification)

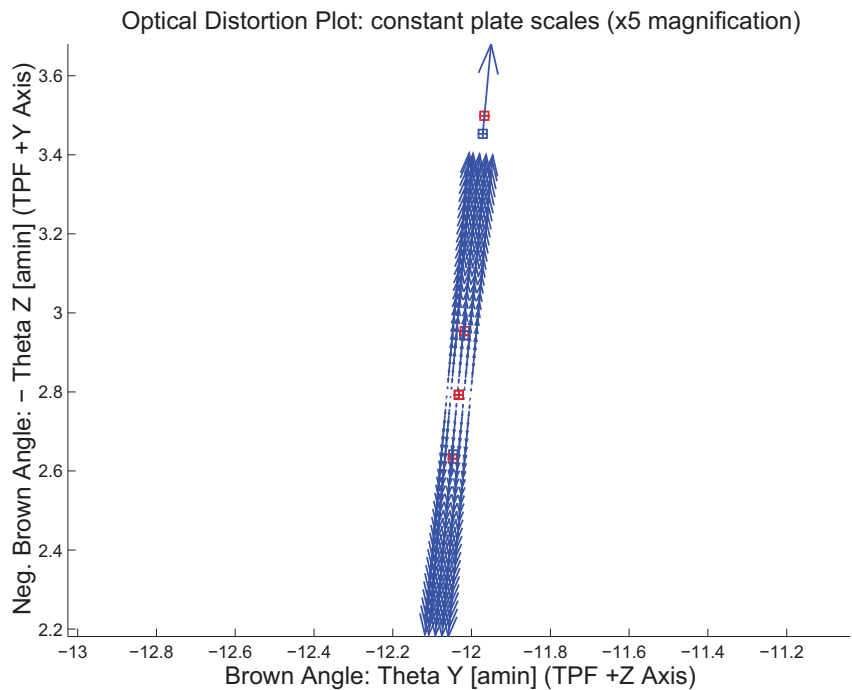


Figure 3.33: Optical Distortion Plot: constant plate scales (x5 magnification)

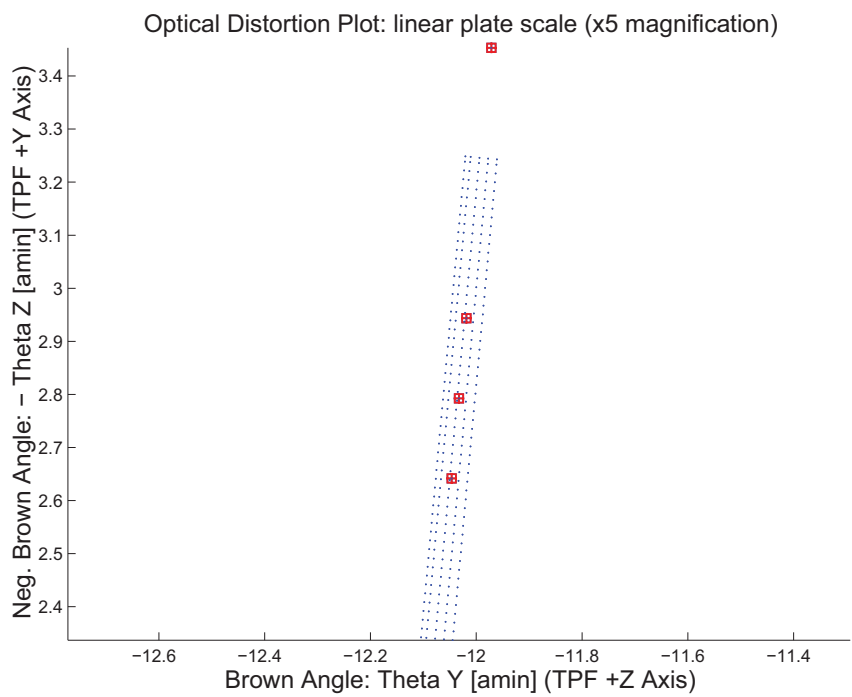


Figure 3.34: Optical Distortion Plot: linear plate scale (x5 magnification)

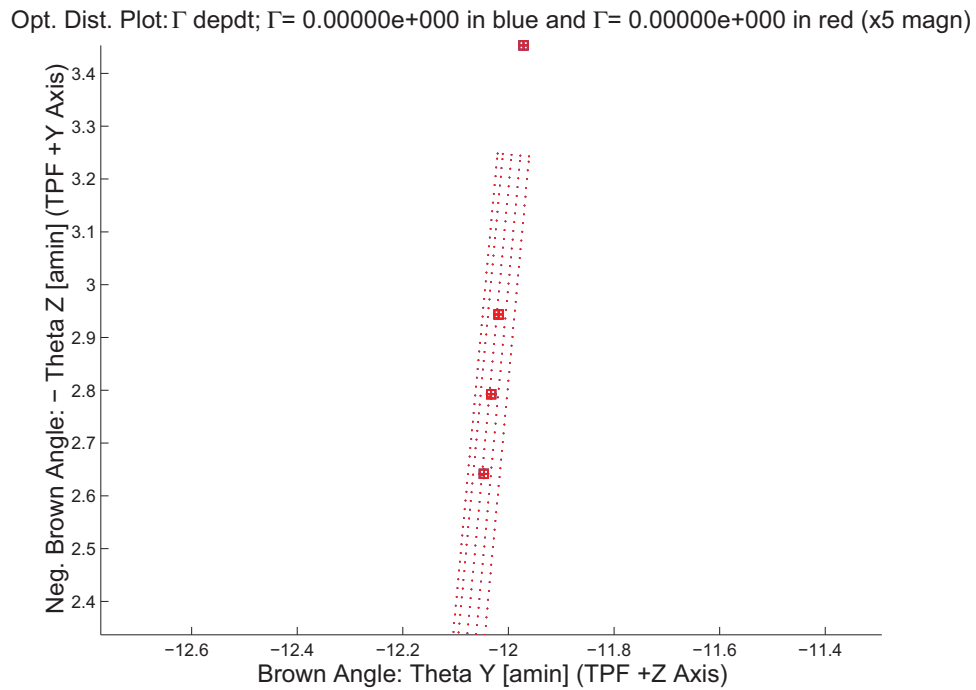


Figure 3.35: Optical Distortion Plot: gamma terms (x5 magnification)

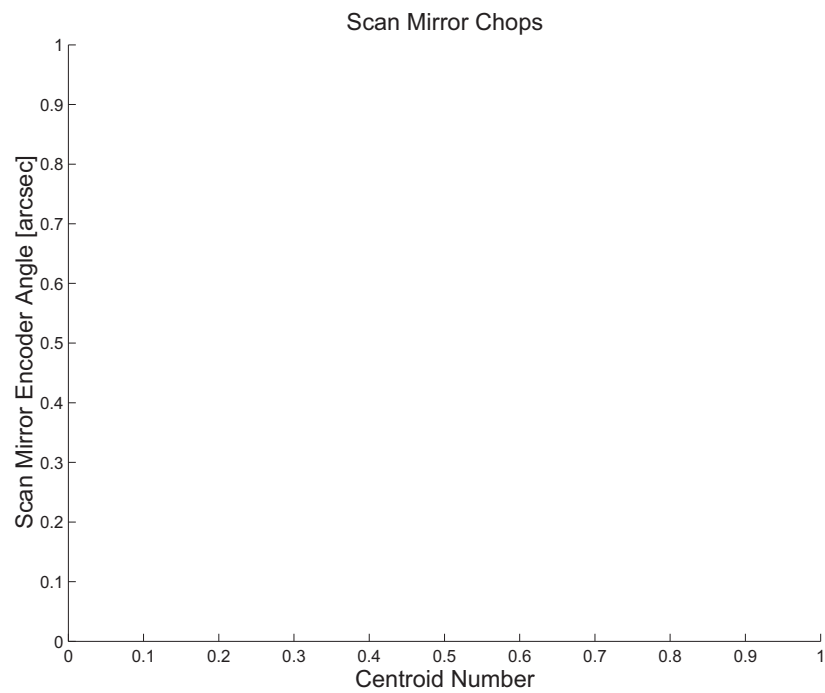


Figure 3.36: Scan Mirror Chops

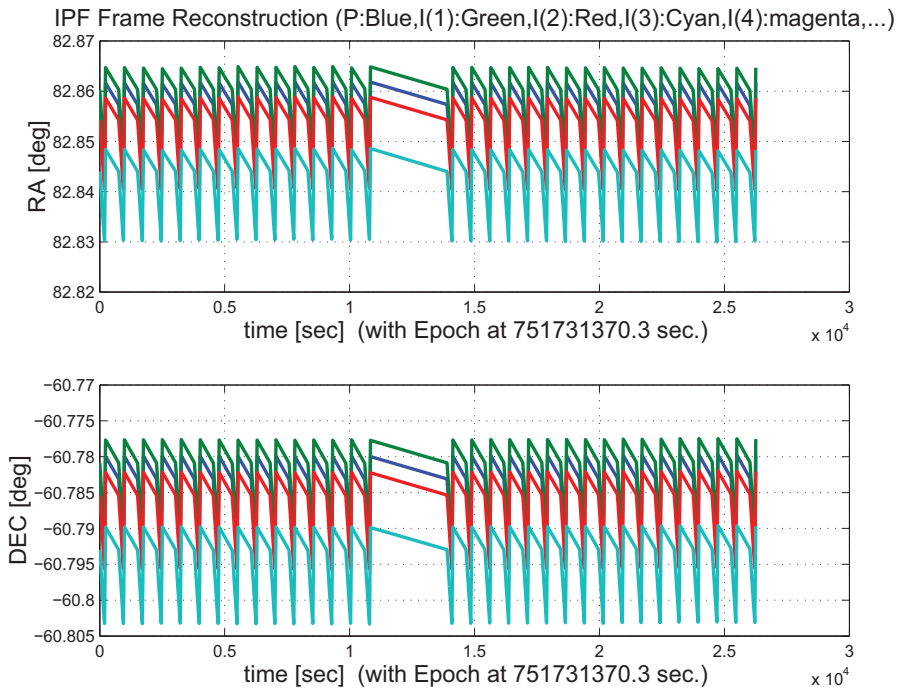


Figure 3.37: IPF Frame Reconstruction

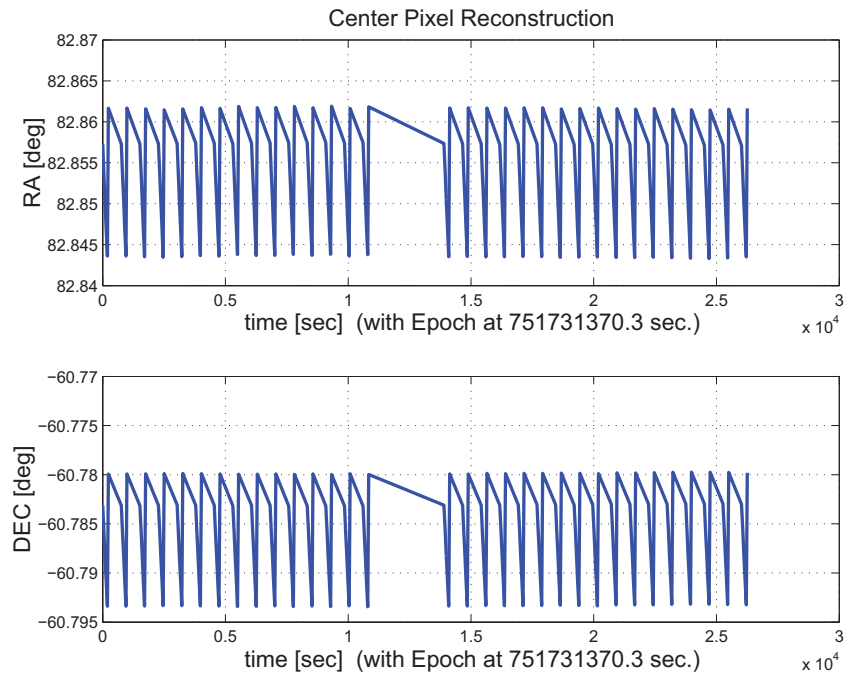


Figure 3.38: Center Pixel Reconstruction

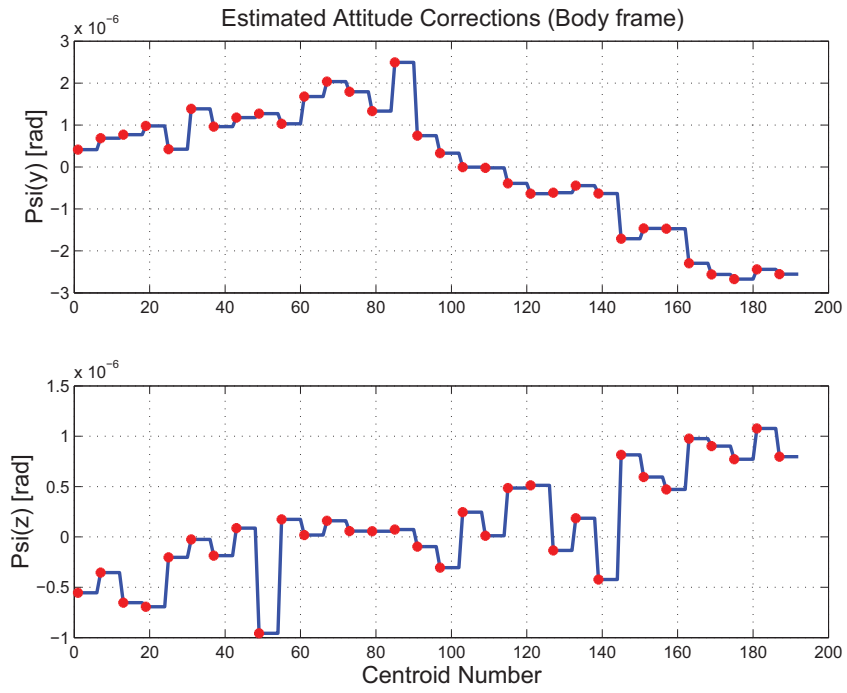


Figure 3.39: Estimated attitude corrections (Body frame)

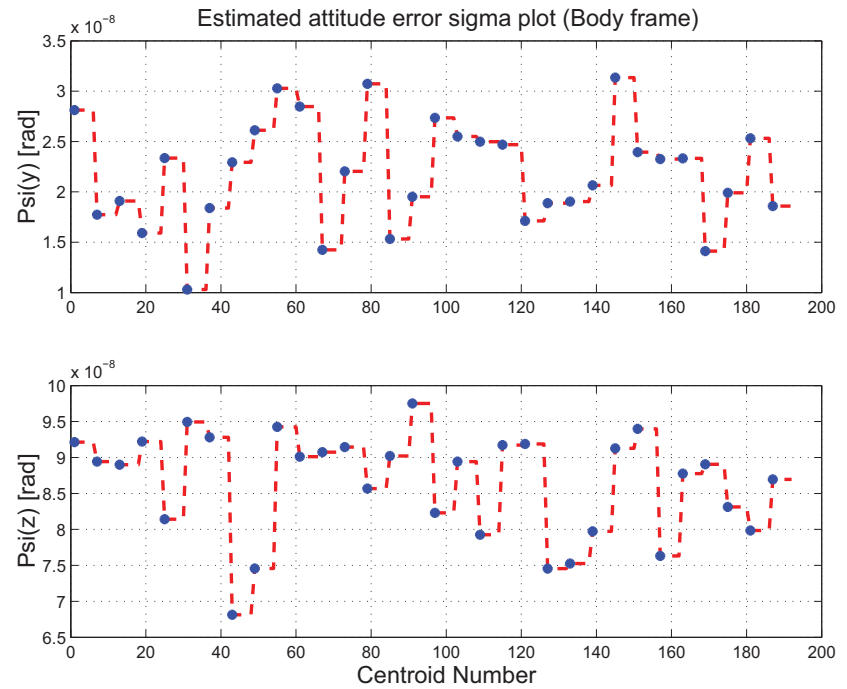


Figure 3.40: Estimated attitude error sigma plot (Body frame)

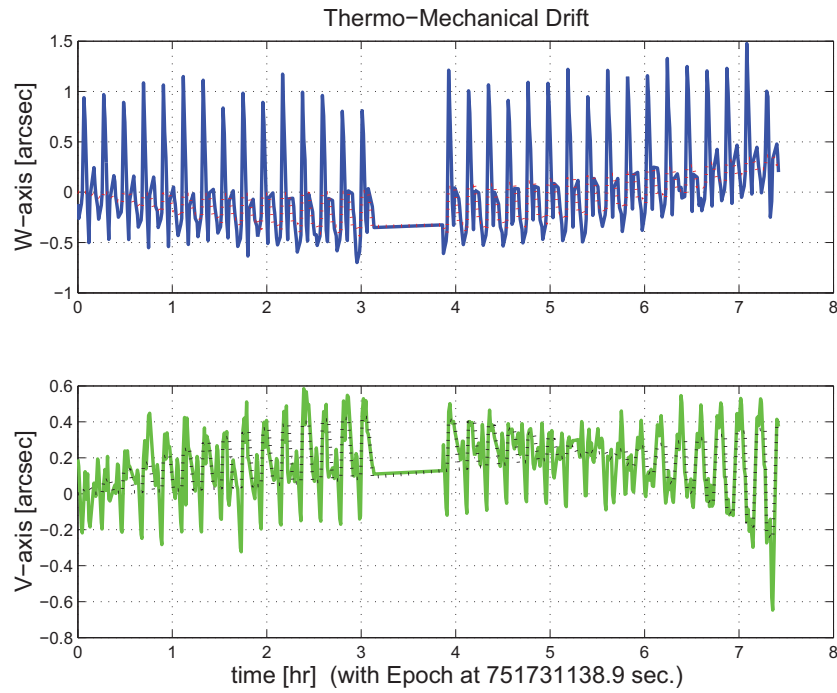


Figure 3.41: Thermo-mechanical boresight drift (equiv. angle in (W,V) coords)

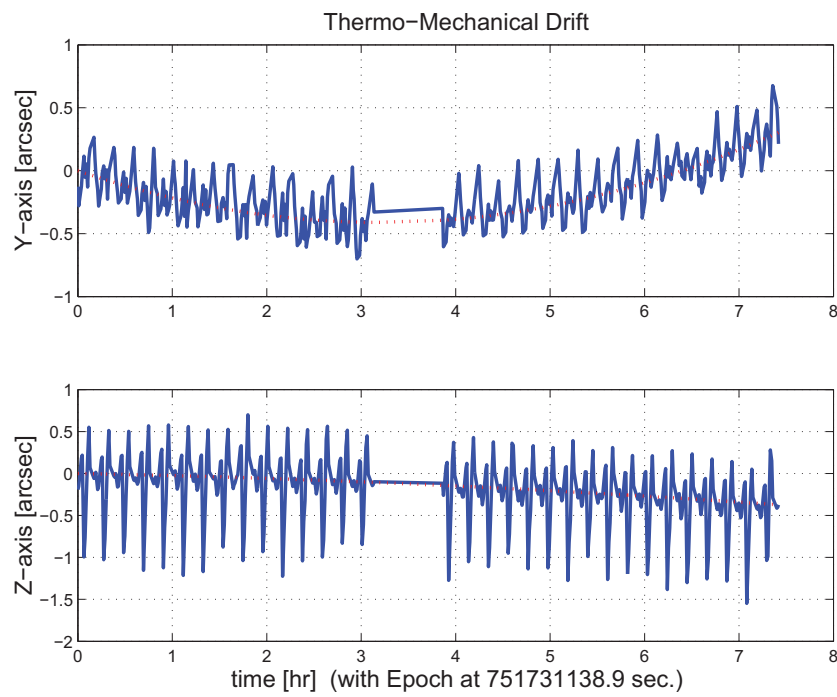


Figure 3.42: Thermo-mechanical boresight drift (equiv. angle in Body frame)

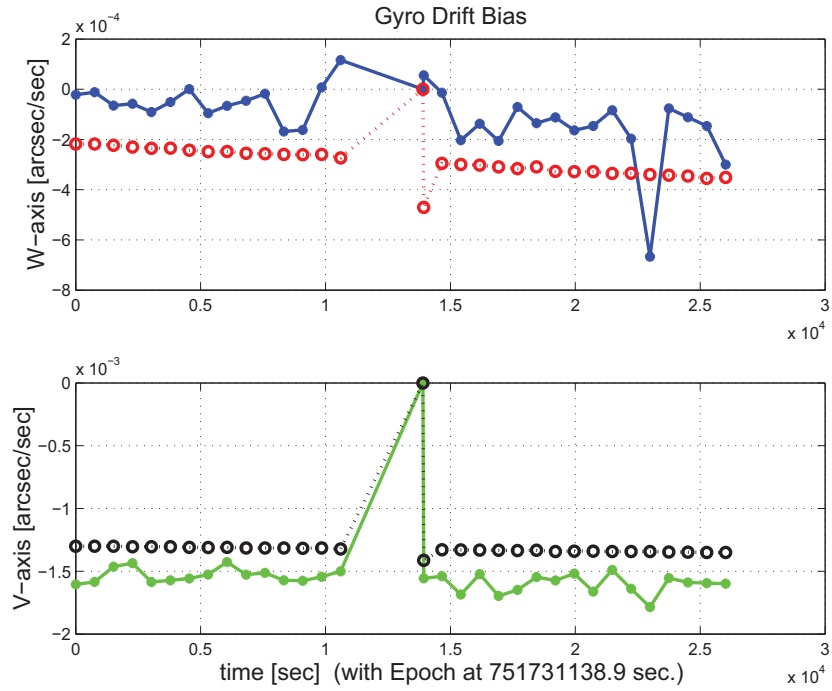


Figure 3.43: Gyro drift bias contribution (equiv. rate in (W,V) coords)

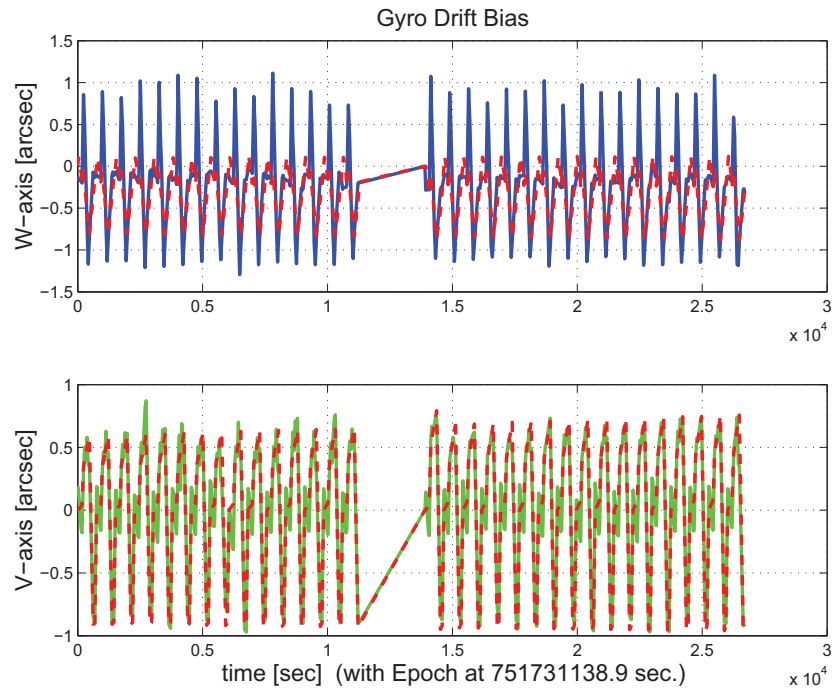


Figure 3.44: Gyro drift bias contribution (equiv. angle in (W,V) coords)

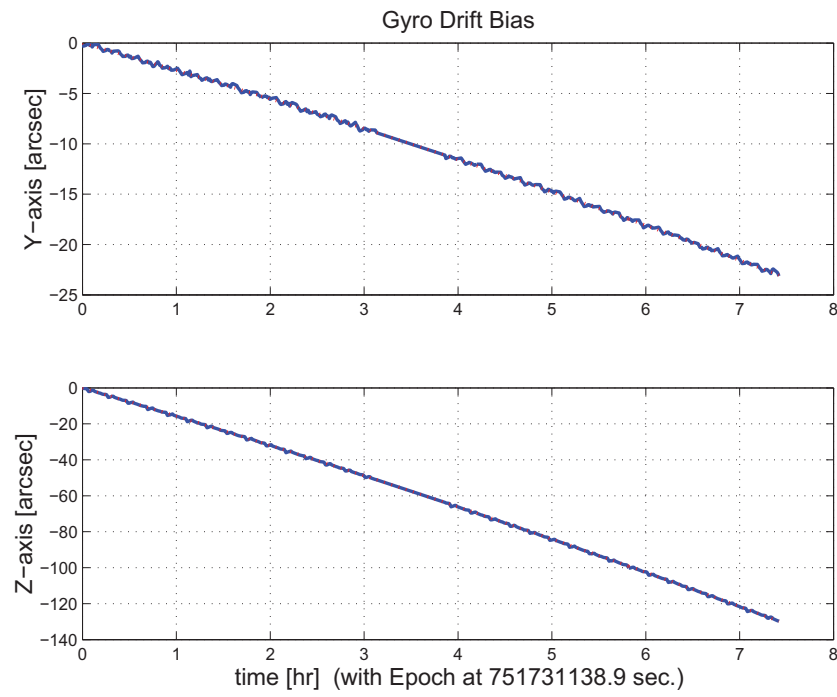


Figure 3.45: Gyro drift bias contribution (equiv. angle in Body frame)

3.2 IPF OUTPUT DATA (IF MINI FILE)

OUTPUT FILE NAME: IFmini502028.dat DATE: 06-Nov-2003 TIME: 14:58
INSTRUMENT NAME: IRS_ShortLo_1st_Ord_Center_Pos NF: 28
IPF FILTER VERSION: IPF.V3.0.0B SW RELEASE DATE: November 3, 2003
FRAME TABLE USED: BodyFrames_FTU_12b

----- IPF BROWN ANGLE SUMMARY -----

WAS			IS			
Frame Number	theta_Y (arcmin)	theta_Z (arcmin)	angle (deg)	theta_Y (arcmin)	theta_Z (arcmin)	angle (deg)
028	-12.031014	-2.776537	-84.719994	-12.032552	-2.792599	-84.719993
026	-12.044971	-2.625513	-84.719994	-12.047468	-2.631200	-84.719993
027	-12.017057	-2.927561	-84.719994	-12.017636	-2.953997	-84.719993
029	-11.969972	-3.437059	-84.719994	-11.967317	-3.498495	-84.719993

OFFSET	NF	Delta_CW	Delta_CV
0	28	+0.000	+0.000 pixels

OFFSET FRAME NAME: IRS_ShortLo_1st_Ord_Center_Pos

Brown Angle	theta_Y(arcmin)	theta_Z(arcmin)	angle(deg)
WAS(FTB)	-12.031014	-2.776537	-84.719994
IS (EST)	-12.032552	-2.792599	-84.719993
dT_EST	-0.001538	-0.016062	+0.000001
T_sSIGMA	+0.000985	+0.000875	+999.999999
dT_EST/T_sSIGMA	-1.561550	-18.349747	+999.999999

OFFSET	NF	Delta_CW	Delta_CV
1	26	-9.100	+0.000 pixels

OFFSET FRAME NAME: IRS_ShortLo_1st_Ord_1st_Pos

Brown Angle	theta_Y(arcmin)	theta_Z(arcmin)	angle(deg)
WAS(FTB)	-12.044971	-2.625513	-84.719994
IS (EST)	-12.047468	-2.631200	-84.719993
dT_EST	-0.002497	-0.005688	+0.000001
T_sSIGMA	+0.001052	+0.000875	+999.999999
dT_EST/T_sSIGMA	-2.372454	-6.497895	+999.999999

OFFSET	NF	Delta_CW	Delta_CV
2	27	+9.100	+0.000 pixels

OFFSET FRAME NAME: IRS_ShortLo_1st_Ord_2nd_Pos

Brown Angle	theta_Y(arcmin)	theta_Z(arcmin)	angle(deg)
WAS(FTB)	-12.017057	-2.927561	-84.719994
IS (EST)	-12.017636	-2.953997	-84.719993
dT_EST	-0.000579	-0.026436	+0.000001
T_sSIGMA	+0.000944	+0.000875	+999.999999
dT_EST/T_sSIGMA	-0.613791	-30.201598	+999.999999

OFFSET	NF	Delta_CW	Delta_CV
3	29	+39.800	+0.000 pixels

OFFSET FRAME NAME: IRS_ShortLo_Module_Center

Brown Angle	theta_Y(arcmin)	theta_Z(arcmin)	angle(deg)
WAS(FTB)	-11.969972	-3.437059	-84.719994
IS (EST)	-11.967317	-3.498495	-84.719993
dT_EST	+0.002655	-0.061435	+0.000001
T_sSIGMA	+0.001026	+0.000875	+999.999999
dT_EST/T_sSIGMA	+2.588876	-70.185304	+999.999999

VARNAME	MEAN	SIGMA	SCALED_SIGMA
a00	+6.8693071855212465E-002	+3.2245121394587015E-004	+1.1238351992073983E-003
del_theta2	-4.7805196201717925E-017	+8.2205919979670894E-008	+2.8651126887024126E-007
del_theta3	-3.6541304423526956E-016	+7.3056749687733810E-008	+2.5462377962249540E-007
del_arx	+1.1644670823299577E-012	+2.4485084374377812E-005	+8.5337559560585665E-005
del_ary	+1.5304131575167917E-014	+1.3202933324997851E-006	+4.6016019049355473E-006

```

del_arz +2.0870360201292440E-014 +1.5702484581173628E-006 +5.4727673905723817E-006
brx +1.2022708092081247E-008 +4.1616301528732299E-009 +1.4504477730596875E-008
bry -3.4727498224045926E-010 +1.6678619583211374E-010 +5.8129785068662596E-010
brz -3.0338480047649187E-011 +2.6013363063410870E-010 +9.0664050237783762E-010
crx -8.9953221186355982E-013 +3.0402621275109410E-013 +1.0596187720625350E-012
cry +3.0101303753606722E-014 +1.2115997783526709E-014 +4.2227736146566088E-014
crz -2.8274678567633319E-015 +1.9291792081932739E-014 +6.7237442626301114E-014
bgx +5.9757865530375755E-006 +2.3988765835818449E-007 +8.3607746740759154E-007
bgy -3.5524184542308187E-009 +2.1385893700580960E-010 +7.4535988911659895E-010
bgz -2.0803344049268431E-008 +1.1630662584746797E-009 +4.0536203424054000E-009
cgx +4.7629401856763607E-011 +1.4712537123479377E-011 +5.1277422363146468E-011
cgy -4.7145226551740444E-014 +1.4450631076012164E-014 +5.0364604478459118E-014
cgz -2.0554865202598213E-013 +7.2492461898416097E-014 +2.5265707441969027E-013

```

LSQF RESIDUAL SIGMA SCALE = +3.4852875430515713E+000

qT	qT(1)	qT(2)	qT(3)	qT(4)
FrmTbl:	-6.7378607921267397E-001	+1.0209060133292000E-003	+1.4774188189635800E-003	+7.3892428194217297E-001
Estim:	-6.7378607535744994E-001	+1.0194972643380847E-003	+1.4792957681896265E-003	+7.3892428364735918E-001
DelTheta	deltheta(1)	deltheta(2)	deltheta(3)	
	-1.7217197886308734E-012	-4.6112570664260272E-006	+8.7545863266075600E-007	[rad]
EulAngT	theta(1)	theta(2)	theta(3)	[rad]
Mean	-1.4786428158489873E+000	+3.5001274979555774E-003	+8.1233407571664037E-004	
SigmaT	+9.9999000000000000E+004	+8.2205919979670894E-008	+7.3056749687733810E-008	

qR	qR(1)	qR(2)	qR(3)	qR(4)
ASFILE:	+7.0888164918869734E-004	+1.2699301587417722E-003	-1.6147216956596822E-004	+9.9999892711639404E-001
Estim:	+6.6093437537587661E-004	+1.2706528124978508E-003	-1.5989120180651706E-004	+9.9999896152045342E-001
DelThetaR	delthetaR(1)	delthetaR(2)	delthetaR(3)	
	-9.5898740407415170E-005	+1.4321214437793184E-006	+3.0390706479952499E-006	[rad]
EulAngR	angR(1)	angR(2)	angR(3)	[rad]
Mean	+1.3214656980879893E-003	+2.5415170771581376E-003	-3.1810346800819315E-004	
SigmaR	+2.4485084374377812E-005	+1.3202933324997851E-006	+1.5702484581173628E-006	

Initial Gyro Bias	Bg0(1)	Bg0(2)	Bg0(3)	
	-3.7722963952546706E-007	-1.9052549760090187E-007	+3.5621116012407583E-007	
Gyro Bias Correction	Bg(1)	Bg(2)	Bg(3)	
	+5.9757865530375755E-006	-3.5524184542308187E-009	-2.0803344049268431E-008	
Total Gyro Bias	BgT(1)	BgT(2)	BgT(3)	
	+5.5985569135121084E-006	-1.9407791605513270E-007	+3.3540781607480738E-007	

Initial Gyro Bias Rate	Cg0(1)	Cg0(2)	Cg0(3)	
	+0.0000000000000000E+000	+0.0000000000000000E+000	+0.0000000000000000E+000	
Gyro Bias Rate Correction	Cg(1)	Cg(2)	Cg(3)	
	+4.7629401856763607E-011	-4.7145226551740444E-014	-2.0554865202598213E-013	
Total Gyro Bias Rate	CgT(1)	CgT(2)	CgT(3)	
	+4.7629401856763607E-011	-4.7145226551740444E-014	-2.0554865202598213E-013	

OFFSET	NF	Delta_CW	Delta_CV	
1	26	-9.100	+0.000	pixels
OFFSET FRAME NAME: IRS_ShortLo_1st_Ord_1st_Pos				
qT	qT(1)	qT(2)	qT(3)	qT(4)
WAS(FTB)	-6.7378605480342335E-001	+1.0372060729182306E-003	+1.4625556765612108E-003	+7.3892431106771239E-001
IS (EST)	-6.7378604929348584E-001	+1.0369170252027796E-003	+1.4634116309533215E-003	+7.3892431480291509E-001

DelTheta	deltheta(1)	deltheta(2)	deltheta(3)	
Units	rad	rad	rad	
	+1.0554517696951005E-008	-1.5806529040657255E-006	+8.7545887496081120E-007	
EulAngT	theta(1)	theta(2)	theta(3)	[rad]
Mean	-1.4786428158489873E+000	+3.5044662605509293E-003	+7.6538519632061096E-004	
sSigmaT	+1.2005167202939043E-011	+3.0613346760988975E-007	+2.5462377729532484E-007	
SigmaT	+3.4445270453719362E-012	+8.7835928550633193E-008	+7.3056749020021165E-008	

OFFSET	NF	Delta_CW	Delta_CV	
--------	----	----------	----------	--

```

2           27      +9.100      +0.000    pixels
OFFSET FRAME NAME: IRS_ShortLo_1st_Ord_2nd_Pos
qT          qT(1)        qT(2)        qT(3)        qT(4)
WAS(FTB)   -6.7378610322816457E-001 +1.0046059510900210E-003 +1.4922819580499510E-003 +7.3892425251716154E-001
IS (EST)   -6.7378610097169700E-001 +1.0020775004472926E-003 +1.4951799016374541E-003 +7.3892425214977420E-001

DelTheta     deltheta(1)      deltheta(2)      deltheta(3)
Units         rad            rad            rad
-1.0532614074516635E-008 -7.6418612286278268E-006 +8.7545745739143687E-007
EulAngT      theta(1)       theta(2)       theta(3)      [rad]
Mean        -1.4786428158489873E+000 +3.4957887276453148E-003 +8.5928295368671007E-004
sSigmaT     +1.2005167202939063E-011 +2.7454753050051110E-007 +2.5462378271809367E-007
SigmaT      +3.4445270453719418E-012 +7.8773279710554042E-008 +7.3056750575924009E-008
-----
-----
```

```

OFFSET      NF      Delta_CW      Delta_CV
3           29      +39.800      +0.000    pixels
OFFSET FRAME NAME: IRS_ShortLo_Module_Center
qT          qT(1)        qT(2)        qT(3)        qT(4)
WAS(FTB)   -6.7378618134247659E-001 +9.4961561267270674E-004 +1.5424246108003514E-003 +7.3892415103881359E-001
IS (EST)   -6.7378618406680668E-001 +9.4330970445350424E-004 +1.5487670042302433E-003 +7.3892414336537915E-001

DelTheta     deltheta(1)      deltheta(2)      deltheta(3)
Units         rad            rad            rad
-4.5872922854547656E-008 -1.7865986856588939E-005 +8.7544663072189450E-007
EulAngT      theta(1)       theta(2)       theta(3)      [rad]
Mean        -1.4786428158489873E+000 +3.4811512811621448E-003 +1.0176709133636844E-003
sSigmaT     +5.2506114840575633E-011 +2.9833497249527714E-007 +2.5462379879768592E-007
SigmaT      +1.5065074026748303E-011 +8.5598381427682025E-008 +7.3056755189486606E-008
-----
```

```

-----
```

```

q(1)          q(2)          q(3)          q(4)
PCRS1A: +5.3371888965461637E-007 +3.7444233778550031E-004 -1.4253684912431913E-003 +9.9999891405806784E-001
PCRS2A: -5.2779261998836216E-007 +3.8462959425181312E-004 +1.3722087221825403E-003 +9.9999898455099423E-001

***** CS-FILE PARAMETERS: ***** AS-FILE PARAMETERS: *****
Row (01) PIX2RADX: +4.8481368110953598E-006 Row (1) TASTART: +7.5173000759077454E+008
Row (02) PIX2RADY: +4.8481368110953598E-006 Row (2) TASTOP: +7.5175899999075925E+008
Row (03) CX0:      +0.0000000000000000E+000 Row (3) S/C TIME: +7.5171031749078369E+008
Row (04) CY0:      +0.0000000000000000E+000 Row (4) QR1:      +7.0888164918869734E-004
Row (05) BETA0:    +9.9999000000000000E+004 Row (5) QR2:      +1.2699301587417722E-003
Row (06) GAMMA_E0: +9.9999000000000000E+004 Row (6) QR3:      -1.6147216956596822E-004
Row (07) D11:      +1.0000000000000000E+000 Row (7) QR4:      +9.9999892711639404E-001
Row (08) D12:      +0.0000000000000000E+000
Row (09) D21:      +0.0000000000000000E+000
Row (10) D22:      +1.0000000000000000E+000
Row (11) DG:       +9.9999000000000000E+004
-----
```

```

-----
```

```

INITIAL STA-TO-PCRS ALIGNMENT (R) KNOWLEDGE (1-SIGMA)
SIGMA(X)      SIGMA(Y)      SIGMA(Z)
5.93149246E+000 3.78252351E-001 3.78761405E-001 [arcsec]

PIX2RADX = 4.848136811095E-006[rad/pixel]
XPIXSIZE = 1.0000[arcsec]
PIX2RADY = 4.848136811095E-006[rad/pixel]
YPIXSIZE = 1.0000[arcsec]
CX0 = 0.0[pixel] = 0.00[arcsec]
CY0 = 0.0[pixel] = 0.00[arcsec]
-----
```

```

NOMINAL BETA0 = 9.999900000000E+004[rad/encoder unit]
ENCODER UNIT SIZE = 99999.00[arcsec]
GAMMA_E0 = 99999.00[encoder unit] = 99999.00[arcsec]
-----
```

```

| +1 | +0 |
FLIP MATRIX D = |----|----| and DG = +99999
| +0 | +1 |
-----
```

3.3 IPF EXECUTION LOG

```
*****
IPF EXECUTION-LOG FILE NAME: LG502028.dat
INSTRUMENT TYPE: IRS_ShortLo_1st_Ord_Center_Pos
IPF FILTER EXECUTION DATE: 06-Nov-2003 TIME: 14:52
IPF FILTER VERSION USED: IPF.V3.0.0B
*****


*****
SLIT FLAG ENABLED! ENTERING SLIT MODE.
*****


----- Loading & Preparing Input Files -----
AAFILE: AA501028 Loaded! AAFILE dimension = 289925 X 21
ASFILE: AS501028 Loaded!
CAFFILE: CA501028 Loaded! CAFFILE dimension = 192 X 15
CBFILE: CB502028 Loaded! CBFILE dimension = 224 X 15
CCFILE: CC502028 Created! CCFILE dimension = 416 X 19
CSFILE: CS501028 Loaded!
Loading Input Files Completed!
-----


----- Selected Mask Vectors -----
index = 1 2 3 4 5 6 7 8 9 10 11 12 13 14 15 16 17 18 19 20
-----
mask1 = [ 1 0 0 0 0 0 0 0 0 0 0 0 0 0 0 0 0 0 0 0 ]
mask2 = [ 0 0 0 1 1 1 1 1 1 1 1 1 1 1 1 1 1 1 1 1 ]
-----


----- Selected Initial Gyro Bias Parameters -----
User Entered 1 : Use AFILE database - from S/C filter
IPF Linearized Using Following Nominal Gyro Bias Estimates
bg0 = [-3.7722963952546706E-007 -1.9052549760090187E-007 +3.5621116012407583E-007 ]
cg0 = [+0.000000000000000E+000 +0.000000000000000E+000 +0.000000000000000E+000 ]
-----


----- Gyro Pre-Processor Run Completed -----
AGFILE CREATED: AG502028.m ACFILE CREATED: AC502028.m
-----


Total Gyro Preprocessor Execution Time: 157 seconds

FRAME TABLE ENTRIES FOR PCRS LOADED TO TPCRS
q_PCRS4 = [ +5.3371888965461637E-007 q_PCRS5 = [ +7.3379987833742897E-007
            +3.7444233778550031E-004 +5.2236196154513707E-004
            -1.4253684912431913E-003 -1.4047712280184723E-003
            +9.9999891405806784E-001 ]; +9.9999887687698918E-001 ];
q_PCRS8 = [ -5.2779261998836216E-007 q_PCRS9 = [ -7.1963421681856818E-007
            +3.8462959425181312E-004 +5.3239763239987400E-004
            +1.3722087221825403E-003 +1.3516841804518383E-003
            +9.9999898455099423E-001 ]; +9.9999894475050310E-001 ];
----- Initial Conditions for State ----- Initial Square-Root Cov (diag) -----
p1(01) = a00 = +0.000000000000000E+000 Sigma_initial(01,01) = 1.000000000000000E+000
p1(02) = b00 = +0.000000000000000E+000 Sigma_initial(02,02) = 9.999900000000000E+004
p1(03) = c00 = +0.000000000000000E+000 Sigma_initial(03,03) = 9.999900000000000E+004
p1(04) = a10 = +0.000000000000000E+000 Sigma_initial(04,04) = 9.999900000000000E+004
p1(05) = b10 = +0.000000000000000E+000 Sigma_initial(05,05) = 9.999900000000000E+004
-----
```

```

p1(06) = c10 = +0.0000000000000000E+000 Sigma_initial(06,06) = 9.999900000000000E+004
p1(07) = d10 = +0.0000000000000000E+000 Sigma_initial(07,07) = 9.999900000000000E+004
p1(08) = a20 = +0.0000000000000000E+000 Sigma_initial(08,08) = 9.999900000000000E+004
p1(09) = b20 = +0.0000000000000000E+000 Sigma_initial(09,09) = 9.999900000000000E+004
p1(10) = c20 = +0.0000000000000000E+000 Sigma_initial(10,10) = 9.999900000000000E+004
p1(11) = d20 = +0.0000000000000000E+000 Sigma_initial(11,11) = 9.999900000000000E+004
p1(12) = a01 = +0.0000000000000000E+000 Sigma_initial(12,12) = 9.999900000000000E+004
p1(13) = b01 = +0.0000000000000000E+000 Sigma_initial(13,13) = 9.999900000000000E+004
p1(14) = c01 = +0.0000000000000000E+000 Sigma_initial(14,14) = 9.999900000000000E+004
p1(15) = d01 = +0.0000000000000000E+000 Sigma_initial(15,15) = 9.999900000000000E+004
p1(16) = e01 = +0.0000000000000000E+000 Sigma_initial(16,16) = 9.999900000000000E+004
p1(17) = f01 = +0.0000000000000000E+000 Sigma_initial(17,17) = 9.999900000000000E+004
-----
p2f(01) = am1 = +0.0000000000000000E+000 Sigma_initial(18,18) = 9.999900000000000E+004
p2f(02) = am2 = +0.0000000000000000E+000 Sigma_initial(19,19) = 9.999900000000000E+004
p2f(03) = am3 = +1.0000000000000000E+000 Sigma_initial(20,20) = 9.999900000000000E+004
p2f(04) = beta = +1.0000000000000000E+000 Sigma_initial(21,21) = 1.000000000000000E-002
p2f(05) = qT1 = -6.7378607921267442E-001 Sigma_initial(22,22) = 1.000000000000000E-002
p2f(06) = qT2 = +1.02090601323292006E-003 Sigma_initial(23,23) = 2.8756686962501117E-004
p2f(07) = aT3 = +1.4774188189635811E-003 Sigma_initial(24,24) = 1.8338191452089435E-005
p2f(08) = qT4 = +7.3892428194217341E-001 Sigma_initial(25,25) = 1.8362871115920518E-005
p2f(09) = qR1 = +7.0888164918869734E-004 Sigma_initial(26,26) = 3.7441965018494723E-005
p2f(10) = qR2 = +1.2699301587417722E-003 Sigma_initial(27,27) = 3.7441965018494723E-005
p2f(11) = qR3 = -1.6147216956596822E-004 Sigma_initial(28,28) = 3.7441965018494723E-005
p2f(12) = qR4 = +9.9999892711639404E-001 Sigma_initial(29,29) = 1.4019007444461827E-009
p2f(13) = brx = +0.0000000000000000E+000 Sigma_initial(30,30) = 1.4019007444461827E-009
p2f(14) = bry = +0.0000000000000000E+000 Sigma_initial(31,31) = 1.4019007444461827E-009
p2f(15) = brz = +0.0000000000000000E+000 Sigma_initial(32,32) = 3.7441965018494723E-005
p2f(16) = crx = +0.0000000000000000E+000 Sigma_initial(33,33) = 3.7441965018494723E-005
p2f(17) = cry = +0.0000000000000000E+000 Sigma_initial(34,34) = 3.7441965018494723E-005
p2f(18) = crz = +0.0000000000000000E+000 Sigma_initial(35,35) = 1.4019007444461827E-009
p2f(19) = bgx = +0.0000000000000000E+000 Sigma_initial(36,36) = 1.4019007444461827E-009
p2f(20) = bgy = +0.0000000000000000E+000 Sigma_initial(37,37) = 1.4019007444461827E-009
p2f(21) = bgz = +0.0000000000000000E+000 Sigma_initial(38,38) = 1.4019007444461827E-009
p2f(22) = cgx = +0.0000000000000000E+000 Sigma_initial(39,39) = 1.4019007444461827E-009
p2f(23) = cgy = +0.0000000000000000E+000 Sigma_initial(40,40) = 1.4019007444461827E-009
p2f(24) = cgz = +0.0000000000000000E+000 Sigma_initial(41,41) = 1.4019007444461827E-009
-----

```

```

----- IPF KALMAN FILTER STARTED -----
Iteration#001: |dp|= +6.389200633002E-002 RMS(|Res|)=+9.941273891199E-006
Iteration#002: |dp|= +4.319427272488E-003 RMS(|Res|)=+2.377998936383E-006
Iteration#003: |dp|= +5.336584864354E-004 RMS(|Res|)=+3.021868906000E-006
Iteration#004: |dp|= +6.716680550602E-005 RMS(|Res|)=+3.045710821361E-006
Iteration#005: |dp|= +8.478576133004E-006 RMS(|Res|)=+3.048649470633E-006
Iteration#006: |dp|= +1.073336248536E-006 RMS(|Res|)=+3.049133586766E-006
Iteration#007: |dp|= +1.356973294263E-007 RMS(|Res|)=+3.049205176196E-006
Iteration#008: |dp|= +1.715168675709E-008 RMS(|Res|)=+3.049214112184E-006
Iteration#009: |dp|= +2.170525319727E-009 RMS(|Res|)=+3.049215156480E-006
Iteration#010: |dp|= +2.744234396924E-010 RMS(|Res|)=+3.049215287306E-006
Iteration#011: |dp|= +3.506198106511E-011 RMS(|Res|)=+3.049215304314E-006
Iteration#012: |dp|= +5.157142714456E-012 RMS(|Res|)=+3.049215306299E-006
Iteration#013: |dp|= +8.975433373278E-013 RMS(|Res|)=+3.049215306641E-006
Iteration#014: |dp|= +1.552476663565E-013 RMS(|Res|)=+3.049215307027E-006
Iteration#015: |dp|= +9.774019721114E-013 RMS(|Res|)=+3.049215306989E-006
Iteration#016: |dp|= +3.381963513109E-013 RMS(|Res|)=+3.049215306566E-006
Iteration#017: |dp|= +5.793120003435E-014 RMS(|Res|)=+3.049215306786E-006
Iteration#018: |dp|= +1.466464293611E-013 RMS(|Res|)=+3.049215306593E-006
Iteration#019: |dp|= +4.543995052808E-013 RMS(|Res|)=+3.049215306992E-006
Iteration#020: |dp|= +3.371954602213E-013 RMS(|Res|)=+3.049215306437E-006
Iteration#021: |dp|= +2.528836376172E-013 RMS(|Res|)=+3.049215306251E-006
Iteration#022: |dp|= +7.674832435137E-013 RMS(|Res|)=+3.049215306147E-006
Iteration#023: |dp|= +4.563426514661E-013 RMS(|Res|)=+3.049215306907E-006
Iteration#024: |dp|= +6.663946751830E-013 RMS(|Res|)=+3.049215306698E-006
Iteration#025: |dp|= +1.513225745004E-012 RMS(|Res|)=+3.049215306712E-006
IPF Kalman Filter Completed with Error |dp1| + |dp2| = +1.5132257450042221E-012
-----
```

----- IPF LEAST SQUARES FILTER STARTED -----

```

Iteration#001 COND#=+6.619149863052E+006, |dp|=+6.389217855252E-002
Iteration#002 COND#=+6.486839552539E+006, |dp|=+4.321467623728E-003
Iteration#003 COND#=+6.475122479694E+006, |dp|=+5.324173477494E-004
Iteration#004 COND#=+6.473756772851E+006, |dp|=+6.704910433369E-005
Iteration#005 COND#=+6.473584764295E+006, |dp|=+8.476698886900E-006
Iteration#006 COND#=+6.473562984299E+006, |dp|=+1.072512062231E-006
Iteration#007 COND#=+6.473560226561E+006, |dp|=+1.357275944117E-007
Iteration#008 COND#=+6.473559877458E+006, |dp|=+1.717749871542E-008
Iteration#009 COND#=+6.473559833269E+006, |dp|=+2.174144494061E-009
Iteration#010 COND#=+6.473559827677E+006, |dp|=+2.750789582699E-010
Iteration#011 COND#=+6.473559826969E+006, |dp|=+3.485641810352E-011
Iteration#012 COND#=+6.473559826879E+006, |dp|=+4.429706913287E-012
Iteration#013 COND#=+6.473559826868E+006, |dp|=+6.147646300597E-013
Iteration#014 COND#=+6.473559826866E+006, |dp|=+3.010765724580E-014
Iteration#015 COND#=+6.473559826866E+006, |dp|=+7.022189355499E-014
Iteration#016 COND#=+6.473559826865E+006, |dp|=+1.819965133604E-015
Iteration#017 COND#=+6.473559826865E+006, |dp|=+5.209894064537E-015
Iteration#018 COND#=+6.473559826865E+006, |dp|=+1.029822200929E-014
Iteration#019 COND#=+6.473559826865E+006, |dp|=+3.679148904569E-014
Iteration#020 COND#=+6.473559826865E+006, |dp|=+9.053371814760E-014
Iteration#021 COND#=+6.473559826866E+006, |dp|=+1.174806370553E-013
Iteration#022 COND#=+6.473559826865E+006, |dp|=+8.334668027799E-014
Iteration#023 COND#=+6.473559826865E+006, |dp|=+3.252525303476E-014
Iteration#024 COND#=+6.473559826865E+006, |dp|=+1.141267788623E-013
Iteration#025 COND#=+6.473559826865E+006, |dp|=+6.679738984011E-014
IPF Least Squares Filter Completed with Error |dp1| + |dp2| = +6.6797389840106698E-014
-----
```

Total Execution Time: 336 seconds

4 COMMENTS

Overall the data looked clean, and the filter converged nicely.

Comments:

1. The run was performed in normal IPF operating mode with the slit mode processing enabled.
2. This run uses IPF version 3.0 where the gyro drift bias estimates make use of the recently corrected GCF signs, (MCR 2521) and now show no sandwich-to-sandwich variations.
3. There were 32 sandwiches maneuvers with 192 science centroids and 224 PCRS measurements.
4. We estimated 18 parameters consisting of: 1 constant plate scale (along W-axis), 2 IPF alignment angles, 3 STA-to-PCRS alignment angles, 6 STA-to-PCRS thermomechanical drift parameters, and 3 gyro bias and 3 gyro bias-drift parameters.

We recommend updating frames 28, 26, 27 and 29 with the new quaternion listed in the IF file IF502028.dat. This contains adjustments of about 0.1 and 0.96 arcseconds in Y and Z. In our best judgement, this fine survey is accurate to 0.1165 arcsecond which satisfies its fine survey requirement of 0.14 arcsecond.

IPF TEAM CONTACT INFORMATION

IPF Team email	ipf@sirtfweb.jpl.nasa.gov	
David S. Bayard	X4-8208	David.S.Bayard@jpl.nasa.gov (TEAM LEADER)
Dhemetrio Boussalis	X4-3977	boussali@grover.jpl.nasa.gov
Paul Brugarolas	X4-9243	Paul.Brugarolas@jpl.nasa.gov
Bryan H. Kang	X4-0541	Bryan.H.Kang@jpl.nasa.gov
Edward.C.Wong	X4-3053	Edward.C.Wong@jpl.nasa.gov (TASK MANAGER)

ACKNOWLEDGEMENTS

This work was performed at the Jet Propulsion Laboratory, California Institute of Technology, under contract with the National Aeronautics and Space Administration.

References

- [1] D.S. Bayard, B.H. Kang, *SIRTF Instrument Pointing Frame Kalman Filter Algorithm*, JPL D-Document D-24809, September 30, 2003.
- [2] B.H. Kang, D.S. Bayard, *SIRTF Instrument Pointing Frame (IPF) Software Description Document and User's Guide*, JPL D-Document D-24808, September 30, 2003.
- [3] D.S. Bayard, B.H. Kang, *SIRTF Instrument Pointing Frame (IPF) Kalman Filter Unit Test Report*, JPL D-Document D-24810, September 30, 2003.
- [4] *Space Infrared Telescope Facility In-Orbit Checkout and Science Verification Mission Plan*, JPL D-Document D-22622, 674-FE-301 Version 1.4, February 8, 2002.
- [5] *Space Infrared Telescope Facility Observatory Description Document*, Lockheed Martin LMMS/P458569, 674-SEIT-300 Version 1.2, November 1, 2002.
- [6] *SIRTF Software Interface Specification for Science Centroid INPUT Files (CAFILe, CS-FILE)*, JPL SOS-SIS-2002, November 18, 2002.
- [7] *SIRTF Software Interface Specification for Inferred Frames Offset INPUT Files (OFILE)*, JPL SOS-SIS-2003, November 18, 2002.
- [8] *SIRTF Software Interface Specification for PCRS Centroid INPUT Files (CBFILE)*, JPL SIS-FES-015, November 18, 2002.
- [9] *SIRTF Software Interface Specification for Attitude INPUT Files (AFILE, ASFILE)*, JPL SIS-FES-014, January 7, 2002.
- [10] *SIRTF Software Interface Specification for IPF Filter Output Files (IFFILE, LGFILE, TARFILE)*, JPL SOS-SIS-2005, November 18, 2002.
- [11] R.J. Brown, *Focal Surface to Object Space Field of View Conversion*. Systems Engineering Report SER No. S20447-OPT-051, Ball Aerospace & Technologies Corp., November 23, 1999.

This page left blank.

JET PROPULSION LABORATORY

SIRTF IPF REPORT

JPL ID502034

November 6, 2003

**SIRTF INSTRUMENT POINTING FRAME
KALMAN FILTER EXECUTION SUMMARY**

IPF RUN NUMBER: 502034

REPORT TYPE: IOC EXECUTION (FINE)

PRIME FRAME: IRS_ShortLo_2nd_Ord_Center_Pos (34)

INFERRRED FRAMES: (32) (33)

IPF TEAM

Autonomy and Control Section (345)

Jet Propulsion Laboratory

California Institute of Technology

4800 Oak Grove Drive

Pasadena, CA 91109

Contents

1 IPF EXECUTION SUMMARY	5
2 IPF INPUT FILE HISTORY	9
3 IPF EXECUTION RESULTS	10
3.1 IPF EXECUTION OUTPUT PLOTS	10
3.2 IPF OUTPUT DATA (IF MINI FILE)	36
3.3 IPF EXECUTION LOG	38
4 COMMENTS	41

List of Figures

1.1 A-priori and a-posteriori IPF frames	5
1.2 A-priori and a-posteriori IPF frames (ZOOMED)	8
2.1 Scenario Plot	9
3.1 TPF coords of measurements and a-priori predicts	12
3.2 Oriented PixelCoords of measurements and a-priori predicts	12
3.3 Oriented (W,V) PixelCoords of A-Priori Prediction Error Quiver Plot	13
3.4 A-priori prediction error (Science Centroids)	13
3.5 Oriented PixelCoords of measurements and a-priori predicts (PCRS only)	14
3.6 Oriented PixelCoords of measurements and a-priori predicts (Zoomed, PCRS only)	14
3.7 Oriented (W,V) PixelCoords of A-Priori PCRS Prediction Error Quiver Plot	15
3.8 A-priori PCRS prediction error	15
3.9 IPF execution convergence, chart 1	16
3.10 IPF execution convergence, chart 2	16
3.11 Parameter uncertainty convergence	17
3.12 IPF parameter symbol table	17
3.13 KF parameter error sigma plots	18
3.14 LS parameter error sigma plot	18
3.15 KF and LS parameter error sigma plot	19
3.16 Oriented PixelCoords of meas. and a-posteriori predicts	20
3.17 Oriented PixelCoords of meas. and a-posteriori predicts (attitude corrected)	20

3.18	KF innovations with (o) and w/o (+) attitude corrections	21
3.19	Histograms of science a-posteriori residuals (or innovations)	21
3.20	A-Posteriori Science Centroid Prediction Error Quiver (Att. Cor.)	22
3.21	Normalized A-Posteriori Science Centroid Prediction Errors	22
3.22	KF innovations with (o) and w/o (+) attitude corrections (PCRS)	23
3.23	Histograms of PCRS a-posteriori residuals (or innovations)	23
3.24	A-posteriori PCRS Prediction Summary	24
3.25	A-posteriori PCRS Prediction (PCRS 1 Only)	25
3.26	A-posteriori PCRS Prediction (PCRS 2 Only)	25
3.27	A-Posteriori PCRS Prediction Errors Quiver (Att. Cor.)	26
3.28	Normalized A-Posteriori PCRS Prediction Errors	26
3.29	W-axis KF innovations and 1-sigma bound	27
3.30	V-axis KF innovations and 1-sigma bound	27
3.31	Array plot with (solid) and w/o (dashed) optical distortion corrections	28
3.32	Optical Distortion Plot: total (x5 magnification)	28
3.33	Optical Distortion Plot: constant plate scales (x5 magnification)	29
3.34	Optical Distortion Plot: linear plate scale (x5 magnification)	29
3.35	Optical Distortion Plot: gamma terms (x5 magnification)	30
3.36	Scan Mirror Chops	30
3.37	IPF Frame Reconstruction	31
3.38	Center Pixel Reconstruction	31
3.39	Estimated attitude corrections (Body frame)	32
3.40	Estimated attitude error sigma plot (Body frame)	32
3.41	Thermo-mechanical boresight drift (equiv. angle in (W,V) coords)	33
3.42	Thermo-mechanical boresight drift (equiv. angle in Body frame)	33
3.43	Gyro drift bias contribution (equiv. rate in (W,V) coords)	34
3.44	Gyro drift bias contribution (equiv. angle in (W,V) coords)	34
3.45	Gyro drift bias contribution (equiv. angle in Body frame)	35

List of Tables

1.1	IPF filter input files	6
1.2	IPF filter execution configuration	6

1.3	IPF filter execution mask vector assignment	6
1.4	IPF calibration error summary ([arcsec], 1-sigma, radial)	7
1.5	Science measurement prediction error summary (1-sigma)	7
1.6	IPF Brown angle summary	8
2.1	IPF input file editing status	9
3.1	Table of figures I (IPF run)	10
3.2	Table of figures II (IPF run)	11
3.3	PCRS measurement prediction error summary	24

1 IPF EXECUTION SUMMARY

This report summarizes the SIRTF Instrument Pointing Frame (IPF) Kalman Filter execution associated with run file: RN502034. In particular, this Focal Point Survey calibrates the instrument: IRS_ShortLo_2nd_Ord_Center_Pos (34), as part of the IOC Fine Survey. The main calibration results from the IPF filter execution have been documented in IF502034 typically stored in the mission archive DOM collection IPF_IF. This report only summarizes the main aspects of the run, and does not substitute for the full information contained in the IF file.

Section 1 summarizes the filter execution results. The filter configurations are tabulated in Table 1.2 and the mask vector assignments are tabulated in Table 1.3. A total of 18 state parameters are estimated in this run. The overall End-to-End pointing performances are tabulated in Table 1.4. The prediction residuals throughout the estimation processes are tabulated in Table 1.5. Section 3 summarizes resulting plots, a mini summary of the IF IPF output file, and the execution log. Section 4 captures the user comments that are specific to this particular run.

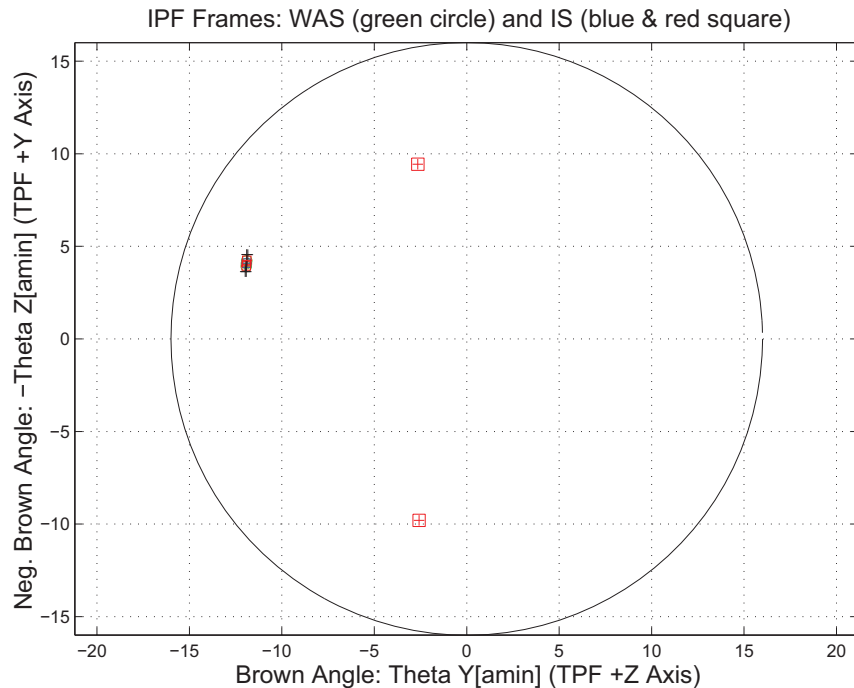


Figure 1.1: A-priori and a-posteriori IPF frames

RAW	FINAL (After Editing)
AA501034	AA501034
AS501034	AS501034
CA501034	CA501034
CB502034	CB502034
CS501034	CS501034

Table 1.1: IPF filter input files

EXECUTION CONFIGURATION ITEM	CURRENT STATUS
IPF Filter Version Used	IPF.V3.0.0B
Frame Table Version Used	BodyFrames_FTU_12b
Scan-Mirror Employed?	NO
IPF Filter Mode	NORMAL-MODE(0)
SLIT-MODE Operation	ENABLED
Kalman Filter Operation	ENABLED
Least-Squares Data Analysis	ENABLED
IBAD Screening	DISABLED
User-Specified Data Editing	DISABLED
Total Number of Iterations	15
LS Residual Sigma Scale	2.45966208E+000
Total Number of Maneuvers	32

Table 1.2: IPF filter execution configuration

Con. Plate Scale			Γ Dependent				Γ^2 Dependent				Linear Plate Scale						Mirror			
a_{00}	b_{00}	c_{00}	a_{10}	b_{10}	c_{10}	d_{10}	a_{20}	b_{20}	c_{20}	d_{20}	a_{01}	b_{01}	c_{01}	d_{01}	e_{01}	f_{01}	α	β		
1	2	3	4	5	6	7	8	9	10	11	12	13	14	15	16	17	18	19		
1	0	0	0	0	0	0	0	0	0	0	0	0	0	0	0	0	0	0		
IPF (T)			Alignment R						Gyro Drift Bias											
θ_1	θ_2	θ_3	a_{rx}	a_{ry}	a_{rz}	b_{rx}	b_{ry}	b_{rz}	c_{rx}	c_{ry}	c_{rz}	b_{gx}	b_{gy}	b_{gz}	c_{gx}	c_{gy}	c_{gz}			
20	21	22	23	24	25	26	27	28	29	30	31	32	33	34	35	36	37			
0	1	1	1	1	1	1	1	1	1	1	1	1	1	1	1	1	1			

Table 1.3: IPF filter execution mask vector assignment

FOCAL PLANE SURVEY ANALYSIS: IOC Fine Survey.

INSTRUMENT NAME: IRS_ShortLo_2nd_Ord_Center_Pos NF: 34

PIX2RADW: 4.84813681E-006 [rad/pixel] = 1.0000E+000 [arcsec/pixel]

PIX2RADV: 4.84813681E-006 [rad/pixel] = 1.0000E+000 [arcsec/pixel]

FRAME	DESCRIPTION	IPF ¹	SF ²	TOTAL	REQ
034(P)	IRS_ShortLo_2nd_Ord_Center_Pos	0.0308	0.0855	0.0909	0.14
032(I)	IRS_ShortLo_2nd_Ord_1st_Pos	0.0346	0.0855	0.0922	N/A
033(I)	IRS_ShortLo_2nd_Ord_2nd_Pos	0.0280	0.0855	0.0900	N/A

Table 1.4: IPF calibration error summary ([arcsec], 1-sigma, radial)

RMS METRIC	A PRIORI ³	A POSTERIORI ³	ATT. CORRECTED ⁴	UNITS
Radial	1.3822	0.9586	0.8421	arcsec
W-Axis	1.2627	0.9165	0.8131	arcsec
V-Axis	0.5623	0.2809	0.2192	arcsec
Radial	1.3822	0.9586	0.8421	pixels
W-Axis	1.2627	0.9165	0.8131	pixels
V-Axis	0.5623	0.2809	0.2192	pixels

Table 1.5: Science measurement prediction error summary (1-sigma)

¹IPF filter removes systematic pointing errors due to: thermomechanical alignment drift (Body to TPF), gyro bias and bias drift, centroiding error, attitude error, and optical distortion. IPF SIGMA presented here is “Scaled” by the Least Squares Scale factor. The Least Squares Scale Factor was: 2.459662. It is assumed that the gyro Angle Random Walk contribution is captured with the Least Squares scaling. The gyro ARW contribution can be approximately calculated as 0.0361 arcseconds, given that ARW = 100 $\mu\text{deg}/\sqrt{\text{hr}}$, with 6.864286e+002 second Maneuver time (max), and 32 independent Maneuvres.

²Gyro Scale Factor(GSF) assumes 95 ppm error over 0.250 degree maneuver.

³This can be interpreted as estimate of ”pixel to sky” pointing reconstruction error if no science data is used.

⁴This can be interpreted as estimate of achieved S/I centroiding error

IPF BROWN ANGLE SUMMARY					
FRAME TABLE USED: BodyFrames_FTU_12b					
NF	NAME	WAS	IS	CHANGE	UNIT
034	theta_Y	-11.911390	-11.913057	-0.001667	arcmin
034	theta_Z	-4.073083	-4.093168	-0.020086	arcmin
034	angle	-84.719995	-84.719994	+0.000001	deg
032	theta_Y	-11.925347	-11.927235	-0.001888	arcmin
032	theta_Z	-3.922059	-3.939748	-0.017689	arcmin
032	angle	-84.719995	-84.719994	+0.000001	deg
033	theta_Y	-11.897433	-11.898879	-0.001445	arcmin
033	theta_Z	-4.224107	-4.246589	-0.022482	arcmin
033	angle	-84.719995	-84.719994	+0.000001	deg

Table 1.6: IPF Brown angle summary

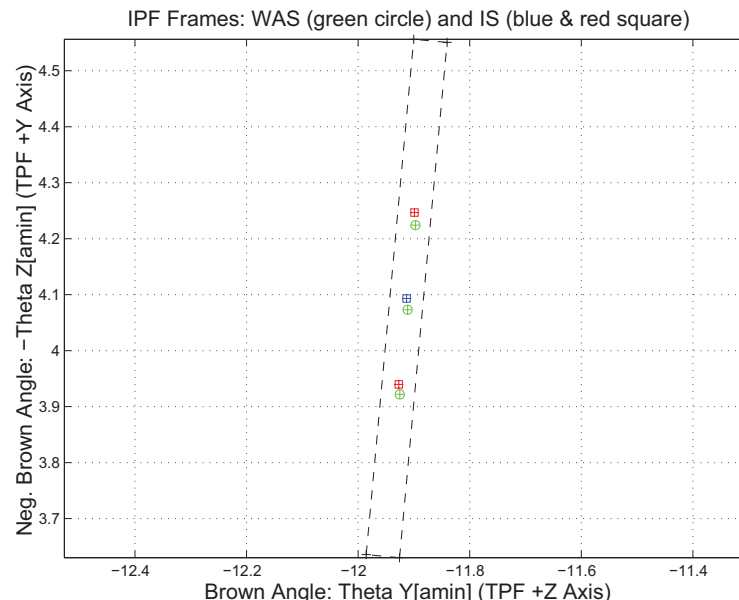


Figure 1.2: A-priori and a-posteriori IPF frames (ZOOMED)

2 IPF INPUT FILE HISTORY

WAS	SIZE	IS	SIZE	REMOVED	PATCHED
AA501034	UNCHANGED	AA501034	UNCHANGED	0	0
CA501034	UNCHANGED	CA501034	UNCHANGED	0	N/A
CB502034	UNCHANGED	CB502034	UNCHANGED	0	N/A

Table 2.1: IPF input file editing status

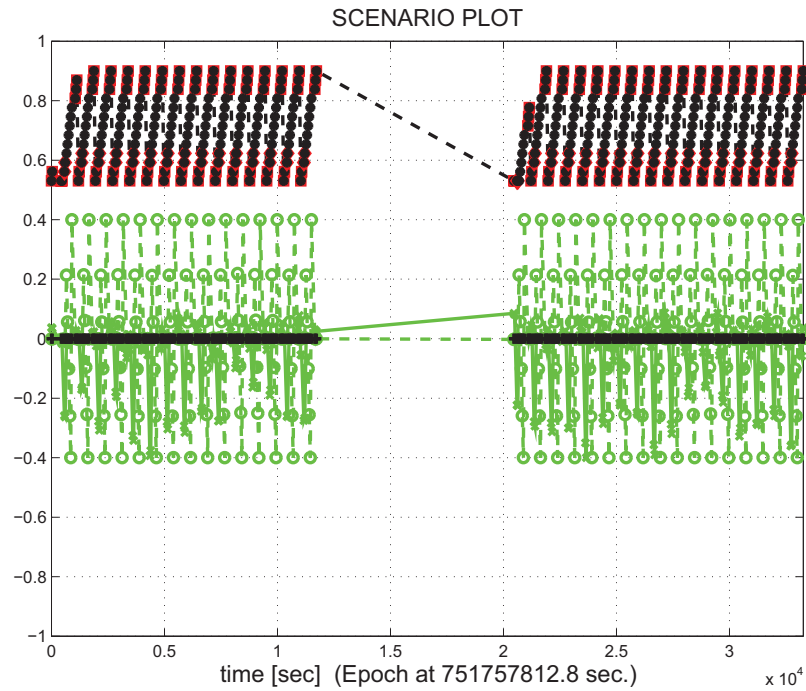


Figure 2.1: Scenario Plot

3 IPF EXECUTION RESULTS

3.1 IPF EXECUTION OUTPUT PLOTS

This subsection summarizes the IPF filter results. As shown in Table 3.1, the output plots are segmented to three groups: predicted performance, post-run results and IPF trending plots.

FIGURE NO.	DESCRIPTION
Predicted performance prior to IPF run	
Figure 3.1	Meas. and a-priori predicts in TPF coords
Figure 3.2	Meas. and a-priori predicts in Oriented Pixel Coords including rectangular array boundary approximation
Figure 3.3	A-Priori Prediction Error Quiver Plot in Oriented Pixel Coords including rectangular array boundary approximation
Figure 3.4	A-priori prediction error
Figure 3.5	Oriented Pixel Coords of measurements and a-priori predicts (PCRS only)
Figure 3.6	Oriented Pixel Coords of measurements and a-priori predicts (Zoomed, PCRS only)
Figure 3.7	Oriented (W,V) Pixel Coords of A-Priori PCRS Prediction Error Quiver Plot
Figure 3.8	A-priori PCRS prediction error
IPF filter performance (post run results)	
Figure 3.9	IPF execution convergence, chart 1: (top) normalized residual error vs. iteration number and (bottom) norm of effective parameter corrections
Figure 3.10	IPF execution convergence, chart 2: parameter correction size vs. iteration number
Figure 3.11	Parameter uncertainty convergence: square-root of diagonal elements of covariance matrix vs. maneuver number
Figure 3.12	IPF parameter symbol table
Figure 3.13	KF parameter error sigma plot (a-priori-dashed, a-posteriori-solid). Includes true parameter errors (FLUTE runs only)
Figure 3.14	LS parameter error sigma plot. Includes true parameter errors (FLUTE runs only)
Figure 3.15	KF and LS parameter errors sigma plot (Figure 3.13 & Figure 3.14 combined)
Figure 3.16	Measurements and a-posteriori predicts in Oriented Pixel Coords including rectangular array boundaries (a-priori-dashed, a-posteriori-solid)
Figure 3.17	Attitude corrected meas. and a-posteriori predicts in Oriented Pixel Coords including rectangular array boundaries (a-priori-dashed, a-posteriori-solid)

Table 3.1: Table of figures I (IPF run)

FIGURE NO.	DESCRIPTION
IPF filter performance (post run results) - CONTINUE	
Figure 3.18	KF innovations with (o) and w/o (+) attitude corrections
Figure 3.19	Histograms of science a-posteriori residuals (or innovations)
Figure 3.20	A-Posteriori Science Centroid Prediction Error Quiver (Att. Cor.)
Figure 3.21	Normalized A-Posteriori Science Centroid Prediction Errors
Figure 3.22	KF innovations with (o) and w/o (+) attitude corrections (PCRS)
Figure 3.23	Histograms of PCRS a-posteriori residuals (or innovations)
Figure 3.24	A-posteriori PCRS Prediction Summary
Figure 3.25	A-posteriori PCRS Prediction (PCRS 1 Only)
Figure 3.26	A-posteriori PCRS Prediction (PCRS 2 Only)
Figure 3.27	A-Posteriori PCRS Prediction Errors Quiver (Att. Cor.)
Figure 3.28	Normalized A-Posteriori PCRS Prediction Errors
Figure 3.29	W-axis KF innovations and 1-sigma bound
Figure 3.30	V-axis KF innovations and 1-sigma bound
Figure 3.31	Array plot with (solid) and w/o (dashed) optical distortion corrections
Figure 3.32	Optical Distortion Plot: total (x5 magnification)
Figure 3.33	Optical Distortion Plot: constant plate scales (x5 magnification)
Figure 3.34	Optical Distortion Plot: linear plate scale (x5 magnification)
Figure 3.35	Optical Distortion Plot: gamma terms (x5 magnification)
Figure 3.36	Scan Mirror Chops
Figure 3.37	IPF Frame Reconstruction
Figure 3.38	Center Pixel Reconstruction
IPF parameter trending plots	
Figure 3.39	Estimated attitude corrections (Body frame)
Figure 3.40	Estimated attitude error sigma plot (Body frame)
Figure 3.41	Systematic error attributed to thermo-mechanical boresight drift (equiv. angle in (W,V) coords)
Figure 3.42	Systematic error attributed to thermo-mechanical boresight drift (equiv. angle in Body frame)
Figure 3.43	Systematic error attributed to gyro drift bias (equiv. rate in (W,V) coords)
Figure 3.44	Systematic error attributed to gyro drift bias (equiv. angle in (W,V) coords)
Figure 3.45	Systematic error attributed to gyro drift bias (equiv. angle in Body frame)

Table 3.2: Table of figures II (IPF run)

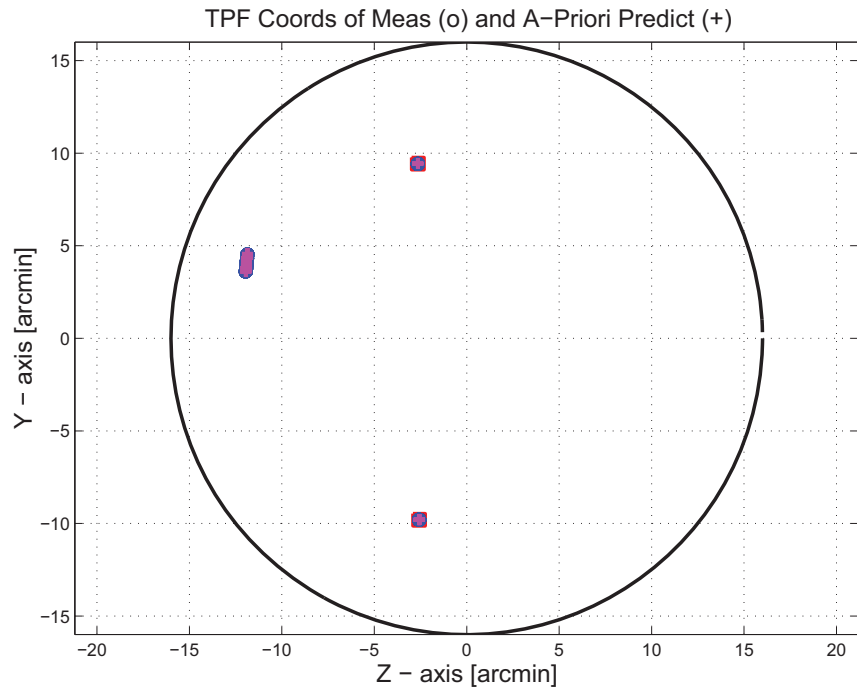


Figure 3.1: TPF coords of measurements and a-priori predicts

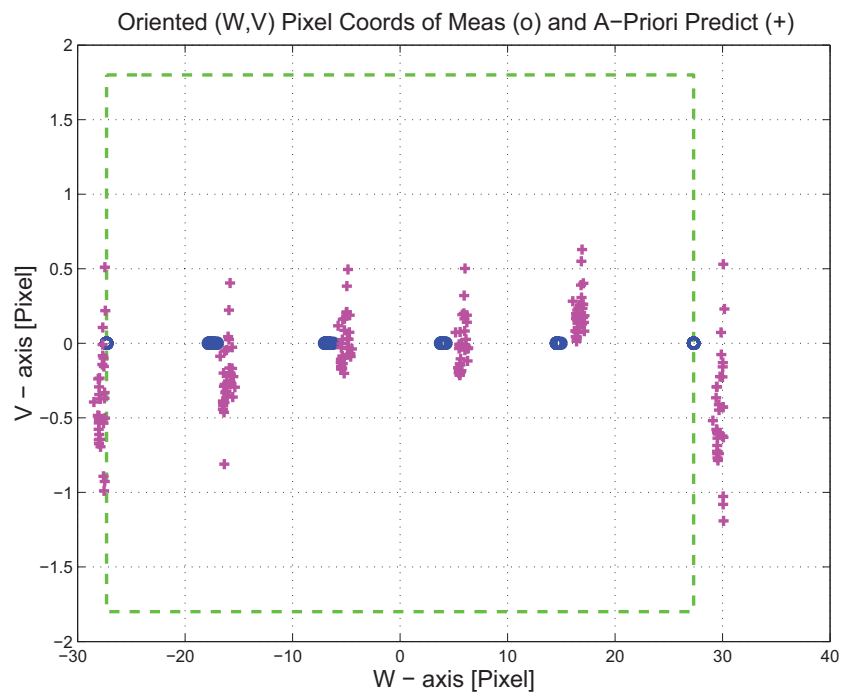


Figure 3.2: Oriented PixelCoords of measurements and a-priori predicts

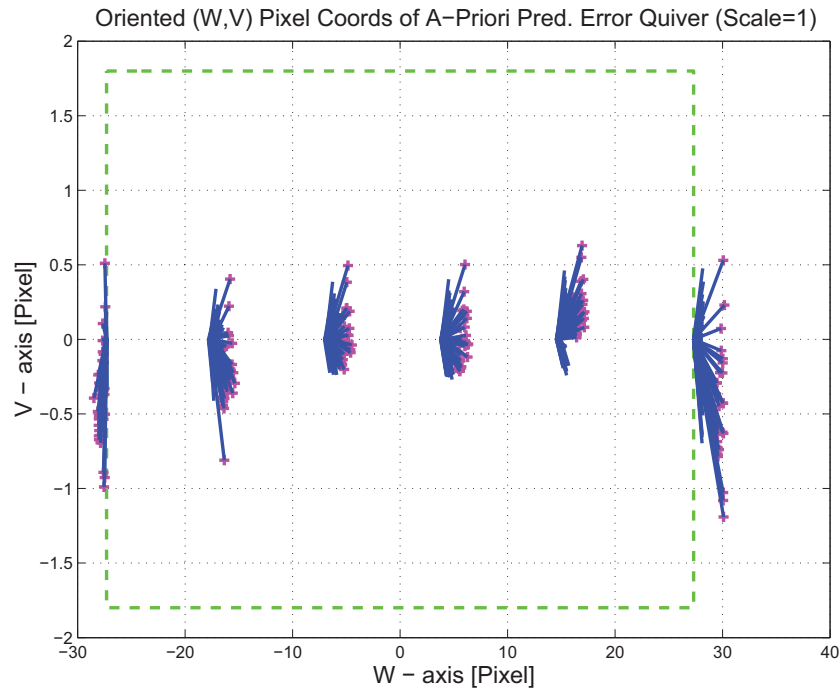


Figure 3.3: Oriented (W,V) Pixel Coords of A-Priori Prediction Error Quiver Plot

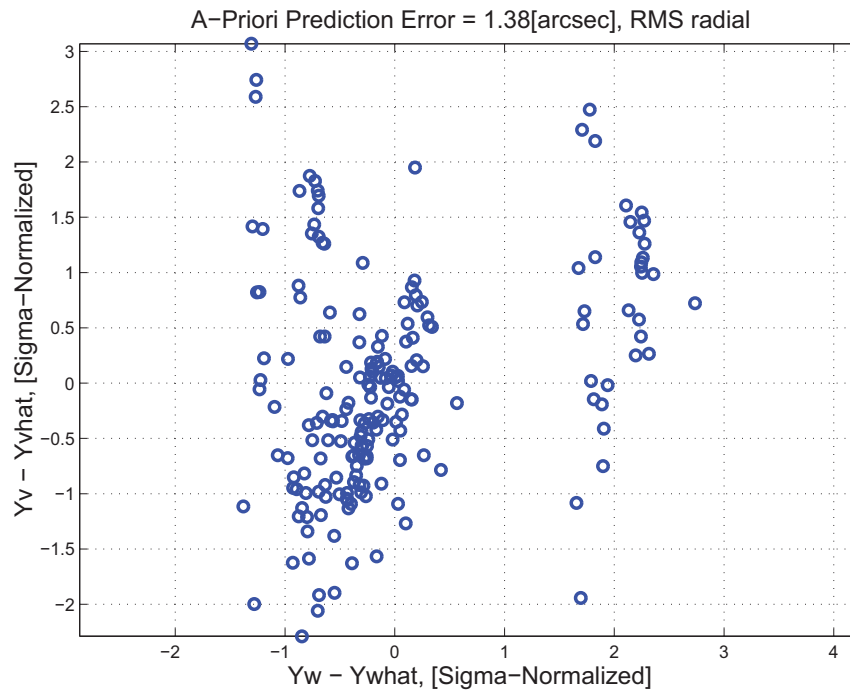


Figure 3.4: A-priori prediction error (Science Centroids)

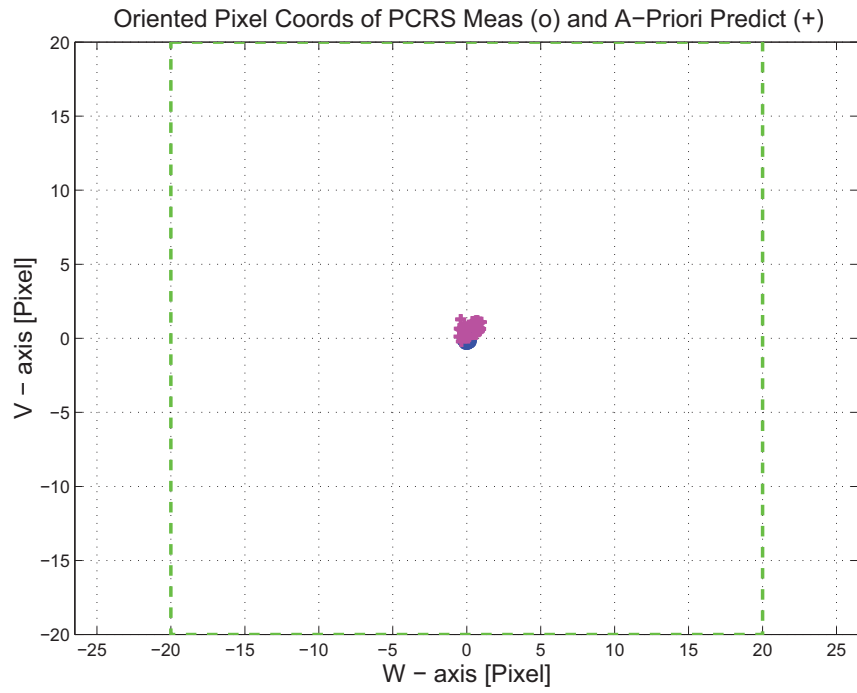


Figure 3.5: Oriented Pixel Coords of measurements and a-priori predicts (PCRS only)

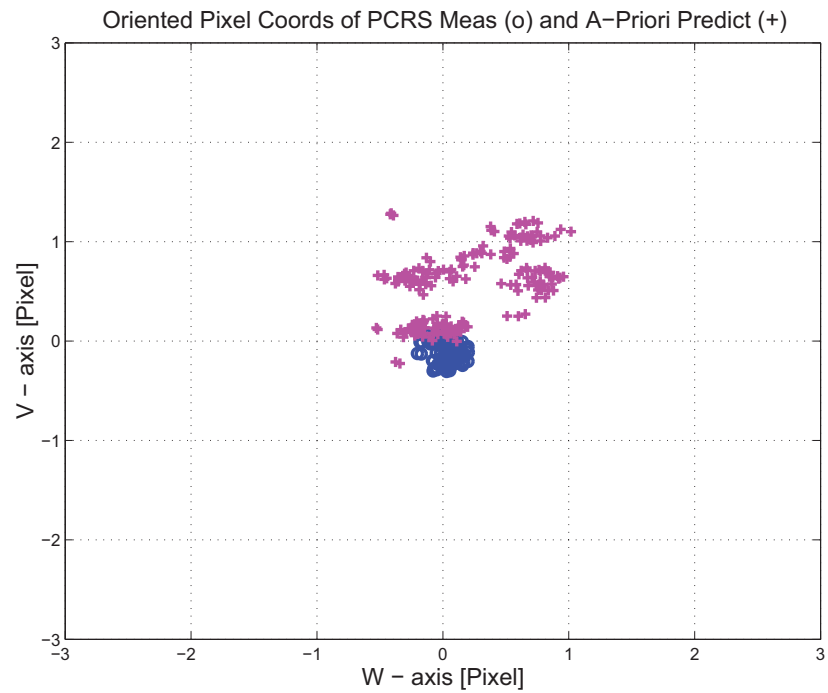


Figure 3.6: Oriented Pixel Coords of measurements and a-priori predicts (Zoomed, PCRS only)

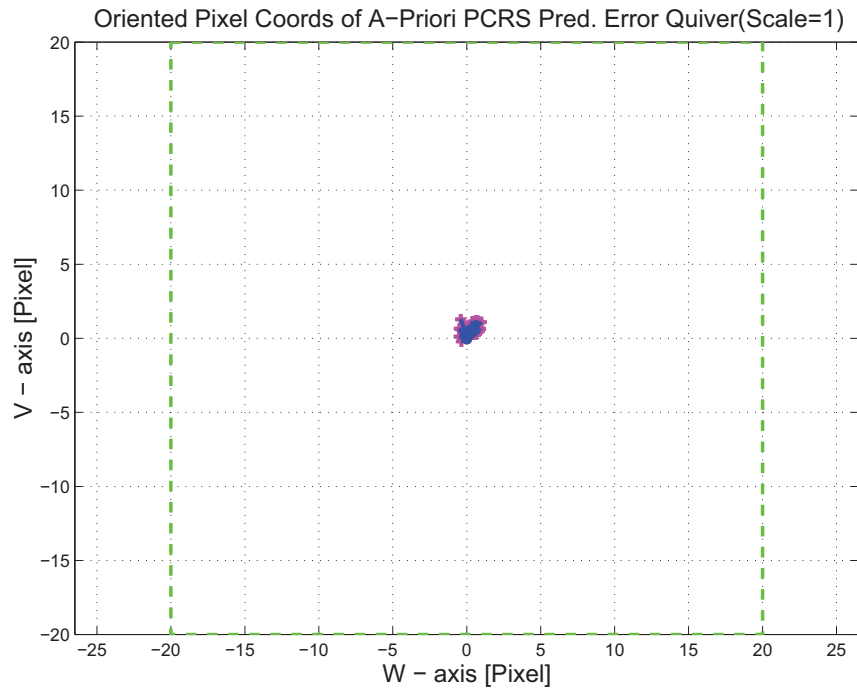


Figure 3.7: Oriented (W,V) Pixel Coords of A-Priori PCRS Prediction Error Quiver Plot

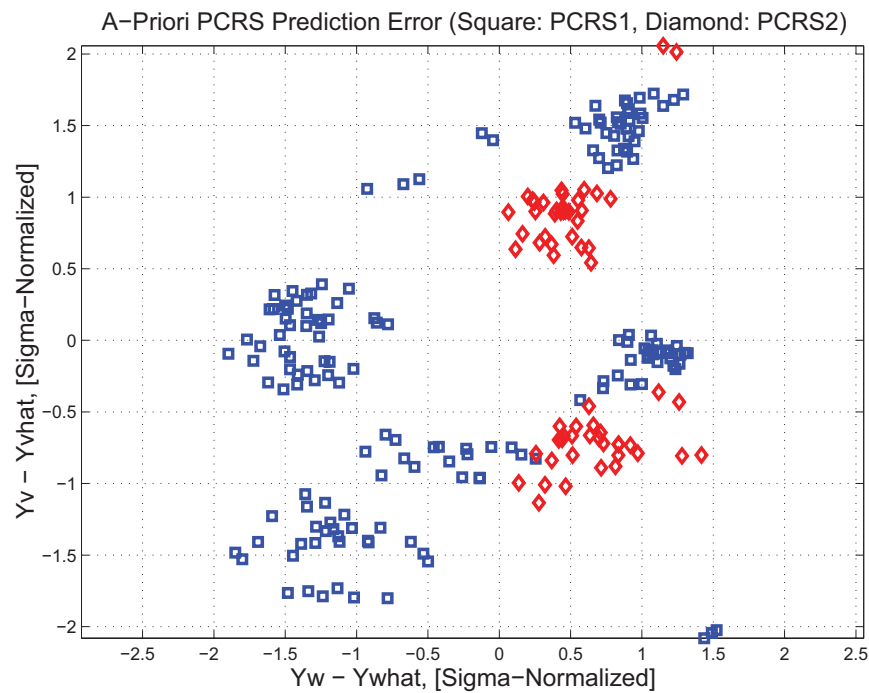


Figure 3.8: A-priori PCRS prediction error

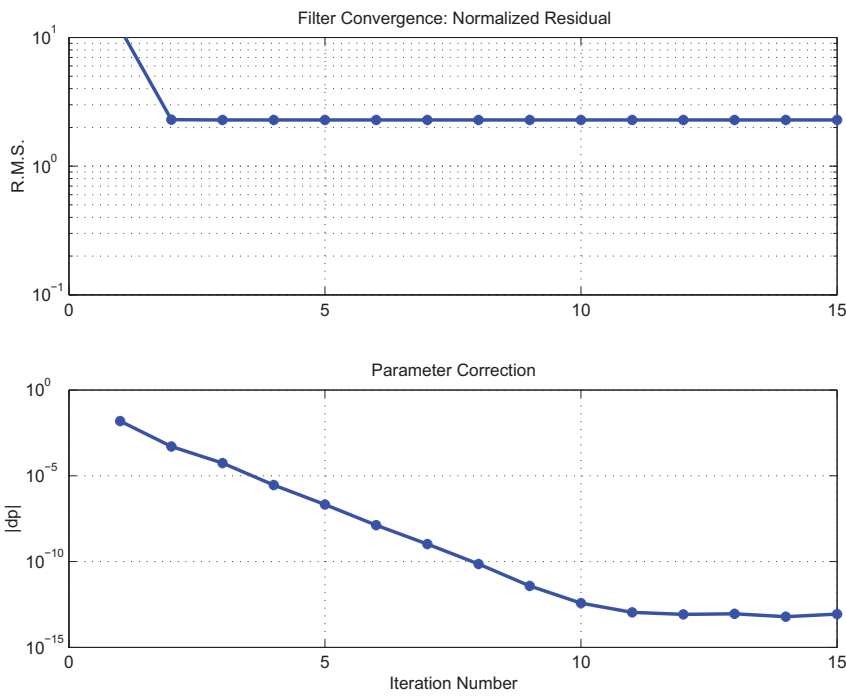


Figure 3.9: IPF execution convergence, chart 1

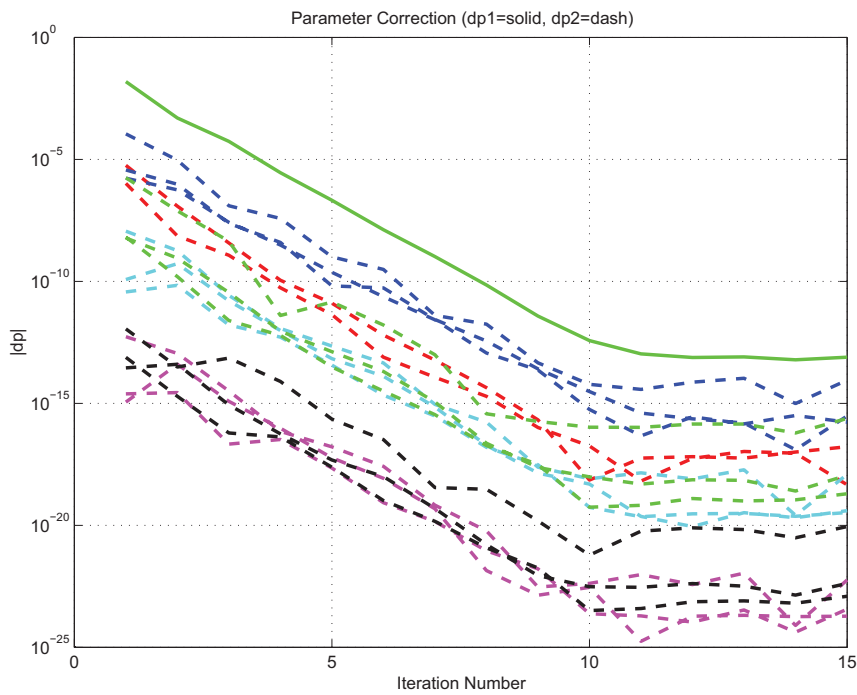


Figure 3.10: IPF execution convergence, chart 2

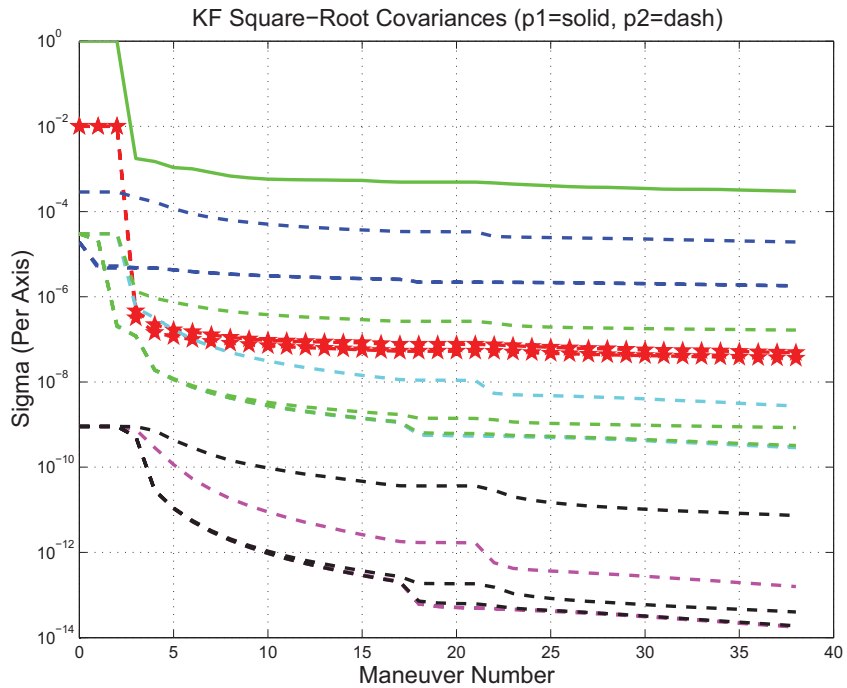


Figure 3.11: Parameter uncertainty convergence

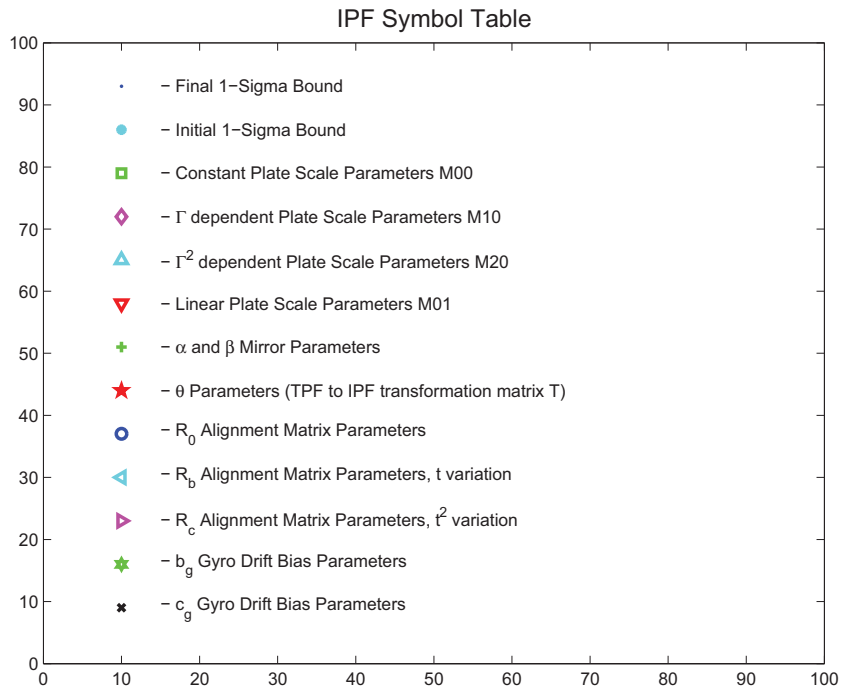


Figure 3.12: IPF parameter symbol table

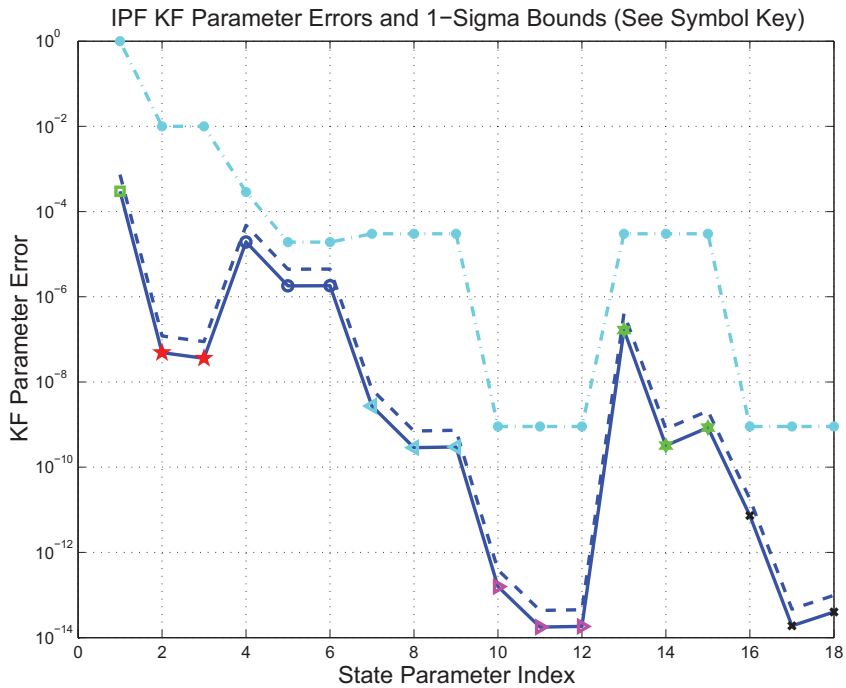


Figure 3.13: KF parameter error sigma plots

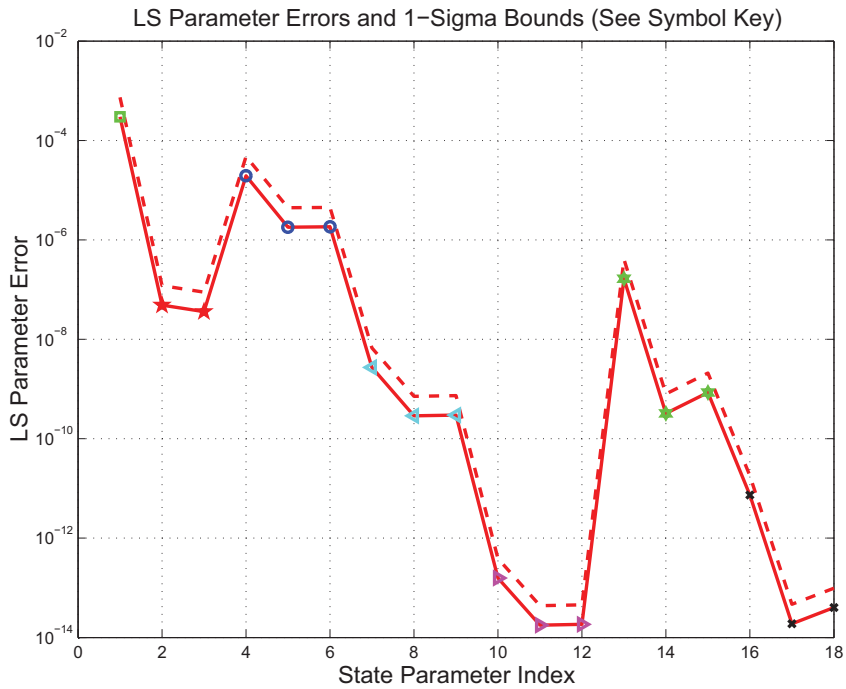


Figure 3.14: LS parameter error sigma plot

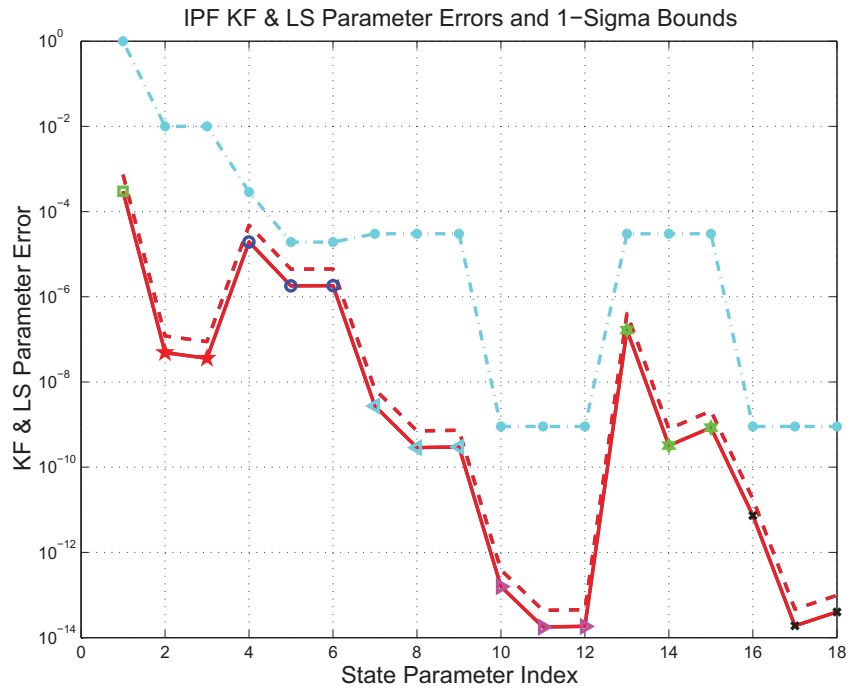


Figure 3.15: KF and LS parameter error sigma plot

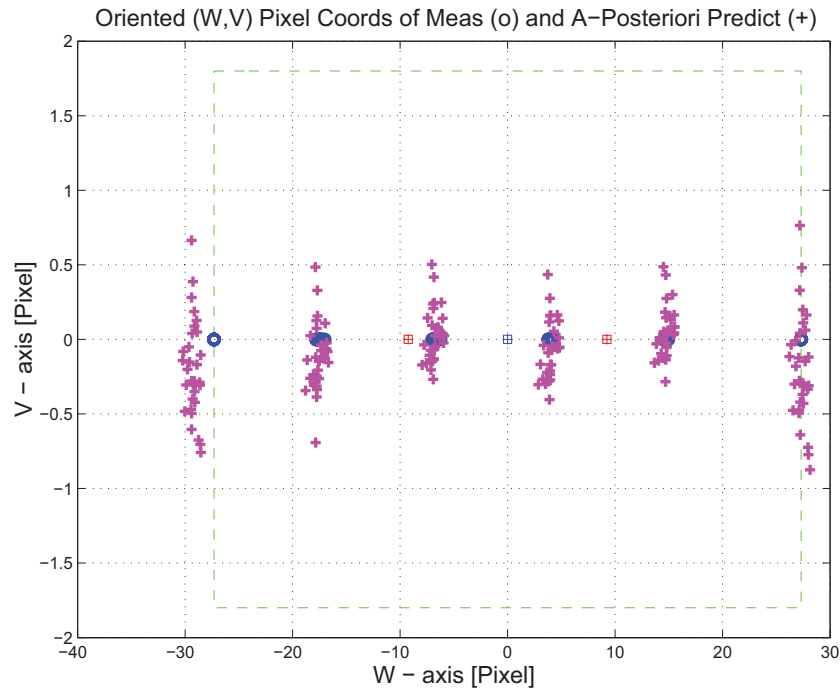


Figure 3.16: Oriented Pixel Coords of meas. and a-posteriori predicts

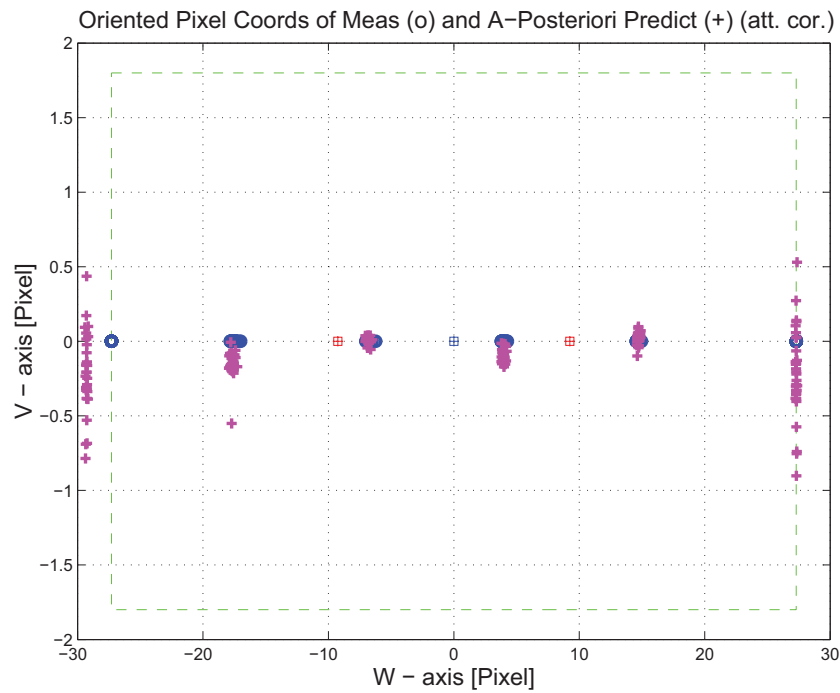


Figure 3.17: Oriented Pixel Coords of meas. and a-posteriori predicts (attitude corrected)

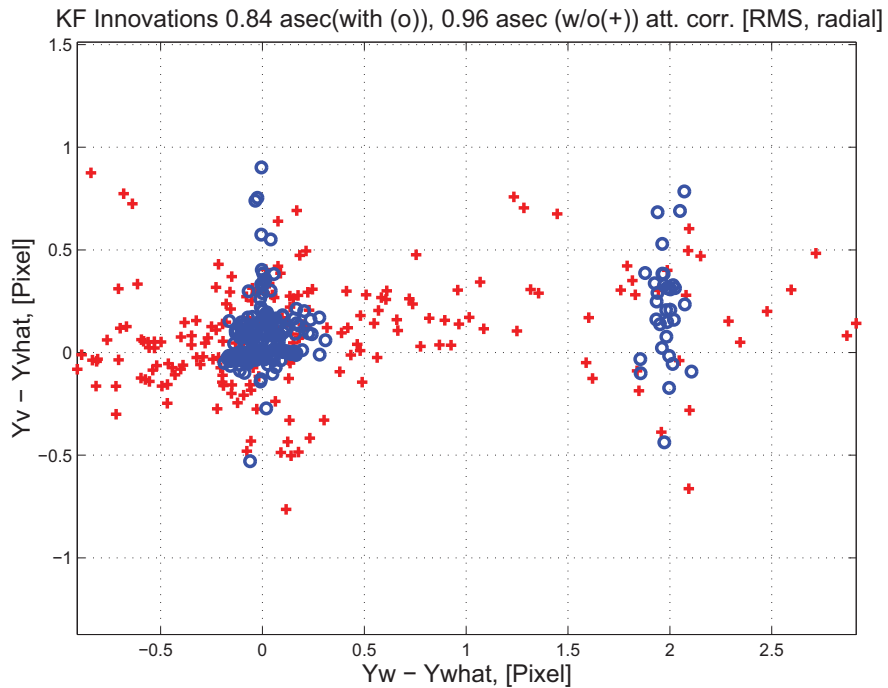


Figure 3.18: KF innovations with (o) and w/o (+) attitude corrections

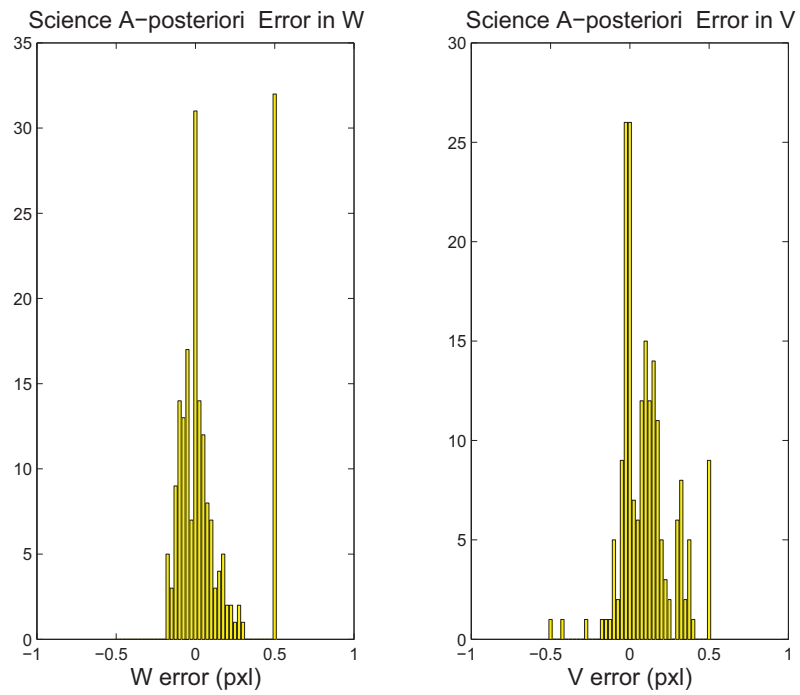


Figure 3.19: Histograms of science a-posteriori residuals (or innovations)

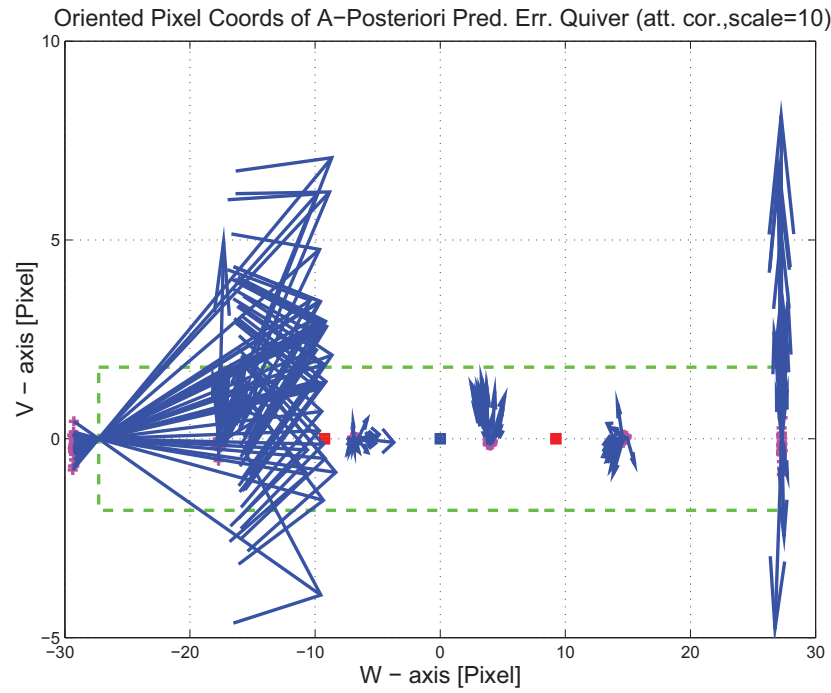


Figure 3.20: A-Posteriori Science Centroid Prediction Error Quiver (Att. Cor.)

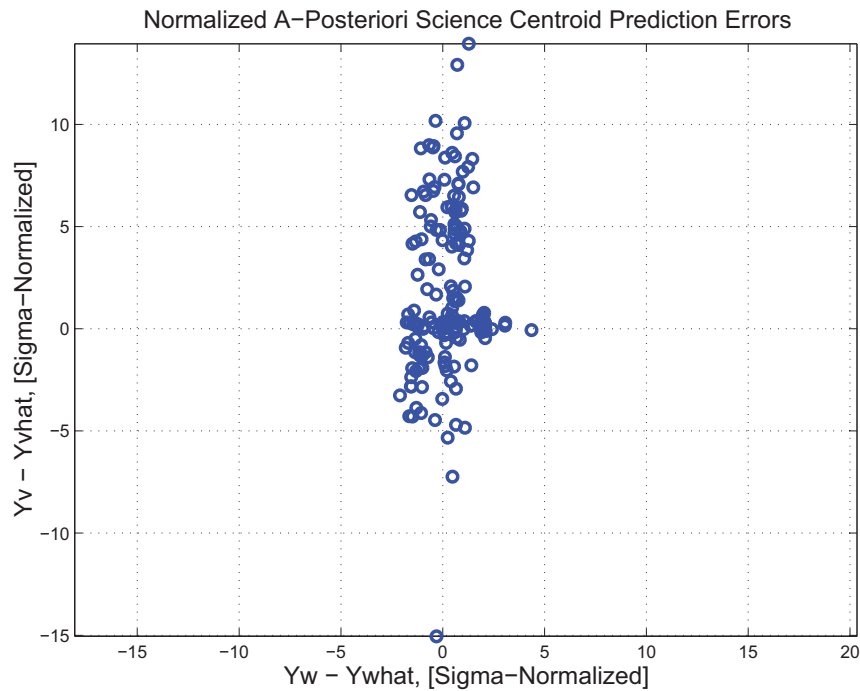


Figure 3.21: Normalized A-Posteriori Science Centroid Prediction Errors

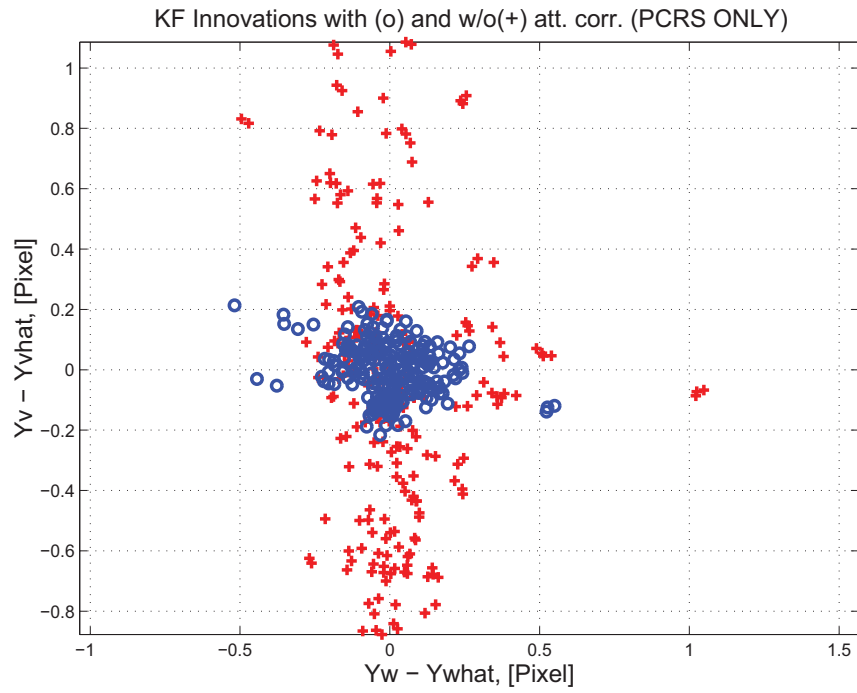


Figure 3.22: KF innovations with (o) and w/o (+) attitude corrections (PCRS)

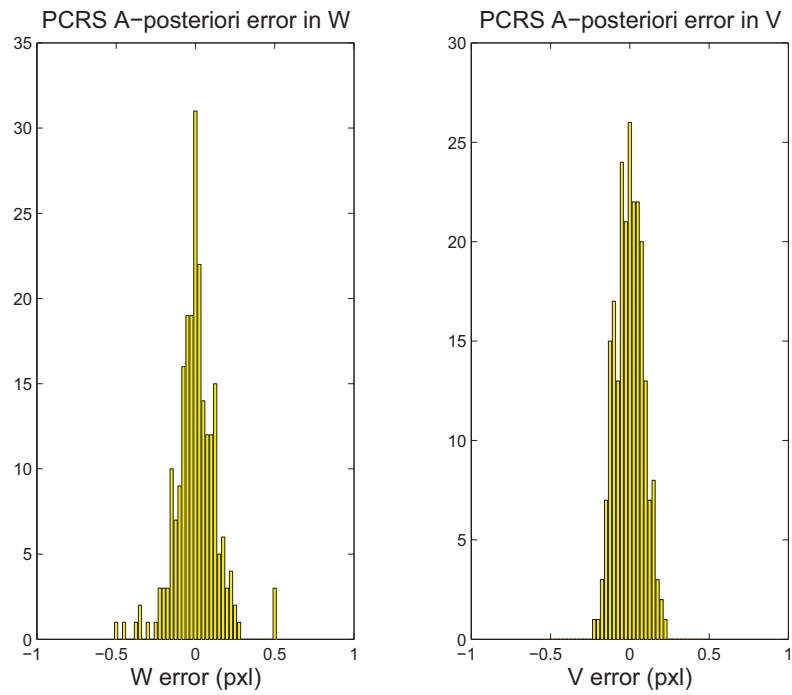


Figure 3.23: Histograms of PCRS a-posteriori residuals (or innovations)

IPF PCRS SUMMARY						
PCRS 1 (Total of 162 centroids)						
RMS	MEAN		SIGMA			
METRIC	APOST.	ATT. COR.	APOST.	ATT. COR.	STAT. CONF.	UNITS
Radial	0.0180	0.0333	0.5177	0.1707	0.0134	arcsec
W-axis	0.0150	0.0059	0.2246	0.1550	0.0122	arcsec
V-axis	0.0100	0.0328	0.4665	0.0715	0.0056	arcsec
PCRS 2 (Total of 64 centroids)						
METRIC	APOST.	ATT. COR.	APOST.	ATT. COR.	STAT. CONF.	UNITS
Radial	0.1280	0.0929	0.4786	0.0752	0.0094	arcsec
W-axis	0.0150	-0.0080	0.1485	0.0553	0.0069	arcsec
V-axis	-0.1271	-0.0926	0.4550	0.0510	0.0064	arcsec
Combined (Total of 226 centroids)						
METRIC	APOST.	ATT. COR.	APOST.	ATT. COR.	STAT. CONF.	UNITS
Radial	0.0325	0.0033	0.5107	0.1604	0.0107	arcsec
W-axis	0.0150	0.0020	0.2059	0.1347	0.0090	arcsec
V-axis	-0.0288	-0.0027	0.4673	0.0871	0.0058	arcsec

Table 3.3: PCRS measurement prediction error summary

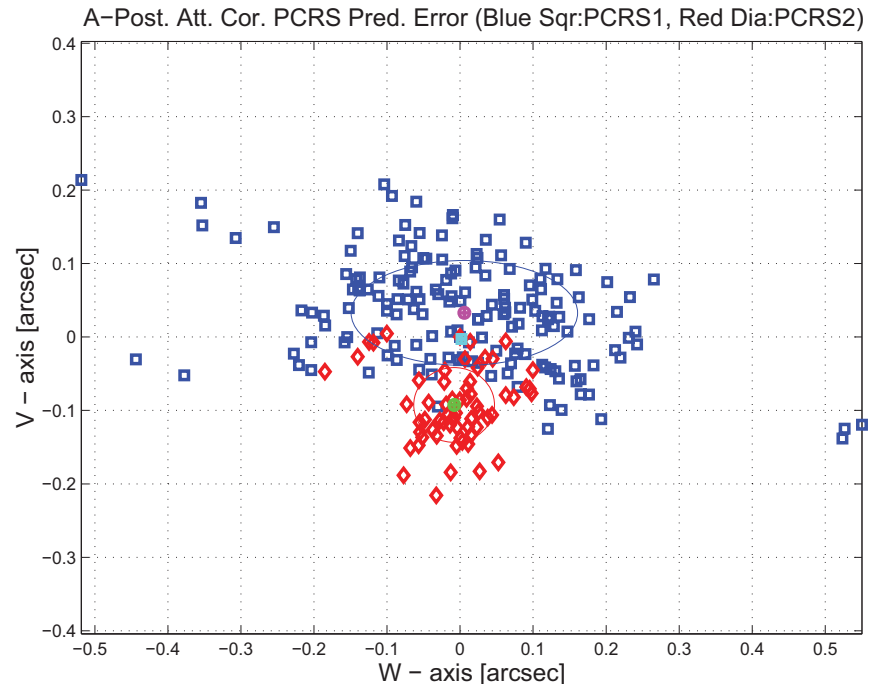


Figure 3.24: A-posteriori PCRS Prediction Summary

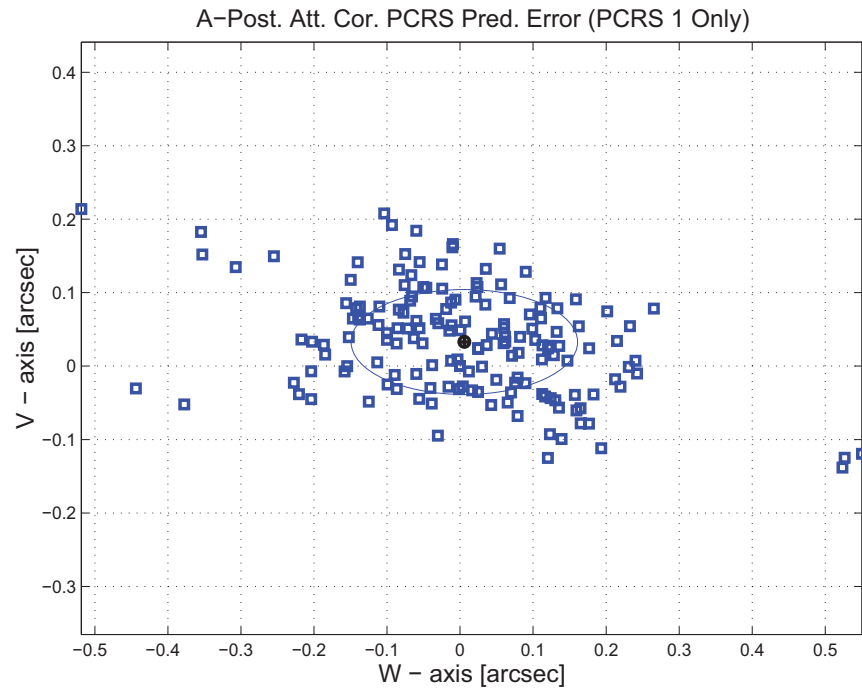


Figure 3.25: A-posteriori PCRS Prediction (PCRS 1 Only)

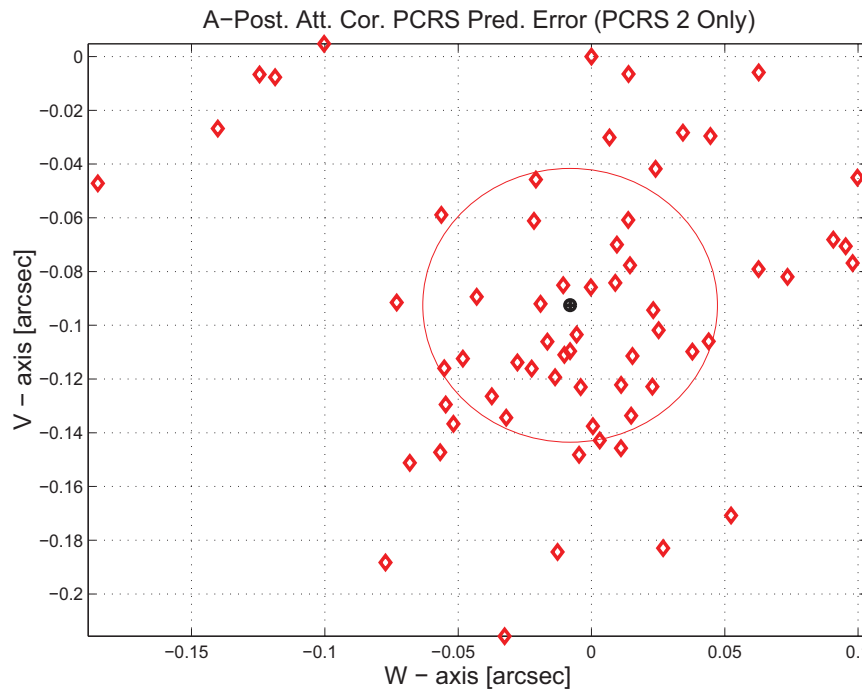


Figure 3.26: A-posteriori PCRS Prediction (PCRS 2 Only)

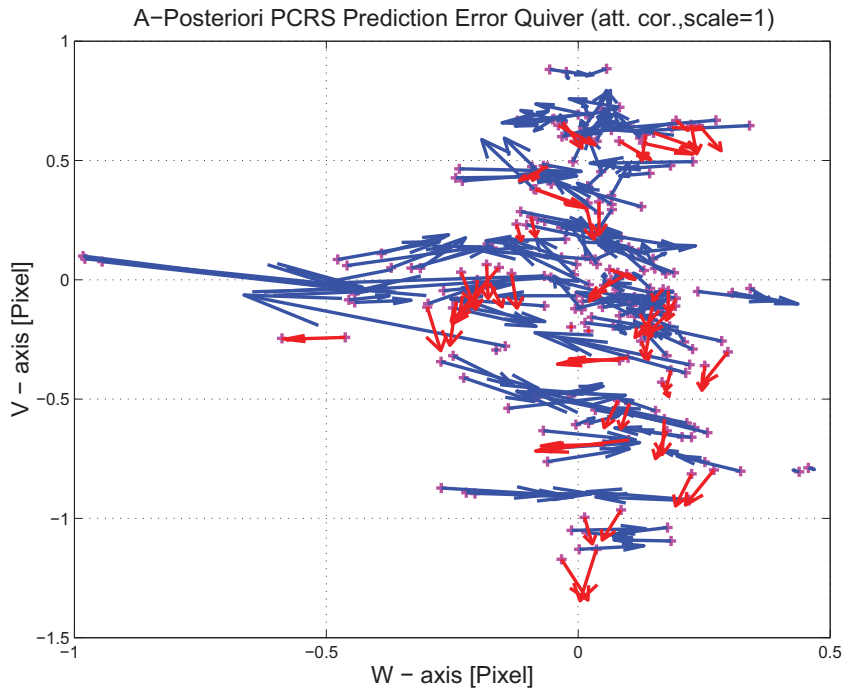


Figure 3.27: A-Posteriori PCRS Prediction Errors Quiver (Att. Cor.)

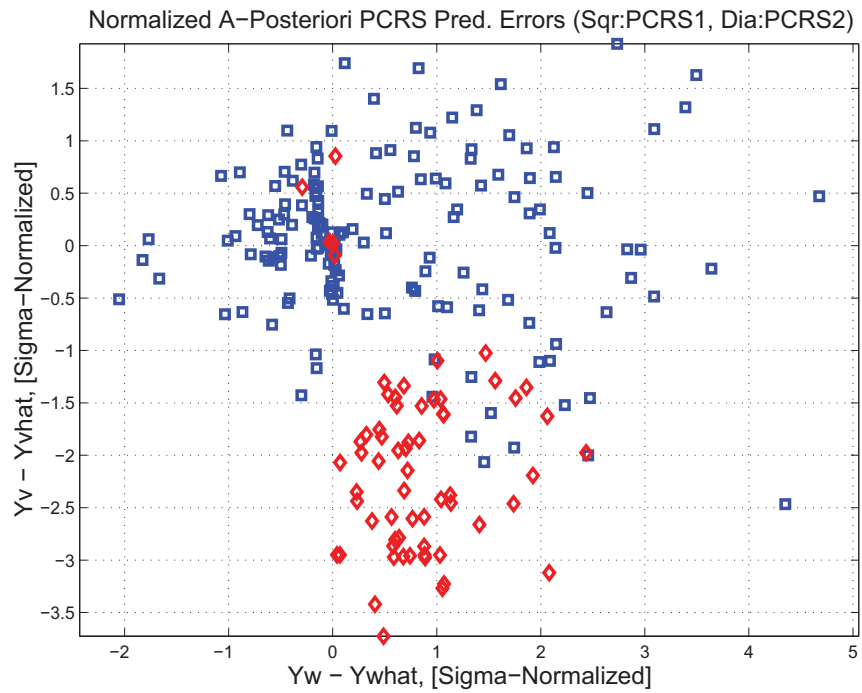


Figure 3.28: Normalized A-Posteriori PCRS Prediction Errors

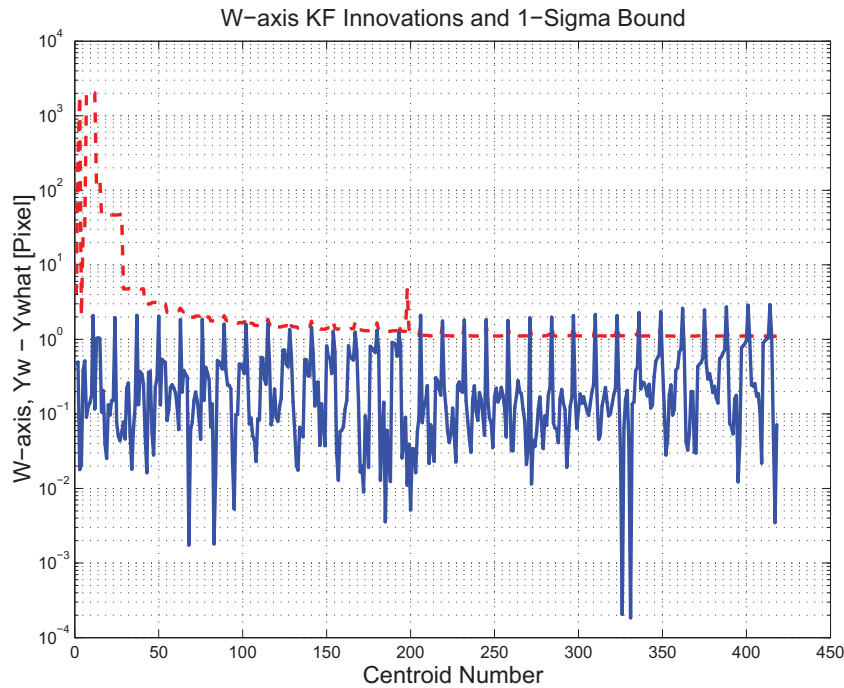


Figure 3.29: W-axis KF innovations and 1-sigma bound

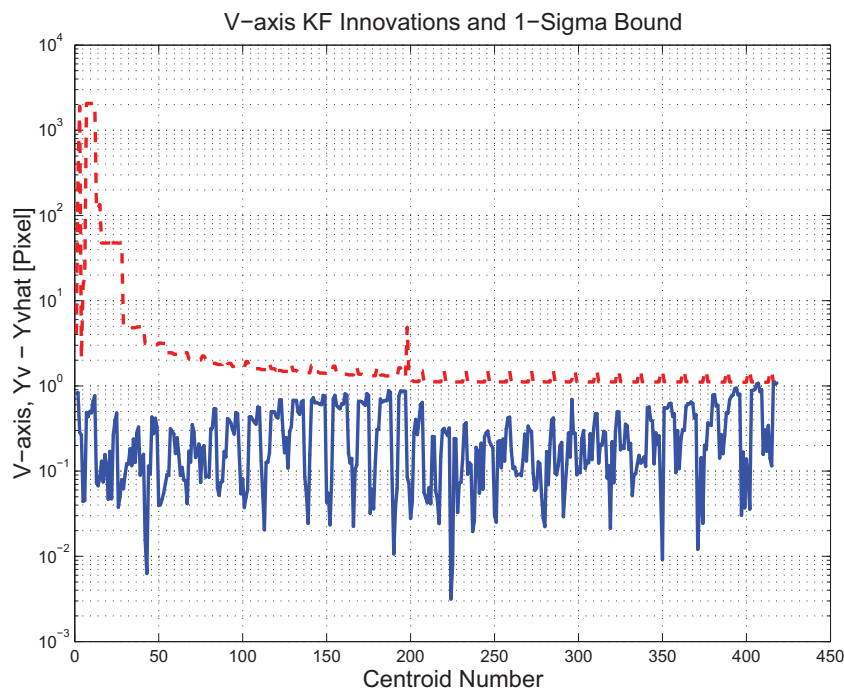


Figure 3.30: V-axis KF innovations and 1-sigma bound

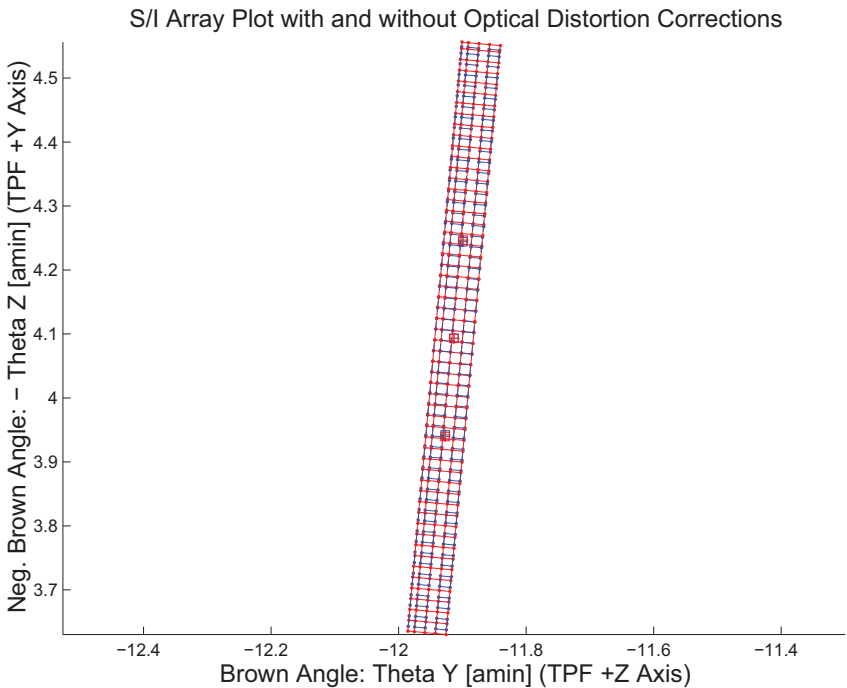


Figure 3.31: Array plot with (solid) and w/o (dashed) optical distortion corrections

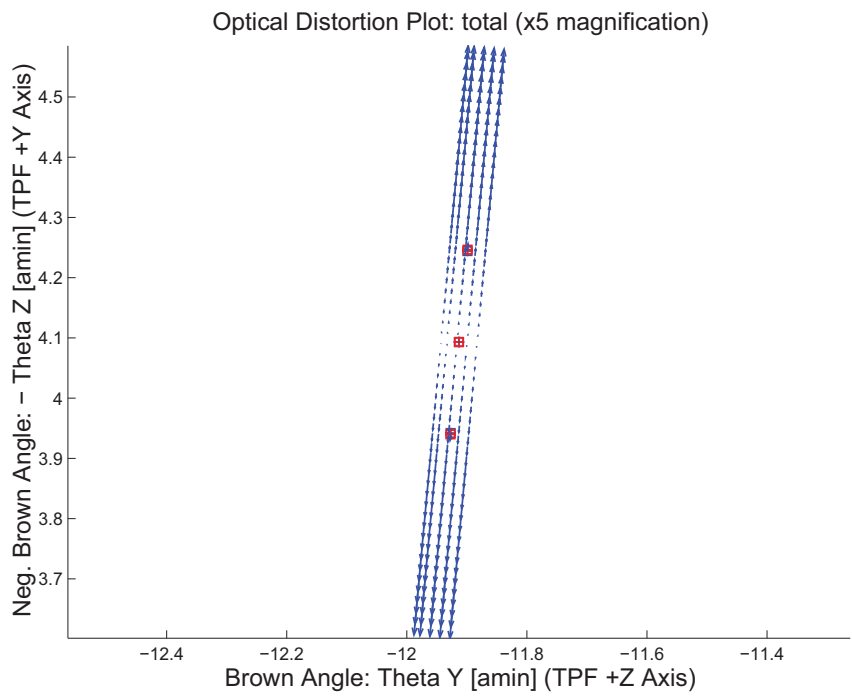


Figure 3.32: Optical Distortion Plot: total (x5 magnification)

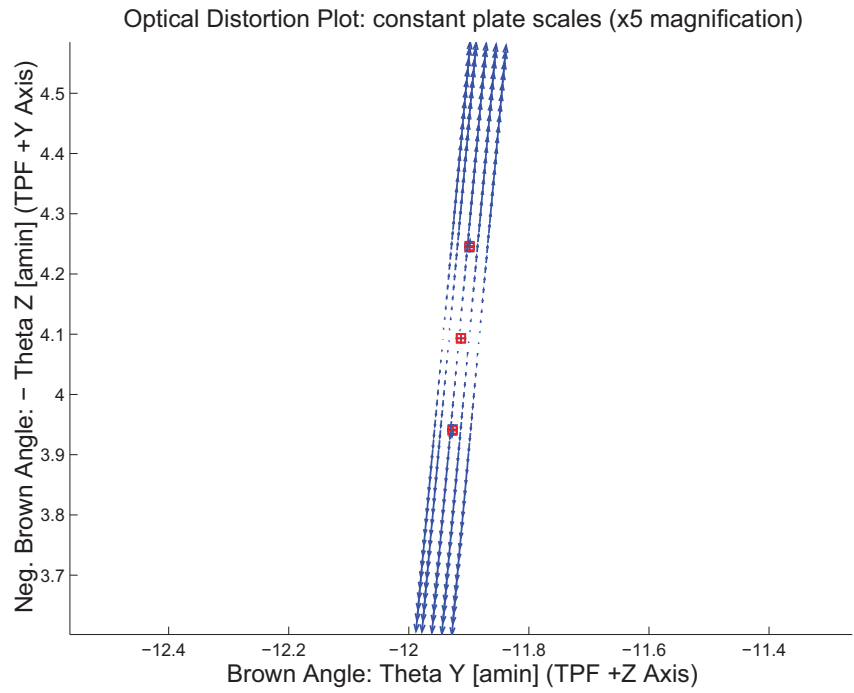


Figure 3.33: Optical Distortion Plot: constant plate scales (x5 magnification)

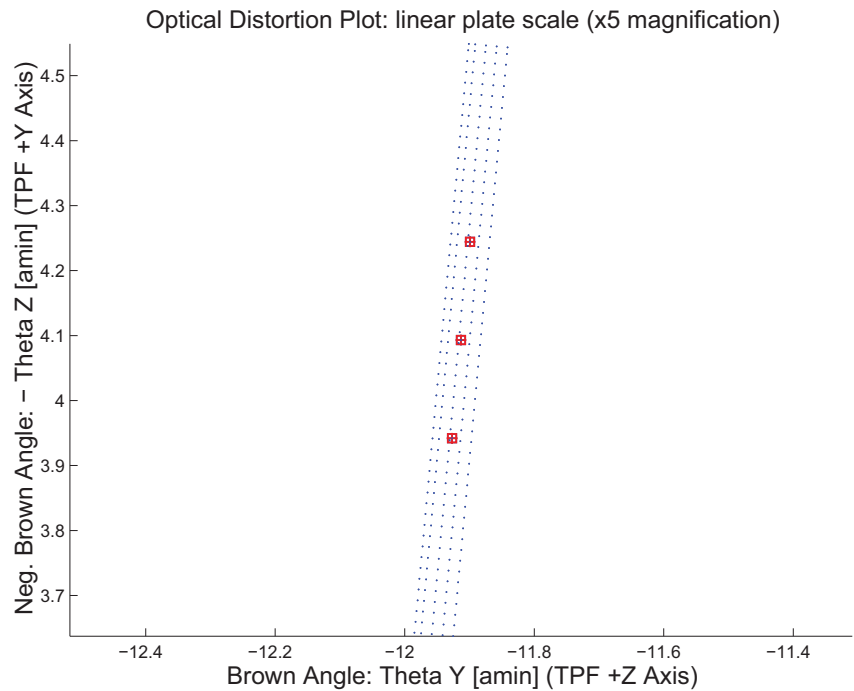


Figure 3.34: Optical Distortion Plot: linear plate scale (x5 magnification)

Opt. Dist. Plot: Γ depdt; $\Gamma = 0.00000e+000$ in blue and $\Gamma = 0.00000e+000$ in red (x5 magn)

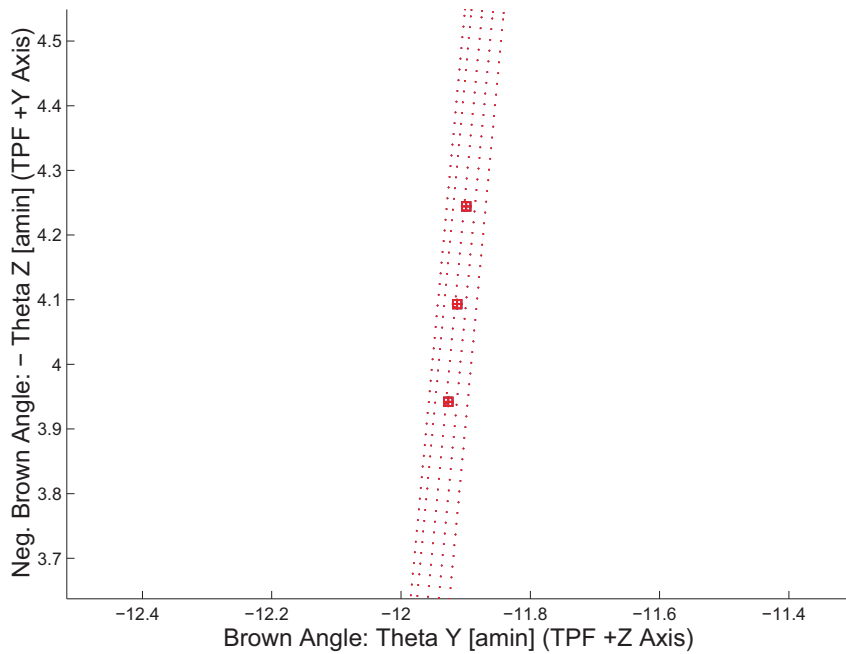


Figure 3.35: Optical Distortion Plot: gamma terms (x5 magnification)

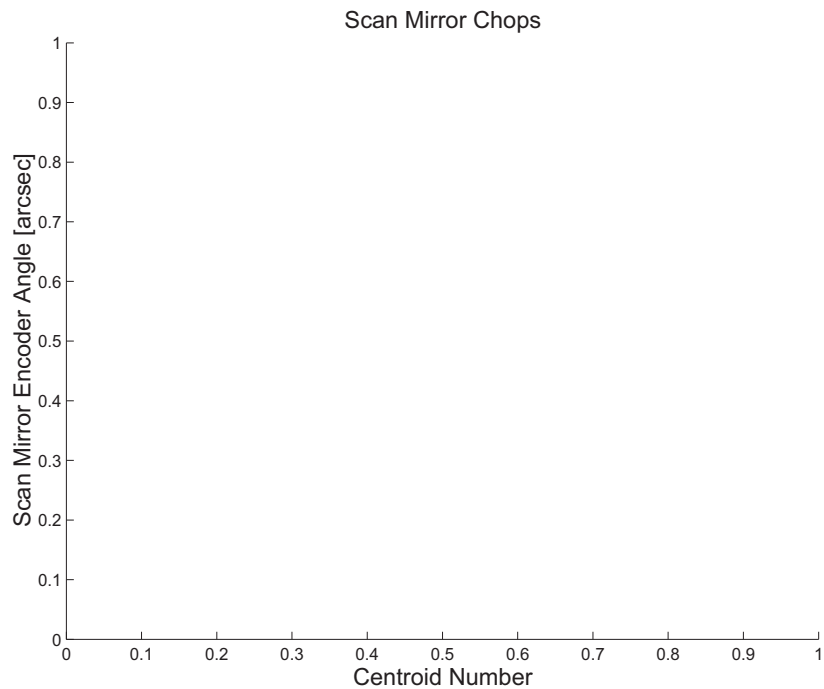


Figure 3.36: Scan Mirror Chops

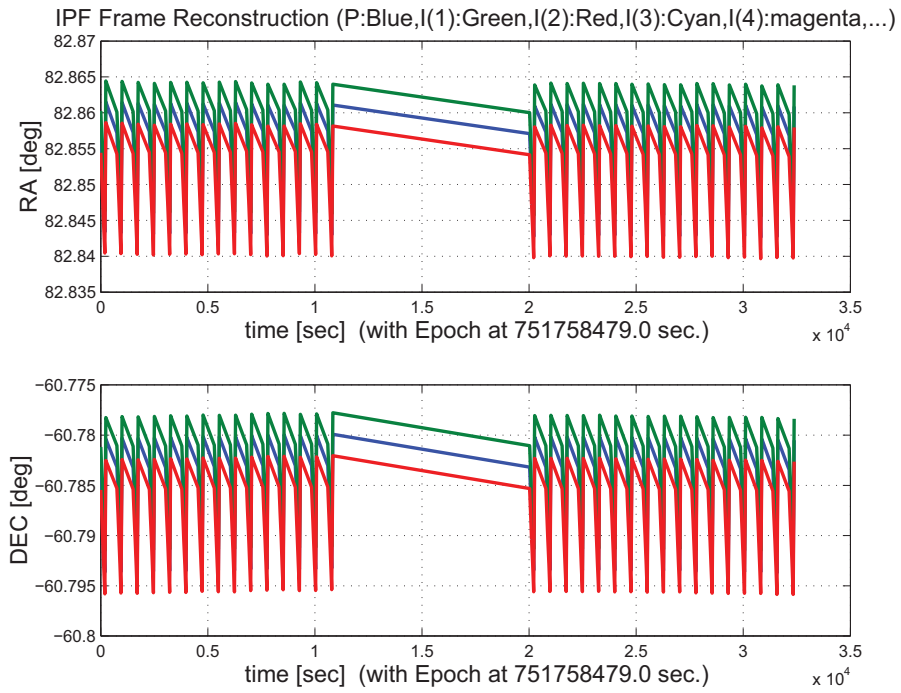


Figure 3.37: IPF Frame Reconstruction

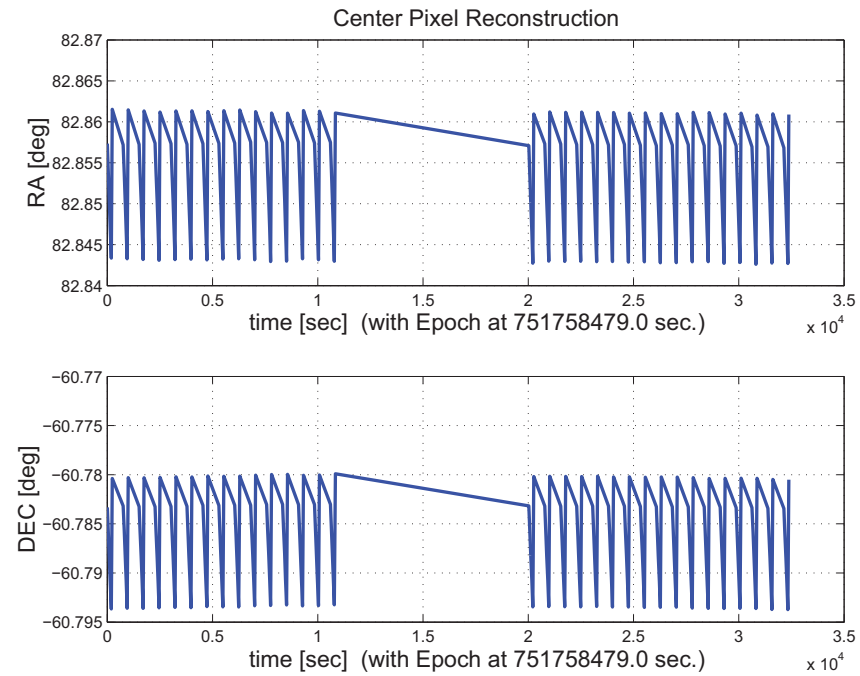


Figure 3.38: Center Pixel Reconstruction

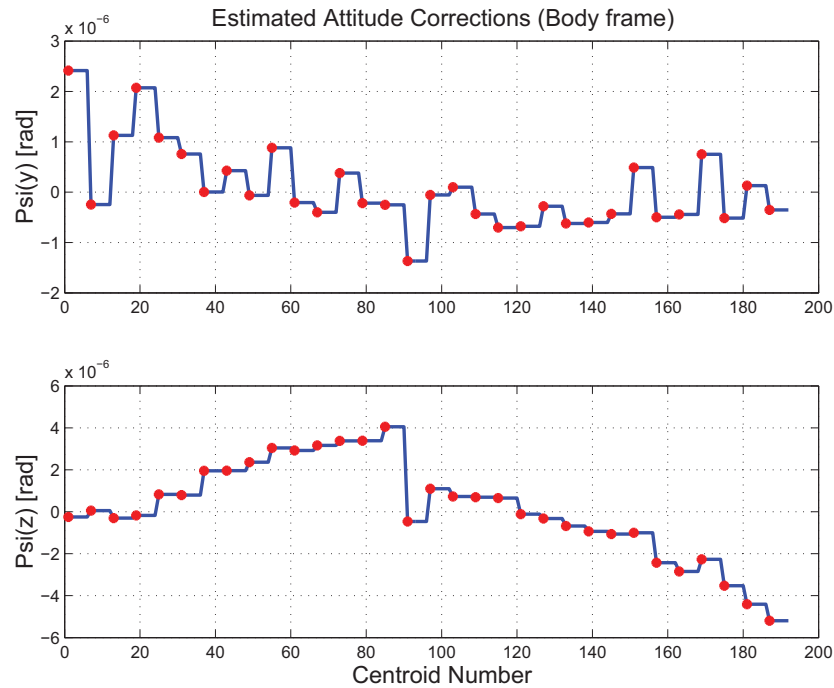


Figure 3.39: Estimated attitude corrections (Body frame)

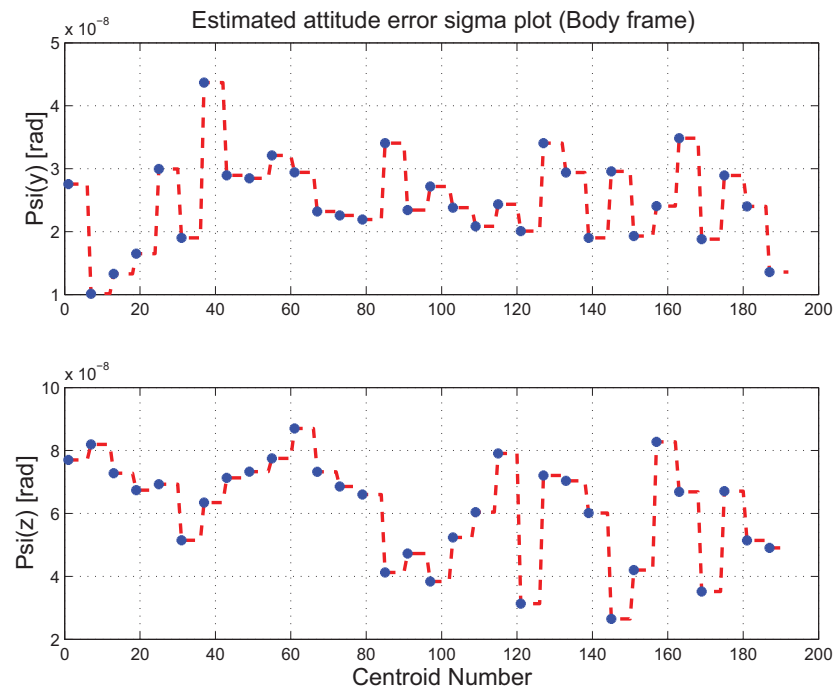


Figure 3.40: Estimated attitude error sigma plot (Body frame)

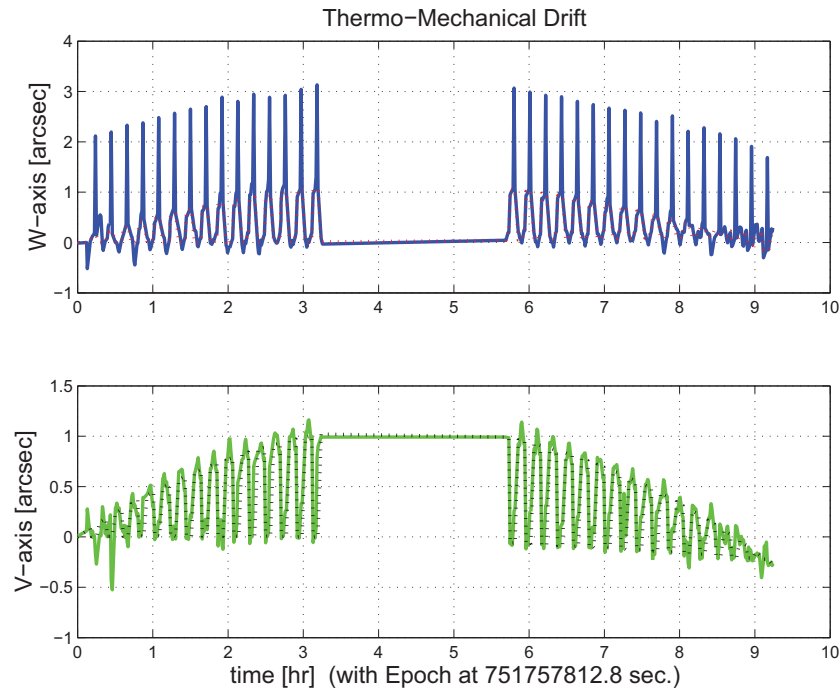


Figure 3.41: Thermo-mechanical boresight drift (equiv. angle in (W,V) coords)

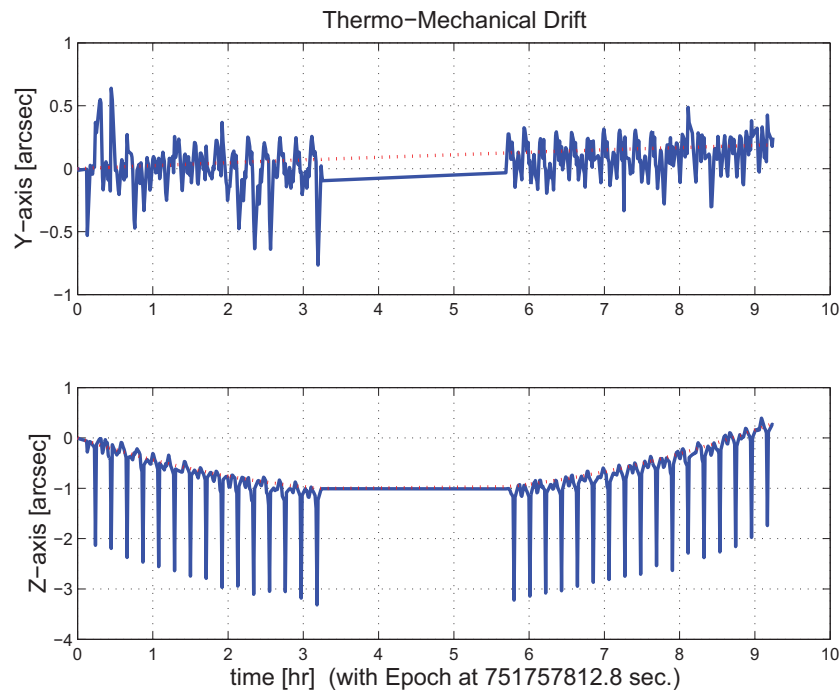


Figure 3.42: Thermo-mechanical boresight drift (equiv. angle in Body frame)

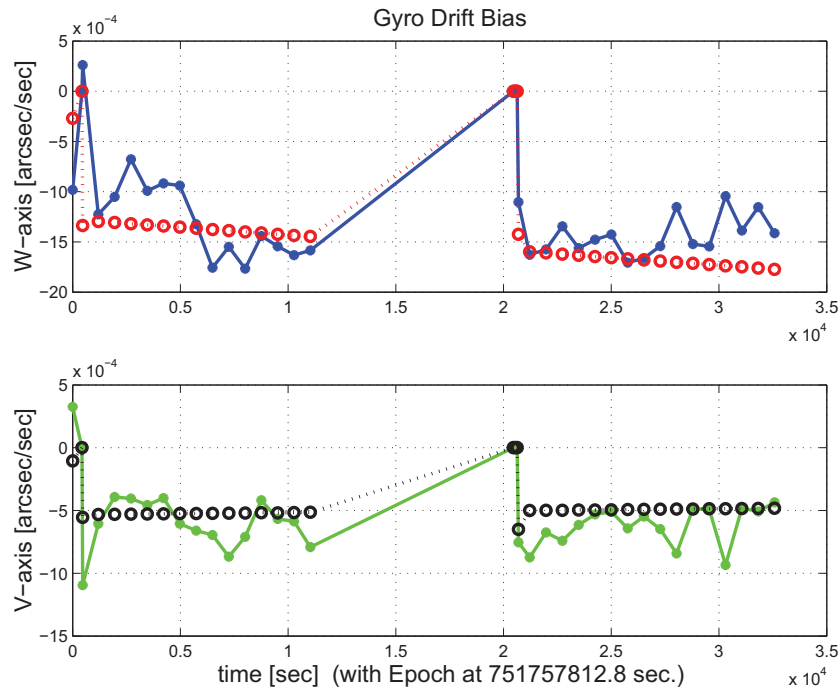


Figure 3.43: Gyro drift bias contribution (equiv. rate in (W,V) coords)

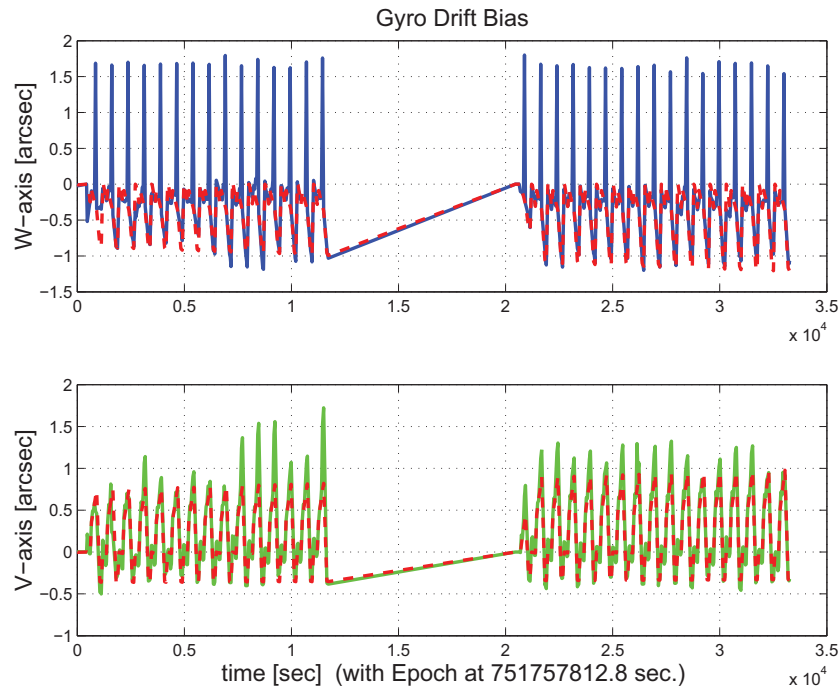


Figure 3.44: Gyro drift bias contribution (equiv. angle in (W,V) coords)

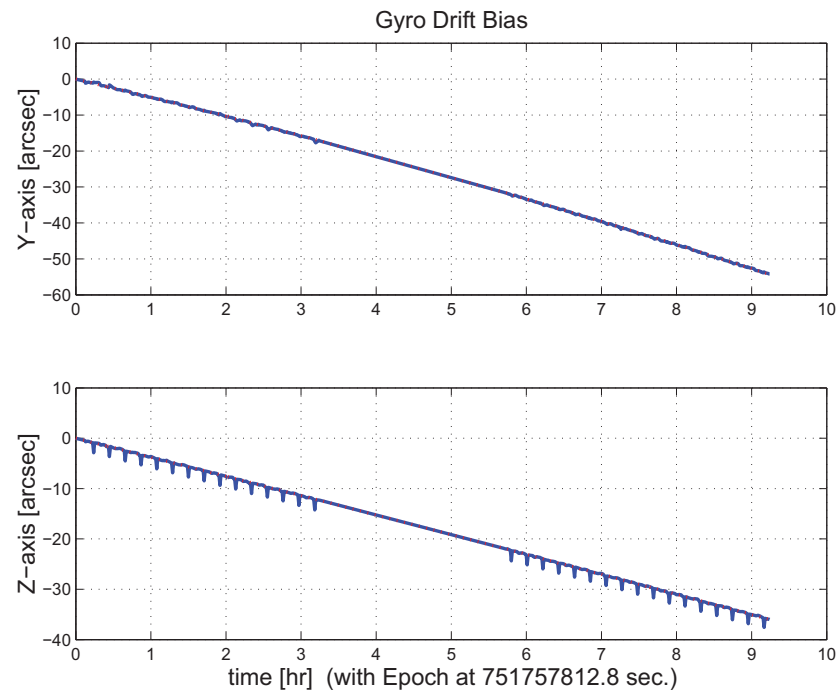


Figure 3.45: Gyro drift bias contribution (equiv. angle in Body frame)

3.2 IPF OUTPUT DATA (IF MINI FILE)

OUTPUT FILE NAME: IFmini502034.dat DATE: 06-Nov-2003 TIME: 09:10
INSTRUMENT NAME: IRS_ShortLo_2nd_Ord_Center_Pos NF: 34
IPF FILTER VERSION: IPF.V3.0.0B SW RELEASE DATE: November 3, 2003
FRAME TABLE USED: BodyFrames_FTU_12b

----- IPF BROWN ANGLE SUMMARY -----

WAS			IS			
Frame Number	theta_Y (arcmin)	theta_Z (arcmin)	angle (deg)	theta_Y (arcmin)	theta_Z (arcmin)	angle (deg)
034	-11.911390	-4.073083	-84.719995	-11.913057	-4.093168	-84.719994
032	-11.925347	-3.922059	-84.719995	-11.927235	-3.939748	-84.719994
033	-11.897433	-4.224107	-84.719995	-11.898879	-4.246589	-84.719994

OFFSET	NF	Delta_CW	Delta_CV
0	34	+0.000	+0.000 pixels

OFFSET FRAME NAME: IRS_ShortLo_2nd_Ord_Center_Pos

Brown Angle	theta_Y(arcmin)	theta_Z(arcmin)	angle(deg)
WAS(FTB)	-11.911390	-4.073083	-84.719995
IS (EST)	-11.913057	-4.093168	-84.719994
dT_EST	-0.001667	-0.020086	+0.000001
T_sSIGMA	+0.000412	+0.000305	+999.999999
dT_EST/T_sSIGMA	-4.041381	-65.814407	+999.999999

OFFSET	NF	Delta_CW	Delta_CV
1	32	-9.100	+0.000 pixels

OFFSET FRAME NAME: IRS_ShortLo_2nd_Ord_1st_Pos

Brown Angle	theta_Y(arcmin)	theta_Z(arcmin)	angle(deg)
WAS(FTB)	-11.925347	-3.922059	-84.719995
IS (EST)	-11.927235	-3.939748	-84.719994
dT_EST	-0.001888	-0.017689	+0.000001
T_sSIGMA	+0.000490	+0.000305	+999.999999
dT_EST/T_sSIGMA	-3.855140	-57.961371	+999.999999

OFFSET	NF	Delta_CW	Delta_CV
2	33	+9.100	+0.000 pixels

OFFSET FRAME NAME: IRS_ShortLo_2nd_Ord_2nd_Pos

Brown Angle	theta_Y(arcmin)	theta_Z(arcmin)	angle(deg)
WAS(FTB)	-11.897433	-4.224107	-84.719995
IS (EST)	-11.898879	-4.246589	-84.719994
dT_EST	-0.001445	-0.022482	+0.000001
T_sSIGMA	+0.000354	+0.000305	+999.999999
dT_EST/T_sSIGMA	-4.084208	-73.667441	+999.999999

VARNAME	MEAN	SIGMA	SCALED_SIGMA
a00	+1.5869176483161697E-002	+2.9935845253503739E-004	+7.3632063285173537E-004
del_theta2	-1.6761989587135778E-017	+4.8777896163896595E-008	+1.1997714134486613E-007
del_theta3	-4.5805126420123907E-019	+3.6092210902652271E-008	+8.8774642398810479E-008
del_arx	+8.9214075512408612E-015	+1.9351289046700310E-005	+4.7597631791257106E-005
del_ary	-1.6843313683622806E-016	+1.7962824734325360E-006	+4.4182478778130435E-006
del_arz	-3.0293752193723787E-016	+1.8207726245966691E-006	+4.4784853738687074E-006
brx	-1.3227445522517075E-008	+2.7188479350550799E-009	+6.6874471564589604E-009
bry	+3.2446525256915202E-011	+2.8814206738590766E-010	+7.0873211566981488E-010
brz	-6.6464980098562955E-010	+2.9803276843996398E-010	+7.3305989795823279E-010
crx	+6.5579227619687570E-013	+1.5761683789046349E-013	+3.8768415870940546E-013
cry	-3.0011346896890972E-016	+1.7722121805382735E-014	+4.3590430912211038E-014
crz	+4.2468509231061945E-014	+1.8394803102879463E-014	+4.5244999588945983E-014
bgx	+1.6868534610963682E-006	+1.6528097784827597E-007	+4.0653535310933736E-007
bgy	-6.6706596122101235E-009	+3.2234045453348027E-010	+7.9284859159949354E-010
bgz	-5.0455155021281773E-009	+8.4985598682678310E-010	+2.0903585409197437E-009
cgx	+1.0050529376805618E-012	+7.3479851119147573E-012	+1.8073560315311135E-011

cgy -7.5022471966270354E-014 +1.8914996057895617E-014 +4.6524498472638531E-014
 cgz -1.2178330312826663E-014 +4.0067841741978710E-014 +9.8553350802760088E-014

LSQF RESIDUAL SIGMA SCALE = +2.4596620760710115E+000

	qT(1)	qT(2)	qT(3)	qT(4)
FrmTbl:	-6.7378628247617900E-001	+8.8099053130865897E-004	+1.6050385638699100E-003	+7.3892401047321599E-001
Estim:	-6.7378627739063246E-001	+8.7920134131392648E-004	+1.6073605424617534E-003	+7.3892401219419157E-001
DelTheta	deltheta(1)	deltheta(2)	deltheta(3)	
	-2.8614297542710135E-012	-5.7732048969180948E-006	+1.0204715524316437E-006	[rad]
EulAngT	theta(1)	theta(2)	theta(3)	[rad]
Mean	-1.4786428388361901E+000	+3.4653678537594629E-003	+1.1906544349402424E-003	
SigmaT	+9.999900000000000E+004	+4.8777896163896595E-008	+3.6092210902652271E-008	

	qR(1)	qR(2)	qR(3)	qR(4)
ASFILE:	+7.0875976234674454E-004	+1.2697187485173345E-003	-1.6123075329232961E-004	+9.9999892711639404E-001
Estim:	+7.6859070931171753E-004	+1.2702636575440285E-003	-1.5898996129461176E-004	+9.9999888520975566E-001
DelThetaR	delthetaR(1)	delthetaR(2)	delthetaR(3)	
	+1.1965596184833106E-004	+1.1121156811694374E-006	+4.6327967610415905E-006	[rad]
EulAngR	angR(1)	angR(2)	angR(3)	[rad]
Mean	+1.5367813519080406E-003	+2.5407716130135169E-003	-3.1602796773958674E-004	
SigmaR	+1.9351289046700310E-005	+1.7962824734325360E-006	+1.8207726245966691E-006	

Initial Gyro Bias	Bg0(1)	Bg0(2)	Bg0(3)	
	-4.1071160694627906E-007	-1.9299631048852461E-007	+3.6002467140860972E-007	
Gyro Bias Correction	Bg(1)	Bg(2)	Bg(3)	
	+1.6868534610963682E-006	-6.6706596122101235E-009	-5.0455155021281773E-009	
Total Gyro Bias	BgT(1)	BgT(2)	BgT(3)	
	+1.2761418541500891E-006	-1.9966697010073472E-007	+3.5497915590648156E-007	

Initial Gyro Bias Rate	Cg0(1)	Cg0(2)	Cg0(3)	
	+0.000000000000000E+000	+0.000000000000000E+000	+0.000000000000000E+000	
Gyro Bias Rate Correction	Cg(1)	Cg(2)	Cg(3)	
	+1.0050529376805618E-012	-7.5022471966270354E-014	-1.217833012826663E-014	
Total Gyro Bias Rate	CgT(1)	CgT(2)	CgT(3)	
	+1.0050529376805618E-012	-7.5022471966270354E-014	-1.217833012826663E-014	

OFFSET	NF	Delta_CW	Delta_CV	
1	32	-9.100	+0.000	pixels
OFFSET FRAME NAME:	IRS_ShortLo_2nd_Ord_1st_Pos			
qT	qT(1)	qT(2)	qT(3)	qT(4)
WAS(FTB)	-6.7378626144690612E-001	+8.9729059354406527E-004	+1.5901754284004005E-003	+7.3892404217016716E-001
IS (EST)	-6.7378625606850673E-001	+8.9576007232856100E-004	+1.5922615414878886E-003	+7.3892404443911619E-001
DelTheta	deltheta(1)	deltheta(2)	deltheta(3)	
Units	rad	rad	rad	
	+2.3921483804712300E-009	-5.0730877009603910E-006	+1.0204723241972602E-006	
EulAngT	theta(1)	theta(2)	theta(3)	[rad]
Mean	-1.4786428388361901E+000	+3.4694921570188261E-003	+1.1460261735683301E-003	
sSigmaT	+3.9787163025556602E-012	+1.4248536525684079E-007	+8.8774641441239097E-008	
SigmaT	+1.6175865543738183E-012	+5.7928837722473867E-008	+3.6092210513342131E-008	

OFFSET	NF	Delta_CW	Delta_CV	
2	33	+9.100	+0.000	pixels
OFFSET FRAME NAME:	IRS_ShortLo_2nd_Ord_2nd_Pos			
qT	qT(1)	qT(2)	qT(3)	qT(4)
WAS(FTB)	-6.7378630311169019E-001	+8.6469046652529928E-004	+1.6199016959987204E-003	+7.3892397847679425E-001
IS (EST)	-6.7378629830639947E-001	+8.6264260767061418E-004	+1.6224595399866929E-003	+7.3892397964021472E-001

DelTheta	deltheta(1)	deltheta(2)	deltheta(3)	
Units	rad	rad	rad	
	-2.3921670238728166E-009	-6.4733220926959718E-006	+1.0204705665179380E-006	
EulAngT	theta(1)	theta(2)	theta(3)	[rad]
Mean	-1.4786428388361901E+000	+3.4612435435982451E-003	+1.2352826950364749E-003	

```

sSigmaT  +3.9787163025556417E-012 +1.0294417450752624E-007 +8.8774645664067963E-008
SigmaT   +1.6175865543738108E-012 +4.1852974645999381E-008 +3.6092212230175067E-008
-----
----- q(1)           q(2)           q(3)           q(4)
PCRS1A: +5.3371888965461637E-007 +3.7444233778550031E-004 -1.4253684912431913E-003 +9.9999891405806784E-001
PCRS2A: -5.2779261998836216E-007 +3.8462959425181312E-004 +1.3722087221825403E-003 +9.9999898455099423E-001
*****
***** CS-FILE PARAMETERS: ***** AS-FILE PARAMETERS: *****
Row (01) PIX2RADX: +4.8481368110953598E-006 Row (1) TASTART: +7.5175700009074402E+008
Row (02) PIX2RADY: +4.8481368110953598E-006 Row (2) TASTOP: +7.5179200009073484E+008
Row (03) CXO: +0.0000000000000000E+000 Row (3) S/C TIME: +7.5174464249078369E+008
Row (04) CYO: +0.0000000000000000E+000 Row (4) QR1: +7.0875976234674454E-004
Row (05) BETA0: +9.9999000000000000E+004 Row (5) QR2: +1.2697187485173345E-003
Row (06) GAMMA_E0: +9.9999000000000000E+004 Row (6) QR3: -1.6123075329232961E-004
Row (07) D11: +1.0000000000000000E+000 Row (7) QR4: +9.9999892711639404E-001
Row (08) D12: +0.0000000000000000E+000
Row (09) D21: +0.0000000000000000E+000
Row (10) D22: +1.0000000000000000E+000
Row (11) DG: +9.9999000000000000E+004
-----
----- INITIAL STA-TO-PCRS ALIGNMENT (R) KNOWLEDGE (1-SIGMA)
      SIGMA(X)      SIGMA(Y)      SIGMA(Z)
5.93092957E+000  3.95658780E-001  3.95875377E-001 [arcsec]
-----
PIX2RADX = 4.848136811095E-006[rad/pixel]
XPIXSIZE = 1.0000[arcsec]
PIX2RADY = 4.848136811095E-006[rad/pixel]
YPIXSIZE = 1.0000[arcsec]
CX0 = 0.0[pixel] = 0.00[arcsec]
CY0 = 0.0[pixel] = 0.00[arcsec]
-----
NOMINAL BETA0 = 9.999900000000E+004[rad/encoder unit]
ENCODER UNIT SIZE = 99999.00[arcsec]
GAMMA_E0 = 99999.00[encoder unit] = 99999.00[arcsec]
-----
| +1 | +0 |
FLIP MATRIX D = |----|----| and DG = +99999
| +0 | +1 |
-----
```

3.3 IPF EXECUTION LOG

```

*****
IPF EXECUTION-LOG FILE NAME: LG502034.dat
INSTRUMENT TYPE: IRS_ShortLo_2nd_Ord_Center_Pos
IPF FILTER EXECUTION DATE: 06-Nov-2003 TIME: 09:04
IPF FILTER VERSION USED: IPF.V3.0.OB
*****
```

```

*****
SLIT FLAG ENABLED! ENTERING SLIT MODE.
*****
```

```

----- Loading & Preparing Input Files -----
AAFILE: AA501034 Loaded! AAFILE dimension = 350001 X 21
ASFILE: AS501034 Loaded!
CAFFILE: CA501034 Loaded! CAFILE dimension = 192 X 15
```

```

CBFILE: CB502034 Loaded!          CBFILe dimension = 226 X 15
CCFILE: CC502034 Created!        CCFILE dimension = 418 X 19
CSFILE: CS501034 Loaded!
Loading Input Files Completed!
-----
----- Selected Mask Vectors -----
index =  1  2  3  4  5  6  7  8  9 10 11 12 13 14 15 16 17 18 19 20
-----
mask1 = [ 1  0  0  0  0  0  0  0  0  0  0  0  0  0  0  0  0  0  0  0 ]
mask2 = [ 0  0  0  1  1  1  1  1  1  1  1  1  1  1  1  1  1  1  1  1 ]
-----
----- Selected Initial Gyro Bias Parameters -----
User Entered 1 : Use AFILE database - from S/C filter
IPF Linearized Using Following Nominal Gyro Bias Estimates
bg0 = [-4.1071160694627906E-007 -1.9299631048852461E-007 +3.6002467140860972E-007 ]
cg0 = [+0.000000000000000E+000 +0.000000000000000E+000 +0.000000000000000E+000 ]
-----
----- Gyro Pre-Processor Run Completed -----
AGFILE CREATED: AG502034.m      ACFILE CREATED: AC502034.m
-----
Total Gyro Preprocessor Execution Time: 214 seconds

FRAME TABLE ENTRIES FOR PCRS LOADED TO TPCRS
q_PCRS4 = [ +5.3371888965461637E-007   q_PCRS5 = [ +7.3379987833742897E-007
             +3.7444233778550031E-004           +5.2236196154513707E-004
             -1.4253684912431913E-003           -1.4047712280184723E-003
             +9.9999891405806784E-001           +9.999887687698918E-001 ];
q_PCRS8 = [ -5.2779261998836216E-007   q_PCRS9 = [ -7.1963421681856818E-007
             +3.8462959425181312E-004           +5.3239763239987400E-004
             +1.3722087221825403E-003           +1.3516841804518383E-003
             +9.9999898455099423E-001           +9.9999894475050310E-001 ];
-----
----- Initial Conditions for State ----- ----- Initial Square-Root Cov (diag) -----
p1(01) = a00 = +0.000000000000000E+000 Sigma_initial(01,01) = 1.000000000000000E+000
p1(02) = b00 = +0.000000000000000E+000 Sigma_initial(02,02) = 9.999900000000000E+004
p1(03) = c00 = +0.000000000000000E+000 Sigma_initial(03,03) = 9.999900000000000E+004
p1(04) = a10 = +0.000000000000000E+000 Sigma_initial(04,04) = 9.999900000000000E+004
p1(05) = b10 = +0.000000000000000E+000 Sigma_initial(05,05) = 9.999900000000000E+004
p1(06) = c10 = +0.000000000000000E+000 Sigma_initial(06,06) = 9.999900000000000E+004
p1(07) = d10 = +0.000000000000000E+000 Sigma_initial(07,07) = 9.999900000000000E+004
p1(08) = a20 = +0.000000000000000E+000 Sigma_initial(08,08) = 9.999900000000000E+004
p1(09) = b20 = +0.000000000000000E+000 Sigma_initial(09,09) = 9.999900000000000E+004
p1(10) = c20 = +0.000000000000000E+000 Sigma_initial(10,10) = 9.999900000000000E+004
p1(11) = d20 = +0.000000000000000E+000 Sigma_initial(11,11) = 9.999900000000000E+004
p1(12) = a01 = +0.000000000000000E+000 Sigma_initial(12,12) = 9.999900000000000E+004
p1(13) = b01 = +0.000000000000000E+000 Sigma_initial(13,13) = 9.999900000000000E+004
p1(14) = c01 = +0.000000000000000E+000 Sigma_initial(14,14) = 9.999900000000000E+004
p1(15) = d01 = +0.000000000000000E+000 Sigma_initial(15,15) = 9.999900000000000E+004
p1(16) = e01 = +0.000000000000000E+000 Sigma_initial(16,16) = 9.999900000000000E+004
p1(17) = f01 = +0.000000000000000E+000 Sigma_initial(17,17) = 9.999900000000000E+004
-----
p2f(01) = am1 = +0.000000000000000E+000 Sigma_initial(18,18) = 9.999900000000000E+004
p2f(02) = am2 = +0.000000000000000E+000 Sigma_initial(19,19) = 9.999900000000000E+004
p2f(03) = am3 = +1.000000000000000E+000 Sigma_initial(20,20) = 9.999900000000000E+004
p2f(04) = beta = +1.000000000000000E+000 Sigma_initial(21,21) = 1.000000000000000E-002
p2f(05) = qT1 = -6.7378628247617944E-001 Sigma_initial(22,22) = 1.000000000000000E-002
p2f(06) = qT2 = +8.8099053130865951E-004 Sigma_initial(23,23) = 2.8753957993070097E-004
p2f(07) = aT3 = +1.605038563869911E-003 Sigma_initial(24,24) = 1.9182078963746193E-005
p2f(08) = qT4 = +7.3892401047321643E-001 Sigma_initial(25,25) = 1.9192579876388130E-005
p2f(09) = qR1 = +7.0875976234674454E-004 Sigma_initial(26,26) = 3.0063795368266617E-005
p2f(10) = qR2 = +1.2697187485173345E-003 Sigma_initial(27,27) = 3.0063795368266617E-005
p2f(11) = qR3 = -1.6123075329232961E-004
p2f(12) = qR4 = +9.9999892711639404E-001
p2f(13) = brx = +0.000000000000000E+000
p2f(14) = bry = +0.000000000000000E+000

```

```

p2f(15) = brz = +0.0000000000000000E+000 Sigma_initial(28,28) = 3.0063795368266617E-005
p2f(16) = crx = +0.0000000000000000E+000 Sigma_initial(29,29) = 9.0383179194500921E-010
p2f(17) = cry = +0.0000000000000000E+000 Sigma_initial(30,30) = 9.0383179194500921E-010
p2f(18) = crz = +0.0000000000000000E+000 Sigma_initial(31,31) = 9.0383179194500921E-010
p2f(19) = bgx = +0.0000000000000000E+000 Sigma_initial(32,32) = 3.0063795368266617E-005
p2f(20) = bgy = +0.0000000000000000E+000 Sigma_initial(33,33) = 3.0063795368266617E-005
p2f(21) = bgz = +0.0000000000000000E+000 Sigma_initial(34,34) = 3.0063795368266617E-005
p2f(22) = cgx = +0.0000000000000000E+000 Sigma_initial(35,35) = 9.0383179194500921E-010
p2f(23) = cgy = +0.0000000000000000E+000 Sigma_initial(36,36) = 9.0383179194500921E-010
p2f(24) = cgz = +0.0000000000000000E+000 Sigma_initial(37,37) = 9.0383179194500921E-010
-----
```

```

----- IPF KALMAN FILTER STARTED -----
Iteration#001: |dp|= +1.542628261155E-002 RMS(|Res|)=+8.895220412358E-006
Iteration#002: |dp|= +5.051962255940E-004 RMS(|Res|)=+4.065897866730E-006
Iteration#003: |dp|= +5.488336525177E-005 RMS(|Res|)=+4.619547886702E-006
Iteration#004: |dp|= +2.880666159878E-006 RMS(|Res|)=+4.644563389253E-006
Iteration#005: |dp|= +2.111346392566E-007 RMS(|Res|)=+4.647101747984E-006
Iteration#006: |dp|= +1.329792437038E-008 RMS(|Res|)=+4.647233977331E-006
Iteration#007: |dp|= +1.035975491900E-009 RMS(|Res|)=+4.647249846006E-006
Iteration#008: |dp|= +7.208998031568E-011 RMS(|Res|)=+4.647250816142E-006
Iteration#009: |dp|= +3.825714355591E-012 RMS(|Res|)=+4.647250839727E-006
Iteration#010: |dp|= +3.788431625068E-013 RMS(|Res|)=+4.647250840767E-006
Iteration#011: |dp|= +1.105110182022E-013 RMS(|Res|)=+4.647250841206E-006
Iteration#012: |dp|= +8.318180019812E-014 RMS(|Res|)=+4.647250841178E-006
Iteration#013: |dp|= +9.055969045638E-014 RMS(|Res|)=+4.647250841275E-006
Iteration#014: |dp|= +6.178802558366E-014 RMS(|Res|)=+4.647250841296E-006
Iteration#015: |dp|= +8.70853582297E-014 RMS(|Res|)=+4.647250841223E-006
IPF Kalman Filter Completed with Error |dp1| + |dp2| = +8.7085358822972741E-014
-----
```

```

----- IPF LEAST SQUARES FILTER STARTED -----
Iteration#001 COND#=+5.886308892341E+006, |dp|=+1.542715433487E-002
Iteration#002 COND#=+5.897154529577E+006, |dp|=+5.034358720748E-004
Iteration#003 COND#=+5.894606247595E+006, |dp|=+5.532483543631E-005
Iteration#004 COND#=+5.894380673638E+006, |dp|=+2.920188628352E-006
Iteration#005 COND#=+5.894365008258E+006, |dp|=+2.347966637846E-007
Iteration#006 COND#=+5.894363946824E+006, |dp|=+1.471367697681E-008
Iteration#007 COND#=+5.894363873502E+006, |dp|=+1.066044990771E-009
Iteration#008 COND#=+5.894363868492E+006, |dp|=+7.092959220175E-011
Iteration#009 COND#=+5.894363868146E+006, |dp|=+4.958499218382E-012
Iteration#010 COND#=+5.894363868123E+006, |dp|=+5.552679989426E-013
Iteration#011 COND#=+5.894363868121E+006, |dp|=+1.830093211357E-013
Iteration#012 COND#=+5.894363868122E+006, |dp|=+1.047509991966E-013
Iteration#013 COND#=+5.894363868121E+006, |dp|=+1.631760146896E-013
Iteration#014 COND#=+5.894363868121E+006, |dp|=+1.835344489484E-013
Iteration#015 COND#=+5.894363868120E+006, |dp|=+1.460190083169E-013
IPF Least Squares Filter Completed with Error |dp1| + |dp2| = +1.4601900831692823E-013
-----
```

Total Execution Time: 353 seconds

4 COMMENTS

Overall the data looked clean, and the filter converged nicely.

Comments:

1. The run was performed in normal IPF operating mode with the slit mode processing enabled.
2. This run uses IPF version 3.0 where the gyro drift bias estimates make use of the recently corrected GCF signs, (MCR 2521) and now show no sandwich-to-sandwich variations.
3. There were 32 sandwiches maneuvers with 192 science centroids and 226 PCRS measurements.
4. We estimated 18 parameters consisting of: 1 constant plate scale (along W-axis), 2 IPF alignment angles, 3 STA-to-PCRS alignment angles, 6 STA-to-PCRS thermomechanical drift parameters, and 3 gyro bias and 3 gyro bias-drift parameters.

We recommend updating frames 34, 32 and 33 with the new quaternion listed in the IF file IF502034.dat. This contains adjustments of about 0.1 and 1.2 arcseconds in Y and Z. In our best judgement, this fine survey is accurate to 0.091 arcsecond which satisfies its fine survey requirement of 0.14 arcsecond by a good margin.

IPF TEAM CONTACT INFORMATION

IPF Team email	ipf@sirtfweb.jpl.nasa.gov	
David S. Bayard	X4-8208	David.S.Bayard@jpl.nasa.gov (TEAM LEADER)
Dhemetrio Boussalis	X4-3977	boussali@grover.jpl.nasa.gov
Paul Brugarolas	X4-9243	Paul.Brugarolas@jpl.nasa.gov
Bryan H. Kang	X4-0541	Bryan.H.Kang@jpl.nasa.gov
Edward.C.Wong	X4-3053	Edward.C.Wong@jpl.nasa.gov (TASK MANAGER)

ACKNOWLEDGEMENTS

This work was performed at the Jet Propulsion Laboratory, California Institute of Technology, under contract with the National Aeronautics and Space Administration.

References

- [1] D.S. Bayard, B.H. Kang, *SIRTF Instrument Pointing Frame Kalman Filter Algorithm*, JPL D-Document D-24809, September 30, 2003.
- [2] B.H. Kang, D.S. Bayard, *SIRTF Instrument Pointing Frame (IPF) Software Description Document and User's Guide*, JPL D-Document D-24808, September 30, 2003.
- [3] D.S. Bayard, B.H. Kang, *SIRTF Instrument Pointing Frame (IPF) Kalman Filter Unit Test Report*, JPL D-Document D-24810, September 30, 2003.
- [4] *Space Infrared Telescope Facility In-Orbit Checkout and Science Verification Mission Plan*, JPL D-Document D-22622, 674-FE-301 Version 1.4, February 8, 2002.
- [5] *Space Infrared Telescope Facility Observatory Description Document*, Lockheed Martin LMMS/P458569, 674-SEIT-300 Version 1.2, November 1, 2002.
- [6] *SIRTF Software Interface Specification for Science Centroid INPUT Files (CAFILe, CS-FILE)*, JPL SOS-SIS-2002, November 18, 2002.
- [7] *SIRTF Software Interface Specification for Inferred Frames Offset INPUT Files (OFILE)*, JPL SOS-SIS-2003, November 18, 2002.
- [8] *SIRTF Software Interface Specification for PCRS Centroid INPUT Files (CBFILE)*, JPL SIS-FES-015, November 18, 2002.
- [9] *SIRTF Software Interface Specification for Attitude INPUT Files (AFILE, ASFILE)*, JPL SIS-FES-014, January 7, 2002.
- [10] *SIRTF Software Interface Specification for IPF Filter Output Files (IFFILE, LGFILE, TARFILE)*, JPL SOS-SIS-2005, November 18, 2002.
- [11] R.J. Brown, *Focal Surface to Object Space Field of View Conversion*. Systems Engineering Report SER No. S20447-OPT-051, Ball Aerospace & Technologies Corp., November 23, 1999.

JET PROPULSION LABORATORY

SIRTF IPF REPORT

JPL ID502040

November 6, 2003

**SIRTF INSTRUMENT POINTING FRAME
KALMAN FILTER EXECUTION SUMMARY**

IPF RUN NUMBER: 502040

REPORT TYPE: IOC EXECUTION (FINE)

PRIME FRAME: IRS_LongLo_1st_Ord_Center_Pos (40)

INFERRRED FRAMES: (38) (39) (41)

IPF TEAM

Autonomy and Control Section (345)

Jet Propulsion Laboratory

California Institute of Technology

4800 Oak Grove Drive

Pasadena, CA 91109

Contents

1 IPF EXECUTION SUMMARY	5
2 IPF INPUT FILE HISTORY	9
3 IPF EXECUTION RESULTS	12
3.1 IPF EXECUTION OUTPUT PLOTS	12
3.2 IPF OUTPUT DATA (IF MINI FILE)	38
3.3 IPF EXECUTION LOG	41
4 COMMENTS	44

List of Figures

1.1 A-priori and a-posteriori IPF frames	5
1.2 A-priori and a-posteriori IPF frames (ZOOMED)	8
2.1 Scenario Plot	9
2.2 Attitude file edit history	10
2.3 Centroid file edit history	10
2.4 Oriented Pixel Coords of Centroid Meas. Edited Centroids	11
3.1 TPF coords of measurements and a-priori predicts	14
3.2 Oriented Pixel Coords of measurements and a-priori predicts	14
3.3 Oriented (W,V) Pixel Coords of A-Priori Prediction Error Quiver Plot	15
3.4 A-priori prediction error (Science Centroids)	15
3.5 Oriented Pixel Coords of measurements and a-priori predicts (PCRS only)	16
3.6 Oriented Pixel Coords of measurements and a-priori predicts (Zoomed, PCRS only) . .	16
3.7 Oriented (W,V) Pixel Coords of A-Priori PCRS Prediction Error Quiver Plot	17
3.8 A-priori PCRS prediction error	17
3.9 IPF execution convergence, chart 1	18
3.10 IPF execution convergence, chart 2	18
3.11 Parameter uncertainty convergence	19
3.12 IPF parameter symbol table	19
3.13 KF parameter error sigma plots	20
3.14 LS parameter error sigma plot	20

3.15 KF and LS parameter error sigma plot	21
3.16 Oriented Pixel Coords of meas. and a-posteriori predicts	22
3.17 Oriented Pixel Coords of meas. and a-posteriori predicts (attitude corrected)	22
3.18 KF innovations with (o) and w/o (+) attitude corrections	23
3.19 Histograms of science a-posteriori residuals (or innovations)	23
3.20 A-Posteriori Science Centroid Prediction Error Quiver (Att. Cor.)	24
3.21 Normalized A-Posteriori Science Centroid Prediction Errors	24
3.22 KF innovations with (o) and w/o (+) attitude corrections (PCRS)	25
3.23 Histograms of PCRS a-posteriori residuals (or innovations)	25
3.24 A-posteriori PCRS Prediction Summary	26
3.25 A-posteriori PCRS Prediction (PCRS 1 Only)	27
3.26 A-posteriori PCRS Prediction (PCRS 2 Only)	27
3.27 A-Posteriori PCRS Prediction Errors Quiver (Att. Cor.)	28
3.28 Normalized A-Posteriori PCRS Prediction Errors	28
3.29 W-axis KF innovations and 1-sigma bound	29
3.30 V-axis KF innovations and 1-sigma bound	29
3.31 Array plot with (solid) and w/o (dashed) optical distortion corrections	30
3.32 Optical Distortion Plot: total (x5 magnification)	30
3.33 Optical Distortion Plot: constant plate scales (x5 magnification)	31
3.34 Optical Distortion Plot: linear plate scale (x5 magnification)	31
3.35 Optical Distortion Plot: gamma terms (x5 magnification)	32
3.36 Scan Mirror Chops	32
3.37 IPF Frame Reconstruction	33
3.38 Center Pixel Reconstruction	33
3.39 Estimated attitude corrections (Body frame)	34
3.40 Estimated attitude error sigma plot (Body frame)	34
3.41 Thermo-mechanical boresight drift (equiv. angle in (W,V) coords)	35
3.42 Thermo-mechanical boresight drift (equiv. angle in Body frame)	35
3.43 Gyro drift bias contribution (equiv. rate in (W,V) coords)	36
3.44 Gyro drift bias contribution (equiv. angle in (W,V) coords)	36
3.45 Gyro drift bias contribution (equiv. angle in Body frame)	37

List of Tables

1.1	IPF filter input files	6
1.2	IPF filter execution configuration	6
1.3	IPF filter execution mask vector assignment	6
1.4	IPF calibration error summary ([arcsec], 1-sigma, radial)	7
1.5	Science measurement prediction error summary (1-sigma)	7
1.6	IPF Brown angle summary	8
2.1	IPF input file begin and end times	9
2.2	IPF input file editing status	9
2.3	List of Removed Centroids (Original CA File Row Index)	11
3.1	Table of figures I (IPF run)	12
3.2	Table of figures II (IPF run)	13
3.3	PCRS measurement prediction error summary	26

1 IPF EXECUTION SUMMARY

This report summarizes the SIRTF Instrument Pointing Frame (IPF) Kalman Filter execution associated with run file: RN502040. In particular, this Focal Point Survey calibrates the instrument: IRS_LongLo_1st_Ord_Center_Pos (40), as part of the IOC Fine Survey. The main calibration results from the IPF filter execution have been documented in IF502040 typically stored in the mission archive DOM collection IPF_IF. This report only summarizes the main aspects of the run, and does not substitute for the full information contained in the IF file.

Section 1 summarizes the filter execution results. The filter configurations are tabulated in Table 1.2 and the mask vector assignments are tabulated in Table 1.3. A total of 18 state parameters are estimated in this run. The overall End-to-End pointing performances are tabulated in Table 1.4. The prediction residuals throughout the estimation processes are tabulated in Table 1.5. Section 3 summarizes resulting plots, a mini summary of the IF IPF output file, and the execution log. Section 4 captures the user comments that are specific to this particular run.

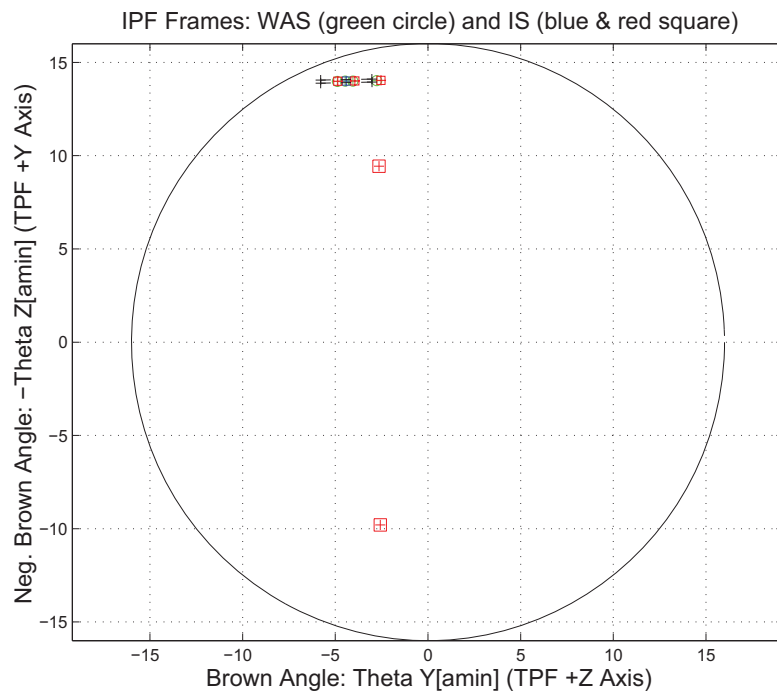


Figure 1.1: A-priori and a-posteriori IPF frames

RAW	FINAL (After Editing)
AA501040	AA501040
AS501040	AS501040
CA501040	CA594040
CB501040	CB501040
CS501040	CS501040

Table 1.1: IPF filter input files

EXECUTION CONFIGURATION ITEM	CURRENT STATUS
IPF Filter Version Used	IPF.V3.0.0B
Frame Table Version Used	BodyFrames_FTU_12b
Scan-Mirror Employed?	NO
IPF Filter Mode	NORMAL-MODE(0)
SLIT-MODE Operation	ENABLED
Kalman Filter Operation	ENABLED
Least-Squares Data Analysis	ENABLED
IBAD Screening	ENABLED
User-Specified Data Editing	DISABLED
Total Number of Iterations	25
LS Residual Sigma Scale	1.48173216E+000
Total Number of Maneuvers	7

Table 1.2: IPF filter execution configuration

Con. Plate Scale			Γ Dependent				Γ^2 Dependent				Linear Plate Scale						Mirror			
a_{00}	b_{00}	c_{00}	a_{10}	b_{10}	c_{10}	d_{10}	a_{20}	b_{20}	c_{20}	d_{20}	a_{01}	b_{01}	c_{01}	d_{01}	e_{01}	f_{01}	α	β		
1	2	3	4	5	6	7	8	9	10	11	12	13	14	15	16	17	18	19		
1	0	0	0	0	0	0	0	0	0	0	0	0	0	0	0	0	0	0		
IPF (T)			Alignment R						Gyro Drift Bias											
θ_1	θ_2	θ_3	a_{rx}	a_{ry}	a_{rz}	b_{rx}	b_{ry}	b_{rz}	c_{rx}	c_{ry}	c_{rz}	b_{gx}	b_{gy}	b_{gz}	c_{gx}	c_{gy}	c_{gz}			
20	21	22	23	24	25	26	27	28	29	30	31	32	33	34	35	36	37			
0	1	1	1	1	1	1	1	1	1	1	1	1	1	1	1	1	1			

Table 1.3: IPF filter execution mask vector assignment

FOCAL PLANE SURVEY ANALYSIS: IOC Fine Survey.

INSTRUMENT NAME: IRS_LongLo_1st_Ord_Center_Pos NF: 40

PIX2RADW: 4.84813681E-006 [rad/pixel] = 1.0000E+000 [arcsec/pixel]

PIX2RADV: 4.84813681E-006 [rad/pixel] = 1.0000E+000 [arcsec/pixel]

FRAME	DESCRIPTION	IPF ¹	SF ²	TOTAL	REQ
040(P)	IRS_LongLo_1st_Ord_Center_Pos	0.0973	0.0855	0.1295	0.28
038(I)	IRS_LongLo_1st_Ord_1st_Pos	0.1013	0.0855	0.1326	N/A
039(I)	IRS_LongLo_1st_Ord_2nd_Pos	0.1025	0.0855	0.1335	N/A
041(I)	IRS_LongLo_Module_Center	0.1548	0.0855	0.1769	N/A

Table 1.4: IPF calibration error summary ([arcsec], 1-sigma, radial)

RMS METRIC	A PRIORI ³	A POSTERIORI ³	ATT. CORRECTED ⁴	UNITS
Radial	4.7663	2.2009	2.1718	arcsec
W-Axis	4.7183	2.1235	2.0956	arcsec
V-Axis	0.6744	0.5784	0.5703	arcsec
Radial	4.7663	2.2009	2.1718	pixels
W-Axis	4.7183	2.1235	2.0956	pixels
V-Axis	0.6744	0.5784	0.5703	pixels

Table 1.5: Science measurement prediction error summary (1-sigma)

¹IPF filter removes systematic pointing errors due to: thermomechanical alignment drift (Body to TPF), gyro bias and bias drift, centroiding error, attitude error, and optical distortion. IPF SIGMA presented here is “Scaled” by the Least Squares Scale factor. The Least Squares Scale Factor was: 1.481732. It is assumed that the gyro Angle Random Walk contribution is captured with the Least Squares scaling. The gyro ARW contribution can be approximately calculated as 0.0844 arcseconds, given that ARW = 100 $\mu\text{deg}/\sqrt{\text{hr}}$, with 6.929620e+002 second Maneuver time (max), and 7 independent Maneuvres.

²Gyro Scale Factor(GSF) assumes 95 ppm error over 0.250 degree maneuver.

³This can be interpreted as estimate of “pixel to sky” pointing reconstruction error if no science data is used.

⁴This can be interpreted as estimate of achieved S/I centroiding error

IPF BROWN ANGLE SUMMARY					
FRAME TABLE USED: BodyFrames_FTU_12b					
NF	NAME	WAS	IS	CHANGE	UNIT
040	theta_Y	-4.467462	-4.405739	+0.061722	arcmin
040	theta_Z	-13.987365	-13.997049	-0.009684	arcmin
040	angle	-1.199998	-1.199998	+0.000000	deg
038	theta_Y	-4.047276	-3.944596	+0.102680	arcmin
038	theta_Z	-13.996167	-14.006709	-0.010542	arcmin
038	angle	-1.199998	-1.199998	+0.000000	deg
039	theta_Y	-4.887647	-4.866882	+0.020765	arcmin
039	theta_Z	-13.978564	-13.987390	-0.008826	arcmin
039	angle	-1.199998	-1.199998	+0.000000	deg
041	theta_Y	-2.763469	-2.535651	+0.227817	arcmin
041	theta_Z	-14.023059	-14.036222	-0.013163	arcmin
041	angle	-1.199998	-1.199998	+0.000000	deg

Table 1.6: IPF Brown angle summary

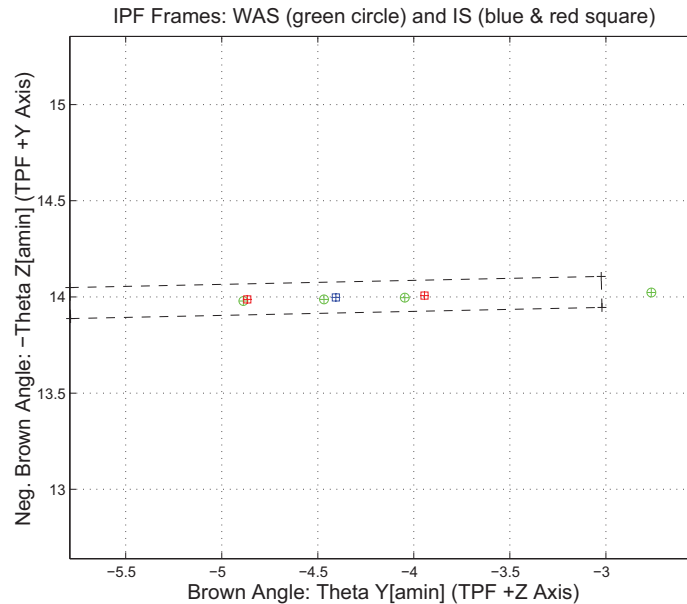


Figure 1.2: A-priori and a-posteriori IPF frames (ZOOMED)

2 IPF INPUT FILE HISTORY

STATUS	FILENAME	START TIME	END TIME
WAS	AA501040	751800000.2	751807000.1
IS	AA501040	751800000.2	751807000.1
WAS	CA501040	751801307.4	751806137.6
IS	CA594040	751801307.4	751806137.6
WAS	CB501040	751801084.0	751806358.3
IS	CB501040	751801084.0	751806358.3

Table 2.1: IPF input file begin and end times

WAS	SIZE	IS	SIZE	REMOVED	PATCHED
AA501040	70000	AA501040	70000	0	0
CA501040	42	CA594040	41	1	N/A
CB501040	49	CB501040	49	0	N/A

Table 2.2: IPF input file editing status

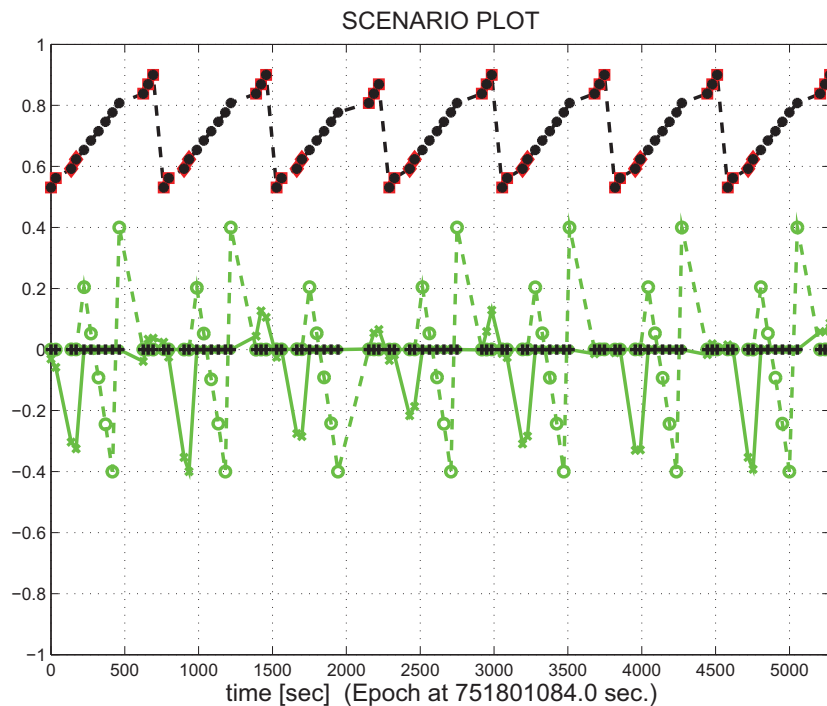


Figure 2.1: Scenario Plot

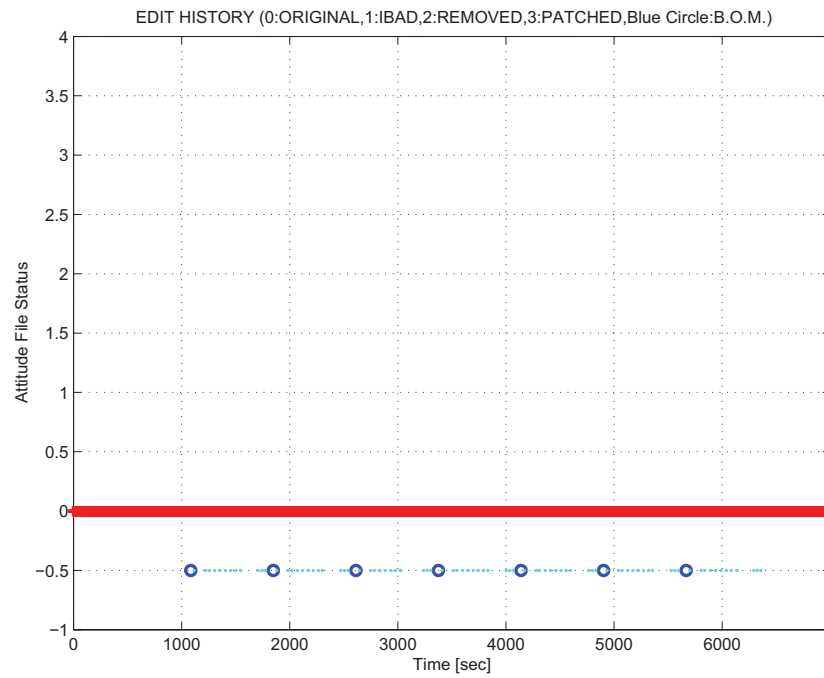


Figure 2.2: Attitude file edit history

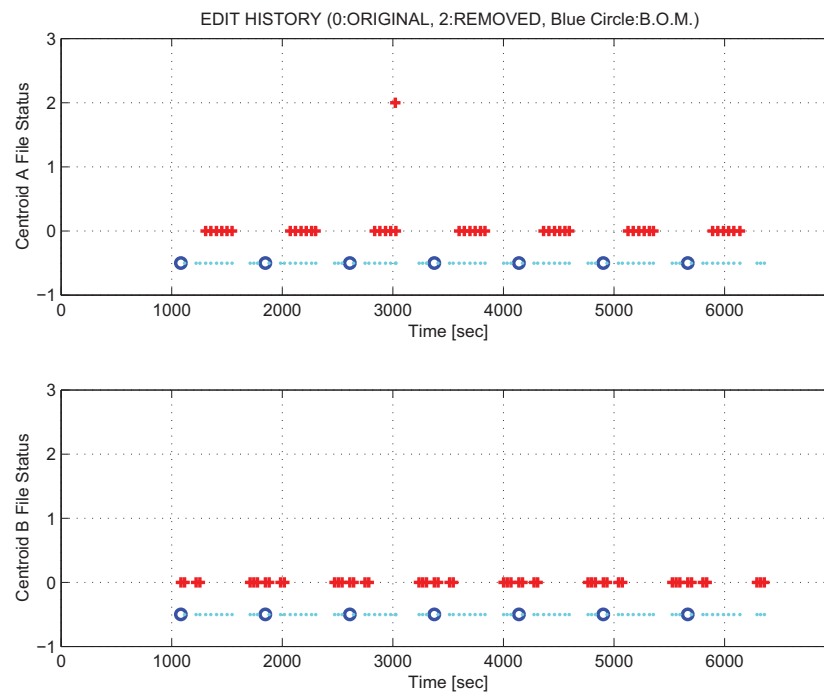


Figure 2.3: Centroid file edit history

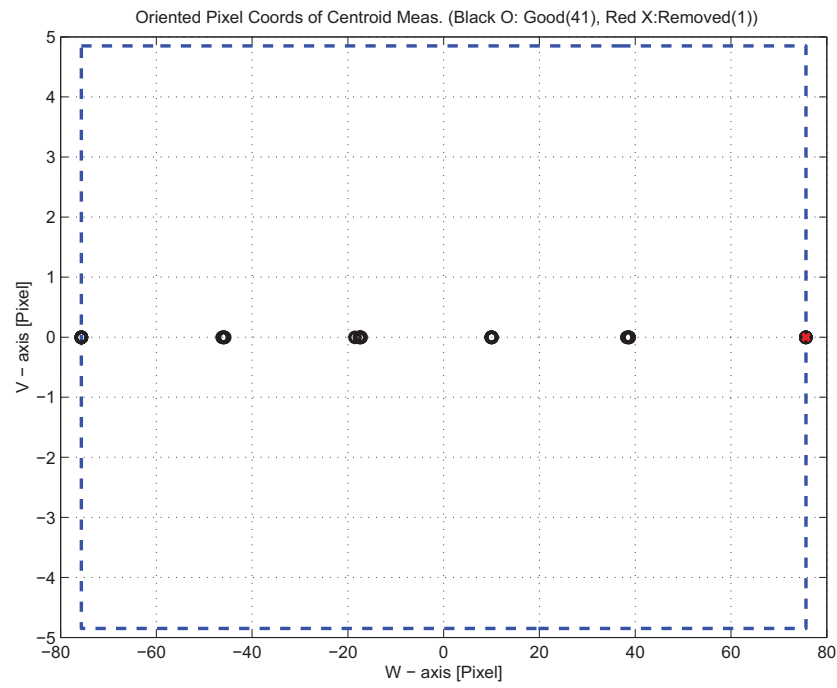


Figure 2.4: Oriented Pixel Coords of Centroid Meas. Edited Centroids

LIST OF REMOVED CENTROIDS										
1	2	3	4	5	6	7	8	9	10	
18										

Table 2.3: List of Removed Centroids (Original CA File Row Index)

3 IPF EXECUTION RESULTS

3.1 IPF EXECUTION OUTPUT PLOTS

This subsection summarizes the IPF filter results. As shown in Table 3.1, the output plots are segmented to three groups: predicted performance, post-run results and IPF trending plots.

FIGURE NO.	DESCRIPTION
Predicted performance prior to IPF run	
Figure 3.1	Meas. and a-priori predicts in TPF coords
Figure 3.2	Meas. and a-priori predicts in Oriented Pixel Coords including rectangular array boundary approximation
Figure 3.3	A-Priori Prediction Error Quiver Plot in Oriented Pixel Coords including rectangular array boundary approximation
Figure 3.4	A-priori prediction error
Figure 3.5	Oriented Pixel Coords of measurements and a-priori predicts (PCRS only)
Figure 3.6	Oriented Pixel Coords of measurements and a-priori predicts (Zoomed, PCRS only)
Figure 3.7	Oriented (W,V) Pixel Coords of A-Priori PCRS Prediction Error Quiver Plot
Figure 3.8	A-priori PCRS prediction error
IPF filter performance (post run results)	
Figure 3.9	IPF execution convergence, chart 1: (top) normalized residual error vs. iteration number and (bottom) norm of effective parameter corrections
Figure 3.10	IPF execution convergence, chart 2: parameter correction size vs. iteration number
Figure 3.11	Parameter uncertainty convergence: square-root of diagonal elements of covariance matrix vs. maneuver number
Figure 3.12	IPF parameter symbol table
Figure 3.13	KF parameter error sigma plot (a-priori-dashed, a-posteriori-solid). Includes true parameter errors (FLUTE runs only)
Figure 3.14	LS parameter error sigma plot. Includes true parameter errors (FLUTE runs only)
Figure 3.15	KF and LS parameter errors sigma plot (Figure 3.13 & Figure 3.14 combined)
Figure 3.16	Measurements and a-posteriori predicts in Oriented Pixel Coords including rectangular array boundaries (a-priori-dashed, a-posteriori-solid)
Figure 3.17	Attitude corrected meas. and a-posteriori predicts in Oriented Pixel Coords including rectangular array boundaries (a-priori-dashed, a-posteriori-solid)

Table 3.1: Table of figures I (IPF run)

FIGURE NO.	DESCRIPTION
IPF filter performance (post run results) - CONTINUE	
Figure 3.18	KF innovations with (o) and w/o (+) attitude corrections
Figure 3.19	Histograms of science a-posteriori residuals (or innovations)
Figure 3.20	A-Posteriori Science Centroid Prediction Error Quiver (Att. Cor.)
Figure 3.21	Normalized A-Posteriori Science Centroid Prediction Errors
Figure 3.22	KF innovations with (o) and w/o (+) attitude corrections (PCRS)
Figure 3.23	Histograms of PCRS a-posteriori residuals (or innovations)
Figure 3.24	A-posteriori PCRS Prediction Summary
Figure 3.25	A-posteriori PCRS Prediction (PCRS 1 Only)
Figure 3.26	A-posteriori PCRS Prediction (PCRS 2 Only)
Figure 3.27	A-Posteriori PCRS Prediction Errors Quiver (Att. Cor.)
Figure 3.28	Normalized A-Posteriori PCRS Prediction Errors
Figure 3.29	W-axis KF innovations and 1-sigma bound
Figure 3.30	V-axis KF innovations and 1-sigma bound
Figure 3.31	Array plot with (solid) and w/o (dashed) optical distortion corrections
Figure 3.32	Optical Distortion Plot: total (x5 magnification)
Figure 3.33	Optical Distortion Plot: constant plate scales (x5 magnification)
Figure 3.34	Optical Distortion Plot: linear plate scale (x5 magnification)
Figure 3.35	Optical Distortion Plot: gamma terms (x5 magnification)
Figure 3.36	Scan Mirror Chops
Figure 3.37	IPF Frame Reconstruction
Figure 3.38	Center Pixel Reconstruction
IPF parameter trending plots	
Figure 3.39	Estimated attitude corrections (Body frame)
Figure 3.40	Estimated attitude error sigma plot (Body frame)
Figure 3.41	Systematic error attributed to thermo-mechanical boresight drift (equiv. angle in (W,V) coords)
Figure 3.42	Systematic error attributed to thermo-mechanical boresight drift (equiv. angle in Body frame)
Figure 3.43	Systematic error attributed to gyro drift bias (equiv. rate in (W,V) coords)
Figure 3.44	Systematic error attributed to gyro drift bias (equiv. angle in (W,V) coords)
Figure 3.45	Systematic error attributed to gyro drift bias (equiv. angle in Body frame)

Table 3.2: Table of figures II (IPF run)

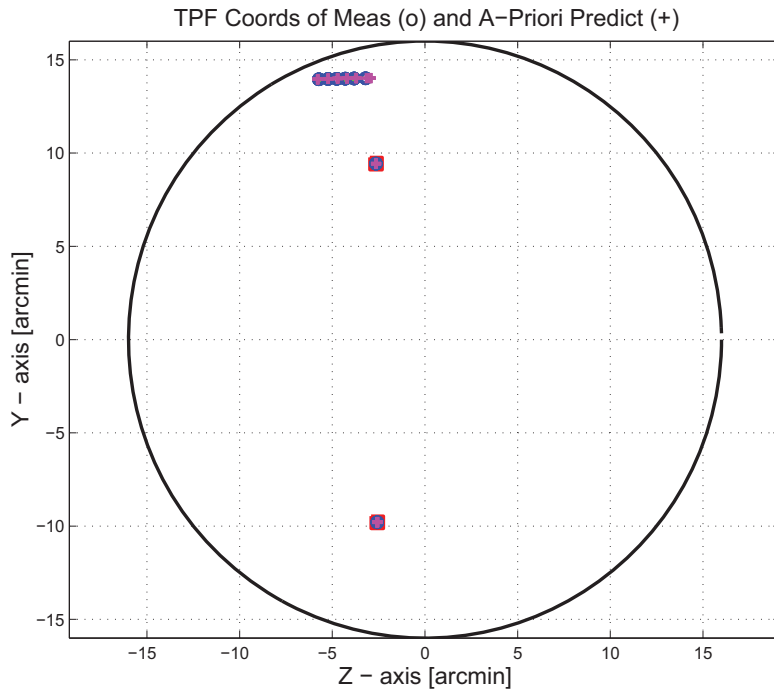


Figure 3.1: TPF coords of measurements and a-priori predicts

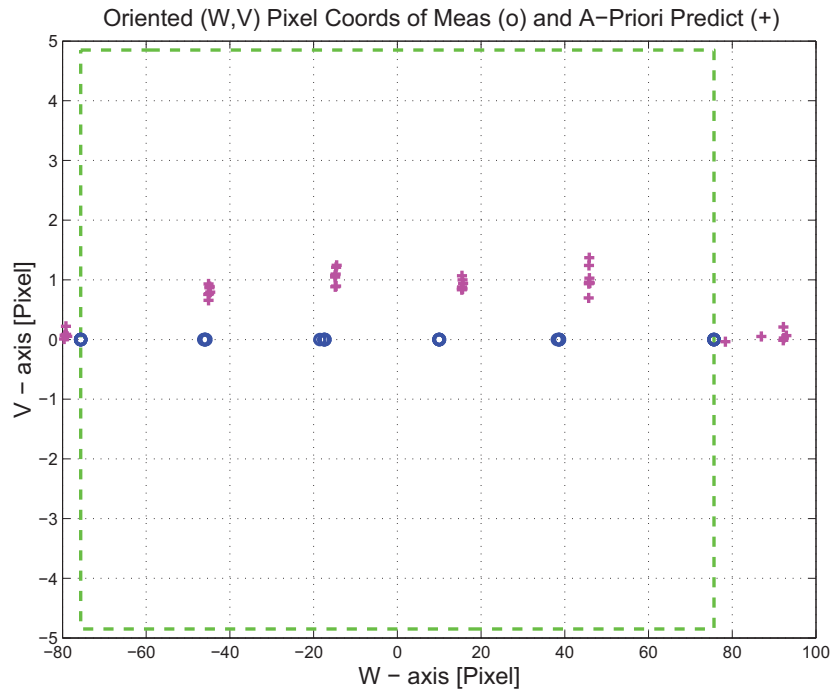


Figure 3.2: Oriented PixelCoords of measurements and a-priori predicts

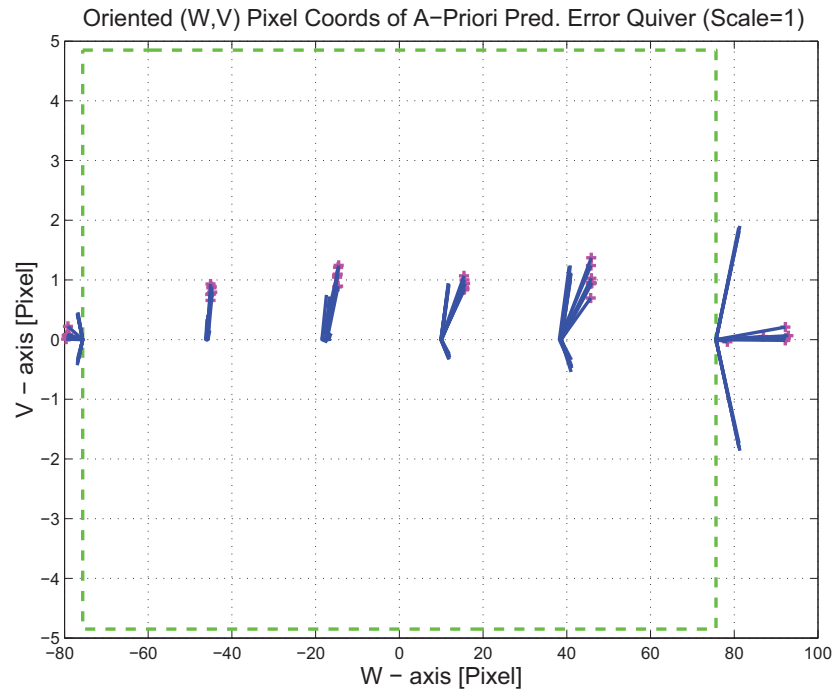


Figure 3.3: Oriented (W,V) Pixel Coords of A-Priori Prediction Error Quiver Plot

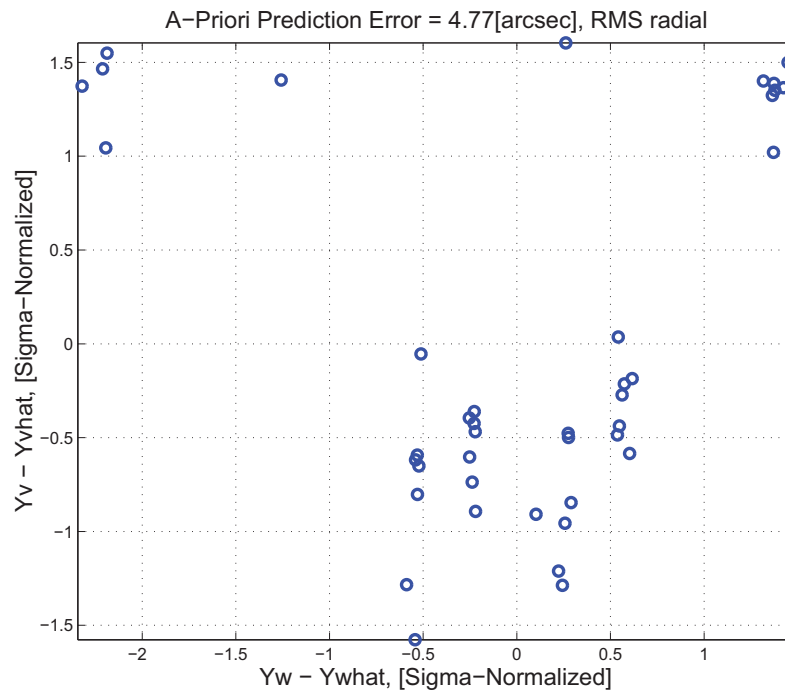


Figure 3.4: A-priori prediction error (Science Centroids)

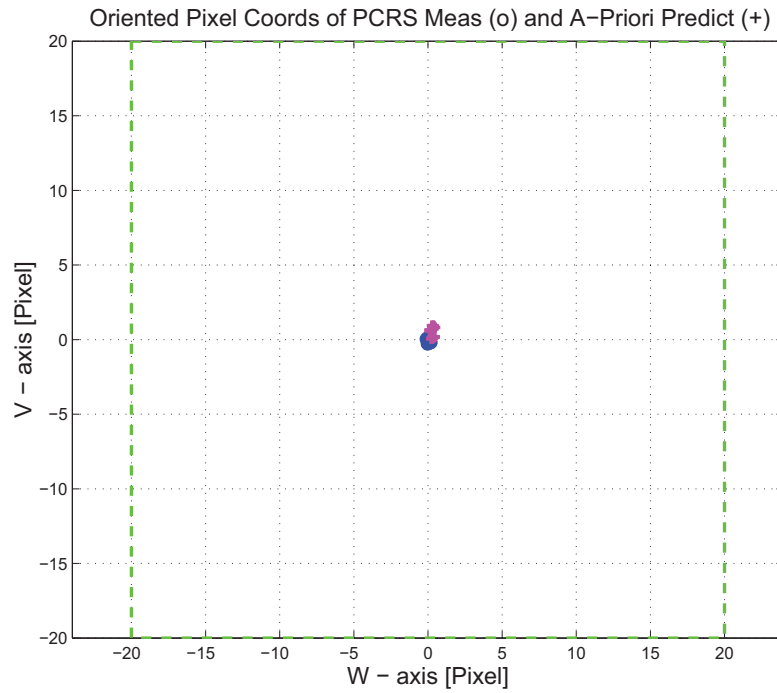


Figure 3.5: Oriented Pixel Coords of measurements and a-priori predicts (PCRS only)

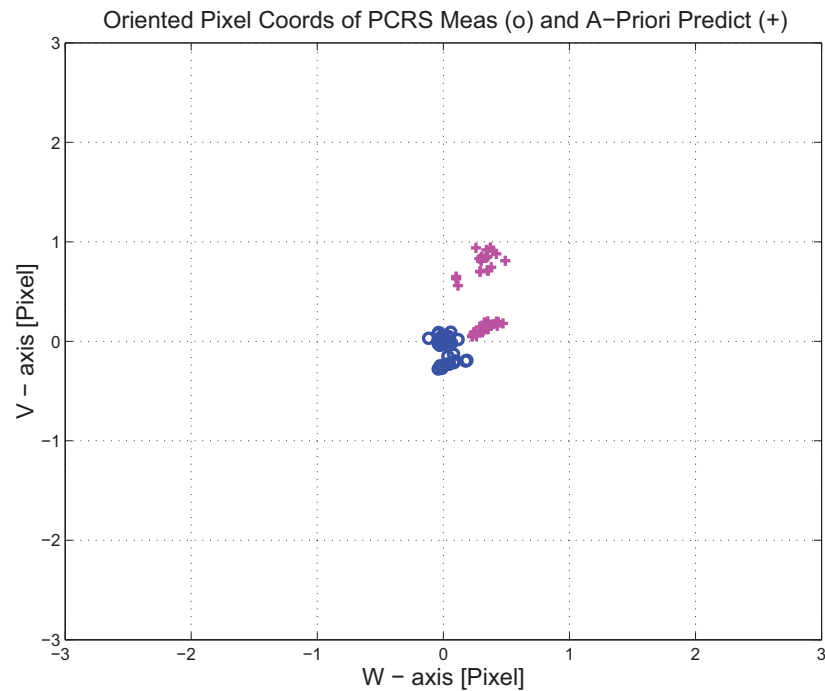


Figure 3.6: Oriented Pixel Coords of measurements and a-priori predicts (Zoomed, PCRS only)

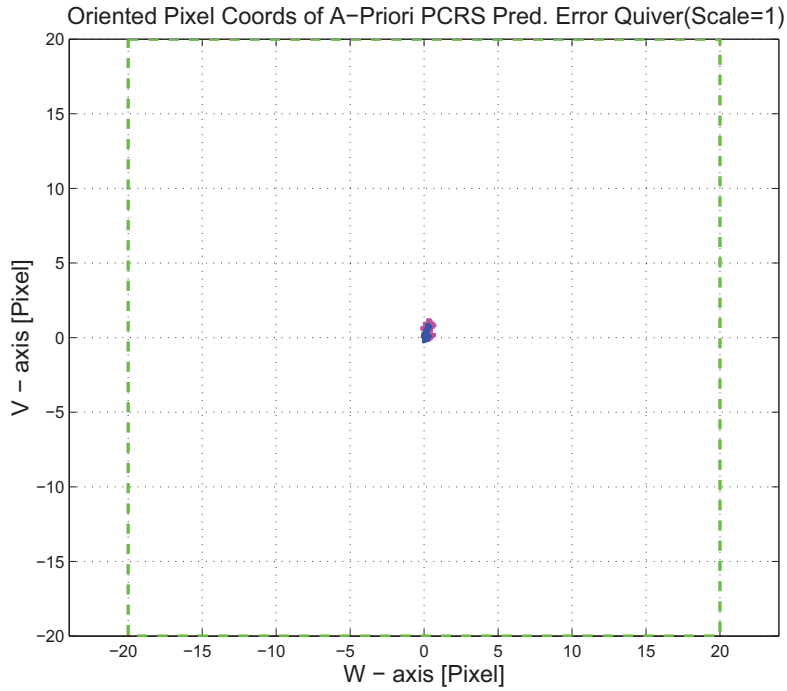


Figure 3.7: Oriented (W,V) Pixel Coords of A-Priori PCRS Prediction Error Quiver Plot

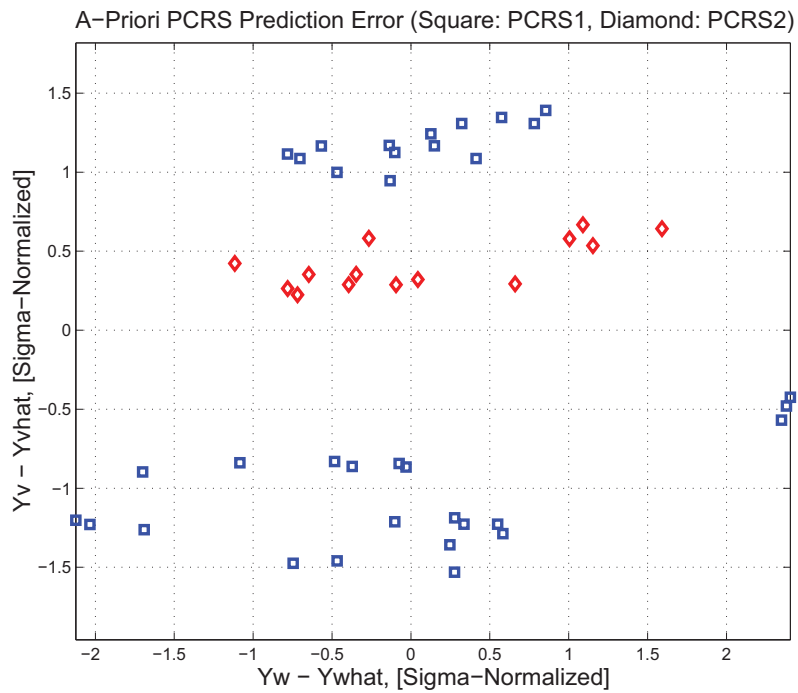


Figure 3.8: A-priori PCRS prediction error

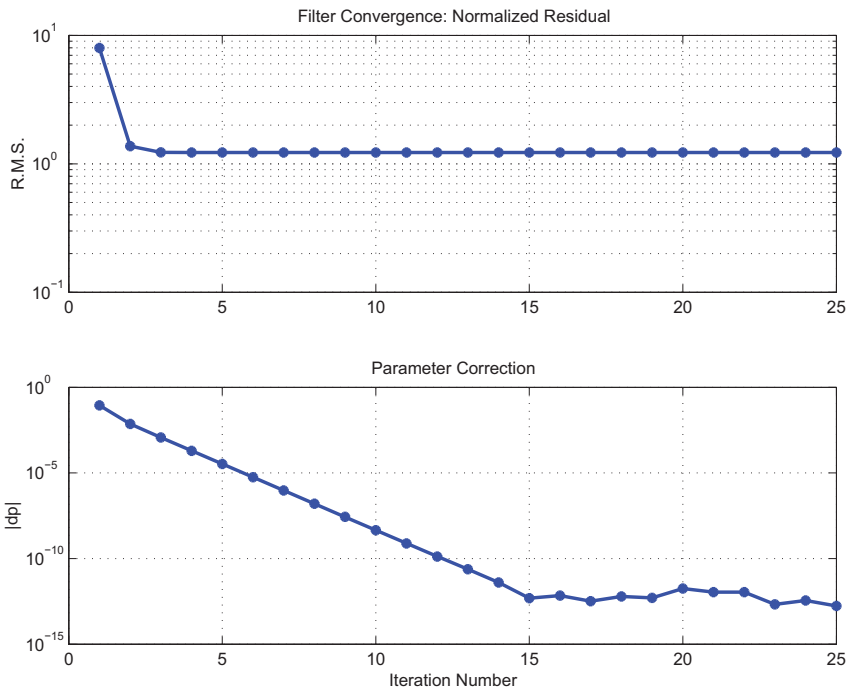


Figure 3.9: IPF execution convergence, chart 1

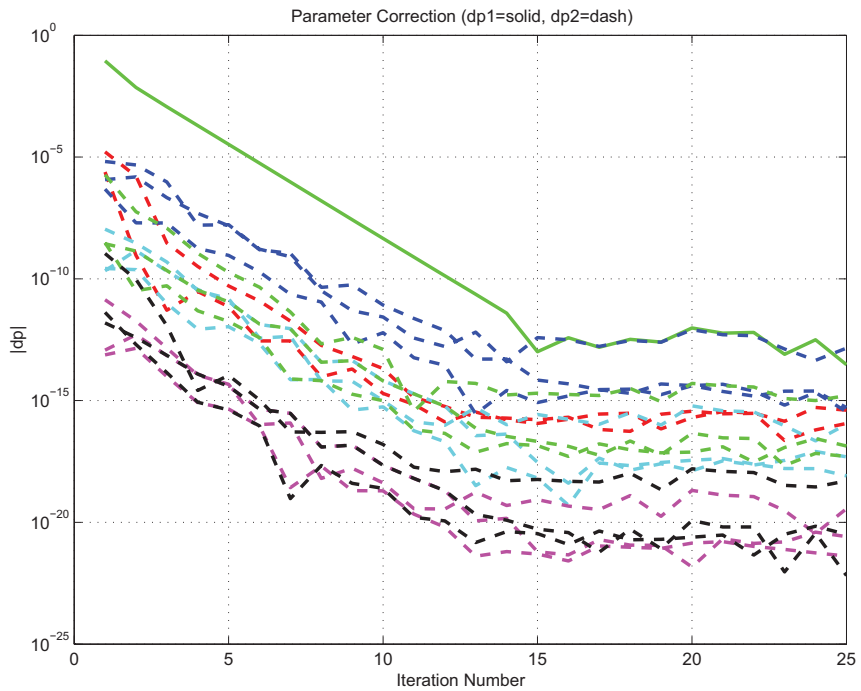


Figure 3.10: IPF execution convergence, chart 2

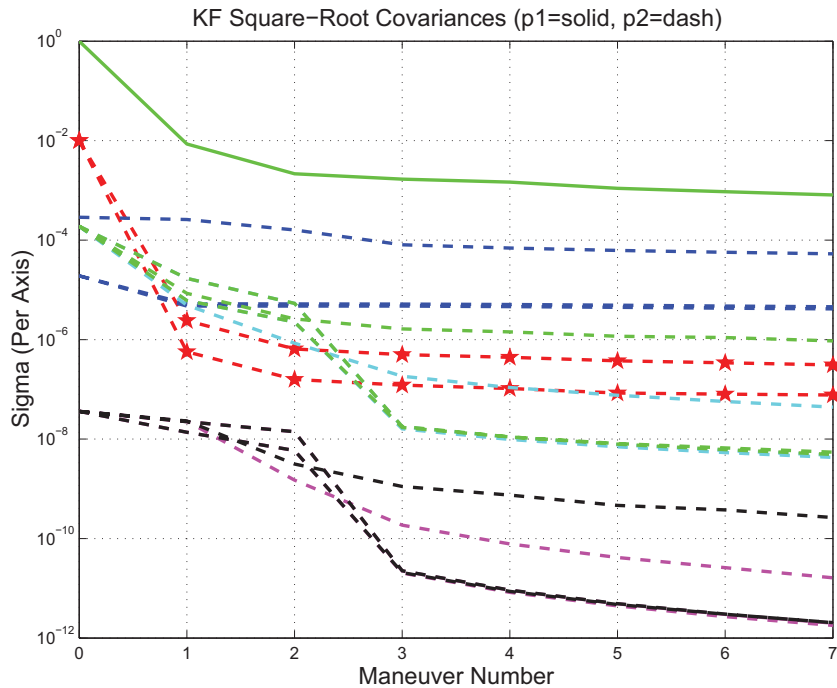


Figure 3.11: Parameter uncertainty convergence

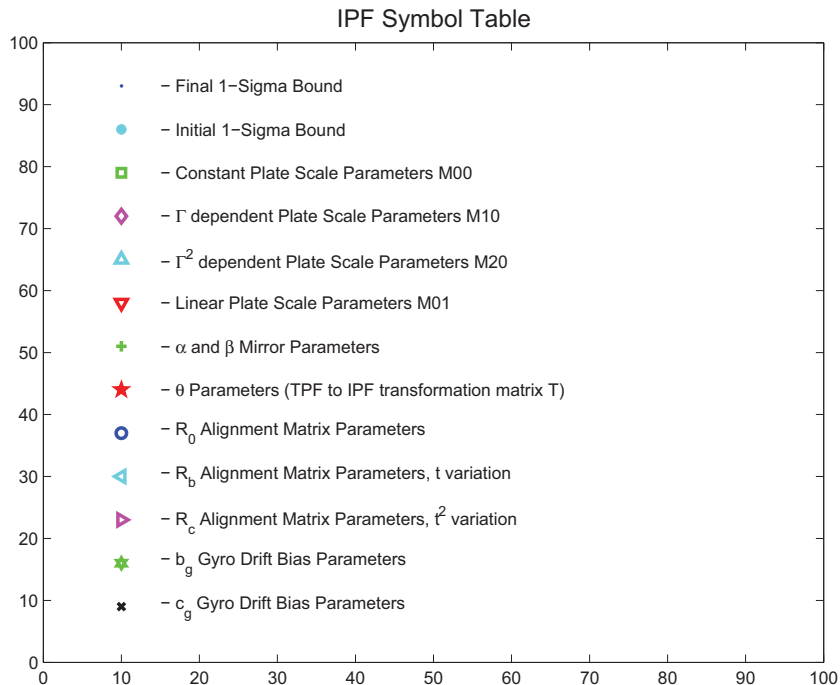


Figure 3.12: IPF parameter symbol table

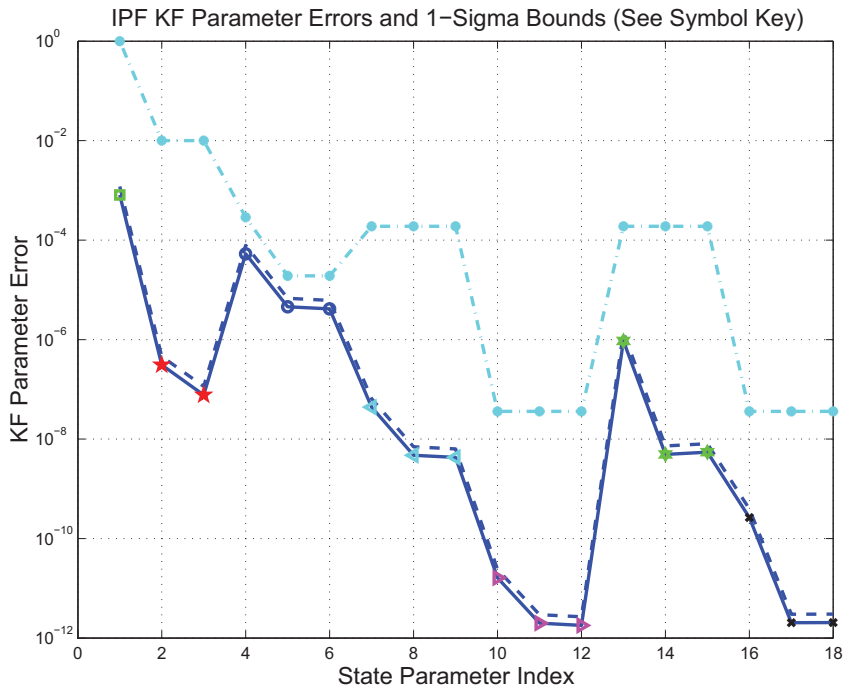


Figure 3.13: KF parameter error sigma plots

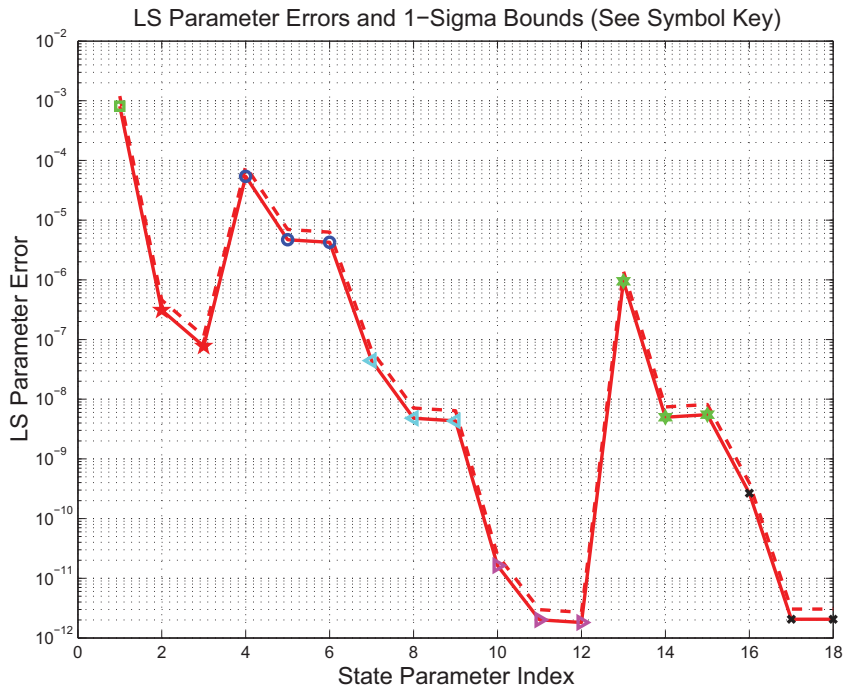


Figure 3.14: LS parameter error sigma plot

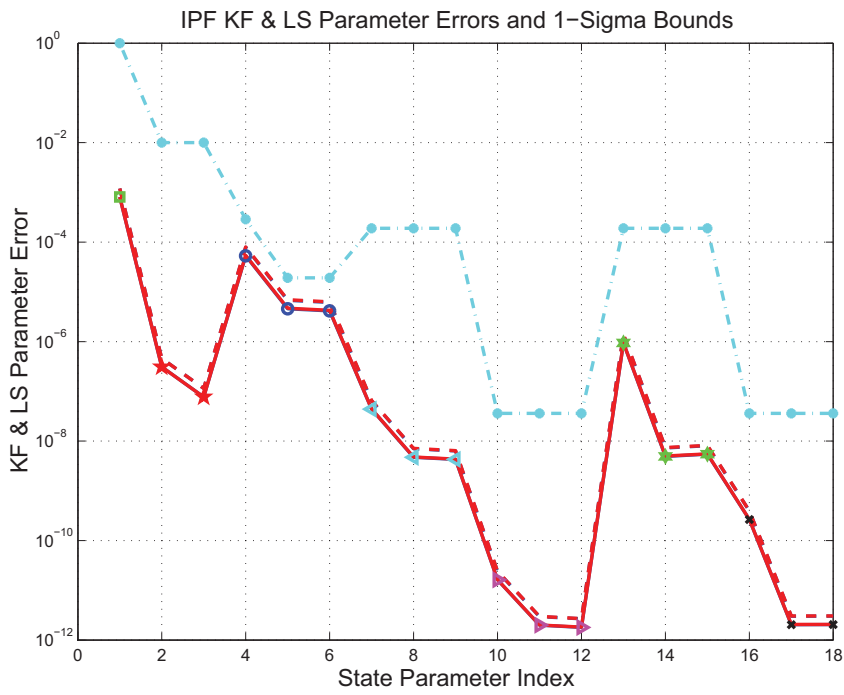


Figure 3.15: KF and LS parameter error sigma plot

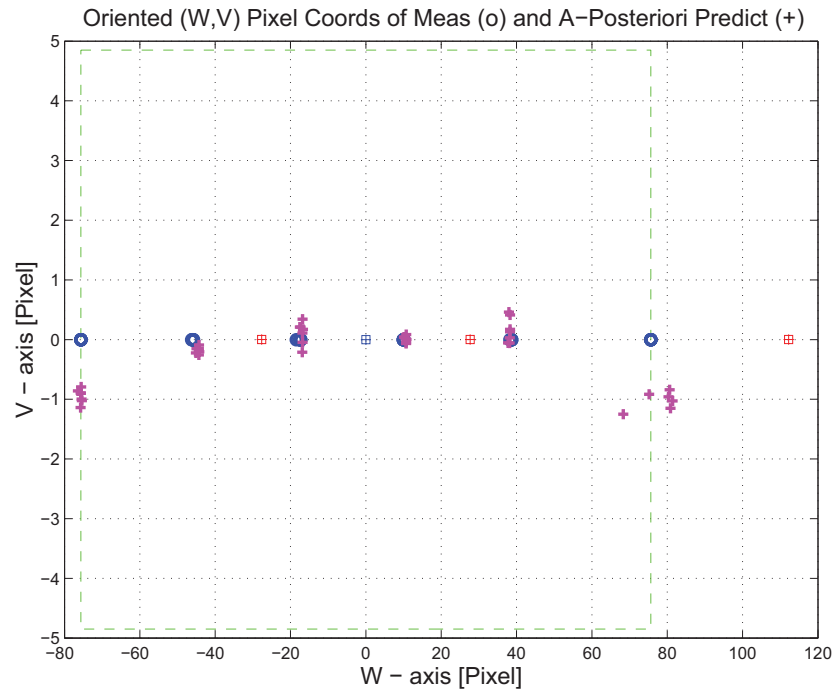


Figure 3.16: Oriented Pixel Coords of meas. and a-posteriori predicts

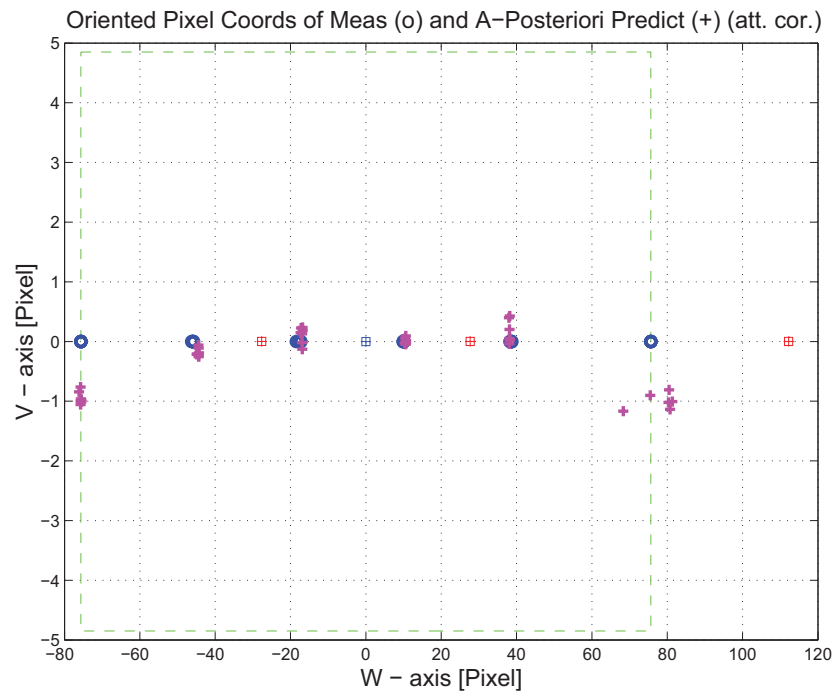


Figure 3.17: Oriented Pixel Coords of meas. and a-posteriori predicts (attitude corrected)

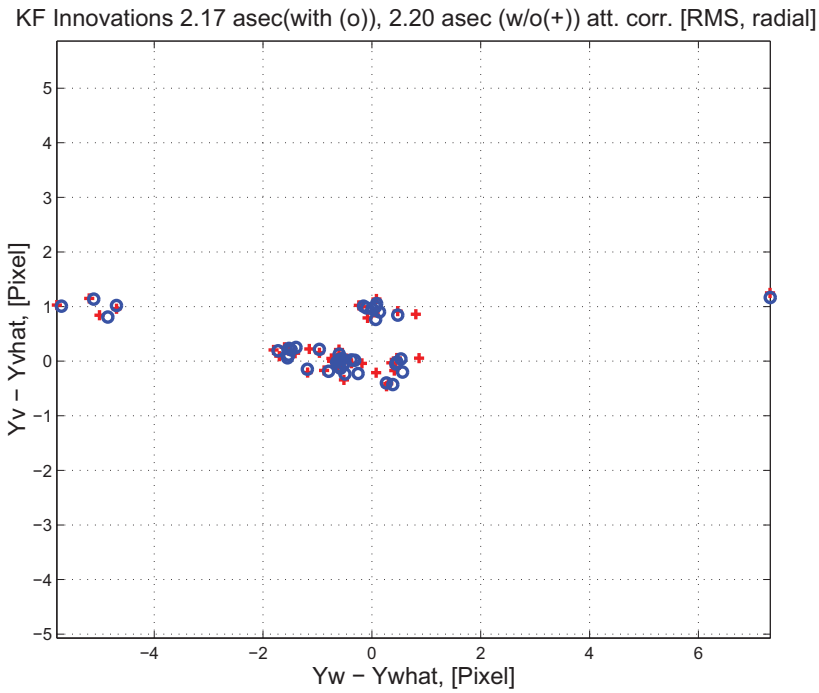


Figure 3.18: KF innovations with (o) and w/o (+) attitude corrections

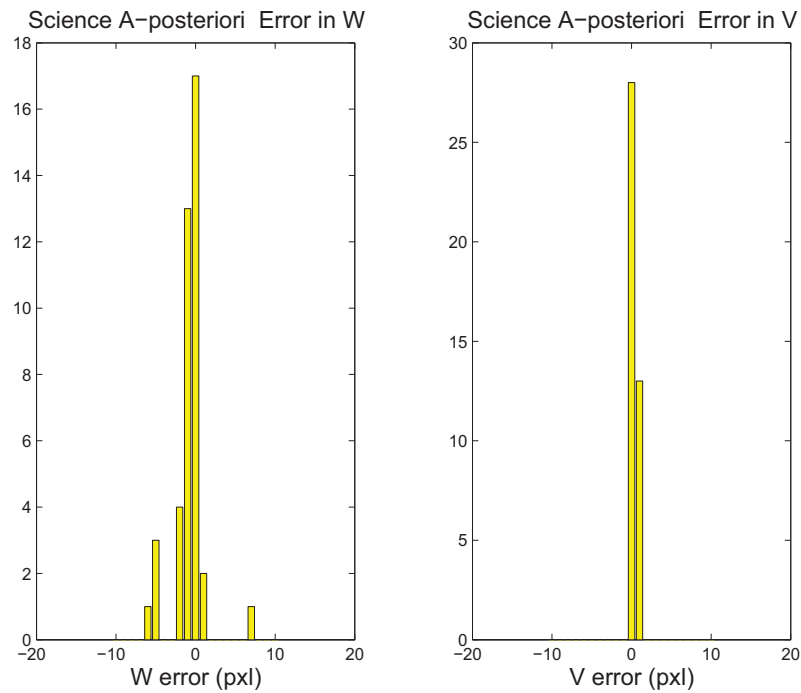


Figure 3.19: Histograms of science a-posteriori residuals (or innovations)

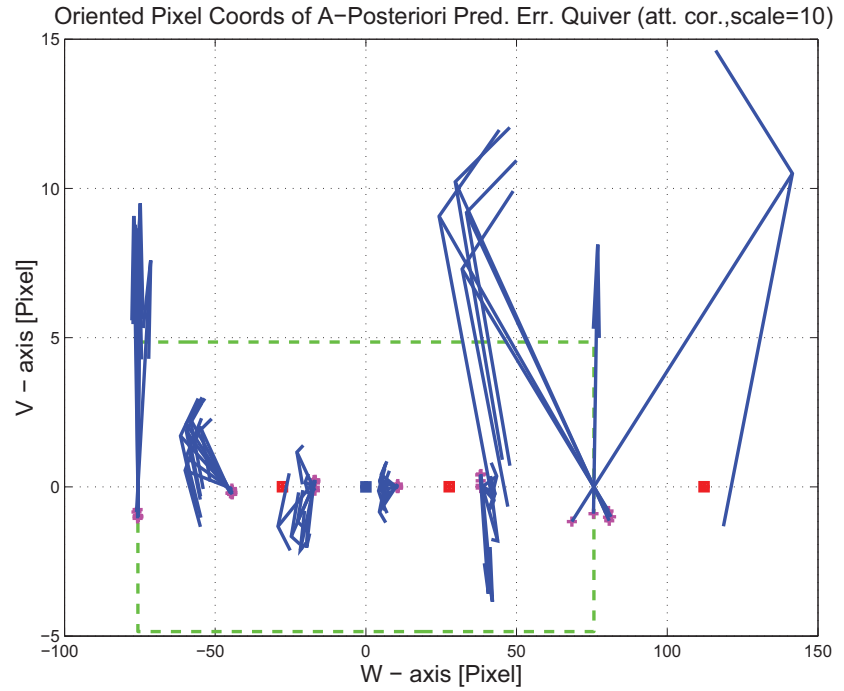


Figure 3.20: A-Posteriori Science Centroid Prediction Error Quiver (Att. Cor.)

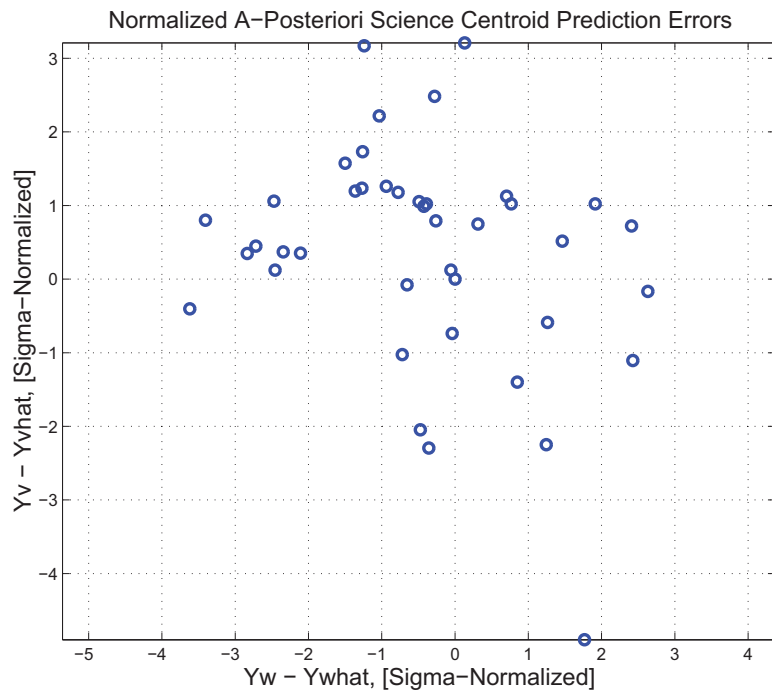


Figure 3.21: Normalized A-Posteriori Science Centroid Prediction Errors

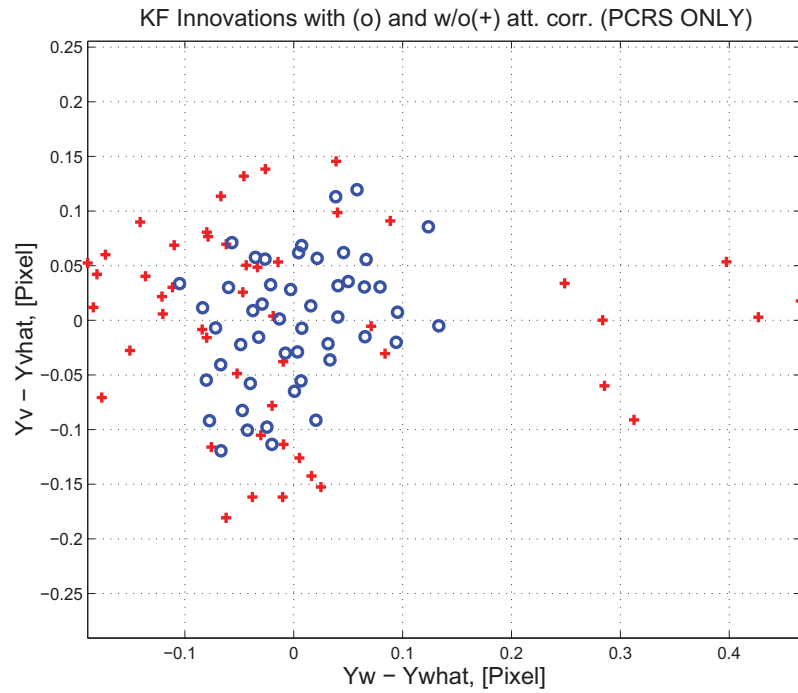


Figure 3.22: KF innovations with (o) and w/o (+) attitude corrections (PCRS)

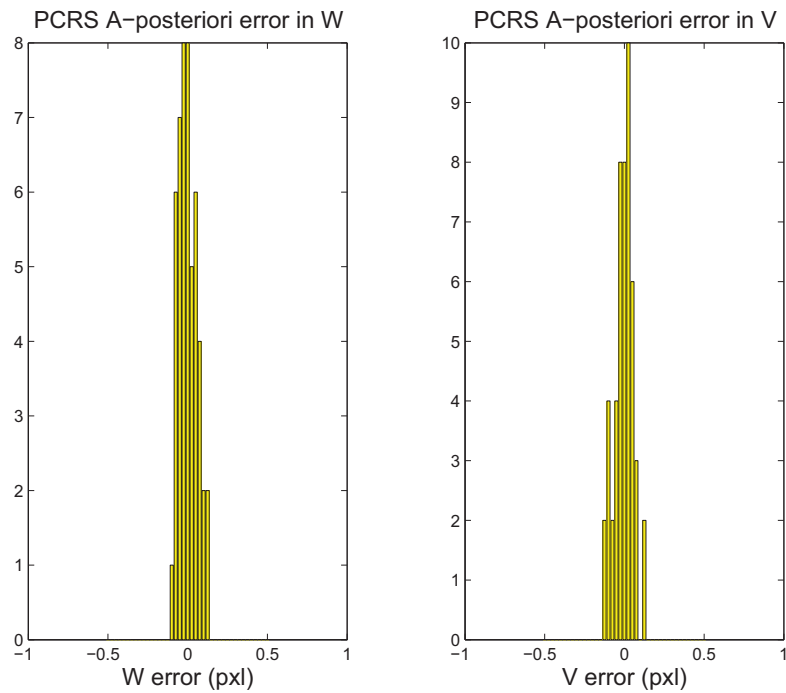


Figure 3.23: Histograms of PCRS a-posteriori residuals (or innovations)

IPF PCRS SUMMARY						
PCRS 1 (Total of 35 centroids)						
RMS	MEAN		SIGMA			
METRIC	APOST.	ATT. COR.	APOST.	ATT. COR.	STAT. CONF.	UNITS
Radial	0.0146	0.0151	0.1874	0.0827	0.0140	arcsec
W-axis	0.0022	0.0031	0.1674	0.0615	0.0104	arcsec
V-axis	0.0144	0.0147	0.0843	0.0554	0.0094	arcsec
PCRS 2 (Total of 14 centroids)						
METRIC	APOST.	ATT. COR.	APOST.	ATT. COR.	STAT. CONF.	UNITS
Radial	0.0417	0.0413	0.1538	0.0569	0.0152	arcsec
W-axis	-0.0051	-0.0042	0.1357	0.0376	0.0100	arcsec
V-axis	-0.0414	-0.0411	0.0723	0.0427	0.0114	arcsec
Combined (Total of 49 centroids)						
METRIC	APOST.	ATT. COR.	APOST.	ATT. COR.	STAT. CONF.	UNITS
Radial	0.0015	0.0016	0.1802	0.0804	0.0115	arcsec
W-axis	0.0001	0.0010	0.1590	0.0558	0.0080	arcsec
V-axis	-0.0015	-0.0012	0.0849	0.0578	0.0083	arcsec

Table 3.3: PCRS measurement prediction error summary

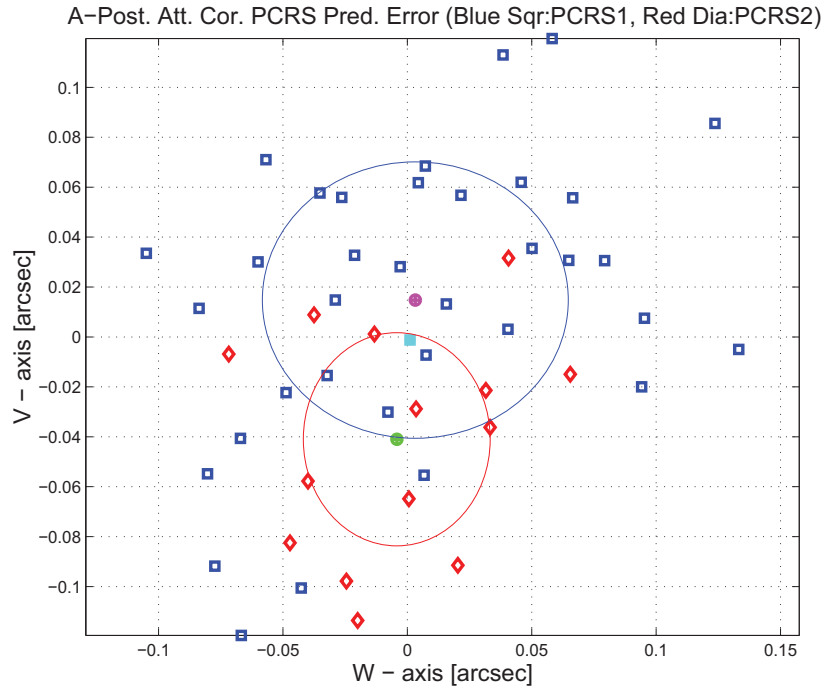


Figure 3.24: A-posteriori PCRS Prediction Summary

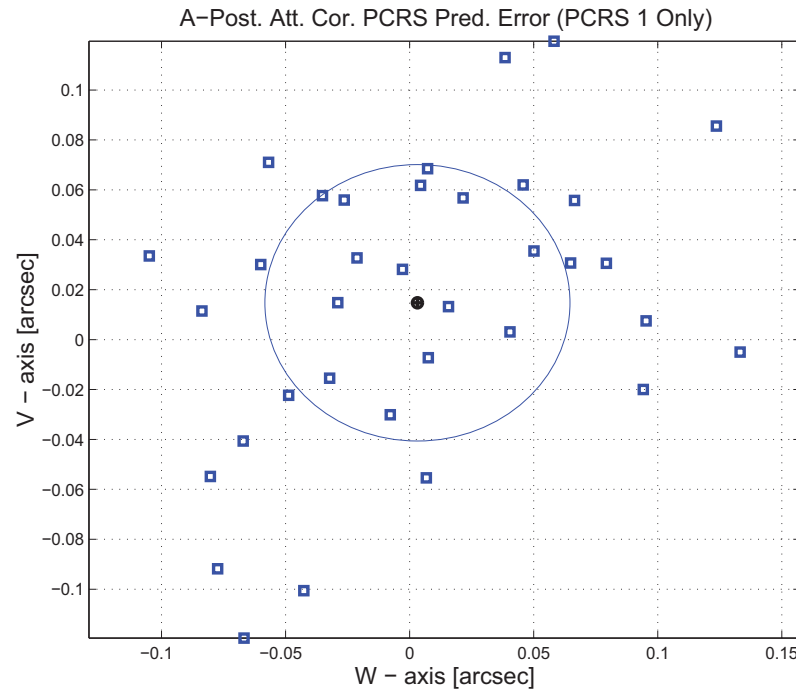


Figure 3.25: A-posteriori PCRS Prediction (PCRS 1 Only)

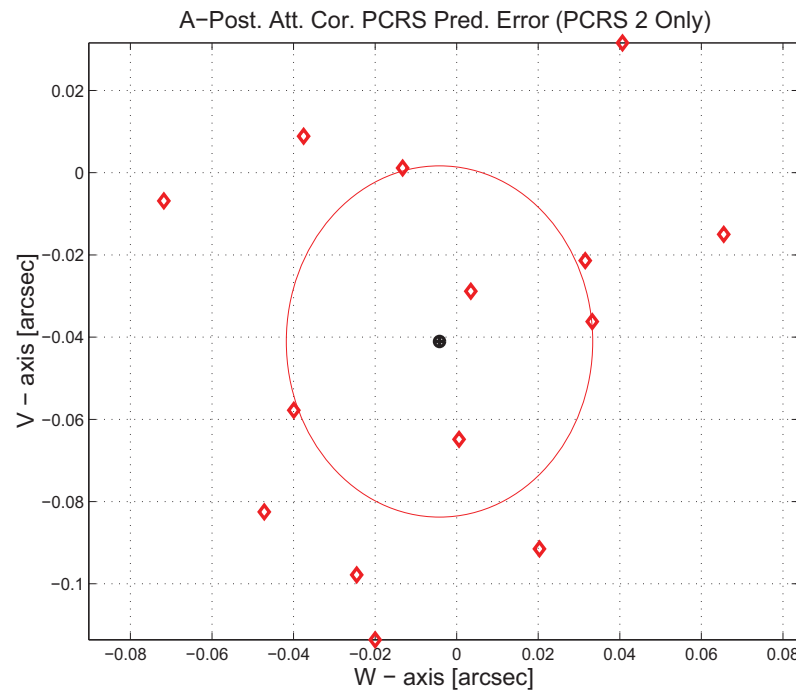


Figure 3.26: A-posteriori PCRS Prediction (PCRS 2 Only)

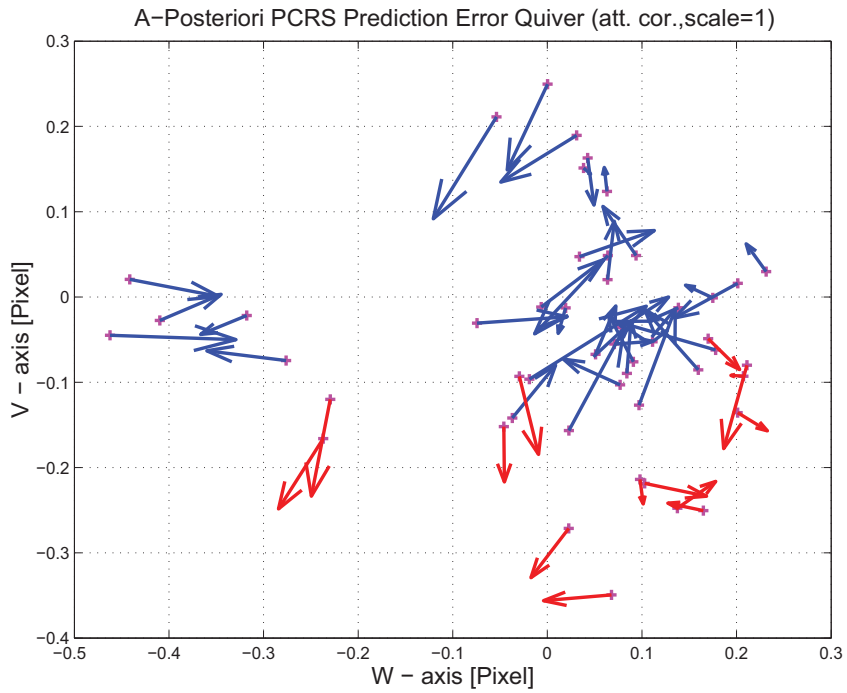


Figure 3.27: A-Posteriori PCRS Prediction Errors Quiver (Att. Cor.)

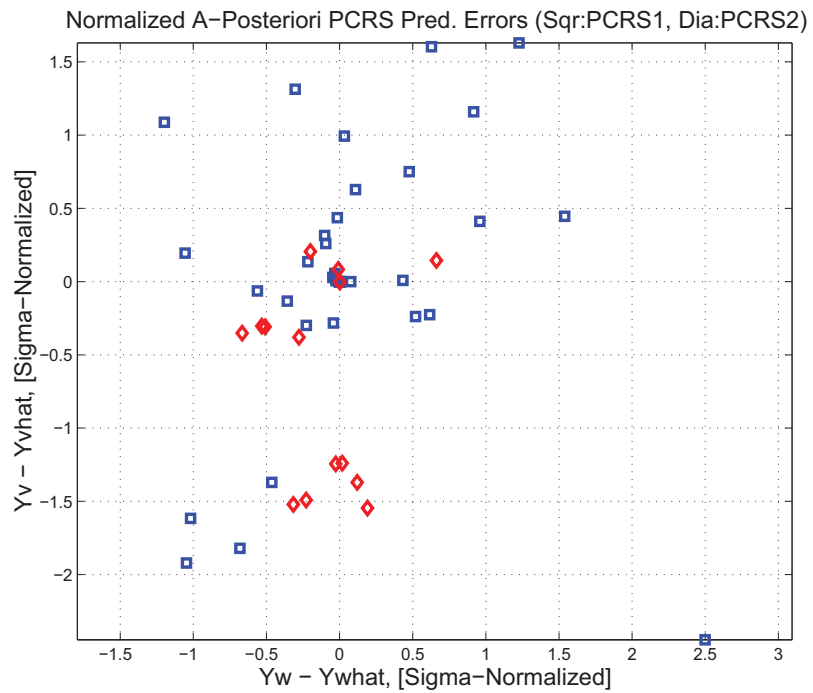


Figure 3.28: Normalized A-Posteriori PCRS Prediction Errors

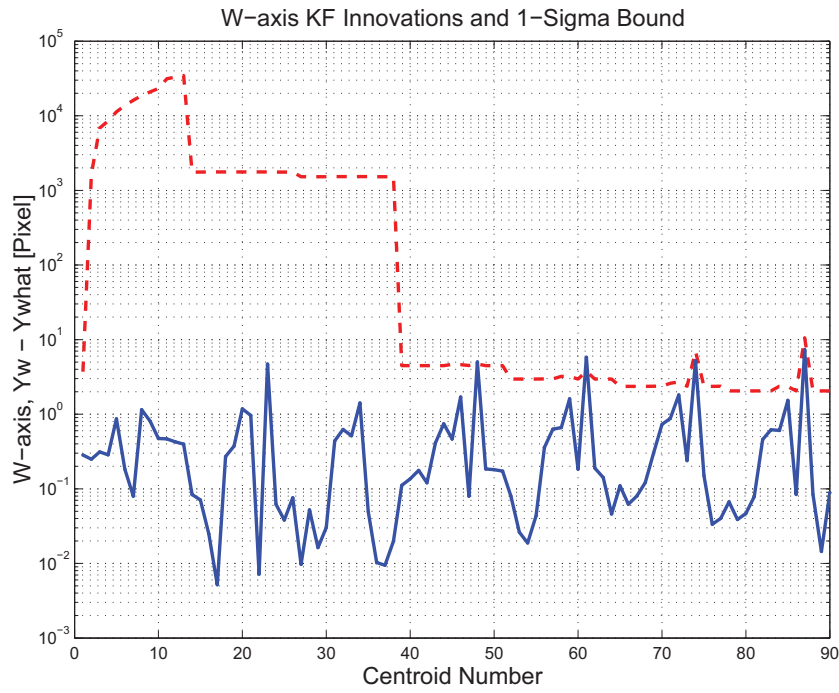


Figure 3.29: W-axis KF innovations and 1-sigma bound

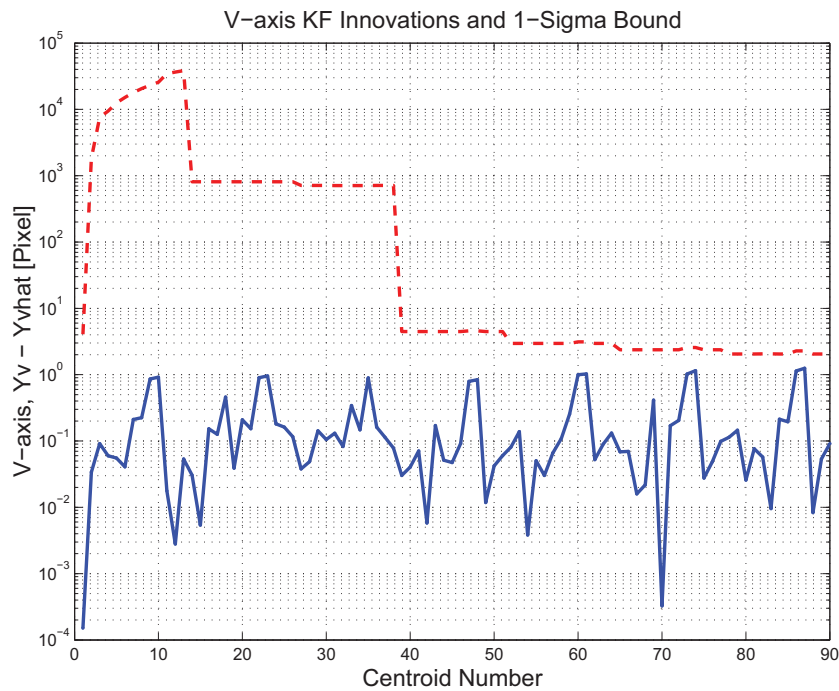


Figure 3.30: V-axis KF innovations and 1-sigma bound

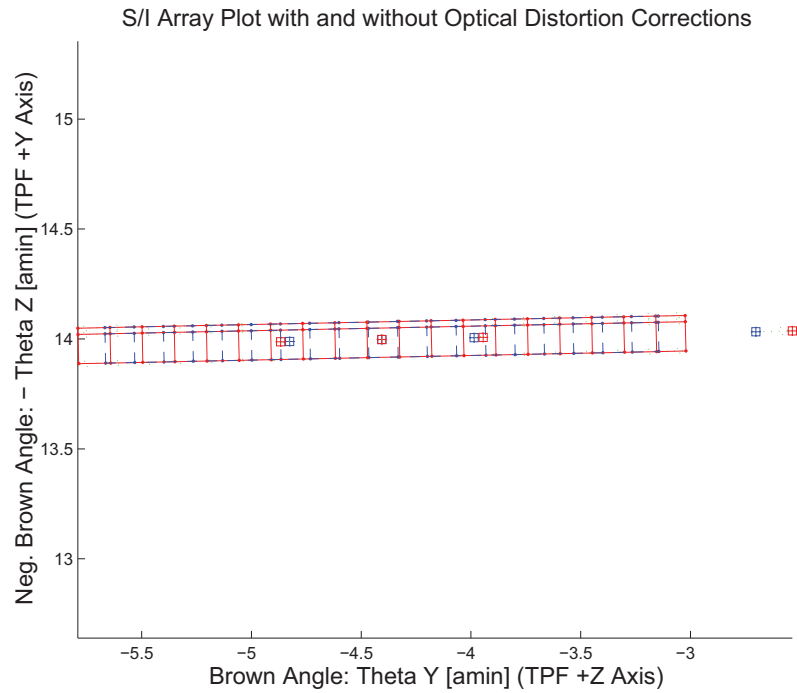


Figure 3.31: Array plot with (solid) and w/o (dashed) optical distortion corrections

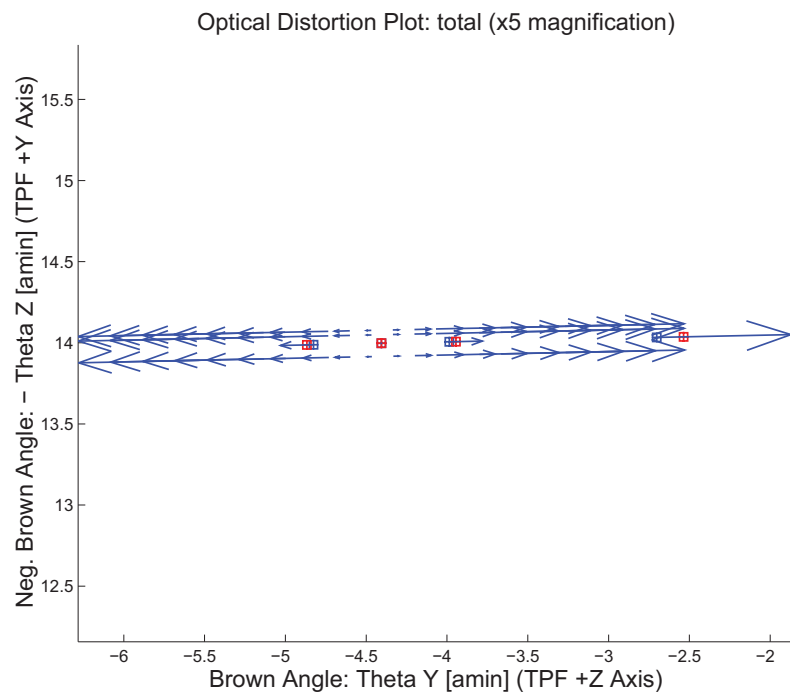


Figure 3.32: Optical Distortion Plot: total (x5 magnification)

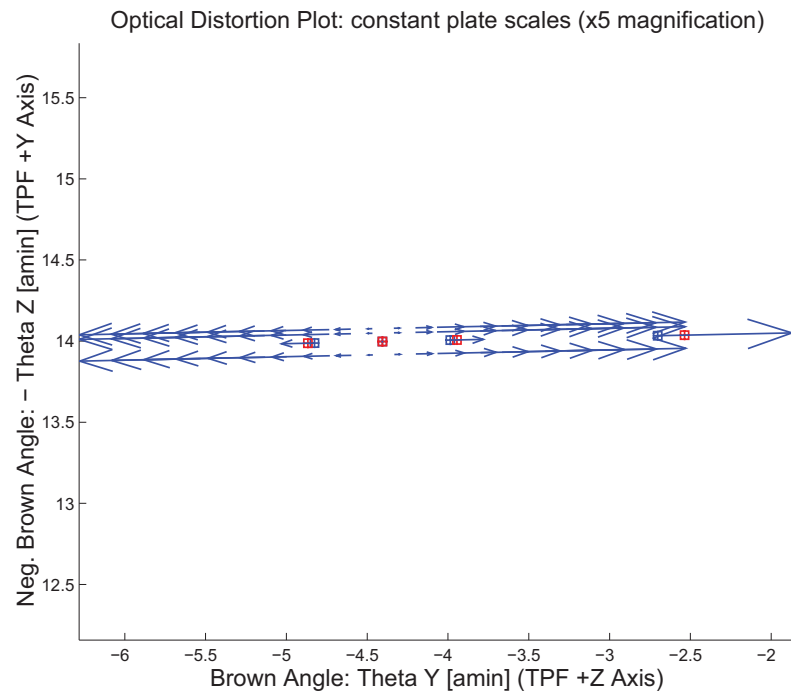


Figure 3.33: Optical Distortion Plot: constant plate scales (x5 magnification)

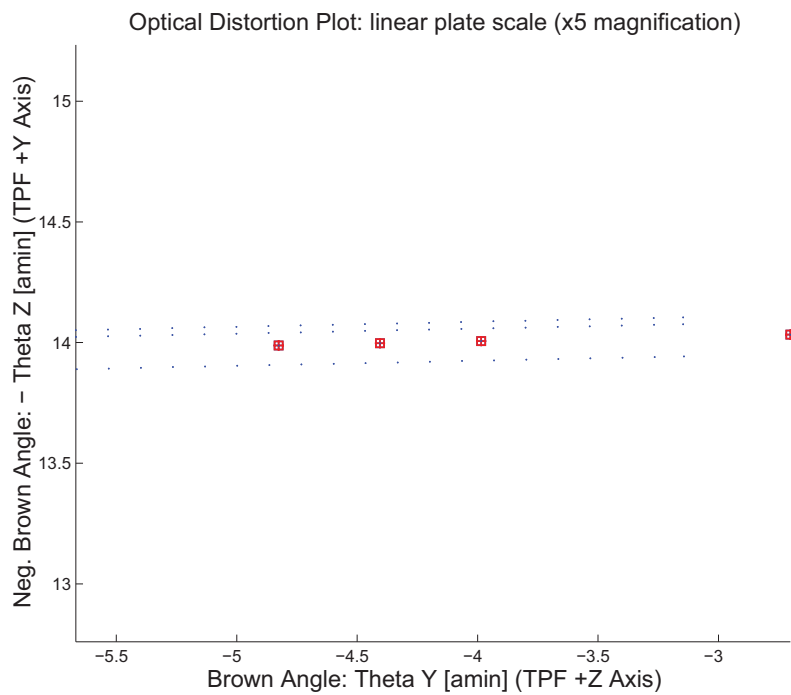


Figure 3.34: Optical Distortion Plot: linear plate scale (x5 magnification)

Opt. Dist. Plot: Γ depdt; $\Gamma = 0.00000e+000$ in blue and $\Gamma = 0.00000e+000$ in red (x5 magn)

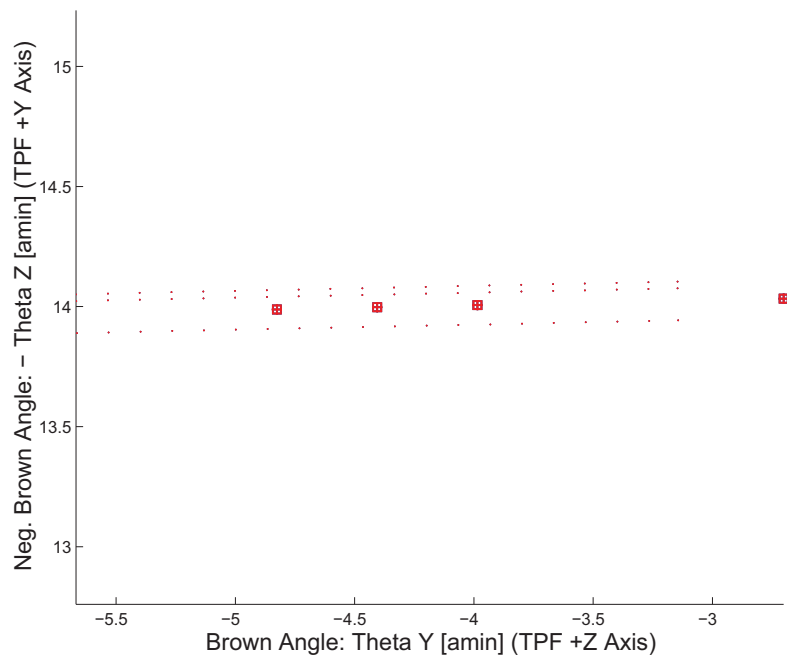


Figure 3.35: Optical Distortion Plot: gamma terms (x5 magnification)

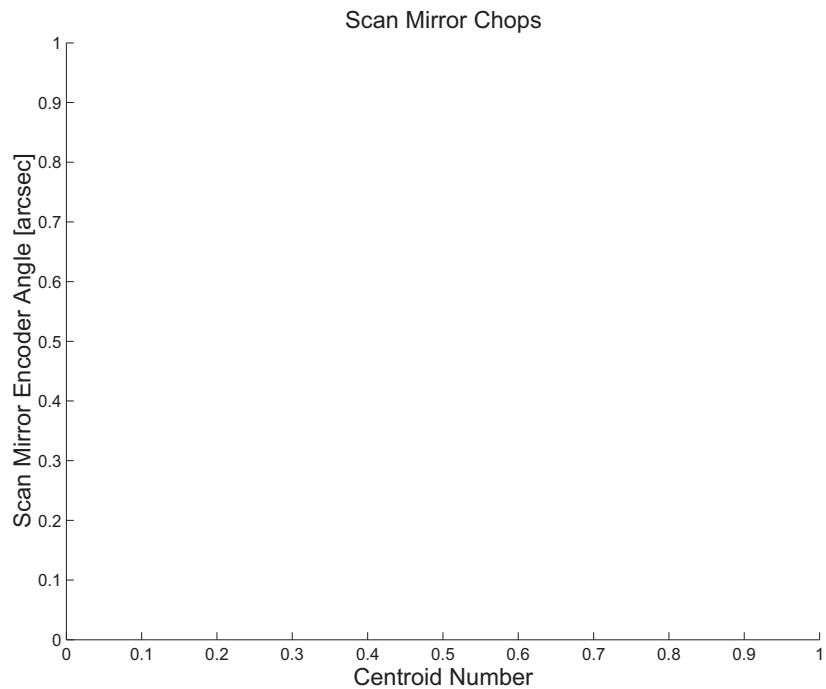


Figure 3.36: Scan Mirror Chops

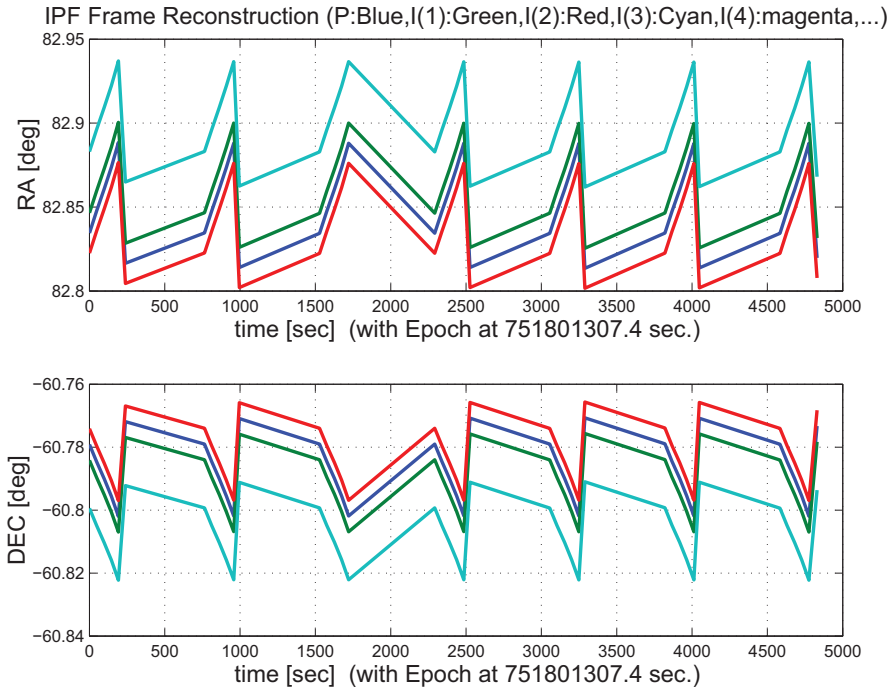


Figure 3.37: IPF Frame Reconstruction

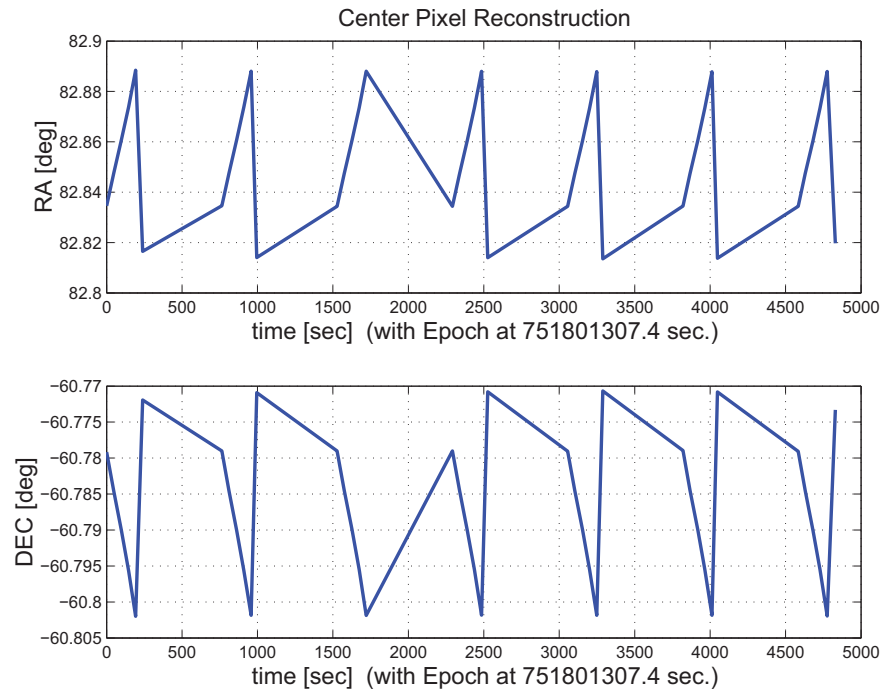


Figure 3.38: Center Pixel Reconstruction

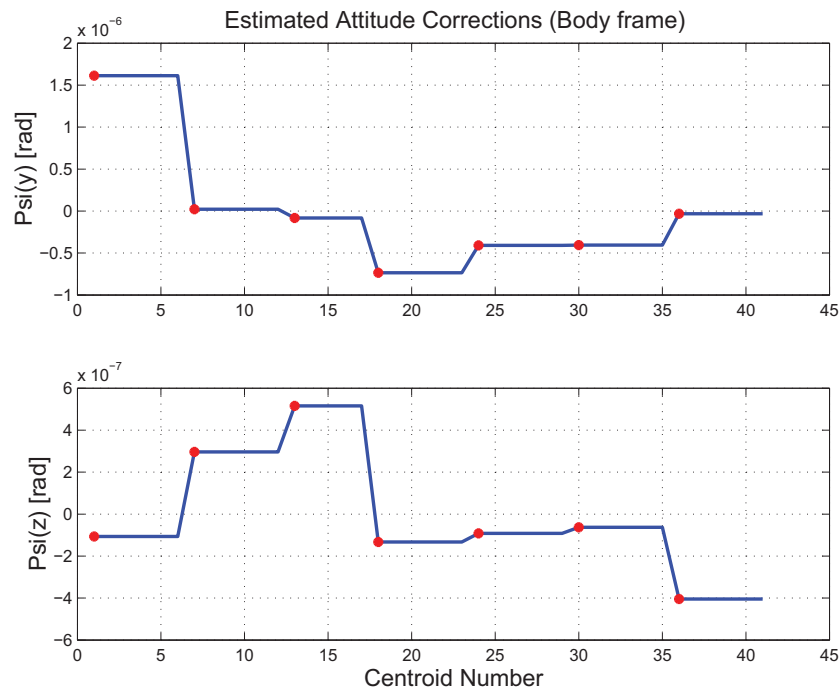


Figure 3.39: Estimated attitude corrections (Body frame)

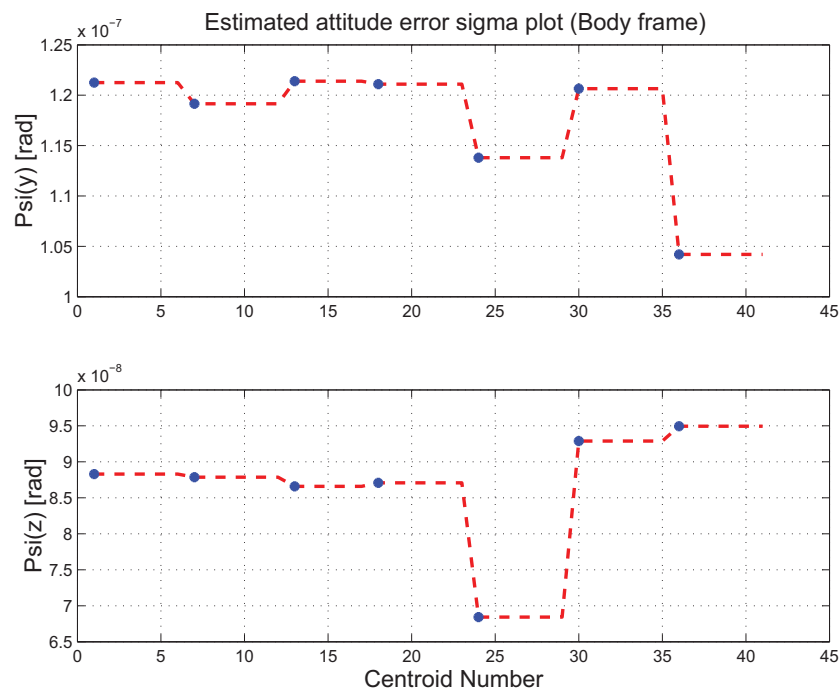


Figure 3.40: Estimated attitude error sigma plot (Body frame)

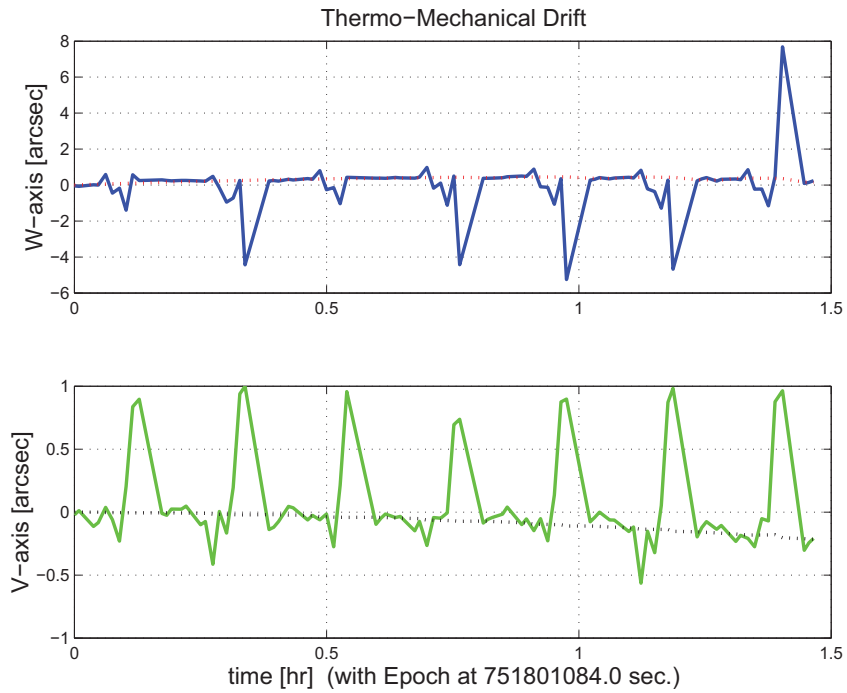


Figure 3.41: Thermo-mechanical boresight drift (equiv. angle in (W,V) coords)

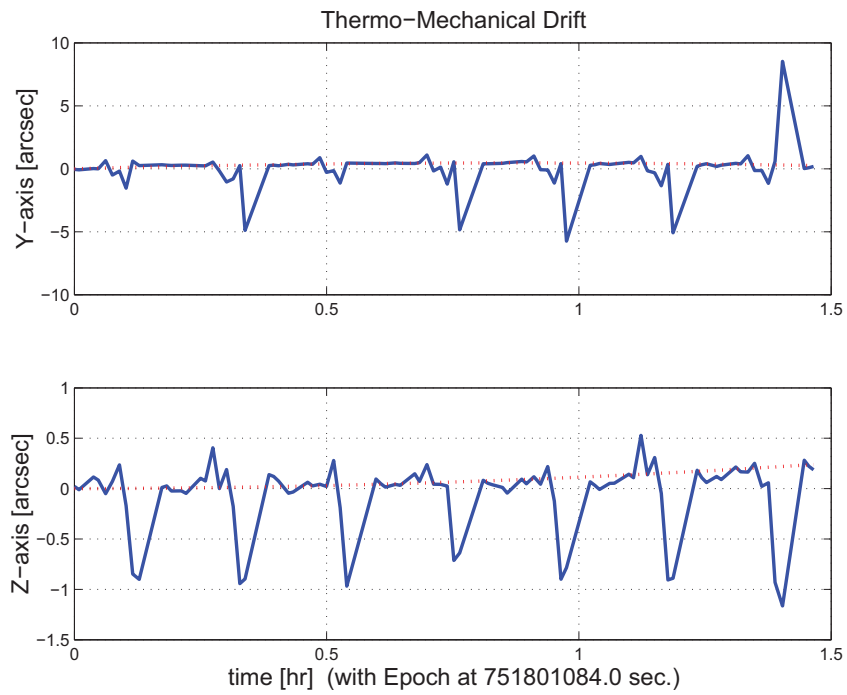


Figure 3.42: Thermo-mechanical boresight drift (equiv. angle in Body frame)

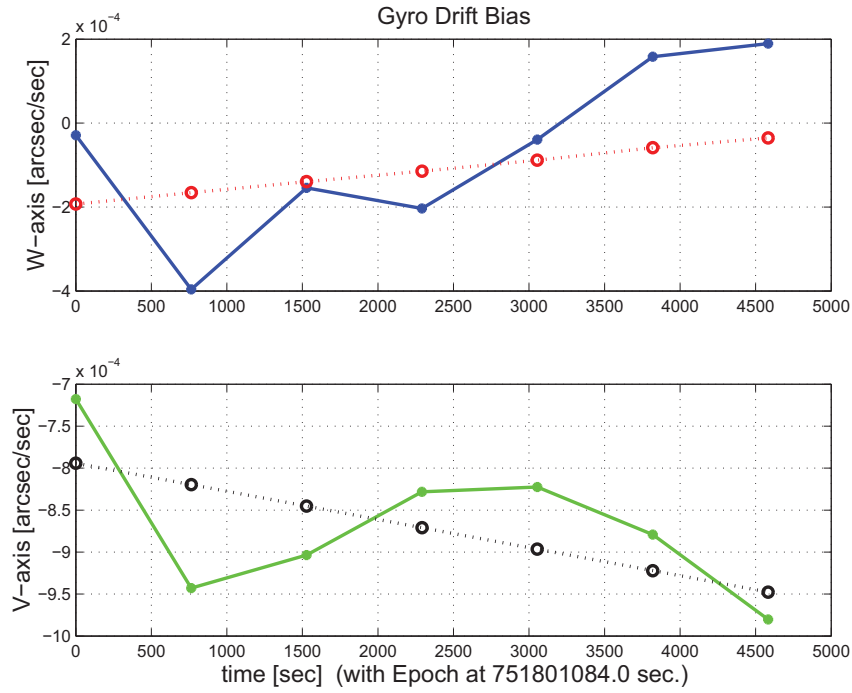


Figure 3.43: Gyro drift bias contribution (equiv. rate in (W,V) coords)

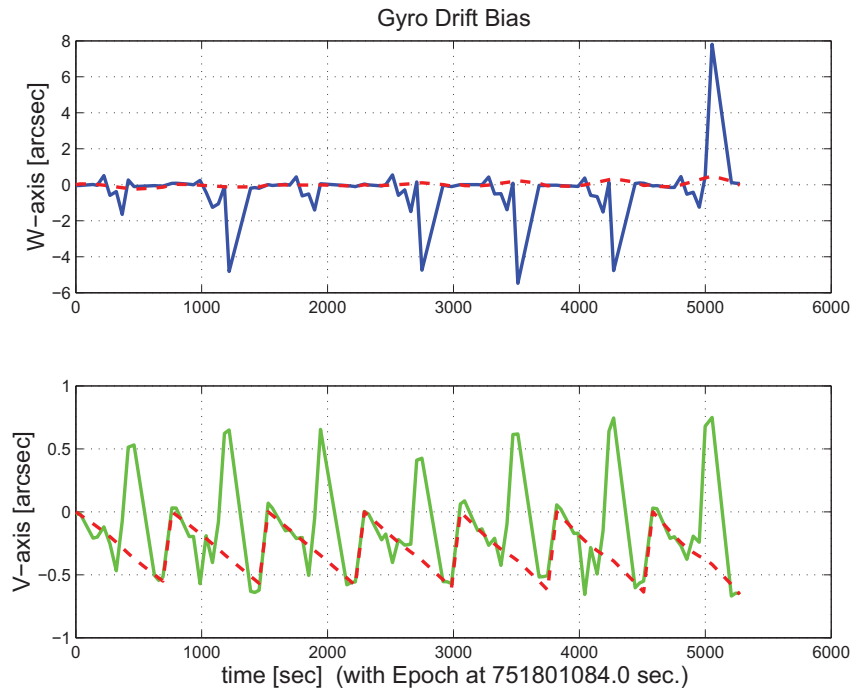


Figure 3.44: Gyro drift bias contribution (equiv. angle in (W,V) coords)

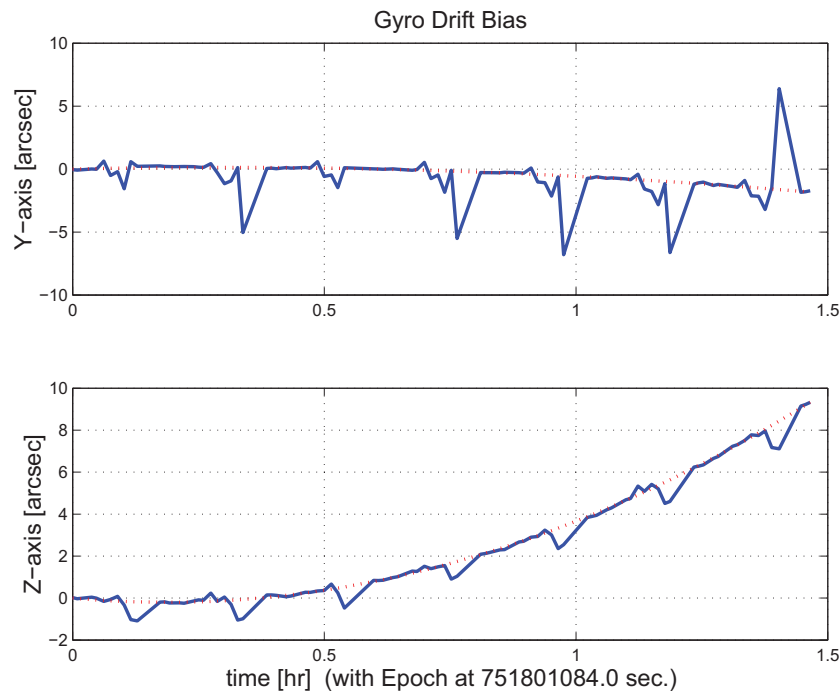


Figure 3.45: Gyro drift bias contribution (equiv. angle in Body frame)

3.2 IPF OUTPUT DATA (IF MINI FILE)

OUTPUT FILE NAME: IFmini502040.dat DATE: 06-Nov-2003 TIME: 14:33
 INSTRUMENT NAME: IRS_LongLo_1st_Ord_Center_Pos NF: 40
 IPF FILTER VERSION: IPF.V3.0.0B SW RELEASE DATE: November 3, 2003
 FRAME TABLE USED: BodyFrames_FTU_12b

----- IPF BROWN ANGLE SUMMARY -----									
Frame Number	WAS			IS					
	theta_Y (arcmin)	theta_Z (arcmin)	angle (deg)	theta_Y (arcmin)	theta_Z (arcmin)	angle (deg)			
040	-4.467462	-13.987365	-1.199998	-4.405739	-13.997049	-1.199998			
038	-4.047276	-13.996167	-1.199998	-3.944596	-14.006709	-1.199998			
039	-4.887647	-13.978564	-1.199998	-4.866882	-13.987390	-1.199998			
041	-2.763469	-14.023059	-1.199998	-2.535651	-14.036222	-1.199998			
<hr/>									
OFFSET 0	NF 40	Delta_CW +0.000	Delta_CV +0.000	pixels					
OFFSET FRAME NAME: IRS_LongLo_1st_Ord_Center_Pos									
Brown Angle	theta_Y(arcmin)	theta_Z(arcmin)	angle(deg)						
WAS(FTB)	-4.467462	-13.987365	-1.199998						
IS (EST)	-4.405739	-13.997049	-1.199998						
dT_EST	+0.061722	-0.009684	+0.000000						
T_sSIGMA	+0.001574	+0.000393	+999.999999						
dT_EST/T_sSIGMA	+39.219614	-24.646548	+999.999999						
<hr/>									
OFFSET 1	NF 38	Delta_CW +25.217	Delta_CV +0.000	pixels					
OFFSET FRAME NAME: IRS_LongLo_1st_Ord_1st_Pos									
Brown Angle	theta_Y(arcmin)	theta_Z(arcmin)	angle(deg)						
WAS(FTB)	-4.047276	-13.996167	-1.199998						
IS (EST)	-3.944596	-14.006709	-1.199998						
dT_EST	+0.102680	-0.010542	+0.000000						
T_sSIGMA	+0.001642	+0.000393	+999.999999						
dT_EST/T_sSIGMA	+62.527218	-26.830042	+999.999999						
<hr/>									
OFFSET 2	NF 39	Delta_CW -25.217	Delta_CV +0.000	pixels					
OFFSET FRAME NAME: IRS_LongLo_1st_Ord_2nd_Pos									
Brown Angle	theta_Y(arcmin)	theta_Z(arcmin)	angle(deg)						
WAS(FTB)	-4.887647	-13.978564	-1.199998						
IS (EST)	-4.866882	-13.987390	-1.199998						
dT_EST	+0.020765	-0.008826	+0.000000						
T_sSIGMA	+0.001662	+0.000393	+999.999999						
dT_EST/T_sSIGMA	+12.492529	-22.463054	+999.999999						
<hr/>									
OFFSET 3	NF 41	Delta_CW +102.262	Delta_CV +0.000	pixels					
OFFSET FRAME NAME: IRS_LongLo_Module_Center									
Brown Angle	theta_Y(arcmin)	theta_Z(arcmin)	angle(deg)						
WAS(FTB)	-2.763469	-14.023059	-1.199998						
IS (EST)	-2.535651	-14.036222	-1.199998						
dT_EST	+0.227817	-0.013163	+0.000000						
T_sSIGMA	+0.002550	+0.000393	+999.999999						
dT_EST/T_sSIGMA	+89.326185	-33.501340	+999.999999						
<hr/>									
<hr/>									
VARNAME	MEAN	SIGMA	SCALED_SIGMA						
a00	+9.7474034472469509E-002	+8.0784400848534540E-004	+1.1970084489630398E-003						
del_theta2	-1.1532157700498247E-016	+3.0895569251553440E-007	+4.5778958612283921E-007						
del_theta3	-4.0356129059723511E-016	+7.7135665794024036E-008	+1.1429439681672288E-007						
del_arx	+1.4206024594523581E-013	+5.3071297719138710E-005	+7.8637448690559099E-005						
del_ary	+5.1730086151965276E-016	+4.5599254091426305E-006	+6.7565881334180742E-006						

del_arz	+3.4707010901111426E-016	+4.1405711615230493E-006	+6.1352174575986925E-006
brx	+1.4243951719815493E-008	+4.3720468087199449E-008	+6.4782023686873755E-008
bry	+1.4067980564249072E-009	+4.7104882311002231E-009	+6.9796819090603125E-009
brz	+1.7091632810602932E-011	+4.2707835246707845E-009	+6.3281573039181810E-009
crx	-1.5881732549309357E-011	+1.6204409601482601E-011	+2.4010594866947437E-011
cry	-4.4646822907070019E-013	+1.9877773393742498E-012	+2.9453536139352475E-012
crz	+7.7171027221494862E-014	+1.7999369125475707E-012	+2.6670244122494776E-012
bgx	+1.8992686485623498E-006	+9.4034631805626587E-007	+1.3933413825462010E-006
bgy	+1.2056324062590971E-009	+4.9199884482857786E-009	+7.2901051720776241E-009
bgz	-2.9288149727522751E-009	+5.4516676041359383E-009	+8.0779112236334545E-009
cgx	-1.1874209429850360E-009	+2.6535120156242397E-010	+3.9317940948556029E-010
cgy	-1.0952748978461174E-012	+2.0313916791882724E-012	+3.0099783839464954E-012
cgz	+4.3635046236627216E-012	+2.0450179328104834E-012	+3.0301688421812246E-012

LSQF RESIDUAL SIGMA SCALE = +1.4817321616426322E+000

qT	qT(1)	qT(2)	qT(3)	qT(4)
FrmTbl:	-1.0473063154003400E-002	+6.2842539206602304E-004	+2.0410706019703198E-003	+9.9994287539863802E-001
Estim:	-1.0473044006579118E-002	+6.1943399183599296E-004	+2.0423850067963476E-003	+9.9994287852569363E-001
DelTheta	deltheta(1)	deltheta(2)	deltheta(3)	
	-1.9989886121699360E-011	-1.8009386982222942E-005	+2.4403357781002783E-006	[rad]
EulAngT	theta(1)	theta(2)	theta(3)	[rad]
Mean	-2.0943909626138728E-002	+1.2815775446346211E-003	+4.0715765598257712E-003	
SigmaT	+9.999900000000000E+004	+3.0895569251553440E-007	+7.7135665794024036E-008	

qR	qR(1)	qR(2)	qR(3)	qR(4)
ASFILE:	+7.0871395291760564E-004	+1.2698702048510313E-003	-1.6122095985338092E-004	+9.9999892711639404E-001
Estim:	+7.0919417171377234E-004	+1.2684389992203750E-003	-1.6098095967680698E-004	+9.9999893109506000E-001
DelThetaR	delthetaR(1)	delthetaR(2)	delthetaR(3)	
	+9.6028217582550430E-007	-2.8619235085193021E-006	+4.8324800999829140E-007	[rad]
EulAngR	angR(1)	angR(2)	angR(3)	[rad]
Mean	+1.4179834771459478E-003	+2.5371063421287710E-003	-3.2016347201672366E-004	
SigmaR	+5.3071297719138710E-005	+4.5599254091426305E-006	+4.1405711615230493E-006	

Initial Gyro Bias	Bg0(1)	Bg0(2)	Bg0(3)
	-4.2146271539422736E-007	-2.0000304346012856E-007	+3.5992636071568995E-007
Gyro Bias Correction	Bg(1)	Bg(2)	Bg(3)
	+1.8992686485623498E-006	+1.2056324062590971E-009	-2.9288149727522751E-009
Total Gyro Bias	BgT(1)	BgT(2)	BgT(3)
	+1.4778059331681224E-006	-1.9879741105386945E-007	+3.5699754574293770E-007

Initial Gyro Bias Rate	Cg0(1)	Cg0(2)	Cg0(3)
	+0.000000000000000E+000	+0.000000000000000E+000	+0.000000000000000E+000
Gyro Bias Rate Correction	Cg(1)	Cg(2)	Cg(3)
	-1.1874209429850360E-009	-1.0952748978461174E-012	+4.3635046236627216E-012
Total Gyro Bias Rate	CgT(1)	CgT(2)	CgT(3)
	-1.1874209429850360E-009	-1.0952748978461174E-012	+4.3635046236627216E-012

OFFSET	NF	Delta_CW	Delta_CV
1	38	+25.217	+0.000 pixels
OFFSET FRAME NAME:	IRS_LongLo_1st_Ord_1st_Pos		
qT	qT(1)	qT(2)	qT(3)
WAS(FTB)	-1.0472939955331610E-002	+5.6730195488904238E-004	+2.0417107851983919E-003
IS (EST)	-1.0472908675373649E-002	+5.5235260646451260E-004	+2.0430875895257007E-003

DelTheta	deltheta(1)	deltheta(2)	deltheta(3)
Units	rad	rad	rad
	+3.6476860206561045E-011	-2.9925962775769315E-005	+2.4403356587288360E-006
EulAngT	theta(1)	theta(2)	theta(3)
Mean	-2.0943909626138728E-002	+1.1474365452086646E-003	+4.0743864094922345E-003
sSigmaT	+1.5334927761000096E-011	+4.7768466308460943E-007	+1.1429439578398670E-007
SigmaT	+1.0349325038608841E-011	+3.2238259751010156E-007	+7.7135665097045054E-008

OFFSET	NF	Delta_CW	Delta_CV
--------	----	----------	----------

2 39 -25.217 +0.000 pixels
 OFFSET FRAME NAME: IRS_LongLo_1st_Ord_2nd_Pos
 qT qT(1) qT(2) qT(3) qT(4)
 WAS(FTB) -1.0473186157083104E-002 +6.8954882721212617E-004 +2.0404304108140908E-003 +9.9994283513502535E-001
 IS (EST) -1.0473179102203828E-002 +6.8651537480213167E-004 +2.0416824145170942E-003 +9.9994283474059242E-001

DelTheta deltheta(1) deltheta(2) deltheta(3)
 Units rad rad rad
 -1.247687791444790E-011 -6.0928111879133950E-006 +2.4403357802281610E-006
 EulAngT theta(1) theta(2) theta(3) [rad]
 Mean -2.0943909626138728E-002 +1.4157185440504595E-003 +4.0687667091932151E-003
 sSigmaT +1.5334927761000077E-011 +4.8351847370619794E-007 +1.1429439574899516E-007
 SigmaT +1.0349325038608828E-011 +3.2631975347702151E-007 +7.7135665073429762E-008

OFFSET NF Delta_CW Delta_CV
 3 41 +102.262 +0.000 pixels
 OFFSET FRAME NAME: IRS_LongLo_Module_Center
 qT qT(1) qT(2) qT(3) qT(4)
 WAS(FTB) -1.0472562330580306E-002 +3.8054946178167815E-004 +2.0436667095949010E-003 +9.9994300039888240E-001
 IS (EST) -1.0472493733959878E-002 +3.4739659760258551E-004 +2.0452341552030105E-003 +9.9994300997999208E-001

DelTheta deltheta(1) deltheta(2) deltheta(3)
 Units rad rad rad
 +6.0536768083363392E-010 -6.6335066984160292E-005 +2.4403346844525034E-006
 EulAngT theta(1) theta(2) theta(3) [rad]
 Mean -2.0943909626138731E-002 +7.3759106955667455E-004 +4.0829714320923180E-003
 sSigmaT +6.2188241824701998E-011 +7.4188114102792216E-007 +1.1429437968345859E-007
 SigmaT +4.1969961531887643E-011 +5.0068504972280604E-007 +7.7135654231027203E-008

q(1) q(2) q(3) q(4)
 PCRS1A: +5.3371888965461637E-007 +3.7444233778550031E-004 -1.4253684912431913E-003 +9.9999891405806784E-001
 PCRS2A: -5.2779261998836216E-007 +3.8462959425181312E-004 +1.3722087221825403E-003 +9.9999898455099423E-001

***** CS-FILE PARAMETERS: ***** AS-FILE PARAMETERS: *****

Row (01) PIX2RADX: +4.8481368110953598E-006 Row (1) TASTART: +7.5180000019071960E+008
 Row (02) PIX2RADY: +4.8481368110953598E-006 Row (2) TASTOP: +7.5180700009071958E+008
 Row (03) CXO: +0.0000000000000000E+000 Row (3) S/C TIME: +7.5177384909075928E+008
 Row (04) CYO: +0.0000000000000000E+000 Row (4) QR1: +7.0871395291760564E-004
 Row (05) BETA0: +9.9999000000000000E+004 Row (5) QR2: +1.2698702048510313E-003
 Row (06) GAMMA_E0: +9.9999000000000000E+004 Row (6) QR3: -1.6122095985338092E-004
 Row (07) D11: +1.0000000000000000E+000 Row (7) QR4: +9.9999892711639404E-001
 Row (08) D12: +0.0000000000000000E+000
 Row (09) D21: +0.0000000000000000E+000
 Row (10) D22: +1.0000000000000000E+000
 Row (11) DG: +9.9999000000000000E+004

INITIAL STA-TO-PCRS ALIGNMENT (R) KNOWLEDGE (1-SIGMA)

SIGMA(X)	SIGMA(Y)	SIGMA(Z)
5.93009073E+000	3.93119736E-001	3.93652091E-001 [arcsec]

PIX2RADX = 4.848136811095E-006 [rad/pixel]
 XPIXSIZE = 1.0000 [arcsec]
 PIX2RADY = 4.848136811095E-006 [rad/pixel]
 YPIXSIZE = 1.0000 [arcsec]
 CXO = 0.0 [pixel] = 0.00 [arcsec]
 CYO = 0.0 [pixel] = 0.00 [arcsec]

NOMINAL BETA0 = 9.999900000000E+004 [rad/encoder unit]
 ENCODER UNIT SIZE = 99999.00 [arcsec]
 GAMMA_E0 = 99999.00 [encoder unit] = 99999.00 [arcsec]

FLIP MATRIX D = | +1 | +0 |
 | --- | --- | and DG = +99999
 | +0 | +1 |

3.3 IPF EXECUTION LOG

```
*****
IPF EXECUTION-LOG FILE NAME: LG502040.dat
INSTRUMENT TYPE: IRS_LongLo_1st_Ord_Center_Pos
IPF FILTER EXECUTION DATE: 06-Nov-2003 TIME: 14:32
IPF FILTER VERSION USED: IPF.V3.0.0B
*****


***** SLIT FLAG ENABLED! ENTERING SLIT MODE.
*****


----- Loading & Preparing Input Files -----
AAFILE: AA501040 Loaded! AAFILE dimension = 70000 X 21
ASFILE: AS501040 Loaded!
CAFIL: CAF594040 Loaded! CAFILE dimension = 41 X 15
CBFILE: CB501040 Loaded! CBFILE dimension = 49 X 15
CCFILE: CC502040 Created! CCFILE dimension = 90 X 19
CSFILE: CS501040 Loaded!
Loading Input Files Completed!
-----


----- Selected Mask Vectors -----
index = 1 2 3 4 5 6 7 8 9 10 11 12 13 14 15 16 17 18 19 20
-----
mask1 = [ 1 0 0 0 0 0 0 0 0 0 0 0 0 0 0 0 0 0 0 0 ]
mask2 = [ 0 0 0 1 1 1 1 1 1 1 1 1 1 1 1 1 1 1 1 1 ]
-----


----- Selected Initial Gyro Bias Parameters -----
User Entered 1 : Use AFILe database - from S/C filter
IPF Linearized Using Following Nominal Gyro Bias Estimates
bg0 = [-4.2146271539422736E-007 -2.0000304346012856E-007 +3.5992636071568995E-007 ]
cg0 = [+0.000000000000000E+000 +0.000000000000000E+000 +0.000000000000000E+000 ]
-----


----- Gyro Pre-Processor Run Completed -----
AGFILE CREATED: AG502040.m ACFILE CREATED: AC502040.m
-----


Total Gyro Preprocessor Execution Time: 21 seconds

FRAME TABLE ENTRIES FOR PCRS LOADED TO TPCRS
q_PCRS4 = [ +5.3371888965461637E-007 q_PCRS5 = [ +7.3379987833742897E-007
+3.7444233778550031E-004 +5.2236196154513707E-004
-1.4253684912431913E-003 -1.4047712280184723E-003
+9.9999891405806784E-001 ]; +9.9999887687698918E-001 ];
q_PCRS8 = [ -5.2779261998836216E-007 q_PCRS9 = [ -7.1963421681856818E-007
+3.8462959425181312E-004 +5.3239763239987400E-004
+1.3722087221825403E-003 +1.3516841804518383E-003
+9.9999898455099423E-001 ]; +9.9999894475050310E-001 ];
----- Initial Conditions for State ----- Initial Square-Root Cov (diag) -----
p1(01) = a00 = +0.000000000000000E+000 Sigma_initial(01,01) = 1.000000000000000E+000
p1(02) = b00 = +0.000000000000000E+000 Sigma_initial(02,02) = 9.999900000000000E+004
p1(03) = c00 = +0.000000000000000E+000 Sigma_initial(03,03) = 9.999900000000000E+004
p1(04) = a10 = +0.000000000000000E+000 Sigma_initial(04,04) = 9.999900000000000E+004
p1(05) = b10 = +0.000000000000000E+000 Sigma_initial(05,05) = 9.999900000000000E+004
-----
```

```

p1(06) = c10 = +0.0000000000000000E+000 Sigma_initial(06,06) = 9.9999000000000000E+004
p1(07) = d10 = +0.0000000000000000E+000 Sigma_initial(07,07) = 9.9999000000000000E+004
p1(08) = a20 = +0.0000000000000000E+000 Sigma_initial(08,08) = 9.9999000000000000E+004
p1(09) = b20 = +0.0000000000000000E+000 Sigma_initial(09,09) = 9.9999000000000000E+004
p1(10) = c20 = +0.0000000000000000E+000 Sigma_initial(10,10) = 9.9999000000000000E+004
p1(11) = d20 = +0.0000000000000000E+000 Sigma_initial(11,11) = 9.9999000000000000E+004
p1(12) = a01 = +0.0000000000000000E+000 Sigma_initial(12,12) = 9.9999000000000000E+004
p1(13) = b01 = +0.0000000000000000E+000 Sigma_initial(13,13) = 9.9999000000000000E+004
p1(14) = c01 = +0.0000000000000000E+000 Sigma_initial(14,14) = 9.9999000000000000E+004
p1(15) = d01 = +0.0000000000000000E+000 Sigma_initial(15,15) = 9.9999000000000000E+004
p1(16) = e01 = +0.0000000000000000E+000 Sigma_initial(16,16) = 9.9999000000000000E+004
p1(17) = f01 = +0.0000000000000000E+000 Sigma_initial(17,17) = 9.9999000000000000E+004
-----
p2f(01) = am1 = +0.0000000000000000E+000 Sigma_initial(18,18) = 9.9999000000000000E+004
p2f(02) = am2 = +0.0000000000000000E+000 Sigma_initial(19,19) = 9.9999000000000000E+004
p2f(03) = am3 = +1.0000000000000000E+000 Sigma_initial(20,20) = 9.9999000000000000E+004
p2f(04) = beta = +1.0000000000000000E+000 Sigma_initial(21,21) = 1.0000000000000000E-002
p2f(05) = qT1 = -1.0473063154003402E-002 Sigma_initial(22,22) = 1.0000000000000000E-002
p2f(06) = qT2 = +6.2842539206602315E-004 Sigma_initial(23,23) = 2.8749891152385988E-004
p2f(07) = aT3 = +2.0410706019703202E-003 Sigma_initial(24,24) = 1.9058982649639287E-005
p2f(08) = qT4 = +9.9994287539863824E-001 Sigma_initial(25,25) = 1.9084791930919871E-005
p2f(09) = qR1 = +7.0871395291760564E-004 Sigma_initial(26,26) = 1.8959725740487208E-004
p2f(10) = qR2 = +1.2698702048510313E-003 Sigma_initial(27,27) = 1.8959725740487208E-004
p2f(11) = qR3 = -1.6122095985338092E-004 Sigma_initial(28,28) = 1.8959725740487208E-004
p2f(12) = qR4 = +9.9999892711639404E-001 Sigma_initial(29,29) = 3.5947120015449321E-008
p2f(13) = brx = +0.0000000000000000E+000 Sigma_initial(30,30) = 3.5947120015449321E-008
p2f(14) = bry = +0.0000000000000000E+000 Sigma_initial(31,31) = 3.5947120015449321E-008
p2f(15) = brz = +0.0000000000000000E+000 Sigma_initial(32,32) = 1.8959725740487208E-004
p2f(16) = crx = +0.0000000000000000E+000 Sigma_initial(33,33) = 1.8959725740487208E-004
p2f(17) = cry = +0.0000000000000000E+000 Sigma_initial(34,34) = 1.8959725740487208E-004
p2f(18) = crz = +0.0000000000000000E+000 Sigma_initial(35,35) = 3.5947120015449321E-008
p2f(19) = bgx = +0.0000000000000000E+000 Sigma_initial(36,36) = 3.5947120015449321E-008
p2f(20) = bgy = +0.0000000000000000E+000 Sigma_initial(37,37) = 3.5947120015449321E-008
p2f(21) = bgz = +0.0000000000000000E+000 Sigma_initial(38,38) = 3.5947120015449321E-008
p2f(22) = cgx = +0.0000000000000000E+000 Sigma_initial(39,39) = 3.5947120015449321E-008
p2f(23) = cgy = +0.0000000000000000E+000 Sigma_initial(40,40) = 3.5947120015449321E-008
p2f(24) = cgz = +0.0000000000000000E+000 Sigma_initial(41,41) = 3.5947120015449321E-008
-----

```

```

----- IPF KALMAN FILTER STARTED -----
Iteration#001: |dp|= +8.888627193757E-002 RMS(|Res|)=+3.407467793117E-005
Iteration#002: |dp|= +7.210748391673E-003 RMS(|Res|)=+1.148608072878E-005
Iteration#003: |dp|= +1.165875629275E-003 RMS(|Res|)=+1.069945862175E-005
Iteration#004: |dp|= +1.956612951525E-004 RMS(|Res|)=+1.067656753398E-005
Iteration#005: |dp|= +3.300011187525E-005 RMS(|Res|)=+1.067133170135E-005
Iteration#006: |dp|= +5.566890048663E-006 RMS(|Res|)=+1.067040804098E-005
Iteration#007: |dp|= +9.437021667188E-007 RMS(|Res|)=+1.067031694398E-005
Iteration#008: |dp|= +1.600763126265E-007 RMS(|Res|)=+1.067031268581E-005
Iteration#009: |dp|= +2.711909671680E-008 RMS(|Res|)=+1.067030955508E-005
Iteration#010: |dp|= +4.548772142555E-009 RMS(|Res|)=+1.067030811254E-005
Iteration#011: |dp|= +7.651616258424E-010 RMS(|Res|)=+1.067030790365E-005
Iteration#012: |dp|= +1.311914752912E-010 RMS(|Res|)=+1.067030792472E-005
Iteration#013: |dp|= +2.383927533431E-011 RMS(|Res|)=+1.067030793251E-005
Iteration#014: |dp|= +3.975173676311E-012 RMS(|Res|)=+1.067030793386E-005
Iteration#015: |dp|= +4.848637176832E-013 RMS(|Res|)=+1.067030793196E-005
Iteration#016: |dp|= +6.907955426811E-013 RMS(|Res|)=+1.067030793084E-005
Iteration#017: |dp|= +3.208289150422E-013 RMS(|Res|)=+1.067030793125E-005
Iteration#018: |dp|= +6.176879041398E-013 RMS(|Res|)=+1.067030793235E-005
Iteration#019: |dp|= +5.034468262820E-013 RMS(|Res|)=+1.067030793025E-005
Iteration#020: |dp|= +1.775110899269E-012 RMS(|Res|)=+1.067030792952E-005
Iteration#021: |dp|= +1.091212075578E-012 RMS(|Res|)=+1.067030793186E-005
Iteration#022: |dp|= +1.089375635357E-012 RMS(|Res|)=+1.067030792905E-005
Iteration#023: |dp|= +2.101383816913E-013 RMS(|Res|)=+1.067030793122E-005
Iteration#024: |dp|= +3.574879103778E-013 RMS(|Res|)=+1.067030793192E-005
Iteration#025: |dp|= +1.719261753694E-013 RMS(|Res|)=+1.067030793001E-005
IPF Kalman Filter Completed with Error |dp1| + |dp2| = +1.7192617536942669E-013
-----
```

```

----- IPF LEAST SQUARES FILTER STARTED -----
Iteration#001 COND#=+7.090363099888E+006, |dp|=+8.888618839293E-002
Iteration#002 COND#=+7.077740886968E+006, |dp|=+7.211375116333E-003
Iteration#003 COND#=+7.076929348000E+006, |dp|=+1.165057127997E-003
Iteration#004 COND#=+7.076756666425E+006, |dp|=+1.956313650856E-004
Iteration#005 COND#=+7.076726384235E+006, |dp|=+3.304837819897E-005
Iteration#006 COND#=+7.076721270580E+006, |dp|=+5.588646701828E-006
Iteration#007 COND#=+7.076720405646E+006, |dp|=+9.452300555585E-007
Iteration#008 COND#=+7.076720259356E+006, |dp|=+1.598753210739E-007
Iteration#009 COND#=+7.076720234607E+006, |dp|=+2.704133898214E-008
Iteration#010 COND#=+7.076720230424E+006, |dp|=+4.573640954667E-009
Iteration#011 COND#=+7.076720229718E+006, |dp|=+7.736817928049E-010
Iteration#012 COND#=+7.076720229598E+006, |dp|=+1.308594389961E-010
Iteration#013 COND#=+7.076720229578E+006, |dp|=+2.205000510472E-011
Iteration#014 COND#=+7.076720229571E+006, |dp|=+3.819229666948E-012
Iteration#015 COND#=+7.076720229572E+006, |dp|=+5.847137995529E-013
Iteration#016 COND#=+7.076720229572E+006, |dp|=+1.954903832276E-013
Iteration#017 COND#=+7.076720229575E+006, |dp|=+3.065838875006E-014
Iteration#018 COND#=+7.076720229571E+006, |dp|=+3.586096943806E-014
Iteration#019 COND#=+7.076720229574E+006, |dp|=+1.194527328257E-013
Iteration#020 COND#=+7.076720229574E+006, |dp|=+1.201873044309E-013
Iteration#021 COND#=+7.076720229571E+006, |dp|=+4.410048057911E-014
Iteration#022 COND#=+7.076720229577E+006, |dp|=+7.327463343695E-014
Iteration#023 COND#=+7.076720229575E+006, |dp|=+3.936043505431E-014
Iteration#024 COND#=+7.076720229573E+006, |dp|=+1.461815120717E-013
Iteration#025 COND#=+7.076720229575E+006, |dp|=+2.436605542300E-013
IPF Least Squares Filter Completed with Error |dp1| + |dp2| = +2.4366055423001228E-013
-----
```

Total Execution Time: 54 seconds

4 COMMENTS

Overall the data looked clean, and the filter converged nicely.

Comments:

1. The run was performed in normal IPF operating mode.
2. This run uses IPF version 3.0 where the gyro drift bias estimates make use of the recently corrected GCF signs, (MCR 2521) and now show no sandwich-to-sandwich variations.
3. There were 7 sandwiches maneuvers with 42 science centroids and 49 PCRS measurements.
Note science centroid number 18 in the CA file CA501040 was removed because the CX value seemed to have the wrong sign.
4. We estimated 18 parameters consisting of: 1 constant plate scales along the slit, 2 IPF alignment angles (no Twist), 3 STA-to-PCRS alignment angles, 6 STA-to-PCRS thermo-mechanical drift parameters, and 3 gyro bias and 3 gyro bias-drift parameters.

We recommend updating frames 38,39,40, and 41 with the new quaternions listed in the IF file IF502040.dat. This contains adjustments of about 3.6 arcseconds in Y, and 0.6 arsecseconds in Z for the prime frame (40). In our best judgement, this fine survey is accurate to 0.13 arcsecond which satisfies its fine survey requirement of 0.28 arcsecond by a good margin.

IPF TEAM CONTACT INFORMATION

IPF Team email	ipf@sirtfweb.jpl.nasa.gov	
David S. Bayard	X4-8208	David.S.Bayard@jpl.nasa.gov (TEAM LEADER)
Dhemetrio Boussalis	X4-3977	boussali@grover.jpl.nasa.gov
Paul Brugarolas	X4-9243	Paul.Brugarolas@jpl.nasa.gov
Bryan H. Kang	X4-0541	Bryan.H.Kang@jpl.nasa.gov
Edward.C.Wong	X4-3053	Edward.C.Wong@jpl.nasa.gov (TASK MANAGER)

ACKNOWLEDGEMENTS

This work was performed at the Jet Propulsion Laboratory, California Institute of Technology, under contract with the National Aeronautics and Space Administration.

References

- [1] D.S. Bayard, B.H. Kang, *SIRTF Instrument Pointing Frame Kalman Filter Algorithm*, JPL D-Document D-24809, September 30, 2003.
- [2] B.H. Kang, D.S. Bayard, *SIRTF Instrument Pointing Frame (IPF) Software Description Document and User's Guide*, JPL D-Document D-24808, September 30, 2003.
- [3] D.S. Bayard, B.H. Kang, *SIRTF Instrument Pointing Frame (IPF) Kalman Filter Unit Test Report*, JPL D-Document D-24810, September 30, 2003.
- [4] *Space Infrared Telescope Facility In-Orbit Checkout and Science Verification Mission Plan*, JPL D-Document D-22622, 674-FE-301 Version 1.4, February 8, 2002.
- [5] *Space Infrared Telescope Facility Observatory Description Document*, Lockheed Martin LMMS/P458569, 674-SEIT-300 Version 1.2, November 1, 2002.
- [6] *SIRTF Software Interface Specification for Science Centroid INPUT Files (CAFILe, CS-FILE)*, JPL SOS-SIS-2002, November 18, 2002.
- [7] *SIRTF Software Interface Specification for Inferred Frames Offset INPUT Files (OFILE)*, JPL SOS-SIS-2003, November 18, 2002.
- [8] *SIRTF Software Interface Specification for PCRS Centroid INPUT Files (CBFILE)*, JPL SIS-FES-015, November 18, 2002.
- [9] *SIRTF Software Interface Specification for Attitude INPUT Files (AFILE, ASFILE)*, JPL SIS-FES-014, January 7, 2002.
- [10] *SIRTF Software Interface Specification for IPF Filter Output Files (IFFILE, LGFILE, TARFILE)*, JPL SOS-SIS-2005, November 18, 2002.
- [11] R.J. Brown, *Focal Surface to Object Space Field of View Conversion*. Systems Engineering Report SER No. S20447-OPT-051, Ball Aerospace & Technologies Corp., November 23, 1999.

This page left blank.

JET PROPULSION LABORATORY

SIRTF IPF REPORT

JPL ID501046

November 6, 2003

**SIRTF INSTRUMENT POINTING FRAME
KALMAN FILTER EXECUTION SUMMARY**

IPF RUN NUMBER: 501046

REPORT TYPE: IOC EXECUTION (FINE)

PRIME FRAME: IRS_LongLo_2nd_Ord_Center_Pos (46)

INFERRRED FRAMES: (44) (45)

IPF TEAM

Autonomy and Control Section (345)

Jet Propulsion Laboratory

California Institute of Technology

4800 Oak Grove Drive

Pasadena, CA 91109

Contents

1 IPF EXECUTION SUMMARY	5
2 IPF INPUT FILE HISTORY	9
3 IPF EXECUTION RESULTS	10
3.1 IPF EXECUTION OUTPUT PLOTS	10
3.2 IPF OUTPUT DATA (IF MINI FILE)	36
3.3 IPF EXECUTION LOG	38
4 COMMENTS	42

List of Figures

1.1 A-priori and a-posteriori IPF frames	5
1.2 A-priori and a-posteriori IPF frames (ZOOMED)	8
2.1 Scenario Plot	9
3.1 TPF coords of measurements and a-priori predicts	12
3.2 Oriented Pixel Coords of measurements and a-priori predicts	12
3.3 Oriented (W,V) Pixel Coords of A-Priori Prediction Error Quiver Plot	13
3.4 A-priori prediction error (Science Centroids)	13
3.5 Oriented Pixel Coords of measurements and a-priori predicts (PCRS only)	14
3.6 Oriented Pixel Coords of measurements and a-priori predicts (Zoomed, PCRS only)	14
3.7 Oriented (W,V) Pixel Coords of A-Priori PCRS Prediction Error Quiver Plot	15
3.8 A-priori PCRS prediction error	15
3.9 IPF execution convergence, chart 1	16
3.10 IPF execution convergence, chart 2	16
3.11 Parameter uncertainty convergence	17
3.12 IPF parameter symbol table	17
3.13 KF parameter error sigma plots	18
3.14 LS parameter error sigma plot	18
3.15 KF and LS parameter error sigma plot	19
3.16 Oriented Pixel Coords of meas. and a-posteriori predicts	20
3.17 Oriented Pixel Coords of meas. and a-posteriori predicts (attitude corrected)	20

3.18	KF innovations with (o) and w/o (+) attitude corrections	21
3.19	Histograms of science a-posteriori residuals (or innovations)	21
3.20	A-Posteriori Science Centroid Prediction Error Quiver (Att. Cor.)	22
3.21	Normalized A-Posteriori Science Centroid Prediction Errors	22
3.22	KF innovations with (o) and w/o (+) attitude corrections (PCRS)	23
3.23	Histograms of PCRS a-posteriori residuals (or innovations)	23
3.24	A-posteriori PCRS Prediction Summary	24
3.25	A-posteriori PCRS Prediction (PCRS 1 Only)	25
3.26	A-posteriori PCRS Prediction (PCRS 2 Only)	25
3.27	A-Posteriori PCRS Prediction Errors Quiver (Att. Cor.)	26
3.28	Normalized A-Posteriori PCRS Prediction Errors	26
3.29	W-axis KF innovations and 1-sigma bound	27
3.30	V-axis KF innovations and 1-sigma bound	27
3.31	Array plot with (solid) and w/o (dashed) optical distortion corrections	28
3.32	Optical Distortion Plot: total (x5 magnification)	28
3.33	Optical Distortion Plot: constant plate scales (x5 magnification)	29
3.34	Optical Distortion Plot: linear plate scale (x5 magnification)	29
3.35	Optical Distortion Plot: gamma terms (x5 magnification)	30
3.36	Scan Mirror Chops	30
3.37	IPF Frame Reconstruction	31
3.38	Center Pixel Reconstruction	31
3.39	Estimated attitude corrections (Body frame)	32
3.40	Estimated attitude error sigma plot (Body frame)	32
3.41	Thermo-mechanical boresight drift (equiv. angle in (W,V) coords)	33
3.42	Thermo-mechanical boresight drift (equiv. angle in Body frame)	33
3.43	Gyro drift bias contribution (equiv. rate in (W,V) coords)	34
3.44	Gyro drift bias contribution (equiv. angle in (W,V) coords)	34
3.45	Gyro drift bias contribution (equiv. angle in Body frame)	35

List of Tables

1.1	IPF filter input files	6
1.2	IPF filter execution configuration	6

1.3	IPF filter execution mask vector assignment	6
1.4	IPF calibration error summary ([arcsec], 1-sigma, radial)	7
1.5	Science measurement prediction error summary (1-sigma)	7
1.6	IPF Brown angle summary	8
2.1	IPF input file editing status	9
3.1	Table of figures I (IPF run)	10
3.2	Table of figures II (IPF run)	11
3.3	PCRS measurement prediction error summary	24

1 IPF EXECUTION SUMMARY

This report summarizes the SIRTF Instrument Pointing Frame (IPF) Kalman Filter execution associated with run file: RN501046. In particular, this Focal Point Survey calibrates the instrument: IRS_LongLo_2nd_Ord_Center_Pos (46), as part of the IOC Fine Survey. The main calibration results from the IPF filter execution have been documented in IF501046 typically stored in the mission archive DOM collection IPF_IF. This report only summarizes the main aspects of the run, and does not substitute for the full information contained in the IF file.

Section 1 summarizes the filter execution results. The filter configurations are tabulated in Table 1.2 and the mask vector assignments are tabulated in Table 1.3. A total of 18 state parameters are estimated in this run. The overall End-to-End pointing performances are tabulated in Table 1.4. The prediction residuals throughout the estimation processes are tabulated in Table 1.5. Section 3 summarizes resulting plots, a mini summary of the IF IPF output file, and the execution log. Section 4 captures the user comments that are specific to this particular run.

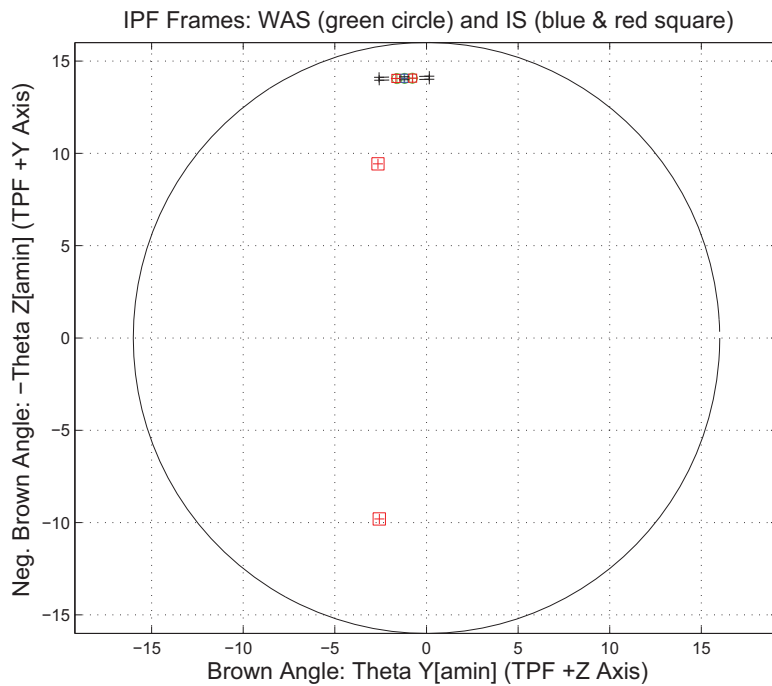


Figure 1.1: A-priori and a-posteriori IPF frames

RAW	FINAL (After Editing)
AA501046	AA501046
AS501046	AS501046
CA501046	CA501046
CB501046	CB501046
CS501046	CS501046

Table 1.1: IPF filter input files

EXECUTION CONFIGURATION ITEM	CURRENT STATUS
IPF Filter Version Used	IPF.V3.0.0B
Frame Table Version Used	BodyFrames_FTU_12b
Scan-Mirror Employed?	NO
IPF Filter Mode	NORMAL-MODE(0)
SLIT-MODE Operation	ENABLED
Kalman Filter Operation	ENABLED
Least-Squares Data Analysis	ENABLED
IBAD Screening	ENABLED
User-Specified Data Editing	DISABLED
Total Number of Iterations	25
LS Residual Sigma Scale	7.59840429E+00
Total Number of Maneuvers	7

Table 1.2: IPF filter execution configuration

Con. Plate Scale			Γ Dependent				Γ^2 Dependent				Linear Plate Scale						Mirror			
a_{00}	b_{00}	c_{00}	a_{10}	b_{10}	c_{10}	d_{10}	a_{20}	b_{20}	c_{20}	d_{20}	a_{01}	b_{01}	c_{01}	d_{01}	e_{01}	f_{01}	α	β		
1	2	3	4	5	6	7	8	9	10	11	12	13	14	15	16	17	18	19		
1	0	0	0	0	0	0	0	0	0	0	0	0	0	0	0	0	0	0		
IPF (T)			Alignment R						Gyro Drift Bias											
θ_1	θ_2	θ_3	a_{rx}	a_{ry}	a_{rz}	b_{rx}	b_{ry}	b_{rz}	c_{rx}	c_{ry}	c_{rz}	b_{gx}	b_{gy}	b_{gz}	c_{gx}	c_{gy}	c_{gz}			
20	21	22	23	24	25	26	27	28	29	30	31	32	33	34	35	36	37			
0	1	1	1	1	1	1	1	1	1	1	1	1	1	1	1	1	1			

Table 1.3: IPF filter execution mask vector assignment

FOCAL PLANE SURVEY ANALYSIS: IOC Fine Survey.

INSTRUMENT NAME: IRS_LongLo_2nd_Ord_Center_Pos NF: 4

PIX2RADW: .8 81 681E-06 [rad/pixel] = 1.0000E 00 [arcsec/pixel]

PIX2RADV: .8 81 681E-06 [rad/pixel] = 1.0000E 00 [arcsec/pixel]

FRAME	DESCRIPTION	IPF ¹	SF ²	TOTAL	REQ
046(P)	IRS_LongLo_2nd_Ord_Center_Pos	0.2542	0.0855	0.2682	0.28
044(I)	IRS_LongLo_2nd_Ord_1st_Pos	0.2534	0.0855	0.2675	N/A
045(I)	IRS_LongLo_2nd_Ord_2nd_Pos	0.2599	0.0855	0.2736	N/A

Table 1.4: IPF calibration error summary ([arcsec], 1-sigma, radial)

RMS METRIC	A PRIORI ³	A POSTERIORI ³	ATT. CORRECTED ⁴	UNITS
Radial	3.5160	1.1167	1.1052	arcsec
W-Axis	3.4550	1.0373	1.0357	arcsec
V-Axis	0.6521	0.4137	0.3858	arcsec
Radial	3.5160	1.1167	1.1052	pixels
W-Axis	3.4550	1.0373	1.0357	pixels
V-Axis	0.6521	0.4137	0.3858	pixels

Table 1.5: Science measurement prediction error summary (1-sigma)

¹IPF filter removes systematic pointing errors due to: thermomechanical alignment drift (Body to TPF), gyro bias and bias drift, centroiding error, attitude error, and optical distortion. IPF SIGMA presented here is “Scaled” by the Least Squares Scale factor. The Least Squares Scale Factor was: 7.598404. It is assumed that the gyro Angle Random Walk contribution is captured with the Least Squares scaling. The gyro ARW contribution can be approximately calculated as 0.0846 arcseconds, given that ARW = 100 $\mu\text{deg}/\sqrt{\text{hr}}$, with 6.955400e+02 second Maneuver time (max), and 7 independent Maneuvres.

²Gyro Scale Factor(GSF) assumes 95 ppm error over 0.250 degree maneuver.

³This can be interpreted as estimate of ”pixel to sky” pointing reconstruction error if no science data is used.

⁴This can be interpreted as estimate of achieved S/I centroiding error

IPF BROWN ANGLE SUMMARY					
FRAME TABLE USED: BodyFrames_FTU_12b					
NF	NAME	WAS	IS	CHANGE	UNIT
046	theta_Y	-1.191436	-1.213355	-0.021919	arcmin
046	theta_Z	-14.057499	-14.066157	-0.008658	arcmin
046	angle	-1.199999	-1.199999	+0.000000	deg
044	theta_Y	-0.771250	-0.756576	+0.014674	arcmin
044	theta_Z	-14.066300	-14.075725	-0.009424	arcmin
044	angle	-1.199999	-1.199999	+0.000000	deg
045	theta_Y	-1.611621	-1.670133	-0.058512	arcmin
045	theta_Z	-14.048697	-14.056588	-0.007891	arcmin
045	angle	-1.199999	-1.199999	+0.000000	deg

Table 1.6: IPF Brown angle summary

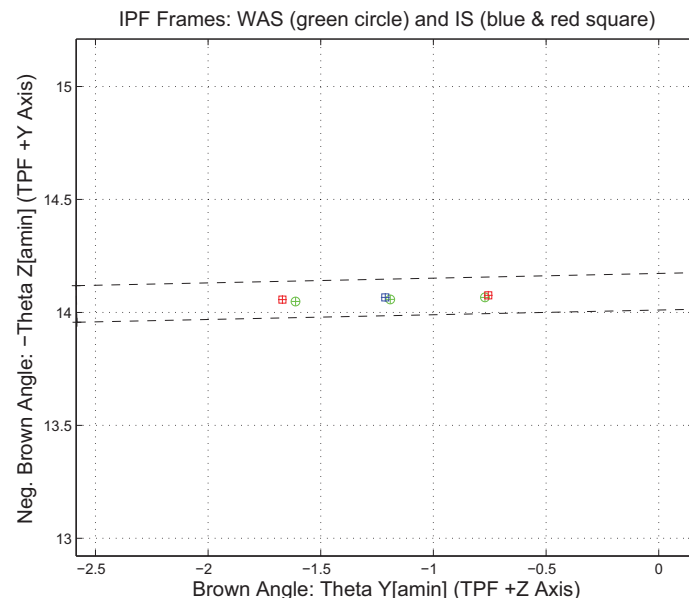


Figure 1.2: A-priori and a-posteriori IPF frames (ZOOMED)

2 IPF INPUT FILE HISTORY

WAS	SIZE	IS	SIZE	REMOVED	PATCHED
AA501046	UNCHANGED	AA501046	UNCHANGED	0	0
CA501046	UNCHANGED	CA501046	UNCHANGED	0	N/A
CB501046	UNCHANGED	CB501046	UNCHANGED	0	N/A

Table 2.1: IPF input file editing status

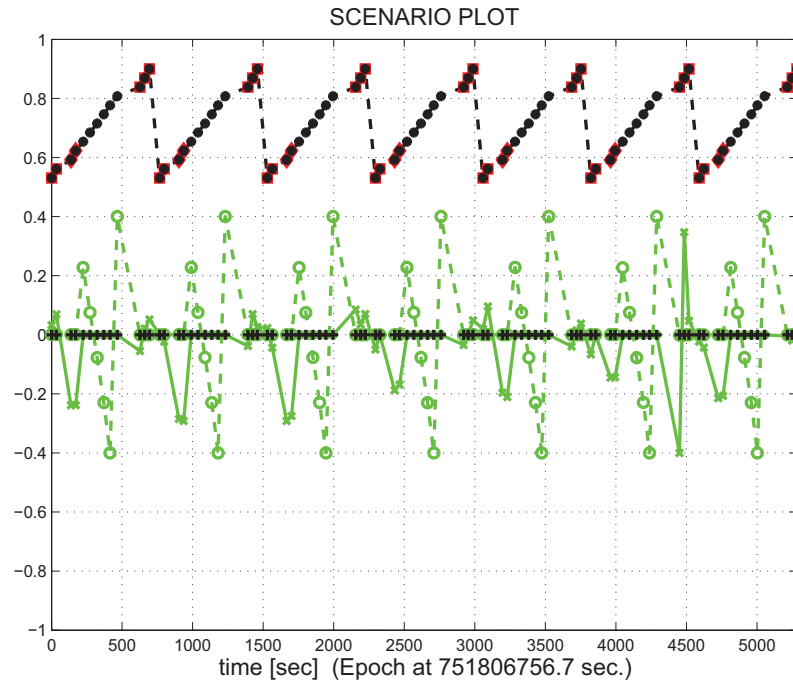


Figure 2.1: Scenario Plot

3 IPF EXECUTION RESULTS

3.1 IPF EXECUTION OUTPUT PLOTS

This subsection summarizes the IPF filter results. As shown in Table 3.1, the output plots are segmented to three groups: predicted performance, post-run results and IPF trending plots.

FIGURE NO.	DESCRIPTION
Predicted performance prior to IPF run	
Figure 3.1	Meas. and a-priori predicts in TPF coords
Figure 3.2	Meas. and a-priori predicts in Oriented Pixel Coords including rectangular array boundary approximation
Figure 3.3	A-Priori Prediction Error Quiver Plot in Oriented Pixel Coords including rectangular array boundary approximation
Figure 3.4	A-priori prediction error
Figure 3.5	Oriented Pixel Coords of measurements and a-priori predicts (PCRS only)
Figure 3.6	Oriented Pixel Coords of measurements and a-priori predicts (Zoomed, PCRS only)
Figure 3.7	Oriented (W,V) Pixel Coords of A-Priori PCRS Prediction Error Quiver Plot
Figure 3.8	A-priori PCRS prediction error
IPF filter performance (post run results)	
Figure 3.9	IPF execution convergence, chart 1: (top) normalized residual error vs. iteration number and (bottom) norm of effective parameter corrections
Figure 3.10	IPF execution convergence, chart 2: parameter correction size vs. iteration number
Figure 3.11	Parameter uncertainty convergence: square-root of diagonal elements of covariance matrix vs. maneuver number
Figure 3.12	IPF parameter symbol table
Figure 3.13	KF parameter error sigma plot (a-priori-dashed, a-posteriori-solid). Includes true parameter errors (FLUTE runs only)
Figure 3.14	LS parameter error sigma plot. Includes true parameter errors (FLUTE runs only)
Figure 3.15	KF and LS parameter errors sigma plot (Figure 3.13 & Figure 3.14 combined)
Figure 3.16	Measurements and a-posteriori predicts in Oriented Pixel Coords including rectangular array boundaries (a-priori-dashed, a-posteriori-solid)
Figure 3.17	Attitude corrected meas. and a-posteriori predicts in Oriented Pixel Coords including rectangular array boundaries (a-priori-dashed, a-posteriori-solid)

Table 3.1: Table of figures I (IPF run)

FIGURE NO.	DESCRIPTION
IPF filter performance (post run results) - CONTINUE	
Figure 3.18	KF innovations with (o) and w/o (+) attitude corrections
Figure 3.19	Histograms of science a-posteriori residuals (or innovations)
Figure 3.20	A-Posteriori Science Centroid Prediction Error Quiver (Att. Cor.)
Figure 3.21	Normalized A-Posteriori Science Centroid Prediction Errors
Figure 3.22	KF innovations with (o) and w/o (+) attitude corrections (PCRS)
Figure 3.23	Histograms of PCRS a-posteriori residuals (or innovations)
Figure 3.24	A-posteriori PCRS Prediction Summary
Figure 3.25	A-posteriori PCRS Prediction (PCRS 1 Only)
Figure 3.26	A-posteriori PCRS Prediction (PCRS 2 Only)
Figure 3.27	A-Posteriori PCRS Prediction Errors Quiver (Att. Cor.)
Figure 3.28	Normalized A-Posteriori PCRS Prediction Errors
Figure 3.29	W-axis KF innovations and 1-sigma bound
Figure 3.30	V-axis KF innovations and 1-sigma bound
Figure 3.31	Array plot with (solid) and w/o (dashed) optical distortion corrections
Figure 3.32	Optical Distortion Plot: total (x5 magnification)
Figure 3.33	Optical Distortion Plot: constant plate scales (x5 magnification)
Figure 3.34	Optical Distortion Plot: linear plate scale (x5 magnification)
Figure 3.35	Optical Distortion Plot: gamma terms (x5 magnification)
Figure 3.36	Scan Mirror Chops
Figure 3.37	IPF Frame Reconstruction
Figure 3.38	Center Pixel Reconstruction
IPF parameter trending plots	
Figure 3.39	Estimated attitude corrections (Body frame)
Figure 3.40	Estimated attitude error sigma plot (Body frame)
Figure 3.41	Systematic error attributed to thermo-mechanical boresight drift (equiv. angle in (W,V) coords)
Figure 3.42	Systematic error attributed to thermo-mechanical boresight drift (equiv. angle in Body frame)
Figure 3.43	Systematic error attributed to gyro drift bias (equiv. rate in (W,V) coords)
Figure 3.44	Systematic error attributed to gyro drift bias (equiv. angle in (W,V) coords)
Figure 3.45	Systematic error attributed to gyro drift bias (equiv. angle in Body frame)

Table 3.2: Table of figures II (IPF run)

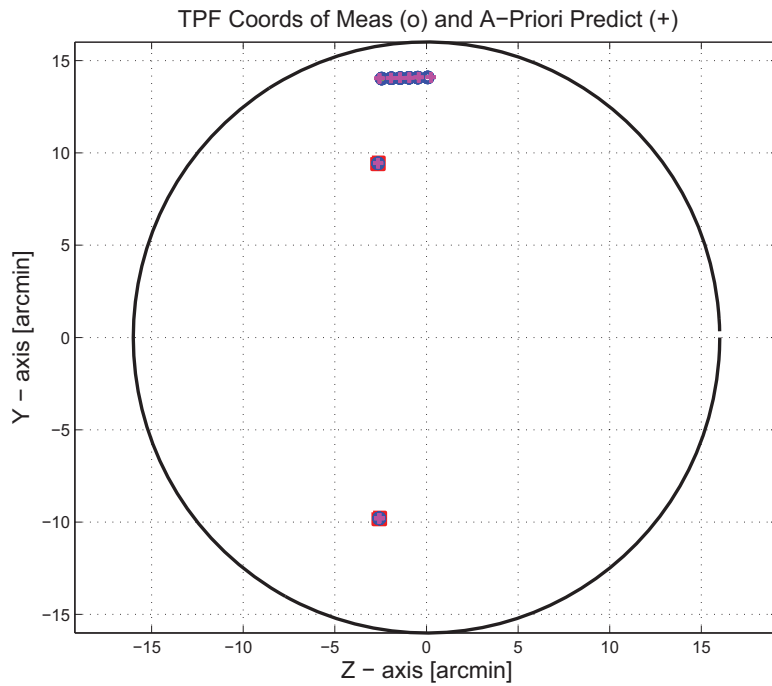


Figure 3.1: TPF coords of measurements and a-priori predicts

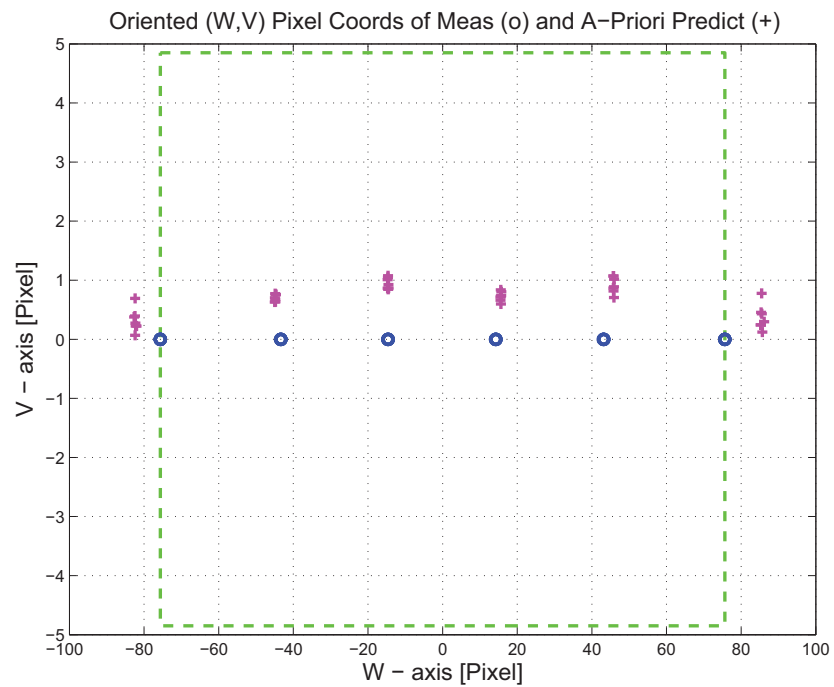


Figure 3.2: Oriented PixelCoords of measurements and a-priori predicts

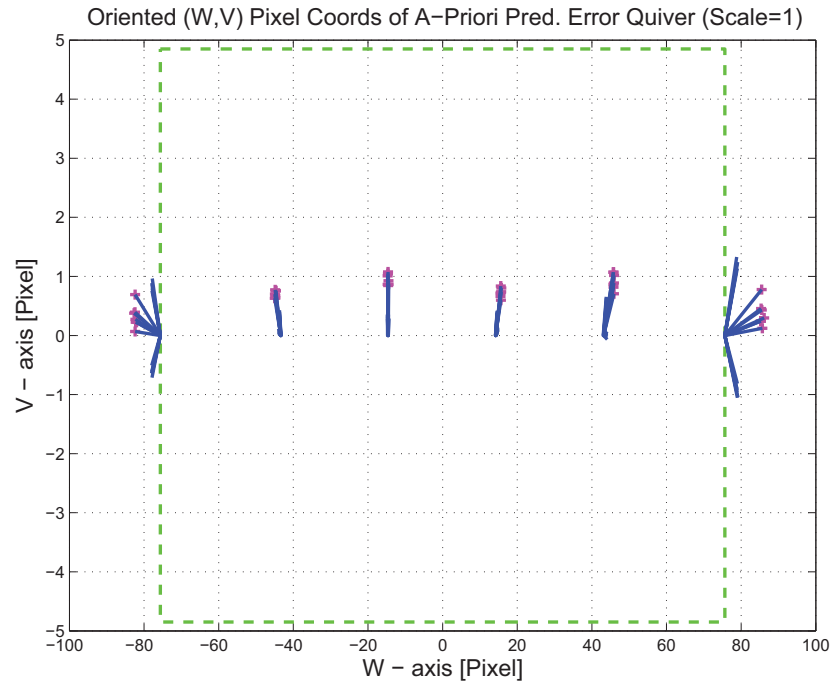


Figure 3.3: Oriented (W,V) Pixel Coords of A-Priori Prediction Error Quiver Plot

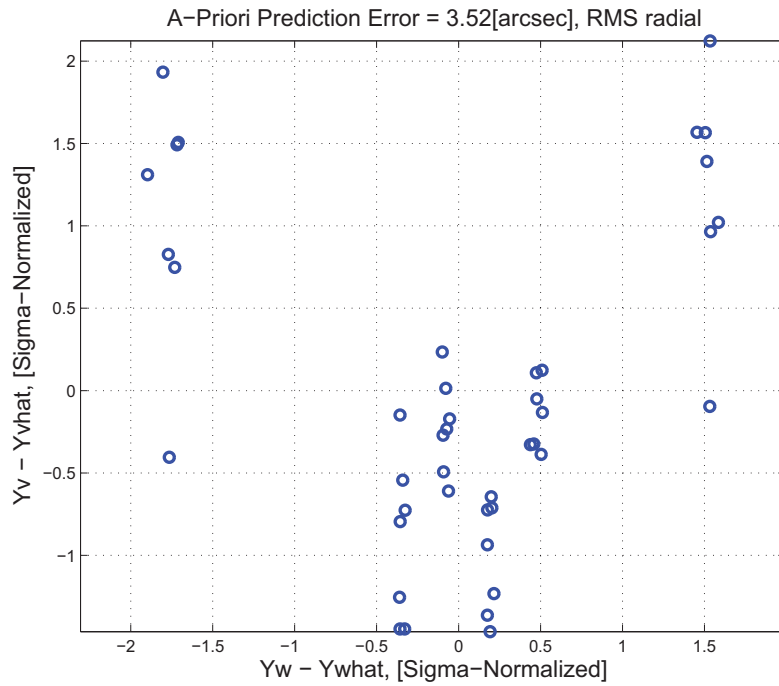


Figure 3.4: A-priori prediction error (Science Centroids)

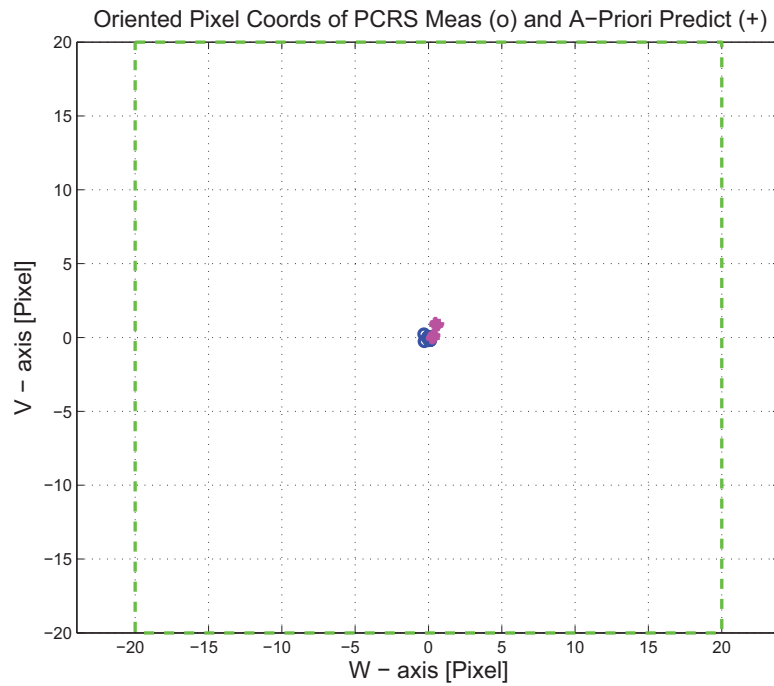


Figure 3.5: Oriented Pixel Coords of measurements and a-priori predicts (PCRS only)

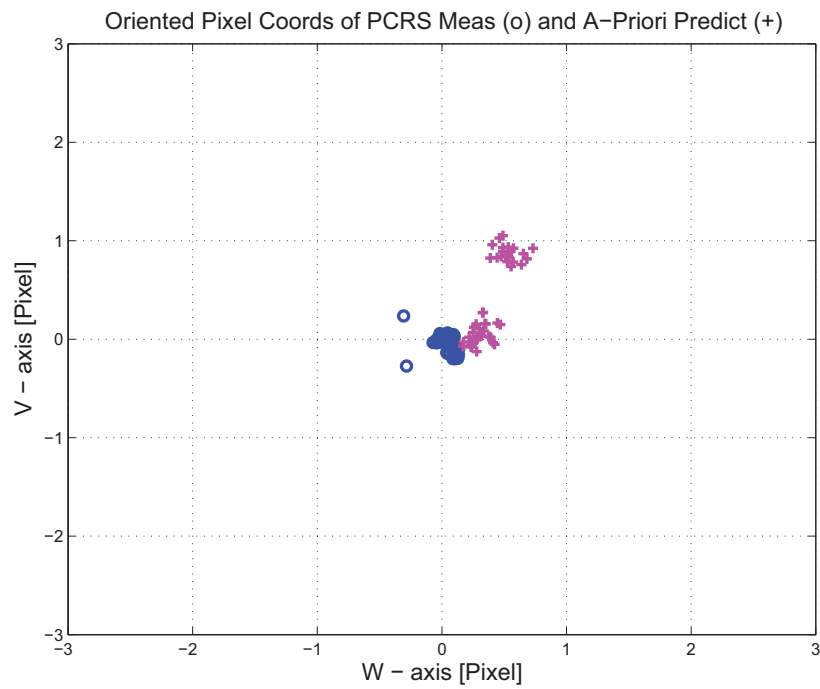


Figure 3.6: Oriented Pixel Coords of measurements and a-priori predicts (Zoomed, PCRS only)

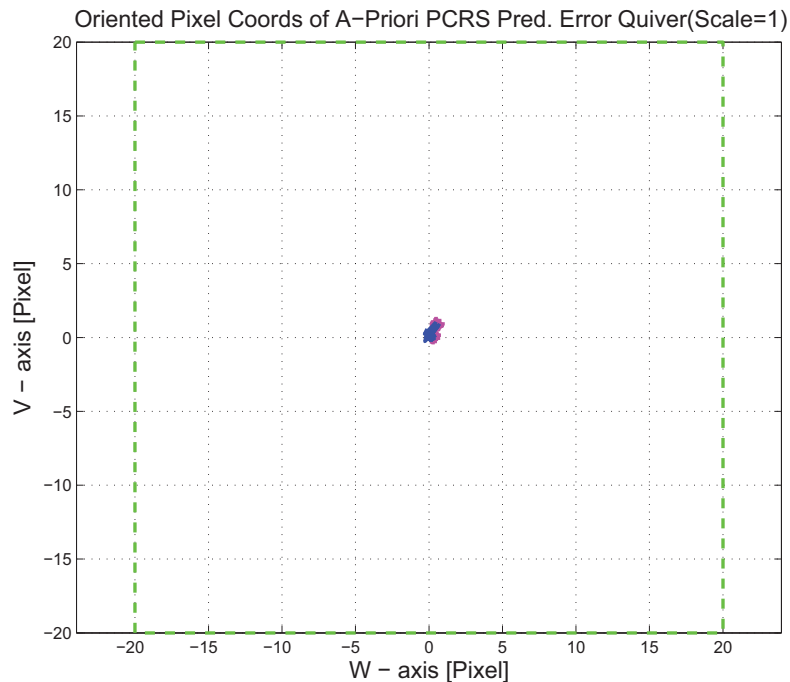


Figure 3.7: Oriented (W,V) Pixel Coords of A-Priori PCRS Prediction Error Quiver Plot

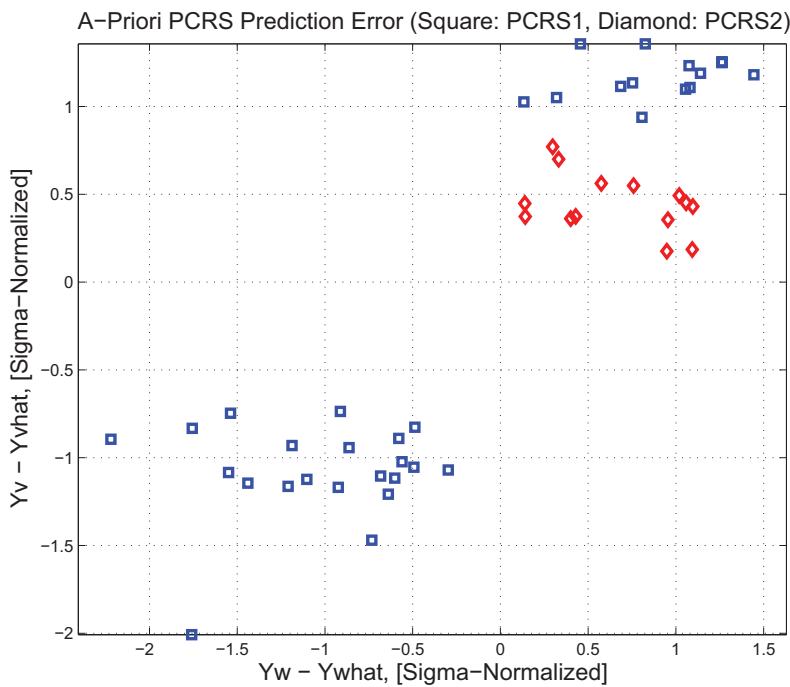


Figure 3.8: A-priori PCRS prediction error

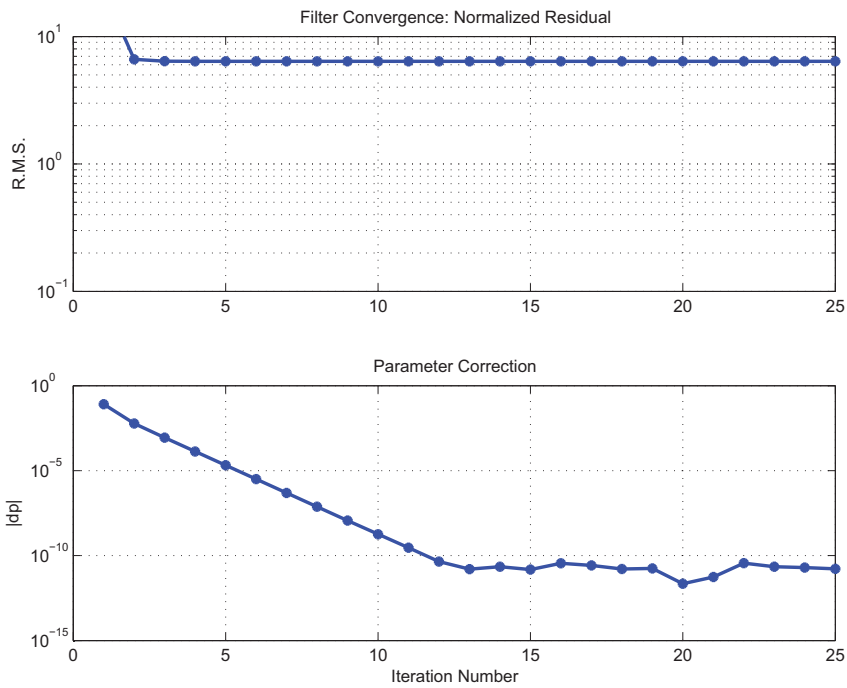


Figure 3.9: IPF execution convergence, chart 1

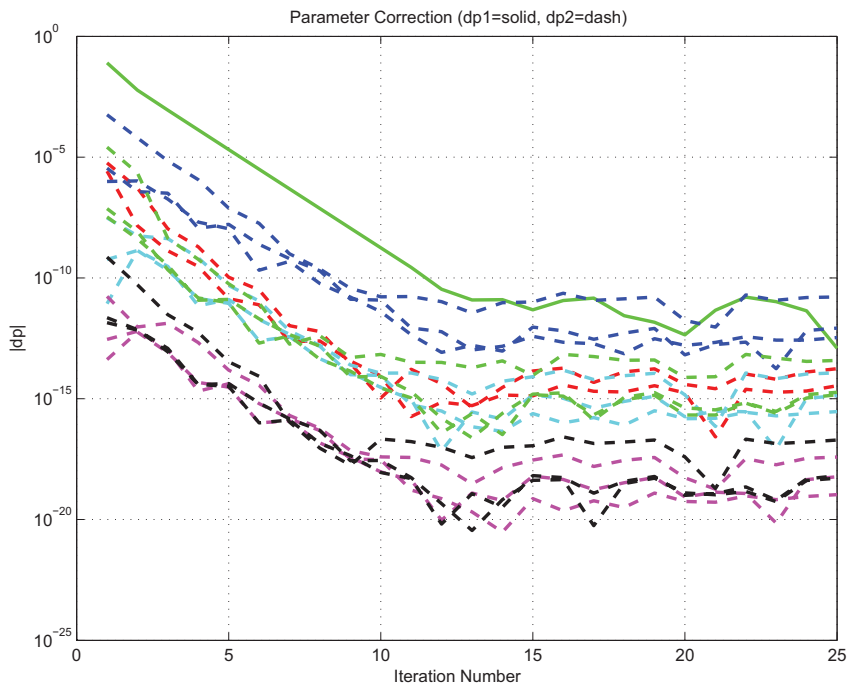


Figure 3.10: IPF execution convergence, chart 2

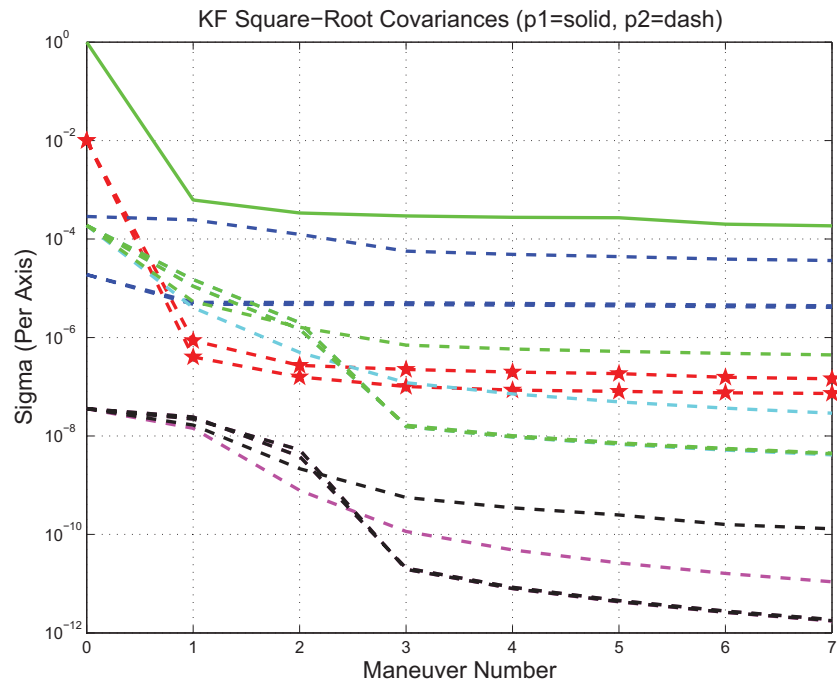


Figure 3.11: Parameter uncertainty convergence

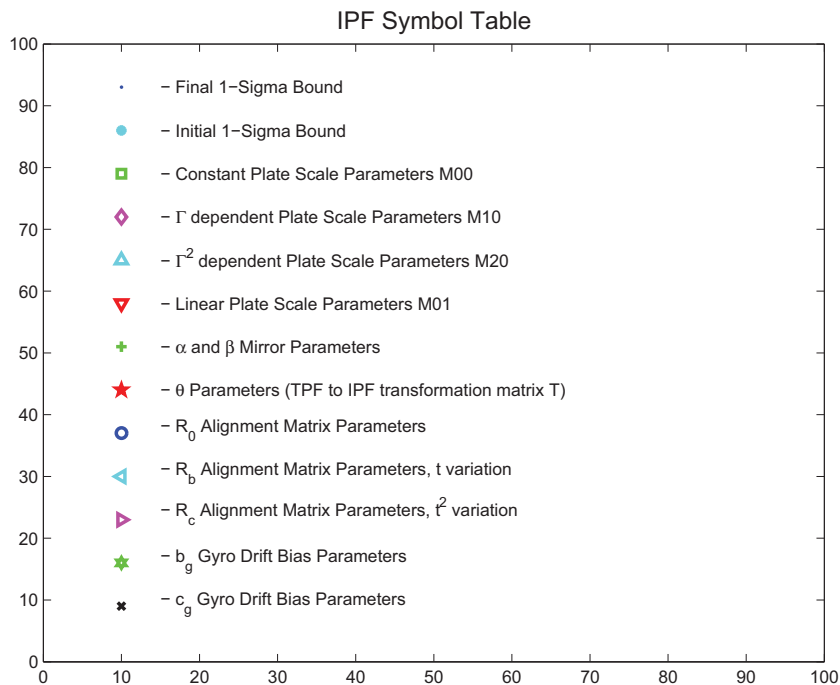


Figure 3.12: IPF parameter symbol table

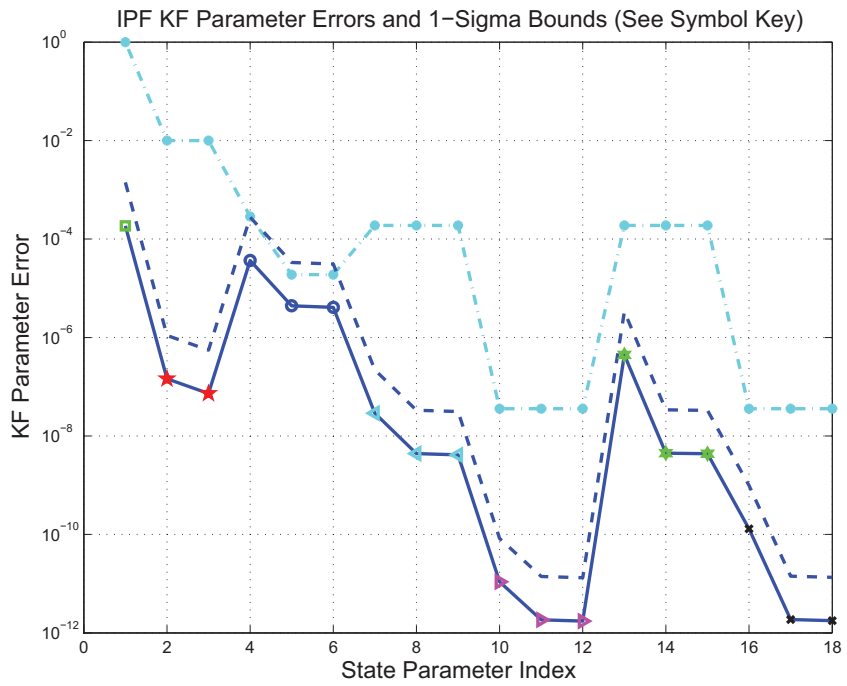


Figure 3.13: KF parameter error sigma plots

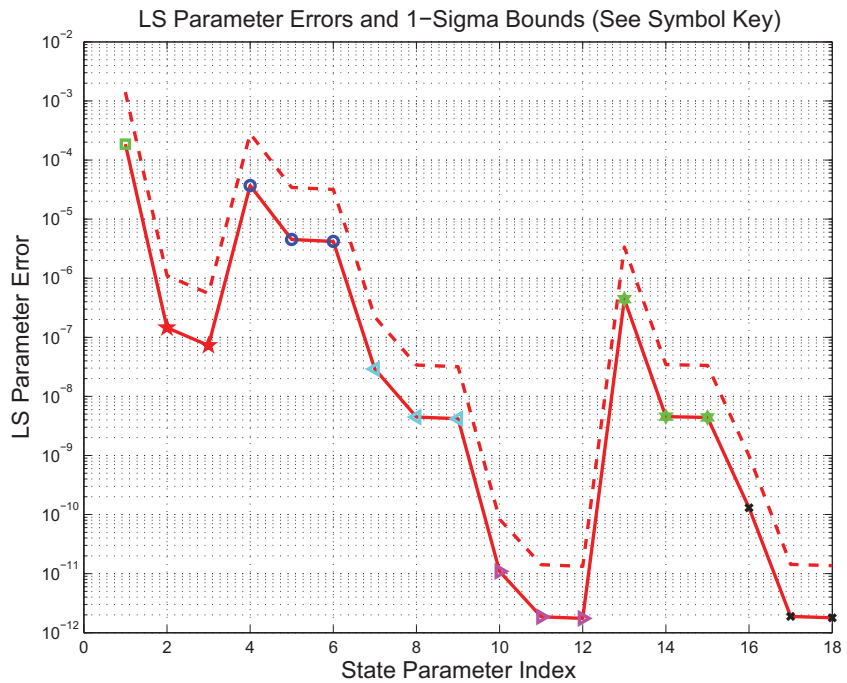


Figure 3.14: LS parameter error sigma plot

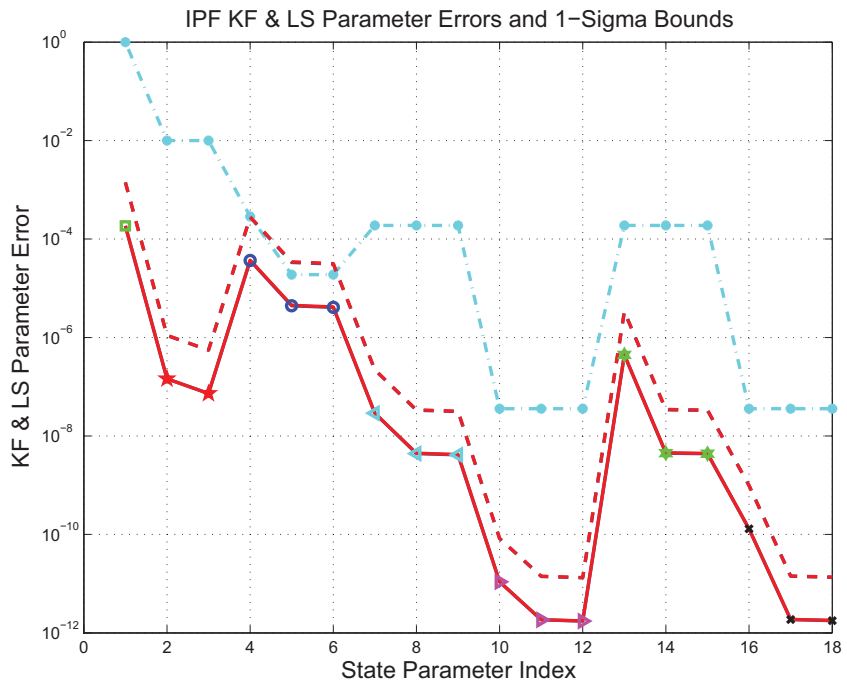


Figure 3.15: KF and LS parameter error sigma plot

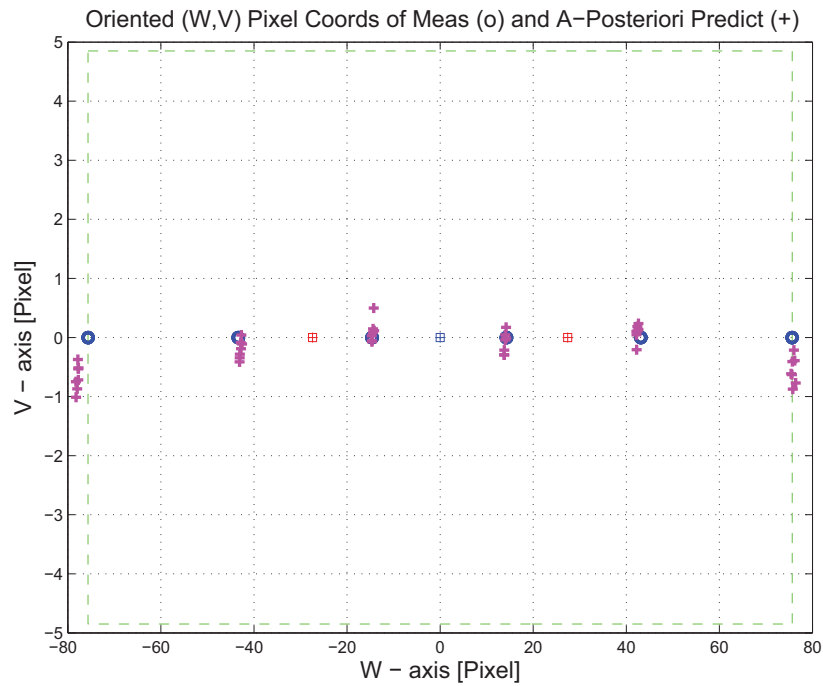


Figure 3.16: Oriented Pixel Coords of meas. and a-posteriori predicts

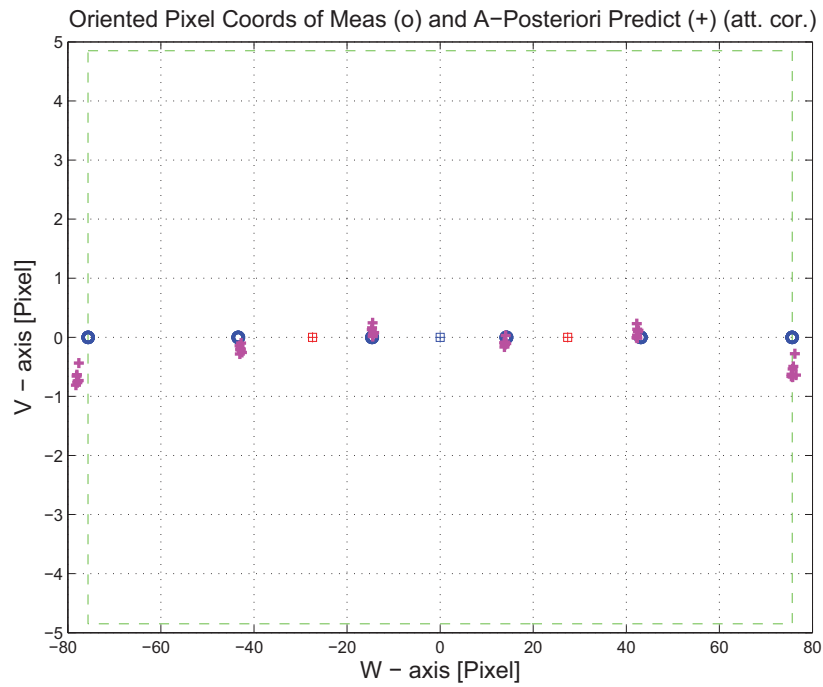


Figure 3.17: Oriented Pixel Coords of meas. and a-posteriori predicts (attitude corrected)

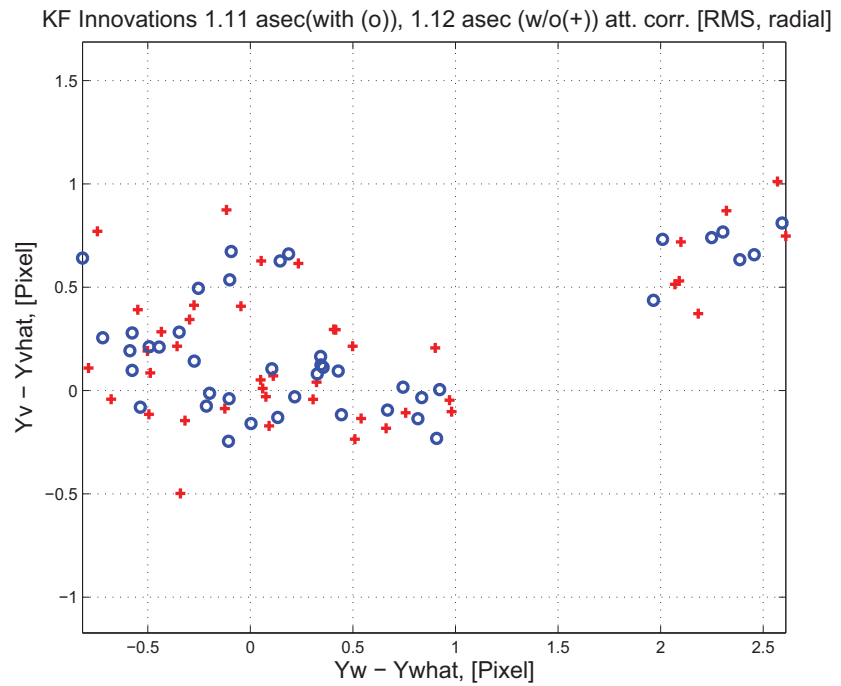


Figure 3.18: KF innovations with (o) and w/o (+) attitude corrections

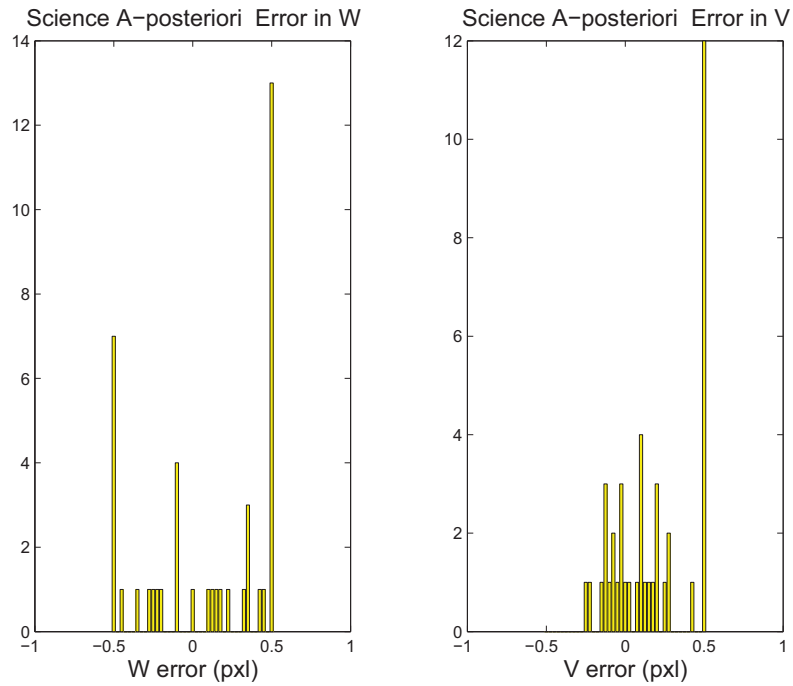


Figure 3.19: Histograms of science a-posteriori residuals (or innovations)

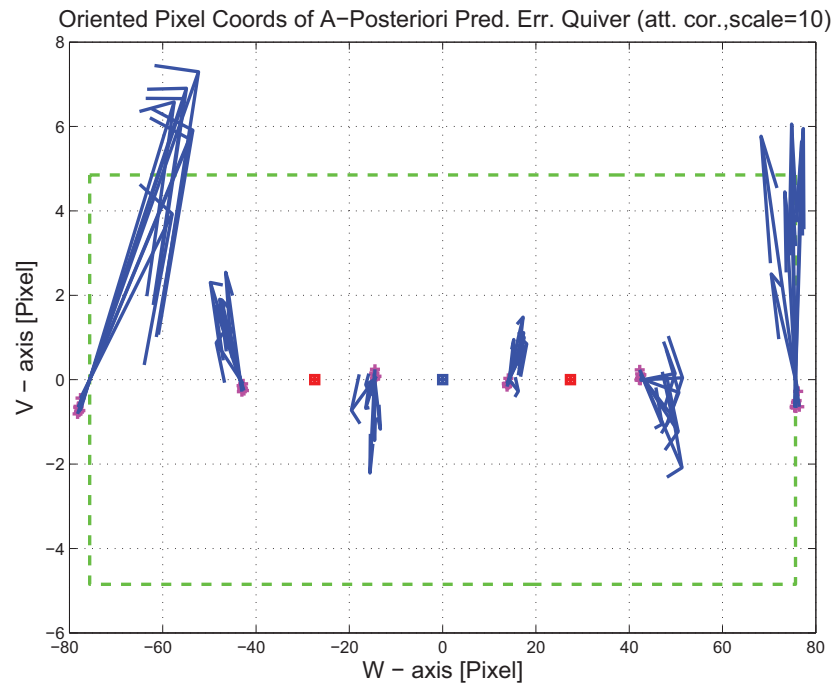


Figure 3.20: A-Posteriori Science Centroid Prediction Error Quiver (Att. Cor.)

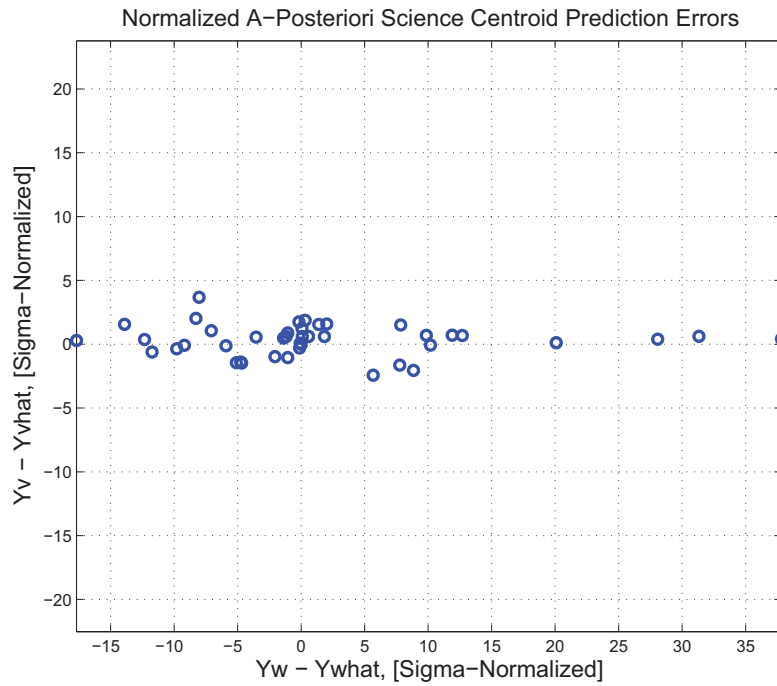


Figure 3.21: Normalized A-Posteriori Science Centroid Prediction Errors

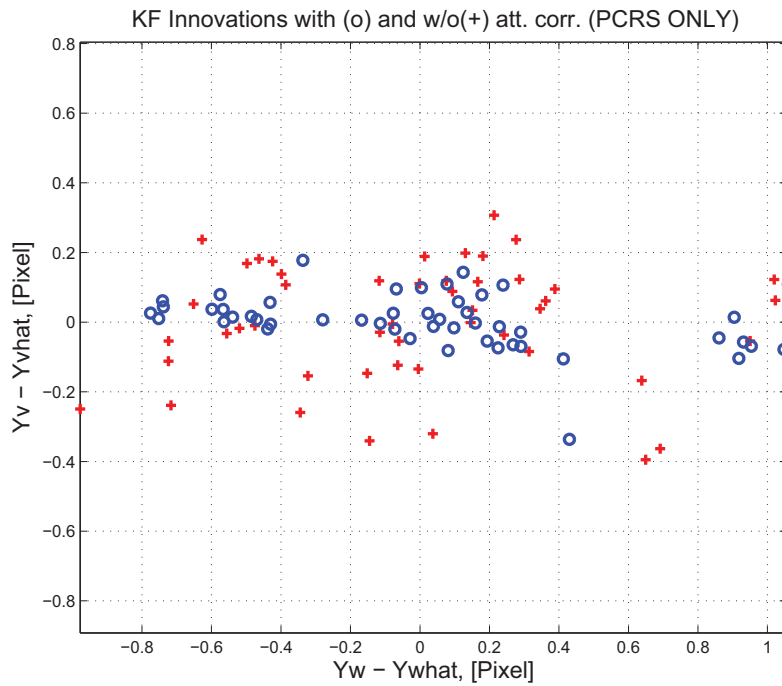


Figure 3.22: KF innovations with (o) and w/o (+) attitude corrections (PCRS)

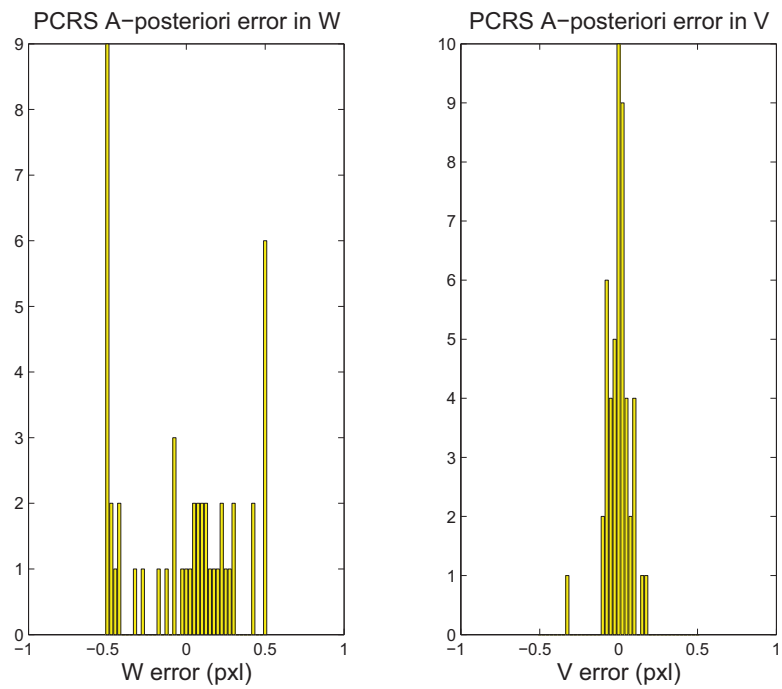


Figure 3.23: Histograms of PCRS a-posteriori residuals (or innovations)

IPF PCRS SUMMARY						
PCRS 1 (Total of 35 centroids)						
RMS	MEAN		SIGMA			
METRIC	APOST.	ATT. COR.	APOST.	ATT. COR.	STAT. CONF.	UNITS
Radial	0.0181	0.0167	0.5918	0.5683	0.0961	arcsec
W-axis	-0.0008	0.0018	0.5668	0.5628	0.0951	arcsec
V-axis	-0.0181	-0.0166	0.1701	0.0792	0.0134	arcsec
PCRS 2 (Total of 14 centroids)						
METRIC	APOST.	ATT. COR.	APOST.	ATT. COR.	STAT. CONF.	UNITS
Radial	0.0449	0.0462	0.2400	0.1479	0.0395	arcsec
W-axis	-0.0051	-0.0025	0.1814	0.1363	0.0364	arcsec
V-axis	0.0446	0.0461	0.1571	0.0573	0.0153	arcsec
Combined (Total of 49 centroids)						
METRIC	APOST.	ATT. COR.	APOST.	ATT. COR.	STAT. CONF.	UNITS
Radial	0.0020	0.0015	0.5171	0.4876	0.0697	arcsec
W-axis	-0.0020	0.0006	0.4888	0.4812	0.0687	arcsec
V-axis	-0.0002	0.0014	0.1689	0.0789	0.0113	arcsec

Table 3.3: PCRS measurement prediction error summary

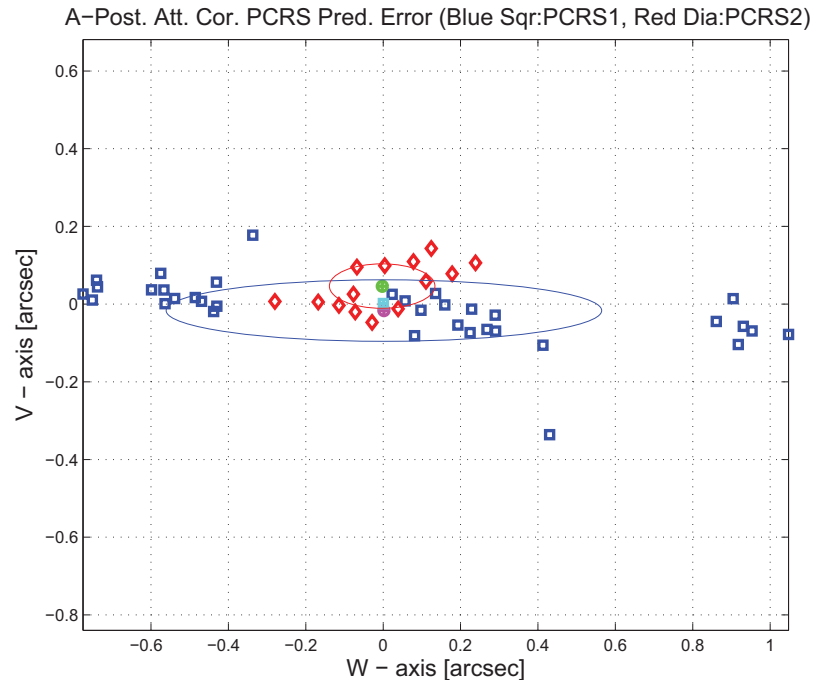


Figure 3.24: A-posteriori PCRS Prediction Summary

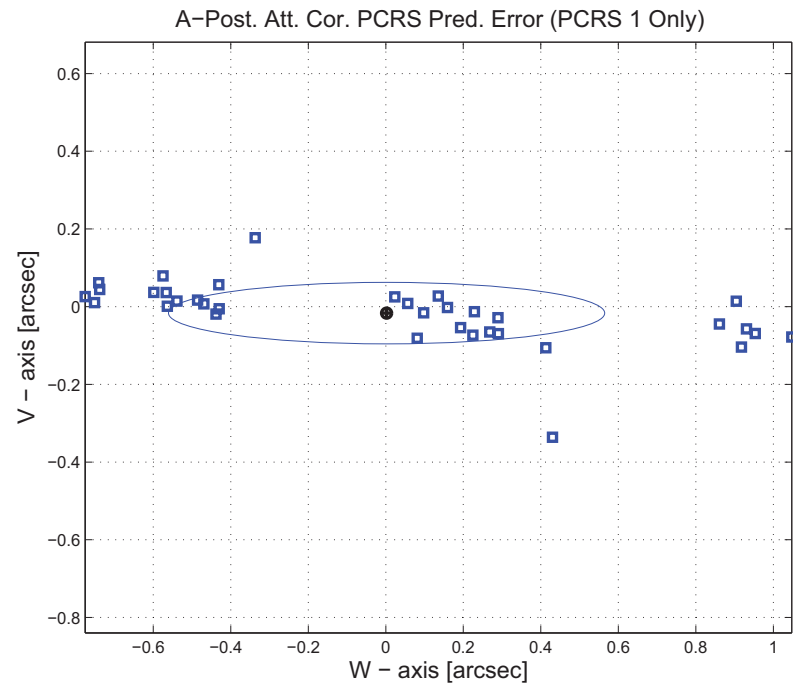


Figure 3.25: A-posteriori PCRS Prediction (PCRS 1 Only)

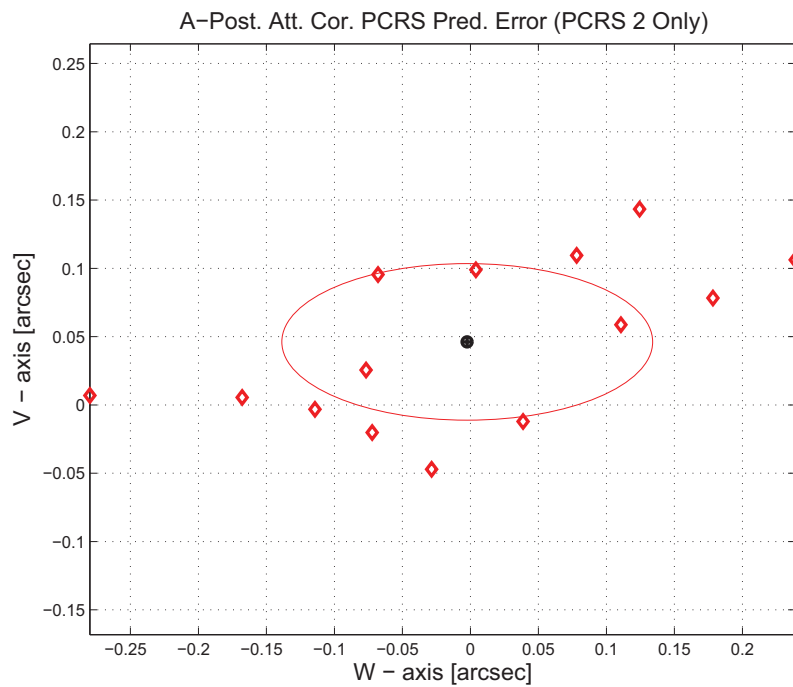


Figure 3.26: A-posteriori PCRS Prediction (PCRS 2 Only)

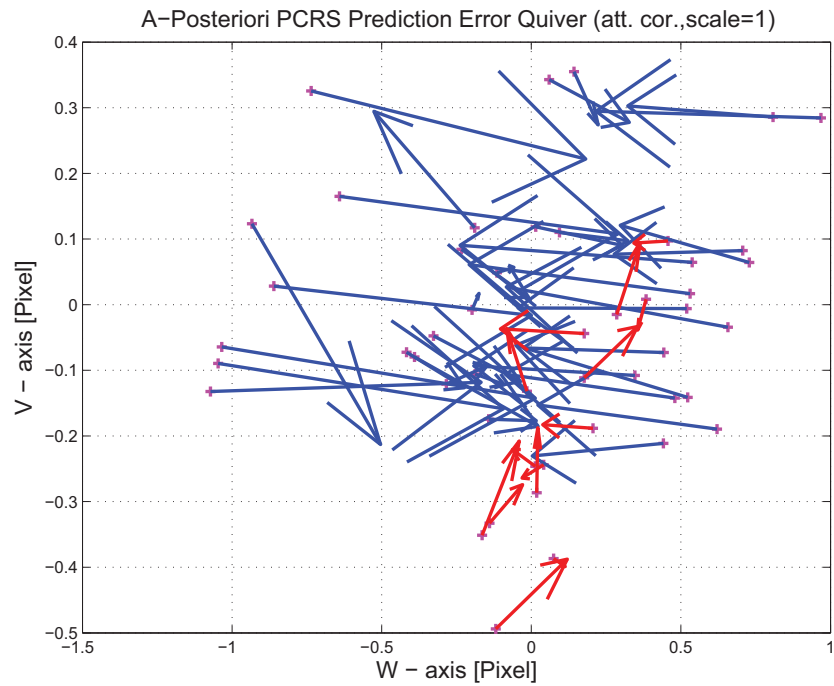


Figure 3.27: A-Posteriori PCRS Prediction Errors Quiver (Att. Cor.)

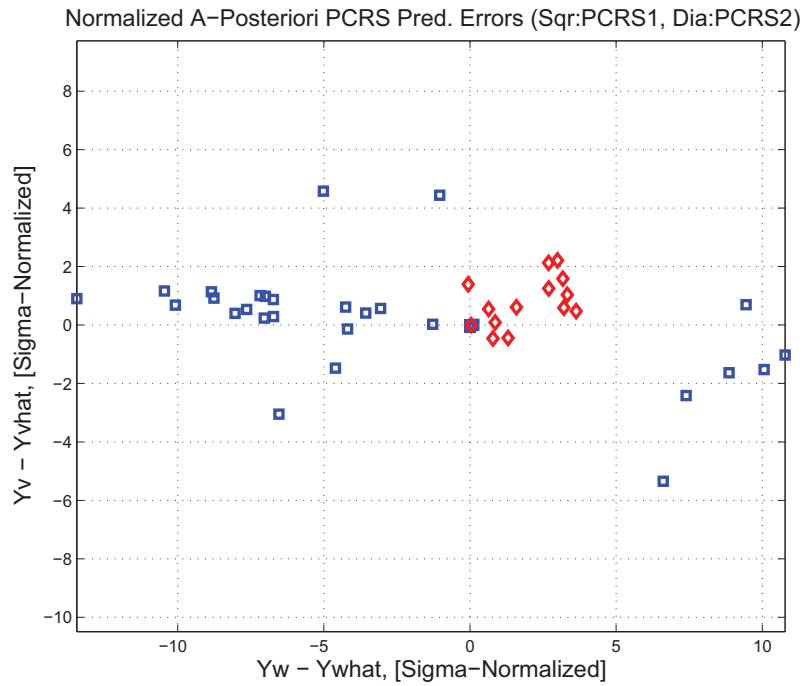


Figure 3.28: Normalized A-Posteriori PCRS Prediction Errors

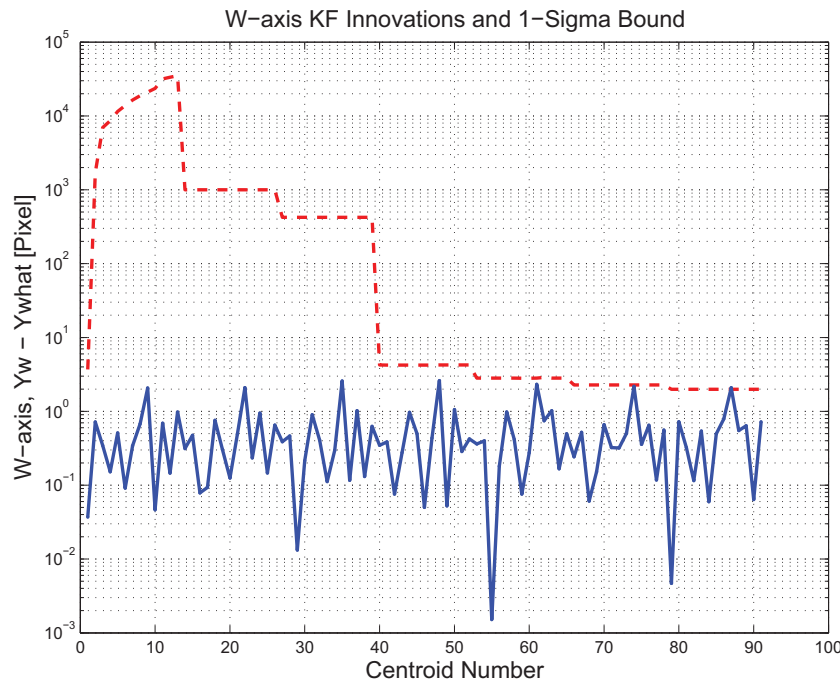


Figure 3.29: W-axis KF innovations and 1-sigma bound

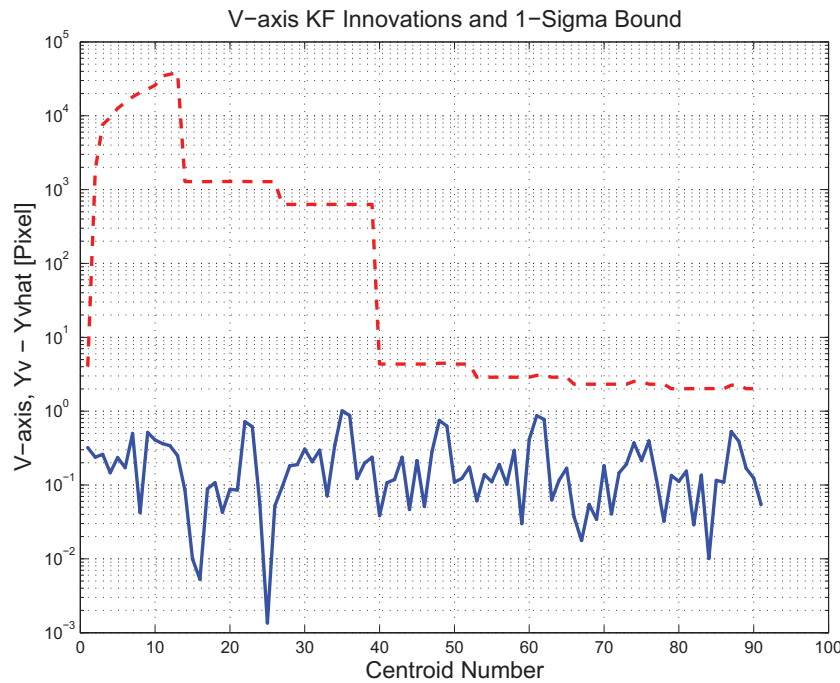


Figure 3.30: V-axis KF innovations and 1-sigma bound

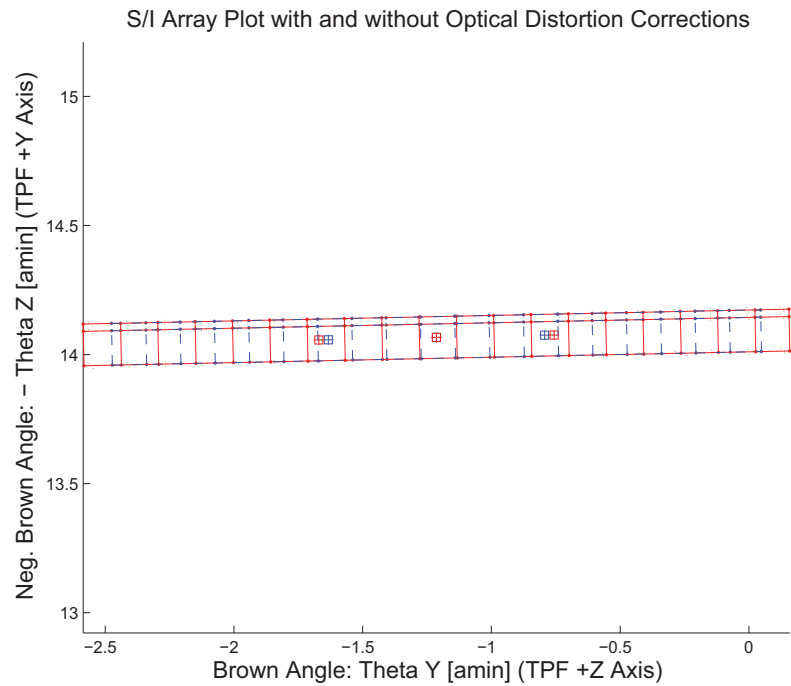


Figure 3.31: Array plot with (solid) and w/o (dashed) optical distortion corrections

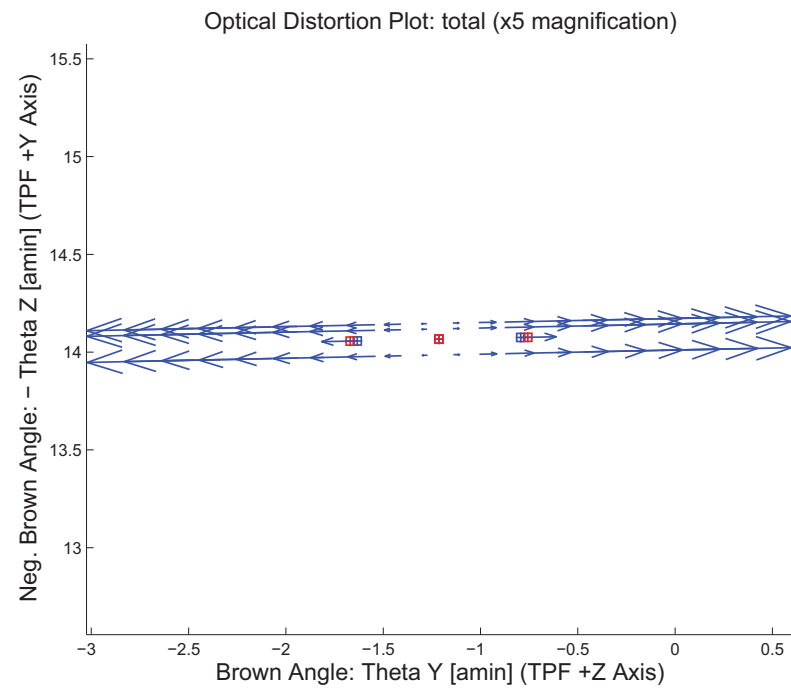


Figure 3.32: Optical Distortion Plot: total (x5 magnification)

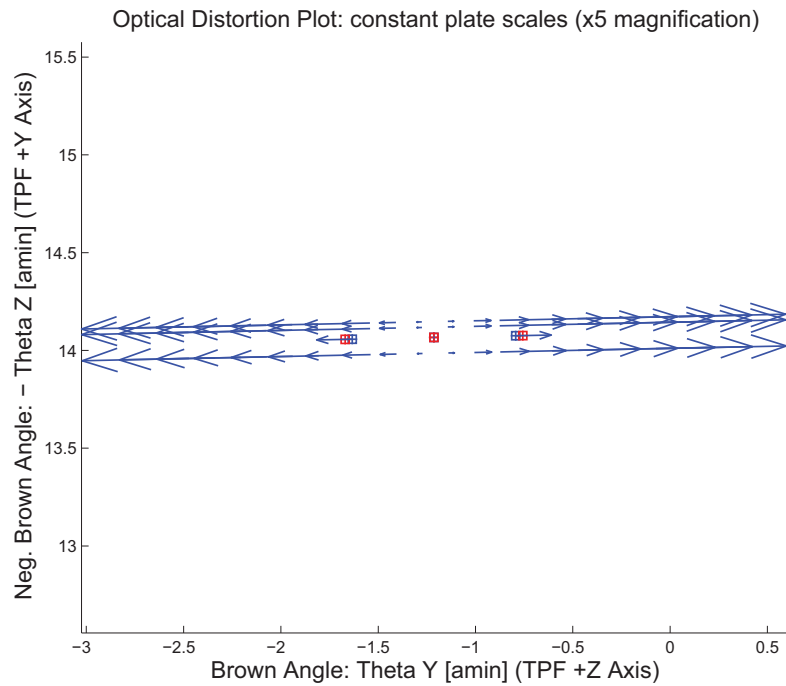


Figure 3.33: Optical Distortion Plot: constant plate scales (x5 magnification)

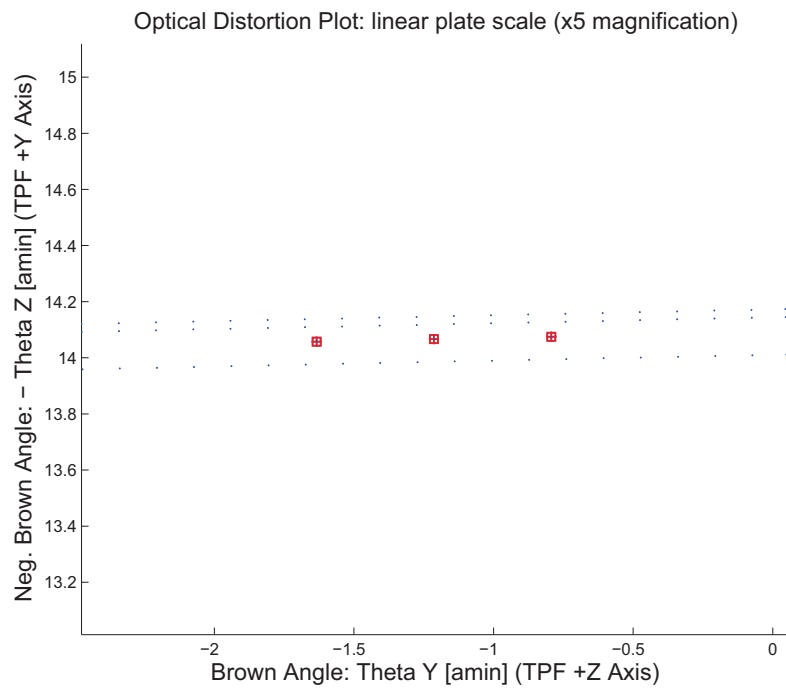


Figure 3.34: Optical Distortion Plot: linear plate scale (x5 magnification)

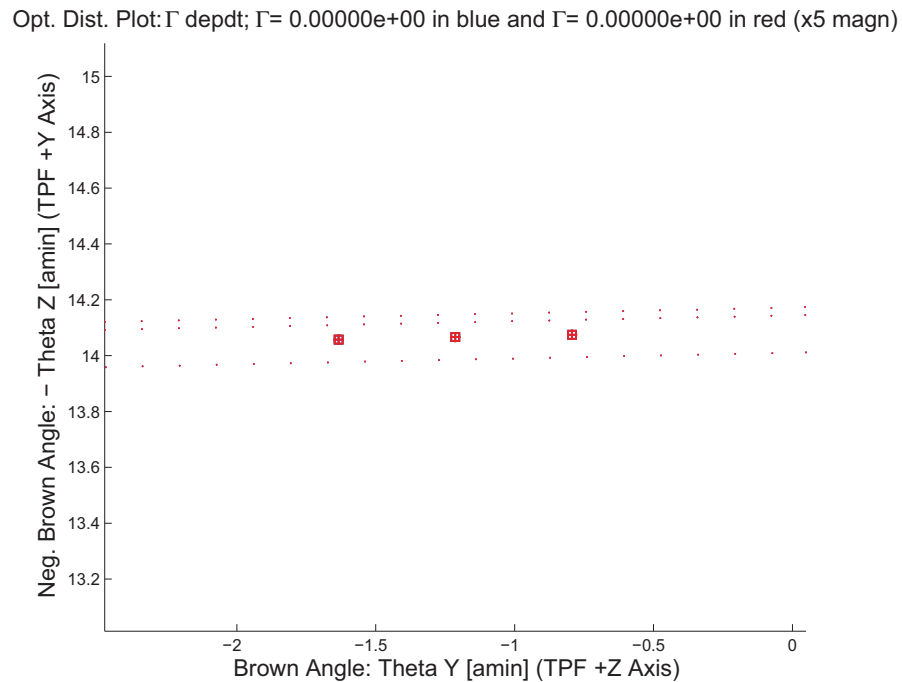


Figure 3.35: Optical Distortion Plot: gamma terms (x5 magnification)

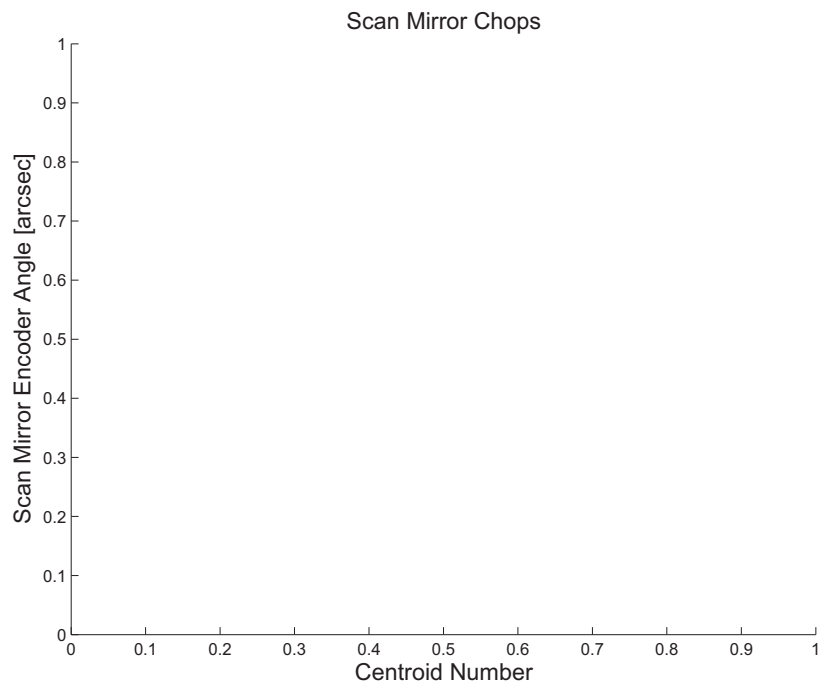


Figure 3.36: Scan Mirror Chops

IPF Frame Reconstruction (P:Blue,I(1):Green,I(2):Red,I(3):Cyan,I(4):magenta,...)

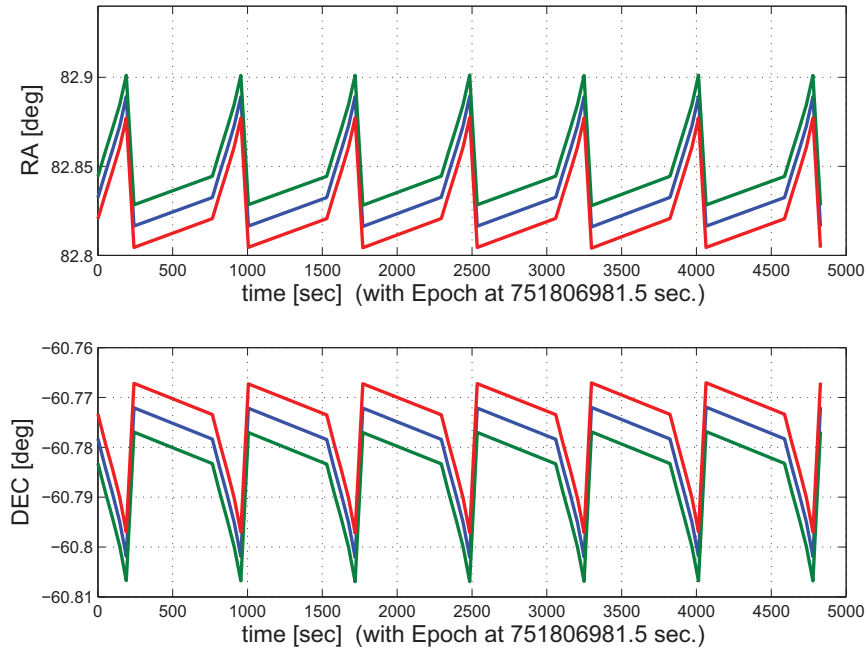


Figure 3.37: IPF Frame Reconstruction

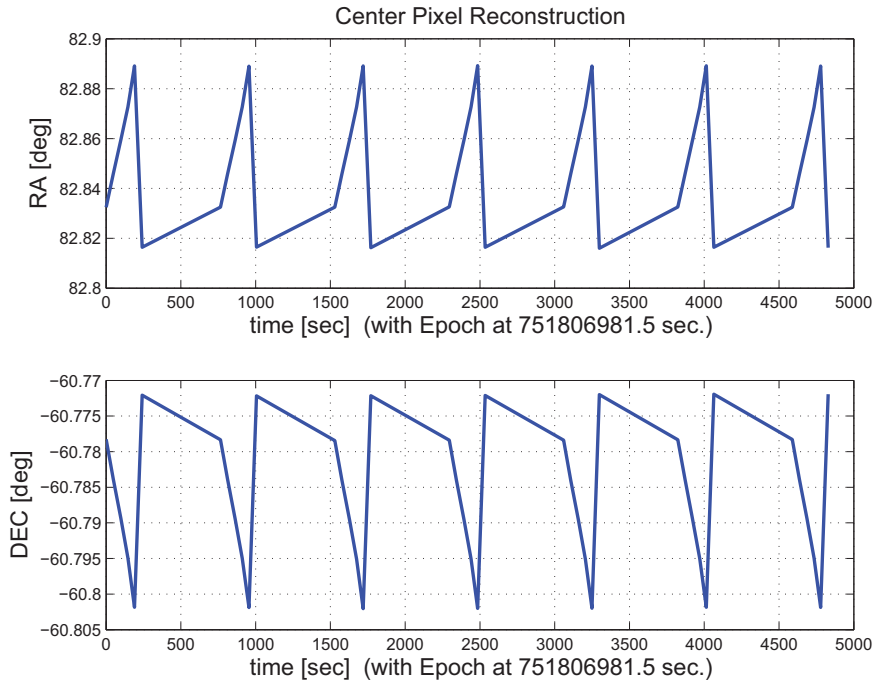


Figure 3.38: Center Pixel Reconstruction

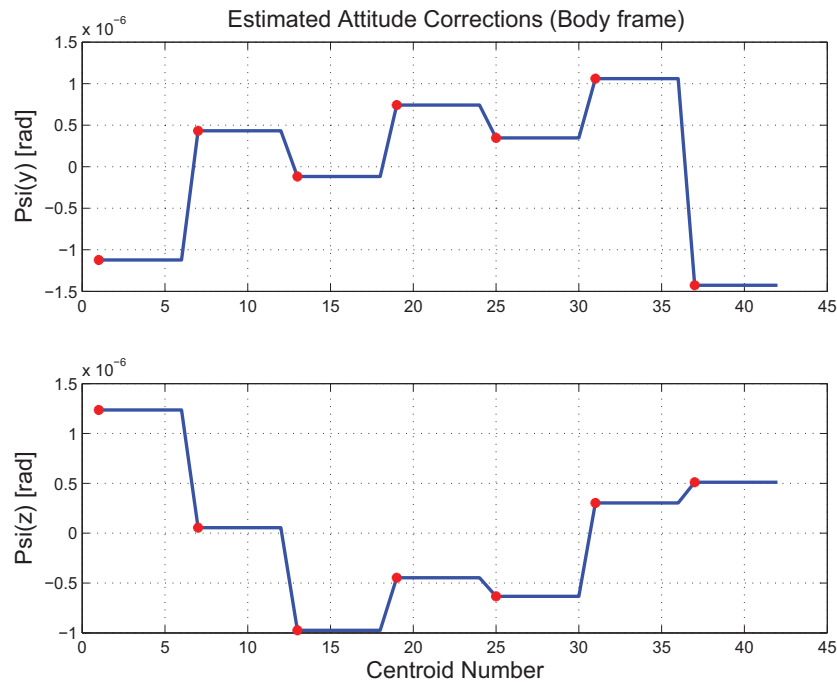


Figure 3.39: Estimated attitude corrections (Body frame)

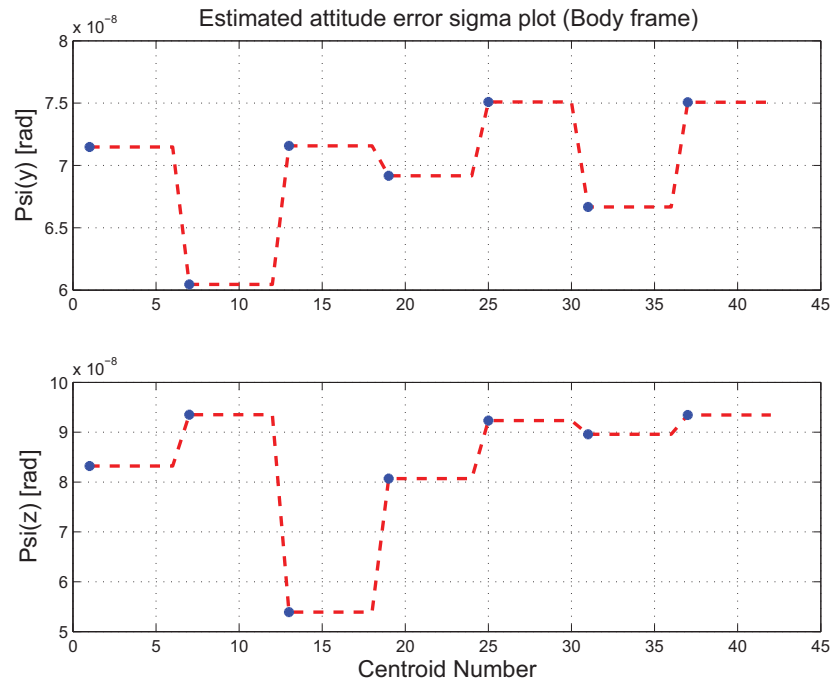


Figure 3.40: Estimated attitude error sigma plot (Body frame)

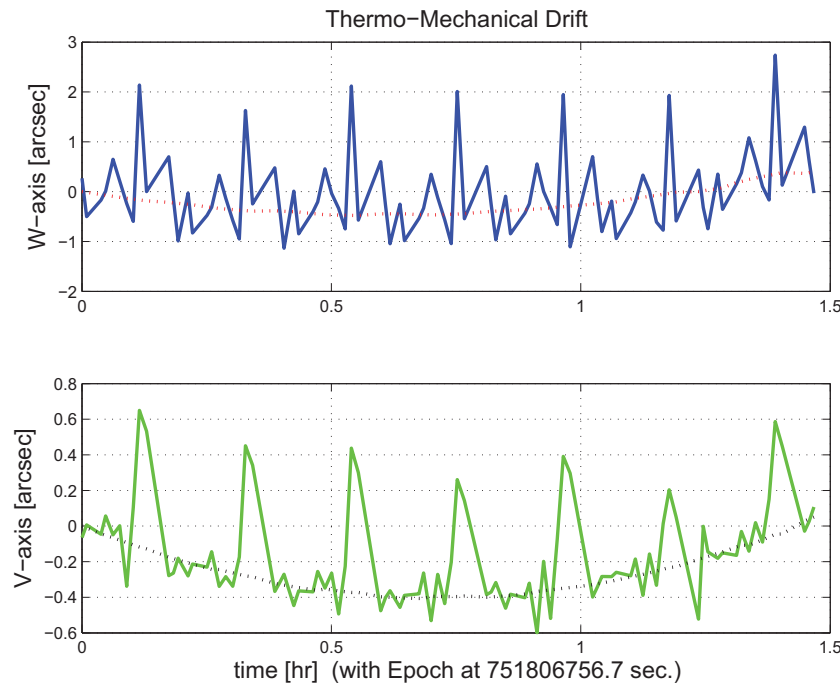


Figure 3.41: Thermo-mechanical boresight drift (equiv. angle in (W,V) coords)

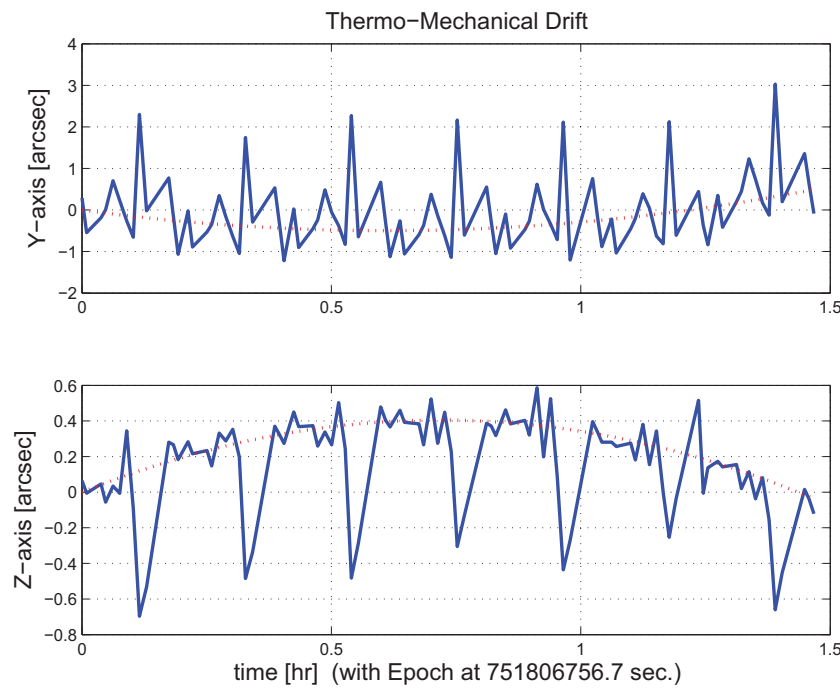


Figure 3.42: Thermo-mechanical boresight drift (equiv. angle in Body frame)

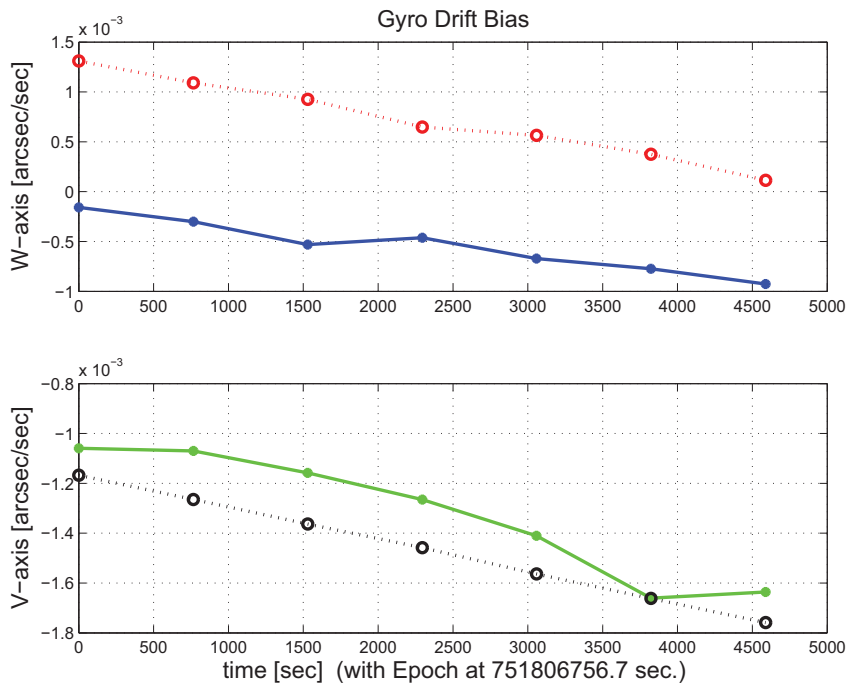


Figure 3.43: Gyro drift bias contribution (equiv. rate in (W,V) coords)

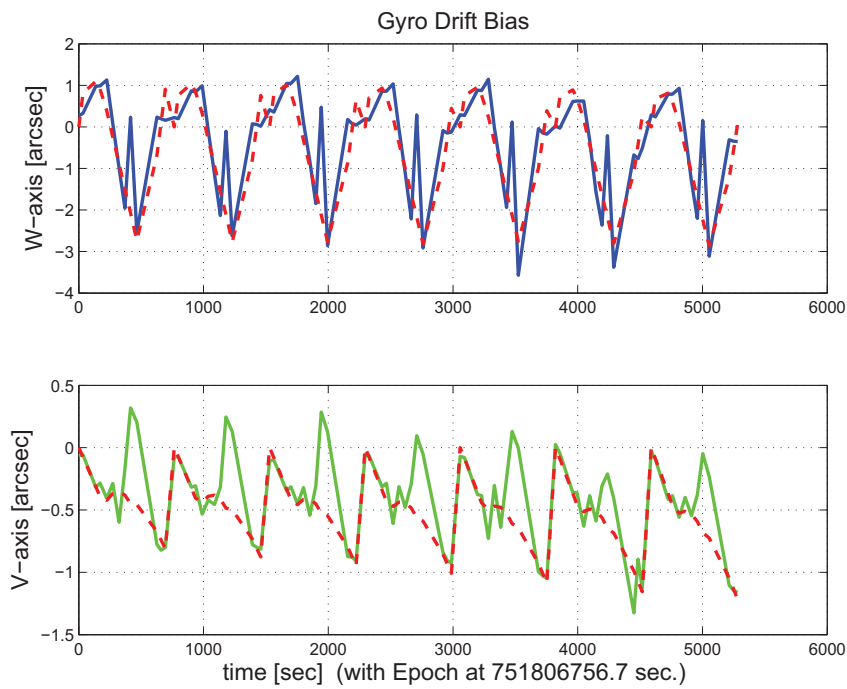


Figure 3.44: Gyro drift bias contribution (equiv. angle in (W,V) coords)

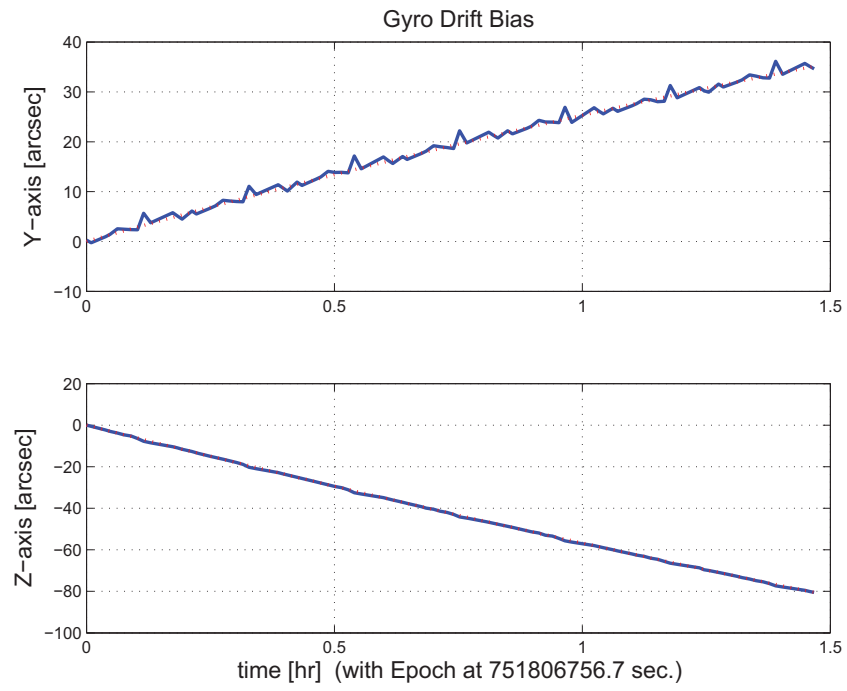


Figure 3.45: Gyro drift bias contribution (equiv. angle in Body frame)

3.2 IPF OUTPUT DATA (IF MINI FILE)

OUTPUT FILE NAME: IFmini501046.dat DATE: 06-Nov-2003 TIME: 16:22
 INSTRUMENT NAME: IRS_LongLo_2nd_Ord_Center_Pos NF: 46
 IPF FILTER VERSION: IPF.V3.0.OB SW RELEASE DATE: November 3, 2003
 FRAME TABLE USED: BodyFrames_FTU_12b

IPF BROWN ANGLE SUMMARY						
Frame Number	WAS			IS		
	theta_Y (arcmin)	theta_Z (arcmin)	angle (deg)	theta_Y (arcmin)	theta_Z (arcmin)	angle (deg)
046	-1.191436	-14.057499	-1.199999	-1.213355	-14.066157	-1.199999
044	-0.771250	-14.066300	-1.199999	-0.756576	-14.075725	-1.199999
045	-1.611621	-14.048697	-1.199999	-1.670133	-14.056588	-1.199999
OFFSET	NF	Delta_CW	Delta_CV			
0	46	+0.000	+0.000	pixels		
OFFSET FRAME NAME: IRS_LongLo_2nd_Ord_Center_Pos						
Brown Angle	theta_Y(arcmin)	theta_Z(arcmin)	angle(deg)			
WAS(FTB)	-1.191436	-14.057499	-1.199999			
IS (EST)	-1.213355	-14.066157	-1.199999			
dT_EST	-0.021919	-0.008658	+0.000000			
T_sSIGMA	+0.003788	+0.001899	+999.999999			
dT_EST/T_sSIGMA	-5.787047	-4.559480	+999.999999			
OFFSET	NF	Delta_CW	Delta_CV			
1	44	+25.217	+0.000	pixels		
OFFSET FRAME NAME: IRS_LongLo_2nd_Ord_1st_Pos						
Brown Angle	theta_Y(arcmin)	theta_Z(arcmin)	angle(deg)			
WAS(FTB)	-0.771250	-14.066300	-1.199999			
IS (EST)	-0.756576	-14.075725	-1.199999			
dT_EST	+0.014674	-0.009424	+0.000000			
T_sSIGMA	+0.003773	+0.001899	+999.999999			
dT_EST/T_sSIGMA	+3.888972	-4.963152	+999.999999			
OFFSET	NF	Delta_CW	Delta_CV			
2	45	-25.217	+0.000	pixels		
OFFSET FRAME NAME: IRS_LongLo_2nd_Ord_2nd_Pos						
Brown Angle	theta_Y(arcmin)	theta_Z(arcmin)	angle(deg)			
WAS(FTB)	-1.611621	-14.048697	-1.199999			
IS (EST)	-1.670133	-14.056588	-1.199999			
dT_EST	-0.058512	-0.007891	+0.000000			
T_sSIGMA	+0.003893	+0.001899	+999.999999			
dT_EST/T_sSIGMA	-15.028950	-4.155808	+999.999999			

VARNAME	MEAN	SIGMA	SCALED_SIGMA			
a00	+8.7087059734473921E-002	+1.8550694274955656E-004	+1.4095567491438092E-003			
del_theta2	-1.7518277313947214E-014	+1.4500085544656167E-007	+1.1017751217120710E-006			
del_theta3	+3.4675495452122054E-015	+7.2692833544583638E-008	+5.5234953807355709E-007			
del_arx	+1.6425949765945178E-011	+3.6633348310265572E-005	+2.7835499086512885E-004			
del_ary	+3.4224666295231570E-013	+4.3993293574104180E-006	+3.3427883051342969E-005			
del_arz	-8.4211713066441692E-013	+4.0792329893131760E-006	+3.0995661435589091E-005			
brx	+2.9656568426812921E-008	+2.8952747476160805E-008	+2.1999468055691628E-007			
bry	-2.233331251775778E-009	+4.3871995196643014E-009	+3.3335715640206553E-008			
brz	+1.5563944305242550E-009	+4.1242772911035891E-009	+3.1337926251439489E-008			
crx	-1.7774342237371903E-011	+1.0898788881032822E-011	+8.2813404161877614E-011			
cry	+1.0143783575591715E-012	+1.8422976924859287E-012	+1.3998522685382428E-011			
crz	-6.0094371338563961E-013	+1.7330505898880320E-012	+1.3168419032608820E-011			
bgx	+2.8232266534456791E-005	+4.4233078301059855E-007	+3.3610081181079968E-006			
bgy	+3.8098926041930816E-008	+4.4745757139576926E-009	+3.3999635289548326E-008			
bgz	-8.1962416925918002E-008	+4.343475666335018E-009	+3.3003484127872590E-008			
cgx	-7.8939947757848371E-010	+1.2993823683863301E-010	+9.8732325590105030E-010			

```

cgx      -2.2141187166949426E-012 +1.8651092587919847E-012 +1.4171854188606285E-011
cgy      +3.0656294541405311E-012 +1.7751701953931605E-012 +1.3488460823665563E-011
-----
LSQF RESIDUAL SIGMA SCALE =      +7.5984042874706841E+000
-----

-----
qT          qT(1)           qT(2)           qT(3)           qT(4)
FrmTbl:   -1.0472111423572201E-002 +1.5186702891322200E-004 +2.0462813840178202E-003 +9.9994306065457295E-001
Estim:    -1.0472117690675119E-002 +1.5504167371163980E-004 +2.0475739086400074E-003 +9.9994305745589374E-001
DelTheta   deltheta(1)       deltheta(2)       deltheta(3)       [rad]
          +7.7442964587631684E-012 +6.3218837687852156E-006 +2.6514037087822358E-006
EulAngT   theta(1)         theta(2)         theta(3)         [rad]
Mean      -2.0943940287392777E-002 +3.5295056771994331E-004 +4.0916790717227996E-003
SigmaT   +9.9999000000000000E+004 +1.4500085544656167E-007 +7.2692833544583638E-008
-----
qR          qR(1)           qR(2)           qR(3)           qR(4)
ASFILE:   +7.0881651481613517E-004 +1.2701130472123623E-003 -1.6120732470881194E-004 +9.9999892711639404E-001
Estim:    +1.0215080139473318E-003 +1.2686557789608512E-003 -1.6268806527535597E-004 +9.9999866028234530E-001
DelThetaR  delthetaR(1)     delthetaR(2)     delthetaR(3)     [rad]
          +6.2538695137703739E-004 -2.8144612110693130E-006 -2.1660711838229870E-006
EulAngR   angR(1)         angR(2)         angR(3)         [rad]
Mean      +2.0426084977168170E-003 +2.5376432565466425E-003 -3.2278485546090535E-004
SigmaR   +3.6633348310265572E-005 +4.3993293574104180E-006 +4.0792329893131760E-006
-----
Initial Gyro Bias   Bg0(1)           Bg0(2)           Bg0(3)
                  -3.9456122635783686E-007 -1.9791467309460131E-007 +3.5724215763366368E-007
Gyro Bias Correction Bg(1)            Bg(2)            Bg(3)
                  +2.8232266534456791E-005 +3.8098926041930816E-008 -8.1962416925918002E-008
Total Gyro Bias     BgT(1)           BgT(2)           BgT(3)
                  +2.7837705308098954E-005 -1.5981574705267051E-007 +2.7527974070774571E-007
-----
Initial Gyro Bias Rate   Cg0(1)           Cg0(2)           Cg0(3)
                  +0.0000000000000000E+000 +0.0000000000000000E+000 +0.0000000000000000E+000
Gyro Bias Rate Correction Cg(1)            Cg(2)            Cg(3)
                  -7.8939947757848371E-010 -2.2141187166949426E-012 +3.0656294541405311E-012
Total Gyro Bias Rate     CgT(1)           CgT(2)           CgT(3)
                  -7.8939947757848371E-010 -2.2141187166949426E-012 +3.0656294541405311E-012
-----
OFFSET        NF        Delta_CW        Delta_CV
1             44        +25.217       +0.000      pixels
OFFSET FRAME NAME: IRS_LongLo_2nd_Ord_1st_Pos
qT          qT(1)           qT(2)           qT(3)           qT(4)
WAS(FTB)   -1.0471986686530507E-002 +9.0743583791269851E-005 +2.0469215081935811E-003 +9.9994306806576672E-001
IS (EST)   -1.0471982004376953E-002 +8.8595167716008834E-005 +2.0482697793983481E-003 +9.9994306554658763E-001
-----
DelTheta   deltheta(1)       deltheta(2)       deltheta(3)
Units      rad              rad              rad
          +2.6530683673238680E-010 -4.3248443909307799E-006 +2.6514036833921420E-006
EulAngT   theta(1)         theta(2)         theta(3)         [rad]
Mean      -2.0943940287392777E-002 +2.2007913751363959E-004 +4.0944623300515123E-003
sSigmaT   +7.3407572358101482E-011 +1.0975571888383877E-006 +5.5234953329671373E-007
SigmaT   +9.6609195274258030E-012 +1.4444574772734773E-007 +7.2692832915919623E-008
-----
OFFSET        NF        Delta_CW        Delta_CV
2             45        -25.217       +0.000      pixels
OFFSET FRAME NAME: IRS_LongLo_2nd_Ord_2nd_Pos
qT          qT(1)           qT(2)           qT(3)           qT(4)
WAS(FTB)   -1.0472235965025410E-002 +2.1299047378733321E-004 +2.0456412521181223E-003 +9.9994304950873003E-001
IS (EST)   -1.0472253145834918E-002 +2.2148817940059127E-004 +2.0468780287463749E-003 +9.9994304495174691E-001
-----
DelTheta   deltheta(1)       deltheta(2)       deltheta(3)
Units      rad              rad              rad
          -1.9293937098254712E-010 +1.6968611929330830E-005 +2.6514036667856604E-006
EulAngT   theta(1)         theta(2)         theta(3)         [rad]
Mean      -2.0943940287392777E-002 +4.8582199792351303E-004 +4.0888958131330352E-003

```

```

sSigmaT +7.3407572358101586E-011 +1.1325087178959285E-006 +5.5234953304428468E-007
SigmaT +9.6609195274258175E-012 +1.4904559892441732E-007 +7.2692832882698302E-008
-----
          q(1)           q(2)           q(3)           q(4)
PCRS1A: +5.3371888965461637E-007 +3.744423778550031E-004 -1.4253684912431913E-003 +9.9999891405806784E-001
PCRS2A: -5.2779261998836216E-007 +3.8462959425181312E-004 +1.3722087221825403E-003 +9.9999898455099423E-001
*****
***** CS-FILE PARAMETERS: ***** AS-FILE PARAMETERS: *****
Row (01) PIX2RADX: +4.8481368110953598E-006 Row (1) TASTART: +7.5180600019071960E+008
Row (02) PIX2RADY: +4.8481368110953598E-006 Row (2) TASTOP: +7.5181300009075010E+008
Row (03) CXO: +0.0000000000000000E+000 Row (3) S/C TIME: +7.5180061489077759E+008
Row (04) CYO: +0.0000000000000000E+000 Row (4) QR1: +7.0881651481613517E-004
Row (05) BETA0: +9.9999000000000000E+004 Row (5) QR2: +1.2701130472123623E-003
Row (06) GAMMA_E0: +9.9999000000000000E+004 Row (6) QR3: -1.6120732470881194E-004
Row (07) D11: +1.0000000000000000E+000 Row (7) QR4: +9.9999892711639404E-001
Row (08) D12: +0.0000000000000000E+000
Row (09) D21: +0.0000000000000000E+000
Row (10) D22: +1.0000000000000000E+000
Row (11) DG: +9.9999000000000000E+004
-----
INITIAL STA-TO-PCRS ALIGNMENT (R) KNOWLEDGE (1-SIGMA)
    SIGMA(X)      SIGMA(Y)      SIGMA(Z)
5.92901382E+000  3.88856458E-001  3.89101386E-001 [arcsec]
-----
PIX2RADX = 4.848136811095E-006 [rad/pixel]
XPIXSIZE = 1.0000 [arcsec]
PIX2RADY = 4.848136811095E-006 [rad/pixel]
YPIXSIZE = 1.0000 [arcsec]
CX0 = 0.0 [pixel] = 0.00 [arcsec]
CY0 = 0.0 [pixel] = 0.00 [arcsec]
-----
NOMINAL BETA0 = 9.99990000000000E+004 [rad/encoder unit]
ENCODER UNIT SIZE = 99999.00 [arcsec]
GAMMA_E0 = 99999.00 [encoder unit] = 99999.00 [arcsec]
-----
| +1 | +0 |
FLIP MATRIX D = |----|----| and DG = +99999
| +0 | +1 |
-----
```

3.3 IPF EXECUTION LOG

```

*****
IPF EXECUTION-LOG FILE NAME: LG501046.dat
INSTRUMENT TYPE: IRS_LongLo_2nd_Ord_Center_Pos
IPF FILTER EXECUTION DATE: 06-Nov-2003 TIME: 16:21
IPF FILTER VERSION USED: IPF.V3.0.OB
*****
```

SLIT FLAG ENABLED! ENTERING SLIT MODE.

```

----- Loading & Preparing Input Files -----
AAFILE: AA501046 Loaded! AAFILE dimension = 70000 X 21
ASFILE: AS501046 Loaded!
CAFFILE: CA501046 Loaded! CAFFILE dimension = 42 X 15
```

```

CBFILE: CB501046 Loaded!          CBFILe dimension = 49 X 15
CCFILE: CC501046 Created!        CCFILE dimension = 91 X 19
CSFILE: CS501046 Loaded!
Loading Input Files Completed!
-----
----- Selected Mask Vectors -----
index =  1  2  3  4  5  6  7  8  9 10 11 12 13 14 15 16 17 18 19 20
-----
mask1 = [ 1  0  0  0  0  0  0  0  0  0  0  0  0  0  0  0  0  0  0  0 ]
mask2 = [ 0  0  0  1  1  1  1  1  1  1  1  1  1  1  1  1  1  1  1  1 ]
-----
----- Selected Initial Gyro Bias Parameters -----
User Entered 1 : Use AFILE database - from S/C filter
IPF Linearized Using Following Nominal Gyro Bias Estimates
bg0 = [-3.9456122635783686E-007 -1.9791467309460131E-007 +3.5724215763366368E-007 ]
cg0 = [+0.0000000000000000E+000 +0.0000000000000000E+000 +0.0000000000000000E+000 ]
-----
----- Gyro Pre-Processor Run Completed -----
AGFILE CREATED: AG501046.m      ACFILE CREATED: AC501046.m
-----
Total Gyro Preprocessor Execution Time: 38 seconds

FRAME TABLE ENTRIES FOR PCRS LOADED TO TPCRS
q_PCRS4 = [ +5.3371888965461637E-007   q_PCRS5 = [ +7.3379987833742897E-007
             +3.7444233778550031E-004           +5.2236196154513707E-004
             -1.4253684912431913E-003           -1.4047712280184723E-003
             +0.9999891405806784E-001 ];       +9.999887687698918E-001 ];
q_PCRS8 = [ -5.2779261998836216E-007   q_PCRS9 = [ -7.1963421681856818E-007
             +3.8462959425181312E-004           +5.3239763239987400E-004
             +1.3722087221825403E-003           +1.3516841804518383E-003
             +9.9999898455099423E-001 ];       +9.9999894475050310E-001 ];
-----
----- Initial Conditions for State ----- ----- Initial Square-Root Cov (diag) -----
p1(01) = a00 = +0.0000000000000000E+000 Sigma_initial(01,01) = 1.0000000000000000E+000
p1(02) = b00 = +0.0000000000000000E+000 Sigma_initial(02,02) = 9.9999000000000000E+004
p1(03) = c00 = +0.0000000000000000E+000 Sigma_initial(03,03) = 9.9999000000000000E+004
p1(04) = a10 = +0.0000000000000000E+000 Sigma_initial(04,04) = 9.9999000000000000E+004
p1(05) = b10 = +0.0000000000000000E+000 Sigma_initial(05,05) = 9.9999000000000000E+004
p1(06) = c10 = +0.0000000000000000E+000 Sigma_initial(06,06) = 9.9999000000000000E+004
p1(07) = d10 = +0.0000000000000000E+000 Sigma_initial(07,07) = 9.9999000000000000E+004
p1(08) = a20 = +0.0000000000000000E+000 Sigma_initial(08,08) = 9.9999000000000000E+004
p1(09) = b20 = +0.0000000000000000E+000 Sigma_initial(09,09) = 9.9999000000000000E+004
p1(10) = c20 = +0.0000000000000000E+000 Sigma_initial(10,10) = 9.9999000000000000E+004
p1(11) = d20 = +0.0000000000000000E+000 Sigma_initial(11,11) = 9.9999000000000000E+004
p1(12) = a01 = +0.0000000000000000E+000 Sigma_initial(12,12) = 9.9999000000000000E+004
p1(13) = b01 = +0.0000000000000000E+000 Sigma_initial(13,13) = 9.9999000000000000E+004
p1(14) = c01 = +0.0000000000000000E+000 Sigma_initial(14,14) = 9.9999000000000000E+004
p1(15) = d01 = +0.0000000000000000E+000 Sigma_initial(15,15) = 9.9999000000000000E+004
p1(16) = e01 = +0.0000000000000000E+000 Sigma_initial(16,16) = 9.9999000000000000E+004
p1(17) = f01 = +0.0000000000000000E+000 Sigma_initial(17,17) = 9.9999000000000000E+004
-----
p2f(01) = am1 = +0.0000000000000000E+000 Sigma_initial(18,18) = 9.9999000000000000E+004
p2f(02) = am2 = +0.0000000000000000E+000
p2f(03) = am3 = +1.0000000000000000E+000
p2f(04) = beta = +1.0000000000000000E+000 Sigma_initial(19,19) = 9.9999000000000000E+004
p2f(05) = qT1 = -1.0472111423572203E-002 Sigma_initial(20,20) = 9.9999000000000000E+004
p2f(06) = qT2 = +1.5186702891322202E-004 Sigma_initial(21,21) = 1.0000000000000000E-002
p2f(07) = aT3 = +2.0462813840178206E-003 Sigma_initial(22,22) = 1.0000000000000000E-002
p2f(08) = qT4 = +9.9994306065457306E-001 Sigma_initial(23,23) = 2.8744670171590572E-004
p2f(09) = qR1 = +7.0881651481613517E-004 Sigma_initial(24,24) = 1.8852293090869427E-005
p2f(10) = qR2 = +1.2701130472123623E-003 Sigma_initial(25,25) = 1.8864167538600070E-005
p2f(11) = qR3 = -1.6120732470881194E-004
p2f(12) = qR4 = +9.9999892711639404E-001
p2f(13) = brx = +0.0000000000000000E+000 Sigma_initial(26,26) = 1.8931761719946324E-004
p2f(14) = bry = +0.0000000000000000E+000 Sigma_initial(27,27) = 1.8931761719946324E-004

```

```

p2f(15) = brz = +0.0000000000000000E+000 Sigma_initial(28,28) = 1.8931761719946324E-004
p2f(16) = crx = +0.0000000000000000E+000 Sigma_initial(29,29) = 3.5841160182082498E-008
p2f(17) = cry = +0.0000000000000000E+000 Sigma_initial(30,30) = 3.5841160182082498E-008
p2f(18) = crz = +0.0000000000000000E+000 Sigma_initial(31,31) = 3.5841160182082498E-008
p2f(19) = bgx = +0.0000000000000000E+000 Sigma_initial(32,32) = 1.8931761719946324E-004
p2f(20) = bgy = +0.0000000000000000E+000 Sigma_initial(33,33) = 1.8931761719946324E-004
p2f(21) = bgz = +0.0000000000000000E+000 Sigma_initial(34,34) = 1.8931761719946324E-004
p2f(22) = cgx = +0.0000000000000000E+000 Sigma_initial(35,35) = 3.5841160182082498E-008
p2f(23) = cgy = +0.0000000000000000E+000 Sigma_initial(36,36) = 3.5841160182082498E-008
p2f(24) = cgz = +0.0000000000000000E+000 Sigma_initial(37,37) = 3.5841160182082498E-008
-----
```

```

----- IPF KALMAN FILTER STARTED -----
Iteration#001: |dp|= +8.068130952310E-002 RMS(|Res|)=+2.480525940856E-005
Iteration#002: |dp|= +6.005977700155E-003 RMS(|Res|)=+5.994619131417E-006
Iteration#003: |dp|= +8.828769125933E-004 RMS(|Res|)=+5.513765426073E-006
Iteration#004: |dp|= +1.348843067015E-004 RMS(|Res|)=+5.427948910205E-006
Iteration#005: |dp|= +2.062901669707E-005 RMS(|Res|)=+5.415362981450E-006
Iteration#006: |dp|= +3.181587726527E-006 RMS(|Res|)=+5.414351443648E-006
Iteration#007: |dp|= +4.878426484961E-007 RMS(|Res|)=+5.414173645299E-006
Iteration#008: |dp|= +7.505738865992E-008 RMS(|Res|)=+5.414093125998E-006
Iteration#009: |dp|= +1.151984081755E-008 RMS(|Res|)=+5.414076050582E-006
Iteration#010: |dp|= +1.796784470290E-009 RMS(|Res|)=+5.414075784435E-006
Iteration#011: |dp|= +2.891133349317E-010 RMS(|Res|)=+5.414076250630E-006
Iteration#012: |dp|= +4.451307595613E-011 RMS(|Res|)=+5.414076285174E-006
Iteration#013: |dp|= +1.578976793399E-011 RMS(|Res|)=+5.414076231698E-006
Iteration#014: |dp|= +2.209383518454E-011 RMS(|Res|)=+5.414076212339E-006
Iteration#015: |dp|= +1.492413819328E-011 RMS(|Res|)=+5.414076217035E-006
Iteration#016: |dp|= +3.500917090701E-011 RMS(|Res|)=+5.414076201622E-006
Iteration#017: |dp|= +2.638249750479E-011 RMS(|Res|)=+5.414076238391E-006
Iteration#018: |dp|= +1.637988778327E-011 RMS(|Res|)=+5.414076218402E-006
Iteration#019: |dp|= +1.757445120150E-011 RMS(|Res|)=+5.414076223332E-006
Iteration#020: |dp|= +2.193712923493E-012 RMS(|Res|)=+5.414076224728E-006
Iteration#021: |dp|= +5.533979227786E-012 RMS(|Res|)=+5.414076227720E-006
Iteration#022: |dp|= +3.568409474479E-011 RMS(|Res|)=+5.414076223925E-006
Iteration#023: |dp|= +2.226582818870E-011 RMS(|Res|)=+5.414076218276E-006
Iteration#024: |dp|= +1.974919574979E-011 RMS(|Res|)=+5.414076223835E-006
Iteration#025: |dp|= +1.657413243961E-011 RMS(|Res|)=+5.414076229161E-006
IPF Kalman Filter Completed with Error |dp1| + |dp2| = +1.6574132439612395E-011
-----
```

```

----- IPF LEAST SQUARES FILTER STARTED -----
Iteration#001 COND#=+2.725773644465E+006, |dp|=+8.068993731765E-002
Iteration#002 COND#=+2.972130056993E+006, |dp|=+5.990684614384E-003
Iteration#003 COND#=+2.993165471176E+006, |dp|=+8.768241574015E-004
Iteration#004 COND#=+2.996153360795E+006, |dp|=+1.339839231422E-004
Iteration#005 COND#=+2.996608280289E+006, |dp|=+2.058298417968E-005
Iteration#006 COND#=+2.996678199306E+006, |dp|=+3.164836698721E-006
Iteration#007 COND#=+2.996688950589E+006, |dp|=+4.866890829264E-007
Iteration#008 COND#=+2.996690603925E+006, |dp|=+7.484449142649E-008
Iteration#009 COND#=+2.996690858193E+006, |dp|=+1.150981159685E-008
Iteration#010 COND#=+2.996690897291E+006, |dp|=+1.769978946903E-009
Iteration#011 COND#=+2.996690903301E+006, |dp|=+2.722645121146E-010
Iteration#012 COND#=+2.996690904215E+006, |dp|=+4.188714975013E-011
Iteration#013 COND#=+2.996690904370E+006, |dp|=+6.411172719765E-012
Iteration#014 COND#=+2.996690904383E+006, |dp|=+9.702082069036E-013
Iteration#015 COND#=+2.996690904389E+006, |dp|=+1.681347696508E-013
Iteration#016 COND#=+2.996690904395E+006, |dp|=+6.673800659022E-014
Iteration#017 COND#=+2.996690904392E+006, |dp|=+2.190900486294E-014
Iteration#018 COND#=+2.996690904388E+006, |dp|=+4.077150015979E-014
Iteration#019 COND#=+2.996690904394E+006, |dp|=+6.192916477591E-014
Iteration#020 COND#=+2.996690904391E+006, |dp|=+3.498550822857E-014
Iteration#021 COND#=+2.996690904392E+006, |dp|=+5.850630606062E-014
Iteration#022 COND#=+2.996690904383E+006, |dp|=+9.066958024912E-015
Iteration#023 COND#=+2.996690904394E+006, |dp|=+3.675333871981E-014
Iteration#024 COND#=+2.996690904391E+006, |dp|=+1.222678482108E-014
Iteration#025 COND#=+2.996690904388E+006, |dp|=+2.812731894265E-015
IPF Least Squares Filter Completed with Error |dp1| + |dp2| = +2.8127318942649906E-015
```

Total Execution Time: 96 seconds

4 COMMENTS

Overall the data looked clean and the filter converged nicely.

The results of this run may be summarized as follows:

- The run was performed in the Normal IPF Mode.
- The data set consisted of 7 sandwich maneuvers yielding 42 science and 48 PCRS centroids.
- This run uses IPF version 3.0 where the gyro drift bias estimates make use of the recently corrected GCF signs, (MCR 2521) and now show no sandwich-to-sandwich variations.
- We estimated 18 parameters consisting of: 1 constant plate scale along the slit, 2 IPF alignment angles (no Twist), 3 STA-to-PCRS alignment angles, 6 STA-to-PCRS thermo-mechanical drift parameters, and 3 gyro bias and 3 gyro bias-drift parameters.

We recommend updating frames 46, 44, and 45 with the new quaternions listed in IF501046.dat. The corrections are on the order of 1.2 arcsec in Y and 0.5 arcsec in Z. The twist angle was not estimated. In our best judgment, these frames will be accurate to 0.26 arcsec. This meets the Fine Focal Plane Survey requirement of 0.28 arcsec.

IPF TEAM CONTACT INFORMATION

IPF Team email	ipf@sirtfweb.jpl.nasa.gov	
David S. Bayard	X4-8208	David.S.Bayard@jpl.nasa.gov (TEAM LEADER)
Dhemetrio Boussalis	X4-3977	boussali@grover.jpl.nasa.gov
Paul Brugarolas	X4-9243	Paul.Brugarolas@jpl.nasa.gov
Bryan H. Kang	X4-0541	Bryan.H.Kang@jpl.nasa.gov
Edward.C.Wong	X4-3053	Edward.C.Wong@jpl.nasa.gov (TASK MANAGER)

ACKNOWLEDGEMENTS

This work was performed at the Jet Propulsion Laboratory, California Institute of Technology, under contract with the National Aeronautics and Space Administration.

References

- [1] D.S. Bayard, B.H. Kang, *SIRTF Instrument Pointing Frame Kalman Filter Algorithm*, JPL D-Document D-24809, September 30, 2003.
- [2] B.H. Kang, D.S. Bayard, *SIRTF Instrument Pointing Frame (IPF) Software Description Document and User's Guide*, JPL D-Document D-24808, September 30, 2003.
- [3] D.S. Bayard, B.H. Kang, *SIRTF Instrument Pointing Frame (IPF) Kalman Filter Unit Test Report*, JPL D-Document D-24810, September 30, 2003.
- [4] *Space Infrared Telescope Facility In-Orbit Checkout and Science Verification Mission Plan*, JPL D-Document D-22622, 674-FE-301 Version 1.4, February 8, 2002.
- [5] *Space Infrared Telescope Facility Observatory Description Document*, Lockheed Martin LMMS/P458569, 674-SEIT-300 Version 1.2, November 1, 2002.
- [6] *SIRTF Software Interface Specification for Science Centroid INPUT Files (CAFFILE, CS-FILE)*, JPL SOS-SIS-2002, November 18, 2002.
- [7] *SIRTF Software Interface Specification for Inferred Frames Offset INPUT Files (OFILE)*, JPL SOS-SIS-2003, November 18, 2002.
- [8] *SIRTF Software Interface Specification for PCRS Centroid INPUT Files (CBFILE)*, JPL SIS-FES-015, November 18, 2002.
- [9] *SIRTF Software Interface Specification for Attitude INPUT Files (AFILE, ASFILE)*, JPL SIS-FES-014, January 7, 2002.
- [10] *SIRTF Software Interface Specification for IPF Filter Output Files (IFFILE, LGFILE, TARFILE)*, JPL SOS-SIS-2005, November 18, 2002.
- [11] R.J. Brown, *Focal Surface to Object Space Field of View Conversion*. Systems Engineering Report SER No. S20447-OPT-051, Ball Aerospace & Technologies Corp., November 23, 1999.

This page left blank.

JET PROPULSION LABORATORY

SIRTF IPF REPORT

JPL ID502052

November 6, 2003

**SIRTF INSTRUMENT POINTING FRAME
KALMAN FILTER EXECUTION SUMMARY**

IPF RUN NUMBER: 502052

REPORT TYPE: IOC EXECUTION (FINE)

PRIME FRAME: IRS_ShortHi_Center_Position (52)

INFERRRED FRAMES: (50) (51)

IPF TEAM

Autonomy and Control Section (345)

Jet Propulsion Laboratory

California Institute of Technology

4800 Oak Grove Drive

Pasadena, CA 91109

Contents

1 IPF EXECUTION SUMMARY	5
2 IPF INPUT FILE HISTORY	9
3 IPF EXECUTION RESULTS	12
3.1 IPF EXECUTION OUTPUT PLOTS	12
3.2 IPF OUTPUT DATA (IF MINI FILE)	38
3.3 IPF EXECUTION LOG	40
4 COMMENTS	43

List of Figures

1.1 A-priori and a-posteriori IPF frames	5
1.2 A-priori and a-posteriori IPF frames (ZOOMED)	8
2.1 Scenario Plot	9
2.2 Attitude file edit history	10
2.3 Centroid file edit history	10
2.4 Oriented PixelCoords of Centroid Meas. Edited Centroids	11
3.1 TPF coords of measurements and a-priori predicts	14
3.2 Oriented PixelCoords of measurements and a-priori predicts	14
3.3 Oriented (W,V) PixelCoords of A-Priori Prediction Error Quiver Plot	15
3.4 A-priori prediction error (Science Centroids)	15
3.5 Oriented PixelCoords of measurements and a-priori predicts (PCRS only)	16
3.6 Oriented PixelCoords of measurements and a-priori predicts (Zoomed, PCRS only) . .	16
3.7 Oriented (W,V) PixelCoords of A-Priori PCRS Prediction Error Quiver Plot	17
3.8 A-priori PCRS prediction error	17
3.9 IPF execution convergence, chart 1	18
3.10 IPF execution convergence, chart 2	18
3.11 Parameter uncertainty convergence	19
3.12 IPF parameter symbol table	19
3.13 KF parameter error sigma plots	20
3.14 LS parameter error sigma plot	20

3.15 KF and LS parameter error sigma plot	21
3.16 Oriented Pixel Coords of meas. and a-posteriori predicts	22
3.17 Oriented Pixel Coords of meas. and a-posteriori predicts (attitude corrected)	22
3.18 KF innovations with (o) and w/o (+) attitude corrections	23
3.19 Histograms of science a-posteriori residuals (or innovations)	23
3.20 A-Posteriori Science Centroid Prediction Error Quiver (Att. Cor.)	24
3.21 Normalized A-Posteriori Science Centroid Prediction Errors	24
3.22 KF innovations with (o) and w/o (+) attitude corrections (PCRS)	25
3.23 Histograms of PCRS a-posteriori residuals (or innovations)	25
3.24 A-posteriori PCRS Prediction Summary	26
3.25 A-posteriori PCRS Prediction (PCRS 1 Only)	27
3.26 A-posteriori PCRS Prediction (PCRS 2 Only)	27
3.27 A-Posteriori PCRS Prediction Errors Quiver (Att. Cor.)	28
3.28 Normalized A-Posteriori PCRS Prediction Errors	28
3.29 W-axis KF innovations and 1-sigma bound	29
3.30 V-axis KF innovations and 1-sigma bound	29
3.31 Array plot with (solid) and w/o (dashed) optical distortion corrections	30
3.32 Optical Distortion Plot: total (x5 magnification)	30
3.33 Optical Distortion Plot: constant plate scales (x5 magnification)	31
3.34 Optical Distortion Plot: linear plate scale (x5 magnification)	31
3.35 Optical Distortion Plot: gamma terms (x5 magnification)	32
3.36 Scan Mirror Chops	32
3.37 IPF Frame Reconstruction	33
3.38 Center Pixel Reconstruction	33
3.39 Estimated attitude corrections (Body frame)	34
3.40 Estimated attitude error sigma plot (Body frame)	34
3.41 Thermo-mechanical boresight drift (equiv. angle in (W,V) coords)	35
3.42 Thermo-mechanical boresight drift (equiv. angle in Body frame)	35
3.43 Gyro drift bias contribution (equiv. rate in (W,V) coords)	36
3.44 Gyro drift bias contribution (equiv. angle in (W,V) coords)	36
3.45 Gyro drift bias contribution (equiv. angle in Body frame)	37

List of Tables

1.1	IPF filter input files	6
1.2	IPF filter execution configuration	6
1.3	IPF filter execution mask vector assignment	6
1.4	IPF calibration error summary ([arcsec], 1-sigma, radial)	7
1.5	Science measurement prediction error summary (1-sigma)	7
1.6	IPF Brown angle summary	8
2.1	IPF input file begin and end times	9
2.2	IPF input file editing status	9
2.3	List of Removed Centroids (Original CA File Row Index)	11
3.1	Table of figures I (IPF run)	12
3.2	Table of figures II (IPF run)	13
3.3	PCRS measurement prediction error summary	26

1 IPF EXECUTION SUMMARY

This report summarizes the SIRTF Instrument Pointing Frame (IPF) Kalman Filter execution associated with run file: RN502052. In particular, this Focal Point Survey calibrates the instrument: IRS_ShortHi_Center_Position (52), as part of the IOC Fine Survey. The main calibration results from the IPF filter execution have been documented in IF502052 typically stored in the mission archive DOM collection IPF_IF. This report only summarizes the main aspects of the run, and does not substitute for the full information contained in the IF file.

Section 1 summarizes the filter execution results. The filter configurations are tabulated in Table 1.2 and the mask vector assignments are tabulated in Table 1.3. A total of 18 state parameters are estimated in this run. The overall End-to-End pointing performances are tabulated in Table 1.4. The prediction residuals throughout the estimation processes are tabulated in Table 1.5. Section 3 summarizes resulting plots, a mini summary of the IF IPF output file, and the execution log. Section 4 captures the user comments that are specific to this particular run.

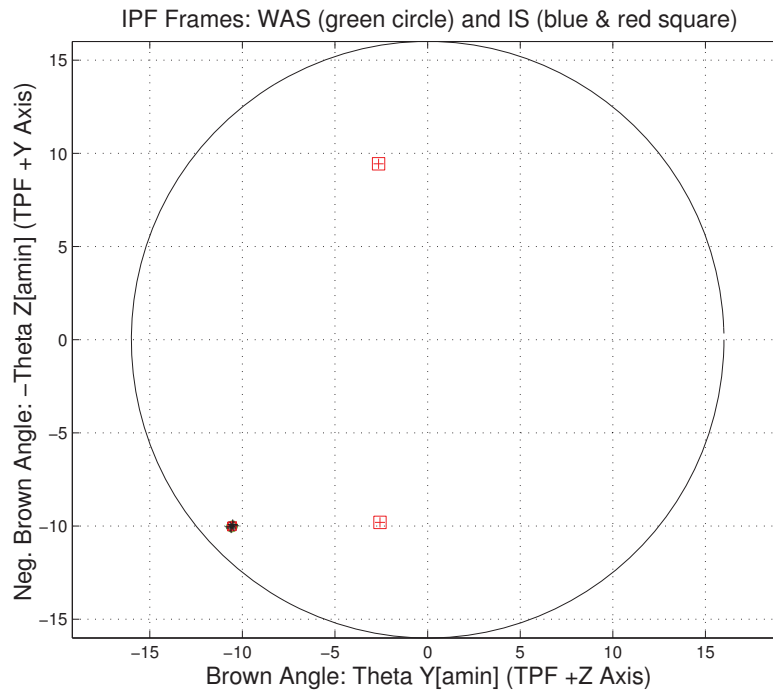


Figure 1.1: A-priori and a-posteriori IPF frames

RAW	FINAL (After Editing)
AA501052	AA501052
AS501052	AS501052
CA502052	CA591052
CB502052	CB502052
CS501052	CS501052

Table 1.1: IPF filter input files

EXECUTION CONFIGURATION ITEM	CURRENT STATUS
IPF Filter Version Used	IPF.V3.0.0B
Frame Table Version Used	BodyFrames_FTU_12b
Scan-Mirror Employed?	NO
IPF Filter Mode	NORMAL-MODE(0)
SLIT-MODE Operation	ENABLED
Kalman Filter Operation	ENABLED
Least-Squares Data Analysis	ENABLED
IBAD Screening	ENABLED
User-Specified Data Editing	DISABLED
Total Number of Iterations	20
LS Residual Sigma Scale	1.64458712E+000
Total Number of Maneuvers	32

Table 1.2: IPF filter execution configuration

Con. Plate Scale			Γ Dependent				Γ^2 Dependent				Linear Plate Scale						Mirror			
a_{00}	b_{00}	c_{00}	a_{10}	b_{10}	c_{10}	d_{10}	a_{20}	b_{20}	c_{20}	d_{20}	a_{01}	b_{01}	c_{01}	d_{01}	e_{01}	f_{01}	α	β		
1	2	3	4	5	6	7	8	9	10	11	12	13	14	15	16	17	18	19		
1	0	0	0	0	0	0	0	0	0	0	0	0	0	0	0	0	0	0		
IPF (T)			Alignment R						Gyro Drift Bias											
θ_1	θ_2	θ_3	a_{rx}	a_{ry}	a_{rz}	b_{rx}	b_{ry}	b_{rz}	c_{rx}	c_{ry}	c_{rz}	b_{gx}	b_{gy}	b_{gz}	c_{gx}	c_{gy}	c_{gz}			
20	21	22	23	24	25	26	27	28	29	30	31	32	33	34	35	36	37			
0	1	1	1	1	1	1	1	1	1	1	1	1	1	1	1	1	1			

Table 1.3: IPF filter execution mask vector assignment

FOCAL PLANE SURVEY ANALYSIS: IOC Fine Survey.

INSTRUMENT NAME: IRS_ShortHi_Center_Position NF: 52

PIX2RADW: 4.84813681E-006 [rad/pixel] = 1.0000E+000 [arcsec/pixel]

PIX2RADV: 4.84813681E-006 [rad/pixel] = 1.0000E+000 [arcsec/pixel]

FRAME	DESCRIPTION	IPF ¹	SF ²	TOTAL	REQ
052(P)	IRS_ShortHi_Center_Position	0.0230	0.0855	0.0885	0.14
050(I)	IRS_ShortHi_1st_Position	0.0231	0.0855	0.0886	N/A
051(I)	IRS_ShortHi_2nd_Position	0.0230	0.0855	0.0885	N/A

Table 1.4: IPF calibration error summary ([arcsec], 1-sigma, radial)

RMS METRIC	A PRIORI ³	A POSTERIORI ³	ATT. CORRECTED ⁴	UNITS
Radial	1.1312	1.0241	0.9296	arcsec
W-Axis	0.7205	0.7654	0.6604	arcsec
V-Axis	0.8720	0.6804	0.6542	arcsec
Radial	1.1312	1.0241	0.9296	pixels
W-Axis	0.7205	0.7654	0.6604	pixels
V-Axis	0.8720	0.6804	0.6542	pixels

Table 1.5: Science measurement prediction error summary (1-sigma)

¹IPF filter removes systematic pointing errors due to: thermomechanical alignment drift (Body to TPF), gyro bias and bias drift, centroiding error, attitude error, and optical distortion. IPF SIGMA presented here is “Scaled” by the Least Squares Scale factor. The Least Squares Scale Factor was: 1.644587. It is assumed that the gyro Angle Random Walk contribution is captured with the Least Squares scaling. The gyro ARW contribution can be approximately calculated as 0.0403 arcseconds, given that ARW = 100 $\mu\text{deg}/\sqrt{\text{hr}}$, with 7.455714e+002 second Maneuver time (max), and 32 independent Maneuvres.

²Gyro Scale Factor(GSF) assumes 95 ppm error over 0.250 degree maneuver.

³This can be interpreted as estimate of ”pixel to sky” pointing reconstruction error if no science data is used.

⁴This can be interpreted as estimate of achieved S/I centroiding error

IPF BROWN ANGLE SUMMARY					
FRAME TABLE USED: BodyFrames_FTU_12b					
NF	NAME	WAS	IS	CHANGE	UNIT
052	theta_Y	-10.562537	-10.564666	-0.002129	arcmin
052	theta_Z	+10.020449	+10.009720	-0.010729	arcmin
052	angle	-41.469994	-41.469994	+0.000001	deg
050	theta_Y	-10.587098	-10.587613	-0.000515	arcmin
050	theta_Z	+10.042156	+10.030000	-0.012156	arcmin
050	angle	-41.469994	-41.469994	+0.000001	deg
051	theta_Y	-10.537977	-10.541720	-0.003743	arcmin
051	theta_Z	+9.998743	+9.989440	-0.009303	arcmin
051	angle	-41.469994	-41.469994	+0.000001	deg

Table 1.6: IPF Brown angle summary

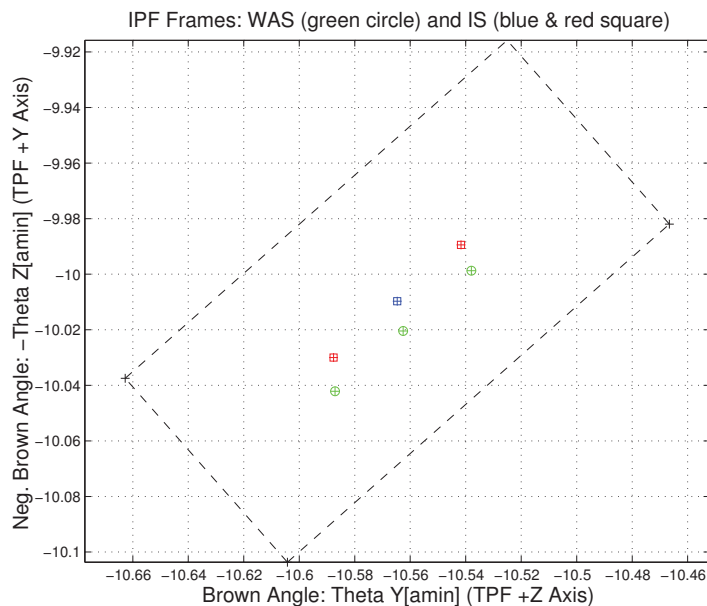


Figure 1.2: A-priori and a-posteriori IPF frames (ZOOMED)

2 IPF INPUT FILE HISTORY

STATUS	FILENAME	START TIME	END TIME
WAS	AA501052	751694000.2	751725500.1
IS	AA501052	751694000.2	751725500.1
WAS	CA502052	751695544.6	751724329.2
IS	CA591052	751695544.6	751724329.2
WAS	CB502052	751695303.1	751724543.0
IS	CB502052	751695303.1	751724543.0

Table 2.1: IPF input file begin and end times

WAS	SIZE	IS	SIZE	REMOVED	PATCHED
AA501052	315000	AA501052	315000	0	0
CA502052	256	CA591052	253	3	N/A
CB502052	224	CB502052	224	0	N/A

Table 2.2: IPF input file editing status

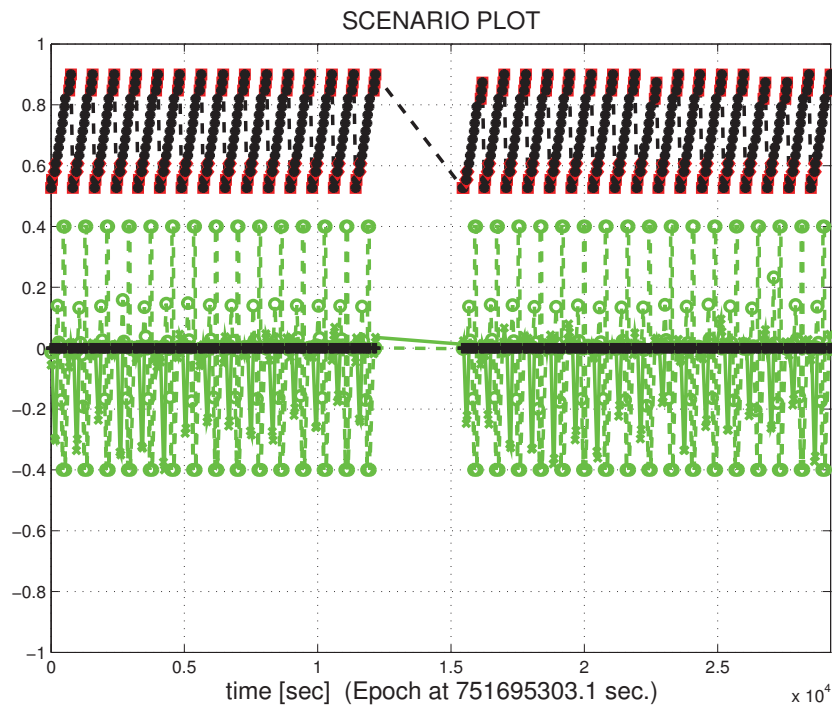


Figure 2.1: Scenario Plot

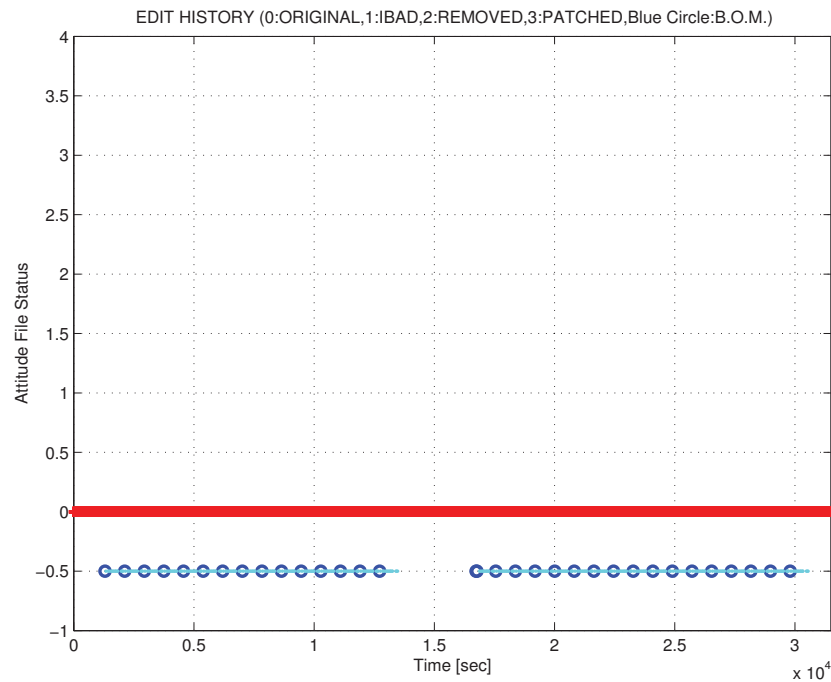


Figure 2.2: Attitude file edit history

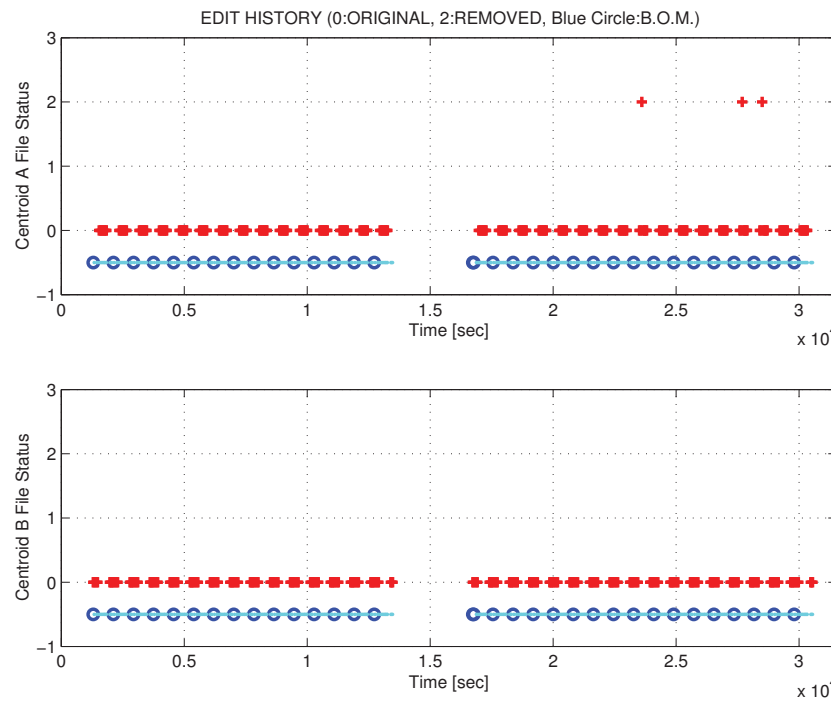


Figure 2.3: Centroid file edit history

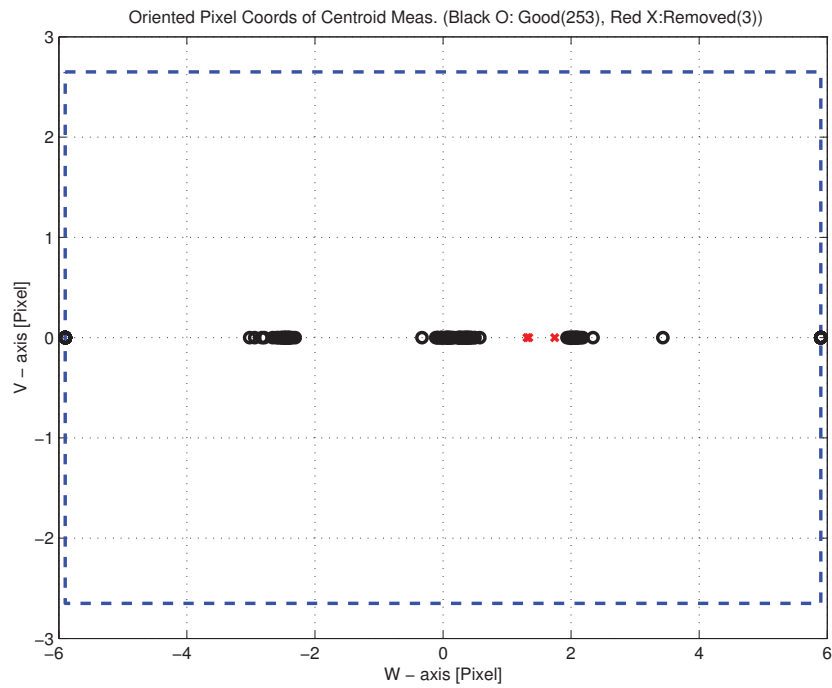


Figure 2.4: Oriented Pixel Coords of Centroid Meas. Edited Centroids

LIST OF REMOVED CENTROIDS									
1	2	3	4	5	6	7	8	9	10
187	227	235							

Table 2.3: List of Removed Centroids (Original CA File Row Index)

3 IPF EXECUTION RESULTS

3.1 IPF EXECUTION OUTPUT PLOTS

This subsection summarizes the IPF filter results. As shown in Table 3.1, the output plots are segmented to three groups: predicted performance, post-run results and IPF trending plots.

FIGURE NO.	DESCRIPTION
Predicted performance prior to IPF run	
Figure 3.1	Meas. and a-priori predicts in TPF coords
Figure 3.2	Meas. and a-priori predicts in Oriented Pixel Coords including rectangular array boundary approximation
Figure 3.3	A-Priori Prediction Error Quiver Plot in Oriented Pixel Coords including rectangular array boundary approximation
Figure 3.4	A-priori prediction error
Figure 3.5	Oriented Pixel Coords of measurements and a-priori predicts (PCRS only)
Figure 3.6	Oriented Pixel Coords of measurements and a-priori predicts (Zoomed, PCRS only)
Figure 3.7	Oriented (W,V) Pixel Coords of A-Priori PCRS Prediction Error Quiver Plot
Figure 3.8	A-priori PCRS prediction error
IPF filter performance (post run results)	
Figure 3.9	IPF execution convergence, chart 1: (top) normalized residual error vs. iteration number and (bottom) norm of effective parameter corrections
Figure 3.10	IPF execution convergence, chart 2: parameter correction size vs. iteration number
Figure 3.11	Parameter uncertainty convergence: square-root of diagonal elements of covariance matrix vs. maneuver number
Figure 3.12	IPF parameter symbol table
Figure 3.13	KF parameter error sigma plot (a-priori-dashed, a-posteriori-solid). Includes true parameter errors (FLUTE runs only)
Figure 3.14	LS parameter error sigma plot. Includes true parameter errors (FLUTE runs only)
Figure 3.15	KF and LS parameter errors sigma plot (Figure 3.13 & Figure 3.14 combined)
Figure 3.16	Measurements and a-posteriori predicts in Oriented Pixel Coords including rectangular array boundaries (a-priori-dashed, a-posteriori-solid)
Figure 3.17	Attitude corrected meas. and a-posteriori predicts in Oriented Pixel Coords including rectangular array boundaries (a-priori-dashed, a-posteriori-solid)

Table 3.1: Table of figures I (IPF run)

FIGURE NO.	DESCRIPTION
IPF filter performance (post run results) - CONTINUE	
Figure 3.18	KF innovations with (o) and w/o (+) attitude corrections
Figure 3.19	Histograms of science a-posteriori residuals (or innovations)
Figure 3.20	A-Posteriori Science Centroid Prediction Error Quiver (Att. Cor.)
Figure 3.21	Normalized A-Posteriori Science Centroid Prediction Errors
Figure 3.22	KF innovations with (o) and w/o (+) attitude corrections (PCRS)
Figure 3.23	Histograms of PCRS a-posteriori residuals (or innovations)
Figure 3.24	A-posteriori PCRS Prediction Summary
Figure 3.25	A-posteriori PCRS Prediction (PCRS 1 Only)
Figure 3.26	A-posteriori PCRS Prediction (PCRS 2 Only)
Figure 3.27	A-Posteriori PCRS Prediction Errors Quiver (Att. Cor.)
Figure 3.28	Normalized A-Posteriori PCRS Prediction Errors
Figure 3.29	W-axis KF innovations and 1-sigma bound
Figure 3.30	V-axis KF innovations and 1-sigma bound
Figure 3.31	Array plot with (solid) and w/o (dashed) optical distortion corrections
Figure 3.32	Optical Distortion Plot: total (x5 magnification)
Figure 3.33	Optical Distortion Plot: constant plate scales (x5 magnification)
Figure 3.34	Optical Distortion Plot: linear plate scale (x5 magnification)
Figure 3.35	Optical Distortion Plot: gamma terms (x5 magnification)
Figure 3.36	Scan Mirror Chops
Figure 3.37	IPF Frame Reconstruction
Figure 3.38	Center Pixel Reconstruction
IPF parameter trending plots	
Figure 3.39	Estimated attitude corrections (Body frame)
Figure 3.40	Estimated attitude error sigma plot (Body frame)
Figure 3.41	Systematic error attributed to thermo-mechanical boresight drift (equiv. angle in (W,V) coords)
Figure 3.42	Systematic error attributed to thermo-mechanical boresight drift (equiv. angle in Body frame)
Figure 3.43	Systematic error attributed to gyro drift bias (equiv. rate in (W,V) coords)
Figure 3.44	Systematic error attributed to gyro drift bias (equiv. angle in (W,V) coords)
Figure 3.45	Systematic error attributed to gyro drift bias (equiv. angle in Body frame)

Table 3.2: Table of figures II (IPF run)

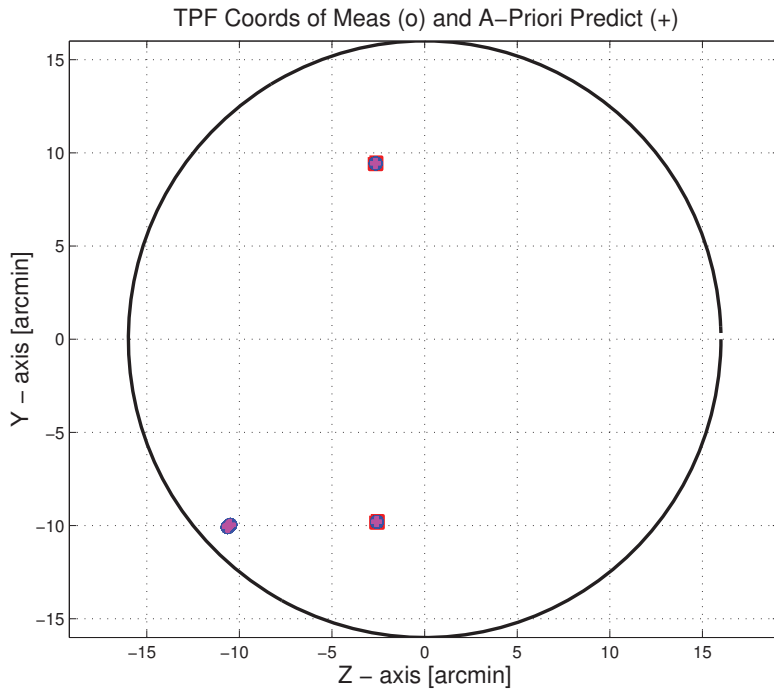


Figure 3.1: TPF coords of measurements and a-priori predicts

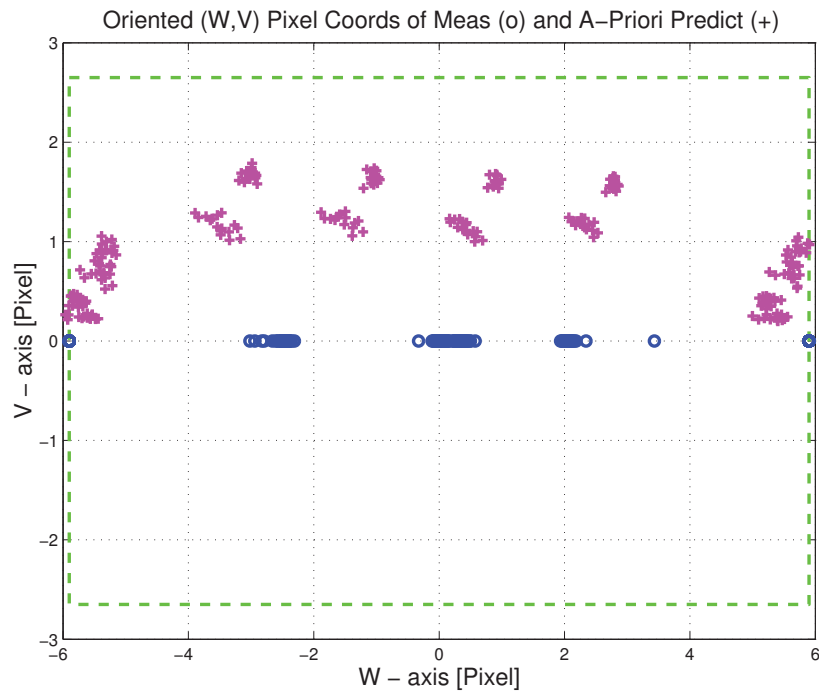


Figure 3.2: Oriented Pixel Coords of measurements and a-priori predicts

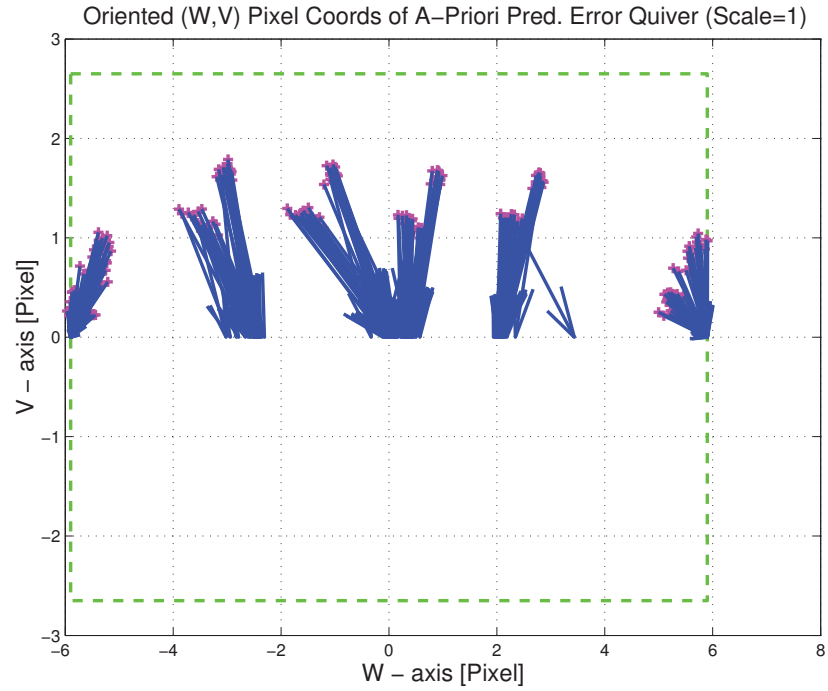


Figure 3.3: Oriented (W,V) Pixel Coords of A-Priori Prediction Error Quiver Plot

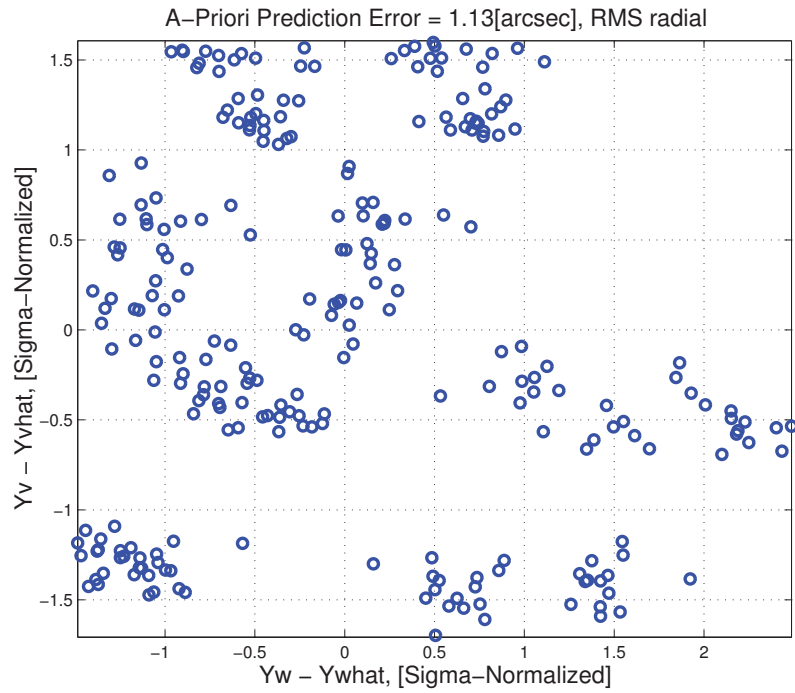


Figure 3.4: A-priori prediction error (Science Centroids)

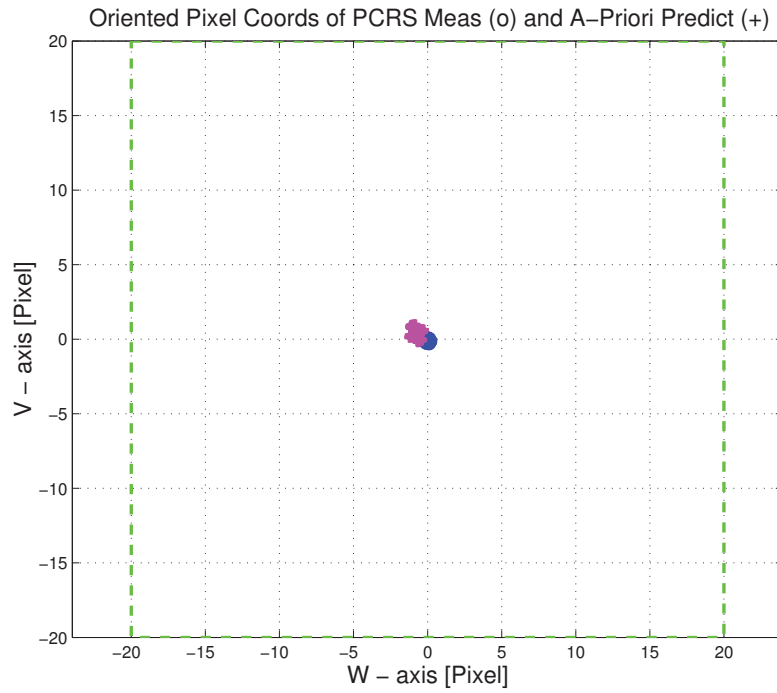


Figure 3.5: Oriented Pixel Coords of measurements and a-priori predicts (PCRS only)

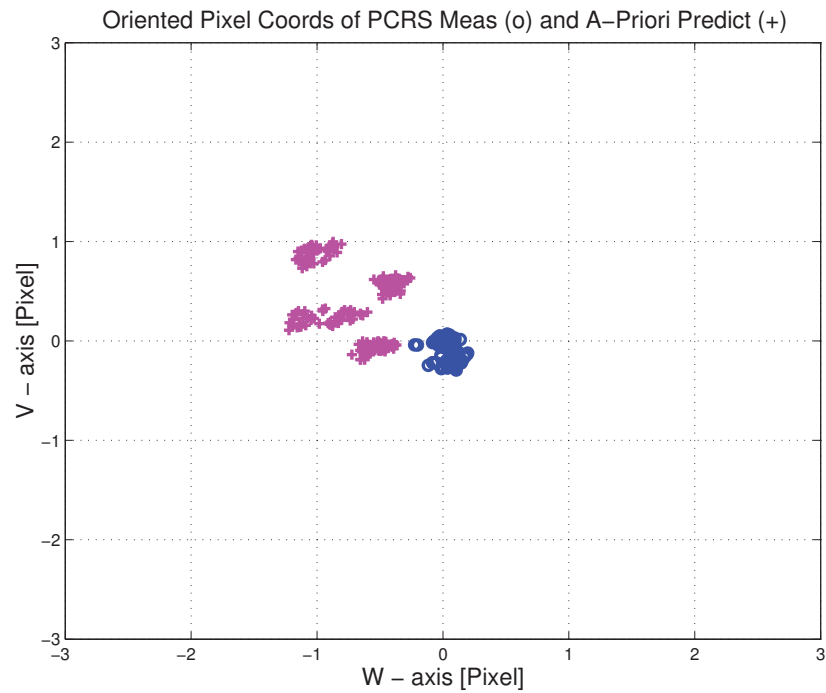


Figure 3.6: Oriented Pixel Coords of measurements and a-priori predicts (Zoomed, PCRS only)

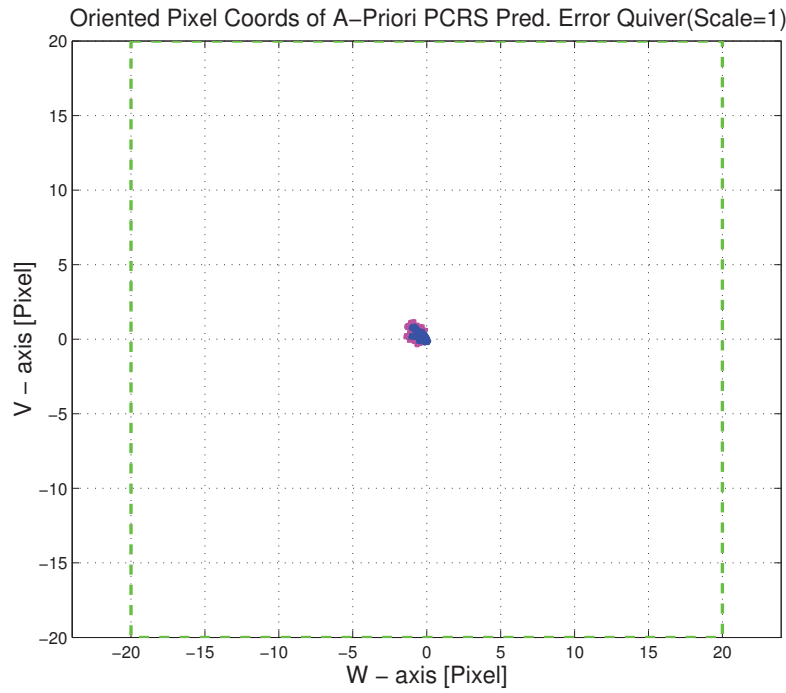


Figure 3.7: Oriented (W,V) Pixel Coords of A-Priori PCRS Prediction Error Quiver Plot

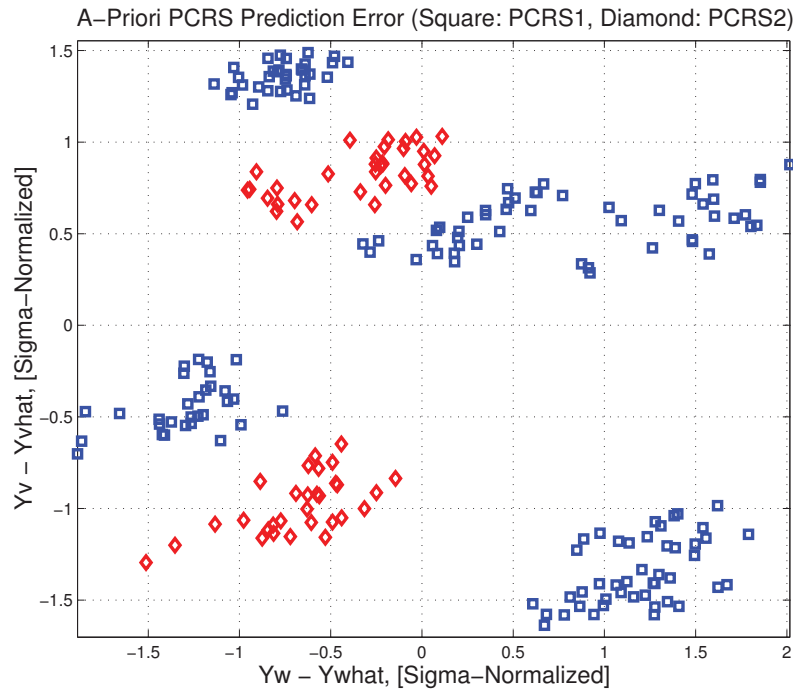


Figure 3.8: A-priori PCRS prediction error

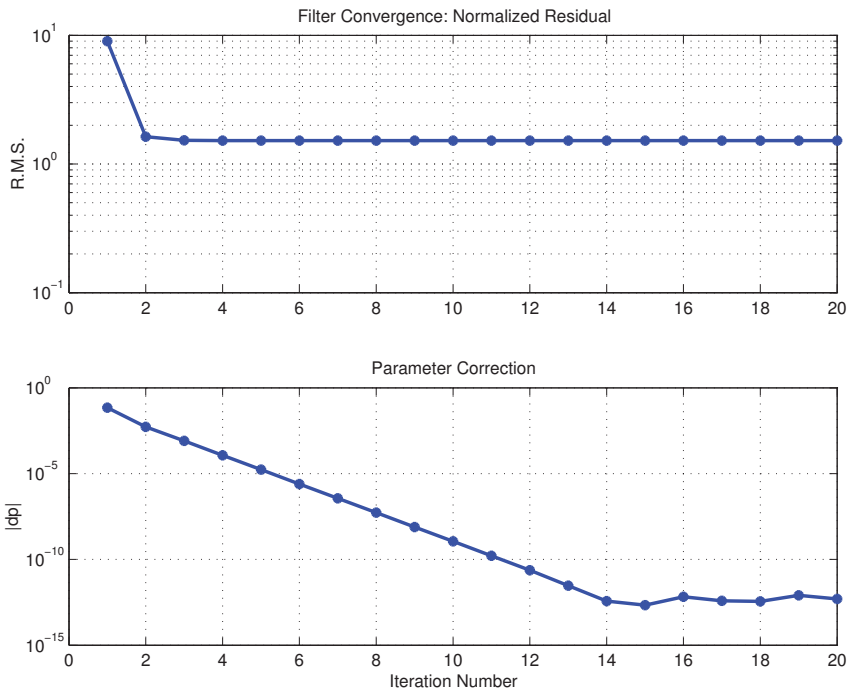


Figure 3.9: IPF execution convergence, chart 1

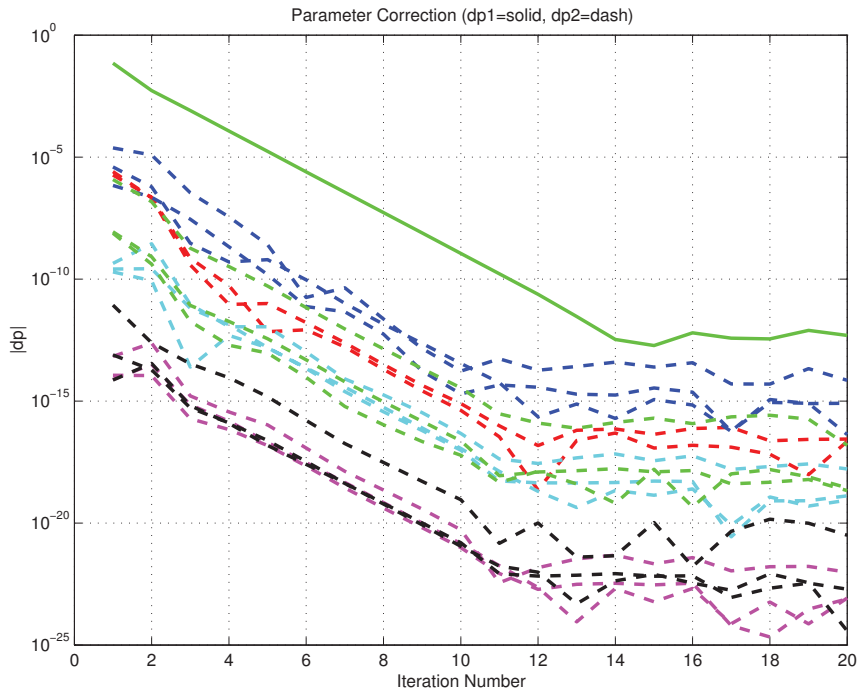


Figure 3.10: IPF execution convergence, chart 2

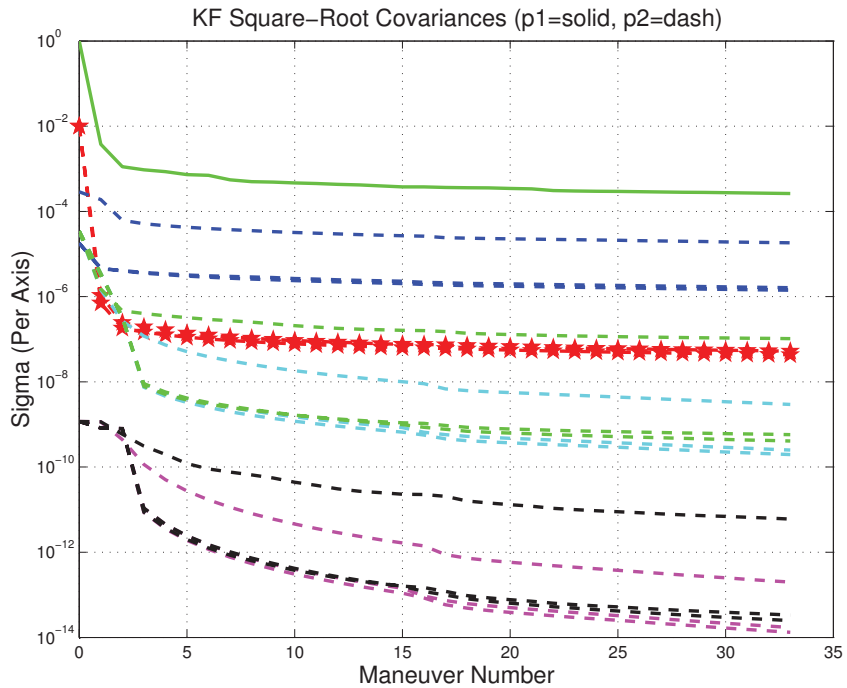


Figure 3.11: Parameter uncertainty convergence

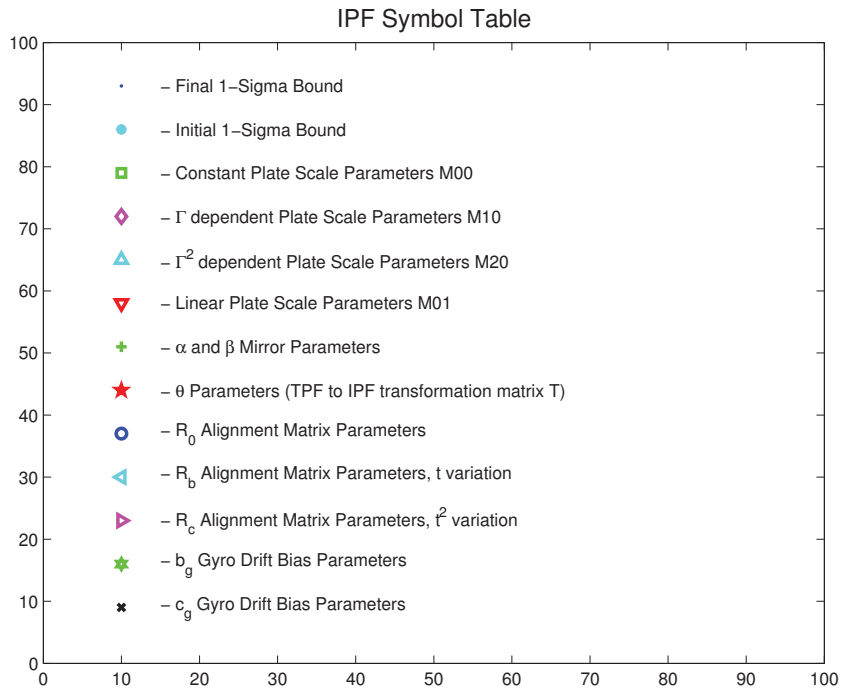


Figure 3.12: IPF parameter symbol table

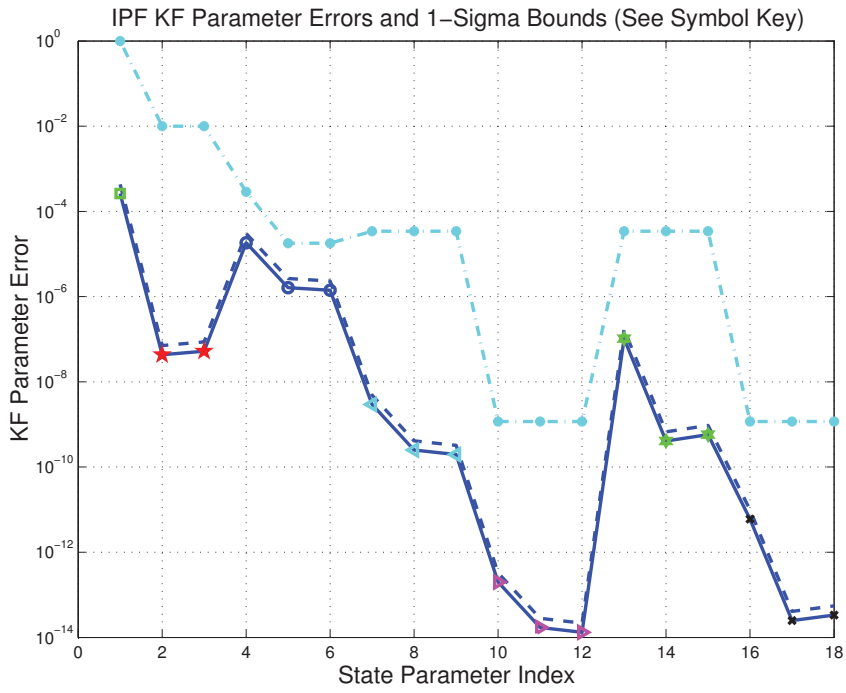


Figure 3.13: KF parameter error sigma plots

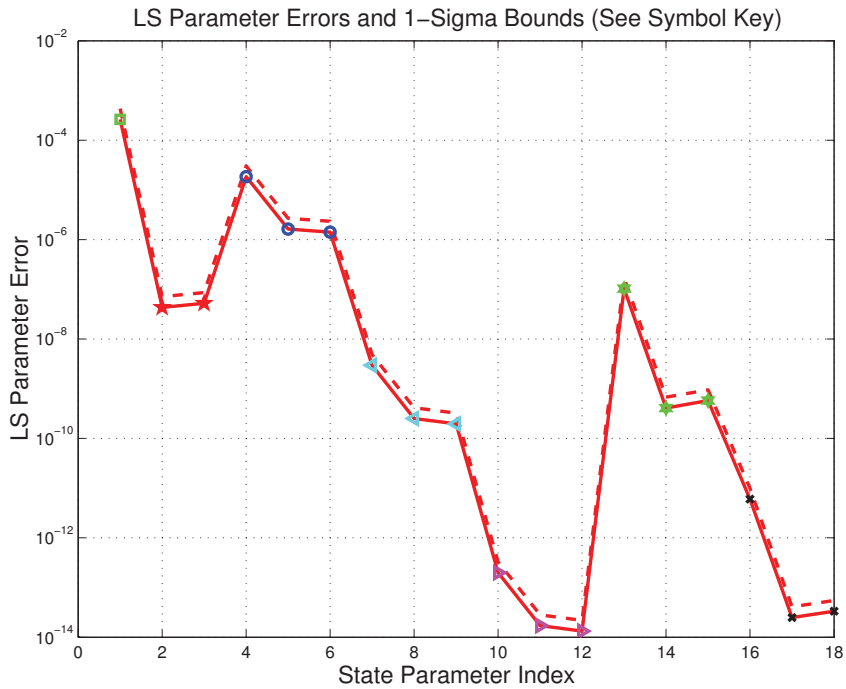


Figure 3.14: LS parameter error sigma plot

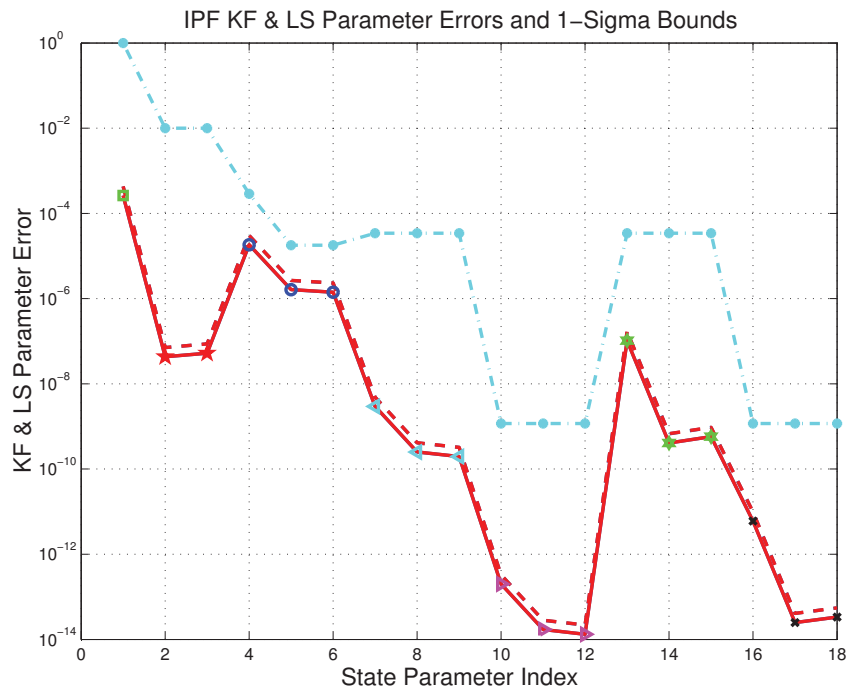


Figure 3.15: KF and LS parameter error sigma plot

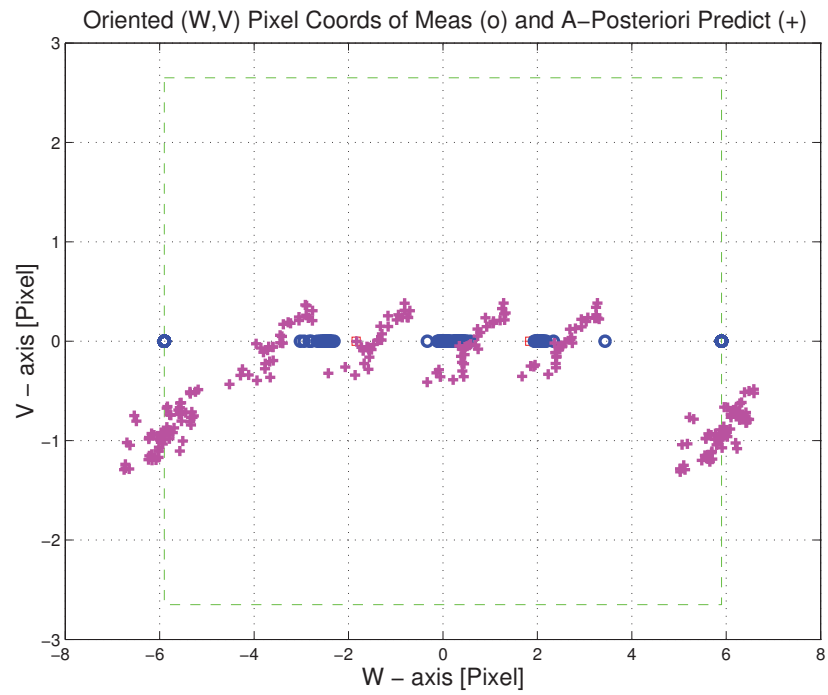


Figure 3.16: Oriented Pixel Coords of meas. and a-posteriori predicts

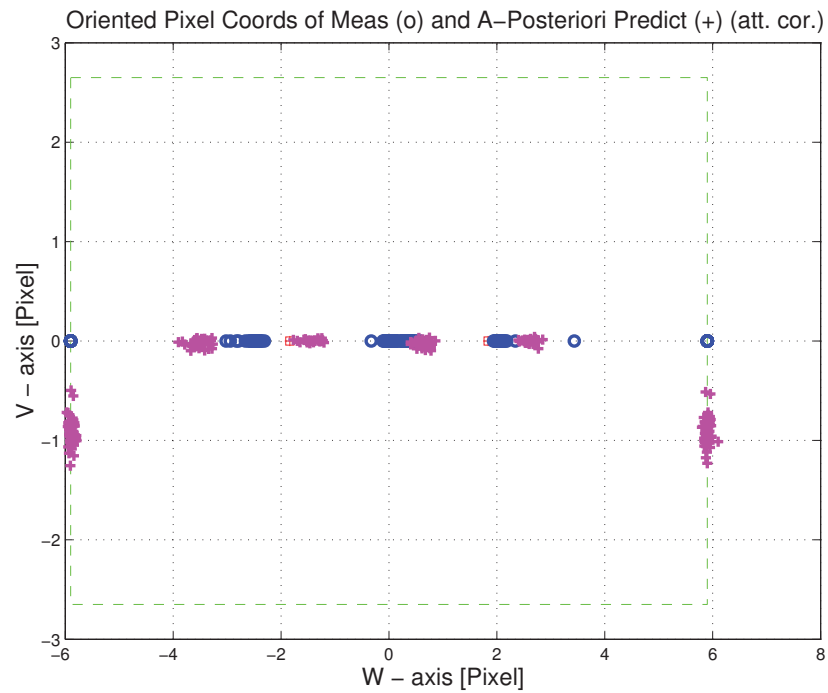


Figure 3.17: Oriented Pixel Coords of meas. and a-posteriori predicts (attitude corrected)

KF Innovations 0.93 asec(with (o)), 1.02 asec (w/o(+)) att. corr. [RMS, radial]

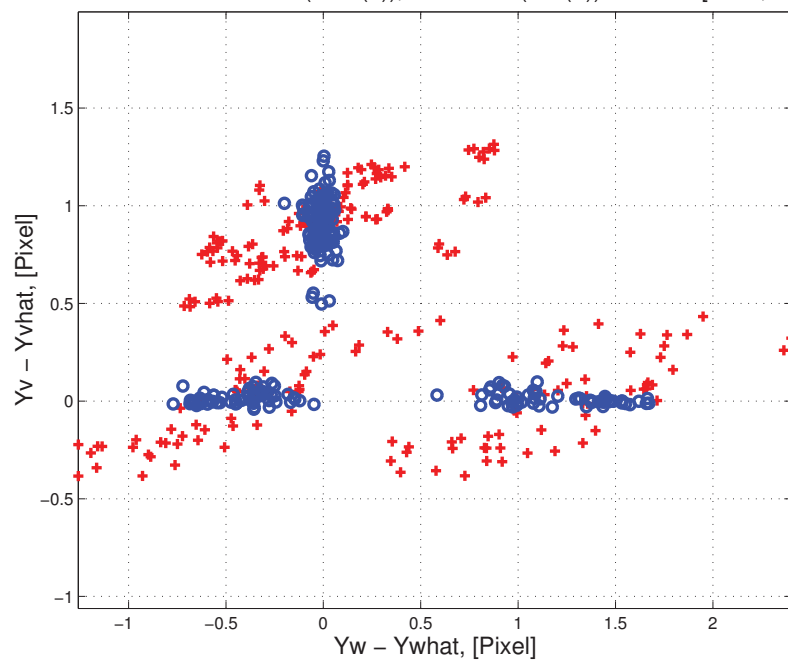


Figure 3.18: KF innovations with (o) and w/o (+) attitude corrections

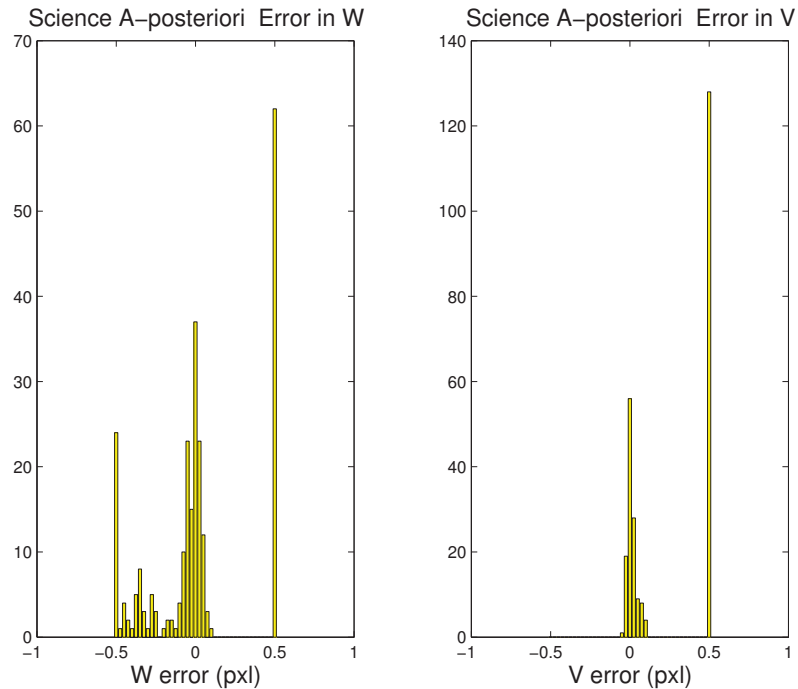


Figure 3.19: Histograms of science a-posteriori residuals (or innovations)

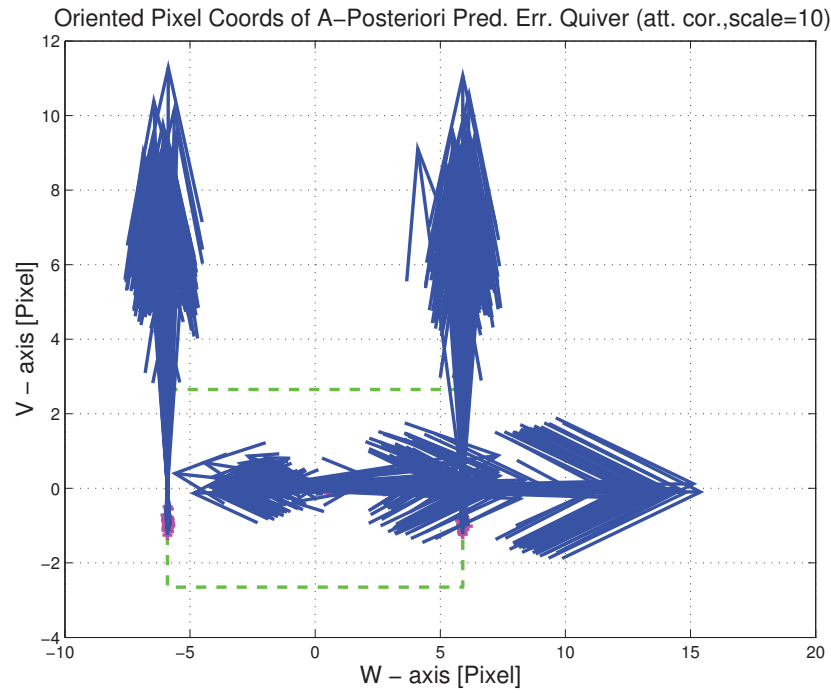


Figure 3.20: A-Posteriori Science Centroid Prediction Error Quiver (Att. Cor.)

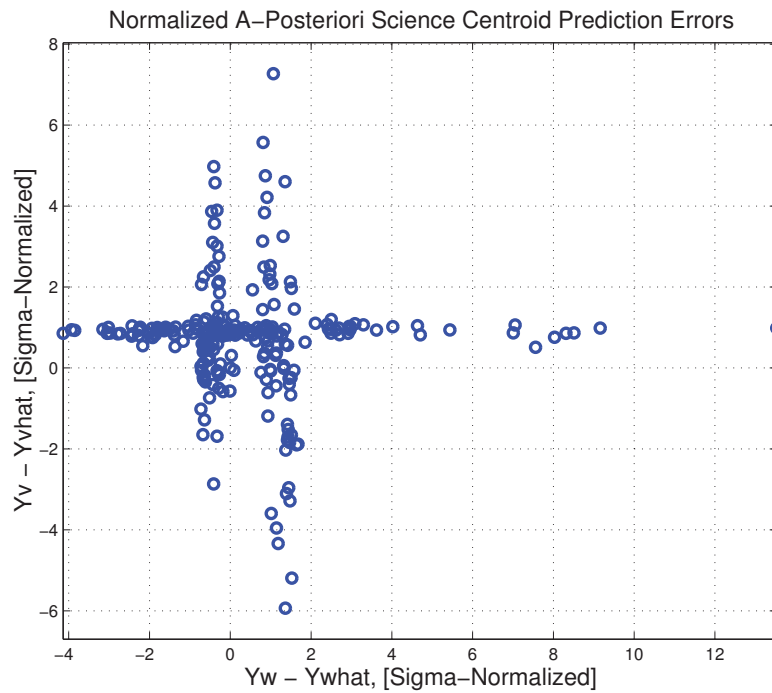


Figure 3.21: Normalized A-Posteriori Science Centroid Prediction Errors

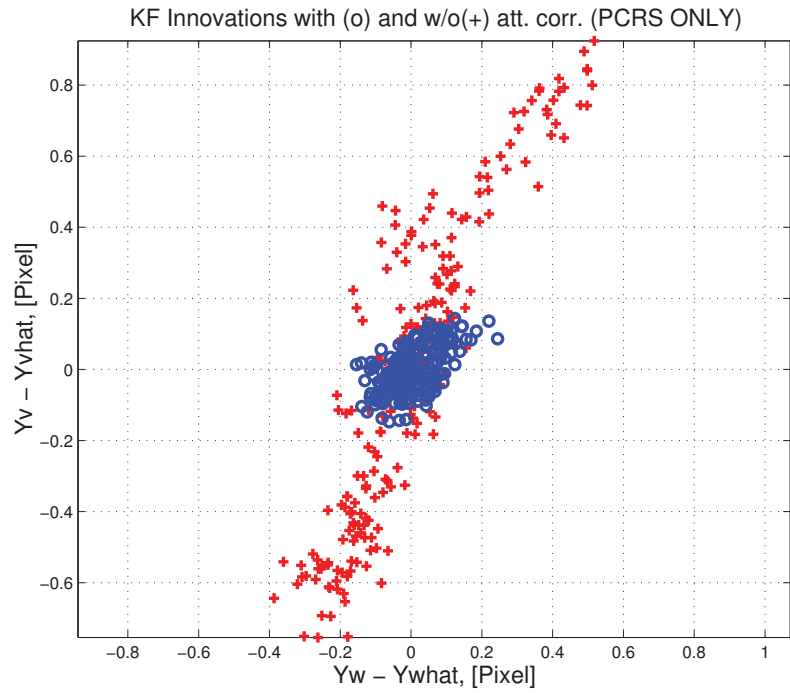


Figure 3.22: KF innovations with (o) and w/o (+) attitude corrections (PCRS)

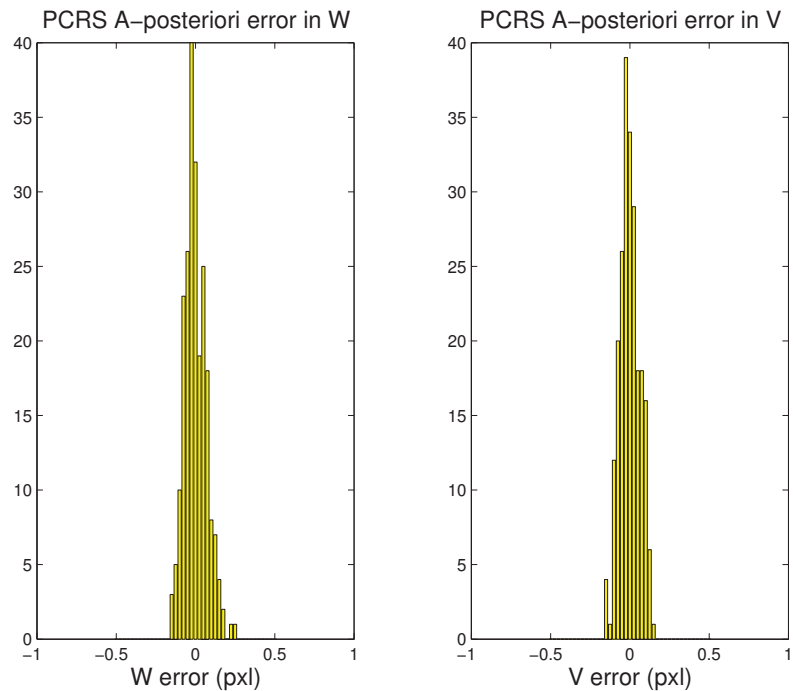


Figure 3.23: Histograms of PCRS a-posteriori residuals (or innovations)

IPF PCRS SUMMARY						
PCRS 1 (Total of 160 centroids)						
RMS	MEAN		SIGMA			
METRIC	APOST.	ATT. COR.	APOST.	ATT. COR.	STAT. CONF.	UNITS
Radial	0.0145	0.0144	0.4643	0.0973	0.0077	arcsec
W-axis	0.0016	-0.0001	0.1953	0.0764	0.0060	arcsec
V-axis	0.0144	0.0144	0.4212	0.0602	0.0048	arcsec
PCRS 2 (Total of 64 centroids)						
METRIC	APOST.	ATT. COR.	APOST.	ATT. COR.	STAT. CONF.	UNITS
Radial	0.0403	0.0401	0.4581	0.0632	0.0079	arcsec
W-axis	0.0019	0.0001	0.1823	0.0445	0.0056	arcsec
V-axis	-0.0402	-0.0401	0.4202	0.0448	0.0056	arcsec
Combined (Total of 224 centroids)						
METRIC	APOST.	ATT. COR.	APOST.	ATT. COR.	STAT. CONF.	UNITS
Radial	0.0021	0.0012	0.4632	0.0923	0.0062	arcsec
W-axis	0.0017	-0.0000	0.1917	0.0688	0.0046	arcsec
V-axis	-0.0012	-0.0012	0.4217	0.0614	0.0041	arcsec

Table 3.3: PCRS measurement prediction error summary

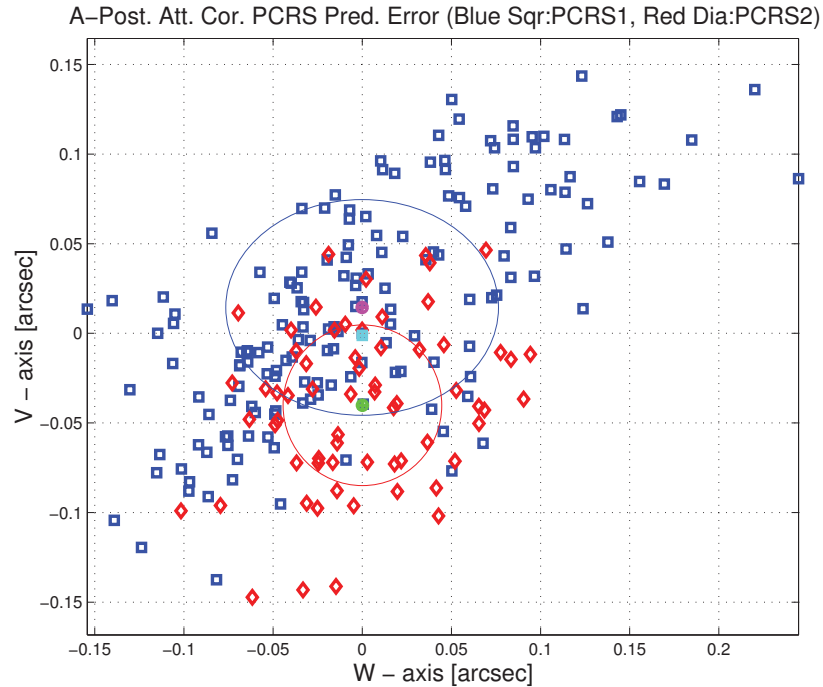


Figure 3.24: A-posteriori PCRS Prediction Summary

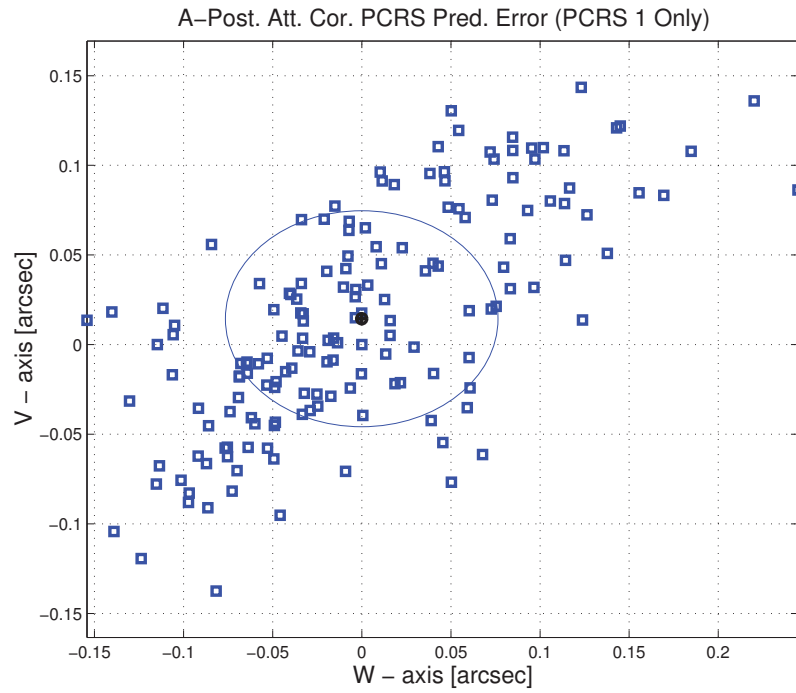


Figure 3.25: A-posteriori PCRS Prediction (PCRS 1 Only)

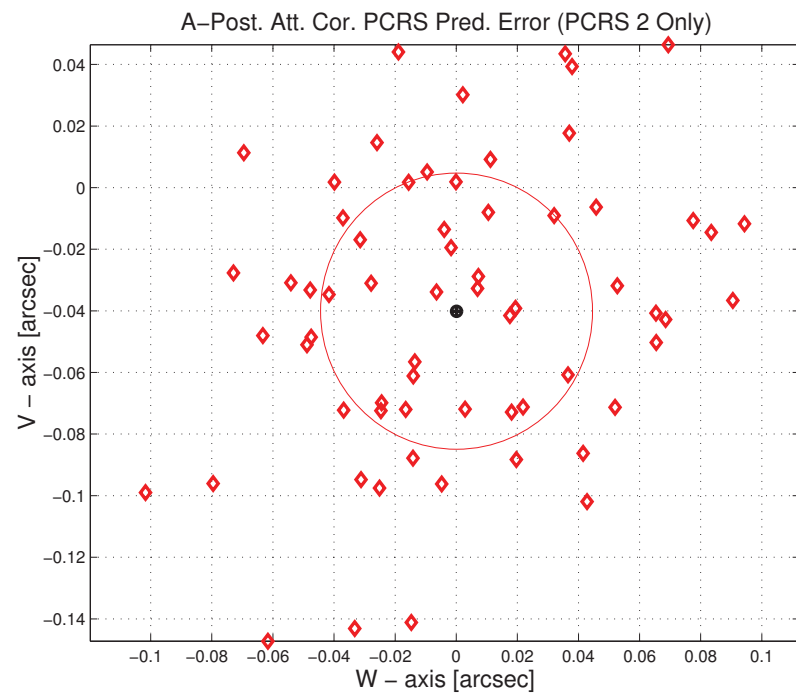


Figure 3.26: A-posteriori PCRS Prediction (PCRS 2 Only)

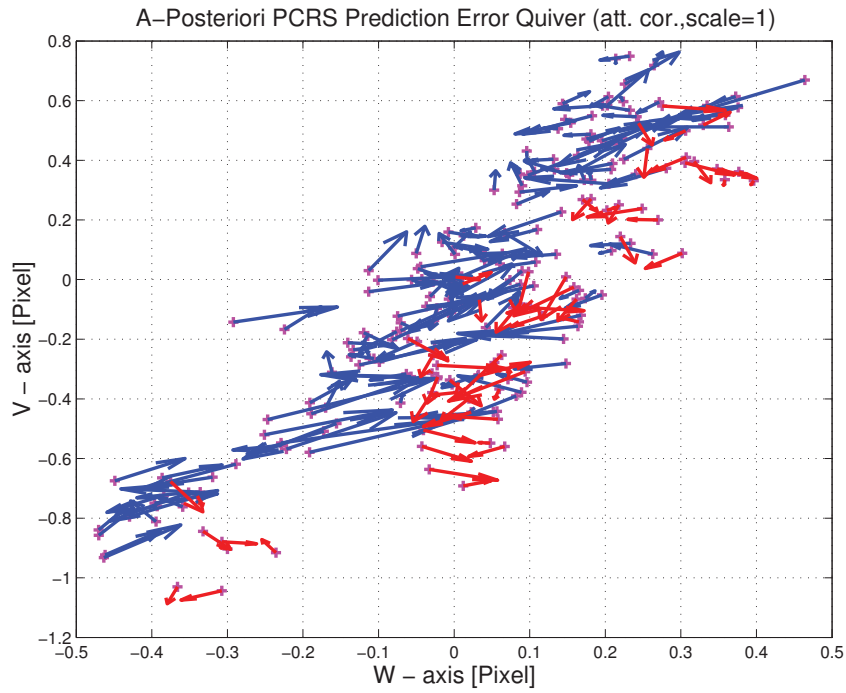


Figure 3.27: A–Posteriori PCRS Prediction Errors Quiver (Att. Cor.)

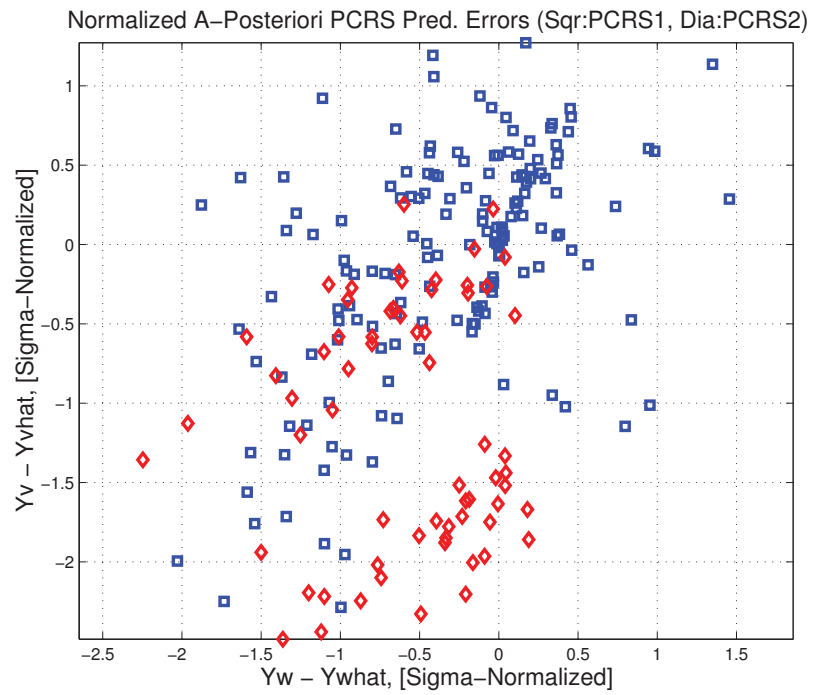


Figure 3.28: Normalized A–Posteriori PCRS Prediction Errors

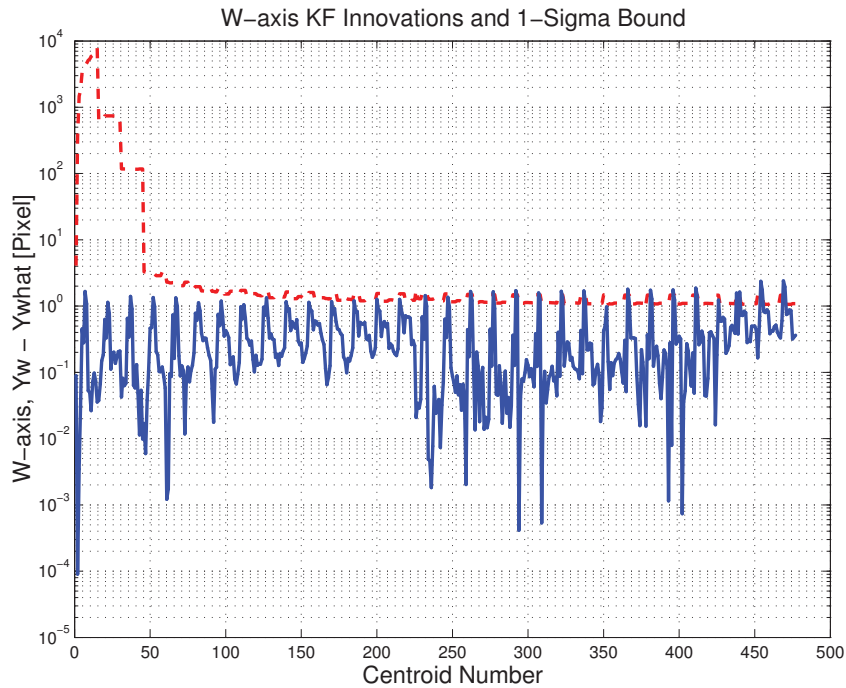


Figure 3.29: W-axis KF innovations and 1-sigma bound

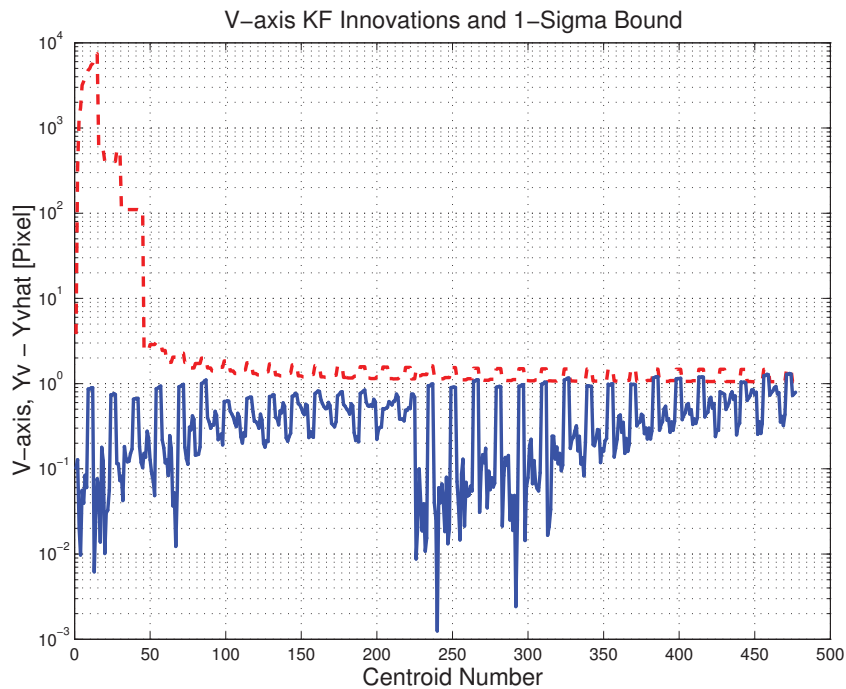


Figure 3.30: V-axis KF innovations and 1-sigma bound

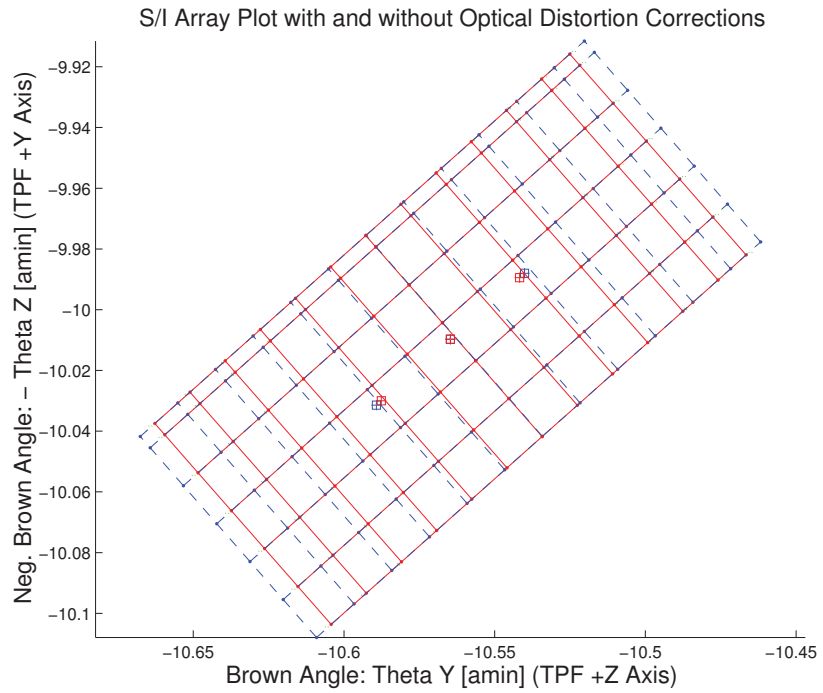


Figure 3.31: Array plot with (solid) and w/o (dashed) optical distortion corrections

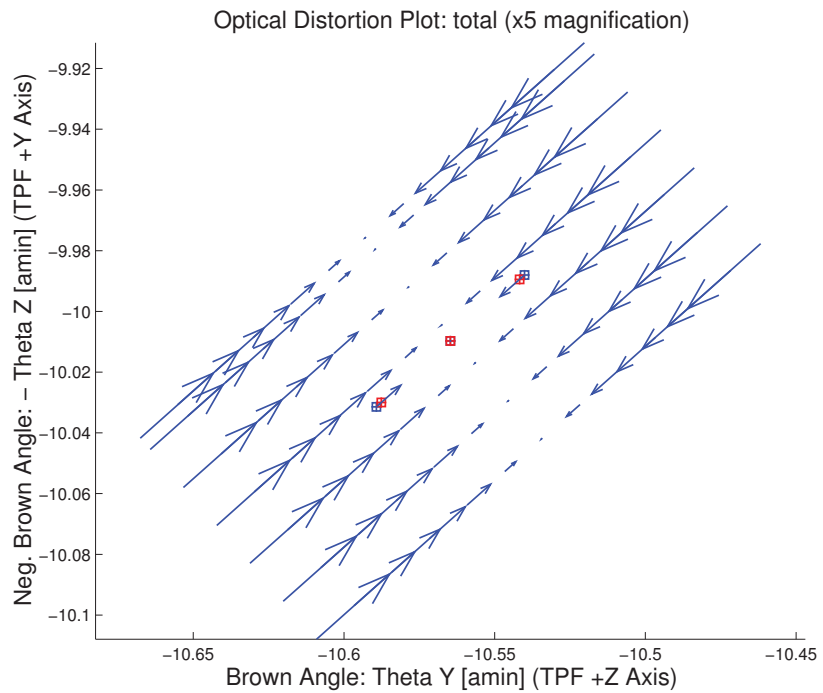


Figure 3.32: Optical Distortion Plot: total (x5 magnification)

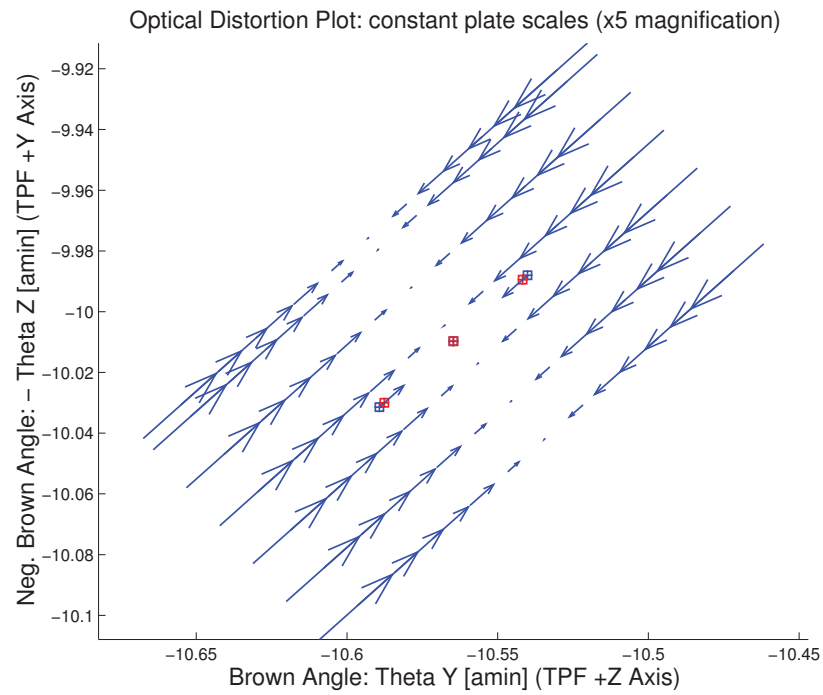


Figure 3.33: Optical Distortion Plot: constant plate scales (x5 magnification)

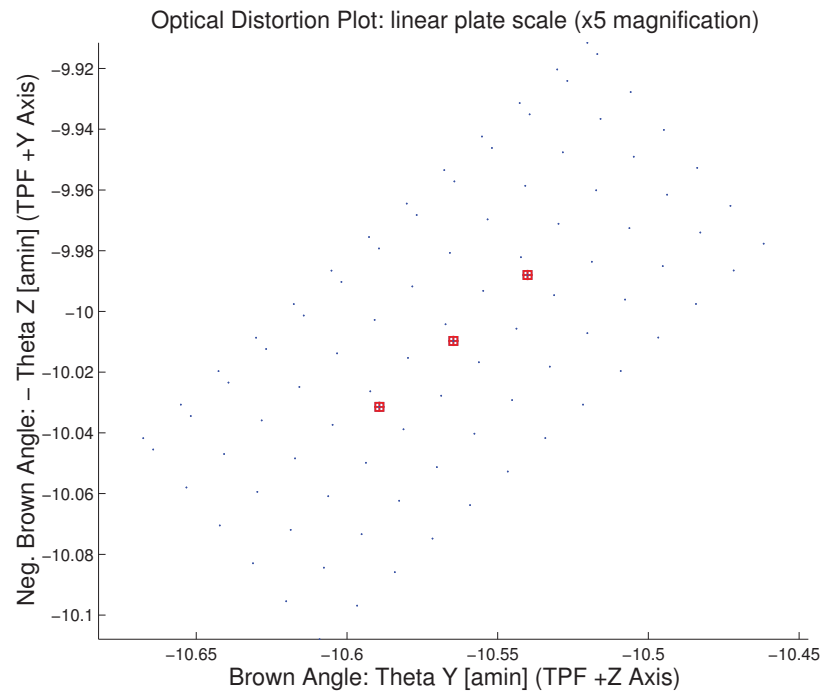


Figure 3.34: Optical Distortion Plot: linear plate scale (x5 magnification)

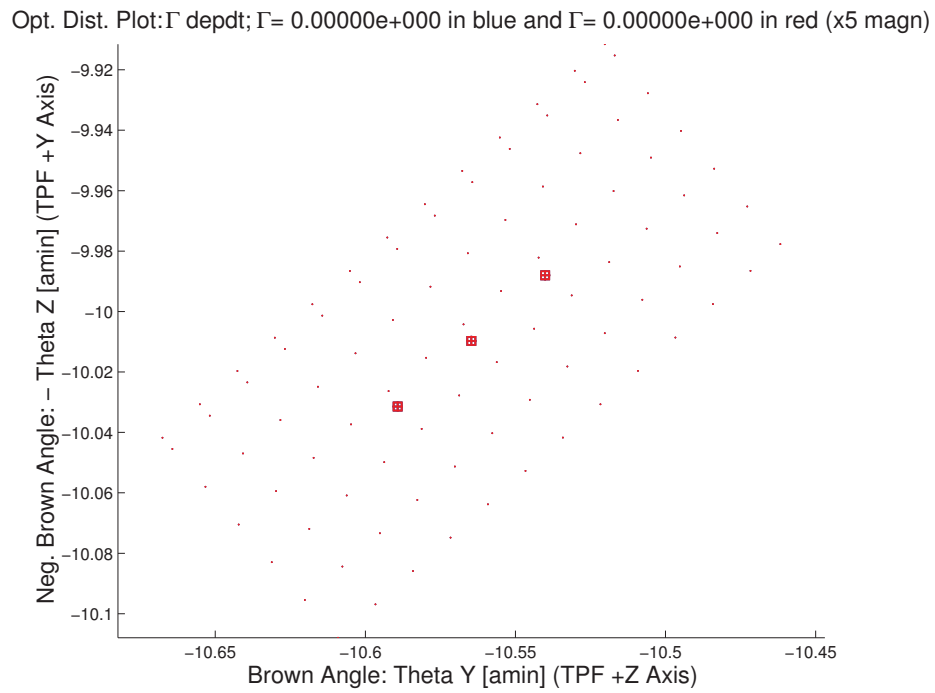


Figure 3.35: Optical Distortion Plot: gamma terms (x5 magnification)

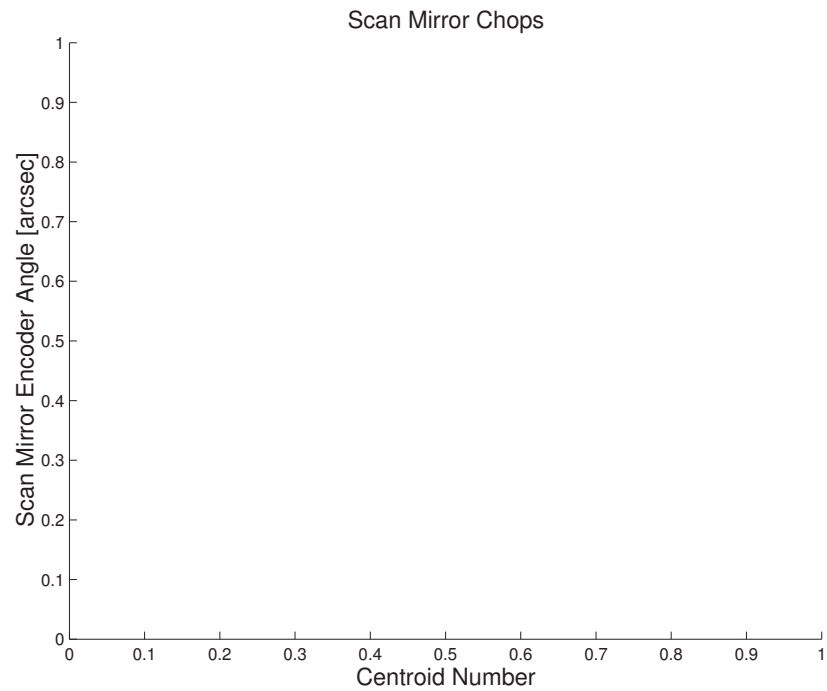


Figure 3.36: Scan Mirror Chops

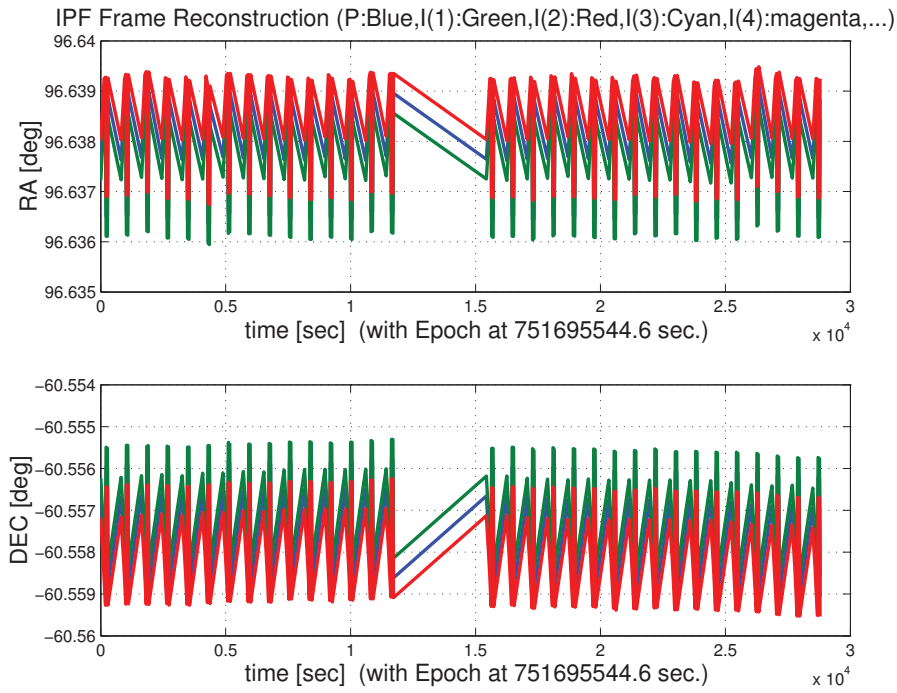


Figure 3.37: IPF Frame Reconstruction

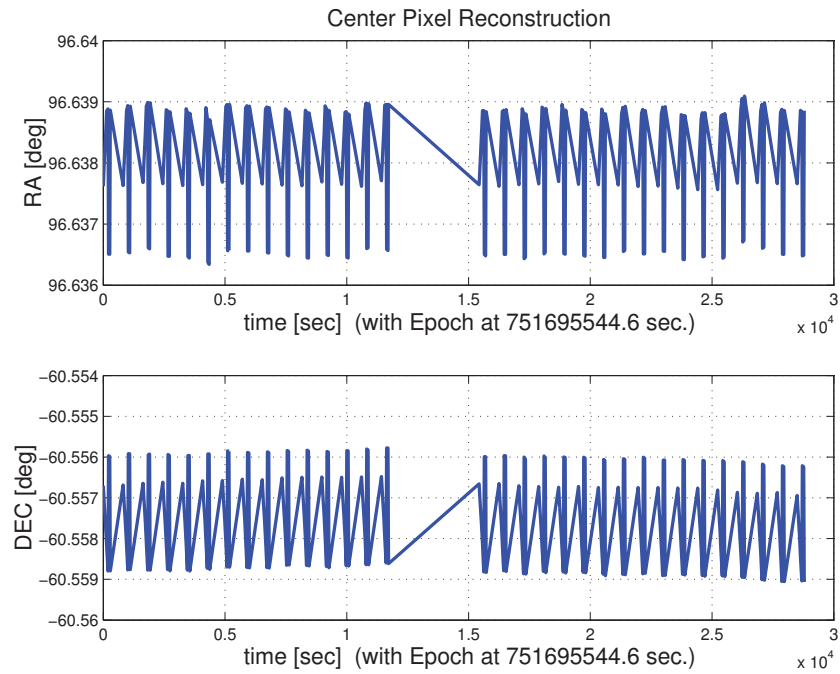


Figure 3.38: Center Pixel Reconstruction

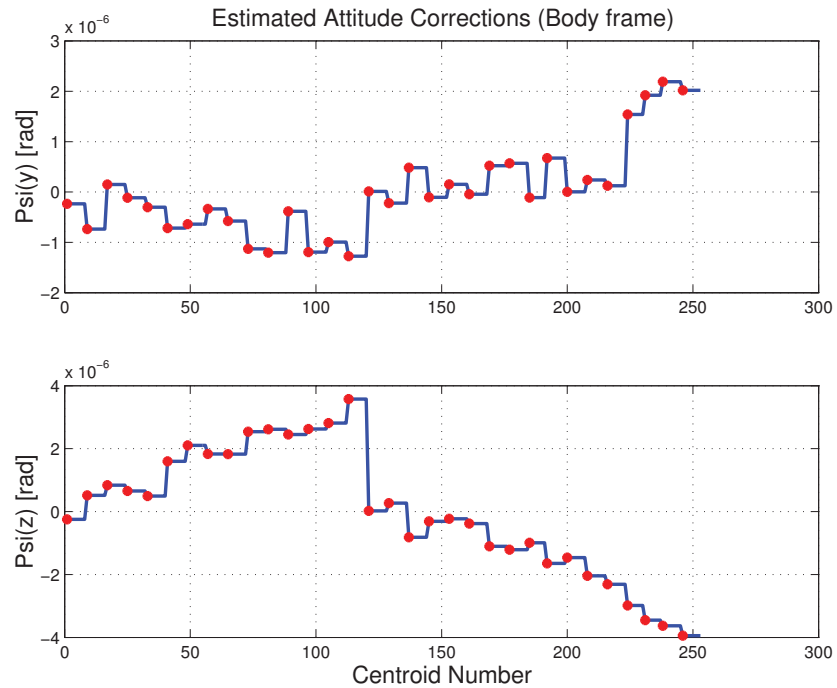


Figure 3.39: Estimated attitude corrections (Body frame)

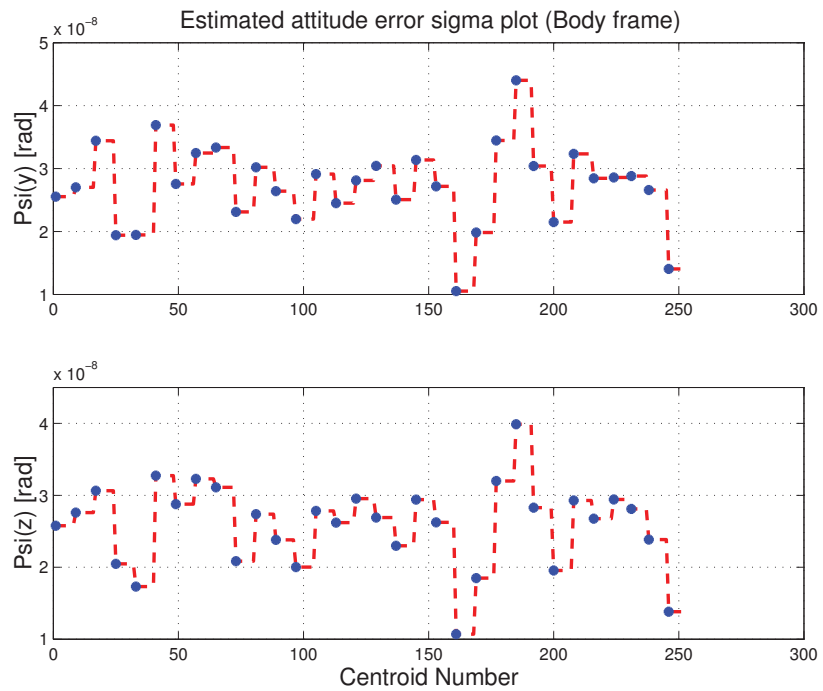


Figure 3.40: Estimated attitude error sigma plot (Body frame)

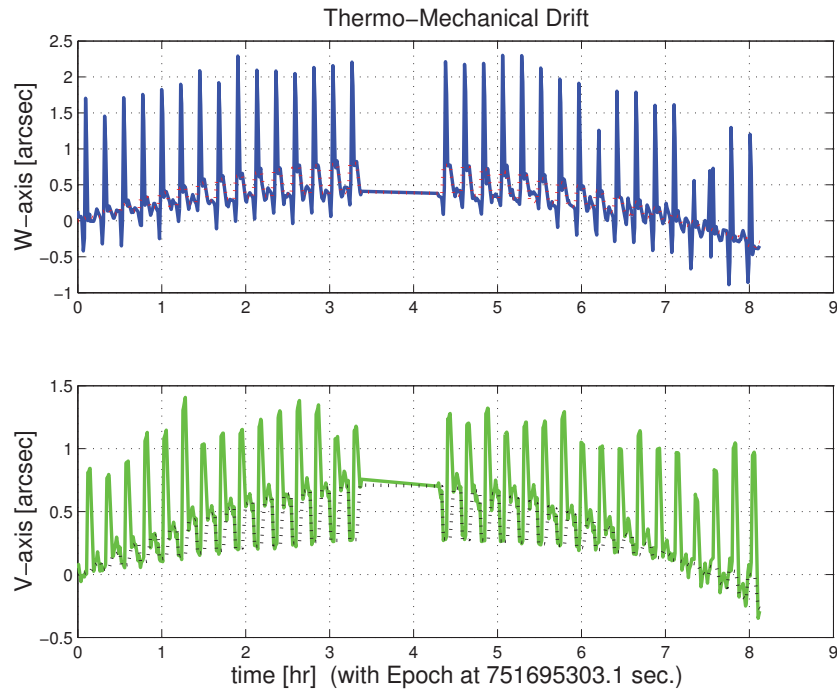


Figure 3.41: Thermo-mechanical boresight drift (equiv. angle in (W,V) coords)

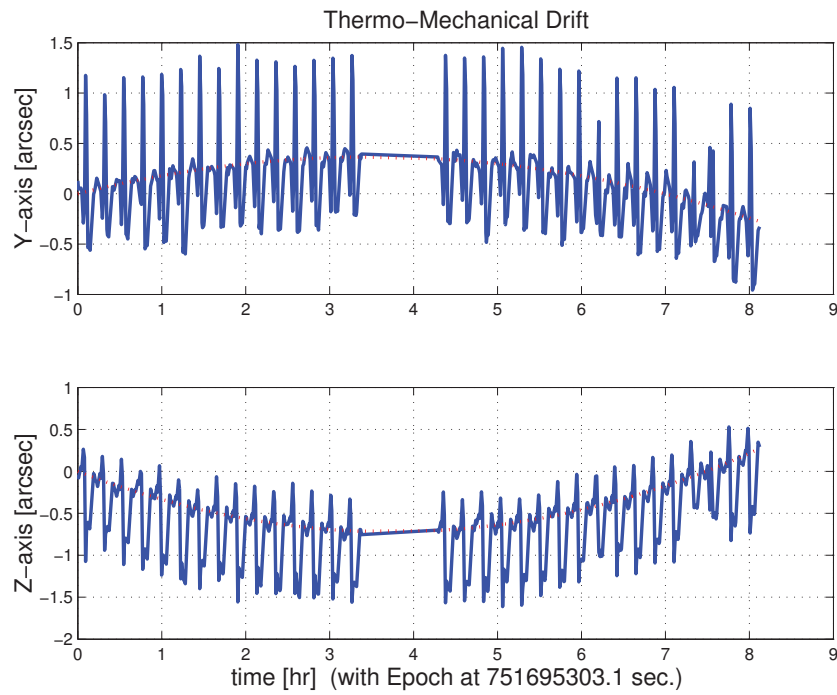


Figure 3.42: Thermo-mechanical boresight drift (equiv. angle in Body frame)

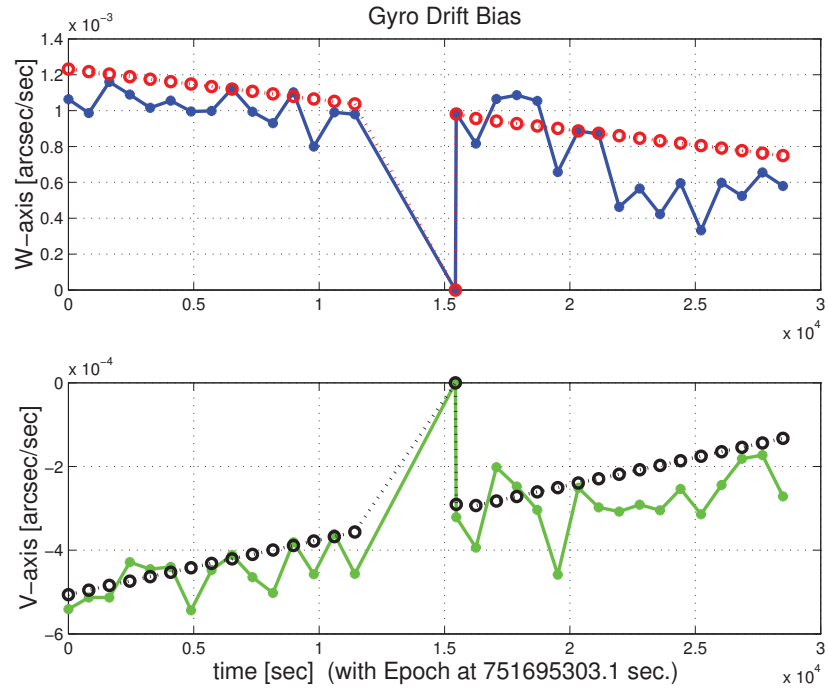


Figure 3.43: Gyro drift bias contribution (equiv. rate in (W,V) coords)

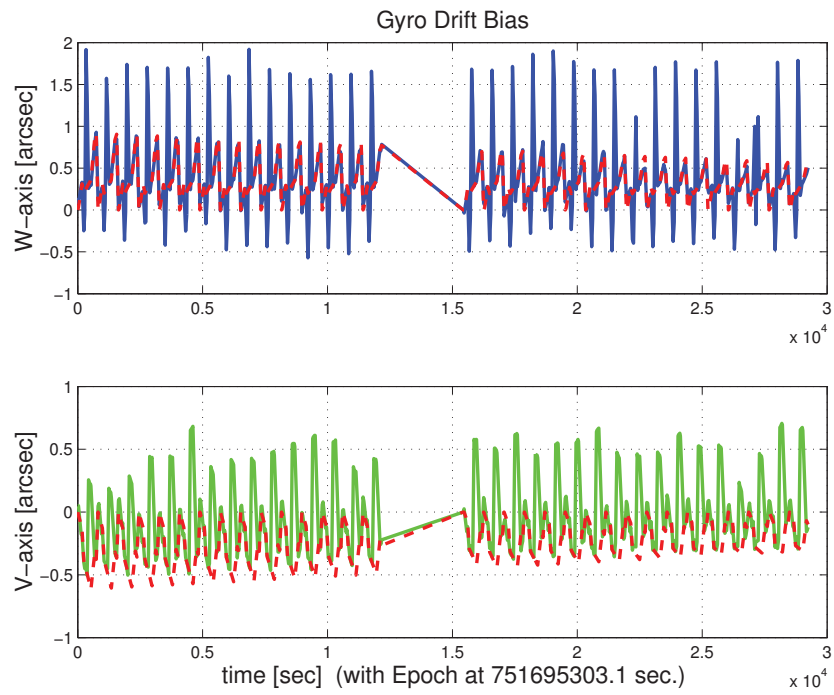


Figure 3.44: Gyro drift bias contribution (equiv. angle in (W,V) coords)

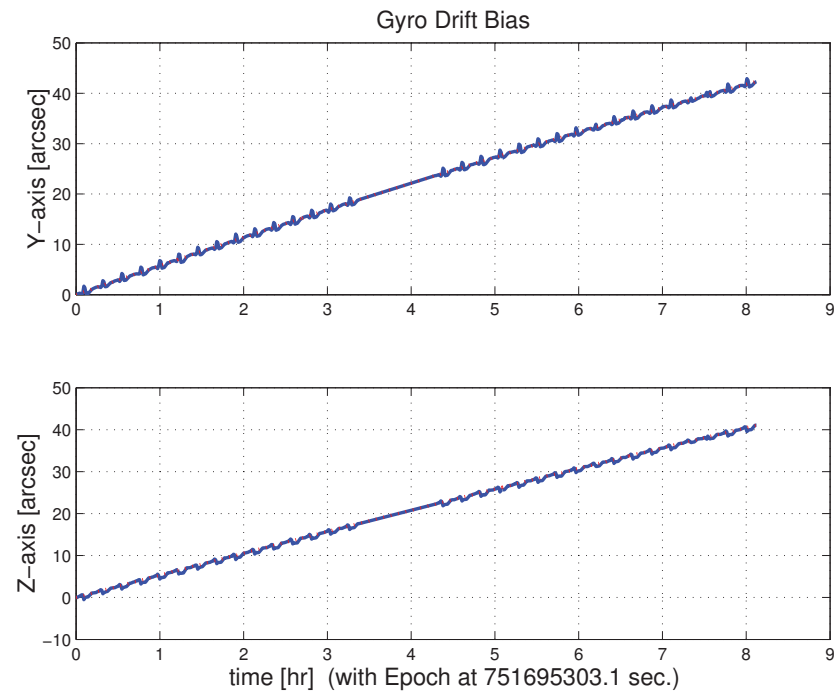


Figure 3.45: Gyro drift bias contribution (equiv. angle in Body frame)

3.2 IPF OUTPUT DATA (IF MINI FILE)

OUTPUT FILE NAME: IFmini502052.dat DATE: 06-Nov-2003 TIME: 15:36
INSTRUMENT NAME: IRS_ShortHi_Center_Position NF: 52
IPF FILTER VERSION: IPF.V3.0.OB SW RELEASE DATE: November 3, 2003
FRAME TABLE USED: BodyFrames_FTU_12b

----- IPF BROWN ANGLE SUMMARY -----

Frame Number	WAS			IS		
	theta_Y (arcmin)	theta_Z (arcmin)	angle (deg)	theta_Y (arcmin)	theta_Z (arcmin)	angle (deg)
052	-10.562537	+10.020449	-41.469994	-10.564666	+10.009720	-41.469994
050	-10.587098	+10.042156	-41.469994	-10.587613	+10.030000	-41.469994
051	-10.537977	+9.998743	-41.469994	-10.541720	+9.989440	-41.469994

OFFSET	NF	Delta_CW	Delta_CV
0	52	+0.000	+0.000 pixels

OFFSET FRAME NAME: IRS_ShortHi_Center_Position

Brown Angle	theta_Y(arcmin)	theta_Z(arcmin)	angle(deg)
WAS(FTB)	-10.562537	+10.020449	-41.469994
IS (EST)	-10.564666	+10.009720	-41.469994
dT_EST	-0.002129	-0.010729	+0.000001
T_sSIGMA	+0.000244	+0.000296	+999.999999
dT_EST/T_sSIGMA	-8.723975	-36.210984	+999.999999

OFFSET	NF	Delta_CW	Delta_CV
1	50	-1.967	+0.000 pixels

OFFSET FRAME NAME: IRS_ShortHi_1st_Position

Brown Angle	theta_Y(arcmin)	theta_Z(arcmin)	angle(deg)
WAS(FTB)	-10.587098	+10.042156	-41.469994
IS (EST)	-10.587613	+10.030000	-41.469994
dT_EST	-0.000515	-0.012156	+0.000001
T_sSIGMA	+0.000246	+0.000296	+999.999999
dT_EST/T_sSIGMA	-2.093937	-41.024396	+999.999999

OFFSET	NF	Delta_CW	Delta_CV
2	51	+1.967	+0.000 pixels

OFFSET FRAME NAME: IRS_ShortHi_2nd_Position

Brown Angle	theta_Y(arcmin)	theta_Z(arcmin)	angle(deg)
WAS(FTB)	-10.537977	+9.998743	-41.469994
IS (EST)	-10.541720	+9.989440	-41.469994
dT_EST	-0.003743	-0.009303	+0.000001
T_sSIGMA	+0.000243	+0.000296	+999.999999
dT_EST/T_sSIGMA	-15.414509	-31.397572	+999.999999

VARNAME	MEAN	SIGMA	SCALED_SIGMA
a00	-6.5705487146102651E-002	+2.6191387008183905E-004	+4.3074017602912843E-004
del_theta2	+2.2273864585491025E-017	+4.3165787164758853E-008	+7.0989897388688794E-008
del_theta3	+2.7528703134662770E-017	+5.2409111796865510E-008	+8.6191349980275216E-008
del_arx	+7.0425940300572042E-015	+1.8382724407847352E-005	+3.0231991703444217E-005
del_ary	+8.1463054889003433E-016	+1.6227957746464321E-006	+2.6688290215868125E-006
del_arz	-4.222903934359957E-017	+1.4128270012491482E-006	+2.3235170822629950E-006
brx	+2.3604735889004068E-009	+2.9550019855455606E-009	+4.8597581908228108E-009
bry	+2.8200257564189934E-010	+2.5101241526822153E-010	+4.1281178390570269E-010
brz	-5.1907500281263906E-010	+1.9577376175246985E-010	+3.2196700607262244E-010
crx	-1.6883873481350253E-013	+1.9929580948029922E-013	+3.2775932038493502E-013
cry	-2.2396366250627404E-014	+1.7136641207161502E-014	+2.8182699327127336E-014
crz	+3.8550434219223248E-014	+1.3239892081674866E-014	+2.1774155924179654E-014
bgx	-1.0600007703919643E-006	+1.0291924858122023E-007	+1.6925967012288573E-007
bgy	+7.8777890409761850E-009	+4.0903062282787342E-010	+6.7268649202552819E-010
bgz	+7.1995246366166518E-009	+5.7672255130505085E-010	+9.4847047692237051E-010
cgx	-8.2645863869215269E-012	+6.0157543817071130E-012	+9.8934321443719405E-012

cgy -5.8515387149980069E-014 +2.4813611173653362E-014 +4.0808145217808047E-014
 cgz -2.6908132548845255E-014 +3.3420365512930413E-014 +5.4962702507886901E-014

LSQF RESIDUAL SIGMA SCALE = +1.6445871152014095E+000

qT	qT(1)	qT(2)	qT(3)	qT(4)
FrmTbl:	-3.5404327280610598E-001	+1.9527415652731701E-003	-8.1910767309139004E-004	+9.3522664463954297E-001
Estim:	-3.5404327077851921E-001	+1.9524786628121128E-003	-8.1753859358548104E-004	+9.3522664732896021E-001
DelTheta	deltheta(1)	deltheta(2)	deltheta(3)	
	-2.6791268705801635E-012	-1.6027980420218137E-006	+2.7487445520394881E-006	[rad]
EulAngT	theta(1)	theta(2)	theta(3)	[rad]
Mean	-7.2378792966003580E-001	+3.0731369094873806E-003	-2.9117094832756549E-003	
SigmaT	+9.999900000000000E+004	+4.3165787164758853E-008	+5.2409111796865510E-008	

qR	qR(1)	qR(2)	qR(3)	qR(4)
ASFILE:	+7.088099955811286E-004	+1.2700363295152783E-003	-1.6170006711035967E-004	+9.9999892711639404E-001
Estim:	+7.1443328514189143E-004	+1.2704772679114627E-003	-1.6004849648910255E-004	+9.9999892492795794E-001
DelThetaR	delthetaR(1)	delthetaR(2)	delthetaR(3)	
	+1.1242233987891900E-005	+8.8602263489922893E-007	+3.3168004594096097E-006	[rad]
EulAngR	angR(1)	angR(2)	angR(3)	[rad]
Mean	+1.4284634562220736E-003	+2.5411832270550833E-003	-3.1828233939970092E-004	
SigmaR	+1.8382724407847352E-005	+1.6227957746464321E-006	+1.4128270012491482E-006	

Initial Gyro Bias	Bg0(1)	Bg0(2)	Bg0(3)
	-4.0464931316819275E-007	-1.9414076746215872E-007	+3.6149171478427883E-007
Gyro Bias Correction	Bg(1)	Bg(2)	Bg(3)
	-1.0600007703919643E-006	+7.8777890409761850E-009	+7.1995246366166518E-009
Total Gyro Bias	BgT(1)	BgT(2)	BgT(3)
	-1.4646500835601571E-006	-1.8626297842118253E-007	+3.6869123942089548E-007

Initial Gyro Bias Rate	Cg0(1)	Cg0(2)	Cg0(3)
	+0.000000000000000E+000	+0.000000000000000E+000	+0.000000000000000E+000
Gyro Bias Rate Correction	Cg(1)	Cg(2)	Cg(3)
	-8.2645863869215269E-012	-5.8515387149980069E-014	-2.6908132548845255E-014
Total Gyro Bias Rate	CgT(1)	CgT(2)	CgT(3)
	-8.2645863869215269E-012	-5.8515387149980069E-014	-2.6908132548845255E-014

OFFSET	NF	Delta_CW	Delta_CV	
1	50	-1.967	+0.000 pixels	
OFFSET FRAME NAME:	IRS_ShortHi_1st_Position			
qT	qT(1)	qT(2)	qT(3)	qT(4)
WAS(FTB)	-3.5404325981473134E-001	+1.9572000955569422E-003	-8.2079553480912985E-004	+9.3522663875781187E-001
IS (EST)	-3.5404325864692332E-001	+1.9566442432193110E-003	-8.191155351555981E-004	+9.3522664183591520E-001
DelTheta	deltheta(1)	deltheta(2)	deltheta(3)	
Units	rad	rad	rad	
	-1.3028069489492143E-009	-2.2292780640205448E-006	+2.7487445952514084E-006	
EulAngT	theta(1)	theta(2)	theta(3)	[rad]
Mean	-7.2378792966003580E-001	+3.0798118389476830E-003	-2.9176087609514832E-003	
sSigmaT	+7.6780883458127753E-013	+7.1583330908168654E-008	+8.6191349805800604E-008	
SigmaT	+4.6687027247397920E-013	+4.3526627593334860E-008	+5.2409111690775289E-008	

OFFSET	NF	Delta_CW	Delta_CV	
2	51	+1.967	+0.000 pixels	
OFFSET FRAME NAME:	IRS_ShortHi_2nd_Position			
qT	qT(1)	qT(2)	qT(3)	qT(4)
WAS(FTB)	-3.5404328576834104E-001	+1.9482830348937904E-003	-8.1741981148557622E-004	+9.3522665050800624E-001
IS (EST)	-3.5404328288467785E-001	+1.9483130823214944E-003	-8.1596163375314439E-004	+9.3522665281042194E-001

DelTheta	deltheta(1)	deltheta(2)	deltheta(3)	
Units	rad	rad	rad	
	+1.2917166136925865E-009	-9.7631801987701761E-007	+2.7487445329969042E-006	
EulAngT	theta(1)	theta(2)	theta(3)	[rad]
Mean	-7.2378792966003580E-001	+3.0664619799201293E-003	-2.9058102058418509E-003	

```

sSigmaT +7.6780883458131883E-013 +7.0630674086003822E-008 +8.6191350149506470E-008
SigmaT +4.6687027247400434E-013 +4.2947359512392755E-008 +5.2409111899767487E-008
-----
          q(1)           q(2)           q(3)           q(4)
PCRS1A: +5.3371888965461637E-007 +3.744423778550031E-004 -1.4253684912431913E-003 +9.9999891405806784E-001
PCRS2A: -5.2779261998836216E-007 +3.8462959425181312E-004 +1.3722087221825403E-003 +9.9999898455099423E-001
*****
***** CS-FILE PARAMETERS: ***** AS-FILE PARAMETERS: *****
Row (01) PIX2RADX: +4.8481368110953598E-006 Row (1) TASTART: +7.5169400019071960E+008
Row (02) PIX2RADY: +4.8481368110953598E-006 Row (2) TASTOP: +7.5172550009073484E+008
Row (03) CX0: +0.0000000000000000E+000 Row (3) S/C TIME: +7.5168484879077148E+008
Row (04) CY0: +0.0000000000000000E+000 Row (4) QR1: +7.0880999555811286E-004
Row (05) BETA0: +9.9999000000000000E+004 Row (5) QR2: +1.2700363295152783E-003
Row (06) GAMMA_E0: +9.9999000000000000E+004 Row (6) QR3: -1.6170006711035967E-004
Row (07) D11: +1.0000000000000000E+000 Row (7) QR4: +9.9999892711639404E-001
Row (08) D12: +0.0000000000000000E+000
Row (09) D21: +0.0000000000000000E+000
Row (10) D22: +1.0000000000000000E+000
Row (11) DG: +9.9999000000000000E+004
-----
INITIAL STA-TO-PCRS ALIGNMENT (R) KNOWLEDGE (1-SIGMA)
  SIGMA(X)      SIGMA(Y)      SIGMA(Z)
5.93215198E+000 3.68186833E-001 3.68475304E-001 [arcsec]
-----
PIX2RADX = 4.848136811095E-006[rad/pixel]
XPIXSIZE = 1.0000[arcsec]
PIX2RADY = 4.848136811095E-006[rad/pixel]
YPIXSIZE = 1.0000[arcsec]
CX0 = 0.0[pixel] = 0.00[arcsec]
CY0 = 0.0[pixel] = 0.00[arcsec]
-----
NOMINAL BETA0 = 9.99990000000000E+004[rad/encoder unit]
ENCODER UNIT SIZE = 99999.00[arcsec]
GAMMA_E0 = 99999.00[encoder unit] = 99999.00[arcsec]
-----
| +1 | +0 |
FLIP MATRIX D = |----|----| and DG = +99999
| +0 | +1 |
-----
```

3.3 IPF EXECUTION LOG

```

*****
IPF EXECUTION-LOG FILE NAME: LG502052.dat
INSTRUMENT TYPE: IRS_ShortHi_Center_Position
IPF FILTER EXECUTION DATE: 06-Nov-2003 TIME: 15:32
IPF FILTER VERSION USED: IPF.V3.0.OB
*****
```

```

*****
SLIT FLAG ENABLED! ENTERING SLIT MODE.
*****
```

```

----- Loading & Preparing Input Files -----
AAFILE: AA501052 Loaded! AAFILE dimension = 315000 X 21
ASFILE: AS501052 Loaded!
CAFFILE: CA591052 Loaded! CAFFILE dimension = 253 X 15
```

```

CBFILE: CB502052 Loaded!          CBFILe dimension = 224 X 15
CCFILE: CC502052 Created!        CCFILE dimension = 477 X 19
CSFILE: CS501052 Loaded!
Loading Input Files Completed!
-----
----- Selected Mask Vectors -----
index =   1  2  3  4  5  6  7  8  9 10 11 12 13 14 15 16 17 18 19 20
-----
mask1 = [ 1  0  0  0  0  0  0  0  0  0  0  0  0  0  0  0  0  0  0  0 ]
mask2 = [ 0  0  0  1  1  1  1  1  1  1  1  1  1  1  1  1  1  1  1  1 ]
-----
----- Selected Initial Gyro Bias Parameters -----
User Entered 1 : Use AFILE database - from S/C filter
IPF Linearized Using Following Nominal Gyro Bias Estimates
bg0 = [-4.0464931316819275E-007 -1.9414076746215872E-007 +3.6149171478427883E-007 ]
cg0 = [+0.000000000000000E+000 +0.000000000000000E+000 +0.000000000000000E+000 ]
-----
----- Gyro Pre-Processor Run Completed -----
AGFILE CREATED: AG502052.m      ACFILE CREATED: AC502052.m
-----
Total Gyro Preprocessor Execution Time: 127 seconds

FRAME TABLE ENTRIES FOR PCRS LOADED TO TPCRS
q_PCRS4 = [ +5.3371888965461637E-007    q_PCRS5 = [ +7.3379987833742897E-007
             +3.7444233778550031E-004           +5.2236196154513707E-004
             -1.4253684912431913E-003           -1.4047712280184723E-003
             +0.9999891405806784E-001 ] ;       +9.9999887687698918E-001 ] ;
q_PCRS8 = [ -5.2779261998836216E-007    q_PCRS9 = [ -7.1963421681856818E-007
             +3.8462959425181312E-004           +5.3239763239987400E-004
             +1.3722087221825403E-003           +1.3516841804518383E-003
             +9.9999898455099423E-001 ] ;       +9.9999894475050310E-001 ] ;
-----
----- Initial Conditions for State ----- ----- Initial Square-Root Cov (diag) -----
p1(01) = a00 = +0.000000000000000E+000 Sigma_initial(01,01) = 1.000000000000000E+000
p1(02) = b00 = +0.000000000000000E+000 Sigma_initial(02,02) = 9.999900000000000E+004
p1(03) = c00 = +0.000000000000000E+000 Sigma_initial(03,03) = 9.999900000000000E+004
p1(04) = a10 = +0.000000000000000E+000 Sigma_initial(04,04) = 9.999900000000000E+004
p1(05) = b10 = +0.000000000000000E+000 Sigma_initial(05,05) = 9.999900000000000E+004
p1(06) = c10 = +0.000000000000000E+000 Sigma_initial(06,06) = 9.999900000000000E+004
p1(07) = d10 = +0.000000000000000E+000 Sigma_initial(07,07) = 9.999900000000000E+004
p1(08) = a20 = +0.000000000000000E+000 Sigma_initial(08,08) = 9.999900000000000E+004
p1(09) = b20 = +0.000000000000000E+000 Sigma_initial(09,09) = 9.999900000000000E+004
p1(10) = c20 = +0.000000000000000E+000 Sigma_initial(10,10) = 9.999900000000000E+004
p1(11) = d20 = +0.000000000000000E+000 Sigma_initial(11,11) = 9.999900000000000E+004
p1(12) = a01 = +0.000000000000000E+000 Sigma_initial(12,12) = 9.999900000000000E+004
p1(13) = b01 = +0.000000000000000E+000 Sigma_initial(13,13) = 9.999900000000000E+004
p1(14) = c01 = +0.000000000000000E+000 Sigma_initial(14,14) = 9.999900000000000E+004
p1(15) = d01 = +0.000000000000000E+000 Sigma_initial(15,15) = 9.999900000000000E+004
p1(16) = e01 = +0.000000000000000E+000 Sigma_initial(16,16) = 9.999900000000000E+004
p1(17) = f01 = +0.000000000000000E+000 Sigma_initial(17,17) = 9.999900000000000E+004
-----
p2f(01) = am1 = +0.000000000000000E+000 Sigma_initial(18,18) = 9.999900000000000E+004
p2f(02) = am2 = +0.000000000000000E+000
p2f(03) = am3 = +1.000000000000000E+000
p2f(04) = beta = +1.000000000000000E+000 Sigma_initial(19,19) = 9.999900000000000E+004
p2f(05) = qT1 = -3.5404327280610642E-001 Sigma_initial(20,20) = 9.999900000000000E+004
p2f(06) = qT2 = +1.9527415652731727E-003 Sigma_initial(21,21) = 1.000000000000000E-002
p2f(07) = aT3 = -8.1910767309139113E-004 Sigma_initial(22,22) = 1.000000000000000E-002
p2f(08) = qT4 = +9.3522664463954419E-001
p2f(09) = qR1 = +7.0880999555811286E-004 Sigma_initial(23,23) = 2.8759884380575061E-004
p2f(10) = qR2 = +1.2700363295152783E-003 Sigma_initial(24,24) = 1.7850201371497795E-005
p2f(11) = qR3 = -1.6170006711035967E-004 Sigma_initial(25,25) = 1.7864186834070523E-005
p2f(12) = qR4 = +9.9999892711639404E-001
p2f(13) = brx = +0.000000000000000E+000 Sigma_initial(26,26) = 3.4199923410131822E-005
p2f(14) = bry = +0.000000000000000E+000 Sigma_initial(27,27) = 3.4199923410131822E-005

```

```

p2f(15) = brz = +0.0000000000000000E+000 Sigma_initial(28,28) = 3.4199923410131822E-005
p2f(16) = crx = +0.0000000000000000E+000 Sigma_initial(29,29) = 1.1696347612588828E-009
p2f(17) = cry = +0.0000000000000000E+000 Sigma_initial(30,30) = 1.1696347612588828E-009
p2f(18) = crz = +0.0000000000000000E+000 Sigma_initial(31,31) = 1.1696347612588828E-009
p2f(19) = bgx = +0.0000000000000000E+000 Sigma_initial(32,32) = 3.4199923410131822E-005
p2f(20) = bgy = +0.0000000000000000E+000 Sigma_initial(33,33) = 3.4199923410131822E-005
p2f(21) = bgz = +0.0000000000000000E+000 Sigma_initial(34,34) = 3.4199923410131822E-005
p2f(22) = cgx = +0.0000000000000000E+000 Sigma_initial(35,35) = 1.1696347612588828E-009
p2f(23) = cgy = +0.0000000000000000E+000 Sigma_initial(36,36) = 1.1696347612588828E-009
p2f(24) = cgz = +0.0000000000000000E+000 Sigma_initial(37,37) = 1.1696347612588828E-009
-----
```

```

----- IPF KALMAN FILTER STARTED -----
Iteration#001: |dp|= +7.035304473914E-002 RMS(|Res|)=+6.192746569781E-006
Iteration#002: |dp|= +5.340758992528E-003 RMS(|Res|)=+4.588057518956E-006
Iteration#003: |dp|= +8.078036632749E-004 RMS(|Res|)=+4.980207813612E-006
Iteration#004: |dp|= +1.171135379293E-004 RMS(|Res|)=+4.961648268860E-006
Iteration#005: |dp|= +1.708650895494E-005 RMS(|Res|)=+4.965471890048E-006
Iteration#006: |dp|= +2.491158786863E-006 RMS(|Res|)=+4.964955767463E-006
Iteration#007: |dp|= +3.633377191562E-007 RMS(|Res|)=+4.965036719099E-006
Iteration#008: |dp|= +5.298407245035E-008 RMS(|Res|)=+4.965024142428E-006
Iteration#009: |dp|= +7.726998202579E-009 RMS(|Res|)=+4.965025964973E-006
Iteration#010: |dp|= +1.126344825022E-009 RMS(|Res|)=+4.965025703642E-006
Iteration#011: |dp|= +1.641712908778E-010 RMS(|Res|)=+4.965025741950E-006
Iteration#012: |dp|= +2.364399517893E-011 RMS(|Res|)=+4.965025736805E-006
Iteration#013: |dp|= +2.946733691273E-012 RMS(|Res|)=+4.965025737407E-006
Iteration#014: |dp|= +3.729283477396E-013 RMS(|Res|)=+4.965025737652E-006
Iteration#015: |dp|= +2.141597851474E-013 RMS(|Res|)=+4.965025737176E-006
Iteration#016: |dp|= +6.641740195310E-013 RMS(|Res|)=+4.965025737133E-006
Iteration#017: |dp|= +3.849759396832E-013 RMS(|Res|)=+4.965025737485E-006
Iteration#018: |dp|= +3.576478413299E-013 RMS(|Res|)=+4.965025737448E-006
Iteration#019: |dp|= +8.043682212241E-013 RMS(|Res|)=+4.965025737422E-006
Iteration#020: |dp|= +4.972818310787E-013 RMS(|Res|)=+4.965025737527E-006
IPF Kalman Filter Completed with Error |dp1| + |dp2| = +4.9728183107868579E-013
-----
```

```

----- IPF LEAST SQUARES FILTER STARTED -----
Iteration#001 COND#=+6.584889771786E+006, |dp|=+7.035311285779E-002
Iteration#002 COND#=+6.637763287133E+006, |dp|=+5.341042164349E-003
Iteration#003 COND#=+6.633342401848E+006, |dp|=+8.075753857731E-004
Iteration#004 COND#=+6.634005680122E+006, |dp|=+1.170941447026E-004
Iteration#005 COND#=+6.633909113754E+006, |dp|=+1.708719355960E-005
Iteration#006 COND#=+6.633923213469E+006, |dp|=+2.491631230291E-006
Iteration#007 COND#=+6.633921156842E+006, |dp|=+3.633894332156E-007
Iteration#008 COND#=+6.633921456809E+006, |dp|=+5.299830437601E-008
Iteration#009 COND#=+6.633921413058E+006, |dp|=+7.729341888773E-009
Iteration#010 COND#=+6.633921419439E+006, |dp|=+1.127260432809E-009
Iteration#011 COND#=+6.633921418506E+006, |dp|=+1.641378111536E-010
Iteration#012 COND#=+6.633921418642E+006, |dp|=+2.385298761950E-011
Iteration#013 COND#=+6.633921418623E+006, |dp|=+3.560617292234E-012
Iteration#014 COND#=+6.633921418624E+006, |dp|=+8.923574599323E-013
Iteration#015 COND#=+6.633921418625E+006, |dp|=+3.864120397288E-013
Iteration#016 COND#=+6.633921418627E+006, |dp|=+2.809497026501E-013
Iteration#017 COND#=+6.633921418628E+006, |dp|=+4.261015156103E-014
Iteration#018 COND#=+6.633921418627E+006, |dp|=+1.857859184083E-013
Iteration#019 COND#=+6.633921418627E+006, |dp|=+7.552667376029E-014
Iteration#020 COND#=+6.633921418627E+006, |dp|=+2.311569587253E-014
IPF Least Squares Filter Completed with Error |dp1| + |dp2| = +2.3115695872532790E-014
-----
```

Total Execution Time: 262 seconds

4 COMMENTS

Overall the data looked clean, and the filter converged nicely.

Comments:

1. The run was performed in normal IPF operating mode.
2. This run uses IPF version 3.0 where the gyro drift bias estimates make use of the recently corrected GCF signs, (MCR 2521) and now show essentially no sandwich-to-sandwich variations.
3. There were 32 sandwiches maneuvers with 253 science centroids and 224 PCRS measurements. Three science centroids (row numbers 227, 187, 235 in the original CA501052.m) were removed due to having large a-posteriori errors from a preliminary run.
4. We estimated 18 parameters consisting of: 1 constant plate scales along the slit, 2 IPF alignment angles (no Twist), 3 STA-to-PCRS alignment angles, 6 STA-to-PCRS thermo-mechanical drift parameters, and 3 gyro bias and 3 gyro bias-drift parameters.
5. The a00 parameter is estimated as -6.77e-2 with high confidence, indicating that the Short-Hi slit is about 7 percent shorter in length than nominally indicated in the CSfile.

We recommend updating frames 52, 50, and 51 with the new quaternions listed in the IF file IF502052.dat. This contains adjustments of about 0.12 arcseconds in theta_Y, and 0.6 arcseconds in theta_Z for the Prime frame 052. In our best judgement, this fine survey is accurate to 0.088 arcsecond which satisfies its fine survey requirement of 0.14 arcsecond by a good margin.

IPF TEAM CONTACT INFORMATION

IPF Team email	ipf@sirtfweb.jpl.nasa.gov	
David S. Bayard	X4-8208	David.S.Bayard@jpl.nasa.gov (TEAM LEADER)
Dhemetrio Boussalis	X4-3977	boussali@grover.jpl.nasa.gov
Paul Brugarolas	X4-9243	Paul.Brugarolas@jpl.nasa.gov
Bryan H. Kang	X4-0541	Bryan.H.Kang@jpl.nasa.gov
Edward.C.Wong	X4-3053	Edward.C.Wong@jpl.nasa.gov (TASK MANAGER)

ACKNOWLEDGEMENTS

This work was performed at the Jet Propulsion Laboratory, California Institute of Technology, under contract with the National Aeronautics and Space Administration.

References

- [1] D.S. Bayard, B.H. Kang, *SIRTF Instrument Pointing Frame Kalman Filter Algorithm*, JPL D-Document D-24809, September 30, 2003.
- [2] B.H. Kang, D.S. Bayard, *SIRTF Instrument Pointing Frame (IPF) Software Description Document and User's Guide*, JPL D-Document D-24808, September 30, 2003.
- [3] D.S. Bayard, B.H. Kang, *SIRTF Instrument Pointing Frame (IPF) Kalman Filter Unit Test Report*, JPL D-Document D-24810, September 30, 2003.
- [4] *Space Infrared Telescope Facility In-Orbit Checkout and Science Verification Mission Plan*, JPL D-Document D-22622, 674-FE-301 Version 1.4, February 8, 2002.
- [5] *Space Infrared Telescope Facility Observatory Description Document*, Lockheed Martin LMMS/P458569, 674-SEIT-300 Version 1.2, November 1, 2002.
- [6] *SIRTF Software Interface Specification for Science Centroid INPUT Files (CAFILe, CS-FILE)*, JPL SOS-SIS-2002, November 18, 2002.
- [7] *SIRTF Software Interface Specification for Inferred Frames Offset INPUT Files (OFILE)*, JPL SOS-SIS-2003, November 18, 2002.
- [8] *SIRTF Software Interface Specification for PCRS Centroid INPUT Files (CBFILE)*, JPL SIS-FES-015, November 18, 2002.
- [9] *SIRTF Software Interface Specification for Attitude INPUT Files (AFILE, ASFILE)*, JPL SIS-FES-014, January 7, 2002.
- [10] *SIRTF Software Interface Specification for IPF Filter Output Files (IFFILE, LGFILE, TARFILE)*, JPL SOS-SIS-2005, November 18, 2002.
- [11] R.J. Brown, *Focal Surface to Object Space Field of View Conversion*. Systems Engineering Report SER No. S20447-OPT-051, Ball Aerospace & Technologies Corp., November 23, 1999.

JET PROPULSION LABORATORY

SIRTF IPF REPORT

JPL ID501058

November 11, 2003

**SIRTF INSTRUMENT POINTING FRAME
KALMAN FILTER EXECUTION SUMMARY**

IPF RUN NUMBER: 501058

REPORT TYPE: IOC EXECUTION (FINE)

PRIME FRAME: IRS_LongHi_Center_Position (58)

INFERRRED FRAMES: (56) (57)

IPF TEAM

Autonomy and Control Section (345)

Jet Propulsion Laboratory

California Institute of Technology

4800 Oak Grove Drive

Pasadena, CA 91109

Contents

1 IPF EXECUTION SUMMARY	5
2 IPF INPUT FILE HISTORY	9
3 IPF EXECUTION RESULTS	10
3.1 IPF EXECUTION OUTPUT PLOTS	10
3.2 IPF OUTPUT DATA (IF MINI FILE)	36
3.3 IPF EXECUTION LOG	38
4 COMMENTS	42

List of Figures

1.1 A-priori and a-posteriori IPF frames	5
1.2 A-priori and a-posteriori IPF frames (ZOOMED)	8
2.1 Scenario Plot	9
3.1 TPF coords of measurements and a-priori predicts	12
3.2 Oriented PixelCoords of measurements and a-priori predicts	12
3.3 Oriented (W,V) PixelCoords of A-Priori Prediction Error Quiver Plot	13
3.4 A-priori prediction error (Science Centroids)	13
3.5 Oriented PixelCoords of measurements and a-priori predicts (PCRS only)	14
3.6 Oriented PixelCoords of measurements and a-priori predicts (Zoomed, PCRS only)	14
3.7 Oriented (W,V) PixelCoords of A-Priori PCRS Prediction Error Quiver Plot	15
3.8 A-priori PCRS prediction error	15
3.9 IPF execution convergence, chart 1	16
3.10 IPF execution convergence, chart 2	16
3.11 Parameter uncertainty convergence	17
3.12 IPF parameter symbol table	17
3.13 KF parameter error sigma plots	18
3.14 LS parameter error sigma plot	18
3.15 KF and LS parameter error sigma plot	19
3.16 Oriented PixelCoords of meas. and a-posteriori predicts	20
3.17 Oriented PixelCoords of meas. and a-posteriori predicts (attitude corrected)	20

3.18	KF innovations with (o) and w/o (+) attitude corrections	21
3.19	Histograms of science a-posteriori residuals (or innovations)	21
3.20	A-Posteriori Science Centroid Prediction Error Quiver (Att. Cor.)	22
3.21	Normalized A-Posteriori Science Centroid Prediction Errors	22
3.22	KF innovations with (o) and w/o (+) attitude corrections (PCRS)	23
3.23	Histograms of PCRS a-posteriori residuals (or innovations)	23
3.24	A-posteriori PCRS Prediction Summary	24
3.25	A-posteriori PCRS Prediction (PCRS 1 Only)	25
3.26	A-posteriori PCRS Prediction (PCRS 2 Only)	25
3.27	A-Posteriori PCRS Prediction Errors Quiver (Att. Cor.)	26
3.28	Normalized A-Posteriori PCRS Prediction Errors	26
3.29	W-axis KF innovations and 1-sigma bound	27
3.30	V-axis KF innovations and 1-sigma bound	27
3.31	Array plot with (solid) and w/o (dashed) optical distortion corrections	28
3.32	Optical Distortion Plot: total (x5 magnification)	28
3.33	Optical Distortion Plot: constant plate scales (x5 magnification)	29
3.34	Optical Distortion Plot: linear plate scale (x5 magnification)	29
3.35	Optical Distortion Plot: gamma terms (x5 magnification)	30
3.36	Scan Mirror Chops	30
3.37	IPF Frame Reconstruction	31
3.38	Center Pixel Reconstruction	31
3.39	Estimated attitude corrections (Body frame)	32
3.40	Estimated attitude error sigma plot (Body frame)	32
3.41	Thermo-mechanical boresight drift (equiv. angle in (W,V) coords)	33
3.42	Thermo-mechanical boresight drift (equiv. angle in Body frame)	33
3.43	Gyro drift bias contribution (equiv. rate in (W,V) coords)	34
3.44	Gyro drift bias contribution (equiv. angle in (W,V) coords)	34
3.45	Gyro drift bias contribution (equiv. angle in Body frame)	35

List of Tables

1.1	IPF filter input files	6
1.2	IPF filter execution configuration	6

1.3	IPF filter execution mask vector assignment	6
1.4	IPF calibration error summary ([arcsec], 1-sigma, radial)	7
1.5	Science measurement prediction error summary (1-sigma)	7
1.6	IPF Brown angle summary	8
2.1	IPF input file editing status	9
3.1	Table of figures I (IPF run)	10
3.2	Table of figures II (IPF run)	11
3.3	PCRS measurement prediction error summary	24

1 IPF EXECUTION SUMMARY

This report summarizes the SIRTF Instrument Pointing Frame (IPF) Kalman Filter execution associated with run file: RN501058. In particular, this Focal Point Survey calibrates the instrument: IRS_LongHi_Center_Position (58), as part of the IOC Fine Survey. The main calibration results from the IPF filter execution have been documented in IF501058 typically stored in the mission archive DOM collection IPF_IF. This report only summarizes the main aspects of the run, and does not substitute for the full information contained in the IF file.

Section 1 summarizes the filter execution results. The filter configurations are tabulated in Table 1.2 and the mask vector assignments are tabulated in Table 1.3. A total of 18 state parameters are estimated in this run. The overall End-to-End pointing performances are tabulated in Table 1.4. The prediction residuals throughout the estimation processes are tabulated in Table 1.5. Section 3 summarizes resulting plots, a mini summary of the IF IPF output file, and the execution log. Section 4 captures the user comments that are specific to this particular run.

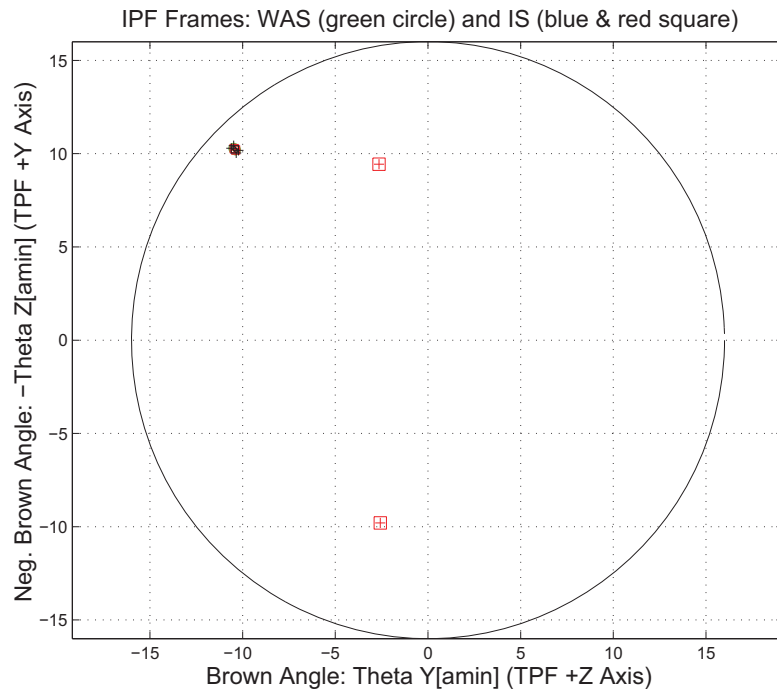


Figure 1.1: A-priori and a-posteriori IPF frames

RAW	FINAL (After Editing)
AA501058	AA501058
AS501058	AS501058
CA501058	CA501058
CB502058	CB502058
CS501058	CS501058

Table 1.1: IPF filter input files

EXECUTION CONFIGURATION ITEM	CURRENT STATUS
IPF Filter Version Used	IPF.V3.0.0B
Frame Table Version Used	BodyFrames_FTU_13a
Scan-Mirror Employed?	NO
IPF Filter Mode	NORMAL-MODE(0)
SLIT-MODE Operation	ENABLED
Kalman Filter Operation	ENABLED
Least-Squares Data Analysis	ENABLED
IBAD Screening	ENABLED
User-Specified Data Editing	DISABLED
Total Number of Iterations	30
LS Residual Sigma Scale	1.74186374E+000
Total Number of Maneuvers	7

Table 1.2: IPF filter execution configuration

Con. Plate Scale			Γ Dependent				Γ^2 Dependent				Linear Plate Scale						Mirror			
a_{00}	b_{00}	c_{00}	a_{10}	b_{10}	c_{10}	d_{10}	a_{20}	b_{20}	c_{20}	d_{20}	a_{01}	b_{01}	c_{01}	d_{01}	e_{01}	f_{01}	α	β		
1	2	3	4	5	6	7	8	9	10	11	12	13	14	15	16	17	18	19		
1	0	0	0	0	0	0	0	0	0	0	0	0	0	0	0	0	0	0		
IPF (T)			Alignment R						Gyro Drift Bias											
θ_1	θ_2	θ_3	a_{rx}	a_{ry}	a_{rz}	b_{rx}	b_{ry}	b_{rz}	c_{rx}	c_{ry}	c_{rz}	b_{gx}	b_{gy}	b_{gz}	c_{gx}	c_{gy}	c_{gz}			
20	21	22	23	24	25	26	27	28	29	30	31	32	33	34	35	36	37			
0	1	1	1	1	1	1	1	1	1	1	1	1	1	1	1	1	1			

Table 1.3: IPF filter execution mask vector assignment

FOCAL PLANE SURVEY ANALYSIS: IOC Fine Survey.

INSTRUMENT NAME: IRS_LongHi_Center_Position NF: 58

PIX2RADW: 4.84813681E-006 [rad/pixel] = 1.0000E+000 [arcsec/pixel]

PIX2RADV: 4.84813681E-006 [rad/pixel] = 1.0000E+000 [arcsec/pixel]

FRAME	DESCRIPTION	IPF ¹	SF ²	TOTAL	REQ
058(P)	IRS_LongHi_Center_Position	0.0569	0.0855	0.1027	0.28
056(I)	IRS_LongHi_1st_Position	0.0578	0.0855	0.1032	N/A
057(I)	IRS_LongHi_2nd_Position	0.0568	0.0855	0.1027	N/A

Table 1.4: IPF calibration error summary ([arcsec], 1-sigma, radial)

RMS METRIC	A PRIORI ³	A POSTERIORI ³	ATT. CORRECTED ⁴	UNITS
Radial	0.9716	0.9682	0.9335	arcsec
W-Axis	0.8113	0.9346	0.9247	arcsec
V-Axis	0.5345	0.2527	0.1279	arcsec
Radial	0.9716	0.9682	0.9335	pixels
W-Axis	0.8113	0.9346	0.9247	pixels
V-Axis	0.5345	0.2527	0.1279	pixels

Table 1.5: Science measurement prediction error summary (1-sigma)

¹IPF filter removes systematic pointing errors due to: thermomechanical alignment drift (Body to TPF), gyro bias and bias drift, centroiding error, attitude error, and optical distortion. IPF SIGMA presented here is “Scaled” by the Least Squares Scale factor. The Least Squares Scale Factor was: 1.741864. It is assumed that the gyro Angle Random Walk contribution is captured with the Least Squares scaling. The gyro ARW contribution can be approximately calculated as 0.0877 arcseconds, given that ARW = 100 $\mu\text{deg}/\sqrt{\text{hr}}$, with 7.477653e+002 second Maneuver time (max), and 7 independent Maneuvres.

²Gyro Scale Factor(GSF) assumes 95 ppm error over 0.250 degree maneuver.

³This can be interpreted as estimate of “pixel to sky” pointing reconstruction error if no science data is used.

⁴This can be interpreted as estimate of achieved S/I centroiding error

IPF BROWN ANGLE SUMMARY					
FRAME TABLE USED: BodyFrames_FTU_13a					
NF	NAME	WAS	IS	CHANGE	UNIT
058	theta_Y	-10.431602	-10.417687	+0.013915	arcmin
058	theta_Z	-10.242024	-10.231851	+0.010173	arcmin
058	angle	+43.340004	+43.340004	-0.000001	deg
056	theta_Y	-10.476856	-10.461402	+0.015453	arcmin
056	theta_Z	-10.284729	-10.273104	+0.011625	arcmin
056	angle	+43.340004	+43.340004	-0.000001	deg
057	theta_Y	-10.386348	-10.373972	+0.012376	arcmin
057	theta_Z	-10.199319	-10.190598	+0.008722	arcmin
057	angle	+43.340004	+43.340004	-0.000001	deg

Table 1.6: IPF Brown angle summary

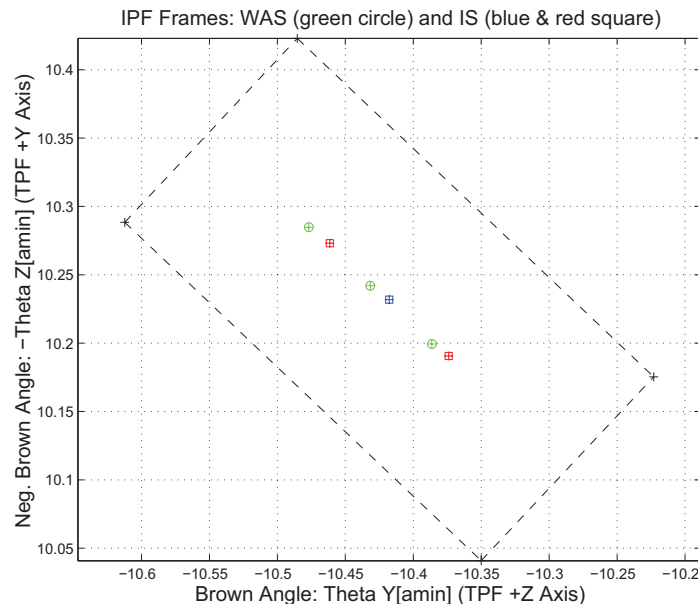


Figure 1.2: A-priori and a-posteriori IPF frames (ZOOMED)

2 IPF INPUT FILE HISTORY

WAS	SIZE	IS	SIZE	REMOVED	PATCHED
AA501058	UNCHANGED	AA501058	UNCHANGED	0	0
CA501058	UNCHANGED	CA501058	UNCHANGED	0	N/A
CB502058	UNCHANGED	CB502058	UNCHANGED	0	N/A

Table 2.1: IPF input file editing status

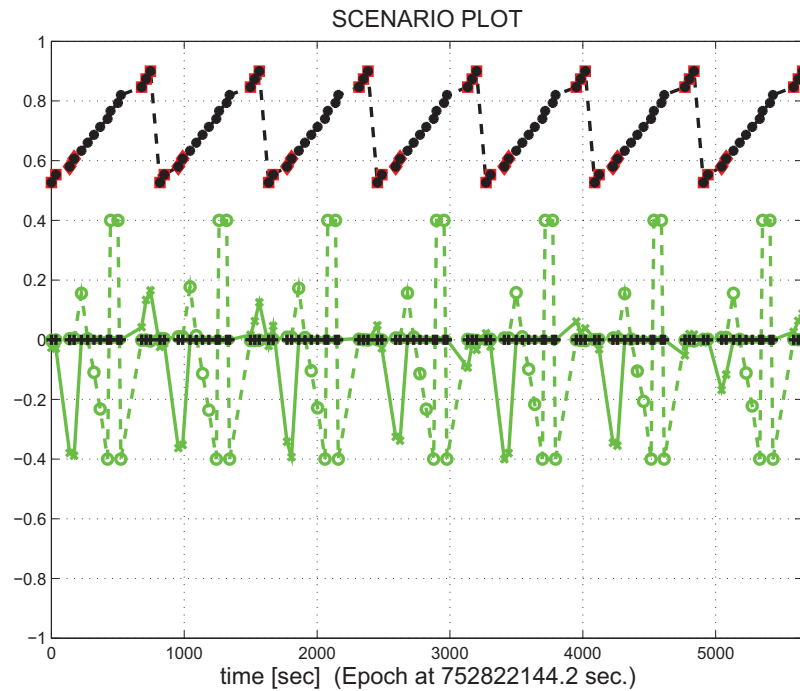


Figure 2.1: Scenario Plot

3 IPF EXECUTION RESULTS

3.1 IPF EXECUTION OUTPUT PLOTS

This subsection summarizes the IPF filter results. As shown in Table 3.1, the output plots are segmented to three groups: predicted performance, post-run results and IPF trending plots.

FIGURE NO.	DESCRIPTION
Predicted performance prior to IPF run	
Figure 3.1	Meas. and a-priori predicts in TPF coords
Figure 3.2	Meas. and a-priori predicts in Oriented Pixel Coords including rectangular array boundary approximation
Figure 3.3	A-Priori Prediction Error Quiver Plot in Oriented Pixel Coords including rectangular array boundary approximation
Figure 3.4	A-priori prediction error
Figure 3.5	Oriented Pixel Coords of measurements and a-priori predicts (PCRS only)
Figure 3.6	Oriented Pixel Coords of measurements and a-priori predicts (Zoomed, PCRS only)
Figure 3.7	Oriented (W,V) Pixel Coords of A-Priori PCRS Prediction Error Quiver Plot
Figure 3.8	A-priori PCRS prediction error
IPF filter performance (post run results)	
Figure 3.9	IPF execution convergence, chart 1: (top) normalized residual error vs. iteration number and (bottom) norm of effective parameter corrections
Figure 3.10	IPF execution convergence, chart 2: parameter correction size vs. iteration number
Figure 3.11	Parameter uncertainty convergence: square-root of diagonal elements of covariance matrix vs. maneuver number
Figure 3.12	IPF parameter symbol table
Figure 3.13	KF parameter error sigma plot (a-priori-dashed, a-posteriori-solid). Includes true parameter errors (FLUTE runs only)
Figure 3.14	LS parameter error sigma plot. Includes true parameter errors (FLUTE runs only)
Figure 3.15	KF and LS parameter errors sigma plot (Figure 3.13 & Figure 3.14 combined)
Figure 3.16	Measurements and a-posteriori predicts in Oriented Pixel Coords including rectangular array boundaries (a-priori-dashed, a-posteriori-solid)
Figure 3.17	Attitude corrected meas. and a-posteriori predicts in Oriented Pixel Coords including rectangular array boundaries (a-priori-dashed, a-posteriori-solid)

Table 3.1: Table of figures I (IPF run)

FIGURE NO.	DESCRIPTION
IPF filter performance (post run results) - CONTINUE	
Figure 3.18	KF innovations with (o) and w/o (+) attitude corrections
Figure 3.19	Histograms of science a-posteriori residuals (or innovations)
Figure 3.20	A-Posteriori Science Centroid Prediction Error Quiver (Att. Cor.)
Figure 3.21	Normalized A-Posteriori Science Centroid Prediction Errors
Figure 3.22	KF innovations with (o) and w/o (+) attitude corrections (PCRS)
Figure 3.23	Histograms of PCRS a-posteriori residuals (or innovations)
Figure 3.24	A-posteriori PCRS Prediction Summary
Figure 3.25	A-posteriori PCRS Prediction (PCRS 1 Only)
Figure 3.26	A-posteriori PCRS Prediction (PCRS 2 Only)
Figure 3.27	A-Posteriori PCRS Prediction Errors Quiver (Att. Cor.)
Figure 3.28	Normalized A-Posteriori PCRS Prediction Errors
Figure 3.29	W-axis KF innovations and 1-sigma bound
Figure 3.30	V-axis KF innovations and 1-sigma bound
Figure 3.31	Array plot with (solid) and w/o (dashed) optical distortion corrections
Figure 3.32	Optical Distortion Plot: total (x5 magnification)
Figure 3.33	Optical Distortion Plot: constant plate scales (x5 magnification)
Figure 3.34	Optical Distortion Plot: linear plate scale (x5 magnification)
Figure 3.35	Optical Distortion Plot: gamma terms (x5 magnification)
Figure 3.36	Scan Mirror Chops
Figure 3.37	IPF Frame Reconstruction
Figure 3.38	Center Pixel Reconstruction
IPF parameter trending plots	
Figure 3.39	Estimated attitude corrections (Body frame)
Figure 3.40	Estimated attitude error sigma plot (Body frame)
Figure 3.41	Systematic error attributed to thermo-mechanical boresight drift (equiv. angle in (W,V) coords)
Figure 3.42	Systematic error attributed to thermo-mechanical boresight drift (equiv. angle in Body frame)
Figure 3.43	Systematic error attributed to gyro drift bias (equiv. rate in (W,V) coords)
Figure 3.44	Systematic error attributed to gyro drift bias (equiv. angle in (W,V) coords)
Figure 3.45	Systematic error attributed to gyro drift bias (equiv. angle in Body frame)

Table 3.2: Table of figures II (IPF run)

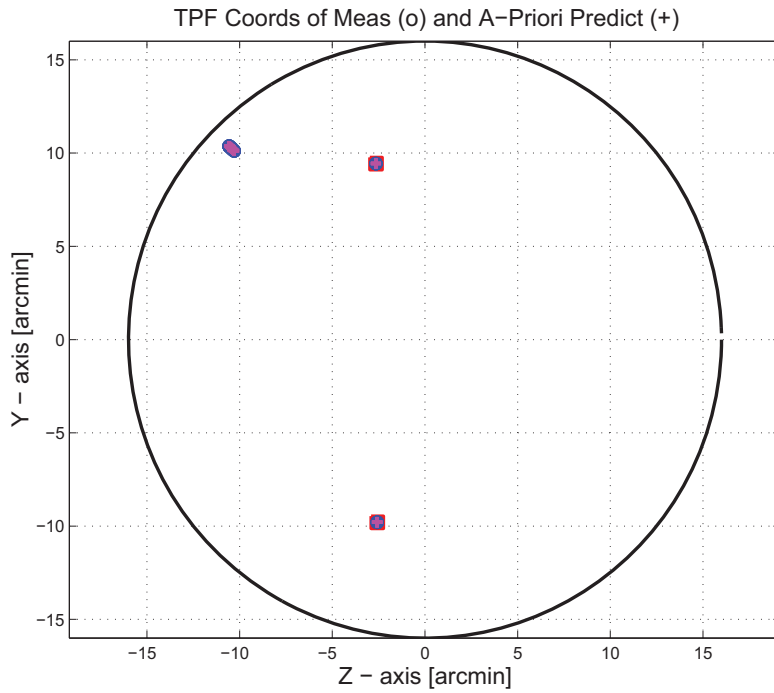


Figure 3.1: TPF coords of measurements and a-priori predicts

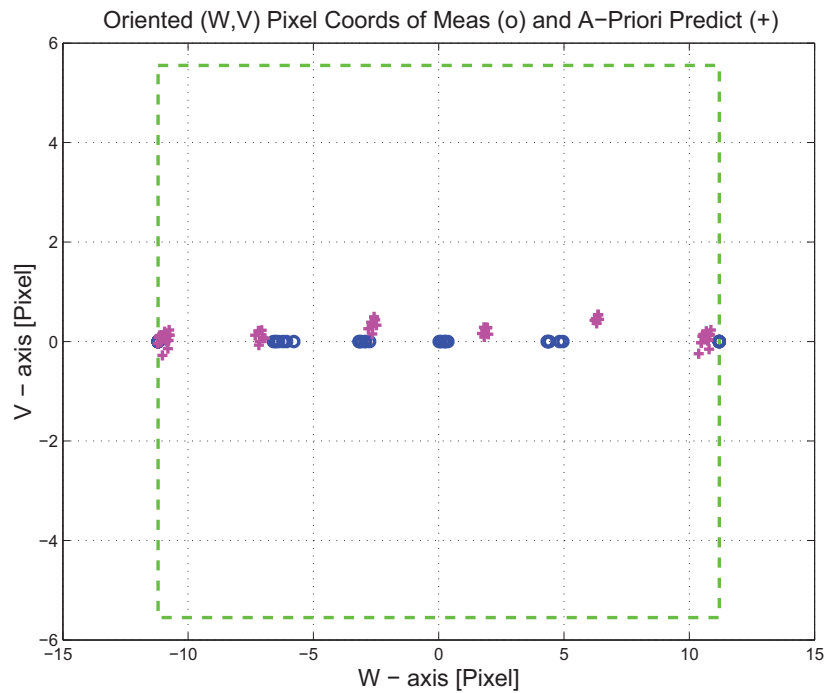


Figure 3.2: Oriented Pixel Coords of measurements and a-priori predicts

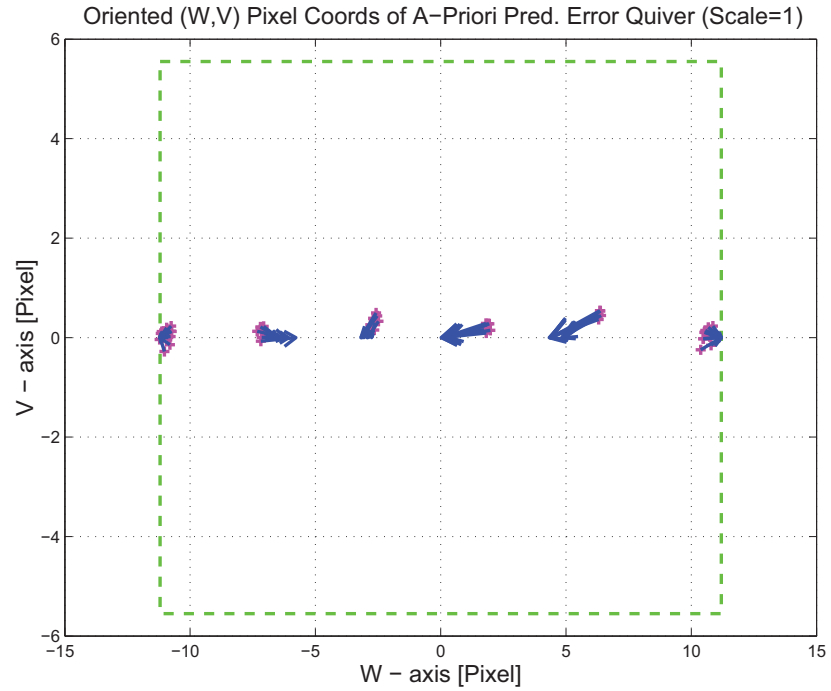


Figure 3.3: Oriented (W,V) Pixel Coords of A-Priori Prediction Error Quiver Plot

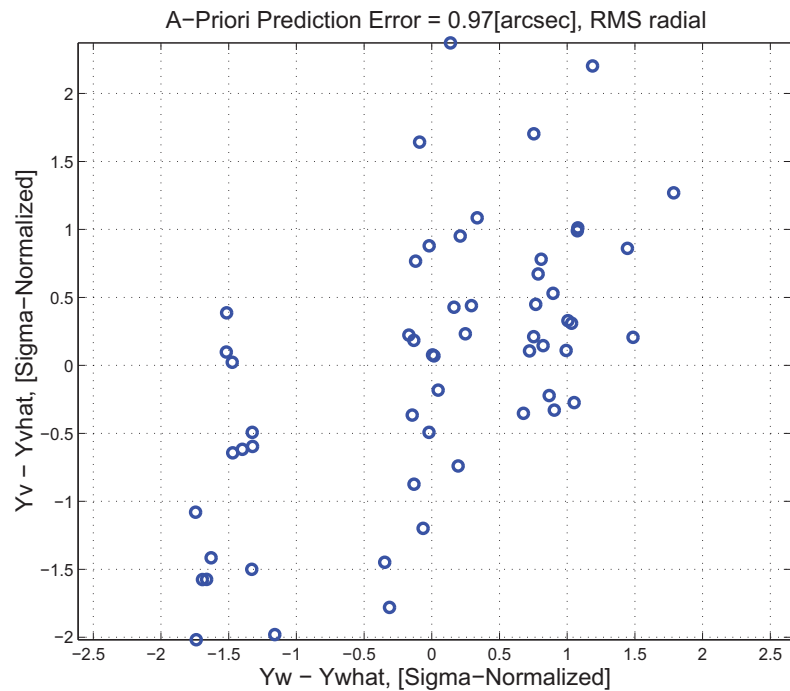


Figure 3.4: A-priori prediction error (Science Centroids)

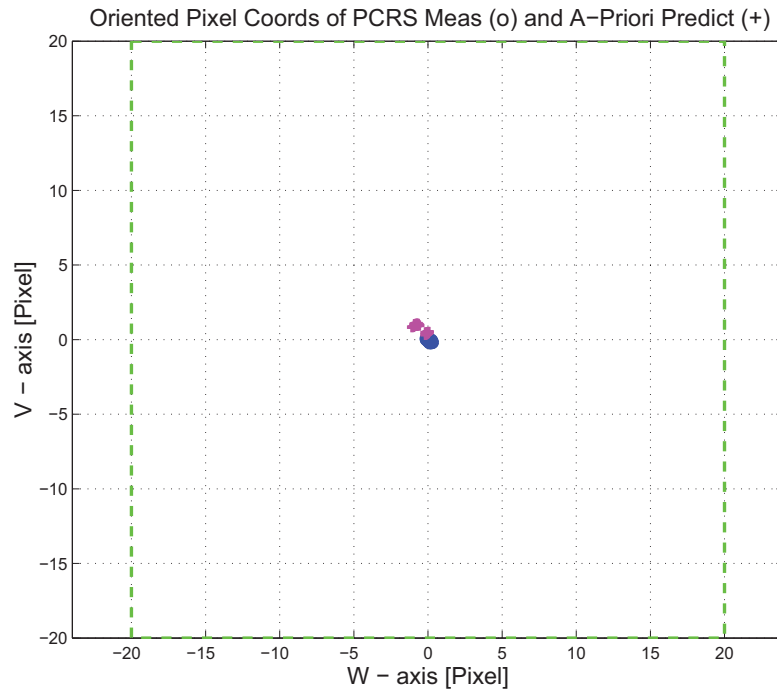


Figure 3.5: Oriented Pixel Coords of measurements and a-priori predicts (PCRS only)

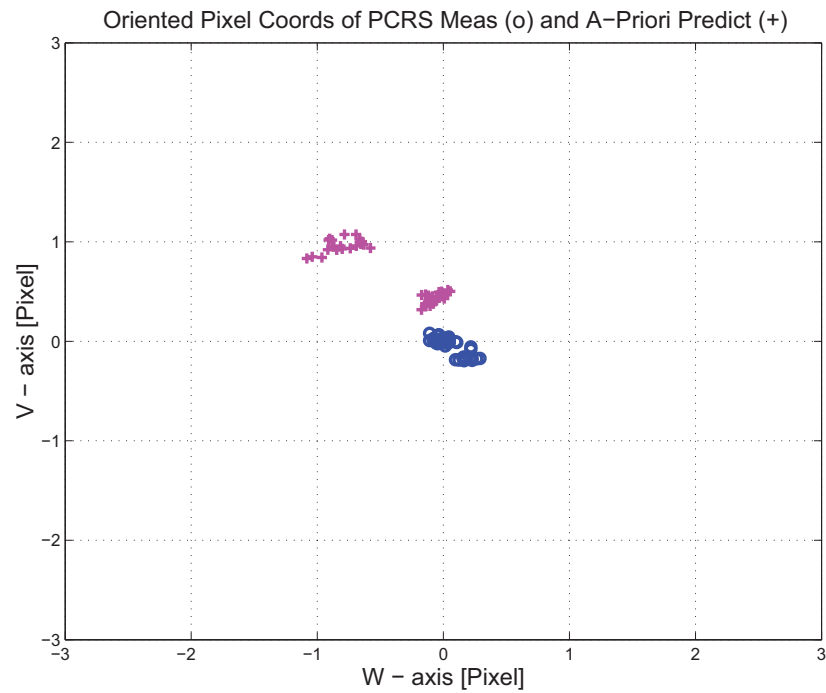


Figure 3.6: Oriented Pixel Coords of measurements and a-priori predicts (Zoomed, PCRS only)

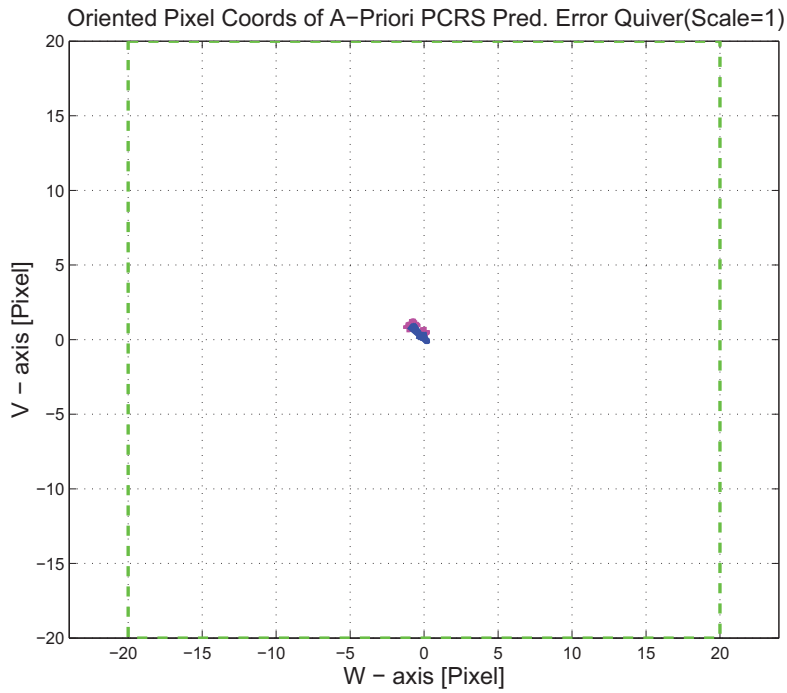


Figure 3.7: Oriented (W,V) Pixel Coords of A-Priori PCRS Prediction Error Quiver Plot

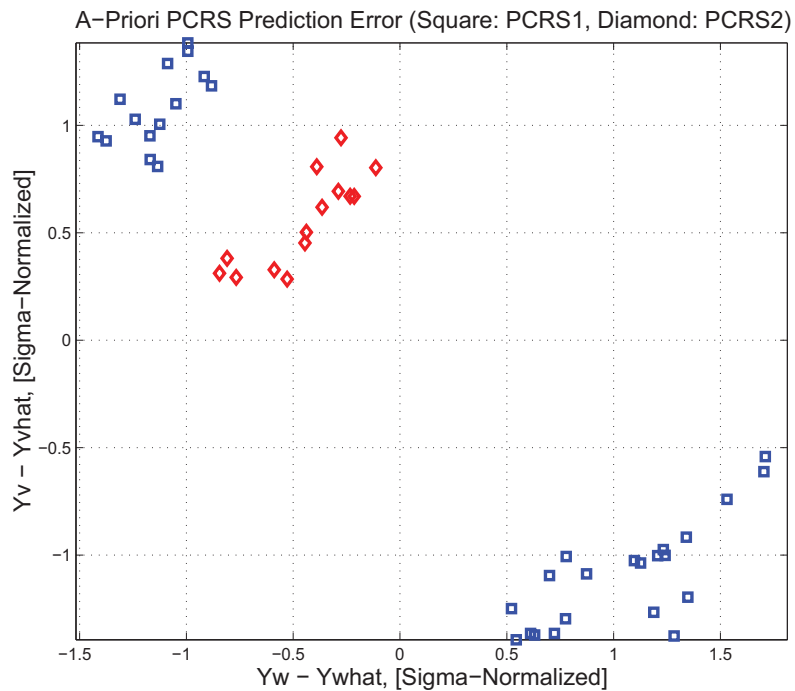


Figure 3.8: A-priori PCRS prediction error

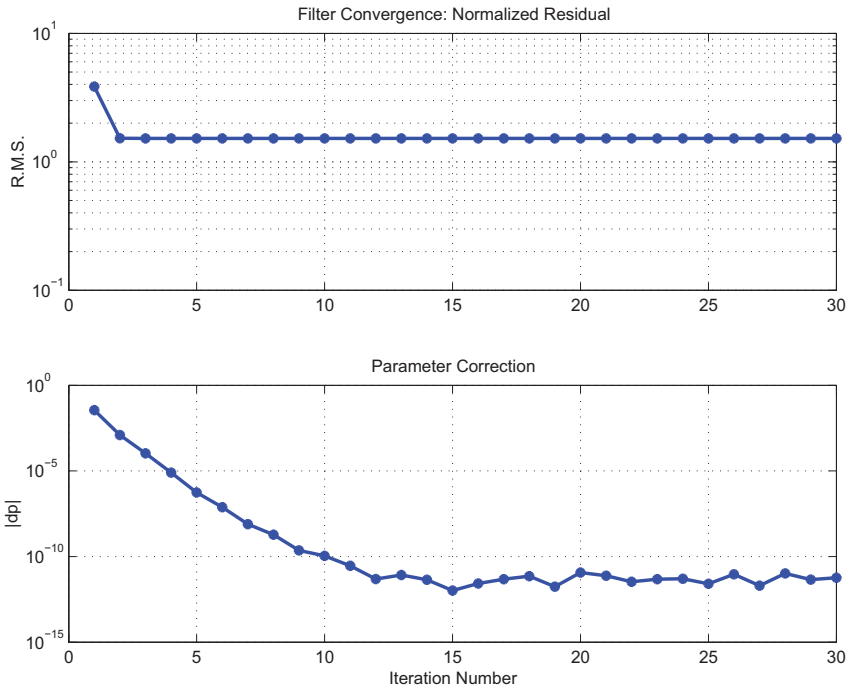


Figure 3.9: IPF execution convergence, chart 1

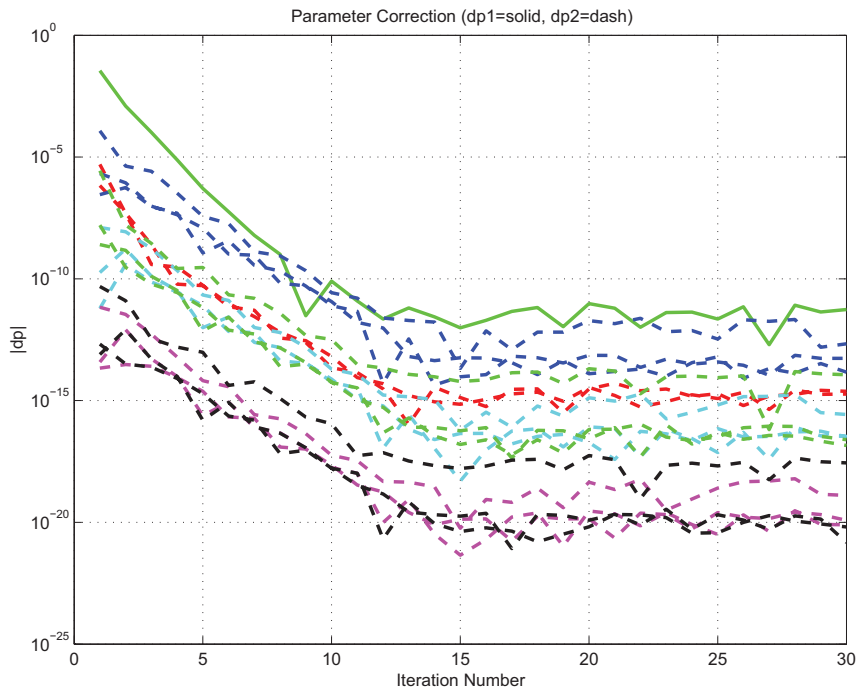


Figure 3.10: IPF execution convergence, chart 2

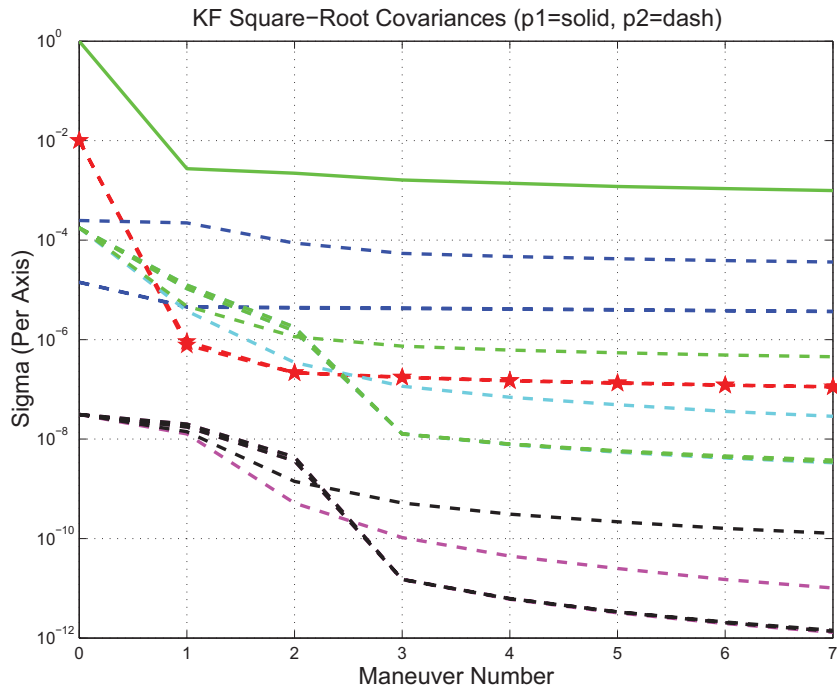


Figure 3.11: Parameter uncertainty convergence

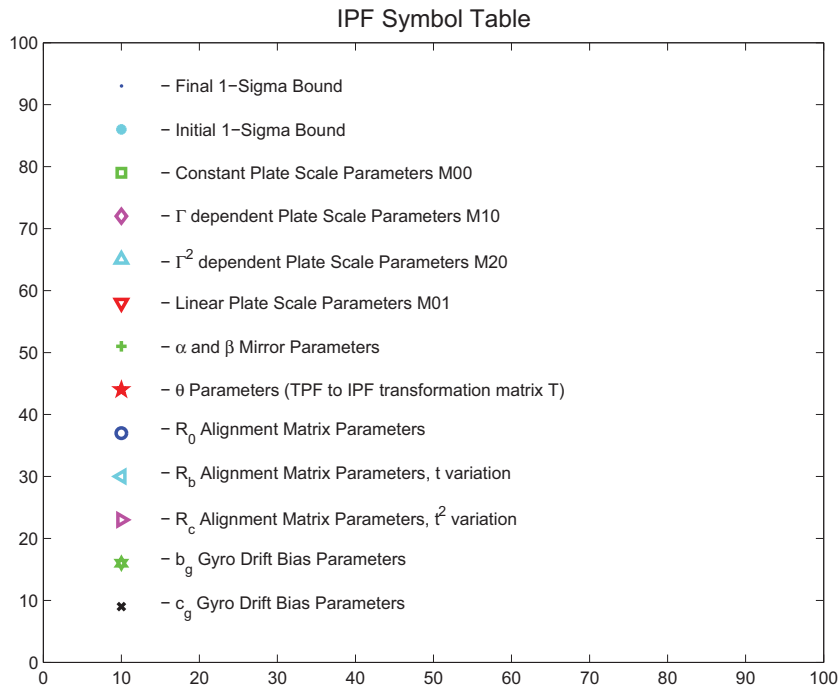


Figure 3.12: IPF parameter symbol table

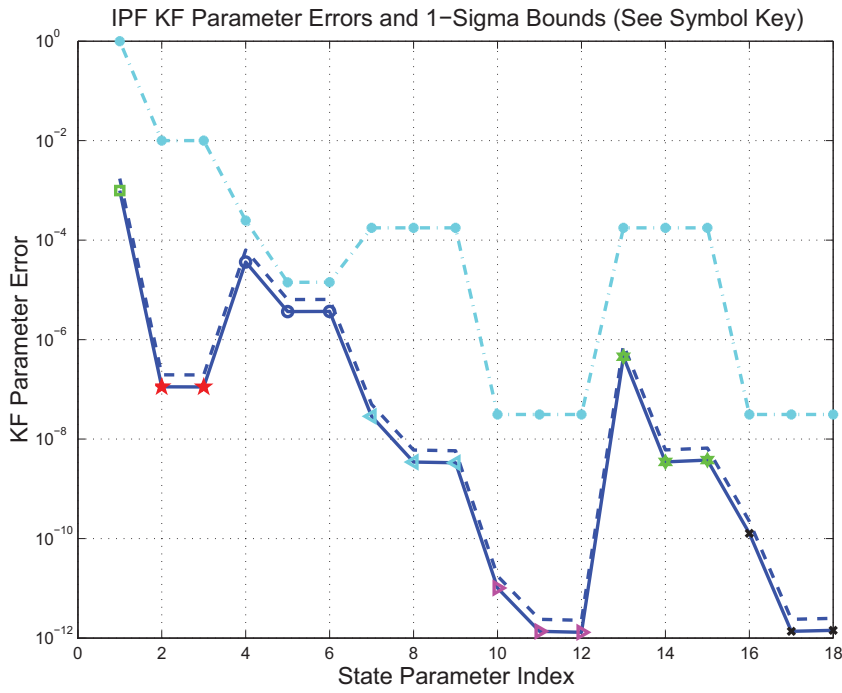


Figure 3.13: KF parameter error sigma plots

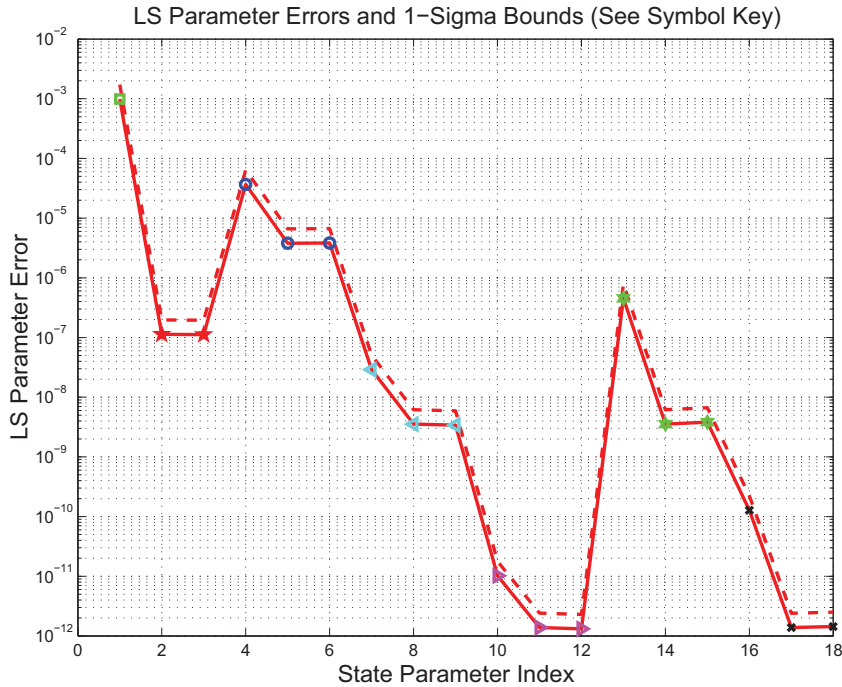


Figure 3.14: LS parameter error sigma plot

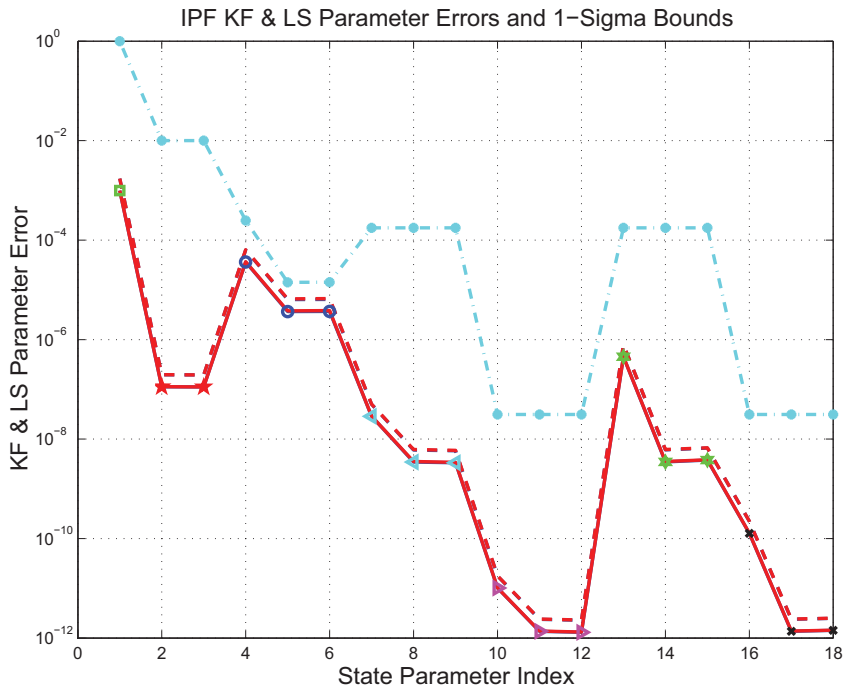


Figure 3.15: KF and LS parameter error sigma plot

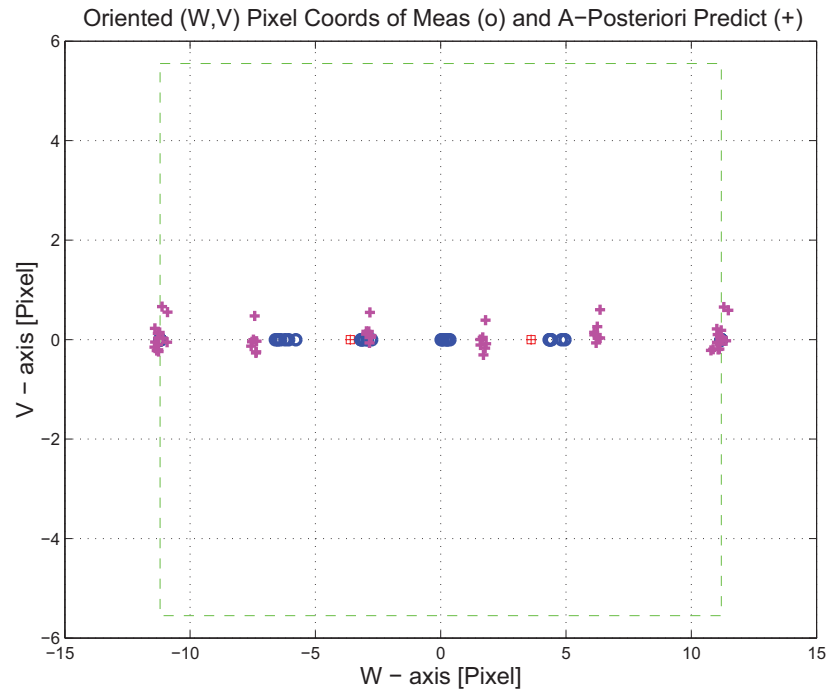


Figure 3.16: Oriented Pixel Coords of meas. and a-posteriori predicts

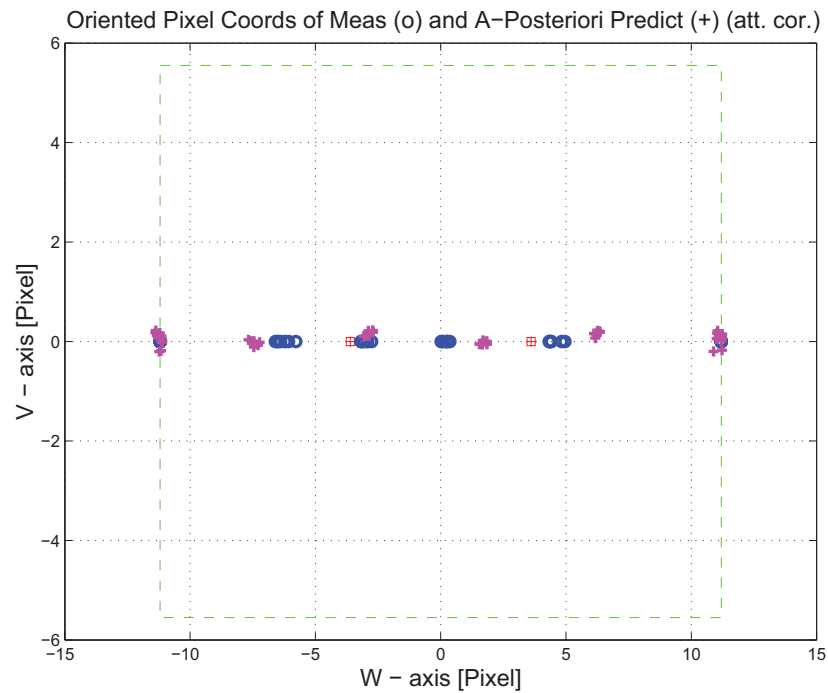


Figure 3.17: Oriented Pixel Coords of meas. and a-posteriori predicts (attitude corrected)

KF Innovations 0.93 asec(with (o)), 0.97 asec (w/o(+)) att. corr. [RMS, radial]

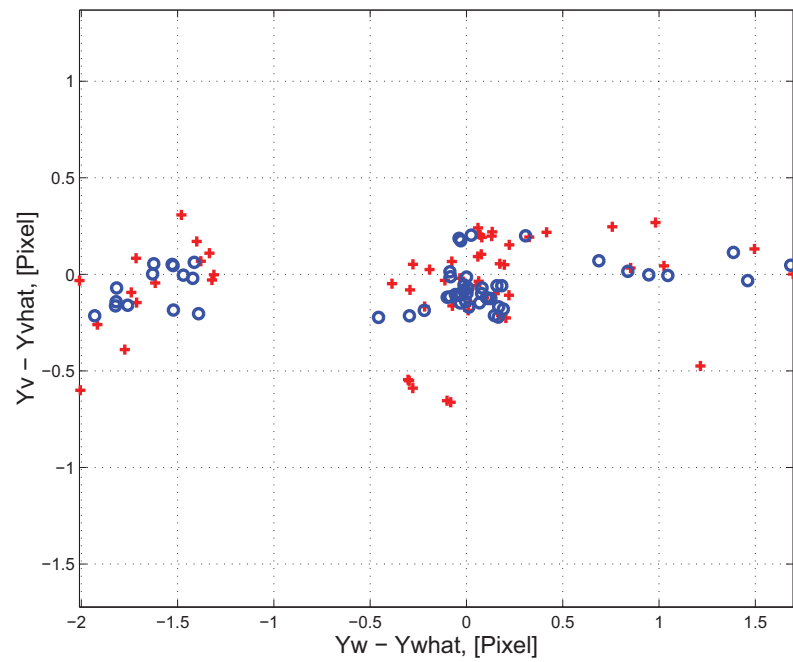


Figure 3.18: KF innovations with (o) and w/o (+) attitude corrections

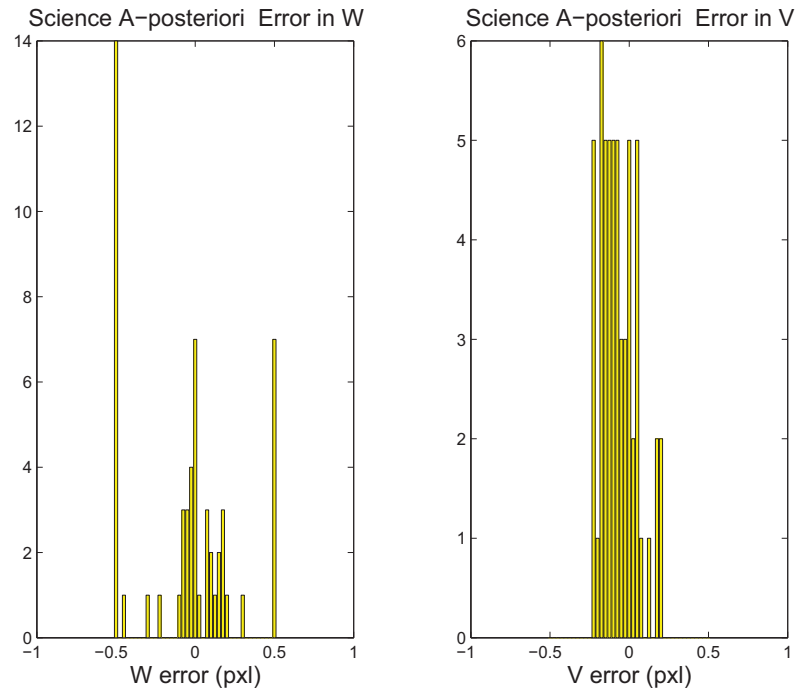


Figure 3.19: Histograms of science a-posteriori residuals (or innovations)

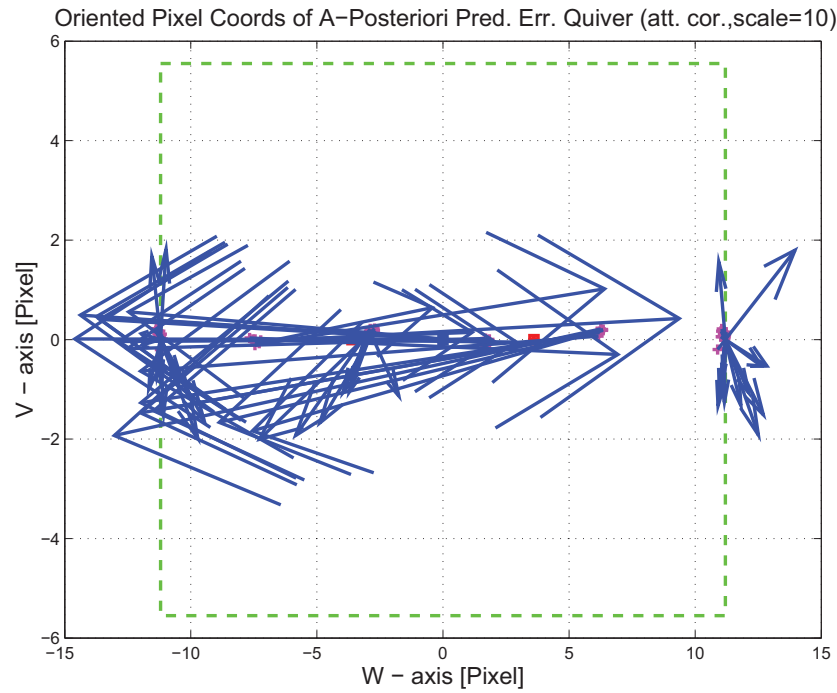


Figure 3.20: A-Posteriori Science Centroid Prediction Error Quiver (Att. Cor.)

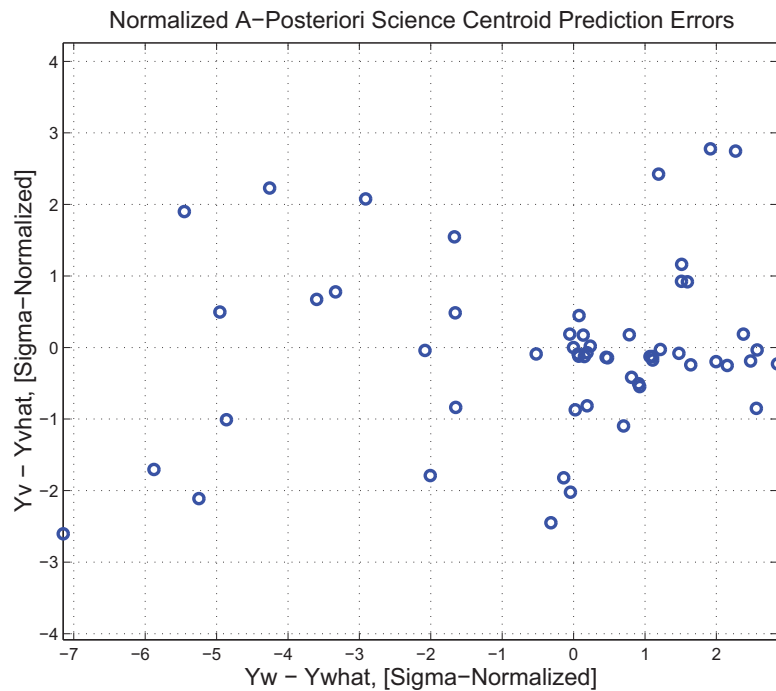


Figure 3.21: Normalized A-Posteriori Science Centroid Prediction Errors

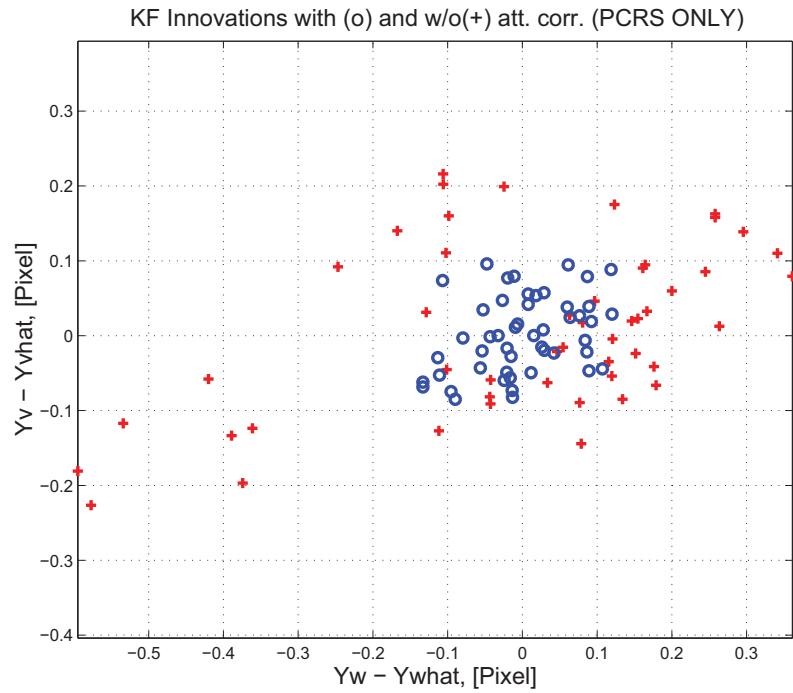


Figure 3.22: KF innovations with (o) and w/o (+) attitude corrections (PCRS)

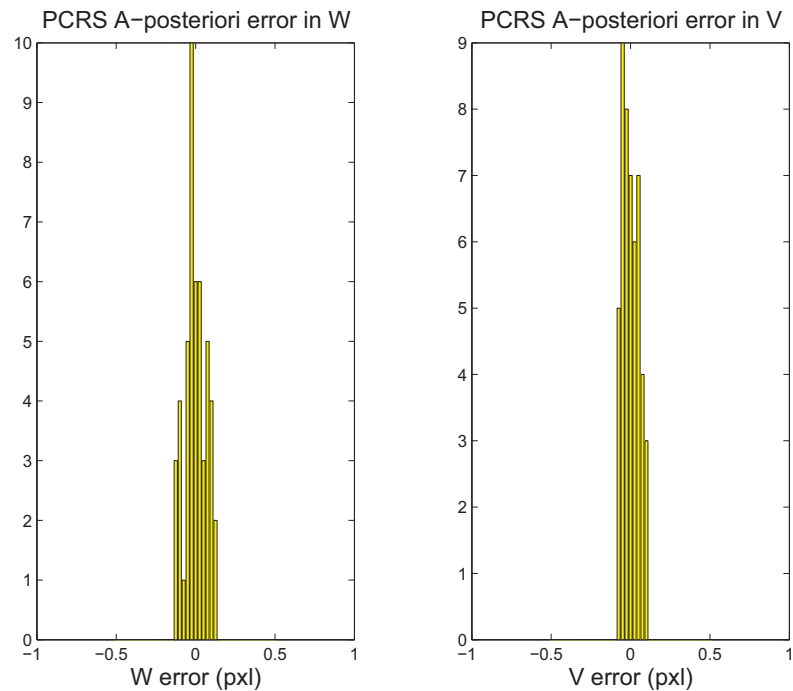


Figure 3.23: Histograms of PCRS a-posteriori residuals (or innovations)

IPF PCRS SUMMARY						
PCRS 1 (Total of 35 centroids)						
RMS	MEAN		SIGMA			
METRIC	APOST.	ATT. COR.	APOST.	ATT. COR.	STAT. CONF.	UNITS
Radial	0.0078	0.0146	0.2672	0.0864	0.0146	arcsec
W-axis	0.0021	0.0003	0.2433	0.0724	0.0122	arcsec
V-axis	-0.0075	-0.0146	0.1105	0.0472	0.0080	arcsec
PCRS 2 (Total of 14 centroids)						
METRIC	APOST.	ATT. COR.	APOST.	ATT. COR.	STAT. CONF.	UNITS
Radial	0.0476	0.0405	0.2369	0.0649	0.0173	arcsec
W-axis	0.0013	-0.0004	0.2135	0.0530	0.0142	arcsec
V-axis	0.0476	0.0405	0.1026	0.0373	0.0100	arcsec
Combined (Total of 49 centroids)						
METRIC	APOST.	ATT. COR.	APOST.	ATT. COR.	STAT. CONF.	UNITS
Radial	0.0084	0.0012	0.2601	0.0846	0.0121	arcsec
W-axis	0.0019	0.0001	0.2351	0.0674	0.0096	arcsec
V-axis	0.0082	0.0012	0.1111	0.0511	0.0073	arcsec

Table 3.3: PCRS measurement prediction error summary

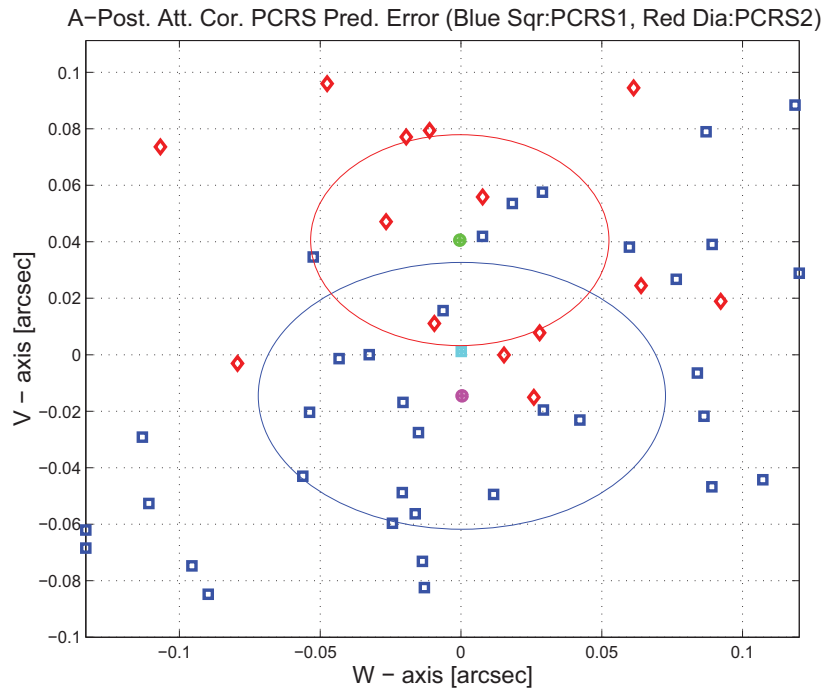


Figure 3.24: A-posteriori PCRS Prediction Summary

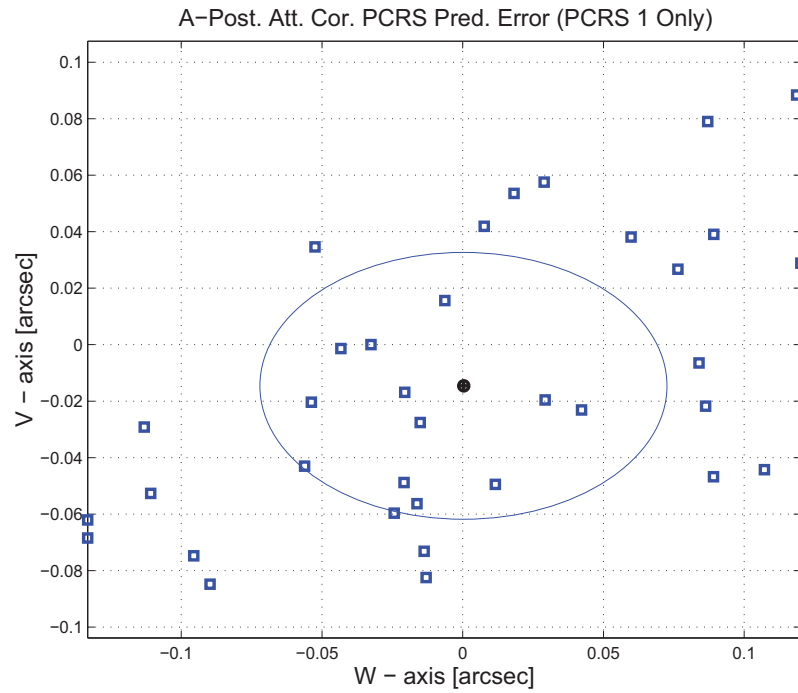


Figure 3.25: A-posteriori PCRS Prediction (PCRS 1 Only)

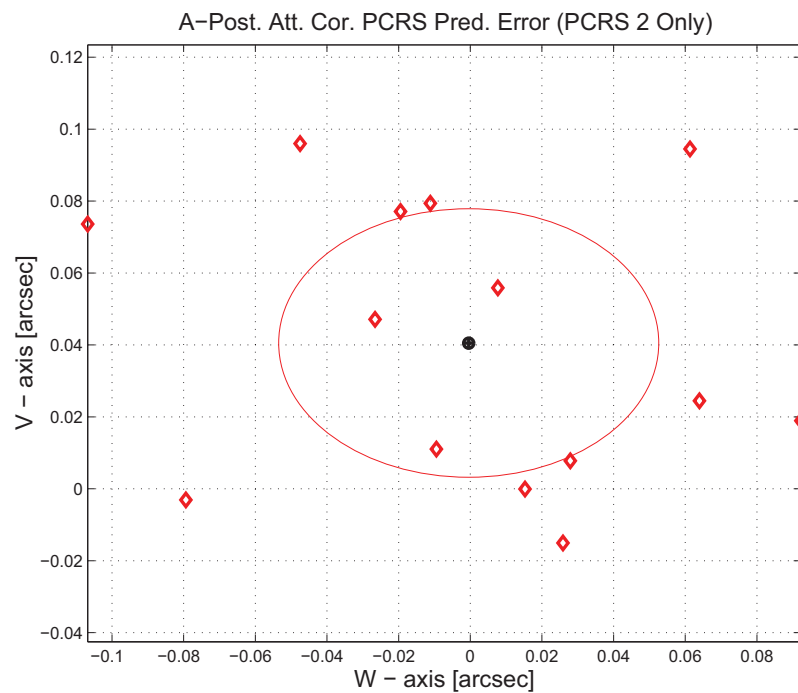


Figure 3.26: A-posteriori PCRS Prediction (PCRS 2 Only)

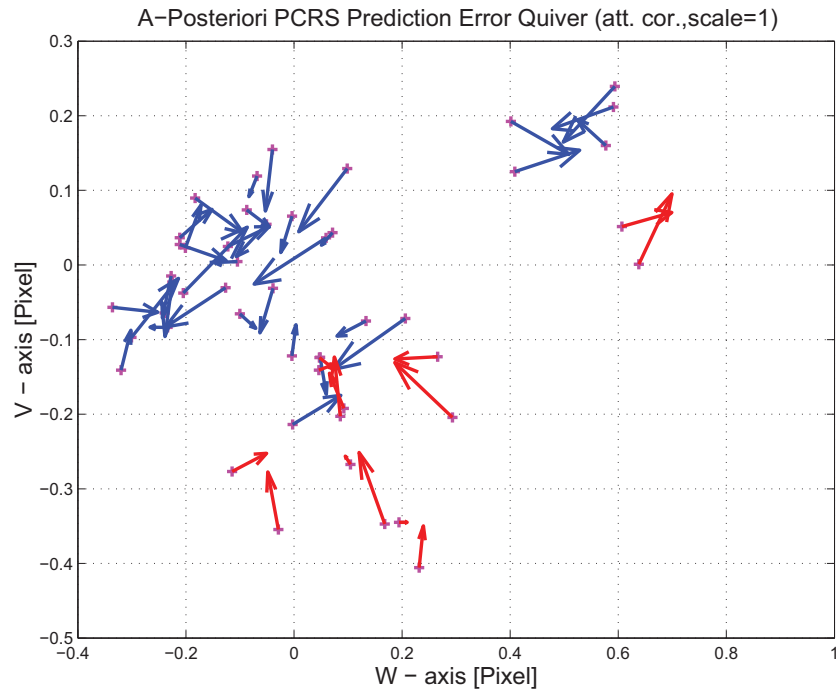


Figure 3.27: A-Posteriori PCRS Prediction Errors Quiver (Att. Cor.)

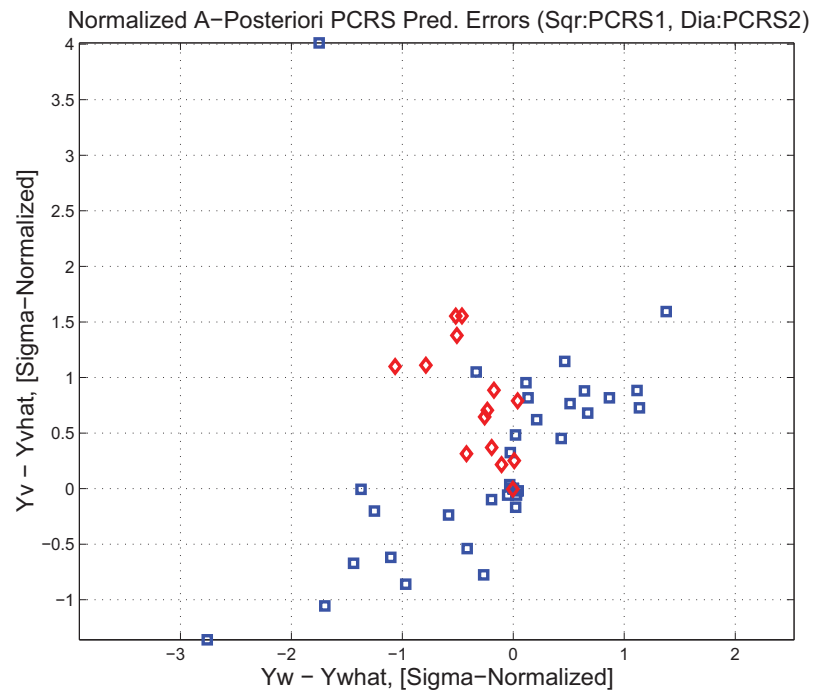


Figure 3.28: Normalized A-Posteriori PCRS Prediction Errors

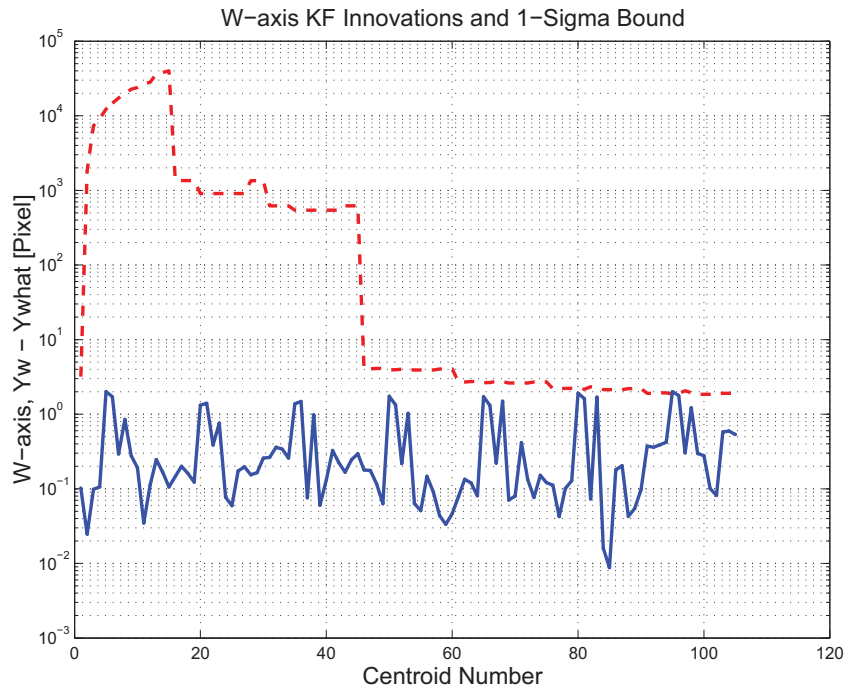


Figure 3.29: W-axis KF innovations and 1-sigma bound

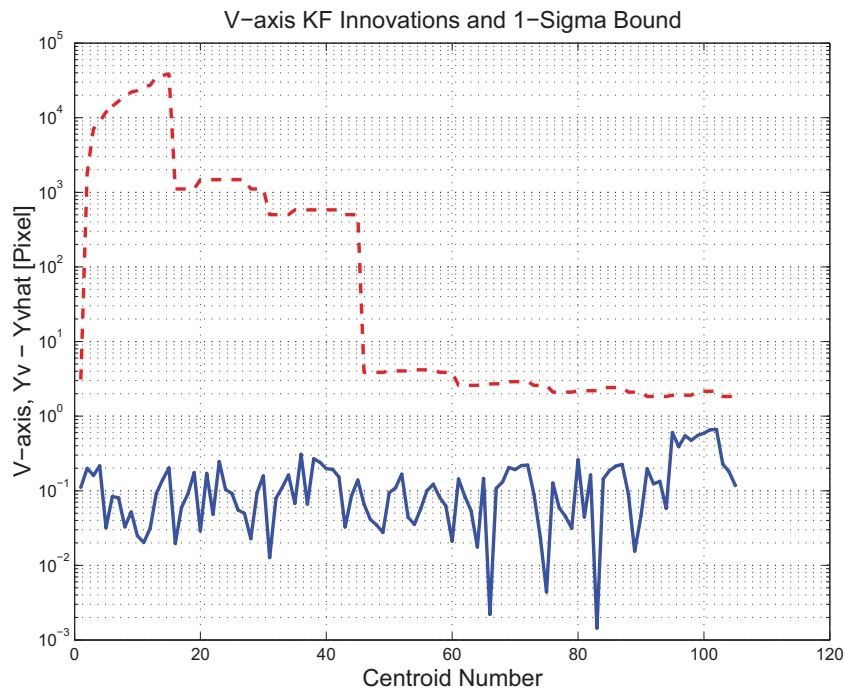


Figure 3.30: V-axis KF innovations and 1-sigma bound

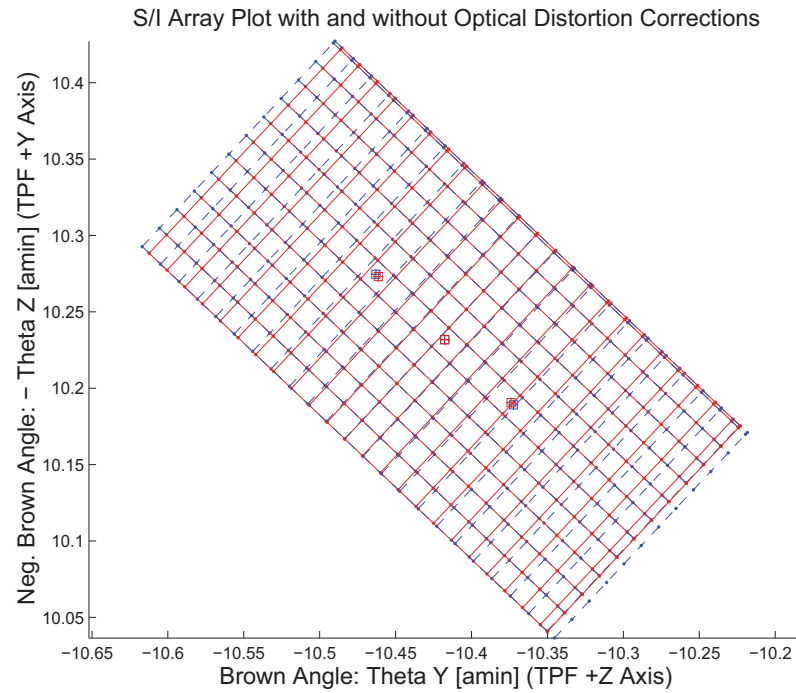


Figure 3.31: Array plot with (solid) and w/o (dashed) optical distortion corrections

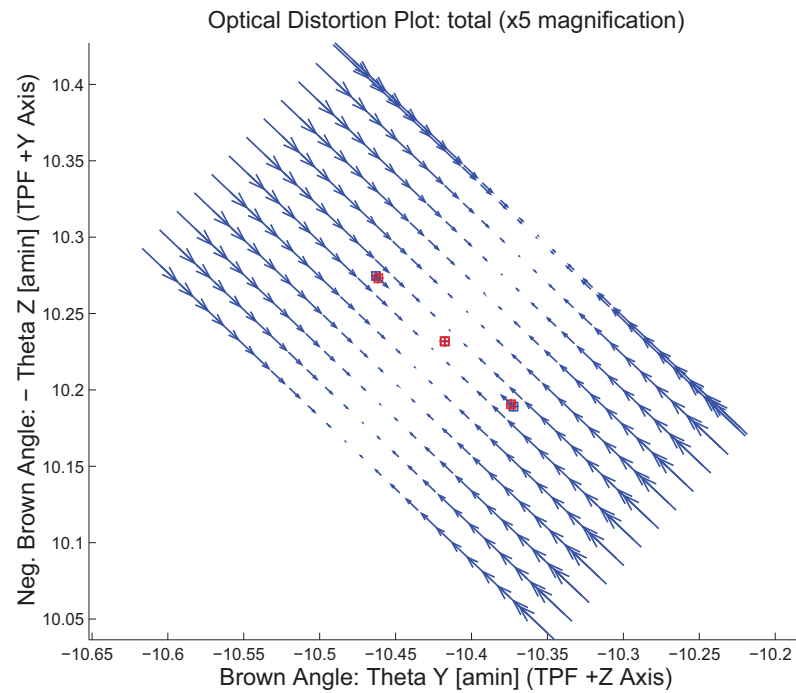


Figure 3.32: Optical Distortion Plot: total (x5 magnification)

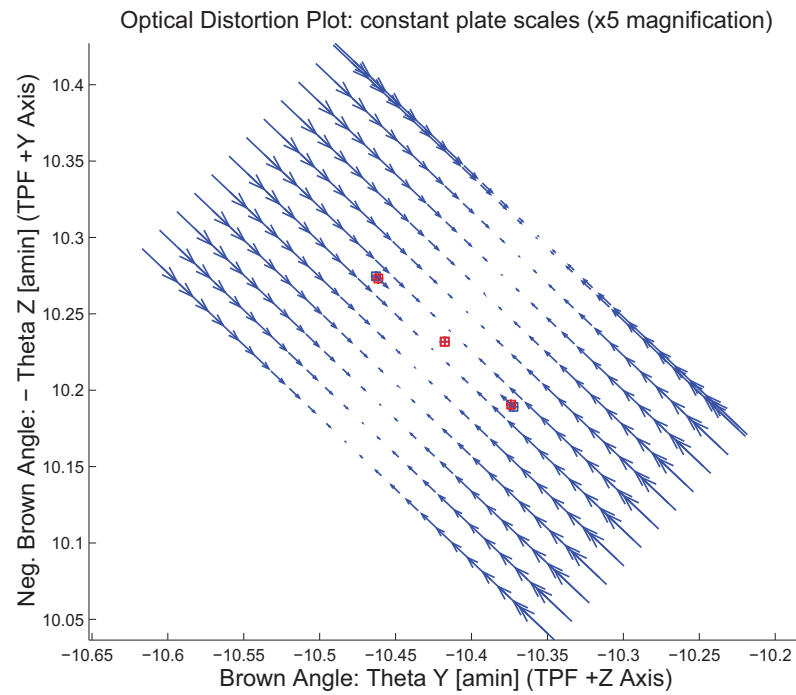


Figure 3.33: Optical Distortion Plot: constant plate scales (x5 magnification)

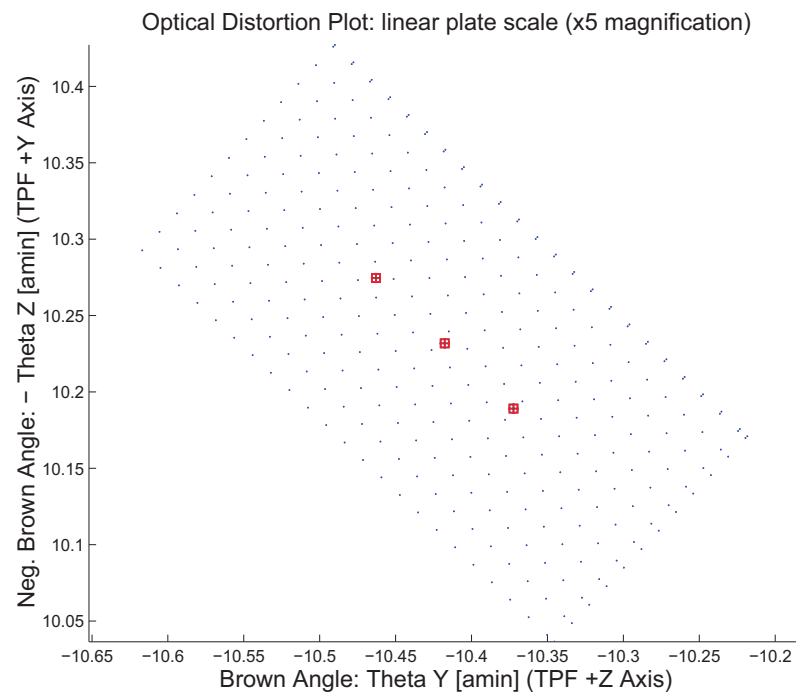


Figure 3.34: Optical Distortion Plot: linear plate scale (x5 magnification)

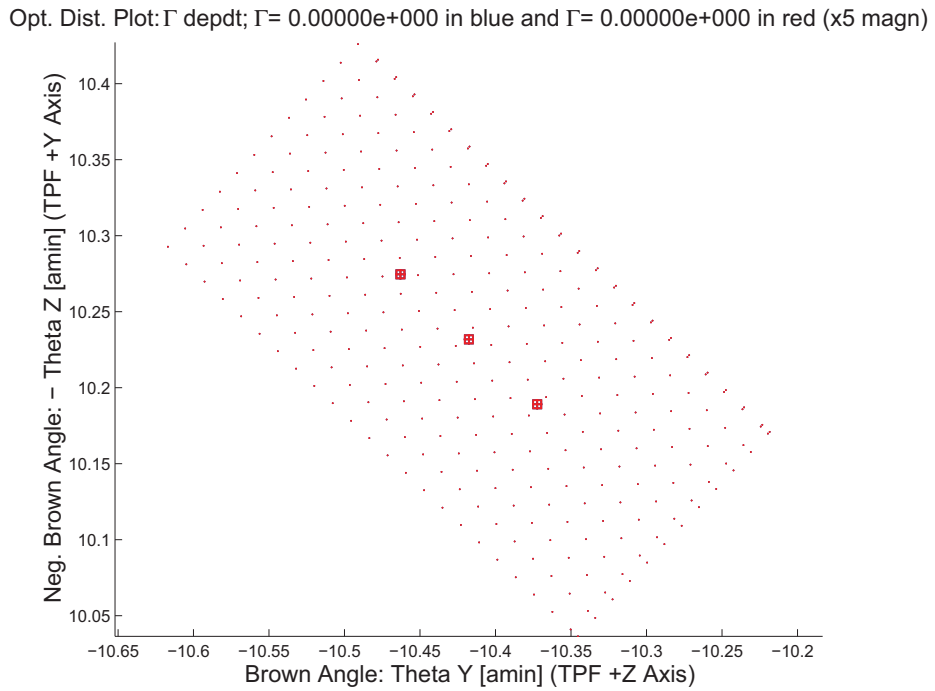


Figure 3.35: Optical Distortion Plot: gamma terms (x5 magnification)

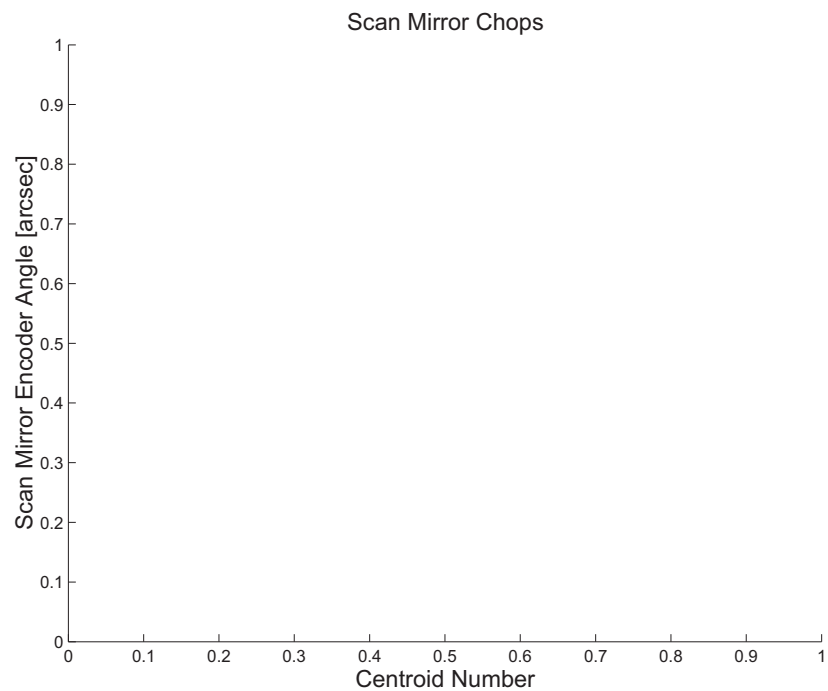


Figure 3.36: Scan Mirror Chops

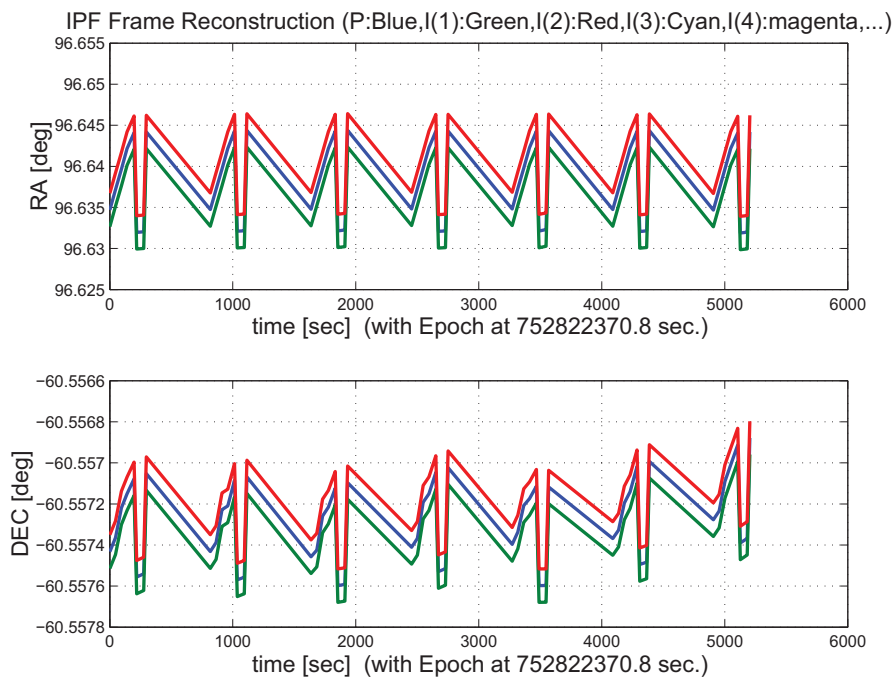


Figure 3.37: IPF Frame Reconstruction

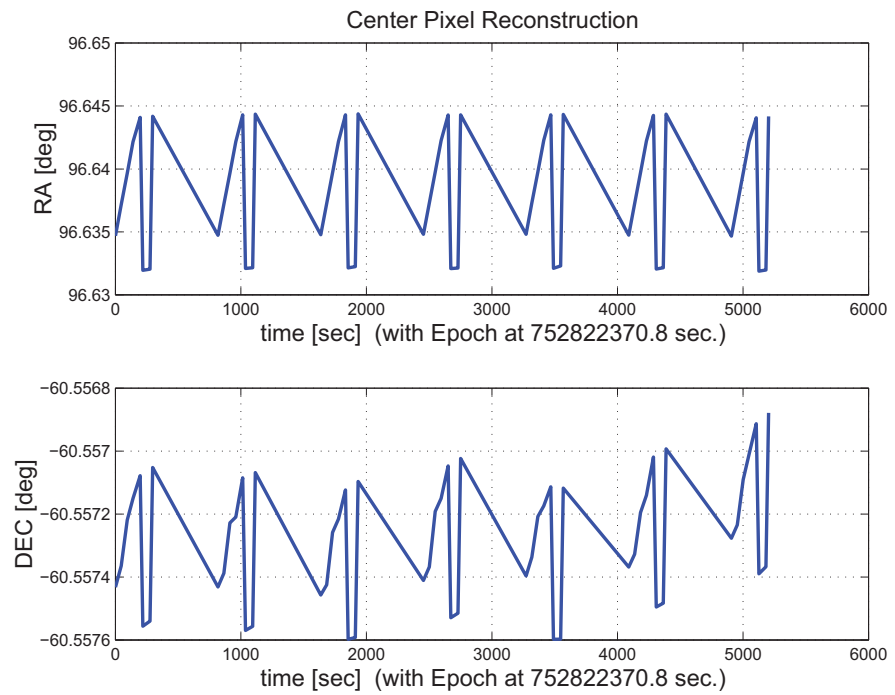


Figure 3.38: Center Pixel Reconstruction

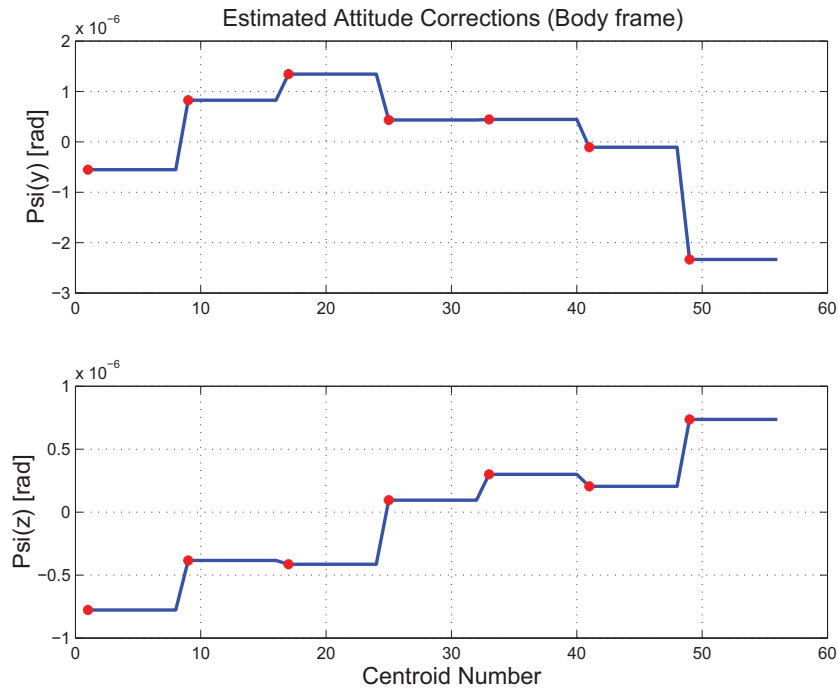


Figure 3.39: Estimated attitude corrections (Body frame)

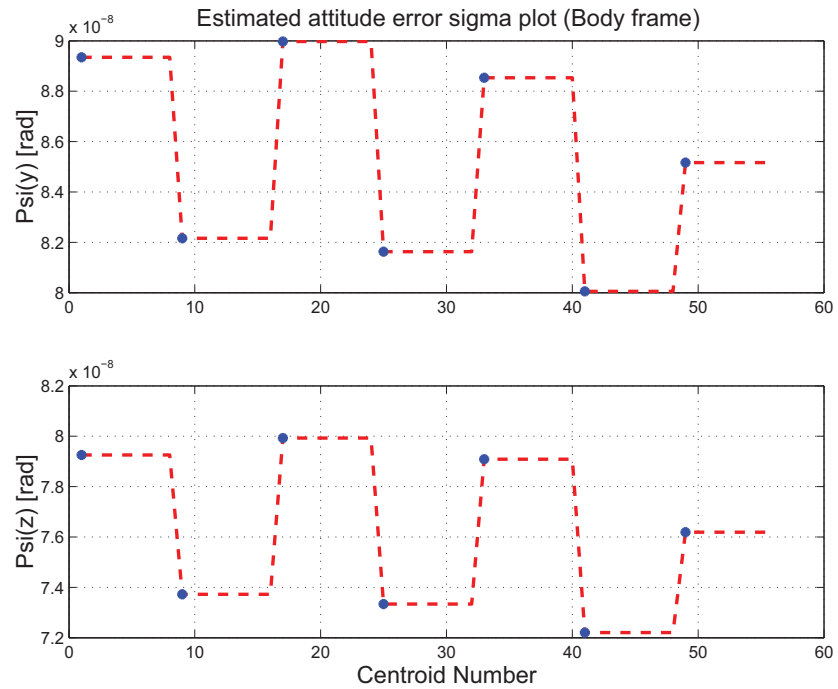


Figure 3.40: Estimated attitude error sigma plot (Body frame)

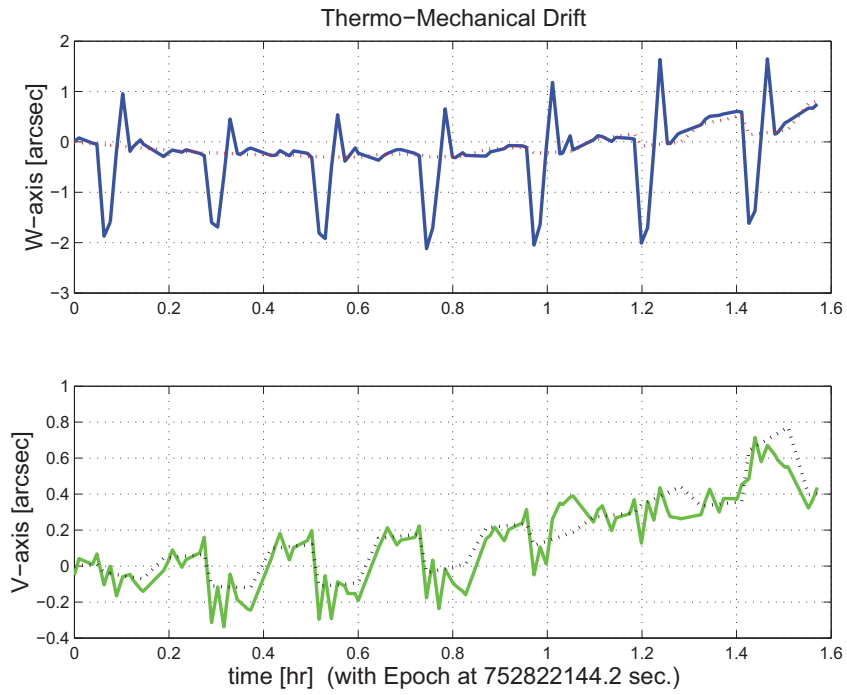


Figure 3.41: Thermo-mechanical boresight drift (equiv. angle in (W,V) coords)

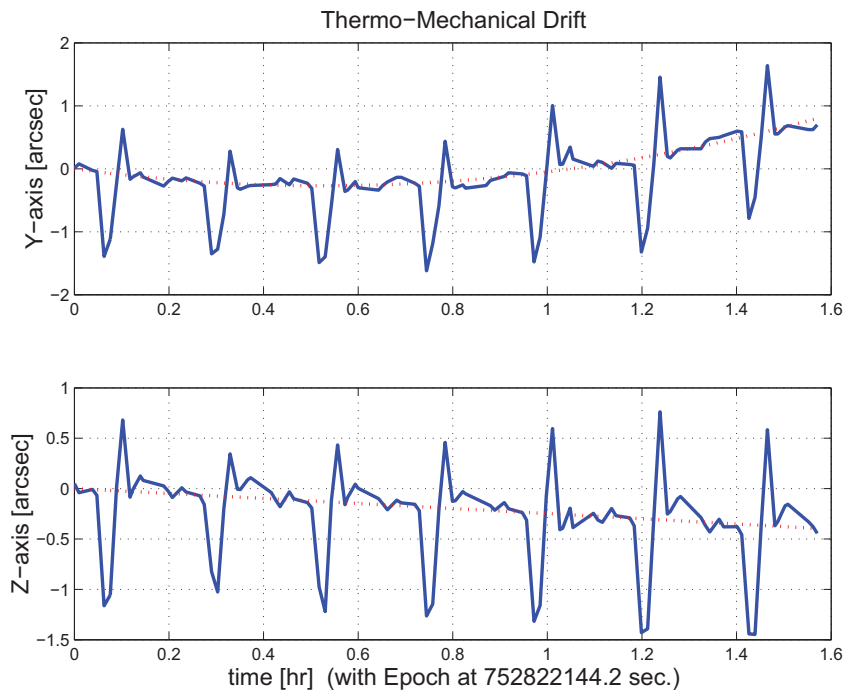


Figure 3.42: Thermo-mechanical boresight drift (equiv. angle in Body frame)

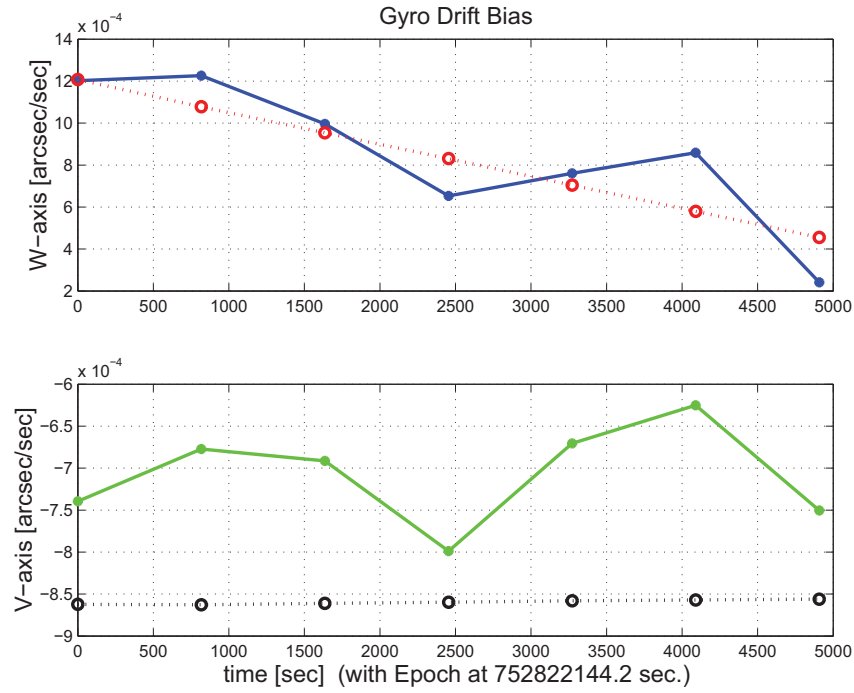


Figure 3.43: Gyro drift bias contribution (equiv. rate in (W,V) coords)

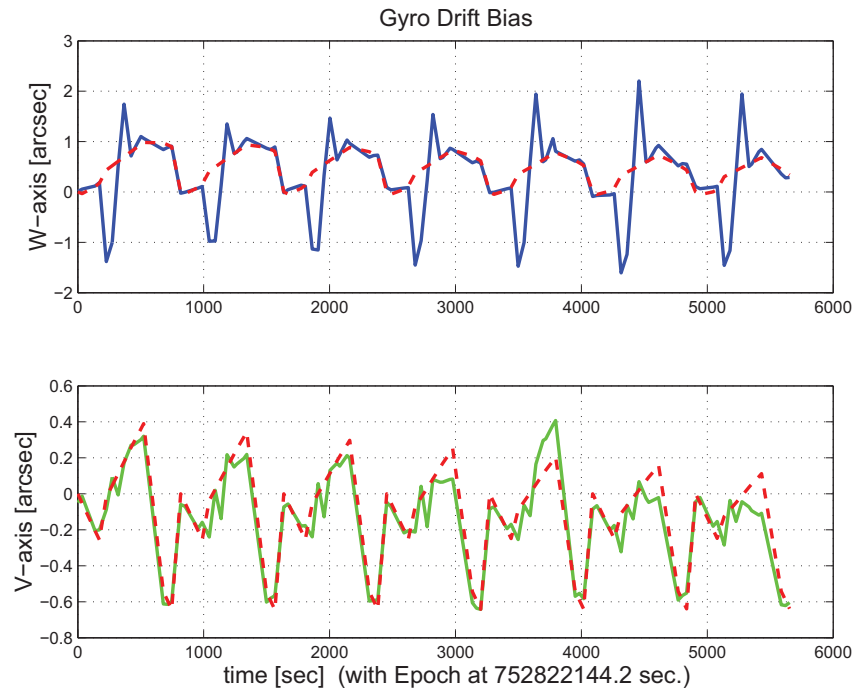


Figure 3.44: Gyro drift bias contribution (equiv. angle in (W,V) coords)

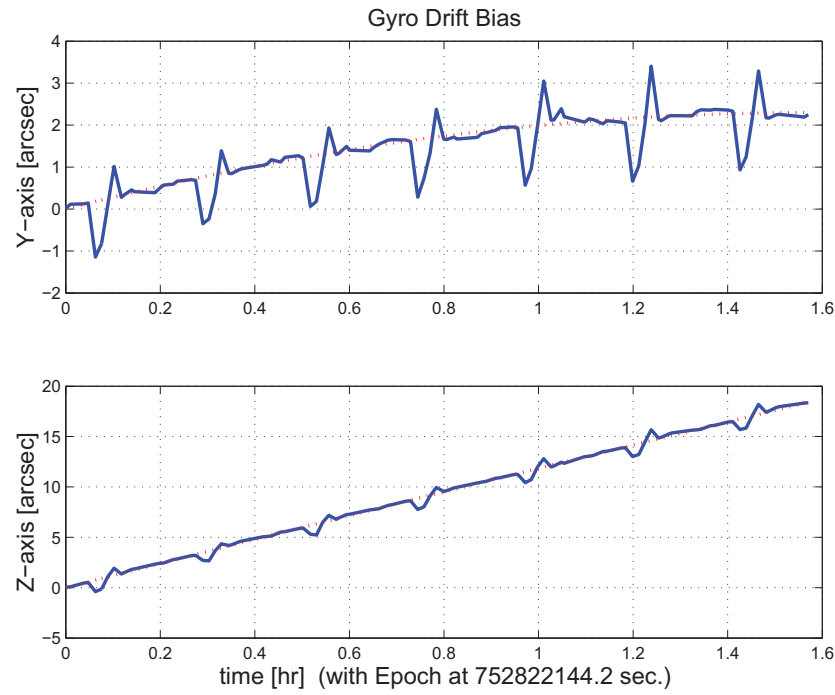


Figure 3.45: Gyro drift bias contribution (equiv. angle in Body frame)

3.2 IPF OUTPUT DATA (IF MINI FILE)

OUTPUT FILE NAME: IFmini501058.dat DATE: 11-Nov-2003 TIME: 14:00
INSTRUMENT NAME: IRS_LongHi_Center_Position NF: 58
IPF FILTER VERSION: IPF.V3.0.0B SW RELEASE DATE: November 3, 2003
FRAME TABLE USED: BodyFrames_FTU_13a

----- IPF BROWN ANGLE SUMMARY -----

Frame Number	WAS			IS		
	theta_Y (arcmin)	theta_Z (arcmin)	angle (deg)	theta_Y (arcmin)	theta_Z (arcmin)	angle (deg)
058	-10.431602	-10.242024	+43.340004	-10.417687	-10.231851	+43.340004
056	-10.476856	-10.284729	+43.340004	-10.461402	-10.273104	+43.340004
057	-10.386348	-10.199319	+43.340004	-10.373972	-10.190598	+43.340004

OFFSET	NF	Delta_CW	Delta_CV
0	58	+0.000	+0.000 pixels

OFFSET FRAME NAME: IRS_LongHi_Center_Position

Brown Angle	theta_Y(arcmin)	theta_Z(arcmin)	angle(deg)
WAS(FTB)	-10.431602	-10.242024	+43.340004
IS (EST)	-10.417687	-10.231851	+43.340004
dT_EST	+0.013915	+0.010173	-0.000001
T_sSIGMA	+0.000675	+0.000667	+999.999999
dT_EST/T_sSIGMA	+20.616104	+15.249726	+999.999999

OFFSET	NF	Delta_CW	Delta_CV
1	56	-3.733	+0.000 pixels

OFFSET FRAME NAME: IRS_LongHi_1st_Position

Brown Angle	theta_Y(arcmin)	theta_Z(arcmin)	angle(deg)
WAS(FTB)	-10.476856	-10.284729	+43.340004
IS (EST)	-10.461402	-10.273104	+43.340004
dT_EST	+0.015453	+0.011625	-0.000001
T_sSIGMA	+0.000694	+0.000667	+999.999999
dT_EST/T_sSIGMA	+22.264145	+17.426096	+999.999999

OFFSET	NF	Delta_CW	Delta_CV
2	57	+3.733	+0.000 pixels

OFFSET FRAME NAME: IRS_LongHi_2nd_Position

Brown Angle	theta_Y(arcmin)	theta_Z(arcmin)	angle(deg)
WAS(FTB)	-10.386348	-10.199319	+43.340004
IS (EST)	-10.373972	-10.190598	+43.340004
dT_EST	+0.012376	+0.008722	-0.000001
T_sSIGMA	+0.000673	+0.000667	+999.999999
dT_EST/T_sSIGMA	+18.399462	+13.073357	+999.999999

VARNAME	MEAN	SIGMA	SCALED_SIGMA
a00	-3.3998474853012106E-002	+9.9159125581899815E-004	+1.7272168506746264E-003
del_theta2	-1.8515478879535657E-015	+1.1271548149668909E-007	+1.9633500984454269E-007
del_theta3	-2.3880356339153045E-015	+1.1140823270551816E-007	+1.9405796057965222E-007
del_arx	+2.1412495528842085E-013	+3.6213021751373178E-005	+6.3078149404572584E-005
del_ary	-5.4508689114610902E-014	+3.6557489413448538E-006	+6.3678165133793237E-006
del_arz	-1.4739070813856890E-014	+3.6926535814163898E-006	+6.4320993676557980E-006
brx	+1.9542544899121899E-008	+2.8652103199168902E-008	+4.9908059558268584E-008
bry	-1.3286826436567504E-009	+3.4610164441035015E-009	+6.0286190379725730E-009
brz	-4.1955128610431331E-010	+3.330375737062398E-009	+5.8056972844947429E-009
crx	-9.6744987240173697E-012	+1.0164378380688718E-011	+1.7704962112900133E-011
cry	+7.1502274025441489E-013	+1.3679935940669178E-012	+2.3828584342807343E-012
crz	+2.3226725489797093E-014	+1.3029068885983878E-012	+2.2694862622487311E-012
bgx	-2.7206733099254488E-006	+4.5262034063521913E-007	+7.8840295808935835E-007
bgy	+3.8688324279918375E-009	+3.4645447682763728E-009	+6.0347648979025217E-009
bgz	+1.6326729952602006E-008	+3.7878587963068638E-009	+6.5979338790695836E-009
cgx	+3.5503968635204746E-011	+1.274256737949476E-010	+2.2195745245635550E-010

cgy -6.7385957723189876E-013 +1.3618504866046581E-012 +2.3721579781582603E-012
cgz -1.9173028861506107E-013 +1.4291916734442240E-012 +2.4894571495367523E-012

LSQF RESIDUAL SIGMA SCALE = +1.7418637372392349E+000

	qT(1)	qT(2)	qT(3)	qT(4)
FrmTbl:	+3.6925731350083602E-001	+1.9600500210806100E-003	+8.2411468409487605E-004	+9.2932476318294999E-001
Estim:	+3.6925731616289736E-001	+1.9576228467781732E-003	+8.2348692625022377E-004	+9.2932476779769835E-001
DelTheta	deltheta(1)	deltheta(2)	deltheta(3)	
	-1.4428822954060074E-012	-4.9748971960906147E-006	+6.2572473338558913E-007	[rad]
EulAngT	theta(1)	theta(2)	theta(3)	[rad]
Mean	+7.5642576340660561E-001	+3.0303822885778759E-003	+2.9763247703501051E-003	
SigmaT	+9.999900000000000E+004	+1.1271548149668909E-007	+1.1140823270551816E-007	

	qR(1)	qR(2)	qR(3)	qR(4)
ASFILE:	+7.1055861189961433E-004	+1.2693599564954638E-003	-1.6143686661962420E-004	+9.9999892711639404E-001
Estim:	+6.5039354876471063E-004	+1.2697216243836105E-003	-1.5985993216695535E-004	+9.9999896961948431E-001
DelThetaR	delthetaR(1)	delthetaR(2)	delthetaR(3)	
	-1.2033417696537401E-004	+7.0622292568579721E-007	+3.0005805477831209E-006	[rad]
EulAngR	angR(1)	angR(2)	angR(3)	[rad]
Mean	+1.3003843621145594E-003	+2.5396513059633419E-003	-3.1806892850188970E-004	
SigmaR	+3.6213021751373178E-005	+3.6557489413448538E-006	+3.6926535814163898E-006	

Initial Gyro Bias	Bg0(1)	Bg0(2)	Bg0(3)	
	-4.0854212102203746E-007	-2.0850968951435789E-007	+3.6856843621535518E-007	
Gyro Bias Correction	Bg(1)	Bg(2)	Bg(3)	
	-2.7206733099254488E-006	+3.8688324279918375E-009	+1.6326729952602006E-008	
Total Gyro Bias	BgT(1)	BgT(2)	BgT(3)	
	-3.1292154309474863E-006	-2.0464085708636604E-007	+3.8489516616795716E-007	

Initial Gyro Bias Rate	Cg0(1)	Cg0(2)	Cg0(3)	
	+0.000000000000000E+000	+0.000000000000000E+000	+0.000000000000000E+000	
Gyro Bias Rate Correction	Cg(1)	Cg(2)	Cg(3)	
	+3.5503968635204746E-011	-6.7385957723189876E-013	-1.9173028861506107E-013	
Total Gyro Bias Rate	CgT(1)	CgT(2)	CgT(3)	
	+3.5503968635204746E-011	-6.7385957723189876E-013	-1.9173028861506107E-013	

OFFSET	NF	Delta_CW	Delta_CV	
1	56	-3.733	+0.000	pixels
OFFSET FRAME NAME:	IRS_LongHi_1st_Position			
qT	qT(1)	qT(2)	qT(3)	qT(4)
WAS(FTB)	+3.6925728847427713E-001	+1.9684602600786309E-003	+8.2745644652694233E-004	+9.2932475238135037E-001
IS (EST)	+3.6925729201700525E-001	+1.9657471505549629E-003	+8.2671507378082650E-004	+9.2932475737634102E-001
DelTheta	deltheta(1)	deltheta(2)	deltheta(3)	
Units	rad	rad	rad	
	+1.3228330183301830E-009	-5.5902597807004995E-006	+6.2572452214378587E-007	
EulAngT	theta(1)	theta(2)	theta(3)	[rad]
Mean	+7.5642576340660561E-001	+3.0430985454184050E-003	+2.9883247941764300E-003	
sSigmaT	+3.3929769532869195E-012	+2.0190365150922200E-007	+1.9405795738422540E-007	
SigmaT	+1.9479003327003148E-012	+1.1591242597955967E-007	+1.1140823087103090E-007	

OFFSET	NF	Delta_CW	Delta_CV	
2	57	+3.733	+0.000	pixels
OFFSET FRAME NAME:	IRS_LongHi_2nd_Position			
qT	qT(1)	qT(2)	qT(3)	qT(4)
WAS(FTB)	+3.6925733842116831E-001	+1.9516397817287217E-003	+8.2077292207259774E-004	+9.2932477393863078E-001
IS (EST)	+3.6925734020966317E-001	+1.9494985426715516E-003	+8.2025877910148692E-004	+9.2932477817620496E-001

DelTheta	deltheta(1)	deltheta(2)	deltheta(3)	
Units	rad	rad	rad	
	-1.3147878598521389E-009	-4.3595346115921732E-006	+6.2572489723914524E-007	
EulAngT	theta(1)	theta(2)	theta(3)	[rad]
Mean	+7.5642576340660572E-001	+3.0176660313009748E-003	+2.9643247474486272E-003	

```

sSigmaT +3.3929769532870706E-012 +1.9566407097298401E-007 +1.9405796368927407E-007
SigmaT +1.9479003327004016E-012 +1.1233029702030628E-007 +1.1140823449074497E-007
-----
----- q(1) q(2) q(3) q(4)
PCRS1A: +5.3371888965461637E-007 +3.7444233778550031E-004 -1.4253684912431913E-003 +9.9999891405806784E-001
PCRS2A: -5.2779261998836216E-007 +3.8462959425181312E-004 +1.3722087221825403E-003 +9.9999898455099423E-001
*****
***** CS-FILE PARAMETERS: ***** AS-FILE PARAMETERS: *****
Row (01) PIX2RADX: +4.8481368110953598E-006 Row (1) TASTART: +7.5282100049076843E+008
Row (02) PIX2RADY: +4.8481368110953598E-006 Row (2) TASTOP: +7.5282900039072263E+008
Row (03) CXO: +0.0000000000000000E+000 Row (3) S/C TIME: +7.5281598359077454E+008
Row (04) CYO: +0.0000000000000000E+000 Row (4) QR1: +7.1055861189961433E-004
Row (05) BETA0: +9.9999000000000000E+004 Row (5) QR2: +1.2693599564954638E-003
Row (06) GAMMA_E0: +9.9999000000000000E+004 Row (6) QR3: -1.6143686661962420E-004
Row (07) D11: -1.0000000000000000E+000 Row (7) QR4: +9.9999892711639404E-001
Row (08) D12: +0.0000000000000000E+000
Row (09) D21: +0.0000000000000000E+000
Row (10) D22: +1.0000000000000000E+000
Row (11) DG: +9.9999000000000000E+004
-----
----- INITIAL STA-TO-PCRS ALIGNMENT (R) KNOWLEDGE (1-SIGMA)
      SIGMA(X)      SIGMA(Y)      SIGMA(Z)
5.11558360E+000  2.92687846E-001  2.93020915E-001 [arcsec]
-----
PIX2RADX = 4.848136811095E-006[rad/pixel]
XPIXSIZE = 1.0000[arcsec]
PIX2RADY = 4.848136811095E-006[rad/pixel]
YPIXSIZE = 1.0000[arcsec]
CX0 = 0.0[pixel] = 0.00[arcsec]
CY0 = 0.0[pixel] = 0.00[arcsec]
-----
NOMINAL BETA0 = 9.999900000000E+004[rad/encoder unit]
ENCODER UNIT SIZE = 99999.00[arcsec]
GAMMA_E0 = 99999.00[encoder unit] = 99999.00[arcsec]
-----
| -1 | +0 |
FLIP MATRIX D = |----|----| and DG = +99999
| +0 | +1 |
-----
```

3.3 IPF EXECUTION LOG

```

*****
IPF EXECUTION-LOG FILE NAME: LG501058.dat
INSTRUMENT TYPE: IRS_LongHi_Center_Position
IPF FILTER EXECUTION DATE: 11-Nov-2003 TIME: 13:59
IPF FILTER VERSION USED: IPF.V3.0.0B
*****
```

```

*****
SLIT FLAG ENABLED! ENTERING SLIT MODE.
*****
```

```

----- Loading & Preparing Input Files -----
AAFILE: AA501058 Loaded! AAFILE dimension = 80000 X 21
ASFILE: AS501058 Loaded!
CAFFILE: CA501058 Loaded! CAFFILE dimension = 56 X 15
```

```

CBFILE: CB502058 Loaded!          CBFILe dimension = 49 X 15
CCFILE: CC501058 Created!        CCFILE dimension = 105 X 19
CSFILE: CS501058 Loaded!
Loading Input Files Completed!
-----
----- Selected Mask Vectors -----
index =  1  2  3  4  5  6  7  8  9 10 11 12 13 14 15 16 17 18 19 20
-----
mask1 = [ 1  0  0  0  0  0  0  0  0  0  0  0  0  0  0  0  0  0  0  0 ]
mask2 = [ 0  0  0  1  1  1  1  1  1  1  1  1  1  1  1  1  1  1  1  1 ]
-----
----- Selected Initial Gyro Bias Parameters -----
User Entered 1 : Use AFILE database - from S/C filter
IPF Linearized Using Following Nominal Gyro Bias Estimates
bg0 = [-4.0854212102203746E-007 -2.0850968951435789E-007 +3.6856843621535518E-007 ]
cg0 = [+0.000000000000000E+000 +0.000000000000000E+000 +0.000000000000000E+000 ]
-----
----- Gyro Pre-Processor Run Completed -----
AGFILE CREATED: AG501058.m      ACFILE CREATED: AC501058.m
-----
Total Gyro Preprocessor Execution Time: 24 seconds

FRAME TABLE ENTRIES FOR PCRS LOADED TO TPCRS
q_PCRS4 = [ +5.3371888965461637E-007   q_PCRS5 = [ +7.3379987833742897E-007
             +3.7444233778550031E-004           +5.2236196154513707E-004
             -1.4253684912431913E-003           -1.4047712280184723E-003
             +9.9999891405806784E-001           +9.999887687698918E-001 ];
q_PCRS8 = [ -5.2779261998836216E-007   q_PCRS9 = [ -7.1963421681856818E-007
             +3.8462959425181312E-004           +5.3239763239987400E-004
             +1.3722087221825403E-003           +1.3516841804518383E-003
             +9.9999898455099423E-001           +9.9999894475050310E-001 ];
-----
----- Initial Conditions for State ----- ----- Initial Square-Root Cov (diag) -----
p1(01) = a00 = +0.000000000000000E+000 Sigma_initial(01,01) = 1.000000000000000E+000
p1(02) = b00 = +0.000000000000000E+000 Sigma_initial(02,02) = 9.999900000000000E+004
p1(03) = c00 = +0.000000000000000E+000 Sigma_initial(03,03) = 9.999900000000000E+004
p1(04) = a10 = +0.000000000000000E+000 Sigma_initial(04,04) = 9.999900000000000E+004
p1(05) = b10 = +0.000000000000000E+000 Sigma_initial(05,05) = 9.999900000000000E+004
p1(06) = c10 = +0.000000000000000E+000 Sigma_initial(06,06) = 9.999900000000000E+004
p1(07) = d10 = +0.000000000000000E+000 Sigma_initial(07,07) = 9.999900000000000E+004
p1(08) = a20 = +0.000000000000000E+000 Sigma_initial(08,08) = 9.999900000000000E+004
p1(09) = b20 = +0.000000000000000E+000 Sigma_initial(09,09) = 9.999900000000000E+004
p1(10) = c20 = +0.000000000000000E+000 Sigma_initial(10,10) = 9.999900000000000E+004
p1(11) = d20 = +0.000000000000000E+000 Sigma_initial(11,11) = 9.999900000000000E+004
p1(12) = a01 = +0.000000000000000E+000 Sigma_initial(12,12) = 9.999900000000000E+004
p1(13) = b01 = +0.000000000000000E+000 Sigma_initial(13,13) = 9.999900000000000E+004
p1(14) = c01 = +0.000000000000000E+000 Sigma_initial(14,14) = 9.999900000000000E+004
p1(15) = d01 = +0.000000000000000E+000 Sigma_initial(15,15) = 9.999900000000000E+004
p1(16) = e01 = +0.000000000000000E+000 Sigma_initial(16,16) = 9.999900000000000E+004
p1(17) = f01 = +0.000000000000000E+000 Sigma_initial(17,17) = 9.999900000000000E+004
-----
p2f(01) = am1 = +0.000000000000000E+000 Sigma_initial(18,18) = 9.999900000000000E+004
p2f(02) = am2 = +0.000000000000000E+000 Sigma_initial(19,19) = 9.999900000000000E+004
p2f(03) = am3 = +1.000000000000000E+000 Sigma_initial(20,20) = 9.999900000000000E+004
p2f(04) = beta = +1.000000000000000E+000 Sigma_initial(21,21) = 1.000000000000000E-002
p2f(05) = qT1 = +3.6925731350083629E-001 Sigma_initial(22,22) = 1.000000000000000E-002
p2f(06) = qT2 = +1.9600500210806117E-003 Sigma_initial(23,23) = 2.4801049141136999E-004
p2f(07) = aT3 = +8.2411468409487670E-004 Sigma_initial(24,24) = 1.4189907179334265E-005
p2f(08) = qT4 = +9.2932476318295076E-001 Sigma_initial(25,25) = 1.4206054839572710E-005
p2f(09) = qR1 = +7.1055861189961433E-004 Sigma_initial(26,26) = 1.7686280828388951E-004
p2f(10) = qR2 = +1.2693599564954638E-003 Sigma_initial(27,27) = 1.7686280828388951E-004
p2f(11) = qR3 = -1.6143686661962420E-004 Sigma_initial(28,28) = 1.7686280828388951E-004
p2f(12) = qR4 = +9.9999892711639404E-001 Sigma_initial(29,29) = 1.7686280828388951E-004
p2f(13) = brx = +0.000000000000000E+000 Sigma_initial(30,30) = 1.7686280828388951E-004
p2f(14) = bry = +0.000000000000000E+000 Sigma_initial(31,31) = 1.7686280828388951E-004

```

```

p2f(15) = brz = +0.0000000000000000E+000 Sigma_initial(28,28) = 1.7686280828388951E-004
p2f(16) = crx = +0.0000000000000000E+000 Sigma_initial(29,29) = 3.1280452954063856E-008
p2f(17) = cry = +0.0000000000000000E+000 Sigma_initial(30,30) = 3.1280452954063856E-008
p2f(18) = crz = +0.0000000000000000E+000 Sigma_initial(31,31) = 3.1280452954063856E-008
p2f(19) = bgx = +0.0000000000000000E+000 Sigma_initial(32,32) = 1.7686280828388951E-004
p2f(20) = bgy = +0.0000000000000000E+000 Sigma_initial(33,33) = 1.7686280828388951E-004
p2f(21) = bgz = +0.0000000000000000E+000 Sigma_initial(34,34) = 1.7686280828388951E-004
p2f(22) = cgx = +0.0000000000000000E+000 Sigma_initial(35,35) = 3.1280452954063856E-008
p2f(23) = cgy = +0.0000000000000000E+000 Sigma_initial(36,36) = 3.1280452954063856E-008
p2f(24) = cgz = +0.0000000000000000E+000 Sigma_initial(37,37) = 3.1280452954063856E-008
-----
```

```

----- IPF KALMAN FILTER STARTED -----
Iteration#001: |dp|= +3.526347505187E-002 RMS(|Res|)=+4.963519105753E-006
Iteration#002: |dp|= +1.246300830477E-003 RMS(|Res|)=+4.544540054409E-006
Iteration#003: |dp|= +1.058046281211E-004 RMS(|Res|)=+4.704851029882E-006
Iteration#004: |dp|= +7.981562917087E-006 RMS(|Res|)=+4.700496904049E-006
Iteration#005: |dp|= +5.530767206222E-007 RMS(|Res|)=+4.694218393813E-006
Iteration#006: |dp|= +7.593062518255E-008 RMS(|Res|)=+4.693330731164E-006
Iteration#007: |dp|= +7.762471588105E-009 RMS(|Res|)=+4.693677688862E-006
Iteration#008: |dp|= +1.907294342344E-009 RMS(|Res|)=+4.693773088045E-006
Iteration#009: |dp|= +2.311770605521E-010 RMS(|Res|)=+4.693762486166E-006
Iteration#010: |dp|= +1.105783028404E-010 RMS(|Res|)=+4.693754986833E-006
Iteration#011: |dp|= +2.912930780740E-011 RMS(|Res|)=+4.693754732121E-006
Iteration#012: |dp|= +4.870557188935E-012 RMS(|Res|)=+4.693755184246E-006
Iteration#013: |dp|= +8.383513355092E-012 RMS(|Res|)=+4.693755262738E-006
Iteration#014: |dp|= +4.429834923077E-012 RMS(|Res|)=+4.693755240395E-006
Iteration#015: |dp|= +1.031421887335E-012 RMS(|Res|)=+4.693755230843E-006
Iteration#016: |dp|= +2.691752781489E-012 RMS(|Res|)=+4.693755230445E-006
Iteration#017: |dp|= +4.765097045884E-012 RMS(|Res|)=+4.693755232595E-006
Iteration#018: |dp|= +7.231113768268E-012 RMS(|Res|)=+4.693755229785E-006
Iteration#019: |dp|= +1.728003844491E-012 RMS(|Res|)=+4.693755231913E-006
Iteration#020: |dp|= +1.151702951633E-011 RMS(|Res|)=+4.693755234378E-006
Iteration#021: |dp|= +7.640576028972E-012 RMS(|Res|)=+4.693755229819E-006
Iteration#022: |dp|= +3.394326367408E-012 RMS(|Res|)=+4.693755228225E-006
Iteration#023: |dp|= +4.785746695967E-012 RMS(|Res|)=+4.693755235744E-006
Iteration#024: |dp|= +5.043962670897E-012 RMS(|Res|)=+4.693755232324E-006
Iteration#025: |dp|= +2.581672610502E-012 RMS(|Res|)=+4.693755233867E-006
Iteration#026: |dp|= +9.135527417462E-012 RMS(|Res|)=+4.693755235717E-006
Iteration#027: |dp|= +1.995255945935E-012 RMS(|Res|)=+4.693755231407E-006
Iteration#028: |dp|= +1.035948149095E-011 RMS(|Res|)=+4.693755227244E-006
Iteration#029: |dp|= +4.523563285809E-012 RMS(|Res|)=+4.693755234905E-006
Iteration#030: |dp|= +5.738631565783E-012 RMS(|Res|)=+4.693755231126E-006
IPF Kalman Filter Completed with Error |dp1| + |dp2| = +5.7386315657825385E-012
-----
```

```

----- IPF LEAST SQUARES FILTER STARTED -----
Iteration#001 COND#=+9.540459911005E+006, |dp|=+3.526632201755E-002
Iteration#002 COND#=+9.575372348010E+006, |dp|=+1.242858012478E-003
Iteration#003 COND#=+9.573960369536E+006, |dp|=+1.032334529942E-004
Iteration#004 COND#=+9.574073924296E+006, |dp|=+7.779596362368E-006
Iteration#005 COND#=+9.574065315728E+006, |dp|=+5.921720332051E-007
Iteration#006 COND#=+9.574065975269E+006, |dp|=+4.505396705635E-008
Iteration#007 COND#=+9.574065925072E+006, |dp|=+3.427673131977E-009
Iteration#008 COND#=+9.574065928893E+006, |dp|=+2.606294894309E-010
Iteration#009 COND#=+9.574065928603E+006, |dp|=+1.987559996742E-011
Iteration#010 COND#=+9.574065928625E+006, |dp|=+1.644691346594E-012
Iteration#011 COND#=+9.574065928624E+006, |dp|=+3.288434155586E-013
Iteration#012 COND#=+9.574065928623E+006, |dp|=+2.677657067311E-013
Iteration#013 COND#=+9.574065928623E+006, |dp|=+1.267217600512E-013
Iteration#014 COND#=+9.574065928625E+006, |dp|=+1.422567799183E-013
Iteration#015 COND#=+9.574065928625E+006, |dp|=+6.646831634304E-014
Iteration#016 COND#=+9.574065928622E+006, |dp|=+1.814230891279E-013
Iteration#017 COND#=+9.574065928625E+006, |dp|=+2.571759029486E-013
Iteration#018 COND#=+9.574065928624E+006, |dp|=+6.853642141772E-014
Iteration#019 COND#=+9.574065928623E+006, |dp|=+1.696608493189E-013
Iteration#020 COND#=+9.574065928626E+006, |dp|=+2.770703443089E-013
Iteration#021 COND#=+9.574065928626E+006, |dp|=+3.965811084234E-014
```

```
Iteration#022 COND#=+9.574065928623E+006, |dp|=+2.178260444563E-013
Iteration#023 COND#=+9.574065928626E+006, |dp|=+2.737607090979E-013
Iteration#024 COND#=+9.574065928625E+006, |dp|=+1.169141639225E-013
Iteration#025 COND#=+9.574065928623E+006, |dp|=+1.574908207199E-013
Iteration#026 COND#=+9.574065928624E+006, |dp|=+1.229997522500E-013
Iteration#027 COND#=+9.574065928626E+006, |dp|=+1.434023005138E-013
Iteration#028 COND#=+9.574065928621E+006, |dp|=+5.262783729141E-013
Iteration#029 COND#=+9.574065928624E+006, |dp|=+3.893754944059E-013
Iteration#030 COND#=+9.574065928624E+006, |dp|=+1.337581131066E-013
IPF Least Squares Filter Completed with Error |dp1| + |dp2| = +1.3375811310662469E-013
```

Total Execution Time: 61 seconds

4 COMMENTS

Overall the data looked clean, and the filter converged nicely.

Comments:

1. The run was performed in normal IPF operating mode.
2. This run uses IPF version 3.0 where the gyro drift bias estimates make use of the recently corrected GCF signs, (MCR 2521) and now show no sandwich-to-sandwich variations.
3. There were 7 sandwiches maneuvers with 56 science centroids and 49 PCRS measurements.
4. We estimated 18 parameters consisting of: 1 constant plate scales along the slit, 2 IPF alignment angles (no Twist), 3 STA-to-PCRS alignment angles, 6 STA-to-PCRS thermo-mechanical drift parameters, and 3 gyro bias and 3 gyro bias-drift parameters.

We recommend updating frames 56, 57, and 58 with the new quaternions listed in the IF file IF501058.dat. This contains adjustments of about 0.6 arcseconds in Y and Z. In our best judgement, these adjustments are accurate to 0.1 arcsecond which satisfies the Fine Focal Plane Survey requirement of 0.28 arcsecond by a good margin.

IPF TEAM CONTACT INFORMATION

IPF Team email	ipf@sirtfweb.jpl.nasa.gov	
David S. Bayard	X4-8208	David.S.Bayard@jpl.nasa.gov (TEAM LEADER)
Dhemetrio Boussalis	X4-3977	boussali@grover.jpl.nasa.gov
Paul Brugarolas	X4-9243	Paul.Brugarolas@jpl.nasa.gov
Bryan H. Kang	X4-0541	Bryan.H.Kang@jpl.nasa.gov
Edward.C.Wong	X4-3053	Edward.C.Wong@jpl.nasa.gov (TASK MANAGER)

ACKNOWLEDGEMENTS

This work was performed at the Jet Propulsion Laboratory, California Institute of Technology, under contract with the National Aeronautics and Space Administration.

References

- [1] D.S. Bayard, B.H. Kang, *SIRTF Instrument Pointing Frame Kalman Filter Algorithm*, JPL D-Document D-24809, September 30, 2003.
- [2] B.H. Kang, D.S. Bayard, *SIRTF Instrument Pointing Frame (IPF) Software Description Document and User's Guide*, JPL D-Document D-24808, September 30, 2003.
- [3] D.S. Bayard, B.H. Kang, *SIRTF Instrument Pointing Frame (IPF) Kalman Filter Unit Test Report*, JPL D-Document D-24810, September 30, 2003.
- [4] *Space Infrared Telescope Facility In-Orbit Checkout and Science Verification Mission Plan*, JPL D-Document D-22622, 674-FE-301 Version 1.4, February 8, 2002.
- [5] *Space Infrared Telescope Facility Observatory Description Document*, Lockheed Martin LMMS/P458569, 674-SEIT-300 Version 1.2, November 1, 2002.
- [6] *SIRTF Software Interface Specification for Science Centroid INPUT Files (CAFILe, CS-FILE)*, JPL SOS-SIS-2002, November 18, 2002.
- [7] *SIRTF Software Interface Specification for Inferred Frames Offset INPUT Files (OFILE)*, JPL SOS-SIS-2003, November 18, 2002.
- [8] *SIRTF Software Interface Specification for PCRS Centroid INPUT Files (CBFILE)*, JPL SIS-FES-015, November 18, 2002.
- [9] *SIRTF Software Interface Specification for Attitude INPUT Files (AFILE, ASFILE)*, JPL SIS-FES-014, January 7, 2002.
- [10] *SIRTF Software Interface Specification for IPF Filter Output Files (IFFILE, LGFILE, TARFILE)*, JPL SOS-SIS-2005, November 18, 2002.
- [11] R.J. Brown, *Focal Surface to Object Space Field of View Conversion*. Systems Engineering Report SER No. S20447-OPT-051, Ball Aerospace & Technologies Corp., November 23, 1999.